ISSN 2218-4333 (online)

World Journal of *Clinical Oncology*

World J Clin Oncol 2024 January 24; 15(1): 1-164

Published by Baishideng Publishing Group Inc

World Journal of Clinical Oncology

Contents

Monthly Volume 15 Number 1 January 24, 2024

World Journal of Clinical Oncology

Monthly Volume 15 Number 1 January 24, 2024

Contents

World Journal of Clinical Oncology

Monthly Volume 15 Number 1 January 24, 2024

Contents

ABOUT COVER

Peer Reviewer of *World Journal of Clinical Oncology*, Hui-Xia Lu, PhD, Professor, Department of Gynecology and Obstetrics, Clinical Medical College, University of Dali, Dali 671003, Yunnan Province, China. haohao021021@foxmail.com

AIMS AND SCOPE

The primary aim of *World Journal of Clinical Oncology* (*WJCO*, *World J Clin Oncol*) is to provide scholars and readers from various fields of oncology with a platform to publish high-quality basic and clinical research articles and communicate their research findings online.

WJCO mainly publishes articles reporting research results and findings obtained in the field of oncology and covering a wide range of topics including art of oncology, biology of neoplasia, breast cancer, cancer prevention and control, cancer-related complications, diagnosis in oncology, gastrointestinal cancer, genetic testing for cancer, gynecologic cancer, head and neck cancer, hematologic malignancy, lung cancer, melanoma, molecular oncology, neurooncology, palliative and supportive care, pediatric oncology, surgical oncology, translational oncology, and urologic oncology.

INDEXING/ABSTRACTING

The *WJCO* is now abstracted and indexed in PubMed, PubMed Central, Emerging Sources Citation Index (Web of Science), Reference Citation Analysis, China Science and Technology Journal Database, and Superstar Journals Database. The 2023 Edition of Journal Citation Reports® cites the 2022 impact factor (IF) for *WJCO* as 2.8; IF without journal self cites: 2.8; 5-year IF: 3.0; Journal Citation Indicator: 0.36.

RESPONSIBLE EDITORS FOR THIS ISSUE

NAME OF JOURNAL
World Journal of Clinical Oncology

ISSN
ISSN 2218-4333 (online)

LAUNCH DATE
November 10, 2010

FREQUENCY
Monthly

EDITORS-IN-CHIEF
Hiten RH Patel, Stephen Safe, Jian-Hua Mao, Ken H Young

EDITORIAL BOARD MEMBERS
https://www.wjgnet.com/2218-4333/editorialboard.htm

PUBLICATION DATE
January 24, 2024

INSTRUCTIONS TO AUTHORS
https://www.wjgnet.com/bpg/gerinfo/204

GUIDELINES FOR ETHICS DOCUMENTS
https://www.wjgnet.com/bpg/GerInfo/287

GUIDELINES FOR NON-NATIVE SPEAKERS OF ENGLISH
https://www.wjgnet.com/bpg/gerinfo/240

PUBLICATION ETHICS
https://www.wjgnet.com/bpg/GerInfo/288

PUBLICATION MISCONDUCT
https://www.wjgnet.com/bpg/gerinfo/208

ARTICLE PROCESSING CHARGE
https://www.wjgnet.com/bpg/gerinfo/242

STEPS FOR SUBMITTING MANUSCRIPTS
https://www.wjgnet.com/bpg/GerInfo/239

ONLINE SUBMISSION
https://www.f6publishing.com

World Journal of Clinical Oncology

Submit a Manuscript: https://www.f6publishing.com

World J Clin Oncol 2024 January 24; 15(1): 1-4

DOI: 10.5306/wjco.v15.i1.1

ISSN 2218-4333 (online)

EDITORIAL

Re-evaluating the role of pelvic radiation in the age of modern precision medicine and systemic therapy

Tao-Wei Ke, Yu-Min Liao, Sheng-Chi Chang, Che-Hung Lin, William Tzu-Liang Chen, Ji-An Liang, Chun-Ru Chien

Specialty type: Oncology

Provenance and peer review: Invited article; Externally peer reviewed.

Peer-review model: Single blind

Peer-review report's scientific quality classification

Grade A (Excellent): 0
Grade B (Very good): B
Grade C (Good): 0
Grade D (Fair): D
Grade E (Poor): 0

P-Reviewer: Chen N, China; Yakar M, Turkey

Received: September 25, 2023
Peer-review started: September 25, 2023
First decision: December 2, 2023
Revised: December 9, 2023
Accepted: December 29, 2023
Article in press: December 29, 2023
Published online: January 24, 2024

Tao-Wei Ke, Sheng-Chi Chang, William Tzu-Liang Chen, Department of Colorectal Surgery, China Medical University Hospital, Taichung 40402, Taiwan

Tao-Wei Ke, School of Chinese Medicine, College of Chinese Medicine, China Medical University, Taichung 40402, Taiwan

Yu-Min Liao, Che-Hung Lin, Division of Hematology and Oncology, Department of Internal Medicine, China Medical University Hospital, Taichung 40402, Taiwan

William Tzu-Liang Chen, Department of Colorectal Surgery, China Medical University Hsinchu Hospital, Hsinchu 30272, Taiwan

William Tzu-Liang Chen, Ji-An Liang, School of Medicine, College of Medicine, China Medical University, Taichung 40402, Taiwan

Ji-An Liang, Chun-Ru Chien, Department of Radiation Oncology, China Medical University Hospital, Taichung 40402, Taiwan

Corresponding author: Chun-Ru Chien, MD, PhD, Doctor, Professor, Department of Radiation Oncology, China Medical University Hospital, No. 91 Hsueh-Shih Road, North District, Taichung 40402, Taiwan. d16181@gmail.com

Abstract

The efficacy of pelvic radiation in the management of locally advanced stage rectal cancer has come under scrutiny in the context of modern precision medicine and systemic therapy as evidenced by recent clinical trials such as FOWARC (*J Clin Oncol* 2019; 37: 3223-3233), NCT04165772 (*N Engl J Med* 2022; 386: 2363-2376), and PROSPECT (*N Engl J Med* 2023; 389: 322-334). In this review, we comprehensively assess these pivotal trials and offer additional insights into the evolving role of pelvic radiation in contemporary oncology.

Key Words: Radiotherapy; Locally advanced stage rectal cancer; Precision medicine; Systemic therapy; Clinical trial

Core Tip: Neoadjuvant systemic therapy alone without radiation represents a viable option for locally advanced rectal cancer patients, particularly when organ preservation is not a priority. Nevertheless, it is crucial to engage in multidisciplinary discussions, especially considering the limited long-term experience.

Citation: Ke TW, Liao YM, Chang SC, Lin CH, Chen WTL, Liang JA, Chien CR. Re-evaluating the role of pelvic radiation in the age of modern precision medicine and systemic therapy. *World J Clin Oncol* 2024; 15(1): 1-4
URL: https://www.wjgnet.com/2218-4333/full/v15/i1/1.htm
DOI: https://dx.doi.org/10.5306/wjco.v15.i1.1

INTRODUCTION

Pelvic radiation has traditionally played an essential role in neoadjuvant therapy for locally advanced rectal cancer (LARC) in the past, either as neoadjuvant concurrent chemoradiotherapy (nCCRT) or neoadjuvant short course radiotherapy (nSCRT)[1-3]. However, its efficacy has come under scrutiny in the context of modern precision medicine and systemic therapy as evidenced by recent clinical trials[4-6] and a systematic review[7]. Consequently, the use of neoadjuvant systemic therapy alone without radiation has emerged as one of the alternatives in contemporary guidelines for patients with certain genetic mutations who achieved a complete clinical response after immunotherapy or patients with a good response (> 20%) after chemotherapy[8]. In addition, patients with high-risk features such as threatened mesorectal fascia, N2 stage, or extramural vascular invasion were not good candidates for the use of chemotherapy without radiation[6,8].

MAIN BODY

In this editorial, we have summarized select relevant trials in Table 1[4-6,9,10], which provide the rationale for employing neoadjuvant systemic therapy alone without radiation in specific LARC cases. However, we would like to highlight two additional considerations regarding the omission of pelvic radiation for LARC.

Table 1 Key characteristic of trials investigating neoadjuvant systemic therapy alone without radiation in locally advanced rectal cancer

Study	ID	Design	LARC	Study group	Comparator group(s)	mFU	pCR (%)	Local control (%)	OS (%)
FOWARC[4]	NCT01211210	Phase 3	Suitable for curative resection	FOLFOX	CCRT	45.2	6.5 *vs* (14 or 27.5); *P* 0.05	3-year LRR 8.3 *vs* (8 or 7); *P* = 0.873	3-year 90.7 *vs* (91.3 or 89.1); *P* = 0.971
PROSPECT [6]	NCT01515787	Phase 3	T2N1, T3N0, T3N1	FOLFOX	CCRT	58	21.9 *vs* 24.3; *P* value NA	5-year LR 1.8% *vs* 1.6%; *P* value > 0.05	5-year 89.5 *vs* 90.2; *P* value > 0.05
GRECCAR4 [9]	NCT01333709	Phase 2 RCT	T3d with predictive CRM 1 mm	FOLFIRINOX	CCRT	65.7	(10 or 13.5) *vs* (58 or 20); *P* value NA	NA	5-year (90 or 84.3) *vs* (93.3 or 86.1); *P* value > 0.05
CONVERT [10]	NCT02288195	Phase 3	cT2N+ or cT3-4Nany uninvolved mesorectal fascia	CAPOX	CCRT	NA	11 *vs* 13.8; *P* = 0.33	NA	NA
19-288[5]	NCT04165772	Phase 2	Mismatch repair–deficient	Dostarlimab	NA	NA	NA	100	100

LARC: Locally advanced rectal cancer; LR: Local recurrence; LRR: Locoregional recurrence; mFU: Median follow up (in months); pCR: Pathological complete response; OS: Overall survival; CCRT: Concurrent chemoradiotherapy; CRM: Circumferential resection margin; NA: Not available; RCT: Randomized controlled trial.

First, it is imperative to await long-term follow-up results from the aforementioned studies. For instance, the initial publication of the RAPIDO trial reported no statistically significant difference in locoregional failure between nSCRT followed by chemotherapy and nCCRT (P = 0.12)[11]. However, the disparity in locoregional failure became more pronounced with borderline statistical significance after extended follow-up (P = 0.07)[12]. This finding has led to nSCRT being less favored by certain experts[13] and in the current guidelines[8]. It is worth noting that the biological equivalent dose in radiotherapy of nCCRT is higher than that of nSCRT [EQD2(10) 50 Gy *vs* 37.5 Gy][14].

Second, one of the potential objectives in modern LARC management is organ preservation, for which nCCRT in the context of total neoadjuvant therapy has shown great promise[15,16]. Therefore, when sphincter or organ preservation is the goal, concerns may arise about the suitability of neoadjuvant systemic therapy alone without radiation[13].

CONCLUSION

In summary, neoadjuvant systemic therapy alone without radiation represents a viable option for LARC patients, particularly when organ preservation is not a priority. Nevertheless, it is crucial to engage in multidisciplinary discussions, especially considering the limited long-term experience. We eagerly anticipate the results of ongoing trials, such as NCT04495088 and NCT04749108, which will provide further insights into this evolving treatment approach.

FOOTNOTES

Co-first authors: Tao-Wei Ke and Yu-Min Liao.

Author contributions: Ke TW and Liao YM contributed equally to this work; Ke TW, Liao YM, Chang SC, Chen WTL, Liang JA, and Chien CR made substantial contribution to the design of the work, to the interpretation of data, and to revise the manuscript; all have read and approve the final manuscript. The choice of these researchers (Ke TW and Liao YM) as co-first authors acknowledges and respects this equal contribution, while recognizing the spirit of teamwork and collaboration of this study. In summary, we believe that designating Ke TW and Liao YM as co-first authors is fitting for our manuscript as it accurately reflects our team's collaborative spirit, equal contributions, and diversity.

Supported by National Science and Technology Council, No. NSTC 112-2314-B-039-048.

Conflict-of-interest statement: We declared no conflict of interest.

Country/Territory of origin: Taiwan

ORCID number: Chun-Ru Chien 0000-0002-2365-7641.

S-Editor: Lin C
L-Editor: A
P-Editor: Zhang XD

REFERENCES

1 **Sauer R**, Becker H, Hohenberger W, Rödel C, Wittekind C, Fietkau R, Martus P, Tschmelitsch J, Hager E, Hess CF, Karstens JH, Liersch T, Schmidberger H, Raab R; German Rectal Cancer Study Group. Preoperative versus postoperative chemoradiotherapy for rectal cancer. *N Engl J Med* 2004; **351**: 1731-1740 [PMID: 15496622 DOI: 10.1056/NEJMoa040694]

2 **Kapiteijn E**, Marijnen CA, Nagtegaal ID, Putter H, Steup WH, Wiggers T, Rutten HJ, Pahlman L, Glimelius B, van Krieken JH, Leer JW, van de Velde CJ; Dutch Colorectal Cancer Group. Preoperative radiotherapy combined with total mesorectal excision for resectable rectal cancer. *N Engl J Med* 2001; **345**: 638-646 [PMID: 11547717 DOI: 10.1056/NEJMoa010580]

3 **Koukourakis GV**. Role of radiation therapy in neoadjuvant era in patients with locally advanced rectal cancer. *World J Gastrointest Oncol* 2012; **4**: 230-237 [PMID: 23443049 DOI: 10.4251/wjgo.v4.i12.230]

4 **Deng Y**, Chi P, Lan P, Wang L, Chen W, Cui L, Chen D, Cao J, Wei H, Peng X, Huang Z, Cai G, Zhao R, Xu L, Zhou H, Wei Y, Zhang H, Zheng J, Huang Y, Zhou Z, Cai Y, Kang L, Huang M, Wu X, Peng J, Ren D, Wang J. Neoadjuvant Modified FOLFOX6 With or Without Radiation Versus Fluorouracil Plus Radiation for Locally Advanced Rectal Cancer: Final Results of the Chinese FOWARC Trial. *J Clin Oncol* 2019; **37**: 3223-3233 [PMID: 31557064 DOI: 10.1200/JCO.18.02309]

5 **Cercek A**, Lumish M, Sinopoli J, Weiss J, Shia J, Lamendola-Essel M, El Dika IH, Segal N, Shcherba M, Sugarman R, Stadler Z, Yaeger R, Smith JJ, Rousseau B, Argiles G, Patel M, Desai A, Saltz LB, Widmar M, Iyer K, Zhang J, Gianino N, Crane C, Romesser PB, Pappou EP, Paty P, Garcia-Aguilar J, Gonen M, Gollub M, Weiser MR, Schalper KA, Diaz LA Jr. PD-1 Blockade in Mismatch Repair-Deficient, Locally Advanced Rectal Cancer. *N Engl J Med* 2022; **386**: 2363-2376 [PMID: 35660797 DOI: 10.1056/NEJMoa2201445]

6 **Schrag D**, Shi Q, Weiser MR, Gollub MJ, Saltz LB, Musher BL, Goldberg J, Al Baghdadi T, Goodman KA, McWilliams RR, Farma JM, George TJ, Kennecke HF, Shergill A, Montemurro M, Nelson GD, Colgrove B, Gordon V, Venook AP, O'Reilly EM, Meyerhardt JA, Dueck AC, Basch E, Chang GJ, Mamon HJ. Preoperative Treatment of Locally Advanced Rectal Cancer. *N Engl J Med* 2023; **389**: 322-334 [PMID: 37272534 DOI: 10.1056/NEJMoa2303269]

7 **Wu P**, Xu HM, Zhu Z. Neoadjuvant chemotherapy without radiation as a potential alternative treatment for locally advanced rectal cancer: A meta-analysis. *World J Gastrointest Oncol* 2021; **13**: 1196-1209 [PMID: 34616523 DOI: 10.4251/wjgo.v13.i9.1196]

8 **National Comprehensive Cancer Network**. Guidelines for Rectal Cancers, version 6.2023. [cited 24 November 2022]. Available from: https://www.nccn.org/professionals/physician_gls/pdf/rectal.pdf

9 **Rouanet P**, Rullier E, Lelong B, Maingon P, Tuech JJ, Pezet D, Castan F, Nougaret S; GRECCAR Study Group*. Tailored Strategy for Locally Advanced Rectal Carcinoma (GRECCAR 4): Long-term Results From a Multicenter, Randomized, Open-Label, Phase II Trial. *Dis Colon Rectum* 2022; **65**: 986-995 [PMID: 34759247 DOI: 10.1097/DCR.0000000000002153]

10 **Mei WJ**, Wang XZ, Li YF, Sun YM, Yang CK, Lin JZ, Wu ZG, Zhang R, Wang W, Li Y, Zhuang YZ, Lei J, Wan XB, Ren YK, Cheng Y, Li WL, Wang ZQ, Xu DB, Mo XW, Ju HX, Ye SW, Zhao JL, Zhang H, Gao YH, Zeng ZF, Xiao WW, Zhang XP, Zhang X, Xie E, Feng YF, Tang JH, Wu XJ, Chen G, Li LR, Lu ZH, Wan DS, Bei JX, Pan ZZ, Ding PR. Neoadjuvant Chemotherapy With CAPOX Versus Chemoradiation for Locally Advanced Rectal Cancer With Uninvolved Mesorectal Fascia (CONVERT): Initial Results of a Phase III Trial. *Ann Surg* 2023; **277**: 557-564 [PMID: 36538627 DOI: 10.1097/SLA.0000000000005780]

11 **Bahadoer RR**, Dijkstra EA, van Etten B, Marijnen CAM, Putter H, Kranenbarg EM, Roodvoets AGH, Nagtegaal ID, Beets-Tan RGH, Blomqvist LK, Fokstuen T, Ten Tije AJ, Capdevila J, Hendriks MP, Edhemovic I, Cervantes A, Nilsson PJ, Glimelius B, van de Velde CJH, Hospers GAP; RAPIDO collaborative investigators. Short-course radiotherapy followed by chemotherapy before total mesorectal excision (TME) versus preoperative chemoradiotherapy, TME, and optional adjuvant chemotherapy in locally advanced rectal cancer (RAPIDO): a randomised, open-label, phase 3 trial. *Lancet Oncol* 2021; **22**: 29-42 [PMID: 33301740 DOI: 10.1016/S1470-2045(20)30555-6]

12 **Dijkstra EA**, Nilsson PJ, Hospers GAP, Bahadoer RR, Meershoek-Klein Kranenbarg E, Roodvoets AGH, Putter H, Berglund Å, Cervantes A, Crolla RMPH, Hendriks MP, Capdevila J, Edhemovic I, Marijnen CAM, van de Velde CJH, Glimelius B, van Etten B; Collaborative Investigators. Locoregional Failure During and After Short-course Radiotherapy Followed by Chemotherapy and Surgery Compared With Long-course Chemoradiotherapy and Surgery: A 5-Year Follow-up of the RAPIDO Trial. *Ann Surg* 2023; **278**: e766-e772 [PMID: 36661037 DOI: 10.1097/SLA.0000000000005799]

13 **Vailati BB**, Cerdán-Santacruz C, São Julião GP, Corbi L, Perez RO. Short-Course Radiation and Consolidation Chemotherapy for Rectal Cancer-The Rise and Fall of a Treatment Strategy-Rest in Peace. *Dis Colon Rectum* 2023; **66**: 1297-1299 [PMID: 37379161 DOI: 10.1097/DCR.0000000000002997]

14 **Bentzen SM**, Dörr W, Gahbauer R, Howell RW, Joiner MC, Jones B, Jones DT, van der Kogel AJ, Wambersie A, Whitmore G. Bioeffect modeling and equieffective dose concepts in radiation oncology--terminology, quantities and units. *Radiother Oncol* 2012; **105**: 266-268 [PMID: 23157980 DOI: 10.1016/j.radonc.2012.10.006]

15 **Garcia-Aguilar J**, Patil S, Gollub MJ, Kim JK, Yuval JB, Thompson HM, Verheij FS, Omer DM, Lee M, Dunne RF, Marcet J, Cataldo P, Polite B, Herzig DO, Liska D, Oommen S, Friel CM, Ternent C, Coveler AL, Hunt S, Gregory A, Varma MG, Bello BL, Carmichael JC, Krauss J, Gleisner A, Paty PB, Weiser MR, Nash GM, Pappou E, Guillem JG, Temple L, Wei IH, Widmar M, Lin S, Segal NH, Cercek A, Yaeger R, Smith JJ, Goodman KA, Wu AJ, Saltz LB. Organ Preservation in Patients With Rectal Adenocarcinoma Treated With Total Neoadjuvant Therapy. *J Clin Oncol* 2022; **40**: 2546-2556 [PMID: 35483010 DOI: 10.1200/JCO.22.00032]

16 **Solé S**, Baeza R, Gabler C, Couñago F. New standard in locally advanced rectal cancer. *World J Clin Oncol* 2020; **11**: 990-995 [PMID: 33437661 DOI: 10.5306/wjco.v11.i12.990]

World Journal of Clinical Oncology

Submit a Manuscript: https://www.f6publishing.com

World J Clin Oncol 2024 January 24; 15(1): 5-8

DOI: 10.5306/wjco.v15.i1.5

ISSN 2218-4333 (online)

EDITORIAL

Prognostic factors of breast cancer brain metastasis

Melek Yakar, Durmuş Etiz

Specialty type: Oncology

Provenance and peer review: Invited article; Externally peer reviewed.

Peer-review model: Single blind

Peer-review report's scientific quality classification

Grade A (Excellent): 0
Grade B (Very good): 0
Grade C (Good): C
Grade D (Fair): 0
Grade E (Poor): 0

P-Reviewer: Zhang JX, China

Received: October 27, 2023
Peer-review started: October 27, 2023
First decision: November 29, 2023
Revised: December 3, 2023
Accepted: December 28, 2023
Article in press: December 28, 2023
Published online: January 24, 2024

Melek Yakar, Department of Radiation Oncology, Osmangazi University, Eskişehir 26040, Turkey

Durmuş Etiz, Department of Radiation Oncology, Eskisehir Osmangazi University Faculty of Medicine, Eskişehir 26040, Turkey

Corresponding author: Melek Yakar, MD, Adjunct Associate Professor, Department of Radiation Oncology, Osmangazi University, Meşelik Campus Büyükdere District Prof. Dr. Nabi AVCI Boulevard No:4 26040 Odunpazarı - Eskişehir, Eskişehir 26040, Turkey.
myakar@ogu.edu.tr

Abstract

In this editorial we comment on the article by Chen *et al* published in the recent issue of the *World Journal of Clinical Oncology*. Brain metastasis is one of the most serious complications of breast cancer and causes high morbidity and mortality. Brain metastases may involve the brain parenchyma and/or leptomeninges. Symptomatic brain metastases develop in 10%-16% of newly recognized cases each year, and this rate increases to 30% in autopsy series. Depending on the size of the metastatic foci, it may be accompanied by extensive vasogenic edema or may occur as small tumor foci. Since brain metastases are a significant cause of morbidity and mortality, early diagnosis can have significant effects on survival and quality of life. The risk of developing brain metastases emerges progressively due to various patient and tumor characteristics. Patient variability may be particularly important in the susceptibility and distribution of brain metastases because malignant blood must cross the brain barrier and move within the brain parenchyma. Some characteristics of the tumor, such as gene expression, may increase the risk of brain metastasis. Clinical growth, tumor stage, tumor grade, growth receptor positivity, HER2 positivity, molecular subtype (such as triple negative status, luminal/nonluminal feature) increase the risk of developing breast cancer metastasis. Factors related to survival due to breast cancer brain metastasis include both tumor/patient characteristics and treatment characteristics, such as patient age, lung metastasis, surgery for brain metastasis, and HER2 positivity. If cases with a high risk of developing brain metastasis can be identified with the help of clinical procedures and artificial intelligence, survival and quality of life can be increased with early diagnosis and treatment. At the same time, it is important to predict the formation of this group in order to develop new treatment methods in cases with low survival expectancy with brain metastases.

Key Words: Breast cancer; Brain metastasis; Prognosis; Artificial intelligence; Clinicopathological features

Core Tip: Breast cancer is still the most common cancer in women. Breast cancer is the second most common cancer causing brain metastasis. In breast cancer, the first metastasis occurs to the brain with a rate of 12%. In recent years, the prognosis of breast cancer-related brain metastases has improved, and survival and the patient's quality of life have increased, thanks to both changes in medical treatments and technological advances in radiotherapy. For this reason, early diagnosis of cases is very important. At the same time, survival is not the same in every case of brain metastasis. Identifying cases with low survival seems to be very important in paving the way for studies to change treatment strategies.

Citation: Yakar M, Etiz D. Prognostic factors of breast cancer brain metastasis. *World J Clin Oncol* 2024; 15(1): 5-8
URL: https://www.wjgnet.com/2218-4333/full/v15/i1/5.htm
DOI: https://dx.doi.org/10.5306/wjco.v15.i1.5

INTRODUCTION

Breast cancer is the most common cancer in women regardless of race and ethnicity. 30% of newly diagnosed patients have breast cancer, and 15% of cancer deaths are caused by breast cancer[1]. While symptomatic brain metastases develop in 10%-16% of newly diagnosed breast cancer patients each year, this rate is 30% in autopsy series[2,3]. In cases diagnosed with breast cancer that develop brain metastases, survival rates may be as low as 2-9 mo despite treatment. Surgical resection, whole brain radiotherapy, stereotactic radiosurgery (SRS), stereotactic body radiotherapy (SBRT), chemotherapy and targeted therapies can improve outcomes in these patients[4,5]. Identifying prognostic factors associated with breast cancer brain metastasis may help identify patients at risk. According to studies, some characteristics of the patient and the tumor have been shown to increase the risk of breast cancer. In most breast cancers, brain metastases occur 2-3 years after initial diagnosis, and only 20% of patients survive after 1 year[6]. After breast cancer develops, some patient, tumor and treatment characteristics that affect the prognosis regarding survival have been determined in studies. If the patient's prognosis can be predicted after developing breast cancer, different treatment options may come to the fore in patients with good prognosis/bad prognosis.

In this editorial we comment on the article by Chen *et al*[7] published in the recent issue of the *World Journal of Clinical Oncology*. Brain metastasis is one of the most serious complications of breast cancer and causes high morbidity and mortality. Brain metastases may involve the brain parenchyma and/or leptomeninges. Symptomatic brain metastases develop in 10%-16% of newly recognized cases each year, and this rate increases to 30% in autopsy series. Depending on the size of the metastatic foci, it may be accompanied by extensive vasogenic edema or may occur as small tumor foci. Since brain metastases are a significant cause of morbidity and mortality, early diagnosis can have significant effects on survival and quality of life. The risk of developing brain metastases emerges progressively due to various patient and tumor characteristics. Patient variability may be particularly important in the susceptibility and distribution of brain metastases because malignant blood must cross the brain barrier and move within the brain parenchyma. Some characteristics of the tumor, such as gene expression, may increase the risk of brain metastasis. Clinical growth, tumor stage, tumor grade, growth receptor positivity, HER2 positivity, molecular subtype (such as triple negative status, luminal/nonluminal feature) increase the risk of developing breast cancer metastasis. Factors related to survival due to breast cancer brain metastasis include both tumor/patient characteristics and treatment characteristics, such as patient age, lung metastasis, surgery for brain metastasis, and HER2 positivity. If cases with a high risk of developing brain metastasis can be identified with the help of clinical procedures and artificial intelligence, survival and quality of life can be increased with early diagnosis and treatment. At the same time, it is important to predict the formation of this group in order to develop new treatment methods in cases with low survival expectancy with brain metastases.

PROGNOSTIC FEATURES IN BREAST CANCER BRAIN METASTASIS

When we look at the literature, many prognostic features in breast cancer have been investigated due to the high incidence of breast cancer. If we look at the prognostic factors related to brain metastasis; We can examine it in two groups: prognostic factors that increase the risk of developing brain metastasis and prognostic factors that affect survival after the development of brain metastasis.

Unlike other metastasis sites, brain metastasis is usually observed after a latent period after diagnosis in breast cancer, and this can be explained by the blood-brain barrier. The blood-brain barrier is a complex structure consisting of endothelial cells, tight junctions, basement membrane, pericytes, astrocytes, microglia, enzymes and transporters. It controls the permeability of the brain to macromolecules and is also involved in the transmission of signals and maintenance of central nervous system homeostasis. For this reason, biological pathways and regulatory molecules formed across the blood-brain barrier are also very important in preventing brain metastasis due to breast cancer[8]. In addition to treating patients with brain metastases, preventing brain metastases due to the primary tumor is also an important clinical goal. Such prevention would require detecting circulating brain-tropic cancer cells before extravasation.

Liquid biopsy is a potential screening tool for the detection of such cells in circulation[9].

Local therapeutic approaches such as surgery and radiotherapy have proven effective for metastatic brain tumors. Systemic treatments to control extracranial disease are developing. However, specific treatments targeting brain metastases in breast cancer patients have not been established, and therefore the prognosis of such patients remains poor. Identification of the cellular and molecular mechanisms underlying brain metastasis of breast cancer will likely provide a basis for the prevention or treatment of such diseases. Breast cancer is divided into several subtypes based on the expression status of human epidermal growth factor receptor 2 (HER2) and estrogen (ER) and progesterone (PR) receptors by immunohistochemical staining or gene expression profiles. These breast cancer subtypes have been found to have different gene signatures, rely on different signaling pathways for metastasis, and show different metastatic site preferences. Patients with HER2-positive breast cancer or triple-negative (HER2− ER− PR−) breast cancer (TNBC) have a higher risk of brain metastasis compared with those with the luminal subtype of breast cancer (ER+ or PR+). Therefore, the frequency of brain metastasis is as high as 20% to 30% in HER2-positive breast cancer and TNBC, but is less than 10% in luminal breast cancer[10].

In a meta-analysis conducted by Hackshaw *et al*[11], 25 studies on this subject and 4097 HER-2 positive breast cancer brain metastasis patients were evaluated. The time between breast cancer diagnosis and the development of brain metastasis was found to be associated with early age, negative hormone receptors, large tumor size, high tumor grade, and not receiving anti-HER-2 treatment. When looking at survival due to brain metastasis, having < 3 metastatic lesions and receiving a local treatment for brain metastasis (SRS, SBRT or surgery) increased survival. At the same time, the longest survival was observed in those treated with trastuzumab and lapatinib or trastuzumab and pertuzumab.

In a study conducted by Leone *et al*[12], prognostic factors were examined in 42 patients who developed brain metastases due to breast cancer and underwent craniotomy. Median survival after brain metastasis develops is 1.33 years. While the only factor affecting the time from breast cancer diagnosis to brain metastasis development is tumor stage, the most important factor affecting survival after brain metastasis is age.

In a study conducted by Castanede *et al*[13] with 215 cases diagnosed with early stage breast cancer, prognostic factors affecting survival due to brain metastasis were investigated. Prognostic factors were found to be nonluminal status, presence of extracrainal metastasis, ≤ 15 mo between breast cancer diagnosis and brain metastasis development, presence of > 3 brain metastasis lesions, and high-grade tumor.

In the literature review by Rostami *et al*[14]; 106 articles and 14599 patients including breast cancer brain metastasis cases were evaluated. Factors affecting prognosis are tumor grade and size, presence of multiple metastases, presence of extracranial metastases, triple negative status, HER2 positivity and Karnofsky score.

Nie *et al*[15] made prognosis prediction with LASSO Cox regression analysis. According to this analysis, the presence of lymph node metastasis, molecular subtype, tumor size, history of chemotherapy and radiotherapy, and the presence of lung metastasis were found to be important variables related to the development of brain metastasis. Li *et al*[16] made prognosis prediction in cases of breast cancer brain metastasis using machine learning method. Among the evaluated algorithms, they reached the highest accuracy rate with the XGBoost model. According to the study, surgery increases survival in HER2+ and triple-negative cases.

CONCLUSION

Breast cancer is the most common cancer in women, and when autopsy series are included, the rate of brain metastasis increases up to 30%. If patients with a high risk of brain metastasis due to breast cancer can be identified, the risk of developing brain metastasis can be reduced and survival can be increased, perhaps with prophylactic brain irradiation, as in small cell lung cancer. Using artificial intelligence, the risky patient group can be predicted through studies with a larger number of patients.

In cases with a high risk of developing brain metastasis and a poor prognosis after the diagnosis of brain metastasis, more effective treatment strategies can be determined if the molecular and cellular mechanisms affecting this can be revealed.

FOOTNOTES

Author contributions: Yakar M and Etiz D contributed to this paper; Yakar M designed the overall concept and outline of the manuscript; Etiz D contributed to the discussion and design of the manuscript; Yakar M and Etiz D contributed to the writing, and editing the manuscript, illustrations, and review of literature.

Conflict-of-interest statement: Authors declare no potential conflict of interests for this article.

Country/Territory of origin: Turkey

ORCID number: Melek Yakar 0000-0002-9042-9489; Durmuş Etiz 0000-0002-2225-0364.

S-Editor: Liu JH
L-Editor: A
P-Editor: Zhang XD

REFERENCES

1 **Miller KD**, Jemal A. Cancer statistics, 2020. *CA Cancer J Clin* 2020; **70**: 7-30 [DOI: 10.3322/caac.21637]
2 **Engel J**, Eckel R, Aydemir U, Aydemir S, Kerr J, Schlesinger-Raab A, Dirschedl P, Hölzel D. Determinants and prognoses of locoregional and distant progression in breast cancer. *Int J Radiat Oncol Biol Phys* 2003; **55**: 1186-1195 [PMID: 12654426 DOI: 10.1016/S0360-3016(02)04476-0]
3 **Lin NU**, Bellon JR, Winer EP. CNS metastases in breast cancer. *J Clin Oncol* 2004; **22**: 3608-3617 [PMID: 15337811 DOI: 10.1200/JCO.2004.01.175]
4 **Duchnowska R**, Dziadziuszko R, Czartoryska-Arłukowicz B, Radecka B, Szostakiewicz B, Sosińska-Mielcarek K, Karpińska A, Starosławska E, Kubiatowski T, Szczylik C. Risk factors for brain relapse in HER2-positive metastatic breast cancer patients. *Breast Cancer Res Treat* 2009; **117**: 297-303 [PMID: 19130219 DOI: 10.1007/s10549-008-0275-z]
5 **Niwińska A**, Pogoda K, Murawska M, Niwiński P. Factors influencing survival in patients with breast cancer and single or solitary brain metastasis. *Eur J Surg Oncol* 2011; **37**: 635-642 [PMID: 21664097 DOI: 10.1016/j.ejso.2011.05.002]
6 **Slimane K**, Andre F, Delaloge S, Dunant A, Perez A, Grenier J, Massard C, Spielmann M. Risk factors for brain relapse in patients with metastatic breast cancer. *Ann Oncol* 2004; **15**: 1640-1644 [PMID: 15520065 DOI: 10.1093/annonc/mdh432]
7 **Chen YR**, Xu ZX, Jiang LX, Dong ZW, Yu PF, Zhang Z, Gu GL. Analysis of clinicopathological features and prognostic factors of breast cancer brain metastasis. *World J Clin Oncol* 2023; **14**: 445-458 [PMID: 38059189 DOI: 10.5306/wjco.v14.i11.445]
8 **Daneman R**, Prat A. The blood-brain barrier. *Cold Spring Harb Perspect Biol* 2015; **7**: a020412 [PMID: 25561720 DOI: 10.1101/cshperspect.a020412]
9 **Boral D**, Vishnoi M, Liu HN, Yin W, Sprouse ML, Scamardo A, Hong DS, Tan TZ, Thiery JP, Chang JC, Marchetti D. Molecular characterization of breast cancer CTCs associated with brain metastasis. *Nat Commun* 2017; **8**: 196 [PMID: 28775303 DOI: 10.1038/s41467-017-00196-1]
10 **Kennecke H**, Yerushalmi R, Woods R, Cheang MC, Voduc D, Speers CH, Nielsen TO, Gelmon K. Metastatic behavior of breast cancer subtypes. *J Clin Oncol* 2010; **28**: 3271-3277 [PMID: 20498394 DOI: 10.1200/JCO.2009.25.9820]
11 **Hackshaw MD**, Danysh HE, Henderson M, Wang E, Tu N, Islam Z, Ladner A, Ritchey ME, Salas M. Prognostic factors of brain metastasis and survival among HER2-positive metastatic breast cancer patients: a systematic literature review. *BMC Cancer* 2021; **21**: 967 [PMID: 34454469 DOI: 10.1186/s12885-021-08708-5]
12 **Leone JP**, Lee AV, Brufsky AM. Prognostic factors and survival of patients with brain metastasis from breast cancer who underwent craniotomy. *Cancer Med* 2015; **4**: 989-994 [PMID: 25756607 DOI: 10.1002/cam4.439]
13 **Castaneda CA**, Flores R, Rojas KY, Castillo M, Dolores-Cerna K, Flores C, Belmar-Lopez C, Milla E, Gomez H. Prognostic factors for patients with newly diagnosed brain metastasis from breast cancer. *CNS Oncol* 2015; **4**: 137-145 [PMID: 25906174 DOI: 10.2217/cns.15.5]
14 **Rostami R**, Mittal S, Rostami P, Tavassoli F, Jabbari B. Brain metastasis in breast cancer: a comprehensive literature review. *J Neurooncol* 2016; **127**: 407-414 [PMID: 26909695 DOI: 10.1007/s11060-016-2075-3]
15 **Nie Y**, Ying B, Lu Z, Sun T, Sun G. Predicting survival and prognosis of postoperative breast cancer brain metastasis: a population-based retrospective analysis. *Chin Med J (Engl)* 2023; **136**: 1699-1707 [PMID: 37257115 DOI: 10.1097/CM9.0000000000002674]
16 **Li C**, Liu M, Zhang Y, Wang Y, Li J, Sun S, Liu X, Wu H, Feng C, Yao P, Jia Y, Wei X, Wu F, Du C, Zhao X, Zhang S, Qu J. Novel models by machine learning to predict prognosis of breast cancer brain metastases. *J Transl Med* 2023; **21**: 404 [PMID: 37344847 DOI: 10.1186/s12967-023-04277-2]

World Journal of Clinical Oncology

Submit a Manuscript: https://www.f6publishing.com

World J Clin Oncol 2024 January 24; 15(1): 9-22

DOI: 10.5306/wjco.v15.i1.9

ISSN 2218-4333 (online)

REVIEW

Inflammatory response in gastrointestinal cancers: Overview of six transmembrane epithelial antigens of the prostate in pathophysiology and clinical implications

Ze-Xuan Fang, Wen-Jia Chen, Zheng Wu, Yan-Yu Hou, Yang-Zheng Lan, Hua-Tao Wu, Jing Liu

Specialty type: Oncology

Provenance and peer review: Invited article; Externally peer reviewed.

Peer-review model: Single blind

Peer-review report's scientific quality classification

Grade A (Excellent): 0
Grade B (Very good): 0
Grade C (Good): C
Grade D (Fair): D
Grade E (Poor): E

P-Reviewer: Gutiérrez-Cuevas J, Mexico; Tantau AI, Romania

Received: October 27, 2023
Peer-review started: October 27, 2023
First decision: November 11, 2023
Revised: November 24, 2023
Accepted: December 19, 2023
Article in press: December 19, 2023
Published online: January 24, 2024

Ze-Xuan Fang, Wen-Jia Chen, Zheng Wu, Yan-Yu Hou, Yang-Zheng Lan, Jing Liu, The Breast Center, Cancer Hospital of Shantou University Medical College, Shantou 515041, Guangdong Province, China

Hua-Tao Wu, Department of General Surgery, First Affiliated Hospital of Shantou University Medical College, Shantou 515041, Guangdong Province, China

Corresponding author: Jing Liu, MD, PhD, Academic Research, Associate Professor, Research Scientist, Senior Scientist, The Breast Center, Cancer Hospital of Shantou University Medical College, No. 22 Xinling Road, Shantou 515041, Guangdong Province, China.
jliu12@stu.edu.cn

Abstract

Chronic inflammation is known to increase the risk of gastrointestinal cancers (GICs), the common solid tumors worldwide. Precancerous lesions, such as chronic atrophic inflammation and ulcers, are related to inflammatory responses *in vivo* and likely to occur in hyperplasia and tumorigenesis. Unfortunately, due to the lack of effective therapeutic targets, the prognosis of patients with GICs is still unsatisfactory. Interestingly, it is found that six transmembrane epithelial antigens of the prostate (STEAPs), a group of metal reductases, are significantly associated with the progression of malignancies, playing a crucial role in systemic metabolic homeostasis and inflammatory responses. The structure and functions of STEAPs suggest that they are closely related to intracellular oxidative stress, responding to inflammatory reactions. Under the imbalance status of abnormal oxidative stress, STEAP members are involved in cell transformation and the development of GICs by inhibiting or activating inflammatory process. This review focuses on STEAPs in GICs along with exploring their potential molecular regulatory mechanisms, with an aim to provide a theoretical basis for diagnosis and treatment strategies for patients suffering from these types of cancers.

Key Words: Six transmembrane epithelial antigens of the prostate; Gastrointestinal cancer; Inflammation

Core Tip: Six transmembrane epithelial antigens of the prostate (STEAPs), a group of metal reductases, are closely related to intracellular oxidative stress, responding to an inflammatory reaction, while chronic inflammation is known to increase the risk of gastrointestinal cancers (GICs). This review of STEAPs in GICs provides a theoretical basis for diagnosis and treatment strategies for patients.

Citation: Fang ZX, Chen WJ, Wu Z, Hou YY, Lan YZ, Wu HT, Liu J. Inflammatory response in gastrointestinal cancers: Overview of six transmembrane epithelial antigens of the prostate in pathophysiology and clinical implications. *World J Clin Oncol* 2024; 15(1): 9-22
URL: https://www.wjgnet.com/2218-4333/full/v15/i1/9.htm
DOI: https://dx.doi.org/10.5306/wjco.v15.i1.9

INTRODUCTION

Gastrointestinal cancers (GICs), such as colorectal cancer (CRC), gastric cancer (GC), and hepatocellular carcinoma (HCC), are one of the leading causes of cancer-related death worldwide, with many cases and wide lesions. Among them, CRC is not only the fourth most common malignancy but also the third main cause of cancer-related death in the United States[1]. GC is the fifth most common cancer and the third leading cause of cancer-related death worldwide[2], while HCC accounts for 90% of liver cancer with 850000 new cases each year[3]. Although effective colonoscopy and upper endoscopy screening can detect precancerous polyps and precancerous lesions in the gastrointestinal tract, many patients have an advanced stage at their first diagnosis and a poor prognosis with current treatment methods[4].

The gastrointestinal tract is exposed to diverse foods and/or drugs daily, which may be related to various degrees of inflammatory response and kinds of diseases. Chronic inflammation is a well-established risk factor for GICs, which is also the molecular and pathophysiological basis of gastritis, inflammatory bowel disease (IBD), and upper and lower GICs[5]. Chronic inflammation initiates tumorigenesis, and mechanisms by which tumor-induced and treatment-related inflammatory processes interact with cancer cells support that inflammatory responses may be closely related to the oncogenesis and/or development of GICs[6]. Inflammatory features involved in the development of CRCs include inflammasome activation and noncanonical nuclear factor-kappaB (NF-κB) pathway activation mediating the production of proinflammatory cytokines, both of which can be activated by changes in the mutant environment or stimulation by microorganisms such as the gut microbiota[7,8]. And smoking, alcohol consumption, various infections, susceptibility gene mutations, and epigenetic changes are associated with the occurrence of GICs[9-11]. Due to the high incidence rates and poor prognosis associated with GICs globally, they represent a significant public health challenge[12].

Recently, the six transmembrane epithelial antigen of the prostate (STEAP) family, a group of key metal oxidoreductases, has been associated with the overexpression of a range of proinflammatory cytokines[13], which are considered promising therapeutic targets for various cancers, especially prostate cancer, due to their role in regulating proinflammatory cytokines[14-16]. However, Gomes *et al*[17] also found that the localization of STEAPs on the cell membrane and their differential expression in normal tissues and gastric, colorectal, and liver cancers make them promising potential targets for the treatment of GICs. Therefore, this review aims to explore the role of STEAPs in inflammatory responses in GICs and provide a new strategy for the prevention and early intervention of GICs.

STRUCTURAL CHARACTERISTICS OF STEAP FAMILY MEMBERS

The STEAP family is composed of four structurally similar members, namely, STEAP1, STEAP2, STEAP3, and STEAP4 [17], as cell-surface transmembrane proteins with six potential transmembrane regions, and intracellular amino and carboxyl termini[18]. It is shown that, unlike STEAP1, the C-terminal and conserved N-terminal domains of STEAP2-4 proteins are similar to the structures of yeast FRE metalloreductase and homologous to the paleontological and bacteriological $F_{420}H_2$:NADP+ oxidoreductase (FNO) binding protein domains, respectively[19]. Normally, STEAPs perform physiological functions as oxidoreductases, involved in the uptake and reduction of iron and copper[19,20] (Figure 1).

STEAP1 is the first reported STEAP family member with a molecular weight of 39.9 kDa (NP_036581.1) and an intramembrane heme binding site[18,21]. Although STEAP1 is widely expressed and co-localizes with transferrin (Tf) and Tf receptor 1 (TfR1), unlike other members, STEAP1 does not independently promote iron or copper reduction or uptake. Although it lacks the FNO-like reductase domain, which is thought to be essential for metal oxidoreductase activity, it is suggested that STEAP1 may play a role in iron or copper metabolism, which may be due to its interaction with the NAPDH-binding FNO domain of STEAP2 or STEAP4[19,22,23]. STEAP1B is a newly discovered member that has an extremely high (88%) identity with STEAP1. What distinguishes it from other proteins is that it only has four potential transmembrane domains without NADPH oxidoreductase domain or heme binding site. Hence, it is not expected to have oxidoreductase activity based on previous studies[15,24].

Besides STEAP1, STEAP2-4 are also composed of six transmembrane α-helices and intracellular hydrophilic N-and C-terminal domains, with the N-terminus containing the intracellular NADPH-binding FNO domain and the C-terminus containing bis-heme with the FRE domain. *In vitro* studies have found that STEAP2-4 perform Fe^{3+} and Cu^{2+} reductase activities and increase intracellular iron and copper uptake[20].

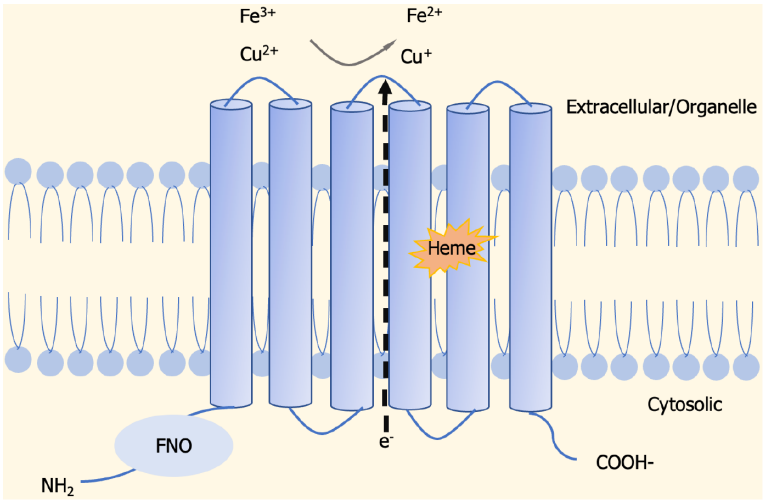

DOI: 10.5306/wjco.v15.i1.9 **Copyright** ©The Author(s) 2024.

Figure 1 Schematic representation of protein structure of six transmembrane epithelial antigens of the prostate. Six transmembrane epithelial antigens of the prostate (STEAPs) are similar in structure, with six transmembrane domains, an intracellular C-terminus, and an intracellular N-terminus containing the intracellular heme group, while STEAP1 Lacks FNO-like domain to perform intrinsic metal reductase activity. STEAP2-4 are involved in cell proliferation, tumor progression, and intercellular communication through their metalloreductase activity. FNO: F420H2:NADP+ oxidoreductase.

STEAP2 is known as STAMP1, which is composed of 490 amino acid residues. It is found that STEAP2 is highly expressed in the androgen-reactive prostate cancer cell line LNCaP, but not in androgen receptor-negative prostate cancer cell lines PC3 and DU145[25,26]. However, the expression of STEAP2 is not regulated by androgen receptors, but requires the presence of an intact androgen receptor[25]. In addition, the characteristics of STEAP2 expression and localization in human microvascular endothelial cells suggest that STEAP2 has a potential role in iron transport across the blood-brain barrier[27], which is further supported by the co-localization of STEAP2 and Tf in primary hippocampal neurons[28]. However, further research is needed to confirm this effect.

STEAP3 was first identified in prostate tissue and proposed as a candidate for prostate cancer immunotherapy, which is also known as tumor suppressor activating pathway 6[29]. STEAP3 co-localizes with Tf, TfR1, and divalent metal transporter 1 (DMT1) to participate in iron-uptake mediated by Tf endosome in erythroid cells and is thus an important component of the Tf-TfR1 cycle[20,30].

STEAP4 is also named STAMP2 because of its sequence similarity to STAMP1. STEAP2 and STEAP4 are highly expressed in the Golgi complex, trans-Golgi network, and plasma membrane, and co-localizes with endosome antigen 1, which is involved in the secretion-endocytosis pathway[25,26,31]. In addition to metal oxidoreductase activity, STEAP4 also plays a role in regulating inflammatory responses, fatty acid metabolism, and glucose metabolism[31-33]. To date, the possible effects of STAMP2 on iron metabolism have not been reported, and more studies are needed to directly evaluate the possible role of STAMP2 in human iron metabolism (Figure 2).

ROLE OF STEAPS IN INFLAMMATORY RESPONSE IN PHYSIOLOGICAL AND PATHOLOGICAL PROCESSES

In mammals, iron and copper metabolism are related. Iron and copper, as important metal ions *in vivo*, are absorbed in the small intestine *via* reduction-state-specific DMT1[34-36] and copper transporter 1[37], respectively. Iron and copper often alternate between two oxidation states and participate in the redox process *in vivo*. Additionally, iron and copper can be used as cofactors of several enzymes to participate in the transformation of substances[34,38,39]. Iron and copper deficiencies are known to cause low-chromium microcell anemia in mammals, while excess iron or copper will lead to organ poisoning, particularly in the liver and brain. More importantly, since tumor cells have stronger proliferative ability than normal cells, their demand for iron and copper exceeds that of normal cells. The imbalance of iron and copper homeostasis is also closely related to cancer progression.

Under physiological conditions, STEAPs are a class of metalloproteinases that play an essential role in iron and copper homeostasis[19]. Iron and its homeostasis are closely related to inflammatory responses and provide a major protective mechanism in human physiology. In the past decades, a series of studies confirmed that iron overload can aggravate inflammatory responses and susceptibility to infection. Persons with hereditary hemochromatosis and iron overload are more susceptible to pathogens, whereas iron deficiency confers relative resistance to infection[40-42]. STEAPs are known to be a participant in iron-copper homeostasis, and their importance in protein functional activity, tissue expression patterns, and subcellular localization in cancer progression has been demonstrated. In addition, STEAPs have also been found to play a role in regulating cell proliferation and apoptosis, alleviating oxidative stress and mediating the Tf cycle [22,43].

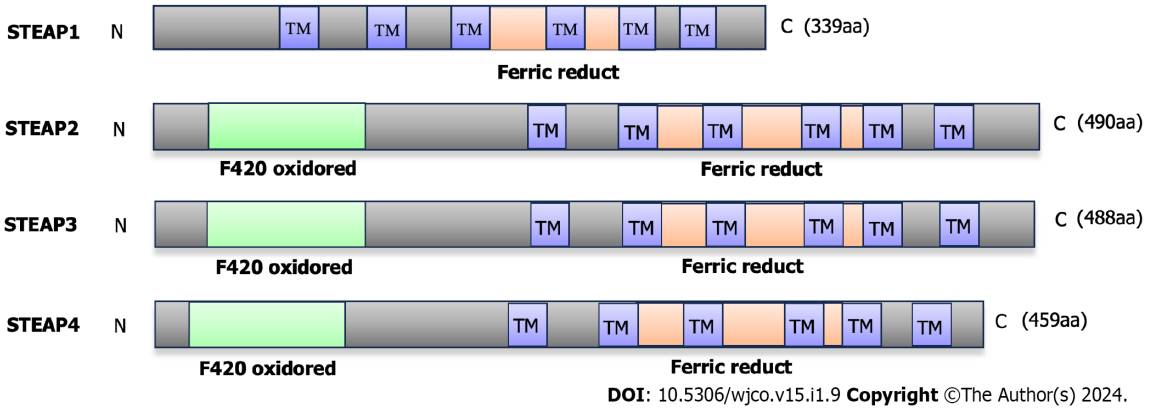

DOI: 10.5306/wjco.v15.i1.9 **Copyright** ©The Author(s) 2024.

Figure 2 Molecular structure diagram of six transmembrane epithelial antigens of the prostate 1-4. The six transmembrane epithelial antigens of the prostate (STEAP) family is composed of a group of cell surface transmembrane proteins with six potential transmembrane domains, one intracellular amino terminus, and a carboxyl terminus that exert physiological functions by acting as oxidoreductases. STEAP1-4 consist of 339, 490, 488, and 459 amino acid residues, respectively. Except STEAP1, the N-terminus of the STEAP2-4 proteins contains the F420H2:NADP+ oxidoreductase binding protein domain. TM: Transmembrane domain; STEAP: Six transmembrane epithelial antigen of the prostate.

Although inflammation is associated with an activated immune system (including immune cells and biological factors) under certain conditions, inflammation is a natural defense response, which is fundamentally different from the immune response[23]. Inflammation is a defense mechanism *in vivo* to remove invading foreign bodies such as bacteria, parasites, and viruses. In the process of inflammatory reaction, excessive or uncontrolled production of inflammatory products will lead to host cell damage, and even lead to chronic inflammation, chronic disease, and tumor transformation[44,45].

STEAP proteins are involved in the regulation of various physiological cellular functions, and plays a potentially important role in various metabolic processes, such as iron uptake and conversion, inflammatory stress response, and glucose metabolism in cells[15,43]. STEAPs have been suggested to play a role in iron metabolism in acute and chronic diseases associated with inflammation, as well as in the oncogenesis and development of malignancies. Liang *et al*[46] reported that STEAP1 and STEAP4 positively regulate the induction of proinflammatory, neutrophil-activated cytokines, such as chemokine (C-X-C motif) ligand (CXCL)1 and interleukin (IL)-8, in pustular skin disorders. More complexly, STEAP4 is found to be regulated by multiple cellular signaling pathways, revealing a positive association of STEAP1 and STEAP4 with the *in vivo* proinflammatory cytokines IL-1, IL-36, CXCL1, and CXCL8 in several neutrophil-driven diseases in humans. In addition, significant changes in genes related to iron biology were observed in patients with pustular skin disorders, suggesting that the inflammatory activity of STEAP has a causal relationship with its regulation of ion metabolism. Timmermans *et al*[47] found that STEAP2 plays a role in pathways involved in a chronic low-grade inflammatory disease state, namely, obesity, and lipid metabolism. Zhang *et al*[13] showed that STEAP3, the only member of this family that is highly expressed in macrophages that play a role in inflammatory immunity, regulates iron homeostasis during inflammatory stress through the translocation-associated membrane protein-dependent pathway. This study provides important insights into the function of STEAP3 as a coordinated regulator of iron homeostasis and inflammation.

In addition to its role as a metal oxidoreductase, STEAP4 is significantly overexpressed in low-grade inflammatory responses[48]. In a study by Gordon *et al*[49], STEAP4 was shown to play a protective role in the face of inflammatory stress in models of metabolic disorders. It is in turn up-regulated by acute inflammation or islet-level cytokine exposure. Even in septic patients, the expression of STEAP4 is elevated in the early stage of sepsis, which can be used to predict the clinical outcome of these patients[50]. These findings point to the complex regulation of STEAP4 that makes its protective role in inflammatory metabolic disorders. It is reported that iron and its homeostasis are closely related to the inflammatory response, which provides a major protective mechanism in human physiology, while iron overload worsens inflammation and infection susceptibility[13].

ROLE OF STEAPS IN INFLAMMATORY RESPONSE IN GICS

In recent years, a large amount of research data have revealed that inflammation is a key component of tumor progression. The oncogenesis of GICs, such as GC, CRC, and HCC, is related to infection and chronic inflammatory stimuli, and the tumor microenvironment, coordinated to a large extent by inflammatory cells, is to a large extent an indispensable participant in tumor formation, promoting tumor cell proliferation, survival, and migration[44]. Clinical studies have revealed that about 15%-20% of cancer patients have an infection, chronic inflammation, or autoimmune disease in the same tissue or organ site before the cancer development[44,51]. This suggests that the pre-cancerous inflammatory response is present before tumor formation. The strongest association between inflammation and malignancy is exemplified by CRC patients with IBD, including chronic ulcerative colitis and Crohn's disease, predispositions to liver cancer in patients with hepatitis, and chronic *Helicobacter pylori* (*H. pylori*) infection as a major cause of GC[52].

Meanwhile, various environmental factors may induce and promote the development of cancer by inducing chronic inflammation, which may accompany tumor development and increase the risk of many different cancers such as liver, pancreatic, colon, and other malignancies[53,54]. So, how does the inflammatory response induce and promote tumorigenesis? It is well known that one of the causes of cancer is the loss of tumor suppressor function, with the most common mutation being the tumor suppressor p53. In the tumor microenvironment, loss of p53 function leads to increased expression of NF-κB dependent inflammatory genes[55,56], which promotes CRC progression and metastasis[56-58]. In addition, oncogene activation leading to excessive production of inflammatory cytokines and chemokines may be another mechanism by which chronic inflammation triggers cancer occurrence[59,60]. Activation of the oncogene K-Ras leads to increased secretion of cytokines and chemokines of "aging-associated secretory phenotypes"[60]. With increasing research on human symbiotic microbiomes, researchers have found that symbiotic microbiomes may be involved in the occurrence and development of many cancers, perhaps through microbial adhesion to cancer cells and translocation or long-distance release of microbial metabolites[61].

As mentioned above, the localization of STEAP proteins on the cell membrane, their differential expression in normal and cancer tissues, and their metal-oxidoreductase activity mechanism make them potential candidate targets for the biomarkers of a variety of cancers, as well as potential targets for the alleviation or treatment of these cancers[62,63]. STEAP4 has been shown to play an important role in the inflammatory response and other physiological metabolic processes[31-33]. Although the role of STEAP1, STEAP2, and STEAP3 in the inflammatory response is rarely reported, it is tempting to speculate that STEAP1-3 may also have similar functions.

GC

GC is one of the most common GICs in humans, and chronic *H. pylori* infection is one of the main risk factors for GC occurrence[64]. The latency of *H. pylori* leads to a variety of changes in the gastric mucosa, such as gastritis, atrophic gastritis, intestinal metaplasia, dysplasia, and eventually GC[65]. Chronic infection with *H. pylori* in the gastric mucosa can occur freely in mucus, by attaching to cells, or intracellularly, requiring iron for bacterial growth[66]. In an iron-deficient medium, *H. pylori* can bind and extract iron from hemoglobin, Tf, and lactoferrin to support its growth, and preferentially bind the iron-free forms of Tf and lactoferrin, limiting its ability to extract iron from normal serum[67]. Hamedi Asl *et al*[68] investigated the expression of genes involved in iron homeostasis and their role in the pathogenesis of *H. pylori* infection. It is found that TfR and ferritin light chain were overexpressed in all *H. pylori*-positive tissues, while increased iron regulatory protein 2 expression was associated with *H. pylori*-positive chronic gastritis and intestinal metaplasia, confirming the role of iron acquisition-related genes in *H. pylori* attachment into the gastric mucosa. On the other hand, the colonization of *H. pylori* induces a substantial production of reactive oxygen species (ROS) and develops various strategies to quench the deleterious effects of ROS, resulting in persistent ROS production. However, excessive ROS will incur chronic inflammation and cellular damage, as the major risk factor for gastric carcinogenesis[69]. These investigations indicate the potential role of STEAPs in inflammatory responses for *H. pylori*-related GC.

The role of STEAP1 in GC was first reported by Wu *et al*[70], who defined the landscape of translationally regulated gene products with differential expression between non-metastatic and metastatic GC cohorts. Interestingly, STEAP1 was identified as the most translationally upregulated gene product, required for cell proliferation, migration/invasion, tumorigenesis, and chemoresistance to docetaxel treatment[70]. To explore the regulatory mechanism, the same research group focused on the potential regulators for STEAP1 expression[71]. They found that the RNA-binding protein poly r(C) binding protein 1 and miR-3978 function as repressors of peritoneal metastasis of GC, partially by downregulating STEAP1, while phosphorylated eIF4E upregulates STEAP1 expression at the level of cap-dependent translation initiation to facilitate the peritoneal metastasis of GC[71]. A similar result was found by Zhang *et al*[72], that STEAP1 performed an oncogenic role in the occurrence and metastasis of GC *via* activating the AKT/FoxO1 pathway and epithelial-mesenchymal transition process.

Besides STEAP1, STEAP4 was also found to be highly expressed in GC tissues, which is associated with advanced clinical stage and poor prognosis of GC patients. Importantly, the expression of STEAP4 was found to be positively correlated with the infiltration levels of B cells, CD4+ T cells, macrophages, neutrophils, and dendritic cells, indicating its contribution to the regulation of the tumor microenvironment[73]. Although the current investigation of STEAPs in GCs is limited, the potential role of STEAPs involved in immune response in GC is emerging and needs further exploration.

CRC

CRC is the third most common cause of cancer death in the United States and other developed countries[1]. It has been well-accepted that chronic inflammation is one of the recognized risk factors for the development of CRC, especially in colon cancer. The accumulation of immune cells and inflammatory factors in the intestinal mucosa constitute a complex chronic inflammatory environment and cause oxidative stress or DNA damage on the epithelial cells[74]. In patients with IBD, the risk for CRC is increased significantly, which is strongly associated with chronic inflammation, and such CRC was named colitis-associated CRC[74]. On the other hand, the gastrointestinal tract is the primary site to absorb copper, which is an essential micronutrient and critical enzyme cofactor for crucial copper-dependent enzymes. Elevated copper concentrations can cause multifaceted responses of pathogenic bacteria when invading the host[75], while in the fish model, Wang *et al*[76] found that copper exposure induced intestinal oxidative stress and inflammation, resulting in enrichment of potentially pathogenic bacteria and reduction of probiotic bacteria. Miller *et al*[77] found a significant difference in copper isotopic composition along with diverse bacterial populations, revealing a host-microbial interaction involved in the regulation of copper transport.

After being identified as a new target for preventative and/or therapeutic vaccine construction and immune monitoring in prostate cancer[78], STEAP1 was found to be highly expressed in CRC, predicting a poor overall survival in CRC patients[79]. Mechanistically, Nakamura *et al*[80] found that silencing STEAP1 suppressed CRC cell growth and

increased ROS production, associated with decreased expression of antioxidant molecules regulated by the transcription factor nuclear erythroid 2-related factor. As an antigen present in various tumors, STEAP1 has the potential to stimulate cytotoxic T lymphocytes (CTLs) involved in antitumor immunotherapy. To explore the specific STEAP1 sequence capable of stimulating naïve HLA-A2-restricted CTLs, Rodeberg *et al*[81] used MHC peptide binding algorithms to predict the potential sequences and verified their abilities to induce antigen-specific CTLs to kill peptide-pulsed HLA-A2 target cells. They provided strong evidence that STEAP1-292 peptide (MIAVFLPIV) is naturally processed by many types of tumors, including CRC, and recognized by CTLs, and the modified STEAP1-292.2L peptide (MLAVFLPIV) is more immunogenic to induce CTL recognition, serving as a potential antitumor peptide vaccine. Soon, Rodeberg *et al*[82] reported another two peptides of STEAP1, which can be used for broad-spectrum-tumor immunotherapy.

As metalloreductases, STEAPs are involved in iron/copper homeostasis[21,83]. Among the copper homeostasis-related genes, STEAP3 was found to be increased in CRC in oligonucleotide microarray analysis, related to copper accumulation [83]. During the polarization of macrophages, the time-dependent change of intracellular Fe(II) during the inflammatory activation was consistent with the expression shifts of TfR, STEAP3, and Fe(II) exporter Slc40a1, indicating the role of Fe(II) in inflammatory-activated macrophages[84]. Even in hypoferric conditions, STEAP3 overexpression increased iron storage, causing resistance to iron deprivation-induced apoptosis[85]. In CRC cells, STEAP3 also facilitates exosomal trafficking to increase the secretion of exosomes[86], which are important interactors between tumor cells and their surroundings[87]. Interestingly, hypoxia-induced antisense long non-coding RNA STEAP3-AS1 increased the expression of STEAP3 by competitively interacting with YTH domain-containing family protein 2 (YTHDF2) and leading to the disassociation of YTHDF2 with STEAP3 mRNA and upregulated STEAP3 mRNA stability in CRC. The enhanced STEAP3 expression increased intracellular Fe(II), which induced the phosphorylation and inactivation of glycogen synthase kinase 3β, releasing β-catenin translocated into the nucleus to activate the Wnt signal with promoted CRC progression[88].

Different from other STEAP family members, STEAP4 expression was found to be low in CRC tissues compared with normal tissues, which is positively correlated with immune infiltration and immune-related biomarkers[89]. However, in colitis animal models and IBD patients, STEAP4 was also highly induced in a hypoxia-dependent manner, leading to a dysregulation in mitochondrial iron balance and enhanced ROS level. Using a colitis-associated colon cancer model, Xue *et al*[90] found that the mitochondrial iron dysregulation related to high STEAP4 level is a key mechanism by which inflammation impacts colon tumorigenesis, indicting STEAP4 as an important regulator of the inflammatory response. In the colitis-associated tumorigenesis model, the copper metabolism can also be mobilized by the pro-inflammatory cytokine IL-17, by inducing STEAP4-dependent cellular copper uptake, which is critical for colon tumor formation[91].

As mentioned above, STEAP1 and STEAP4 function as metalloreductases to regulate the iron/copper homeostasis during the oncogenesis and development of CRC related to inflammation. Although there are no reports of STEAP2 nor STEAP3 in CRC, the structural similarity of STEAP family proteins has prompted a further investigation of the potential role of STEAP2 or STEAP3 in CRC.

HCC

HCC is the most common type of primary liver cancer, listed as the third leading cause of cancer-related death worldwide[92]. The increased incidence of primary liver cancer in several developed countries will likely continue for decades. Since primary liver cancer is mostly related to the infection with hepatitis B and C viruses (HBV and HCV), it is the first human cancer enormously amendable to prevention with HBV vaccines[93,94]. Although serum copper concentration is not a specific diagnostic biomarker for liver disease, serum copper isotope ratio has been proven to be an assistant monitor for the diagnosis, prognosis, and follow-up of chronic liver diseases, as the imbalanced copper homeostasis exists in liver diseases[95,96].

Interestingly, STEAP1 was considered as a targeted tumor antigen with the cytotoxic potency of chemotherapeutic drugs for designing antibody-drug conjugates (ADCs). Boswell *et al*[97] constructed a humanized anti-STEAP1 antibody-linked ADC, and evaluated its pharmacokinetics, tissue distribution, and/or potential organ toxicity in rats, finding a general trend toward increased hepatic uptake and reduced levels in other highly vascularized organs. Another research group constructed a radio-labeled anti-STEAP1-conjugated probe for positron emission tomography detection, and the highest mean absorbed dose to the normal organ was found in the liver at 1.18 mGy/MBq[98]. The above results indicate the ability of uptake for anti-STEAP1 ADCs in the liver, predicting the therapeutic potential for liver malignancies. Not surprisingly, the expression of STEAP1 was found to be high in liver tumors and associated with poor clinical outcomes, suggesting that STEAP1 is a druggable target in liver cancer[99].

Related to inflammatory responses, STEAP3 is a mediator and protector of hepatic ischemia-reperfusion injury through TAK1-dependent activation of the JNK/p38 pathways in hepatocytes[100]. Interestingly, after HCV infection, STEAP3 was found to be downregulated in HCC and associated with the progression to cirrhosis and HCC, and it thus can be used as a potential monitoring biomarker for the development of HCC[101]. The decreased expression of STEAP3 in HCC was also confirmed by Yi *et al*[102], which is associated with the abnormal expression of ferroptosis-related genes. However, at the cellular level, Wang *et al*[101] found that nuclear STEAP3 was highly expressed in HCC, which was an independent prognostic factor for HCC patients. Mechanically, increased nuclear STEAP3 expression significantly promoted the stemness phenotype, cell cycle progression, and cellular proliferation of HCC cells, through RAC1-ERK-STAT3 and RAC1-JNK-STAT6 signaling axes, while STEAP3 also upregulated the expression and nuclear trafficking of epidermal growth factor receptor (EGFR) to promote EGFR-mediated STAT3 transcription activity in a positive feedback manner[101]. As the matrix stiffness is a key factor impairing tumor immunity, Wang *et al*[103] analyzed the effect of stiffness in HCV-infected cirrhotic HCC, finding that stiffer matrix decreased STEAP3 in the invasive front region of HCC and the cirrhotic tissue, suppressing STEAP3-mediated immune infiltration of CD4+ and CD8+ T cells, macrophages, neutrophils, and dendritic cells, along with decreased ferroptosis.

As a plasma membrane metalloreductase, STEAP4 is controlled by inflammatory cytokines in the liver, such as IL-6, which significantly induced the transcription activity of STEAP4 through STAT3 and CCAAT/enhancer-binding protein alpha, playing a critical role in the response to nutritional and inflammatory stress[104]. Hepatic STEAP4 decreases the stability of HBV X protein (HBx) by physically interacting with HBx, subsequentially suppressing HBx-mediated transcription of lipogenic and adipogenic genes and protecting hepatocytes from HBV gene expression[105]. In a non-alcoholic fatty liver disease (NAFLD) animal model, recombinant fibroblast growth factor 21 treatment ameliorated hepatic steatosis and insulin resistance by increasing STEAP4-mediated hepatic iron overload and ferroportin expression, indicating STEAP4 as a suitable therapeutic intervention for NAFLD patients[106]. However, in HCC tissues, genome-wide DNA methylation analysis revealed significantly hypermethylated and downregulated STEAP4 compared to the non-tumor liver tissues, which may be associated with the development of HCC[107], while STEAP4 methylation in plasma DNA was not associated with HCC risk[108]. Not surprisingly, Zhou *et al*[88] reported that the methylation level of the STEAP4 promoter was correlated with the downregulation of STEAP4, functioning as a tumor suppressor in HCC by inhibiting the PI3K/AKT/mTOR pathway. The reduced STEAP4 expression is significantly associated with tumor aggressiveness and poor prognosis in HCC patients, likely due to its link to various biological processes and induction of HCC immune evasion[109].

As mentioned above, STEAPs, through iron/copper metabolism or different cytokines, participate in the inflammatory process of the gastrointestinal tract, and then induce GIC occurrence and promote GIC development accordingly (Table 1).

CLINICAL IMPLICATION OF STEAPS IN GICS

The strict maintenance of a specific microbial consortium in the gastrointestinal tract is critical for health, while gut microbiota alteration and dysbiosis will cause inflammation and pathogenic intestinal conditions[110]. The connection between inflammation and tumorigenesis has been well-established for decades based on genetic, pharmacological, and epidemiological evidence. Even obstructive sleep apnea-induced hypertension is found to be associated with gut dysbiosis, which may serve as the trigger for gut and neuroinflammation, and preventing or reversing gut dysbiosis may reduce neuroinflammation and hypertension accordingly[111]. Therefore, monitoring microbiota alteration or inflammation in the gastrointestinal tract is a research hotspot for the diagnosis or treatment of gastrointestinal inflammation-related diseases, including GICs.

Gopalakrishnan *et al*[112] implemented a miniaturized smart capsule to monitor inflammatory lesions throughout the gastrointestinal tract by detecting ROS level, a biomarker of inflammation, which provided a new milestone of smart ingestible electronics for improving the diagnosis and treatment of digestive disease. The exosomes derived from human placental mesenchymal stem cells used in the myocardial infarction model, notably modulated gut microbial community, increased the gut microbiota metabolites short chain fatty acids (SCFAs), and decreased lipopolysaccharide[113]. By sorting and sequencing of immunoglobulin (Ig) A-coated microbiota to define immune-reactive microbiota, Lima *et al* [114] identified that transferable IgA-coated *Odoribacter splanchnicus* in responders to fecal microbiota transplantation for patients with ulcerative colitis increases mucosal regulatory T cells, and induces the production of IL-10 and SCFAs, resulting in the resolution of colitis. Such investigation provided potential strategies or vectors for the treatment of the gastrointestinal tract, as well as inflammation-related GICs.

As a common oncogene in diverse malignancies, STEAP1 was considered a promising candidate therapeutic target, with abundant expression in malignancies[17,18]. Importantly, STEAP1 is also found to be a transporter, participating in intercellular communication[115,116]. Since the first prostate cancer-specific immunotherapy was licensed in 2010, immunotherapy represents a promising approach to harness the host's immune system with an anti-tumor effect[117, 118]. ^{89}Zr-DFO-MSTP2109A, a radiolabeled antibody targeting STEAP1, was well tolerated and showed good visualization in the study, thus establishing its potential role as a potential biomarker for STEAP1 directed therapy and confirming its diagnostic value[119]. Given STEAP1's mechanism in cancers, therapeutic strategies targeting STEAP1, such as monoclonal antibodies (mAbs), DNA vaccines, and ADCs, have been developed. Challita-Eid *et al*[115] identified STEAP1 mediating the transfer of small molecules between adjacent cells and first generated two mAbs that bind to STEAP1 epitopes at the cell surface, which significantly inhibited STEAP-1-induced intercellular communication in a dose-dependent manner. Soon, an anti-STEAP4 mAb that binds to the extracellular domain of STEAP4 was also shown to cause insulin resistance in adipocytes by disrupting cellular mitochondrial function, in addition to inducing apoptosis and inhibiting preadipocyte proliferation and glucose uptake without affecting human preadipocyte differentiation[120], while anti-STEAP1 based ADCs performed exciting anti-tumor function by regulating the immune response[97,121].

One of the goals of current tumor immunotherapy research is to design and validate multi-epitope/multi-antigen vaccines that can induce multi-specific anti-tumor responses and reduce the risk of selection of antigen loss escape variants *in vivo*[122,123]. The multivalent vaccine should be composed of a variety of epitopes of widely expressed tumor antigens for the purpose of wide application. Recently, many of the same tumor antigens expressed in most human tumors have been described, such as survivin[124], EphA2[125], pan-MAGE-A HLA-A* 0201-restricted epitopes, and Hsp70[126,127]. STEAP1 protein was found to be overexpressed in prostate cancer, pancreatic cancer, CRC, HCC, breast cancer, bladder cancer, ovarian cancer, acute lymphoblastic leukemia, and Ewing sarcoma[18]. This wide expression pattern strongly suggests the utility of this tumor antigen in broad-spectrum antitumor immunotherapy. It has been demonstrated that STEAP1 is a tumor antigen target of CD8+ T cells by identifying two HLA-A* 0201-restricted antigen peptides, STEAP86-94 and STEAP262-270[82].

Table 1 Functions/mechanisms of six transmembrane epithelial antigens of the prostate involved in gastrointestinal cancers

Protein	Organ	Function/mechanism	Ref.
STEAP1	Stomach	Promoting peritoneal metastasis of GC	[113]
		Regulated at the level of cap-dependent translation initiation by phosphorylated eIF4E in GC	[114]
		Increasing cell proliferation, migration, and invasion of GC, *via* the activation of AKT/FoxO1 pathway and epithelial-mesenchymal transition	[72]
	Colon/rectum	Inducing cytotoxic T lymphocytes to recognize colon cancer with STEAP1 by specific STEAP1 peptide	[81]
		Reducing ROS and preventing apoptosis of CRC cells *via* NRF2 pathway	[115]
	Liver	Increased hepatic uptake of STEAP1 antibody-drug conjugates	[116]
		Accelerating cell proliferation by targeting c-Myc in liver cancer cells	[100]
STEAP3	Colon/rectum	Increased in CRC, along with CTR1 to induce copper accumulation	[84]
		Facilitating iron uptake and resistance to iron deprivation-induced apoptosis under hypoferric condition	[86]
		Time-dependent change of STEAP3 during inflammatory activation, along with specific accumulation of Fe (II) in inflammatory-activated macrophages	[85]
		Increasing exosome secretion in CRC, which can be cleaved by RHBDD1 in a dose/activity dependent manner	[87]
		Protected by hypoxia-induced lncRNA STEAP3-AS1 by preventing m^6A-mediated degradation of STEAP3 mRNA	[89]
	Liver	Decreased expression in liver, associated with the transition from cirrhosis to HCC	[117]
		Increased in HCC cell nucleus, promoting proliferation *via* RAC1-ERK-STAT3 and RAC1-JNK-STAT6 signaling axes	[102]
		Ferroptosis-related differential gene in HCV-infected cirrhotic HCC, impaired by matrix stiffness	[105]
STEAP4	Stomach	Highly expressed in GC, associated with infiltration of immune cells	[73]
	Colon/rectum	Decreased in CRC and positively correlated with immune-related biomarkers	[118]
		Highly induced in mouse models of colitis and inflammatory bowel disease patients, increasing ROS production in a hypoxia-dependent manner	[91]
		Induced by the inflammatory cytokine IL-17 to drive copper uptake, critical for colon tumor formation	[119]
	Liver	Lowly expressed in HCC, controlled by hypermethylation in STEAP4 promoter region	[109]
		Inhibiting proliferation and metastasis of HCC through PI3K/AKT/mTOR pathway inhibition	[111]
		Low level in HCC, associated with advanced HCC stage, poor survival, and immunosuppressive microenvironment	[112]
		Stimulated by the inflammatory cytokine IL-6, through STAT3 and CCAAT/enhancer-binding protein alpha in liver	[106]
		Hepatic STEAP4 antagonizes HBx-mediated hepatocyte dysfunction by interacting with and decreasing the stability of HBx	[107]
		Therapeutic effect of recombinant FGF21 on NAFLD is performed by increasing hepatic STEAP4 to protect hepatocytes	[108]

STEAP: Six transmembrane epithelial antigen of the prostate; GICs: Gastrointestinal cancers; GC: Gastric cancer; eIF4E: Eukaryotic initiation factor 4E; ROS: Reactive oxygen species; CRC: Colorectal cancer; NRF2: Nuclear erythroid 2-related factor; CTR1: Copper transporter 1; RHBDD1: Rhomboid domain containing 1; HCV: Hepatitis C virus; IL-17: Interleukin-17; HCC: Hepatocellular carcinoma; STAT3: Signal transducer and activator of transcription 3; PI3K: Phosphoinositide 3-kinase; mTOR: Mammalian target of rapamycin; JNK: c-Jun N-terminal kinase; ERK: Extracellular signal-regulated kinase; IL-6: Interleukin-6; HBx: Hepatitis B virus x protein; FGF21: Fibroblast growth factor 21; NAFLD: Non-alcoholic fatty liver disease.

In addition, immunotherapy has proved to be an effective treatment for a variety of cancers, especially for patients with tumors with overexpressed antigens that can be recognized by immune T/B cells. The use of STEAP peptides to induce helper T cells in the context of multiple major histocompatibility complex class II alleles have been studied for T cell immunotherapy against STEAP-expressing renal cell carcinoma and bladder cancer[128]. These studies confirm that targeting STEAP family proteins in a variety of solid tumors is an attractive and promising effective approach. Although current therapeutic strategies targeting STEAPs have not been applied in clinical practice, their molecular transport mechanism and involvement in cancer progression make them promising targets for the treatment of patients with GICs.

CONCLUSION

STEAP family members share similar structural features and function as metal oxidoreductases involved in a variety of cellular processes, such as copper/iron uptake, response to inflammation, fatty acid and glucose metabolism, and oxidative stress regulation. STEAPs are irregularly expressed in different cancers, which are involved in the proliferation, migration, invasion, and metastasis of cancer cells, and play a role in promoting or suppressing cancer. In addition, the inflammatory response may be caused by necrosis of rapidly growing tumor cells due to hypoxia and lack of nutrients. ROS and reactive nitrogen species produced by inflammatory cells can cause oxidative DNA damage in gastrointestinal cells, leading to the activation of oncogenes and/or inactivation of tumor suppressor genes, as well as various epigenetic changes that are conducive to the progression of GICs. Thus, molecules that affect cell survival or the subsequent inflammatory response are likely to have an impact on the course of GIC development. In conclusion, based on the increasing use of STEAPs as cancer therapeutic targets, inflammatory therapeutic strategies in GICs will be more considered in the future, most likely including STEAP family proteins.

FOOTNOTES

Author contributions: Liu J and Fang ZX designed this study; Fang ZX, Chen WJ, and Wu Z searched the publications; Fang ZX, Chen WJ, Wu Z, Hou YY, Lan YZ, Wu HT, and Liu J interpreted the results, constructed the structure of the review, and prepared the tables; Fang ZX prepared the draft of the manuscript; Fang ZX and Chen WJ prepared the figures; Liu J revised the manuscript critically; and all authors have read and approved the final manuscript.

Supported by the National Natural Science Foundation of China, No. 82273457; the Natural Science Foundation of Guangdong Province, No. 2021A1515012180, 2023A1515012762 and No. 2019A1515010962; Special Grant for Key Area Programs of Guangdong Department of Education, No. 2021ZDZX2040; Science and Technology Special Project of Guangdong Province, No. 210715216902829.

Conflict-of-interest statement: All the authors report no relevant conflicts of interest for this article.

Country/Territory of origin: China

ORCID number: Ze-Xuan Fang 0000-0002-6100-9012; Wen-Jia Chen 0000-0001-7157-3242; Zheng Wu 0000-0002-1393-7586; Yan-Yu Hou 0000-0002-4249-8770; Yang-Zheng Lan 0009-0000-4241-228X; Hua-Tao Wu 0000-0002-1640-6094; Jing Liu 0000-0002-7483-4572.

S-Editor: Wang JJ
L-Editor: Wang TQ
P-Editor: Zhang XD

REFERENCES

1 **Siegel RL**, Miller KD, Fuchs HE, Jemal A. Cancer statistics, 2022. *CA Cancer J Clin* 2022; **72**: 7-33 [PMID: 35020204 DOI: 10.3322/caac.21708]

2 **Smyth EC**, Nilsson M, Grabsch HI, van Grieken NC, Lordick F. Gastric cancer. *Lancet* 2020; **396**: 635-648 [PMID: 32861308 DOI:

10.1016/S0140-6736(20)31288-5]
3 **Forner A**, Reig M, Bruix J. Hepatocellular carcinoma. *Lancet* 2018; **391**: 1301-1314 [PMID: 29307467 DOI: 10.1016/S0140-6736(18)30010-2]
4 **Wang D**, Cabalag CS, Clemons NJ, DuBois RN. Cyclooxygenases and Prostaglandins in Tumor Immunology and Microenvironment of Gastrointestinal Cancer. *Gastroenterology* 2021; **161**: 1813-1829 [PMID: 34606846 DOI: 10.1053/j.gastro.2021.09.059]
5 **Man SM**. Inflammasomes in the gastrointestinal tract: infection, cancer and gut microbiota homeostasis. *Nat Rev Gastroenterol Hepatol* 2018; **15**: 721-737 [PMID: 30185915 DOI: 10.1038/s41575-018-0054-1]
6 **Schmitt M**, Greten FR. The inflammatory pathogenesis of colorectal cancer. *Nat Rev Immunol* 2021; **21**: 653-667 [PMID: 33911231 DOI: 10.1038/s41577-021-00534-x]
7 **Elinav E**, Nowarski R, Thaiss CA, Hu B, Jin C, Flavell RA. Inflammation-induced cancer: crosstalk between tumours, immune cells and microorganisms. *Nat Rev Cancer* 2013; **13**: 759-771 [PMID: 24154716 DOI: 10.1038/nrc3611]
8 **Karin M**, Greten FR. NF-kappaB: linking inflammation and immunity to cancer development and progression. *Nat Rev Immunol* 2005; **5**: 749-759 [PMID: 16175180 DOI: 10.1038/nri1703]
9 **Duan F**, Song C, Zhang J, Wang P, Ye H, Dai L, Wang K. Evaluation of the Epidemiologic Efficacy of Eradicating Helicobacter pylori on Development of Gastric Cancer. *Epidemiol Rev* 2019; **41**: 97-108 [PMID: 31497856 DOI: 10.1093/epirev/mxz006]
10 **Jin G**, Lv J, Yang M, Wang M, Zhu M, Wang T, Yan C, Yu C, Ding Y, Li G, Ren C, Ni J, Zhang R, Guo Y, Bian Z, Zheng Y, Zhang N, Jiang Y, Chen J, Wang Y, Xu D, Zheng H, Yang L, Chen Y, Walters R, Millwood IY, Dai J, Ma H, Chen K, Chen Z, Hu Z, Wei Q, Shen H, Li L. Genetic risk, incident gastric cancer, and healthy lifestyle: a meta-analysis of genome-wide association studies and prospective cohort study. *Lancet Oncol* 2020; **21**: 1378-1386 [PMID: 33002439 DOI: 10.1016/S1470-2045(20)30460-5]
11 **Ponziani FR**, Bhoori S, Castelli C, Putignani L, Rivoltini L, Del Chierico F, Sanguinetti M, Morelli D, Paroni Sterbini F, Petito V, Reddel S, Calvani R, Camisaschi C, Picca A, Tuccitto A, Gasbarrini A, Pompili M, Mazzaferro V. Hepatocellular Carcinoma Is Associated With Gut Microbiota Profile and Inflammation in Nonalcoholic Fatty Liver Disease. *Hepatology* 2019; **69**: 107-120 [PMID: 29665135 DOI: 10.1002/hep.30036]
12 **Tourelle KM**, Boutin S, Weigand MA, Schmitt FCF. The Association of Gut Microbiota and Complications in Gastrointestinal-Cancer Therapies. *Biomedicines* 2021; **9** [PMID: 34680424 DOI: 10.3390/biomedicines9101305]
13 **Zhang F**, Tao Y, Zhang Z, Guo X, An P, Shen Y, Wu Q, Yu Y, Wang F. Metalloreductase Steap3 coordinates the regulation of iron homeostasis and inflammatory responses. *Haematologica* 2012; **97**: 1826-1835 [PMID: 22689674 DOI: 10.3324/haematol.2012.063974]
14 **Wu HT**, Chen WJ, Xu Y, Shen JX, Chen WT, Liu J. The Tumor Suppressive Roles and Prognostic Values of STEAP Family Members in Breast Cancer. *Biomed Res Int* 2020; **2020**: 9578484 [PMID: 32802887 DOI: 10.1155/2020/9578484]
15 **Grunewald TG**, Bach H, Cossarizza A, Matsumoto I. The STEAP protein family: versatile oxidoreductases and targets for cancer immunotherapy with overlapping and distinct cellular functions. *Biol Cell* 2012; **104**: 641-657 [PMID: 22804687 DOI: 10.1111/boc.201200027]
16 **Xu M**, Evans L, Bizzaro CL, Quaglia F, Verrillo CE, Li L, Stieglmaier J, Schiewer MJ, Languino LR, Kelly WK. STEAP1-4 (Six-Transmembrane Epithelial Antigen of the Prostate 1-4) and Their Clinical Implications for Prostate Cancer. *Cancers (Basel)* 2022; **14** [PMID: 36011027 DOI: 10.3390/cancers14164034]
17 **Gomes IM**, Maia CJ, Santos CR. STEAP proteins: from structure to applications in cancer therapy. *Mol Cancer Res* 2012; **10**: 573-587 [PMID: 22522456 DOI: 10.1158/1541-7786.MCR-11-0281]
18 **Hubert RS**, Vivanco I, Chen E, Rastegar S, Leong K, Mitchell SC, Madraswala R, Zhou Y, Kuo J, Raitano AB, Jakobovits A, Saffran DC, Afar DE. STEAP: a prostate-specific cell-surface antigen highly expressed in human prostate tumors. *Proc Natl Acad Sci U S A* 1999; **96**: 14523-14528 [PMID: 10588738 DOI: 10.1073/pnas.96.25.14523]
19 **Ohgami RS**, Campagna DR, McDonald A, Fleming MD. The Steap proteins are metalloreductases. *Blood* 2006; **108**: 1388-1394 [PMID: 16609065 DOI: 10.1182/blood-2006-02-003681]
20 **Ohgami RS**, Campagna DR, Greer EL, Antiochos B, McDonald A, Chen J, Sharp JJ, Fujiwara Y, Barker JE, Fleming MD. Identification of a ferrireductase required for efficient transferrin-dependent iron uptake in erythroid cells. *Nat Genet* 2005; **37**: 1264-1269 [PMID: 16227996 DOI: 10.1038/ng1658]
21 **Chen WJ**, Wu HT, Li CL, Lin YK, Fang ZX, Lin WT, Liu J. Regulatory Roles of Six-Transmembrane Epithelial Antigen of the Prostate Family Members in the Occurrence and Development of Malignant Tumors. *Front Cell Dev Biol* 2021; **9**: 752426 [PMID: 34778263 DOI: 10.3389/fcell.2021.752426]
22 **Gomes IM**, Rocha SM, Gaspar C, Alvelos MI, Santos CR, Socorro S, Maia CJ. Knockdown of STEAP1 inhibits cell growth and induces apoptosis in LNCaP prostate cancer cells counteracting the effect of androgens. *Med Oncol* 2018; **35**: 40 [PMID: 29464393 DOI: 10.1007/s12032-018-1100-0]
23 **Amaral L**, Viveiros M, Kristiansen JE. "Non-Antibiotics": alternative therapy for the management of MDRTB and MRSA in economically disadvantaged countries. *Curr Drug Targets* 2006; **7**: 887-891 [PMID: 16842219 DOI: 10.2174/138945006777709539]
24 **Gomes IM**, Santos CR, Maia CJ. Expression of STEAP1 and STEAP1B in prostate cell lines, and the putative regulation of STEAP1 by post-transcriptional and post-translational mechanisms. *Genes Cancer* 2014; **5**: 142-151 [PMID: 25053991 DOI: 10.18632/genesandcancer.13]
25 **Korkmaz KS**, Elbi C, Korkmaz CG, Loda M, Hager GL, Saatcioglu F. Molecular cloning and characterization of STAMP1, a highly prostate-specific six transmembrane protein that is overexpressed in prostate cancer. *J Biol Chem* 2002; **277**: 36689-36696 [PMID: 12095985 DOI: 10.1074/jbc.M202414200]
26 **Porkka KP**, Helenius MA, Visakorpi T. Cloning and characterization of a novel six-transmembrane protein STEAP2, expressed in normal and malignant prostate. *Lab Invest* 2002; **82**: 1573-1582 [PMID: 12429817 DOI: 10.1097/01.lab.0000038554.26102.c6]
27 **McCarthy RC**, Kosman DJ. Mechanistic analysis of iron accumulation by endothelial cells of the BBB. *Biometals* 2012; **25**: 665-675 [PMID: 22434419 DOI: 10.1007/s10534-012-9538-6]
28 **Ji C**, Kosman DJ. Molecular mechanisms of non-transferrin-bound and transferring-bound iron uptake in primary hippocampal neurons. *J Neurochem* 2015; **133**: 668-683 [PMID: 25649872 DOI: 10.1111/jnc.13040]
29 **Machlenkin A**, Paz A, Bar Haim E, Goldberger O, Finkel E, Tirosh B, Volovitz I, Vadai E, Lugassy G, Cytron S, Lemonnier F, Tzehoval E, Eisenbach L. Human CTL epitopes prostatic acid phosphatase-3 and six-transmembrane epithelial antigen of prostate-3 as candidates for prostate cancer immunotherapy. *Cancer Res* 2005; **65**: 6435-6442 [PMID: 16024648 DOI: 10.1158/0008-5472.Can-05-0133]
30 **Yanatori I**, Kishi F. DMT1 and iron transport. *Free Radic Biol Med* 2019; **133**: 55-63 [PMID: 30055235 DOI: 10.1016/j.freeradbiomed.2018.07.020]

31 **Korkmaz CG**, Korkmaz KS, Kurys P, Elbi C, Wang L, Klokk TI, Hammarstrom C, Troen G, Svindland A, Hager GL, Saatcioglu F. Molecular cloning and characterization of STAMP2, an androgen-regulated six transmembrane protein that is overexpressed in prostate cancer. *Oncogene* 2005; **24**: 4934-4945 [PMID: 15897894 DOI: 10.1038/sj.onc.1208677]

32 **Scarl RT**, Lawrence CM, Gordon HM, Nunemaker CS. STEAP4: its emerging role in metabolism and homeostasis of cellular iron and copper. *J Endocrinol* 2017; **234**: R123-R134 [PMID: 28576871 DOI: 10.1530/JOE-16-0594]

33 **Moldes M**, Lasnier F, Gauthereau X, Klein C, Pairault J, Fève B, Chambaut-Guérin AM. Tumor necrosis factor-alpha-induced adipose-related protein (TIARP), a cell-surface protein that is highly induced by tumor necrosis factor-alpha and adipose conversion. *J Biol Chem* 2001; **276**: 33938-33946 [PMID: 11443137 DOI: 10.1074/jbc.M105726200]

34 **Gunshin H**, Mackenzie B, Berger UV, Gunshin Y, Romero MF, Boron WF, Nussberger S, Gollan JL, Hediger MA. Cloning and characterization of a mammalian proton-coupled metal-ion transporter. *Nature* 1997; **388**: 482-488 [PMID: 9242408 DOI: 10.1038/41343]

35 **Fleming MD**, Romano MA, Su MA, Garrick LM, Garrick MD, Andrews NC. Nramp2 is mutated in the anemic Belgrade (b) rat: evidence of a role for Nramp2 in endosomal iron transport. *Proc Natl Acad Sci U S A* 1998; **95**: 1148-1153 [PMID: 9448300 DOI: 10.1073/pnas.95.3.1148]

36 **Fleming MD**, Trenor CC 3rd, Su MA, Foernzler D, Beier DR, Dietrich WF, Andrews NC. Microcytic anaemia mice have a mutation in Nramp2, a candidate iron transporter gene. *Nat Genet* 1997; **16**: 383-386 [PMID: 9241278 DOI: 10.1038/ng0897-383]

37 **Kuo YM**, Zhou B, Cosco D, Gitschier J. The copper transporter CTR1 provides an essential function in mammalian embryonic development. *Proc Natl Acad Sci U S A* 2001; **98**: 6836-6841 [PMID: 11391004 DOI: 10.1073/pnas.111057298]

38 **Lee PL**, Gelbart T, West C, Halloran C, Beutler E. The human Nramp2 gene: characterization of the gene structure, alternative splicing, promoter region and polymorphisms. *Blood Cells Mol Dis* 1998; **24**: 199-215 [PMID: 9642100 DOI: 10.1006/bcmd.1998.0186]

39 **Harris ED**. Iron-copper interactions: some new revelations. *Nutr Rev* 1994; **52**: 311-315 [PMID: 7984346 DOI: 10.1111/j.1753-4887.1994.tb01462.x]

40 **Bullen JJ**, Spalding PB, Ward CG, Gutteridge JM. Hemochromatosis, iron and septicemia caused by Vibrio vulnificus. *Arch Intern Med* 1991; **151**: 1606-1609 [PMID: 1872665]

41 **Doherty CP**. Host-pathogen interactions: the role of iron. *J Nutr* 2007; **137**: 1341-1344 [PMID: 17449603 DOI: 10.1093/jn/137.5.1341]

42 **Gerhard GS**, Levin KA, Price Goldstein J, Wojnar MM, Chorney MJ, Belchis DA. Vibrio vulnificus septicemia in a patient with the hemochromatosis HFE C282Y mutation. *Arch Pathol Lab Med* 2001; **125**: 1107-1109 [PMID: 11473471 DOI: 10.5858/2001-125-1107-vvsiap]

43 **Gakis G**. The role of inflammation in bladder cancer. *Adv Exp Med Biol* 2014; **816**: 183-196 [PMID: 24818724 DOI: 10.1007/978-3-0348-0837-8_8]

44 **Mantovani A**, Allavena P, Sica A, Balkwill F. Cancer-related inflammation. *Nature* 2008; **454**: 436-444 [PMID: 18650914 DOI: 10.1038/nature07205]

45 **Simmons DL**. What makes a good anti-inflammatory drug target? *Drug Discov Today* 2006; **11**: 210-219 [PMID: 16580598 DOI: 10.1016/s1359-6446(05)03721-9]

46 **Liang Y**, Xing X, Beamer MA, Swindell WR, Sarkar MK, Roberts LW, Voorhees JJ, Kahlenberg JM, Harms PW, Johnston A, Gudjonsson JE. Six-transmembrane epithelial antigens of the prostate comprise a novel inflammatory nexus in patients with pustular skin disorders. *J Allergy Clin Immunol* 2017; **139**: 1217-1227 [PMID: 27884600 DOI: 10.1016/j.jaci.2016.10.021]

47 **Timmermans S**, Van Hauwermeiren F, Puimège L, Dejager L, Van Wonterghem E, Vanhooren V, Mestdagh P, Libert C, Vandenbroucke RE. Determining differentially expressed miRNAs and validating miRNA--target relationships using the SPRET/Ei mouse strain. *Mamm Genome* 2015; **26**: 94-107 [PMID: 25491574 DOI: 10.1007/s00335-014-9550-y]

48 **Sharma PR**, Mackey AJ, Dejene EA, Ramadan JW, Langefeld CD, Palmer ND, Taylor KD, Wagenknecht LE, Watanabe RM, Rich SS, Nunemaker CS. An Islet-Targeted Genome-Wide Association Scan Identifies Novel Genes Implicated in Cytokine-Mediated Islet Stress in Type 2 Diabetes. *Endocrinology* 2015; **156**: 3147-3156 [PMID: 26018251 DOI: 10.1210/en.2015-1203]

49 **Gordon HM**, Majithia N, MacDonald PE, Fox JEM, Sharma PR, Byrne FL, Hoehn KL, Evans-Molina C, Langman L, Brayman KL, Nunemaker CS. STEAP4 expression in human islets is associated with differences in body mass index, sex, HbA1c, and inflammation. *Endocrine* 2017; **56**: 528-537 [PMID: 28405880 DOI: 10.1007/s12020-017-1297-2]

50 **Jiang H**, Dong Y, Yan D, Wu Y, Wang Y, Ren Y, Mao G, Liang G, Liu W, Zhou Y, Huang Z, Qi L. The expression of STEAP4 in peripheral blood predicts the outcome of septic patients. *Ann Transl Med* 2021; **9**: 1519 [PMID: 34790725 DOI: 10.21037/atm-21-2794]

51 **Grivennikov SI**, Greten FR, Karin M. Immunity, inflammation, and cancer. *Cell* 2010; **140**: 883-899 [PMID: 20303878 DOI: 10.1016/j.cell.2010.01.025]

52 **Macarthur M**, Hold GL, El-Omar EM. Inflammation and Cancer II. Role of chronic inflammation and cytokine gene polymorphisms in the pathogenesis of gastrointestinal malignancy. *Am J Physiol Gastrointest Liver Physiol* 2004; **286**: G515-G520 [PMID: 15010360 DOI: 10.1152/ajpgi.00475.2003]

53 **Quail DF**, Dannenberg AJ. The obese adipose tissue microenvironment in cancer development and progression. *Nat Rev Endocrinol* 2019; **15**: 139-154 [PMID: 30459447 DOI: 10.1038/s41574-018-0126-x]

54 **Quail DF**, Olson OC, Bhardwaj P, Walsh LA, Akkari L, Quick ML, Chen IC, Wendel N, Ben-Chetrit N, Walker J, Holt PR, Dannenberg AJ, Joyce JA. Obesity alters the lung myeloid cell landscape to enhance breast cancer metastasis through IL5 and GM-CSF. *Nat Cell Biol* 2017; **19**: 974-987 [PMID: 28737771 DOI: 10.1038/ncb3578]

55 **Komarova EA**, Krivokrysenko V, Wang K, Neznanov N, Chernov MV, Komarov PG, Brennan ML, Golovkina TV, Rokhlin OW, Kuprash DV, Nedospasov SA, Hazen SL, Feinstein E, Gudkov AV. p53 is a suppressor of inflammatory response in mice. *FASEB J* 2005; **19**: 1030-1032 [PMID: 15811878 DOI: 10.1096/fj.04-3213fje]

56 **Schwitalla S**, Ziegler PK, Horst D, Becker V, Kerle I, Begus-Nahrmann Y, Lechel A, Rudolph KL, Langer R, Slotta-Huspenina J, Bader FG, Prazeres da Costa O, Neurath MF, Meining A, Kirchner T, Greten FR. Loss of p53 in enterocytes generates an inflammatory microenvironment enabling invasion and lymph node metastasis of carcinogen-induced colorectal tumors. *Cancer Cell* 2013; **23**: 93-106 [PMID: 23273920 DOI: 10.1016/j.ccr.2012.11.014]

57 **Elyada E**, Pribluda A, Goldstein RE, Morgenstern Y, Brachya G, Cojocaru G, Snir-Alkalay I, Burstain I, Haffner-Krausz R, Jung S, Wiener Z, Alitalo K, Oren M, Pikarsky E, Ben-Neriah Y. CKIα ablation highlights a critical role for p53 in invasiveness control. *Nature* 2011; **470**: 409-413 [PMID: 21331045 DOI: 10.1038/nature09673]

58 **Pribluda A**, Elyada E, Wiener Z, Hamza H, Goldstein RE, Biton M, Burstain I, Morgenstern Y, Brachya G, Billauer H, Biton S, Snir-Alkalay I, Vucic D, Schlereth K, Mernberger M, Stiewe T, Oren M, Alitalo K, Pikarsky E, Ben-Neriah Y. A senescence-inflammatory switch from cancer-inhibitory to cancer-promoting mechanism. *Cancer Cell* 2013; **24**: 242-256 [PMID: 23890787 DOI: 10.1016/j.ccr.2013.06.005]

59 **Liao W**, Overman MJ, Boutin AT, Shang X, Zhao D, Dey P, Li J, Wang G, Lan Z, Tang M, Jiang S, Ma X, Chen P, Katkhuda R, Korphaisarn

K, Chakravarti D, Chang A, Spring DJ, Chang Q, Zhang J, Maru DM, Maeda DY, Zebala JA, Kopetz S, Wang YA, DePinho RA. KRAS-IRF2 Axis Drives Immune Suppression and Immune Therapy Resistance in Colorectal Cancer. *Cancer Cell* 2019; **35**: 559-572.e7 [PMID: 30905761 DOI: 10.1016/j.ccell.2019.02.008]

60 **Davalos AR**, Coppe JP, Campisi J, Desprez PY. Senescent cells as a source of inflammatory factors for tumor progression. *Cancer Metastasis Rev* 2010; **29**: 273-283 [PMID: 20390322 DOI: 10.1007/s10555-010-9220-9]

61 **Bullman S**, Pedamallu CS, Sicinska E, Clancy TE, Zhang X, Cai D, Neuberg D, Huang K, Guevara F, Nelson T, Chipashvili O, Hagan T, Walker M, Ramachandran A, Diosdado B, Serna G, Mulet N, Landolfi S, Ramon Y Cajal S, Fasani R, Aguirre AJ, Ng K, Élez E, Ogino S, Tabernero J, Fuchs CS, Hahn WC, Nuciforo P, Meyerson M. Analysis of Fusobacterium persistence and antibiotic response in colorectal cancer. *Science* 2017; **358**: 1443-1448 [PMID: 29170280 DOI: 10.1126/science.aal5240]

62 **Finegold AA**, Shatwell KP, Segal AW, Klausner RD, Dancis A. Intramembrane bis-heme motif for transmembrane electron transport conserved in a yeast iron reductase and the human NADPH oxidase. *J Biol Chem* 1996; **271**: 31021-31024 [PMID: 8940093 DOI: 10.1074/jbc.271.49.31021]

63 **Valenti MT**, Dalle Carbonare L, Donatelli L, Bertoldo F, Giovanazzi B, Caliari F, Lo Cascio V. STEAP mRNA detection in serum of patients with solid tumours. *Cancer Lett* 2009; **273**: 122-126 [PMID: 18793824 DOI: 10.1016/j.canlet.2008.07.037]

64 **Krzysiek-Maczka G**, Brzozowski T, Ptak-Belowska A. Helicobacter pylori-activated fibroblasts as a silent partner in gastric cancer development. *Cancer Metastasis Rev* 2023 [PMID: 37460910 DOI: 10.1007/s10555-023-10122-1]

65 **Ajani JA**, D'Amico TA, Bentrem DJ, Chao J, Cooke D, Corvera C, Das P, Enzinger PC, Enzler T, Fanta P, Farjah F, Gerdes H, Gibson MK, Hochwald S, Hofstetter WL, Ilson DH, Keswani RN, Kim S, Kleinberg LR, Klempner SJ, Lacy J, Ly QP, Matkowskyj KA, McNamara M, Mulcahy MF, Outlaw D, Park H, Perry KA, Pimiento J, Poultsides GA, Reznik S, Roses RE, Strong VE, Su S, Wang HL, Wiesner G, Willett CG, Yakoub D, Yoon H, McMillian N, Pluchino LA. Gastric Cancer, Version 2.2022, NCCN Clinical Practice Guidelines in Oncology. *J Natl Compr Canc Netw* 2022; **20**: 167-192 [PMID: 35130500 DOI: 10.6004/jnccn.2022.0008]

66 **Boyanova L**. Role of Helicobacter pylori virulence factors for iron acquisition from gastric epithelial cells of the host and impact on bacterial colonization. *Future Microbiol* 2011; **6**: 843-846 [PMID: 21861616 DOI: 10.2217/fmb.11.75]

67 **Senkovich O**, Ceaser S, McGee DJ, Testerman TL. Unique host iron utilization mechanisms of Helicobacter pylori revealed with iron-deficient chemically defined media. *Infect Immun* 2010; **78**: 1841-1849 [PMID: 20176792 DOI: 10.1128/IAI.01258-09]

68 **Hamedi Asl D**, Naserpour Farivar T, Rahmani B, Hajmanoochehri F, Emami Razavi AN, Jahanbin B, Soleimani Dodaran M, Peymani A. The role of transferrin receptor in the Helicobacter pylori pathogenesis; L-ferritin as a novel marker for intestinal metaplasia. *Microb Pathog* 2019; **126**: 157-164 [PMID: 30391537 DOI: 10.1016/j.micpath.2018.10.039]

69 **Wu S**, Chen Y, Chen Z, Wei F, Zhou Q, Li P, Gu Q. Reactive oxygen species and gastric carcinogenesis: The complex interaction between Helicobacter pylori and host. *Helicobacter* 2023; **28**: e13024 [PMID: 37798959 DOI: 10.1111/hel.13024]

70 **Wu YY**, Jiang JN, Fang XD, Ji FJ. STEAP1 Regulates Tumorigenesis and Chemoresistance During Peritoneal Metastasis of Gastric Cancer. *Front Physiol* 2018; **9**: 1132 [PMID: 30246786 DOI: 10.3389/fphys.2018.01132]

71 **Jiang JN**, Wu YY, Fang XD, Ji FJ. EIF4E regulates STEAP1 expression in peritoneal metastasis. *J Cancer* 2020; **11**: 990-996 [PMID: 31949502 DOI: 10.7150/jca.29105]

72 **Zhang Z**, Hou WB, Zhang C, Tan YE, Zhang DD, An W, Pan SW, Wu WD, Chen QC, Xu HM. A research of STEAP1 regulated gastric cancer cell proliferation, migration and invasion in vitro and in vivos. *J Cell Mol Med* 2020; **24**: 14217-14230 [PMID: 33128353 DOI: 10.1111/jcmm.16038]

73 **Fang ZX**, Hou YY, Wu Z, Wu BX, Deng Y, Wu HT, Liu J. Immune responses of six-transmembrane epithelial antigen of the prostate 4 functions as a novel biomarker in gastric cancer. *World J Clin Oncol* 2023; **14**: 297-310 [PMID: 37700807 DOI: 10.5306/wjco.v14.i8.297]

74 **Yin Y**, Wan J, Yu J, Wu K. Molecular Pathogenesis of Colitis-associated Colorectal Cancer: Immunity, Genetics, and Intestinal Microecology. *Inflamm Bowel Dis* 2023; **29**: 1648-1657 [PMID: 37202830 DOI: 10.1093/ibd/izad081]

75 **Focarelli F**, Giachino A, Waldron KJ. Copper microenvironments in the human body define patterns of copper adaptation in pathogenic bacteria. *PLoS Pathog* 2022; **18**: e1010617 [PMID: 35862345 DOI: 10.1371/journal.ppat.1010617]

76 **Wang L**, Hu C, Wang B, Wang H, Wang C, Shu Y, Gao C, Yan Y. Chronic environmentally relevant concentration of copper exposure induces intestinal oxidative stress, inflammation, and microbiota disturbance in freshwater grouper (Acrossocheilus fasciatus). *Aquat Toxicol* 2023; **263**: 106702 [PMID: 37741225 DOI: 10.1016/j.aquatox.2023.106702]

77 **Miller KA**, Vicentini FA, Hirota SA, Sharkey KA, Wieser ME. Antibiotic treatment affects the expression levels of copper transporters and the isotopic composition of copper in the colon of mice. *Proc Natl Acad Sci U S A* 2019; **116**: 5955-5960 [PMID: 30850515 DOI: 10.1073/pnas.1814047116]

78 **Yang D**, Holt GE, Velders MP, Kwon ED, Kast WM. Murine six-transmembrane epithelial antigen of the prostate, prostate stem cell antigen, and prostate-specific membrane antigen: prostate-specific cell-surface antigens highly expressed in prostate cancer of transgenic adenocarcinoma mouse prostate mice. *Cancer Res* 2001; **61**: 5857-5860 [PMID: 11479226]

79 **Moreaux J**, Kassambara A, Hose D, Klein B. STEAP1 is overexpressed in cancers: a promising therapeutic target. *Biochem Biophys Res Commun* 2012; **429**: 148-155 [PMID: 23142226 DOI: 10.1016/j.bbrc.2012.10.123]

80 **Nakamura H**, Takada K, Arihara Y, Hayasaka N, Murase K, Iyama S, Kobune M, Miyanishi K, Kato J. Six-transmembrane epithelial antigen of the prostate 1 protects against increased oxidative stress *via* a nuclear erythroid 2-related factor pathway in colorectal cancer. *Cancer Gene Ther* 2019; **26**: 313-322 [PMID: 30401882 DOI: 10.1038/s41417-018-0056-8]

81 **Rodeberg DA**, Nuss RA, Elsawa SF, Celis E. Recognition of six-transmembrane epithelial antigen of the prostate-expressing tumor cells by peptide antigen-induced cytotoxic T lymphocytes. *Clin Cancer Res* 2005; **11**: 4545-4552 [PMID: 15958640 DOI: 10.1158/1078-0432.Ccr-04-2235]

82 **Alves PM**, Faure O, Graff-Dubois S, Cornet S, Bolonakis I, Gross DA, Miconnet I, Chouaib S, Fizazi K, Soria JC, Lemonnier FA, Kosmatopoulos K. STEAP, a prostate tumor antigen, is a target of human CD8+ T cells. *Cancer Immunol Immunother* 2006; **55**: 1515-1523 [PMID: 16622681 DOI: 10.1007/s00262-006-0165-3]

83 **Barresi V**, Trovato-Salinaro A, Spampinato G, Musso N, Castorina S, Rizzarelli E, Condorelli DF. Transcriptome analysis of copper homeostasis genes reveals coordinated upregulation of SLC31A1,SCO1, and COX11 in colorectal cancer. *FEBS Open Bio* 2016; **6**: 794-806 [PMID: 27516958 DOI: 10.1002/2211-5463.12060]

84 **Ma H**, Shu Q, Li D, Wang T, Li L, Song X, Lou K, Xu H. Accumulation of Intracellular Ferrous Iron in Inflammatory-Activated Macrophages. *Biol Trace Elem Res* 2023; **201**: 2303-2310 [PMID: 35852674 DOI: 10.1007/s12011-022-03362-9]

85 **Isobe T**, Baba E, Arita S, Komoda M, Tamura S, Shirakawa T, Ariyama H, Takaishi S, Kusaba H, Ueki T, Akashi K. Human STEAP3

maintains tumor growth under hypoferric condition. *Exp Cell Res* 2011; **317**: 2582-2591 [PMID: 21871451 DOI: 10.1016/j.yexcr.2011.07.022]

86 **Wan C**, Fu J, Wang Y, Miao S, Song W, Wang L. Exosome-related multi-pass transmembrane protein TSAP6 is a target of rhomboid protease RHBDD1-induced proteolysis. *PLoS One* 2012; **7**: e37452 [PMID: 22624035 DOI: 10.1371/journal.pone.0037452]

87 **Wu Z**, Fang ZX, Hou YY, Wu BX, Deng Y, Wu HT, Liu J. Exosomes in metastasis of colorectal cancers: Friends or foes? *World J Gastrointest Oncol* 2023; **15**: 731-756 [PMID: 37275444 DOI: 10.4251/wjgo.v15.i5.731]

88 **Zhou L**, Jiang J, Huang Z, Jin P, Peng L, Luo M, Zhang Z, Chen Y, Xie N, Gao W, Nice EC, Li JQ, Chen HN, Huang C. Hypoxia-induced lncRNA STEAP3-AS1 activates Wnt/β-catenin signaling to promote colorectal cancer progression by preventing m(6)A-mediated degradation of STEAP3 mRNA. *Mol Cancer* 2022; **21**: 168 [PMID: 35986274 DOI: 10.1186/s12943-022-01638-1]

89 **Fang ZX**, Li CL, Chen WJ, Wu HT, Liu J. Potential of six-transmembrane epithelial antigen of the prostate 4 as a prognostic marker for colorectal cancer. *World J Gastrointest Oncol* 2022; **14**: 1675-1688 [PMID: 36187390 DOI: 10.4251/wjgo.v14.i9.1675]

90 **Xue X**, Bredell BX, Anderson ER, Martin A, Mays C, Nagao-Kitamoto H, Huang S, Győrffy B, Greenson JK, Hardiman K, Spence JR, Kamada N, Shah YM. Quantitative proteomics identifies STEAP4 as a critical regulator of mitochondrial dysfunction linking inflammation and colon cancer. *Proc Natl Acad Sci U S A* 2017; **114**: E9608-E9617 [PMID: 29078383 DOI: 10.1073/pnas.1712946114]

91 **Liao Y**, Zhao J, Bulek K, Tang F, Chen X, Cai G, Jia S, Fox PL, Huang E, Pizarro TT, Kalady MF, Jackson MW, Bao S, Sen GC, Stark GR, Chang CJ, Li X. Inflammation mobilizes copper metabolism to promote colon tumorigenesis *via* an IL-17-STEAP4-XIAP axis. *Nat Commun* 2020; **11**: 900 [PMID: 32060280 DOI: 10.1038/s41467-020-14698-y]

92 **Gutiérrez-Cuevas J**, Lucano-Landeros S, López-Cifuentes D, Santos A, Armendariz-Borunda J. Epidemiologic, Genetic, Pathogenic, Metabolic, Epigenetic Aspects Involved in NASH-HCC: Current Therapeutic Strategies. *Cancers (Basel)* 2022; **15** [PMID: 36612019 DOI: 10.3390/cancers15010023]

93 **Bosch FX**, Ribes J, Díaz M, Cléries R. Primary liver cancer: worldwide incidence and trends. *Gastroenterology* 2004; **127**: S5-S16 [PMID: 15508102 DOI: 10.1053/j.gastro.2004.09.011]

94 **Tong MJ**, el-Farra NS, Reikes AR, Co RL. Clinical outcomes after transfusion-associated hepatitis C. *N Engl J Med* 1995; **332**: 1463-1466 [PMID: 7739682 DOI: 10.1056/nejm199506013322202]

95 **Costas-Rodríguez M**, Anoshkina Y, Lauwens S, Van Vlierberghe H, Delanghe J, Vanhaecke F. Isotopic analysis of Cu in blood serum by multi-collector ICP-mass spectrometry: a new approach for the diagnosis and prognosis of liver cirrhosis? *Metallomics* 2015; **7**: 491-498 [PMID: 25644127 DOI: 10.1039/c4mt00319e]

96 **Lauwens S**, Costas-Rodríguez M, Van Vlierberghe H, Vanhaecke F. Cu isotopic signature in blood serum of liver transplant patients: a follow-up study. *Sci Rep* 2016; **6**: 30683 [PMID: 27468898 DOI: 10.1038/srep30683]

97 **Boswell CA**, Mundo EE, Zhang C, Bumbaca D, Valle NR, Kozak KR, Fourie A, Chuh J, Koppada N, Saad O, Gill H, Shen BQ, Rubinfeld B, Tibbitts J, Kaur S, Theil FP, Fielder PJ, Khawli LA, Lin K. Impact of drug conjugation on pharmacokinetics and tissue distribution of anti-STEAP1 antibody-drug conjugates in rats. *Bioconjug Chem* 2011; **22**: 1994-2004 [PMID: 21913715 DOI: 10.1021/bc200212a]

98 **O'Donoghue JA**, Danila DC, Pandit-Taskar N, Beylergil V, Cheal SM, Fleming SE, Fox JJ, Ruan S, Zanzonico PB, Ragupathi G, Lyashchenko SK, Williams SP, Scher HI, Fine BM, Humm JL, Larson SM, Morris MJ, Carrasquillo JA. Pharmacokinetics and Biodistribution of a [(89)Zr]Zr-DFO-MSTP2109A Anti-STEAP1 Antibody in Metastatic Castration-Resistant Prostate Cancer Patients. *Mol Pharm* 2019; **16**: 3083-3090 [PMID: 31117485 DOI: 10.1021/acs.molpharmaceut.9b00326]

99 **Iijima K**, Nakamura H, Takada K, Hayasaka N, Kubo T, Umeyama Y, Iyama S, Miyanishi K, Kobune M, Kato J. Six-transmembrane epithelial antigen of the prostate 1 accelerates cell proliferation by targeting c-Myc in liver cancer cells. *Oncol Lett* 2021; **22**: 546 [PMID: 34335918 DOI: 10.3892/ol.2021.12807]

100 **Guo WZ**, Fang HB, Cao SL, Chen SY, Li J, Shi JH, Tang HW, Zhang Y, Wen PH, Zhang JK, Wang ZH, Shi XY, Pang C, Yang H, Hu BW, Zhang SJ. Six-Transmembrane Epithelial Antigen of the Prostate 3 Deficiency in Hepatocytes Protects the Liver Against Ischemia-Reperfusion Injury by Suppressing Transforming Growth Factor-β-Activated Kinase 1. *Hepatology* 2020; **71**: 1037-1054 [PMID: 31393024 DOI: 10.1002/hep.30882]

101 **Wang LL**, Luo J, He ZH, Liu YQ, Li HG, Xie D, Cai MY. STEAP3 promotes cancer cell proliferation by facilitating nuclear trafficking of EGFR to enhance RAC1-ERK-STAT3 signaling in hepatocellular carcinoma. *Cell Death Dis* 2021; **12**: 1052 [PMID: 34741044 DOI: 10.1038/s41419-021-04329-9]

102 **Yi Q**, Liang Q, Liu Y, Gong Z, Yan Y. Application of genomic selection and experimental techniques to predict cell death and immunotherapeutic efficacy of ferroptosis-related CXCL2 in hepatocellular carcinoma. *Front Oncol* 2022; **12**: 998736 [PMID: 36276119 DOI: 10.3389/fonc.2022.998736]

103 **Wang S**, Chen L, Liu W. Matrix stiffness-dependent STEAP3 coordinated with PD-L2 identify tumor responding to sorafenib treatment in hepatocellular carcinoma. *Cancer Cell Int* 2022; **22**: 318 [PMID: 36229881 DOI: 10.1186/s12935-022-02634-7]

104 **Ramadoss P**, Chiappini F, Bilban M, Hollenberg AN. Regulation of hepatic six transmembrane epithelial antigen of prostate 4 (STEAP4) expression by STAT3 and CCAAT/enhancer-binding protein alpha. *J Biol Chem* 2010; **285**: 16453-16466 [PMID: 20304921 DOI: 10.1074/jbc.M109.066936]

105 **Kim HY**, Cho HK, Yoo SK, Cheong JH. Hepatic STAMP2 decreases hepatitis B virus X protein-associated metabolic deregulation. *Exp Mol Med* 2012; **44**: 622-632 [PMID: 23095254 DOI: 10.3858/emm.2012.44.10.071]

106 **Kim HY**, Kwon WY, Park JB, Lee MH, Oh YJ, Suh S, Baek YH, Jeong JS, Yoo YH. Hepatic STAMP2 mediates recombinant FGF21-induced improvement of hepatic iron overload in nonalcoholic fatty liver disease. *FASEB J* 2020; **34**: 12354-12366 [PMID: 32721044 DOI: 10.1096/fj.202000790R]

107 **Yamada N**, Yasui K, Dohi O, Gen Y, Tomie A, Kitaichi T, Iwai N, Mitsuyoshi H, Sumida Y, Moriguchi M, Yamaguchi K, Nishikawa T, Umemura A, Naito Y, Tanaka S, Arii S, Itoh Y. Genome-wide DNA methylation analysis in hepatocellular carcinoma. *Oncol Rep* 2016; **35**: 2228-2236 [PMID: 26883180 DOI: 10.3892/or.2016.4619]

108 **Wu HC**, Yang HI, Wang Q, Chen CJ, Santella RM. Plasma DNA methylation marker and hepatocellular carcinoma risk prediction model for the general population. *Carcinogenesis* 2017; **38**: 1021-1028 [PMID: 28981677 DOI: 10.1093/carcin/bgx078]

109 **Ju MH**, Jang EJ, Kang SH, Roh YH, Jeong JS, Han SH. Six-Transmembrane Epithelial Antigen of Prostate 4: An Indicator of Prognosis and Tumor Immunity in Hepatocellular Carcinoma. *J Hepatocell Carcinoma* 2023; **10**: 643-658 [PMID: 37101765 DOI: 10.2147/JHC.S394973]

110 **Abril AG**, Carrera M, Sánchez-Pérez Á, Villa TG. Gut Microbiome Proteomics in Food Allergies. *Int J Mol Sci* 2023; **24** [PMID: 36768555 DOI: 10.3390/ijms24032234]

111 **Ayyaswamy S**, Shi H, Zhang B, Bryan RM Jr, Durgan DJ. Obstructive Sleep Apnea-Induced Hypertension Is Associated With Increased Gut and Neuroinflammation. *J Am Heart Assoc* 2023; **12**: e029218 [PMID: 37260032 DOI: 10.1161/JAHA.122.029218]

112 **Gopalakrishnan S**, Thomas R, Sedaghat S, Krishnakumar A, Khan S, Meyer T, Ajieren H, Nejati S, Wang J, Verma MS, Irazoqui P, Rahimi R. Smart capsule for monitoring inflammation profile throughout the gastrointestinal tract. *Biosens Bioelectron X* 2023; **14** [PMID: 37799507 DOI: 10.1016/j.biosx.2023.100380]

113 **Yang L**, Wang T, Zhang X, Zhang H, Yan N, Zhang G, Yan R, Li Y, Yu J, He J, Jia S, Wang H. Exosomes derived from human placental mesenchymal stem cells ameliorate myocardial infarction *via* anti-inflammation and restoring gut dysbiosis. *BMC Cardiovasc Disord* 2022; **22**: 61 [PMID: 35172728 DOI: 10.1186/s12872-022-02508-w]

114 **Lima SF**, Gogokhia L, Viladomiu M, Chou L, Putzel G, Jin WB, Pires S, Guo CJ, Gerardin Y, Crawford CV, Jacob V, Scherl E, Brown SE, Hambor J, Longman RS. Transferable Immunoglobulin A-Coated Odoribacter splanchnicus in Responders to Fecal Microbiota Transplantation for Ulcerative Colitis Limits Colonic Inflammation. *Gastroenterology* 2022; **162**: 166-178 [PMID: 34606847 DOI: 10.1053/j.gastro.2021.09.061]

115 **Challita-Eid PM**, Morrison K, Etessami S, An Z, Morrison KJ, Perez-Villar JJ, Raitano AB, Jia XC, Gudas JM, Kanner SB, Jakobovits A. Monoclonal antibodies to six-transmembrane epithelial antigen of the prostate-1 inhibit intercellular communication in vitro and growth of human tumor xenografts in vivo. *Cancer Res* 2007; **67**: 5798-5805 [PMID: 17575147 DOI: 10.1158/0008-5472.Can-06-3849]

116 **Yamamoto T**, Tamura Y, Kobayashi J, Kamiguchi K, Hirohashi Y, Miyazaki A, Torigoe T, Asanuma H, Hiratsuka H, Sato N. Six-transmembrane epithelial antigen of the prostate-1 plays a role for in vivo tumor growth *via* intercellular communication. *Exp Cell Res* 2013; **319**: 2617-2626 [PMID: 23916873 DOI: 10.1016/j.yexcr.2013.07.025]

117 **Barroca-Ferreira J**, Pais JP, Santos MM, Goncalves AM, Gomes IM, Sousa I, Rocha SM, Passarinha LA, Maia CJ. Targeting STEAP1 Protein in Human Cancer: Current Trends and Future Challenges. *Curr Cancer Drug Targets* 2018; **18**: 222-230 [PMID: 28460619 DOI: 10.2174/1568009617666170427103732]

118 **Cole G**, McCaffrey J, Ali AA, McCarthy HO. DNA vaccination for prostate cancer: key concepts and considerations. *Cancer Nanotechnol* 2015; **6**: 2 [PMID: 26161151 DOI: 10.1186/s12645-015-0010-5]

119 **Carrasquillo JA**, Fine BM, Pandit-Taskar N, Larson SM, Fleming SE, Fox JJ, Cheal SM, O'Donoghue JA, Ruan S, Ragupathi G, Lyashchenko SK, Humm JL, Scher HI, Gönen M, Williams SP, Danila DC, Morris MJ. Imaging Patients with Metastatic Castration-Resistant Prostate Cancer Using (89)Zr-DFO-MSTP2109A Anti-STEAP1 Antibody. *J Nucl Med* 2019; **60**: 1517-1523 [PMID: 31053681 DOI: 10.2967/jnumed.118.222844]

120 **Qin DN**, Kou CZ, Ni YH, Zhang CM, Zhu JG, Zhu C, Wang YP, Zhu GZ, Shi C, Ji CB, Guo XR. Monoclonal antibody to the six-transmembrane epithelial antigen of prostate 4 promotes apoptosis and inhibits proliferation and glucose uptake in human adipocytes. *Int J Mol Med* 2010; **26**: 803-811 [PMID: 21042773 DOI: 10.3892/ijmm_00000528]

121 **Lin TY**, Park JA, Long A, Guo HF, Cheung NV. Novel potent anti-STEAP1 bispecific antibody to redirect T cells for cancer immunotherapy. *J Immunother Cancer* 2021; **9** [PMID: 34497115 DOI: 10.1136/jitc-2021-003114]

122 **Bai XF**, Liu J, Li O, Zheng P, Liu Y. Antigenic drift as a mechanism for tumor evasion of destruction by cytolytic T lymphocytes. *J Clin Invest* 2003; **111**: 1487-1496 [PMID: 12750398 DOI: 10.1172/jci17656]

123 **Melief CJ**, Toes RE, Medema JP, van der Burg SH, Ossendorp F, Offringa R. Strategies for immunotherapy of cancer. *Adv Immunol* 2000; **75**: 235-282 [PMID: 10879286 DOI: 10.1016/s0065-2776(00)75006-1]

124 **Andersen MH**, Pedersen LO, Becker JC, Straten PT. Identification of a cytotoxic T lymphocyte response to the apoptosis inhibitor protein survivin in cancer patients. *Cancer Res* 2001; **61**: 869-872 [PMID: 11221872]

125 **Alves PM**, Faure O, Graff-Dubois S, Gross DA, Cornet S, Chouaib S, Miconnet I, Lemonnier FA, Kosmatopoulos K. EphA2 as target of anticancer immunotherapy: identification of HLA-A*0201-restricted epitopes. *Cancer Res* 2003; **63**: 8476-8480 [PMID: 14679012]

126 **Faure O**, Graff-Dubois S, Bretaudeau L, Derré L, Gross DA, Alves PM, Cornet S, Duffour MT, Chouaib S, Miconnet I, Grégoire M, Jotereau F, Lemonnier FA, Abastado JP, Kosmatopoulos K. Inducible Hsp70 as target of anticancer immunotherapy: Identification of HLA-A*0201-restricted epitopes. *Int J Cancer* 2004; **108**: 863-870 [PMID: 14712489 DOI: 10.1002/ijc.11653]

127 **Graff-Dubois S**, Faure O, Gross DA, Alves P, Scardino A, Chouaib S, Lemonnier FA, Kosmatopoulos K. Generation of CTL recognizing an HLA-A*0201-restricted epitope shared by MAGE-A1, -A2, -A3, -A4, -A6, -A10, and -A12 tumor antigens: implication in a broad-spectrum tumor immunotherapy. *J Immunol* 2002; **169**: 575-580 [PMID: 12077290 DOI: 10.4049/jimmunol.169.1.575]

128 **Azumi M**, Kobayashi H, Aoki N, Sato K, Kimura S, Kakizaki H, Tateno M. Six-transmembrane epithelial antigen of the prostate as an immunotherapeutic target for renal cell and bladder cancer. *J Urol* 2010; **183**: 2036-2044 [PMID: 20303532 DOI: 10.1016/j.juro.2009.12.094]

World Journal of Clinical Oncology

Submit a Manuscript: https://www.f6publishing.com

World J Clin Oncol 2024 January 24; 15(1): 23-31

DOI: 10.5306/wjco.v15.i1.23

ISSN 2218-4333 (online)

MINIREVIEWS

Uveal melanoma: Recent advances in immunotherapy

Francesco Saverio Sorrentino, Francesco De Rosa, Patrick Di Terlizzi, Giacomo Toneatto, Andrea Gabai, Lucia Finocchio, Carlo Salati, Leopoldo Spadea, Marco Zeppieri

Specialty type: Oncology

Provenance and peer review: Invited article; Externally peer reviewed.

Peer-review model: Single blind

Peer-review report's scientific quality classification

Grade A (Excellent): 0
Grade B (Very good): B
Grade C (Good): C
Grade D (Fair): 0
Grade E (Poor): 0

P-Reviewer: Luo Y, China; Yu HP, China

Received: November 1, 2023
Peer-review started: November 1, 2023
First decision: November 29, 2023
Revised: December 7, 2023
Accepted: January 2, 2024
Article in press: January 2, 2024
Published online: January 24, 2024

Francesco Saverio Sorrentino, Patrick Di Terlizzi, Department of Surgical Sciences, Unit of Ophthalmology, Ospedale Maggiore, Bologna 40100, Italy

Francesco De Rosa, Department of Oncology, IRCCS Istituto Romagnolo per lo Studio dei Tumori "Dino Amadori", Meldola 47014, Italy

Giacomo Toneatto, Andrea Gabai, Lucia Finocchio, Carlo Salati, Marco Zeppieri, Department of Ophthalmology, University Hospital of Udine, Udine 33100, Italy

Leopoldo Spadea, Eye Clinic, Policlinico Umberto I, "Sapienza" University of Rome, Rome 00142, Italy

Corresponding author: Marco Zeppieri, BSc, MD, PhD, Doctor, Department of Ophthalmology, University Hospital of Udine, p.le S. Maria della Misericordia 15, Udine 33100, Italy. markzeppieri@hotmail.com

Abstract

Uveal melanoma (UM) is the most common primary intraocular cancer in adults. The incidence in Europe and the United States is 6-7 per million population per year. Although most primary UMs can be successfully treated and locally controlled by irradiation therapy or local tumor resection, up to 50% of UM patients develop metastases that usually involve the liver and are fatal within 1 year. To date, chemotherapy and targeted treatments only obtain minimal responses in patients with metastatic UM, which is still characterized by poor prognosis. No standard therapeutic approaches for its prevention or treatment have been established. The application of immunotherapy agents, such as immune checkpoint inhibitors that are effective in cutaneous melanoma, has shown limited effects in the treatment of ocular disease. This is due to UM's distinct genetics, natural history, and complex interaction with the immune system. Unlike cutaneous melanomas characterized mainly by BRAF or NRAS mutations, UMs are usually triggered by a mutation in GNAQ or GNA11. As a result, more effective immunotherapeutic approaches, such as cancer vaccines, adoptive cell transfer, and other new molecules are currently being studied. In this review, we examine novel immunotherapeutic strategies in clinical and preclinical studies and highlight the latest insight in immunotherapy and the development of tailored treatment of UM.

Key Words: Uveal melanoma; Immunotherapy; Ocular oncology; Tumor; Metastatic disease; Genetic mutations

Core Tip: Our minireview will cover the latest studies about immunotherapy for uveal melanoma (UM) metastatic disease. Driver genes and oncogenic mutations have been largely investigated. Up to half of affected patients develop metastases that are the leading single cause of death after diagnosis of UM. Precise systemic therapy addressing metastatic UM and significantly improving the surveillance is not available for each single case. However, identifying predictive factors, achieving international consensus on surveillance protocols, aiming to inactivate micrometastases, and standardizing outcomes would be crucial to be able to effectively cure metastatic UM.

Citation: Sorrentino FS, De Rosa F, Di Terlizzi P, Toneatto G, Gabai A, Finocchio L, Salati C, Spadea L, Zeppieri M. Uveal melanoma: Recent advances in immunotherapy. *World J Clin Oncol* 2024; 15(1): 23-31
URL: https://www.wjgnet.com/2218-4333/full/v15/i1/23.htm
DOI: https://dx.doi.org/10.5306/wjco.v15.i1.23

INTRODUCTION

Uveal melanoma (UM) is a rare ocular tumor regarded as the most common primary malignancy in the adult eye. The annual incidence is approximately 6-7 per million in the United States, accounting for 3.7% of all melanomas[1]. UM derives from the pigmented uveal zone, which comprises the choroid, ciliary body, and iris, and is featured by characteristic cytogenetic changes, oncogenic mutations in GNAQ or GNA11, and tropism to aggressively metastasize to the liver resulting in a poor prognosis[2,3]. At this time, UM has no established and effective treatments once metastases arise or have been detected. Although several immunotherapies have demonstrated efficacy in metastatic melanoma of cutaneous origin, these immune-based therapies have disappointing outcomes in UM[3,4]. Some authors have speculated that ocular melanomas, arising from the uveal tract, might be regarded as an immunotherapy-resistant variant of ocular melanomas[5].

Numerous studies in scientific medical literature continually show that tumor-associated cell therapy tends to be an effective alternative and innovative method to fight metastasis. In the last decades, studies have shown that immunotherapies therapies can bring substantial benefits to patients suffering from a wide range of neoplasia and metastatic disease[6,7]. For this reason, huge investments, resources, and important clinical trials have been performed for immunotherapy research and its potential benefit on UM metastatic disease.

Before undertaking this study, we searched PubMed (https://pubmed.ncbi.nlm.nih.gov) and Reference Citation Analysis (RCA) (https://www.referencecitationanalysis.com) for the terms "metastatic uveal melanoma" (1788 papers) and "uveal melanoma immunotherapy" (367 papers) for articles published between January 1, 2000, to August 31, 2023. We considered only studies in English, with abstracts and structured text, and those referring to humans, whereas we excluded "case reports", "case series", "conference papers", "letters" and "*in vitro*" studies. The reference lists of all retrieved articles were scanned to detect further relevant papers.

Genetics and pathways involved in UM

Differently from cutaneous melanoma, which usually harbors an activating BRAF (52%) or NRAS (10%-25%) mutation or inactivation of the *NF1* gene, UMs, as well as uveal nevi, are commonly characterized by a mutation in GNAQ or GNA11 [8-10]. These genetic alterations, however, are not sufficient to drive the full malignant transformation to melanoma, being rather an initiating event[11]. GNAQ/11 activates mitogen activating protein kinase (MAPK) pathway, present in most UM, as well as PKC, AKT, and Yes-associated protein 1, associated with tumor growth in some UM models[12,13].

Another genetic pathway implicated in UM involve schromosome 3, specifically the BAP1 tumor suppressor gene. The loss of one copy of chromosome 3 is indeed an established negative prognostic factor associated with metastasis and poor clinical outcome, while BAP1 mutation leads to malignant transformation when associated with chromosome 3 monosomy, as the other gene copy is already lost[14,15].

Immune checkpoint inhibitors

Activation of T cells by antigen-presenting cells (dendritic cells) is the key point of an effective immune reaction against cancer cell antigens. This process is enhanced by co-stimulatory molecules like CD28 and B-7, and hampered by immune checkpoints like cytotoxic T-lymphocyte-associated protein 4 (CTLA-4) and programmed cell death protein 1 (PD-1). These molecules modulate the immune response, preventing inappropriate activation of T cells and controlling excessive immune reaction[16]. CTLA-4, when expressed, binds B-7 with a higher affinity than CD28, thus way blocking CD28-mediated co-stimulation; conversely, PD-1 interacts mainly with programmed death-ligand 1 (PD-L1) and mostly affects the effector phase of the immune response[17].

Immune checkpoint inhibitors (ICIs) are antibodies suppressing the negative immunomodulatory activities of their targets (*i.e.*, CTLA-4 and PD-1). The consequent activation of T cell-mediated response can result in lysis and degradation of cancer cells, ultimately leading to long-term tumor control. This practice-changing concept was first demonstrated by the studies by James P Allison and Tasuku Honjo, awarded the Nobel Prize in Physiology or Medicine in 2018[18].

Malignant melanoma was the first indication for which ipilimumab, an antibody targeting the CTLA-4, was approved by the Food and Drug Administration (FDA) in 2011[19,20]. Few years later, the anti-PD-1 antibodies nivolumab and pembrolizumab were also approved. ICIs have been subsequently tested in metastatic UM (mUM); however, robust conclusions regarding their efficacy are difficult to draw given the many limitations of the available data[21-30].

Anti CTLA-4 antibodies

Ipilimumab, whose efficacy in mUM was evaluated in just a few studies, is a humanized monoclonal antibody blocking the CTLA-4 receptor, enhancing T-cell activation, and amplifying T-cell-mediated immunity. Tremelimumab is an anti-CTLA-4 antibody that has also been proposed for mUM[22]. A recent systematic review and meta-analysis of Pham *et al* [31] showed that the objective response rate (ORR) was 4.1% for anti-CTLA4, with a median overall survival (OS) of 8.0 mo, and a 12-mo OS rate of 34.7%[31]. The progression-free survival (PFS) was longer in treatment-naïve patients than in pretreated patients, with a median value of 3.3 mo. The side effect profile was similar to studies of CTLA-4 inhibitors in cutaneous melanoma, with an overall adverse event (AE) rate of 64.5% and a grade 3-4 AE rate of 17.5% (more commonly hepatitis and diarrhea). No deaths secondary to AEs were reported[32]. Overall, CTLA-4 inhibitors appear to have limited activity in mUM; consequently, their use is generally restricted to selected cases.

Anti PD-1 antibodies

After nivolumab and pembrolizumab were first approved by the FDA for melanoma in 2014, the number of agents acting on the PD-1/PD-L1 axis and their indications across malignancies have been rapidly rising[33]. Concerning mUM, pembrolizumab and nivolumab have been the most studied, but atezolizumab and avelumab have also been proposed [34].

Pham *et al*[31] reported anORR of 7.1% for anti-PD-1 antibodies. Median OS was 11.7 mo, 12-mo OS probability was 48.9%, and PFS was 3.2 mo. These data, similar toanti-CTLA-4 antibodies, suggest that their activity is modest, with only a few patients benefiting from them. Anyway, a better toxicity profile (AE rate of 50.2%; grade 3-4 AE rate of 13.2%) favors them with respect to ipilimumab.

Combined therapies

The dramatic efficacy of the combination of iplimumab and nivolumab in metastatic cutaneous melanoma prompted studies also in mUM: However, as already reported for monotherapies, efficacy was substantially lower[35]. Indeed, the recent meta-analysis of Pham *et al*[31] showed an ORR dropped to 13.5%, with a median OS of 16.0 mo, a 12-mo OS rate of 60.3%, and a median PFS of 3.2 mo. Although these data were slightly better, they are not sufficient to support a clear benefit for mUM patients. Moreover, toxicity is also higher and can be substantial, as shown by an overall AE rate of 85.8% and a grade 3-4 AE rate of 33.9%.

The mechanisms determining a substantially reduced efficacy of ICIs in mUM *vs* metastatic cutaneous melanoma are not completely understood. The studies have shown an immune privilege of UM inside the eye through multiple strategies, including expression of PD-L1 and indoleamine dioxygenase-1: These are also allegedly active at metastatic deposits, particularly in the liver, creating a microenvironment particularly resistant to immunotherapy. A low tumor mutational burden has also been suggested to contribute[36,37].

ICIs in combination with liver-directed therapies

The liver is the most common site for UM metastases, and about 50% of the patients will have isolated liver metastases. High lactate dehydrogenase and liver metastases are dominant predictors for ICI failure in cancer therapy since hepatic disease in mUM is particularly resistant to immunotherapy[38]. Therefore, liver-directed therapies in combination with ICIs have a strong rationale.

Treatment with ipilimumab/nivolumab in combination with percutaneous hepatic perfusion with melphalan has been explored in a phase Ibtrialona small number of patients. The authors found 1 complete response, 5 partial responses, and 1 stable disease. Grade III/IV AEs were observed in 5/7 patients without dose-limiting toxicities or death[39].

Minor *et al*[40] conducted a pilot study on 26 patients with hepatic metastases of UM treated with two cycles of selective internal radiation therapy (SIRT) with yttrium-90 (90Y) resin microspheres, one to each lobe of the liver, followed in 2-4 wk by immunotherapy with ipilimumab/nivolumab every 3 wk for four doses, then maintenance immunotherapy with nivolumab alone. Initial dosing of both 90Y and immunotherapy resulted in excessive toxicity but, after decreasing the dosage of 90Y microspheres to limit the radiation dose to normal liver to 35 Gy and lowering the ipilimumab dose to 1 mg/kg, the treatment was tolerable. Reported ORR was 20%, median OS 15 mo, and median PFS 5.5 mo[40].

Aedo-Lopez *et al*[41] conducted a retrospective study of 32 patients with mUM divided into two groups based on the treatment received: SIRT with 90Y microspheres and ipilimumab/nivolumab before or after the SIRT (18 patients) *vs* SIRT without combined immunotherapy (14 patients). Median OS was 49.6 and 13.6 mo in the two groups respectively. The presence of extra hepatic-metastases at the time of SIRT, a liver lesion over 8 cm, and a high liver tumor volume negatively impacted survival[41].

A case series of 8 patients treated with ipilimumab/nivolumab combination along with transarterial chemoembolization (TACE), followed by nivolumab maintenance and monthly TACE procedures, demonstrated a median OS of 14.2 mo. Two/8 patients had partial response, 4/8 stable disease, 2/8 disease progression[42]. A phase Ib/II study was conducted to assess the safety and efficacy of radiofrequency ablation (RFA) of one liver metastatic lesion plus ipilimumab. Recommended phase II dose was ipilimumab 3 mg/kg + RFA. No confirmed objective responses were observed. Median OS was 14.2 mo for the 10 mg/kg ipilimumab cohort *vs* 9.7 mo for the 3 mg/kg cohort. Median PFS

was 3 mo comparable for both cohorts. Combining RFA with ipilimumab 3 mg/kg was well tolerated but showed very limited clinical activity in UM[43].

An ongoing phase II trial (NCT03472586) studies ipilimumab and nivolumab in combination with immunoembolization with lipiodol and granulocyte-macrophage colony-stimulating factor in patients with liver metastases from UM. Similarly, a phase I randomized controlled multicenter trial (NCT04463368) is evaluating the effectiveness of isolated hepatic perfusion with melphalan in combination with ipilimumab and nivolumab. The isolation of the liver from the systemic circulation allows a high concentration of the chemotherapeutic agent to be delivered to the liver in conjunction with hyperthermia, allowing a higher efficacy with minimal systemic exposure to the drug.

Other strategies

The phase Ib, open-label CLEVER study evaluated treatment with intravenous coxsackievirus A21 (V937) in combination with ipilimumab in patients with mUM, based on the rationale that the combination of V937 and ipilimumab might result in augmented T-cell responses with consequent improved clinical activity. However, the combination regimen did not result in objective responses, although 3 patients obtained a stable disease[44].

Drugs targeting epigenetic regulators such as histone deacetylases (HDACs) show promise as cancer therapies by reversing oncogene transcription and modifying the tumor microenvironment. A phase II trial was conducted to evaluate if anti-PD-1 therapies and HDAC inhibitors (entinostat) could synergize. ORR was 14%, median OS was 13.4 mo and median PFS was 2.1 mo, slightly higher than that of anti-PD-1 monotherapy[45]. Arginine deprivation with ADI PEG-20 with ipilimumab/nivolumab was also studied in a phase I trial; however, there were no objective responses, and the median OS was only 8.6 mo[46].

Lymphocyte-activation gene 3 (LAG-3) is another immune checkpoint that negatively regulates T-cell proliferation and effector T-cell function. LAG-3 and PD-1 are often co-expressed on tumor-infiltrating lymphocytes, thus contributing to tumor-mediated T-cell exhaustion: Upon this rationale, the phase III RELATIVITY-047 trial validated LAG-3 blockade as a relevant biological target and established it as the third clinically relevant immune checkpoint, demonstrating improved antitumor activity for the combination of the anti-LAG-3 antibody relatlimab and nivolumab concerning nivolumab alone [47]. After these results, the combination nivolumab/relatlimab (Opdualag) was approved for medical use in the United States in March 2022 for the first-line therapy of patients with metastatic melanoma. Whether the combination is effective also in rare melanoma subtypes remains to be elucidated: An ongoing trial (NCT04552223) aims to test it in mUM patients. A study from a southern French patient cohort confirmed LAG-3 and PRAME (PReferentially expressed Antigen in MElanoma) as potentially important immunotherapy targets in the treatment of UM patients while proposing V-domain Ig suppressor of T-cell activation as a novel relevant immune checkpoint molecule in primary UM[48].

Immunotherapy has proven to be an interesting and viable option in UM metastatic disease, even though much has still to be studied to have scientific and clinical effectiveness. Despite optimal management of primary tumors, about half of patients will eventually develop distant metastatic disease. Differently from cutaneous melanoma, the liver is involved in the vast majority of cases: This led to the employment of liver-directed therapies with encouraging results in carefully selected patients[49]. However, a randomized trial comparing hepatic artery infusion *vs* systemic fotemustine was stopped early for futility after failure to show improved OS despite improvement in PFS[50]. This observation, considering also that most patients either progress after or are not candidates for locoregional therapy, suggests that effective systemic treatments may represent the therapeutic mainstay.

Historically, patients with ocular or UM were excluded from clinical trials on cutaneous melanoma because of the biological and clinical differences: Therefore, there has been no widely accepted standard treatment, and patients were generally managed with drugs and regimens approved for cutaneous melanoma (*i.e.*, dacarbazine, temozolomide, or fotemustine). However, despite some responses being observed, none of them was demonstrated to be effective[51].

The discovery of the presence of activating mutation in GNAQ/GNA11 in the majority of UM patients, resulting in constitutional activation of MAPK pathways, led to the development of the MEK inhibitor selumetinib in this setting. A first randomized, phase II clinical trial compared it with chemotherapy (dacarbazine or temozolomide); the primary endpoint was PFS. Selumetinib improved PFS concerning the comparator, but the AE rate was high and OS was similar between the two arms[52]. A subsequent randomized, placebo-controlled, phase III study evaluated its combination with dacarbazine concerning dacarbazine monotherapy and failed to show any improvement in either PFS or OS[53].

The ICIs proved very effective in cutaneous melanoma and were subsequently tested in ocular melanoma; however, the results were not as good as expected. Despite retrospective reports suggesting potential efficacy ipilimumab, an anti-CTLA4 antibody, did not show any response in a phase II clinical trial; PFS and OS were comparable with historical controls treated with chemotherapy[54].

The anti-PD1 agents nivolumab and pembrolizumab were also tested as monotherapies in phase II clinical trials. Both agents showed clinical responses that were sometimes durable; however, PFS and OS were highly variable and, overall, not so different from those obtained with chemotherapy[55]. Other two studies evaluated the combination of ipilimumab and nivolumab, after the very good results observed in cutaneous melanoma. A first study on 55 patients showed a high rate (51.9%) of disease stabilization; however, PFS and OS were still comparable to historical controls treated with chemotherapy[56]. Data from the second one were more promising, observing a median PFS of 5.5 mo and OS of 19.1 mo, but only 33 patients were evaluable for efficacy[57]. Overall, these data demonstrate that ICIs, and especially the combination of ipilimumab and nivolumab, may achieve durable responses, but with a limited prognostic impact.

Tebentafusp

ImmTAC, short for immune-mobilizing monoclonal T-cell receptors against cancer, represents a novel category of T-cell–redirecting bispecific fusion proteins. These innovative molecules utilize an engineered high-affinity T-cell receptor to effectively target any protein, including intracellular antigens, displayed as a peptide-HLA complex on the surface of

Table 1 Drug therapies for metastatic uveal melanoma disease

Drug	Target	Action
Ipilimumab	CTLA-4	Blocking the CTLA-4 receptor, enhancing T-cell activation, amplifying T-cell-mediated immunity
Tremelimumab	CTLA-4	Blocking the CTLA-4 receptor, amplifying T-cell-mediated immunity
Nivolumab	PD-1	Activation of T cell-mediated response. Lysis and degradation of cancer cells
Pembrolizumab	PD-1	Activation of T cell-mediated response. Lysis and degradation of cancer cells
Coxsackievirus A21 (V937)		Augmented T-cell responses with consequent improved clinical activity
Lymphocyte-activation gene 3		Negatively regulation T-cell proliferation and effector T-cell function
Tebentafusp	T-cell-redirecting bispecific fusion proteins	Enhancing HLA-A*0201-restricted T-cell receptor specifically recognizing the glycoprotein 100

CTLA-4: Cytotoxic T-lymphocyte-associated protein 4; PD-1: Programmed cell death protein 1.

the target cell[58]. Tebentafusp, previously known as IMCgp100, is an example of such a molecule, featuring a soluble, enhanced HLA-A*0201-restricted T-cell receptor specifically recognizing the glycoprotein 100 (gp100) peptide YLEPGPVTA, that is highly express on UM cells. This receptor is fused with an anti-CD3 single-chain variable fragment. When the ImmTAC binds to its designated peptide–HLA complexes on the surface of the target cell, it enlists and stimulates polyclonal T cells *via* CD3, to kill these cells. In addition to its T cell cytotoxic effects, IMCgp100 stimulates T cells to secrete a diverse array of cytokines and chemokines, such as interleukin-6 (IL-6), IL-2, and tumor necrosis factor-alpha, thereby amplifying its potential as an anti-cancer immune agent[59,60]. The activation of T-cells by IMCgp100 occurs at a concentration of 1 pM, with the most significant reaction observed at 1 nM. Off-target effects are observable solely at concentrations significantly exceeding 1 nM, highlighting the high specificity of the tumor antigen and a broad therapeutic range, and IMCgp100 activity *in vitro* correlates with the cellular expression levels of gp100-HLA-A*01[61].

The drug was tested in a phase III randomized trial (2:1) against a comparator chosen by the investigator among pembrolizumab, ipilimumab, or dacarbazine (Table 1). PFS was not significantly different among the two arms, but OS was superior in the tebentafusp arm (21.7 *vs* 16 mo; hazard ratio = 0.51). The decoupling between PFS and OS was explained by the observation that, while responding patients had similar outcomes in both arms, the prognosis of unresponsive patients was better in the tebentafusp arm, suggesting that treatment-induced immune activation slows disease progression even in the absence of an objective response. The toxicity observed is mild or moderate in most cases, with the cytokine-release syndrome and cutaneous reaction being the most characteristic drug-related AEs[62].

Tebentafusp has undoubtedly marked a significant advancement in the treatment of metastatic UM, offering a survival benefit over conventional therapies. Its preferential binding to HLA-A0201 has limited its applicability to patients with this specific subtype, prompting a need for the development of alternative treatments for individuals with other HLA subtypes. Although subgroup analyses in the phase III trial raised questions regarding its potential efficacy in certain patient groups, including those with high tumor burden and poorer performance status, its overall benefit still positions it as a preferred therapeutic option for most HLA-A0201-positive patients. Regarding the optimal duration of treatment, current data suggest that continuing tebentafusp until confirmed radiological progression might be a reasonable approach, given its manageable and predictable toxicities. However, more extensive studies are required to establish the most suitable duration for treatment. Additionally, the challenge of evaluating treatment response necessitates the exploration of alternative markers beyond traditional response measures. The correlation between rash appearance and improved survival warrants further investigation, while circulating tumor DNA reduction holds promise as a potential indicator of treatment benefit.

The investigation of tebentafusp in conjunction with liver-directed therapies is also a significant area of interest, considering the potential benefit for patients with bulky disease. Furthermore, the exploration of other therapeutic targets, such as PRAME, through alternative treatments like IMC-F106C, presents a promising direction for future research efforts.

In this scenario, while certain limitations exist, tebentafusp represents a groundbreaking development in the field of metastatic UM treatment. Unanswered questions regarding response monitoring and application in diverse treatment settings warrant further exploration to optimize its therapeutic potential and expand its applicability to a broader patient population. Future research objectives should include the determination of theoptimal treatment sequence between tebentafusp and checkpoint blockade, as well as the potential benefits of combining these therapies. Ongoing studies focusing on the combination of tebentafusp with other immunotherapies and the assessment of its role in the adjuvant setting after primary disease therapy are critical in further delineating its therapeutic scope. Further research and a comprehensive understanding of tebentafusp's mechanisms will undoubtedly pave the way for improved treatment strategies and outcomes in the management of metastatic UM.

CONCLUSION

To conclude, research on immunotherapy for UM metastatic disease has vast supporting scientific and clinically applicable literature but is just at the beginning of a new era for effective treatment to practically increase the surveillance of affected patients. Predictive biomarkers, mechanisms of resistance, treatment duration and treatment beyond progression, immune-related toxicities, and clinical trial design are key concepts in need of further consideration to optimize the anticancer potential treatments. Future studies based on longer follow-up with homogenous criteria, preferably on human subjects, can pave the way to tailoring immunotherapy for patients affected by ultraviolet metastatic disease.

FOOTNOTES

Author contributions: De Rosa F and Zeppieri M wrote the outline; De Rosa F assisted in the revisions of the manuscript; Salati C and Spadea L assisted in the editing of the manuscript; Zeppieri M assisted in the conception and design of the study, and completed the English and scientific editing (a native English speaking MD, PhD); Sorrentino FS, De Rosa F, Di Terlizzi P, Toneatto G, Gabai A, Finocchio L, Salati C, Spadea L, and Zeppieri M participated in the manuscript writing; Sorrentino FS, De Rosa F, Di Terlizzi P, Toneatto G, and Gabai A contributed to the research; Sorrentino FS and Zeppieri M provided the final approval of the version of the article.

Conflict-of-interest statement: All the authors report no relevant conflicts of interest for this article.

Country/Territory of origin: Italy

ORCID number: Francesco De Rosa 0000-0003-0511-1298; Carlo Salati 0000-0003-4736-5296; Leopoldo Spadea 0000-0002-1190-3956; Marco Zeppieri 0000-0003-0999-5545.

S-Editor: Wang JJ
L-Editor: A
P-Editor: Zhang XD

REFERENCES

1 **Krantz BA**, Dave N, Komatsubara KM, Marr BP, Carvajal RD. Uveal melanoma: epidemiology, etiology, and treatment of primary disease. *Clin Ophthalmol* 2017; **11**: 279-289 [PMID: 28203054 DOI: 10.2147/OPTH.S89591]

2 **Chattopadhyay C**, Kim DW, Gombos DS, Oba J, Qin Y, Williams MD, Esmaeli B, Grimm EA, Wargo JA, Woodman SE, Patel SP. Uveal melanoma: From diagnosis to treatment and the science in between. *Cancer* 2016; **122**: 2299-2312 [PMID: 26991400 DOI: 10.1002/cncr.29727]

3 **Jager MJ**, Shields CL, Cebulla CM, Abdel-Rahman MH, Grossniklaus HE, Stern MH, Carvajal RD, Belfort RN, Jia R, Shields JA, Damato BE. Uveal melanoma. *Nat Rev Dis Primers* 2020; **6**: 24 [PMID: 32273508 DOI: 10.1038/s41572-020-0158-0]

4 **Rossi E**, Croce M, Reggiani F, Schinzari G, Ambrosio M, Gangemi R, Tortora G, Pfeffer U, Amaro A. Uveal Melanoma Metastasis. *Cancers (Basel)* 2021; **13** [PMID: 34830841 DOI: 10.3390/cancers13225684]

5 **Chandran SS**, Somerville RPT, Yang JC, Sherry RM, Klebanoff CA, Goff SL, Wunderlich JR, Danforth DN, Zlott D, Paria BC, Sabesan AC, Srivastava AK, Xi L, Pham TH, Raffeld M, White DE, Toomey MA, Rosenberg SA, Kammula US. Treatment of metastatic uveal melanoma with adoptive transfer of tumour-infiltrating lymphocytes: a single-centre, two-stage, single-arm, phase 2 study. *Lancet Oncol* 2017; **18**: 792-802 [PMID: 28395880 DOI: 10.101/S1470-2045(17)30251-6]

6 **Feng X**, Arang N, Rigiracciolo DC, Lee JS, Yeerna H, Wang Z, Lubrano S, Kishore A, Pachter JA, König GM, Maggiolini M, Kostenis E, Schlaepfer DD, Tamayo P, Chen Q, Ruppin E, Gutkind JS. A Platform of Synthetic Lethal Gene Interaction Networks Reveals that the GNAQ Uveal Melanoma Oncogene Controls the Hippo Pathway through FAK. *Cancer Cell* 2019; **35**: 457-472.e5 [PMID: 30773340 DOI: 10.1016/j.ccell.2019.01.009]

7 **Fu Y**, Xiao W, Mao Y. Recent Advances and Challenges in Uveal Melanoma Immunotherapy. *Cancers (Basel)* 2022; **14** [PMID: 35804863 DOI: 10.3390/cancers14133094]

8 **Bauer J**, Kilic E, Vaarwater J, Bastian BC, Garbe C, de Klein A. Oncogenic GNAQ mutations are not correlated with disease-free survival in uveal melanoma. *Br J Cancer* 2009; **101**: 813-815 [PMID: 19654573 DOI: 10.1038/sj.bjc.6605226]

9 **Jensen DE**, Rauscher FJ 3rd. BAP1, a candidate tumor suppressor protein that interacts with BRCA1. *Ann N Y Acad Sci* 1999; **886**: 191-194 [PMID: 10667217 DOI: 10.1111/j.1749-6632.1999.tb09414.x]

10 **Davies H**, Bignell GR, Cox C, Stephens P, Edkins S, Clegg S, Teague J, Woffendin H, Garnett MJ, Bottomley W, Davis N, Dicks E, Ewing R, Floyd Y, Gray K, Hall S, Hawes R, Hughes J, Kosmidou V, Menzies A, Mould C, Parker A, Stevens C, Watt S, Hooper S, Wilson R, Jayatilake H, Gusterson BA, Cooper C, Shipley J, Hargrave D, Pritchard-Jones K, Maitland N, Chenevix-Trench G, Riggins GJ, Bigner DD, Palmieri G, Cossu A, Flanagan A, Nicholson A, Ho JW, Leung SY, Yuen ST, Weber BL, Seigler HF, Darrow TL, Paterson H, Marais R, Marshall CJ, Wooster R, Stratton MR, Futreal PA. Mutations of the BRAF gene in human cancer. *Nature* 2002; **417**: 949-954 [PMID: 12068308 DOI: 10.1038/nature00766]

11 **Van Raamsdonk CD**, Bezrookove V, Green G, Bauer J, Gaugler L, O'Brien JM, Simpson EM, Barsh GS, Bastian BC. Frequent somatic mutations of GNAQ in uveal melanoma and blue naevi. *Nature* 2009; **457**: 599-602 [PMID: 19078957 DOI: 10.1038/nature07586]

12 **Feng X**, Degese MS, Iglesias-Bartolome R, Vaque JP, Molinolo AA, Rodrigues M, Zaidi MR, Ksander BR, Merlino G, Sodhi A, Chen Q, Gutkind JS. Hippo-independent activation of YAP by the GNAQ uveal melanoma oncogene through a trio-regulated rho GTPase signaling circuitry. *Cancer Cell* 2014; **25**: 831-845 [PMID: 24882515 DOI: 10.1016/j.ccr.2014.04.016]

13 **Vaqué JP**, Dorsam RT, Feng X, Iglesias-Bartolome R, Forsthoefel DJ, Chen Q, Debant A, Seeger MA, Ksander BR, Teramoto H, Gutkind JS. A genome-wide RNAi screen reveals a Trio-regulated Rho GTPase circuitry transducing mitogenic signals initiated by G protein-coupled receptors. *Mol Cell* 2013; **49**: 94-108 [PMID: 23177739 DOI: 10.1016/j.molcel.2012.10.018]

14 **Scholes AG**, Damato BE, Nunn J, Hiscott P, Grierson I, Field JK. Monosomy 3 in uveal melanoma: correlation with clinical and histologic predictors of survival. *Invest Ophthalmol Vis Sci* 2003; **44**: 1008-1011 [PMID: 12601021 DOI: 10.1167/iovs.02-0159]

15 **Harbour JW**, Onken MD, Roberson ED, Duan S, Cao L, Worley LA, Council ML, Matatall KA, Helms C, Bowcock AM. Frequent mutation of BAP1 in metastasizing uveal melanomas. *Science* 2010; **330**: 1410-1413 [PMID: 21051595 DOI: 10.1126/science.1194472]

16 **Han Y**, Liu D, Li L. PD-1/PD-L1 pathway: current researches in cancer. *Am J Cancer Res* 2020; **10**: 727-742 [PMID: 32266087]

17 **Salmaninejad A**, Valilou SF, Shabgah AG, Aslani S, Alimardani M, Pasdar A, Sahebkar A. PD-1/PD-L1 pathway: Basic biology and role in cancer immunotherapy. *J Cell Physiol* 2019; **234**: 16824-16837 [PMID: 30784085 DOI: 10.1002/jcp.28358]

18 **Ljunggren HG**, Jonsson R, Höglund P. Seminal immunologic discoveries with direct clinical implications: The 2018 Nobel Prize in Physiology or Medicine honours discoveries in cancer immunotherapy. *Scand J Immunol* 2018; **88**: e12731 [PMID: 30485497 DOI: 10.1111/sji.12731]

19 **Beaver JA**, Tzou A, Blumenthal GM, McKee AE, Kim G, Pazdur R, Philip R. An FDA Perspective on the Regulatory Implications of Complex Signatures to Predict Response to Targeted Therapies. *Clin Cancer Res* 2017; **23**: 1368-1372 [PMID: 27993967 DOI: 10.1158/1078-0432.CCR-16-1098]

20 **Davis AA**, Patel VG. The role of PD-L1 expression as a predictive biomarker: an analysis of all US Food and Drug Administration (FDA) approvals of immune checkpoint inhibitors. *J Immunother Cancer* 2019; **7**: 278 [PMID: 31655605 DOI: 10.1186/s40425-019-0768-9]

21 **Maio M**, Danielli R, Chiarion-Sileni V, Pigozzo J, Parmiani G, Ridolfi R, De Rosa F, Del Vecchio M, Di Guardo L, Queirolo P, Picasso V, Marchetti P, De Galitiis F, Mandalà M, Guida M, Simeone E, Ascierto PA. Efficacy and safety of ipilimumab in patients with pre-treated, uveal melanoma. *Ann Oncol* 2013; **24**: 2911-2915 [PMID: 24067719 DOI: 10.1093/annonc/mdt376]

22 **Joshua AM**, Monzon JG, Mihalcioiu C, Hogg D, Smylie M, Cheng T. A phase 2 study of tremelimumab in patients with advanced uveal melanoma. *Melanoma Res* 2015; **25**: 342-347 [PMID: 26050146 DOI: 10.1097/CMR.0000000000000175]

23 **Karydis I**, Chan PY, Wheater M, Arriola E, Szlosarek PW, Ottensmeier CH. Clinical activity and safety of Pembrolizumab in Ipilimumab pre-treated patients with uveal melanoma. *Oncoimmunology* 2016; **5**: e1143997 [PMID: 27467964 DOI: 10.1080/2162402X.2016.1143997]

24 **Kirchberger MC**, Moreira A, Erdmann M, Schuler G, Heinzerling L. Real world experience in low-dose ipilimumab in combination with PD-1 blockade in advanced melanoma patients. *Oncotarget* 2018; **9**: 28903-28909 [PMID: 29988983 DOI: 10.18632/oncotarget.25627]

25 **Heppt MV**, Amaral T, Kähler KC, Heinzerling L, Hassel JC, Meissner M, Kreuzberg N, Loquai C, Reinhardt L, Utikal J, Dabrowski E, Gesierich A, Pföhler C, Terheyden P, Thoms KM, Zimmer L, Eigentler TK, Kirchberger MC, Stege HM, Meier F, Schlaak M, Berking C. Combined immune checkpoint blockade for metastatic uveal melanoma: a retrospective, multi-center study. *J Immunother Cancer* 2019; **7**: 299 [PMID: 31722735 DOI: 10.1186/s40425-019-0800-0]

26 **Johnson DB**, Bao R, Ancell KK, Daniels AB, Wallace D, Sosman JA, Luke JJ. Response to Anti-PD-1 in Uveal Melanoma Without High-Volume Liver Metastasis. *J Natl Compr Canc Netw* 2019; **17**: 114-117 [PMID: 30787124 DOI: 10.6004/jnccn.2018.7070]

27 **Rossi E**, Pagliara MM, Orteschi D, Dosa T, Sammarco MG, Caputo CG, Petrone G, Rindi G, Zollino M, Blasi MA, Cassano A, Bria E, Tortora G, Schinzari G. Pembrolizumab as first-line treatment for metastatic uveal melanoma. *Cancer Immunol Immunother* 2019; **68**: 1179-1185 [PMID: 31175402 DOI: 10.1007/s00262-019-02352-6]

28 **Namikawa K**, Takahashi A, Mori T, Tsutsumida A, Suzuki S, Motoi N, Jinnai S, Kage Y, Mizuta H, Muto Y, Nakano E, Yamazaki N. Nivolumab for patients with metastatic uveal melanoma previously untreated with ipilimumab: a single-institution retrospective study. *Melanoma Res* 2020; **30**: 76-84 [PMID: 31095037 DOI: 10.1097/CMR.0000000000000617]

29 **Piulats JM**, Espinosa E, de la Cruz Merino L, Varela M, Alonso Carrión L, Martín-Algarra S, López Castro R, Curiel T, Rodríguez-Abreu D, Redrado M, Gomà M, Rullán AJ, Calvo González A, Berrocal-Jaime A. Nivolumab Plus Ipilimumab for Treatment-Naïve Metastatic Uveal Melanoma: An Open-Label, Multicenter, Phase II Trial by the Spanish Multidisciplinary Melanoma Group (GEM-1402). *J Clin Oncol* 2021; **39**: 586-598 [PMID: 33417511 DOI: 10.1200/JCO.20.00550]

30 **Salaün H**, de Koning L, Saint-Ghislain M, Servois V, Ramtohul T, Garcia A, Matet A, Cassoux N, Mariani P, Piperno-Neumann S, Rodrigues M. Nivolumab plus ipilimumab in metastatic uveal melanoma: a real-life, retrospective cohort of 47 patients. *Oncoimmunology* 2022; **11**: 2116845 [PMID: 36092639 DOI: 10.1080/2162402X.2022.2116845]

31 **Pham JP**, On L, Ardolino L, Hurwitz J, Salaun H, Sim HW, Joshua AM. Efficacy of immune checkpoint inhibition in metastatic uveal melanoma: a systematic review and meta-analysis. *Melanoma Res* 2023; **33**: 316-325 [PMID: 37199712 DOI: 10.1097/CMR.0000000000000900]

32 **Larkin J**, Chiarion-Sileni V, Gonzalez R, Grob JJ, Rutkowski P, Lao CD, Cowey CL, Schadendorf D, Wagstaff J, Dummer R, Ferrucci PF, Smylie M, Hogg D, Hill A, Márquez-Rodas I, Haanen J, Guidoboni M, Maio M, Schöffski P, Carlino MS, Lebbé C, McArthur G, Ascierto PA, Daniels GA, Long GV, Bastholt L, Rizzo JI, Balogh A, Moshyk A, Hodi FS, Wolchok JD. Five-Year Survival with Combined Nivolumab and Ipilimumab in Advanced Melanoma. *N Engl J Med* 2019; **381**: 1535-1546 [PMID: 31562797 DOI: 10.1056/NEJMoa1910836]

33 **Gong J**, Chehrazi-Raffle A, Reddi S, Salgia R. Development of PD-1 and PD-L1 inhibitors as a form of cancer immunotherapy: a comprehensive review of registration trials and future considerations. *J Immunother Cancer* 2018; **6**: 8 [PMID: 29357948 DOI: 10.1186/s40425-018-0316-z]

34 **Keilholz U**, Mehnert JM, Bauer S, Bourgeois H, Patel MR, Gravenor D, Nemunaitis JJ, Taylor MH, Wyrwicz L, Lee KW, Kasturi V, Chin K, von Heydebreck A, Gulley JL. Avelumab in patients with previously treated metastatic melanoma: phase 1b results from the JAVELIN Solid Tumor trial. *J Immunother Cancer* 2019; **7**: 12 [PMID: 30651126 DOI: 10.1186/s40425-018-0459-y]

35 **Wolchok JD**, Chiarion-Sileni V, Gonzalez R, Rutkowski P, Grob JJ, Cowey CL, Lao CD, Wagstaff J, Schadendorf D, Ferrucci PF, Smylie M, Dummer R, Hill A, Hogg D, Haanen J, Carlino MS, Bechter O, Maio M, Marquez-Rodas I, Guidoboni M, McArthur G, Lebbé C, Ascierto PA, Long GV, Cebon J, Sosman J, Postow MA, Callahan MK, Walker D, Rollin L, Bhore R, Hodi FS, Larkin J. Overall Survival with Combined Nivolumab and Ipilimumab in Advanced Melanoma. *N Engl J Med* 2017; **377**: 1345-1356 [PMID: 28889792 DOI: 10.1056/NEJMoa1709684]

36 **Luke JJ**, Triozzi PL, McKenna KC, Van Meir EG, Gershenwald JE, Bastian BC, Gutkind JS, Bowcock AM, Streicher HZ, Patel PM, Sato T, Sossman JA, Sznol M, Welch J, Thurin M, Selig S, Flaherty KT, Carvajal RD. Biology of advanced uveal melanoma and next steps for clinical therapeutics. *Pigment Cell Melanoma Res* 2015; **28**: 135-147 [PMID: 25113308 DOI: 10.1111/pcmr.12304]

37 **Rothermel LD**, Sabesan AC, Stephens DJ, Chandran SS, Paria BC, Srivastava AK, Somerville R, Wunderlich JR, Lee CC, Xi L, Pham TH, Raffeld M, Jailwala P, Kasoji M, Kammula US. Identification of an Immunogenic Subset of Metastatic Uveal Melanoma. *Clin Cancer Res* 2016; **22**: 2237-2249 [PMID: 26712692 DOI: 10.1158/1078-0432.CCR-15-2294]

38 **Dercle L**, Ammari S, Roblin E, Bigorgne A, Champiat S, Taihi L, Plaian A, Hans S, Lakiss S, Tselikas L, Rouanne M, Deutsch E, Schwartz LH, Gönen M, Flynn J, Massard C, Soria JC, Robert C, Marabelle A. High serum LDH and liver metastases are the dominant predictors of primary cancer resistance to anti-PD(L)1 immunotherapy. *Eur J Cancer* 2022; **177**: 80-93 [PMID: 36332438 DOI: 10.1016/j.ejca.2022.08.034]

39 **Tong TML**, Burgmans MC, Speetjens FM, van Erkel AR, van der Meer RW, van Rijswijk CSP, Jonker-Bos MA, Roozen CFM, Sporrel-Blokland M, Lutjeboer J, van Persijn van Meerten EL, Martini CH, Zoethout RWM, Tijl FGJ, Blank CU, Kapiteijn E. Combining Melphalan Percutaneous Hepatic Perfusion with Ipilimumab Plus Nivolumab in Advanced Uveal Melanoma: First Safety and Efficacy Data from the Phase Ib Part of the Chopin Trial. *Cardiovasc Intervent Radiol* 2023; **46**: 350-359 [PMID: 36624292 DOI: 10.1007/s00270-022-03338-1]

40 **Minor DR**, Kim KB, Tong RT, Wu MC, Kashani-Sabet M, Orloff M, Eschelman DJ, Gonsalves CF, Adamo RD, Anne PR, Luke JJ, Char D, Sato T. A Pilot Study of Hepatic Irradiation with Yttrium-90 Microspheres Followed by Immunotherapy with Ipilimumab and Nivolumab for Metastatic Uveal Melanoma. *Cancer Biother Radiopharm* 2022; **37**: 11-16 [PMID: 35021863 DOI: 10.1089/cbr.2021.0366]

41 **Aedo-Lopez V**, Gérard CL, Boughdad S, Gautron Moura B, Berthod G, Digklia A, Homicsko K, Schaefer N, Duran R, Cuendet MA, Michielin O. Safety and Efficacy of Ipilimumab plus Nivolumab and Sequential Selective Internal Radiation Therapy in Hepatic and Extrahepatic Metastatic Uveal Melanoma. *Cancers (Basel)* 2022; **14** [PMID: 35267470 DOI: 10.3390/cancers14051162]

42 **Karivedu V**, Eldessouki I, Taftaf A, Zhu Z, Makramalla A, Karim NA. Nivolumab and Ipilimumab in the Treatment of Metastatic Uveal Melanoma: A Single-Center Experience. *Case Rep Oncol Med* 2019; **2019**: 3560640 [PMID: 31179139 DOI: 10.1155/2019/3560640]

43 **Rozeman EA**, Prevoo W, Meier MAJ, Sikorska K, Van TM, van de Wiel BA, van der Wal JE, Mallo HA, Grijpink-Ongering LG, Broeks A, Lalezari F, Reeves J, Warren S, van Thienen JV, van Tinteren H, Haanen JBAG, Kapiteijn E, Blank CU. Phase Ib/II trial testing combined radiofrequency ablation and ipilimumab in uveal melanoma (SECIRA-UM). *Melanoma Res* 2020; **30**: 252-260 [PMID: 31895753 DOI: 10.1097/CMR.0000000000000653]

44 **Lutzky J**, Sullivan RJ, Cohen JV, Ren Y, Li A, Haq R. Phase 1b study of intravenous coxsackievirus A21 (V937) and ipilimumab for patients with metastatic uveal melanoma. *J Cancer Res Clin Oncol* 2023; **149**: 6059-6066 [PMID: 36651961 DOI: 10.1007/s00432-022-04510-3]

45 **Ny L**, Jespersen H, Karlsson J, Alsén S, Filges S, All-Eriksson C, Andersson B, Carneiro A, Helgadottir H, Levin M, Ljuslinder I, Olofsson Bagge R, Sah VR, Stierner U, Ståhlberg A, Ullenhag G, Nilsson LM, Nilsson JA. The PEMDAC phase 2 study of pembrolizumab and entinostat in patients with metastatic uveal melanoma. *Nat Commun* 2021; **12**: 5155 [PMID: 34453044 DOI: 10.1038/s41467-021-25332-w]

46 **Kraehenbuehl L**, Holland A, Armstrong E, O'Shea S, Mangarin L, Chekalil S, Johnston A, Bomalaski JS, Erinjeri JP, Barker CA, Francis JH, Wolchok JD, Merghoub T, Shoushtari AN. Pilot Trial of Arginine Deprivation Plus Nivolumab and Ipilimumab in Patients with Metastatic Uveal Melanoma. *Cancers (Basel)* 2022; **14** [PMID: 35681616 DOI: 10.3390/cancers14112638]

47 **Tawbi HA**, Schadendorf D, Lipson EJ, Ascierto PA, Matamala L, Castillo Gutiérrez E, Rutkowski P, Gogas HJ, Lao CD, De Menezes JJ, Dalle S, Arance A, Grob JJ, Srivastava S, Abaskharoun M, Hamilton M, Keidel S, Simonsen KL, Sobiesk AM, Li B, Hodi FS, Long GV; RELATIVITY-047 Investigators. Relatlimab and Nivolumab versus Nivolumab in Untreated Advanced Melanoma. *N Engl J Med* 2022; **386**: 24-34 [PMID: 34986285 DOI: 10.1056/NEJMoa2109970]

48 **Lamas NJ**, Lassalle S, Martel A, Nahon-Estève S, Macocco A, Zahaf K, Lalvee S, Fayada J, Lespinet-Fabre V, Bordone O, Pedeutour F, Baillif S, Hofman P. Characterisation of the protein expression of the emerging immunotherapy targets VISTA, LAG-3 and PRAME in primary uveal melanoma: insights from a southern French patient cohort. *Pathology* 2023; **55**: 929-944 [PMID: 37863710 DOI: 10.1016/j.pathol.2023.08.003]

49 **Khan SA**, Almalki WH, Arora S, Kesharwani P. Recent approaches for the treatment of uveal melanoma: Opportunities and challenges. *Crit Rev Oncol Hematol* 2023; **193**: 104218 [PMID: 38040071 DOI: 10.1016/j.critrevonc.2023.104218]

50 **Leyvraz S**, Piperno-Neumann S, Suciu S, Baurain JF, Zdzienicki M, Testori A, Marshall E, Scheulen M, Jouary T, Negrier S, Vermorken JB, Kaempgen E, Durando X, Schadendorf D, Gurunath RK, Keilholz U. Hepatic intra-arterial versus intravenous fotemustine in patients with liver metastases from uveal melanoma (EORTC 18021): a multicentric randomized trial. *Ann Oncol* 2014; **25**: 742-746 [PMID: 24510314 DOI: 10.1093/annonc/mdt585]

51 **Carvajal RD**, Schwartz GK, Tezel T, Marr B, Francis JH, Nathan PD. Metastatic disease from uveal melanoma: treatment options and future prospects. *Br J Ophthalmol* 2017; **101**: 38-44 [PMID: 27574175 DOI: 10.1136/bjophthalmol-2016-309034]

52 **Carvajal RD**, Sosman JA, Quevedo JF, Milhem MM, Joshua AM, Kudchadkar RR, Linette GP, Gajewski TF, Lutzky J, Lawson DH, Lao CD, Flynn PJ, Albertini MR, Sato T, Lewis K, Doyle A, Ancell K, Panageas KS, Bluth M, Hedvat C, Erinjeri J, Ambrosini G, Marr B, Abramson DH, Dickson MA, Wolchok JD, Chapman PB, Schwartz GK. Effect of selumetinib vs chemotherapy on progression-free survival in uveal melanoma: a randomized clinical trial. *JAMA* 2014; **311**: 2397-2405 [PMID: 24938562 DOI: 10.1001/jama.2014.6096]

53 **Carvajal RD**, Piperno-Neumann S, Kapiteijn E, Chapman PB, Frank S, Joshua AM, Piulats JM, Wolter P, Cocquyt V, Chmielowski B, Evans TRJ, Gastaud L, Linette G, Berking C, Schachter J, Rodrigues MJ, Shoushtari AN, Clemett D, Ghiorghiu D, Mariani G, Spratt S, Lovick S, Barker P, Kilgour E, Lai Z, Schwartz GK, Nathan P. Selumetinib in Combination With Dacarbazine in Patients With Metastatic Uveal Melanoma: A Phase III, Multicenter, Randomized Trial (SUMIT). *J Clin Oncol* 2018; **36**: 1232-1239 [PMID: 29528792 DOI: 10.1200/JCO.2017.74.1090]

54 **Zimmer L**, Vaubel J, Mohr P, Hauschild A, Utikal J, Simon J, Garbe C, Herbst R, Enk A, Kämpgen E, Livingstone E, Bluhm L, Rompel R, Griewank KG, Fluck M, Schilling B, Schadendorf D. Phase II DeCOG-study of ipilimumab in pretreated and treatment-naïve patients with metastatic uveal melanoma. *PLoS One* 2015; **10**: e0118564 [PMID: 25761109 DOI: 10.1371/journal.pone.0118564]

55 **Petzold A**, Steeb T, Wessely A, Koch EAT, Vera J, Berking C, Heppt MV. Is tebentafusp superior to combined immune checkpoint blockade and other systemic treatments in metastatic uveal melanoma? A comparative efficacy analysis with population adjustment. *Cancer Treat Rev* 2023; **115**: 102543 [PMID: 36931146 DOI: 10.1016/j.ctrv.2023.102543]

56 **Seth R**, Agarwala SS, Messersmith H, Alluri KC, Ascierto PA, Atkins MB, Bollin K, Chacon M, Davis N, Faries MB, Funchain P, Gold JS, Guild S, Gyorki DE, Kaur V, Khushalani NI, Kirkwood JM, McQuade JL, Meyers MO, Provenzano A, Robert C, Santinami M, Sehdev A, Sondak VK, Spurrier G, Swami U, Truong TG, Tsai KK, van Akkooi A, Weber J. Systemic Therapy for Melanoma: ASCO Guideline Update. *J Clin Oncol* 2023; **41**: 4794-4820 [PMID: 37579248 DOI: 10.1200/JCO.23.01136]

57 **Lowe KL**, Cole D, Kenefeck R, OKelly I, Lepore M, Jakobsen BK. Novel TCR-based biologics: mobilising T cells to warm 'cold' tumours.

Cancer Treat Rev 2019; **77**: 35-43 [PMID: 31207478 DOI: 10.1016/j.ctrv.2019.06.001]

58 **Boudousquie C**, Bossi G, Hurst JM, Rygiel KA, Jakobsen BK, Hassan NJ. Polyfunctional response by ImmTAC (IMCgp100) redirected CD8(+) and CD4(+) T cells. *Immunology* 2017; **152**: 425-438 [PMID: 28640942 DOI: 10.1111/imm.12779]

59 **Middleton MR**, McAlpine C, Woodcock VK, Corrie P, Infante JR, Steven NM, Evans TRJ, Anthoney A, Shoushtari AN, Hamid O, Gupta A, Vardeu A, Leach E, Naidoo R, Stanhope S, Lewis S, Hurst J, O'Kelly I, Sznol M. Tebentafusp, A TCR/Anti-CD3 Bispecific Fusion Protein Targeting gp100, Potently Activated Antitumor Immune Responses in Patients with Metastatic Melanoma. *Clin Cancer Res* 2020; **26**: 5869-5878 [PMID: 32816891 DOI: 10.1158/1078-0432.CCR-20-1247]

60 **Harper J**, Adams KJ, Bossi G, Wright DE, Stacey AR, Bedke N, Martinez-Hague R, Blat D, Humbert L, Buchanan H, Le Provost GS, Donnellan Z, Carreira RJ, Paston SJ, Weigand LU, Canestraro M, Sanderson JP, Botta Gordon-Smith S, Lowe KL, Rygiel KA, Powlesland AS, Vuidepot A, Hassan NJ, Cameron BJ, Jakobsen BK, Dukes J. An approved in vitro approach to preclinical safety and efficacy evaluation of engineered T cell receptor anti-CD3 bispecific (ImmTAC) molecules. *PLoS One* 2018; **13**: e0205491 [PMID: 30321203 DOI: 10.1371/journal.pone.0205491]

61 **Chen LN**, Carvajal RD. Tebentafusp for the treatment of HLA-A*02:01-positive adult patients with unresectable or metastatic uveal melanoma. *Expert Rev Anticancer Ther* 2022; **22**: 1017-1027 [PMID: 36102132 DOI: 10.1080/14737140.2022.2124971]

62 **Carvajal RD**, Butler MO, Shoushtari AN, Hassel JC, Ikeguchi A, Hernandez-Aya L, Nathan P, Hamid O, Piulats JM, Rioth M, Johnson DB, Luke JJ, Espinosa E, Leyvraz S, Collins L, Goodall HM, Ranade K, Holland C, Abdullah SE, Sacco JJ, Sato T. Clinical and molecular response to tebentafusp in previously treated patients with metastatic uveal melanoma: a phase 2 trial. *Nat Med* 2022; **28**: 2364-2373 [PMID: 36229663 DOI: 10.1038/s41591-022-02015-7]

World Journal of Clinical Oncology

Submit a Manuscript: https://www.f6publishing.com

World J Clin Oncol 2024 January 24; 15(1): 32-44

DOI: 10.5306/wjco.v15.i1.32

ISSN 2218-4333 (online)

ORIGINAL ARTICLE

Clinical and Translational Research

Scinderin promotes glioma cell migration and invasion *via* remodeling actin cytoskeleton

Xin Lin, Zhao Zhao, Shu-Peng Sun, Wei Liu

Specialty type: Clinical neurology

Provenance and peer review: Unsolicited article; Externally peer reviewed.

Peer-review model: Single blind

Peer-review report's scientific quality classification

Grade A (Excellent): 0
Grade B (Very good): B
Grade C (Good): C
Grade D (Fair): 0
Grade E (Poor): 0

P-Reviewer: El-Shishtawy MM, Egypt; Ma Z, United States

Received: September 8, 2023
Peer-review started: September 8, 2023
First decision: October 17, 2023
Revised: November 20, 2023
Accepted: December 19, 2023
Article in press: December 19, 2023
Published online: January 24, 2024

Xin Lin, Zhao Zhao, Shu-Peng Sun, Wei Liu, Department of Neurosurgery, Tianjin Huanhu Hospital, Tianjin 300000, China

Corresponding author: Xin Lin, PhD, Associate Chief Physician, Department of Neurosurgery, Tianjin Huanhu Hospital, No. 6 Jizhao Road, Jinnan District, Tianjin 300000, China.
xnln69@aliyun.com

Abstract

BACKGROUND

Glioma is one of the most common intracranial tumors, characterized by invasive growth and poor prognosis. Actin cytoskeletal rearrangement is an essential event of tumor cell migration. The actin dynamics-related protein scinderin (SCIN) has been reported to be closely related to tumor cell migration and invasion in several cancers.

AIM

To investigate the role and mechanism of SCIN in glioma.

METHODS

The expression and clinical significance of SCIN in glioma were analyzed based on public databases. SCIN expression was examined using real-time quantitative polymerase chain reaction and Western blotting. Gene silencing was performed using short hairpin RNA transfection. Cell viability, migration, and invasion were assessed using cell counting kit 8 assay, wound healing, and Matrigel invasion assays, respectively. F-actin cytoskeleton organization was assessed using F-actin staining.

RESULTS

SCIN expression was significantly elevated in glioma, and high levels of SCIN were associated with advanced tumor grade and wild-type isocitrate dehydrogenase. Furthermore, SCIN-deficient cells exhibited decreased proliferation, migration, and invasion in U87 and U251 cells. Moreover, knockdown of SCIN inhibited the RhoA/focal adhesion kinase (FAK) signaling to promote F-actin depolymerization in U87 and U251 cells.

CONCLUSION

SCIN modulates the actin cytoskeleton *via* activating RhoA/FAK signaling, thereby promoting the migration and invasion of glioma cells. This study

identified the cancer-promoting effect of SCIN and provided a potential therapeutic target for the treatment of glioma.

Key Words: Glioma; Scinderin; Actin cytoskeleton; RhoA/FAK signaling; Depolymerization

Core Tip: Actin dynamics-related protein scinderin (SCIN) was found to be significantly upregulated in glioma, and high SCIN expression was associated with advanced tumor grade and wild-type isocitrate dehydrogenase. Furthermore, silenced-SCIN cells exhibited decreased proliferation, migration, and invasion. Besides, knockdown of SCIN inhibited RhoA/focal adhesion kinase signaling to promote F-actin depolymerization in glioma cells.

Citation: Lin X, Zhao Z, Sun SP, Liu W. Scinderin promotes glioma cell migration and invasion *via* remodeling actin cytoskeleton. *World J Clin Oncol* 2024; 15(1): 32-44
URL: https://www.wjgnet.com/2218-4333/full/v15/i1/32.htm
DOI: https://dx.doi.org/10.5306/wjco.v15.i1.32

INTRODUCTION

Glioma is the most frequent and deadly tumor of the central nervous system, accounting for about 40%-60% of human intracranial tumors[1]. Based on the histologic types and malignancy grades, gliomas are classified into low-grade gliomas (LGGs) [World Health Organization (WHO) grade I-II] and high-grade gliomas (WHO III-IV grade)[2]. Low-grade gliomas are well-differentiated, while high-grade gliomas are poorly differentiated. The incidence rate of glioma in China ranged from 3 to 6 per 100000 people, most of which are grade III (anaplastic glioma) and IV gliomas [glioblastoma multiforme (GBM)]. Despite remarkable advances in microsurgery, radiotherapy, chemotherapy, and biotherapy, the prognosis of glioma patients remains unsatisfactory. Thus, exploring the molecular mechanism of glioma progression is of great significance for developing new prognostic indicators and therapeutic targets.

Actin dynamics-related protein scinderin (SCIN) (also known as adseverin) belongs to the gelsolin superfamily and is an important actin-severing protein[3]. SCIN regulates the reorganization of F-actin and participates in cell polarity, cell secretion, cell differentiation, and cell motility[4-6]. SCIN has been demonstrated to play diverse roles in chronic inflammation, coagulation processes, immune diseases, and tumors. The role of SCIN in tumors was first reported by Zunino in 2001[7]. They found that SCIN induced cell differentiation, maturation, and apoptosis by releasing platelet-like granules, and inhibited tumor cell formation and proliferation in megakaryoblastic leukemia. Since then, a growing body of studies have uncovered the biological roles of SCIN in various kinds of cancers[8-10]. For instance, in the cytotoxic lymphocyte-resistant mutants of non-small cell lung cancer, upregulated SCIN reduces the killing effect of cytotoxic T lymphocytes on tumor cells[11]. In a study of bladder cancer, SCIN was found to bind to mitochondrial voltage-dependent anion channel (VDAC) oligomers, thereby preventing VADC-induced mitochondrial apoptosis pathways. Besides, SCIN promotes the proliferation and metastasis of bladder, stomach, lung, and prostate cancers[12,13]. However, the biological role and molecular mechanism of SCIN in glioma remain unclear.

In this study, we analyzed the expression and clinical significance of SCIN in glioma based on public databases. Then, we utilized SCIN-specific short hairpin RNAs (shRNAs) to knock down SCIN expression in glioma cell lines and observed the effects of SCIN silencing on the proliferative, migrative, and invasive abilities of glioma cells. Furthermore, the effect of SCIN silencing on the cytoskeleton of glioma cells was also investigated. These experimental results will help us to further explore the mechanism of SCIN in glioma and lay a solid experimental foundation for glioma treatment.

MATERIALS AND METHODS

Data collection

Based on the Gene Expression Profiling Interactive Analysis (GEPIA) database (http://gepia.cancer-pku.cn/), we analyzed the difference in SCIN mRNA expression between 163 GBM samples or 518 LGG samples and 207 normal brain tissue samples and analyzed the relationship between SCIN expression and overall survival of glioma patients[14]. Based on the Chinese Glioma Genome Atlas (CGGA) database (http://www.cgga.org.cn/), we further analyzed the relationship between SCIN expression and the clinical features of gliomas[15]. RNA sequencing data of 325 patients including 203 males and 122 females based on the CGGA database were analyzed. According to pathological features, these patients included 4 normal, 103 WHO grade II, 79 WHO grade III, and 139 WHO grade IV gliomas. In total, 53.85 % of patients (n = 175) had IDH mutations and 45.85% (n = 149) had IDH wildtype. Only 20.62% of patients (n = 67) showed a 1p19q co-deletion, whereas 76.92% (n = 250) did not have this genotype.

Cell culture
U87 MG and U251 cell lines were provided by Procell (Wuhan, China). U87 MG cells were cultured in Minimum Essential Medium. U251 cells were cultured in Dulbecco's modified Eagle medium. All culture medium was supplemented with 10% fetal bovine serum and 1% penicillin/streptomycin. Cells were maintained in an incubator containing 5% CO_2 at 37 °C.

Cell transfection
shRNAs targeting SCIN (sh-SCIN) were obtained from Shanghai Gene Pharmaceutical Co., LTD. (Shanghai, China). RNA double-stranded random sequences were used as the negative control for shRNA (sh-NC). Lipofectamine® 2000 (ThermoFisher Scientific, Waltham, MA, United States) was used to transfect these plasmids into U87 MG and U251 cells at a concentration of 50 nM. The transfected cells were screened with puromycin. The clones were then selected and cultured for further experiments.

Western blot
Cells were lysed by RIPA buffer (Solarbio, Beijing, China). The protein concentration was determined by the BCA Protein Assay Kit (Solarbio). Protein samples (20 μg) were loaded into 10% sodium dodecyl sulfate-polyacrylamide gel electrophoresis (SDS-PAGE) gel and electrophoresis was performed at 100 V for 1-2 h. Then, the protein was transferred from the gel to the polyvinylidene fluoride membrane (Whatman, Maidstone, United Kingdom). After sealing the membrane with sealing buffer for 1 h, the membranes were incubated with primary antibody at 4 °C overnight. The membranes were then incubated with HRP-IgG antibody (1: 5000; Proteintech, Wuhan, China). Image J software was used to analyze the data. Anti-SCIN, anti-RhoA, and anti-GAPDH antibodies were obtained from Proteintech. Focal adhesion kinase (FAK), phospho-FAK, phospho-Cofilin (Ser3), Cofilin, and Talin antibodies were obtained from Cell Signaling Technology (Boston, MA, United States).

Quantitative real-time polymerase chain reaction
TRIzol reagent (ThermoFisher) was used to isolate total RNAs from cells. The purity of total RNAs was detected by agarose gel electrophoresis. The cDNA was synthesized using SuperScript® III Reverse Transcriptase (ThermoFisher). Polymerase chain reaction (PCR) amplification kit (ThermoFisher) was used for PCR amplification. SCIN primers were provided by Sangon Biotech (Shanghai, China), with sequences (forward primer, 5′-ACTGAGTGGCAGTTGCATTAT-3′, reverse primer, 5′-TGTGGGATGAATTGTTGGACCC-3′).

Cell Counting Kit-8 assay
Cell proliferation was measured using Cell Counting Kit-8 Cell Proliferation and Cytotoxicity Assay Kit (Solarbio).

Colony formation assay
Cells were seeded into Petri dishes at 1 × 10^3 cells per well. After incubation at 37 °C and 5% CO_2, the cells were saturated with humidity for 14 d. Cells were rinsed twice with phosphate buffered saline buffer. Cells were incubated with paraformaldehyde for 30 min, and stained with the crystal violet solution for 30 min. Finally, the clones were counted under a microscope.

Wound-healing assay
The wound-healing experiment was carried out for migration ability. Glioma cells were plated on 6-well plates. Pipettes (200 μL) were used to draw a straight wound. After incubation in a serum-free medium for 24 h or 48 h, cell images were taken under a microscope.

Transwell invasion assay
Transwell chambers were precoated with Matrigel (Corning Costar, Cambridge, MA, United States). Transfected (1 × 10^3) cells in 100 μL serum-free medium were added to the upper Transwell chamber. The lower chamber was added with medium of 10% fetal bovine serum. After incubation for 6 h, the invading cells that adhered to the lower surface of the membrane were fixed and stained. Finally, the number of invading cells was counted under an inverted microscope (Olympus, Tokyo, Japan).

F-actin labeling
F-actin staining was performed using an F-actin Staining Kit (Phalloidin-Green; AmyJet Scientific, Wuhan, China). Cells were first inoculated on 96-well cover slides and grown to 70% confluence. Next, the cells were fixed with precooled 4% paraformaldehyde on ice for 20 min and permeabilized with 0.1% Triton X-100 for 10 min at room temperature. Then, after cells were incubated with 100 μL staining solution for 30 min, a 4′,6-diamidino-2-phenylindole solution (100 mL) was applied to stain the nuclei. The immediate observation was carried out under a fluorescence microscope (200 cells counted per field): excitation wavelength 488 nm, emission wavelength 530 nm (F-actin staining) or 350 nm excitation wavelength, 460 nm emission wavelength (nuclear staining).

Statistical analysis
SPSS 22.0 (IBM Corp., Armonk, NY, United States) was applied for statistical analysis. Data were expressed as mean ± SD. Two-tailed Student *t*-test and one-way analysis of variance (ANOVA) were used to analyze the statistical difference. Each

experiment was replicated at least three times independently. $P < 0.05$ was considered to be statistically significant.

RESULTS

SCIN is highly expressed in glioma

Based on the GEPIA database, we found that the SCIN abundance was remarkably higher in both LGG and GBM than that of normal tissues (Figure 1A). Consistently, the Clinical Proteomic Tumor Analysis Consortium data showed higher SCIN protein levels in primary GBM tissues than in normal tissues (Figure 1B). Furthermore, analysis results of the overall survival curve showed that high levels of SCIN predicted poor prognosis of LGG patients (Figure 1C). However, SCIN expression was not associated with the prognosis of patients with GBM (Figure 1D).

Relationship between SCIN expression and clinical features of glioma

Then, we analyzed SCIN expression in gliomas with different characteristics based on the CGGA dataset. As displayed in Figure 2A, SCIN expression was higher in various types of gliomas than in normal tissues. Moreover, the expression of SCIN increased with advanced tumor grades (Figure 2B). Furthermore, a significant decrease in SCIN expression was observed in gliomas with IDH mutation and 1p/19q co-deletion (Figures 2C and D). Furthermore, we examined the expression of SCIN in glioma by qRT-PCR and Immunohistochemical staining. As shown in Figure 2E, the expression levels of SCIN mRNA were positively correlated with the tumor grades of glioma, and the highest expression was found in grade IV glioma. In line with these results, Immunohistochemical staining showed strong staining of SCIN in grade IV glioma tissues, whereas low and moderate staining was observed in grade I-III gliomas (Figure 2F).

Silenced SCIN inhibits malignant behaviors of glioma cells

We constructed three shRNAs targeting SCIN and found that sh-SCIN#3 showed the strongest inhibitory effect on SCIN expression in both U87 and U251 cells (Supplementary Figure 1A and B). Furthermore, cell viability was most significantly inhibited by sh-SCIN#3, compared to the other two shRNAs (Supplementary Figure 1C). Thus, sh-SCIN#3 was used in the further experiments. CCK8 assay indicated that cell proliferation was decreased after silencing endogenous SCIN (Figure 3A), which was also confirmed by colony formation assay in U87 and U251 cells (Figure 3B). Moreover, the wound-healing assay showed that the SCIN-deficient cells migrated into the scratching area at a significantly slower rate than those in the sh-NC groups (Figure 3C). Besides, the knockdown of SCIN could inhibit cell invasive ability (Figure 3D). Therefore, these results suggested that SCIN had a promoting effect on migration and invasion in glioma cells.

Knockdown of SCIN promotes F-actin depolymerization and inhibits RhoA/FAK signaling in glioma cells

SCIN is an actin severing and capping protein and controls actin organization. Therefore, we investigated the effect of SCIN on F-actin polymerization in glioma cells. Immunofluorescence with F-actin staining indicated the actin stress fibers were clustered and arranged in the negative control cells, while the SCIN-deficient cells showed significant morphological changes, showing sparse disorder of actin stress fibers and less dendrite-like structures (Figure 4A), suggesting that the mobility activity of the cells was weakened. Consistently, western blot results demonstrated that knockdown of SCIN suppressed RhoA, Talin, and phosphorylated cofilin and FAK levels in U87 and U251 cells (Figure 4B), indicating that silenced SCIN inhibited the activation of RhoA/FAK signaling pathway. Notably, the RhoA/FAK pathway is a well-known F-actin polymerization-related signaling pathway, and its inactivation indicated the weakness of F-actin polymerization[16]. This phenomenon indicates that SCIN regulates F-actin polymerization *via* RhoA/FAK signaling.

Inhibition of RhoA/FAK signaling reverses SCIN-mediated malignant behaviors in glioma cells

To shed light on the role of RhoA/FAK signaling in SCIN-mediated glioma cell migration and invasion, a selective FAK inhibitor, PF-573228, and a RhoA inhibitor, CCG1423, were used in SCIN-overexpressed U87 and U251 cells. The wound healing assays demonstrated that SCIN overexpression promoted the motility of the cells, which was inhibited after treatment with PF-573228 or CCG1423 (Figure 5A). The Transwell assays revealed that either PF-573228 or CCG1423 treatment reversed the excessive cell invasion induced by SCIN overexpression (Figure 5B). These data indicated that SCIN promotes malignant behaviors in glioma cells *via* RhoA/FAK signaling pathway.

DISCUSSION

Glioma is one of the most common brain tumors with rapid progression and dismal prognosis. The occurrence and development of glioma is a complex process involving multiple factors, levels, and genes. In current study, we found that SCIN expression was upregulated in glioma tissues and that high levels of SCIN were associated with high tumor grade and poor prognosis. The depletion of SCIN inhibited the proliferation, invasion, and migration of glioma cells. Mechanistically, SCIN affected cytoskeleton remodeling and inhibited the formation of lamellipodia *via* RhoA/FAK signaling pathway. This study identifies the cancer-promoting role of SCIN and provides a potential therapeutic target of SCIN for glioma treatment.

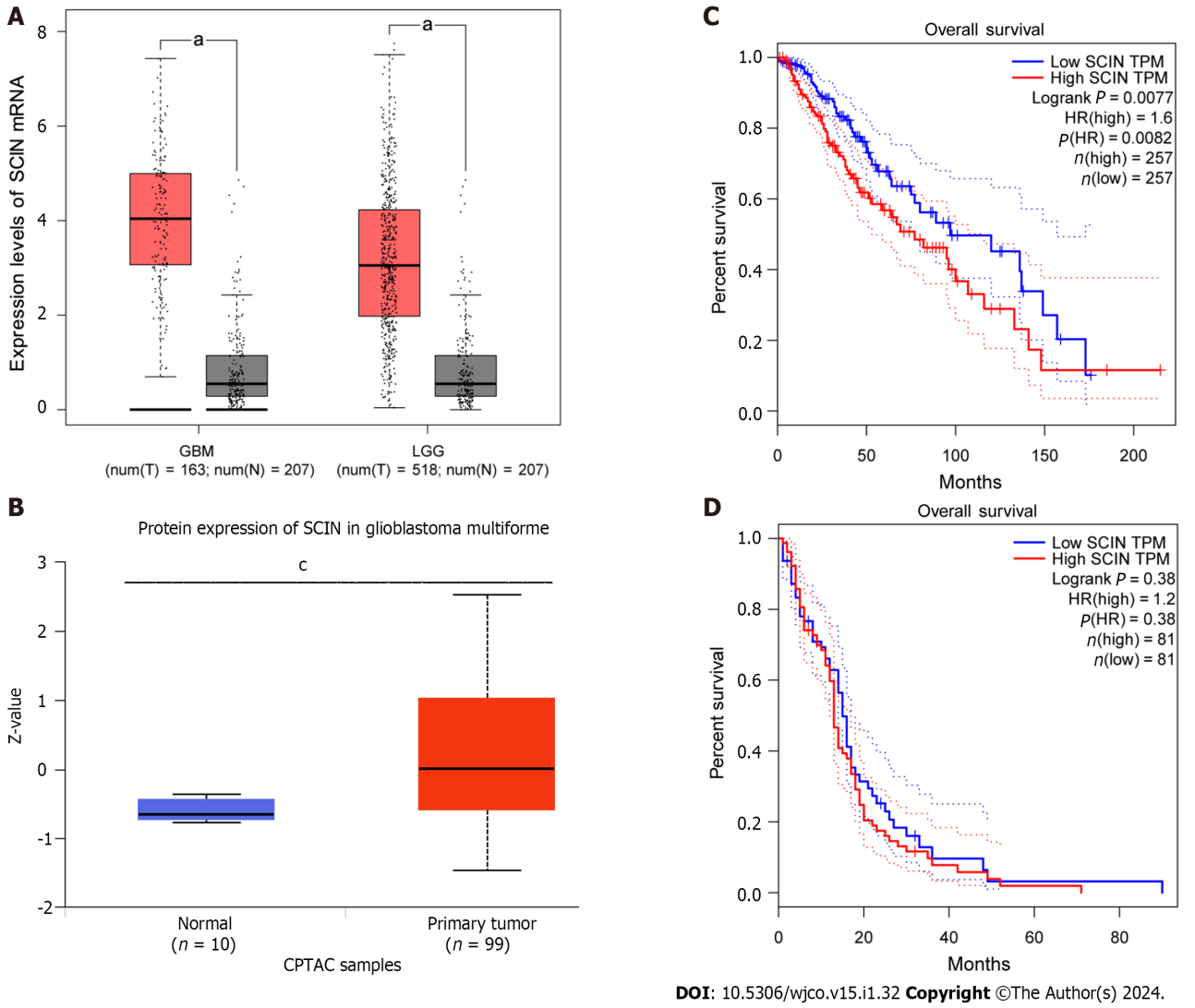

DOI: 10.5306/wjco.v15.i1.32

Figure 1 Scinderin expression is upregulated in gliomas and associated with the prognosis of patients with lower-grade glioma. A: mRNA expression of scinderin (SCIN) in lower-grade glioma (LGG), glioblastoma multiforme (GBM), and corresponding normal tissues, was demonstrated by the Gene Expression Profiling Interactive Analysis database. [a]*P* < 0.05; B: Protein expression of SCIN in GBM and normal tissues was revealed by the UALCAN database. [c]*P* < 0.001; C: Relationship between SCIN mRNA expression and overall survival of LGG patients; D: Relationship between SCIN mRNA expression and overall survival of GBM patients.

Numerous studies revealed aberrant expression of SCIN in several human cancers[17]. It was reported that SCIN was upregulated in gastric cancer tissues and increased SCIN expression was related to metastasis and poor overall survival [18]. Overexpression of SCIN was an independent predictor of poor prognosis in colorectal cancer patients[8]. Consistent with these findings, we found that the expression of SCIN was upregulated in LGG and GBM, and the overexpression of SCIN correlated with a poor prognosis in LGG patients. Further analysis of data from the CGGA database showed that higher levels of SCIN correlated with advanced tumor grade, while lower levels of SCIN were associated with IDH mutation and 1p/19q co-deletion in glioma. Currently, IDH mutation and 1p/19q co-deletion are considered to be good prognostic factors for patients with glioma[19]. Thus, these results support that SCIN is a potential prognostic biomarker for glioma.

Further, SCIN has been reported to participate in a variety of cellular biological processes in human cancer cells. Some studies have shown that SCIN promotes proliferation, inhibits apoptosis, and regulates the cell cycle in several cancers, including prostate, breast, lung, and hepatocellular cancers[10,20,21]. For example, SCIN is identified as a functional apoptosis regulator in hepatocellular carcinoma (HCC). Overexpression of SCIN inhibited apoptotic death and promoted xenografted HCC cell growth, while SCIN knockdown enhanced the chemosensitivity of HCC cells and suppressed tumor growth *in vivo*[22]. Other studies revealed the positive role of SCIN in cell migration, invasion, and metastasis[18,23]. Herein, CCK8 and colony-forming assays were used to verify that SCIN silencing suppressed cell proliferative ability in glioma cells. Meanwhile, wound healing and Transwell invasion assays revealed that SCIN silencing repressed cell migratory and invasive capabilities of glioma cells. These findings were consistent with previous reports, confirming the carcinogenic activity of SCIN in glioma cells.

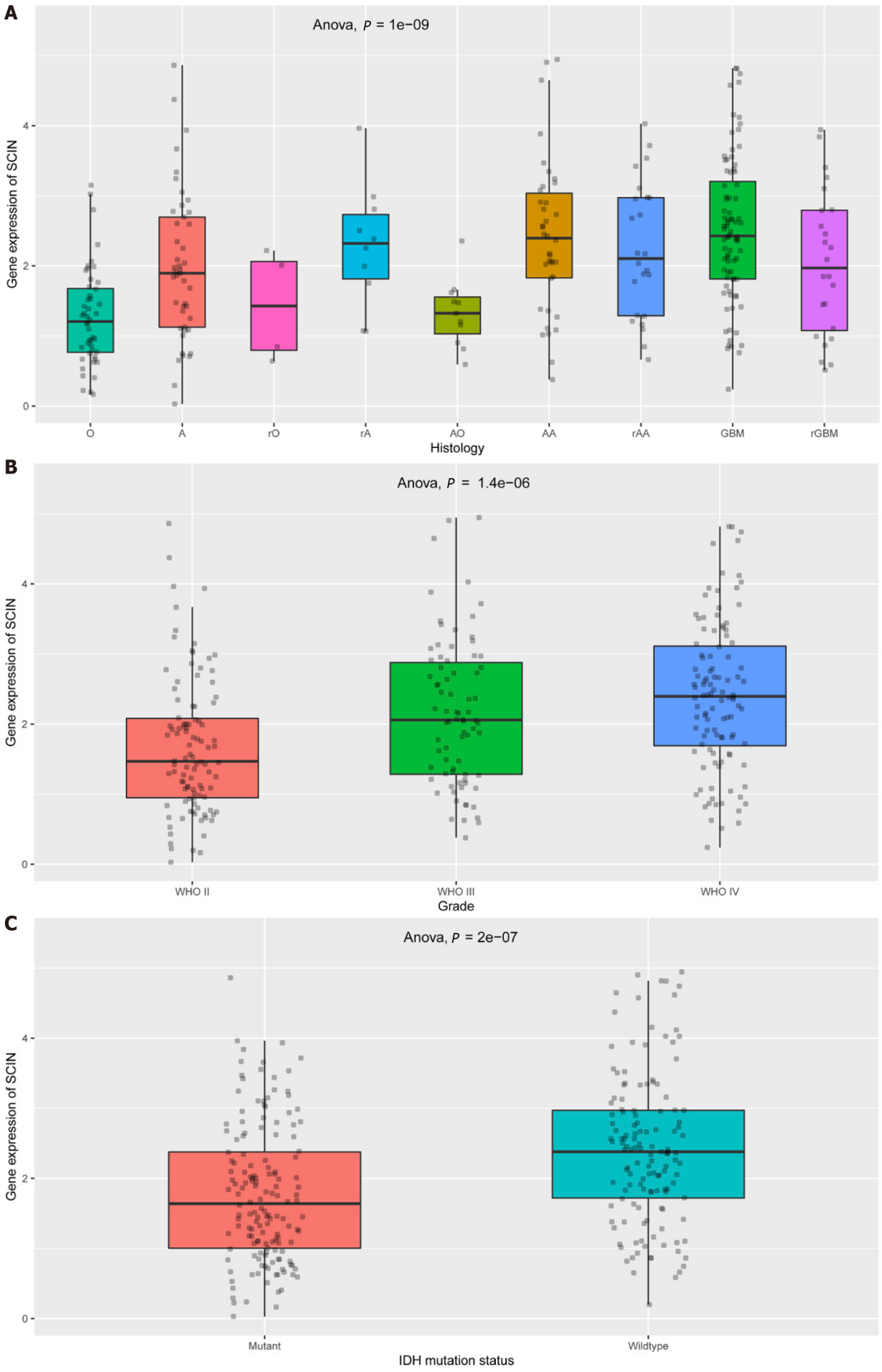
A
Anova, P = 1e−09
Gene expression of SCIN
0
2
4
O
A
rO
rA
AO
AA
rAA
GBM
rGBM
Histology
B
Anova, P = 1.4e−06
Gene expression of SCIN
0
2
4
WHO II
WHO III
WHO IV
Grade
C
Anova, P = 2e−07
Gene expression of SCIN
0
2
4
Mutant
Wildtype
IDH mutation status

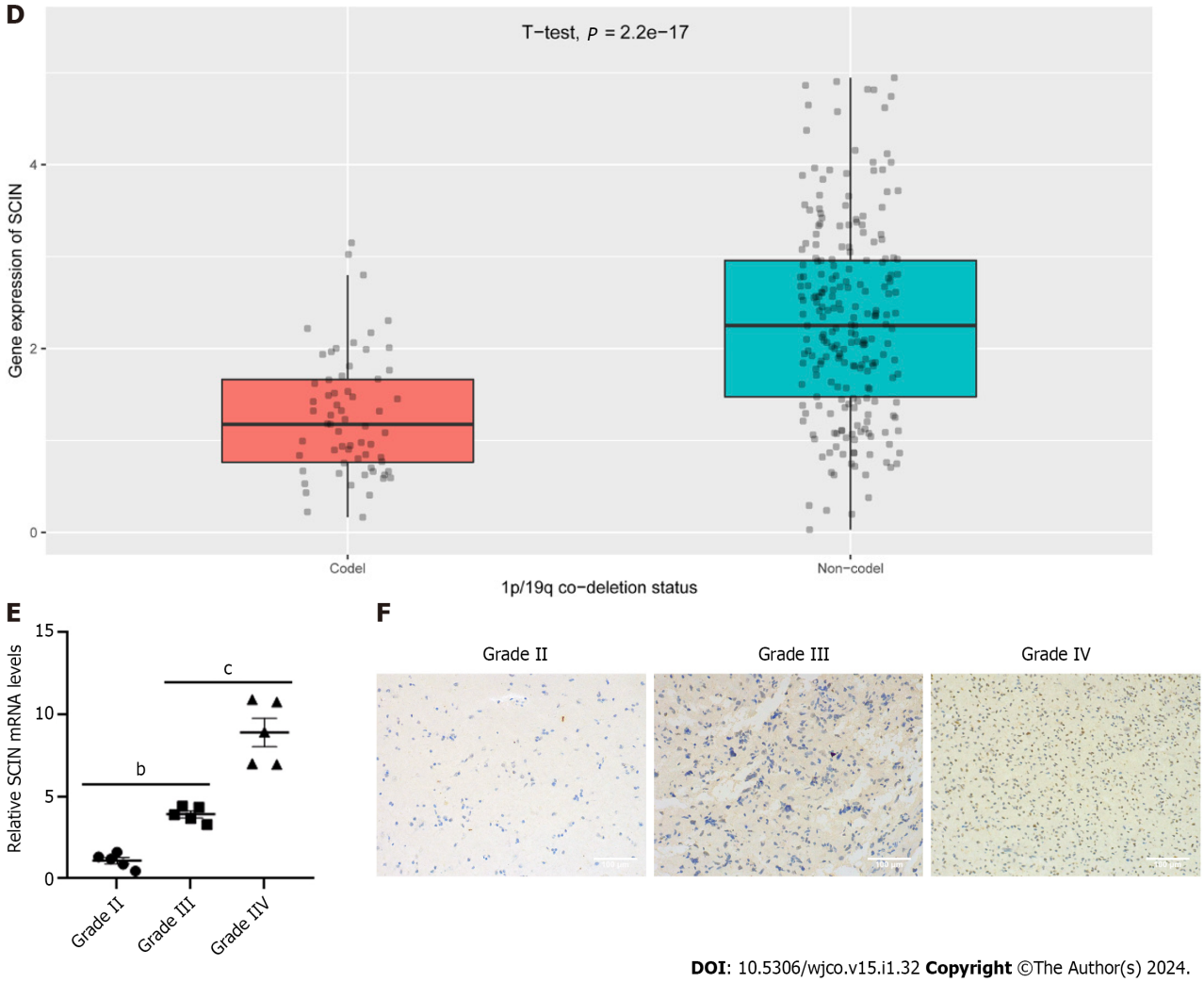

DOI: 10.5306/wjco.v15.i1.32

Figure 2 Relationship between scinderin mRNA expression and clinical features of glioma. A: Expression of scinderin (SCIN) in various types of gliomas; B: Expression of SCIN in World Health Organization II-IV gliomas; C: Expression of SCIN was reduced in gliomas with IDH mutation; D: Expression of SCIN was reduced in gliomas with 1p/19q co-deletion; E: Quantitative real-time polymerase chain reaction analysis of the transcriptional levels of SCIN in clinical tissues of Grade II-IV gliomas. $^{b}P < 0.01$, $^{c}P < 0.001$; F: Representative images of the SCIN protein expression in clinical tissues of Grade II-IV gliomas by immunohistochemical staining. Scale bar: 100 μm.

Cytoskeleton constituents, including F-actin, maintain epithelial integrity and their disruption is a major cause of cancer progression[24]. SCIN, as an important regulator of F-actin organization, regulates actin filament dynamics[6]. Previous studies showed that the dysfunction of SCIN promoted cytoskeleton remodeling, resulting in changes in cellular behaviors. High levels of SCIN were observed in gastric cancer and silenced SCIN suppressed metastasis of gastric cancer cells, and decreased filopodium formation[18]. SCIN is involved in subcortical actin remodeling and promotes the formation of cell extensions and collagen degradation in MCF7 cells, thereby affecting matrix invasion and metastasis [25]. In this study, aggregated and arranged actin stress fibers were observed in the glioma cells, while the knockdown of SCIN caused the formation of sparse and disordered actin stress fibers. Accordingly, we suggest that SCIN may play a key role in F-actin polymerization. The reduction of actin stress fibers indicates that cell migration is inhibited, which explains the phenomenon of inhibited cell migration caused by SCIN loss at the subcellular levels.

FAK and RhoA have been shown to play critical roles in the F-actin reorganization, leading to tumor invasion[26]. The role of RhoA in regulating actin-filament formation has been well described[27]. RhoA promotes F-actin formation in various cancer cells[28,29]. FAK serves as a scaffolding protein for the binding sites of multiple oncogenic tyrosine kinases and regulates diverse cellular processes, including adhesion, migration, invasion, and metastasis[30]. Our investigation showed that SCIN silencing inhibited the expression levels of RhoA, p-cofilin, p-FAK, and Talin. To further clarify whether the FAK/RhoA signaling axis may be involved in SCIN-mediated migration and invasive activity of glioma cells, PF-573228 or CCG1423 was used to inhibit the FAK or RhoA activity in SCIN-overexpressed glioma cells. Expectedly, PF-573228 or CCG1423 suppressed the migration and invasiveness of glioma cells. Collectively, SCIN has the potential to promote malignant behaviors and F-actin polymerization in human glioma cells, and the underlying mechanism is related to the activation of the RhoA/FAK signaling axis.

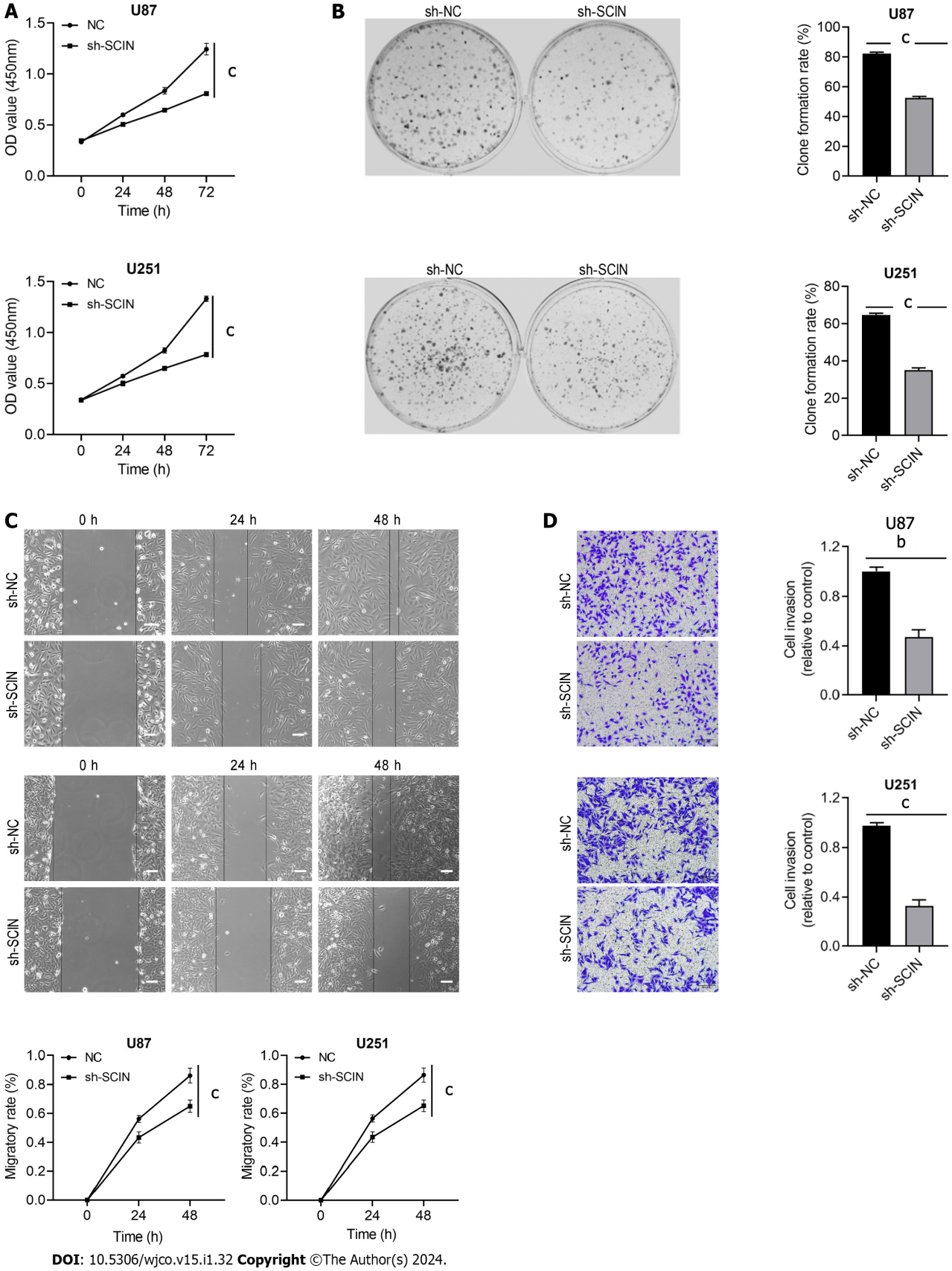

DOI: 10.5306/wjco.v15.i1.32 **Copyright** ©The Author(s) 2024.

Figure 3 Scinderin silencing inhibits glioma cell malignant behaviors. A: Cell proliferation was assessed using the Cell Counting Kit-8; B: U87 and U251 cells were transfected with scinderin (SCIN) short hairpin RNAs (shRNAs) to determine cell proliferation by colony formation assay; C: Effect of downregulated SCIN on the migration of U87 and U251 was evaluated by a wound-healing assay. Scale bar = 100 μm; D: Transwell assay with Matrigel was performed to examine the invasion property. $^{b}P < 0.01$, $^{c}P < 0.001$.

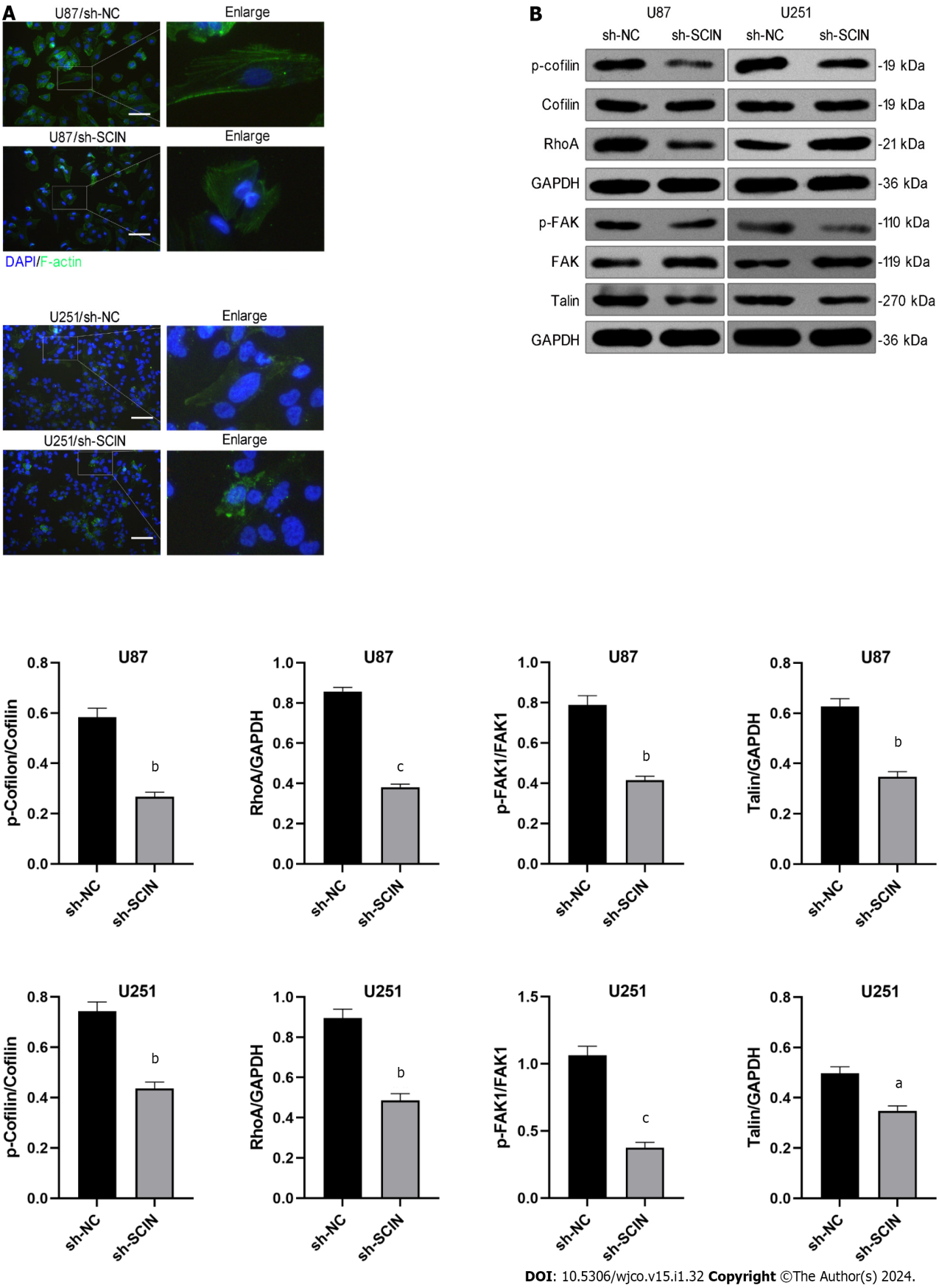

DOI: 10.5306/wjco.v15.i1.32

Figure 4 Scinderin silencing promotes F-actin depolymerization and inhibits RhoA/focal adhesion kinase signaling of glioma cells. A: F-actin cytoskeleton in glioma cells was visualized using Phalloidin staining (green). Scinderin (SCIN) led to a diminution of ruffles and pseudopods on the cell surface; B: Knockdown of SCIN reduced the expression of p-cofilin, RhoA, p-focal adhesion kinase, and Talin, as demonstrated by western blotting. $^{a}P < 0.05$, $^{b}P < 0.01$, $^{c}P < 0.001$.

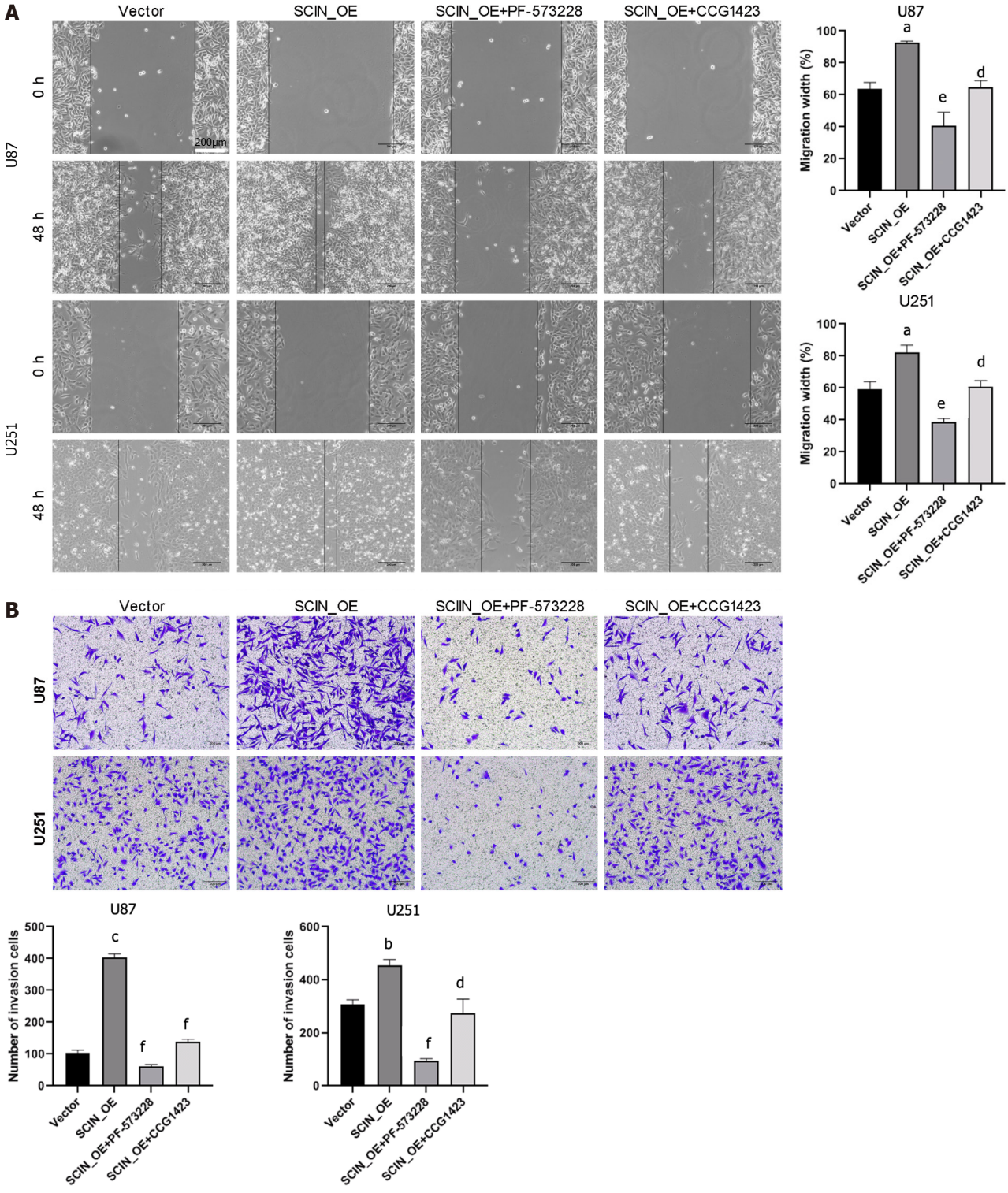

DOI: 10.5306/wjco.v15.i1.32

Figure 5 Inhibition of RhoA-focal adhesion kinase signaling reverses scinderin -mediated malignant behaviors in glioma cells. A: Effects of PF-573228 and Y-27632 on the migration of U87 and U251 cells, evaluated by wound healing assay; B: Transwell assay with Matrigel was performed to examine the invasion property. $^{a}P < 0.05$, $^{b}P < 0.01$, $^{c}P < 0.001$ *vs* the Vector groups; $^{d}P < 0.05$, $^{e}P < 0.01$, $^{f}P < 0.001$ *vs* the SCIN_OE groups.

CONCLUSION

In summary, SCIN promotes cell proliferation, migration, and invasion of glioma cells through remodeling the actin cytoskeleton. Our work illustrates a novel mechanism of SCIN-mediated glioma progression and suggests the possibility that SCIN might be a potential therapeutic target for glioma treatment.

ARTICLE HIGHLIGHTS

Research background

Glioma is one of the most common intracranial tumors, characterized by invasive growth and poor prognosis. Actin cytoskeletal rearrangement is an essential event of tumor cell migration. The actin dynamics-related protein scinderin (SCIN) has been reported to be closely related to tumor cell mobility and invasion in several cancers.

Research motivation

The biological role and molecular mechanism of SCIN in glioma remain unclear.

Research objectives

This study aims to investigate the role and mechanism of SCIN in glioma.

Research methods

The expression and clinical significance of SCIN were analyzed in glioma based on public databases. Then, we utilized SCIN-specific short hairpin RNAs to knock down SCIN expression in glioma cell lines and observed the effects of SCIN silencing on the proliferative, migrative, and invasive abilities of glioma cells. Furthermore, the effect of SCIN silencing on the cytoskeleton of glioma cells was also investigated.

Research results

SCIN expression was significantly elevated in glioma, and high levels of SCIN were associated with advanced tumor grade and wild-type dehydrogenase. SCIN-deficient cells exhibited repressed proliferation, migration, and invasion in U87 and U251 cells. The knockdown of SCIN promotes F-actin depolymerization in U87 and U251 cells *via* inhibiting RhoA/FAK signaling.

Research conclusions

Our work illustrates a novel mechanism of SCIN-mediated glioma progression and suggests the possibility that SCIN might be a potential therapeutic target for glioma treatment.

Research perspectives

To explore SCIN as a biomarker for glioma diagnosis in more clinical samples. To investigate the potential anticancer value of SCIN as an intervention target *in vivo*.

FOOTNOTES

Author contributions: Lin X designed the research study; Lin X, Zhao Z, Sun S, and Liu W performed the research; Zhao Z and Sun S contributed new reagents and analytic tools; Lin X analyzed the data and wrote the manuscript; All authors have read and approved the final manuscript.

Institutional review board statement: The study was reviewed and approved by the Institutional Review Board of Tianjin Huanhu Hospital.

Informed consent statement: All study participants or their legal guardians provided informed written consent about personal and medical data collection before study enrollment.

Conflict-of-interest statement: The authors have no relevant financial or non-financial interests to disclose.

Data sharing statement: The mRNA expression and clinical data of glioma analyzed during the current study are available on the GEPIA database (http://gepia.cancer-pku.cn/) and CGGA) database (http://www.cgga.org.cn/). The protein expression of glioma analyzed in this study is also available on the UALCAN database (https://ualcan.path.uab.edu/). Other datasets during and/or analyzed during the current study are available from the corresponding author upon reasonable request.

Country/Territory of origin: China

ORCID number: Xin Lin 0000-0003-0597-5942.

S-Editor: Liu JH
L-Editor: Filipodia

P-Editor: Zhang XD

REFERENCES

1 **Wen PY**, Kesari S. Malignant gliomas in adults. *N Engl J Med* 2008; **359**: 492-507 [PMID: 18669428 DOI: 10.1056/NEJMra0708126]

2 **Louis DN**, Perry A, Wesseling P, Brat DJ, Cree IA, Figarella-Branger D, Hawkins C, Ng HK, Pfister SM, Reifenberger G, Soffietti R, von Deimling A, Ellison DW. The 2021 WHO Classification of Tumors of the Central Nervous System: a summary. *Neuro Oncol* 2021; **23**: 1231-1251 [PMID: 34185076 DOI: 10.1093/neuonc/noab106]

3 **Lejen T**, Pene TD, Rosé SD, Trifaró JM. The role of different Scinderin domains in the control of F-actin cytoskeleton during exocytosis. *Ann N Y Acad Sci* 2002; **971**: 248-250 [PMID: 12438125 DOI: 10.1111/j.1749-6632.2002.tb04469.x]

4 **Wang K**, Kong F, Qiu Y, Chen T, Fu J, Jin X, Su Y, Gu Y, Hu Z, Li J. Autophagy regulation and protein kinase activity of PIK3C3 controls sertoli cell polarity through its negative regulation on SCIN (scinderin). *Autophagy* 2023; **19**: 2934-2957 [PMID: 37450577 DOI: 10.1080/15548627.2023.2235195]

5 **Wang X**, Shelton SD, Bordieanu B, Frank AR, Yi Y, Venigalla SSK, Gu Z, Lenser NP, Glogauer M, Chandel NS, Zhao H, Zhao Z, McFadden DG, Mishra P. Scinderin promotes fusion of electron transport chain dysfunctional muscle stem cells with myofibers. *Nat Aging* 2022; **2**: 155-169 [PMID: 35342888 DOI: 10.1038/s43587-021-00164-x]

6 **Zhang J**, Yu Q, Jiang D, Yu K, Yu W, Chi Z, Chen S, Li M, Yang D, Wang Z, Xu T, Guo X, Zhang K, Fang H, Ye Q, He Y, Zhang X, Wang D. Epithelial Gasdermin D shapes the host-microbial interface by driving mucus layer formation. *Sci Immunol* 2022; **7**: eabk2092 [PMID: 35119941 DOI: 10.1126/sciimmunol.abk2092]

7 **Zunino R**, Li Q, Rosé SD, Romero-Benítez MM, Lejen T, Brandan NC, Trifaró JM. Expression of scinderin in megakaryoblastic leukemia cells induces differentiation, maturation, and apoptosis with release of plateletlike particles and inhibits proliferation and tumorigenesis. *Blood* 2001; **98**: 2210-2219 [PMID: 11568009 DOI: 10.1182/blood.v98.7.2210]

8 **Lin Q**, Li J, Zhu D, Niu Z, Pan X, Xu P, Ji M, Wei Y, Xu J. Aberrant Scinderin Expression Correlates With Liver Metastasis and Poor Prognosis in Colorectal Cancer. *Front Pharmacol* 2019; **10**: 1183 [PMID: 31736743 DOI: 10.3389/fphar.2019.01183]

9 **Jian W**, Zhang X, Wang J, Liu Y, Hu C, Wang X, Liu R. Scinderin-knockdown inhibits proliferation and promotes apoptosis in human breast carcinoma cells. *Oncol Lett* 2018; **16**: 3207-3214 [PMID: 30127916 DOI: 10.3892/ol.2018.9009]

10 **Liu H**, Shi D, Liu T, Yu Z, Zhou C. Lentivirus-mediated silencing of SCIN inhibits proliferation of human lung carcinoma cells. *Gene* 2015; **554**: 32-39 [PMID: 25303873 DOI: 10.1016/j.gene.2014.10.013]

11 **Abouzahr S**, Bismuth G, Gaudin C, Caroll O, Van Endert P, Jalil A, Dausset J, Vergnon I, Richon C, Kauffmann A, Galon J, Raposo G, Mami-Chouaib F, Chouaib S. Identification of target actin content and polymerization status as a mechanism of tumor resistance after cytolytic T lymphocyte pressure. *Proc Natl Acad Sci U S A* 2006; **103**: 1428-1433 [PMID: 16432193 DOI: 10.1073/pnas.0510454103]

12 **Zhou B**, Chen TW, Jiang YB, Wei XB, Lu CD, Li JJ, Xie D, Cheng SQ. Scinderin suppresses cell proliferation and predicts the poor prognosis of hepatocellular carcinoma. *Oncol Lett* 2020; **19**: 2011-2020 [PMID: 32194697 DOI: 10.3892/ol.2020.11262]

13 **Tavabe Ghavami TS**, Irani S, Mirfakhrai R, Shirkoohi R. Differential expression of Scinderin and Gelsolin in gastric cancer and comparison with clinical and morphological characteristics. *EXCLI J* 2020; **19**: 750-761 [PMID: 32636728 DOI: 10.17179/excli2020-1335]

14 **Tang Z**, Li C, Kang B, Gao G, Zhang Z. GEPIA: a web server for cancer and normal gene expression profiling and interactive analyses. *Nucleic Acids Res* 2017; **45**: W98-W102 [PMID: 28407145 DOI: 10.1093/nar/gkx247]

15 **Zhao Z**, Zhang KN, Wang Q, Li G, Zeng F, Zhang Y, Wu F, Chai R, Wang Z, Zhang C, Zhang W, Bao Z, Jiang T. Chinese Glioma Genome Atlas (CGGA): A Comprehensive Resource with Functional Genomic Data from Chinese Glioma Patients. *Genomics Proteomics Bioinformatics* 2021; **19**: 1-12 [PMID: 33662628 DOI: 10.1016/j.gpb.2020.10.005]

16 **Tang J**, Kang Y, Huang L, Wu L, Peng Y. TIMP1 preserves the blood-brain barrier through interacting with CD63/integrin β 1 complex and regulating downstream FAK/RhoA signaling. *Acta Pharm Sin B* 2020; **10**: 987-1003 [PMID: 32642407 DOI: 10.1016/j.apsb.2020.02.015]

17 **Zhang ZH**, Zhang W, Zhou JD, Zhang TJ, Ma JC, Xu ZJ, Lian XY, Wu DH, Wen XM, Deng ZQ, Lin J, Qian J. Decreased SCIN expression, associated with promoter methylation, is a valuable predictor for prognosis in acute myeloid leukemia. *Mol Carcinog* 2018; **57**: 735-744 [PMID: 29457658 DOI: 10.1002/mc.22794]

18 **Liu JJ**, Liu JY, Chen J, Wu YX, Yan P, Ji CD, Wang YX, Xiang DF, Zhang X, Zhang P, Cui YH, Wang JM, Bian XW, Qian F. Scinderin promotes the invasion and metastasis of gastric cancer cells and predicts the outcome of patients. *Cancer Lett* 2016; **376**: 110-117 [PMID: 27033455 DOI: 10.1016/j.canlet.2016.03.035]

19 **Yang Z**, Ling F, Ruan S, Hu J, Tang M, Sun X, Long W. Clinical and Prognostic Implications of 1p/19q, IDH, BRAF, MGMT Promoter, and TERT Promoter Alterations, and Expression of Ki-67 and p53 in Human Gliomas. *Cancer Manag Res* 2021; **13**: 8755-8765 [PMID: 34849029 DOI: 10.2147/CMAR.S336213]

20 **Wang D**, Sun SQ, Yu YH, Wu WZ, Yang SL, Tan JM. Suppression of SCIN inhibits human prostate cancer cell proliferation and induces G0/G1 phase arrest. *Int J Oncol* 2014; **44**: 161-166 [PMID: 24212916 DOI: 10.3892/ijo.2013.2170]

21 **Lai X**, Su W, Zhao H, Yang S, Zeng T, Wu W, Wang D. Loss of scinderin decreased expression of epidermal growth factor receptor and promoted apoptosis of castration-resistant prostate cancer cells. *FEBS Open Bio* 2018; **8**: 743-750 [PMID: 29744289 DOI: 10.1002/2211-5463.12412]

22 **Qiao X**, Zhou Y, Xie W, Wang Y, Zhang Y, Tian T, Dou J, Yang X, Shen S, Hu J, Qiao S, Wu Y. Scinderin is a novel transcriptional target of BRMS1 involved in regulation of hepatocellular carcinoma cell apoptosis. *Am J Cancer Res* 2018; **8**: 1008-1018 [PMID: 30034938 DOI: 10.3892/ijo.2017.3930]

23 **Chen XM**, Guo JM, Chen P, Mao LG, Feng WY, Le DH, Li KQ. Suppression of scinderin modulates epithelialmesenchymal transition markers in highly metastatic gastric cancer cell line SGC7901. *Mol Med Rep* 2014; **10**: 2327-2333 [PMID: 25174406 DOI: 10.3892/mmr.2014.2523]

24 **Best M**, Gale ME, Wells CM. PAK-dependent regulation of actin dynamics in breast cancer cells. *Int J Biochem Cell Biol* 2022; **146**: 106207 [PMID: 35385780 DOI: 10.1016/j.biocel.2022.106207]

25 **Tanic J**, Wang Y, Lee W, Coelho NM, Glogauer M, McCulloch CA. Adseverin modulates morphology and invasive function of MCF7 cells. *Biochim Biophys Acta Mol Basis Dis* 2019; **1865**: 2716-2725 [PMID: 31369818 DOI: 10.1016/j.bbadis.2019.07.015]

26 **Schaks M**, Giannone G, Rottner K. Actin dynamics in cell migration. *Essays Biochem* 2019; **63**: 483-495 [PMID: 31551324 DOI: 10.1042/EBC20190015]

27 **Kim JG**, Islam R, Cho JY, Jeong H, Cap KC, Park Y, Hossain AJ, Park JB. Regulation of RhoA GTPase and various transcription factors in the RhoA pathway. *J Cell Physiol* 2018; **233**: 6381-6392 [PMID: 29377108 DOI: 10.1002/jcp.26487]

28 **Denk-Lobnig M**, Totz JF, Heer NC, Dunkel J, Martin AC. Combinatorial patterns of graded RhoA activation and uniform F-actin depletion promote tissue curvature. *Development* 2021; **148** [PMID: 34124762 DOI: 10.1242/dev.199232]

29 **Ma TJ**, Zhang ZW, Lu YL, Zhang YY, Tao DC, Liu YQ, Ma YX. CLOCK and BMAL1 stabilize and activate RHOA to promote F-actin formation in cancer cells. *Exp Mol Med* 2018; **50**: 1-15 [PMID: 30287810 DOI: 10.1038/s12276-018-0156-4]

30 **Hong KO**, Ahn CH, Yang IH, Han JM, Shin JA, Cho SD, Hong SD. Norcantharidin Suppresses YD-15 Cell Invasion Through Inhibition of FAK/Paxillin and F-Actin Reorganization. *Molecules* 2019; **24** [PMID: 31109130 DOI: 10.3390/molecules24101928]

World Journal of Clinical Oncology

Submit a Manuscript: https://www.f6publishing.com

World J Clin Oncol 2024 January 24; 15(1): 45-61

DOI: 10.5306/wjco.v15.i1.45

ISSN 2218-4333 (online)

ORIGINAL ARTICLE

Clinical and Translational Research

Prognostic and immunological roles of heat shock protein A4 in lung adenocarcinoma

Xuan Wu, Shen-Ying Yang, Yi-Hua Zhang, Jin-Zhou Fang, Shuai Wang, Zhi-Wei Xu, Xiao-Ju Zhang

Specialty type: Oncology

Provenance and peer review: Unsolicited article; Externally peer reviewed.

Peer-review model: Single blind

Peer-review report's scientific quality classification

Grade A (Excellent): A
Grade B (Very good): 0
Grade C (Good): 0
Grade D (Fair): 0
Grade E (Poor): 0

P-Reviewer: Sultana N, Bangladesh

Received: September 11, 2023
Peer-review started: September 11, 2023
First decision: November 23, 2023
Revised: December 3, 2023
Accepted: December 29, 2023
Article in press: December 29, 2023
Published online: January 24, 2024

Xuan Wu, Shen-Ying Yang, Jin-Zhou Fang, Shuai Wang, Zhi-Wei Xu, Department of Respiratory and Critical Care Medicine, Zhengzhou University People's Hospital, Zhengzhou 450008, Henan Province, China

Yi-Hua Zhang, Graduate School, Xinxiang Medical University, Xinxiang 453003, Henan Province, China

Xiao-Ju Zhang, Department of Pulmonary and Critical Care Medicine, Zhengzhou University People's Hospital, Zhengzhou 450008, Henan Province, China

Corresponding author: Xiao-Ju Zhang, Doctor, PhD, Academic Research, Additional Professor, Chief Physician, Department of Pulmonary and Critical Care Medicine, Zhengzhou University People's Hospital, No. 7 Weiwu Road, Jinshui District, Zhengzhou 450008, Henan Province, China. zhangxiaoju@zzu.edu.cn

Abstract

BACKGROUND

Heat shock protein A4 (HSPA4) belongs to molecular chaperone protein family which plays important roles within variable cellular activities, including cancer initiation and progression. However, the prognostic and immunological significance of HSPA4 in lung adenocarcinoma (LUAD) has not been revealed yet.

AIM

To explore the prognostic and immunological roles of HSPA4 to identify a novel prognostic biomarker and therapeutic target for LUAD.

METHODS

We assessed the prognostic and immunological significance of HSPA4 in LUAD using data from The Cancer Genome Atlas database. The association between HSPA4 expression and clinical-pathological features was assessed through Kruskal-Wallis and Wilcoxon signed-rank test. Univariate/multivariate Cox regression analyses and Kaplan-Meier curves were employed to evaluate prognostic factors, including HSPA4, in LUAD. Gene set enrichment analysis (GSEA) was conducted to identify the key signaling pathways associated with HSPA4. The correlation between HSPA4 expression and cancer immune infiltration was evaluated using single-sample gene set enrichment analysis (ssGSEA).

RESULTS

Overexpressing HSPA4 was significantly related to advanced pathologic TNM stage, advanced pathologic stage, progression disease status of primary therapy outcome and female subgroups with LUAD. In addition, increased HSPA4 expression was found to be related to worse disease-specific survival and overall survival. GSEA analysis indicated a significant correlation between HSPA4 and cell cycle regulation and immune response, particularly through diminishing the function of cytotoxicity cells and CD8 T cells. The ssGSEA algorithm showed a positive correlation between HSPA4 expression and infiltrating levels of Th2 cells, while a negative correlation was observed with cytotoxic cell infiltration levels.

CONCLUSION
Our findings indicate HSPA4 is related to prognosis and immune cell infiltrates and may act as a novel prognostic biomarker and therapeutic target for LUAD.

Key Words: Heat shock protein A4; Lung adenocarcinoma; Tumor-infiltration; Prognosis; T helper cells

Core Tip: Overexpressing heat shock protein A4 (HSPA4) was significantly related to advanced pathologic TNM stage, advanced pathologic stage, progression disease status of primary therapy outcome and female subgroups with lung adenocarcinoma. In addition, increased HSPA4 expression was also found to be related to worse disease-specific survival and overall survival. Gene set enrichment analysis indicated a significant correlation between HSPA4 and cell cycle regulation and immune response, particularly through diminishing the function of cytotoxicity cells and CD8 T cells. The single-sample gene set enrichment analysis algorithm showed a positive correlation between HSPA4 expression and infiltrating levels of Th2 cells, while a negative correlation was observed with cytotoxic cell infiltration levels.

Citation: Wu X, Yang SY, Zhang YH, Fang JZ, Wang S, Xu ZW, Zhang XJ. Prognostic and immunological roles of heat shock protein A4 in lung adenocarcinoma. *World J Clin Oncol* 2024; 15(1): 45-61
URL: https://www.wjgnet.com/2218-4333/full/v15/i1/45.htm
DOI: https://dx.doi.org/10.5306/wjco.v15.i1.45

INTRODUCTION

Lung cancer remains a highly prevalent and deadly disease, causing the most cancer-related deaths globally. It is estimated that there are 2 million new diagnosed cases and more than 1.7 million deaths from lung cancer each year[1]. Lung adenocarcinoma (LUAD), the most prevalent histological subtype of lung cancer, exhibits significant morphological diversity and consists of tumor cells representing various histological subtypes[2]. The discovery of actionable oncogenic mutations has revolutionized cancer treatment, leading to the development of targeted therapies that specifically inhibit driver mutations. For instance, epidermal growth factor receptor (EGFR)-tyrosine kinase inhibitors have demonstrated superior tumor response and longer progression-free survival in patients with EGFR-mutated LUAD compared to traditional chemotherapy[3-5]. However, despite these advancements, advanced-stage LUAD remains largely incurable due to the emergence of therapeutic resistance mechanisms[6-8]. Identifying new oncogenic driver genes, and understanding their roles can assist us better comprehend the biological characteristics of the disease and provide new targets for precision therapy[9]. Through analyzing large-scale tumor genomic data, the researchers can find new oncogenic driver genes and further study their roles to promote the development of personalized treatments and make therapies more precise and effective[10,11]. Additionally, the search for novel prognostic markers is also important avenue to help predict the outcomes and disease progression, and make early predictions of treatment efficacy and prognosis, thereby adjusting treatment strategies and developing personalized treatment plans[12]. Some prognostic biomarkers, such as tumor staging and gene expression profiles, are already widely used in clinical practice[13]. However, due to the high heterogeneity of LUAD, existing prognostic biomarkers are not sufficient to accurately predict disease progression and prognosis for every individual patient. Therefore, the search for novel prognostic biomarkers is crucial for guiding treatment strategies and evaluating treatment efficacy in LUAD[14]. Elevated levels of structurally unstable proteins contribute to the genetic instability and continuous proliferation observed in cancer cells[15]. Additionally, cancer cells experience heightened metabolism and protein synthesis, leading to a persistent state of cellular stress that must be counterbalanced[16,17]. As a result, tumor cells heavily rely on the maintenance of protein homeostasis through molecular chaperones. As we all know, the 70-kDa heat shock proteins (HSP70s), which are present throughout the cell, play a vital role in the folding and remodeling of all cellular proteins[18,19]. In turn, the HSP70s released by cancer cells can affect the malignant characteristics through receptor-mediated signaling pathways[20,21]. Several studies have demonstrated an upregulation of HSP70 expression in various human malignant tumors[22,23]. Heat shock protein A4 (HSPA4) is a heat shock protein that acts as a co-chaperone for HSP70. HSPA4 overexpression has been associated with increased cell survival, enhanced metastatic potential, and resistance to apoptosis, and acts as potential prognostic markers in various cancers[24-26]. HSPA4 has been found to regulate the function of many immune

cells involved in the anti-tumor immune response, and modulates the activity of macrophages, dendritic cells, and natural killer cells, among others, influencing their ability to recognize and eliminate cancer cells[26,27]. However, the functional role of HSPA4 in LUAD has not been explored. Therefore, we conducted this comprehensive study to explore the prognostic and immunological significance of HSPA4 and the potential molecular mechanisms involved in LUAD development, in order to provide novel prognostic markers and potential therapeutic targets for this malignancy disease.

MATERIALS AND METHODS

Data collection and preparation

RNA-Seq profile and related clinical information of 539 LUAD samples and 59 adjacent normal tissues were obtained from The Cancer Genome Atlas (TCGA) database (https://portal.gdc.cancer.gov/). Then, the RNA-seq data in FPKM format was transformed to TPM format. Our analysis strictly adhered to the publication guidelines provided by the TCGA database.

Differentially expressed gene analysis

The LUAD samples included in this study were assigned into two groups according to the median value of HSPA4 expression. Subsequently, we performed further analysis using the student's t-test through the DESeq2 R package (version 3.6.3) to identify genes that showed differential expression between these two groups. To determine significant differential expression, we applied a threshold of adjusted *P* value < 0.05 and |log2-fold change (FC)| > 1.5. Genes that met the criteria were considered as the differentially expressed genes (DEGs).

Enrichment analysis

To explore the functional implications of DEGs between the above high HSPA4 expression group and the low HSPA4 expression group, we conducted gene ontology (GO) and gene set enrichment analysis (GSEA) functional enrichment analyses. These analyses were conducted using the ClusterProfiler package in R (version 3.6.3). For GO analysis, which encompasses cellular component, molecular function, and biological process, we identified significantly enriched GO terms associated with these DEGs. GSEA, on the other hand, is a computational method that assesses whether a defined gene set shows concordant differences and statistically significant between two biological states. In our study, we utilized GSEA to identify signaling pathways and gene sets that were enriched in each phenotype. To sort the enriched pathways, we employed the normalized enrichment score and adjusted p-value. In both GO analysis and GSEA, we considered gene sets with an adjusted *P* value < 0.05 and a false discovery rate (FDR) < 0.25 as significantly enriched, indicating their potential relevance to the phenotypic differences observed.

Immune infiltration analysis

To examine the association between HSPA4 and the hub genes of 24 different types of the immune cells, we employed single-sample gene set enrichment analysis (ssGSEA) within the R GSVA package. This approach allowed us to assess the correlation between HSPA4 expression status and immune cell signatures. Additionally, we systematically analyzed the published literature to investigate the immune infiltrates associated with HSPA4. To compare the immune cell infiltrates between the HSPA4 high and low expression groups, we utilized two statistical methods. Firstly, we conducted the Spearman correlation analysis to evaluate the relationship between HSPA4 expression and the abundance of immunocytes. Secondly, we applied the Wilcoxon rank-sum test to determine any significant differences in immune cell infiltrates between the two expression groups of HSPA4. By employing these methods, we aimed to gain insights into the potential role of HSPA4 in modulating immune cell infiltrates and its implications in the context of the published literature.

Protein–protein interaction network

To explore the protein-protein interactions (PPIs) among co-regulated DEGs, we utilized the Search Tool for the Retrieval of Interacting Genes (STRING) database (http://string-db.org). The PPI network was constructed based on the functional interactions between the proteins encoded by these DEGs. In our study, we set a combined score threshold of 0.7 to determine the reliability of the protein interactions. The STRING database provides a comprehensive score for each protein pair relationship, ranging from 0 to 1. The higher total score always indicates the more reliable PPI networks. To visualize and analyze the PPI network, we utilized the STRING database interface, which offers interactive visualizations and various tools for exploring the functional associations among proteins. By employing the STRING database, we aimed to gain insights into the protein interactions and functional associations among the co-regulated DEGs in our study.

Validation analysis

We evaluated the prognostic value of HSPA4 expressions in three independent datasets (GSE31210, GSE13213, and HARVARD-LC).

Statistical analysis

We performed the analyses in this study by R 3.6.3. First, Wilcoxon rank-sum test and Wilcoxon signed-rank test were performed to evaluate HSPA4 expression between LUAD tissues and the adjacent normal lung tissues. The correlation

Table 1 Demographic and clinicopathological parameters of high and low HSPA4 expression group patients in The Cancer Genome Atlas - lung adenocarcinoma, *n* (%)

Characteristics	Low expression of HSPA4	High expression of HSPA4	*P* value
n	269	270	
Pathologic T stage			0.141
T1	99 (18.5)	77 (14.4)	
T2	137 (25.6)	155 (28.9)	
T3 & T4	33 (6.2)	35 (6.5)	
Pathologic N stage			0.028
N0	189 (36.1)	161 (30.8)	
N1	41 (7.8)	56 (10.7)	
N2 & N3	31 (5.9)	45 (8.6)	
Pathologic stage			0.012
Stage I	163 (30.7)	133 (25)	
Stage II	58 (10.9)	67 (12.6)	
Stage III & Stage IV	43 (8.1)	67 (12.6)	
Gender			0.410
Female	149 (27.6)	140 (26)	
Male	120 (22.3)	130 (24.1)	
Primary therapy outcome			< 0.001
PD	22 (4.9)	49 (10.9)	
SD & PR	22 (4.9)	22 (4.9)	
CR	186 (41.4)	148 (33)	
OS event			0.002
Alive	190 (35.3)	157 (29.1)	
Dead	79 (14.7)	113 (21)	

CR: Complete response; PD: Progressive disease; SD: Stable disease; PR: Partial response; OS: Overall survival.

between clinicopathological factors and HSPA4 expression was assessed by Welch one-way ANOVA. Univariate logistic regression analysis was conducted to evaluate the effect of clinicopathological features on HSPA4 expression. Moreover, univariate and multivariate Cox regression analyses in this study were used to evaluate the prognostic significance of clinicopathological features and HSPA4 expression on survival of LUAD patients. The prognostic significance of HSPA4 was estimated by the Kaplan–Meier curves. Two-tailed $P \leq 0.05$ was considered as the statistical significance.

RESULTS

Baseline characteristics

The clinical information, including the age, gender, T stage, pathologic stage, primary therapy outcome, and overall survival (OS) event, of 539 LUAD samples was shown in Table 1. After excluding the samples without complete information, a total of 539 samples were analyzed in this study. The result of Fisher's exact test revealed that HSPA4 was significantly associated with the OS event of LUAD patients ($P = 0.02$). And the result of chi-square test showed that HSPA4 significantly correlated with N stage ($P = 0.028$), pathologic stage ($P = 0.012$), and primary therapy outcome ($P < 0.001$). However, no significant correlation was observed between HSPA4 expression and other clinicopathological variables.

Differential expression analysis of HSPA4 in LUAD

Based on the HTSeq-Counts data of HSPA4-related genes obtained from TCGA, we conducted a differential expression analysis to identify DEGs using a cut-off criterion of $|\log FC| > 1.5$ and adjusted P value < 0.05. A total of 150 DEGs were detected, with 40 genes upregulated and 110 genes downregulated. To visually represent the expression patterns of these

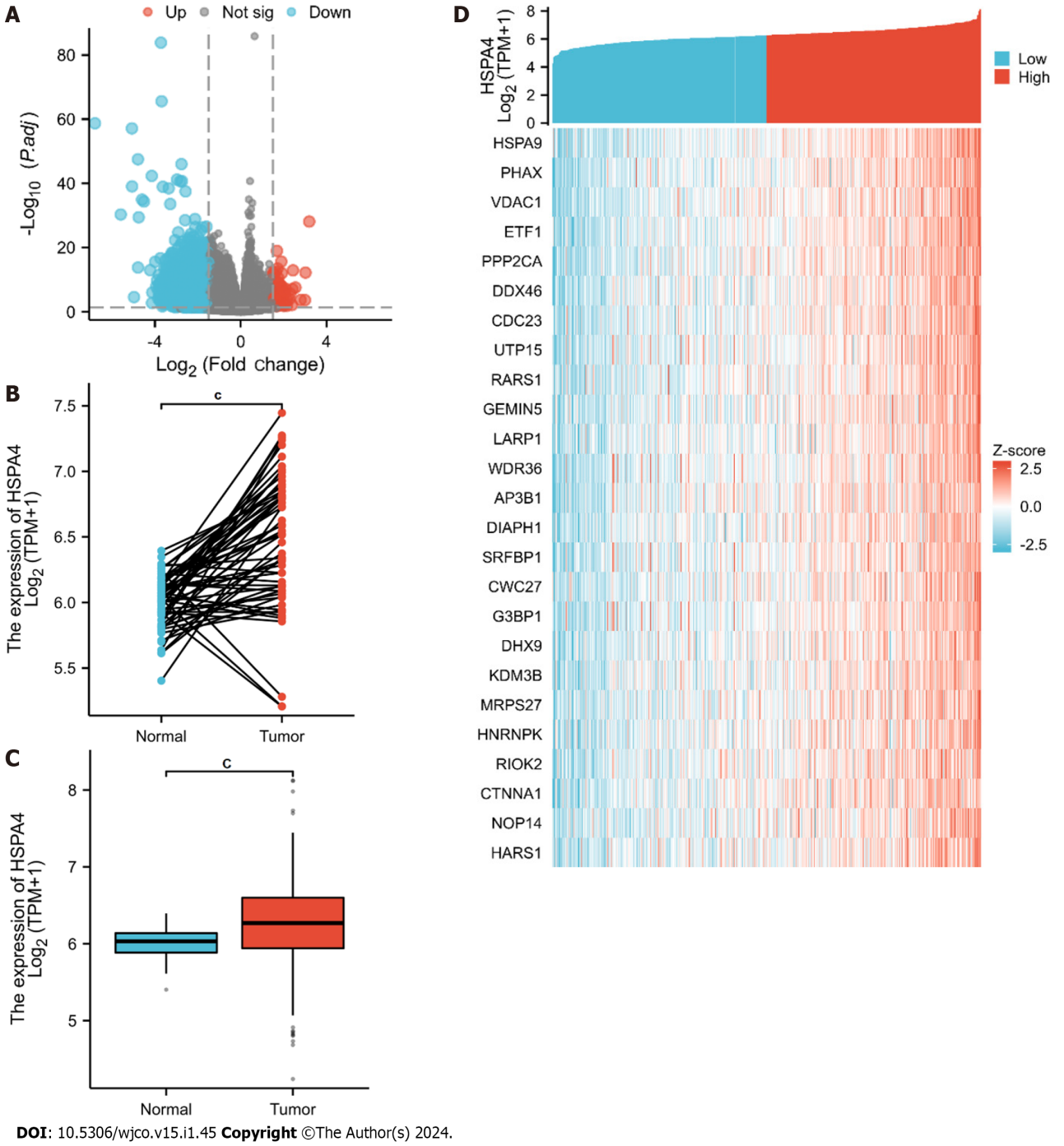

DOI: 10.5306/wjco.v15.i1.45 **Copyright** ©The Author(s) 2024.

Figure 1 The results of differentially expressed genes analysis. A: The volcano plot of differentially expressed RNAs; B and C: The different expressions of HSPA4 between lung adenocarcinoma and adjacent normal tissues; D: Heatmap of the 25 genes correlated to HSPA4. Statistical significance is expressed as $^{c}P < 0.0001$.

DEGs, we created a volcano plot (Figure 1A). Further analyses were conducted to explore the expression of HSPA4 specifically. Both unpaired and paired differential expression analyses were conducted to compare HSPA4 expression between the normal and LUAD groups. The results indicated that HSPA4 was significantly upregulated in tumor samples compared with normal tissues (Figure 1B and C). To investigate the correlation between HSPA4 and other genes, we generated a heatmap depicting the expression levels of HSPA4 along with 25 selected genes (Figure 1D). This heatmap provides a visual representation of the relationship between HSPA4 and these genes.

In addition, we also evaluated the protein level of HSPA4 between LUAD samples and adjacent normal tissues based on the UALCAN database which provides protein expression analysis option using data from CPTAC and ICPC datasets. The results showed that both the total- and phosphor-protein levels of HSPA4 were significantly increased in LUAD tissues than those in adjacent normal tissues (Supplementary Figure 1).

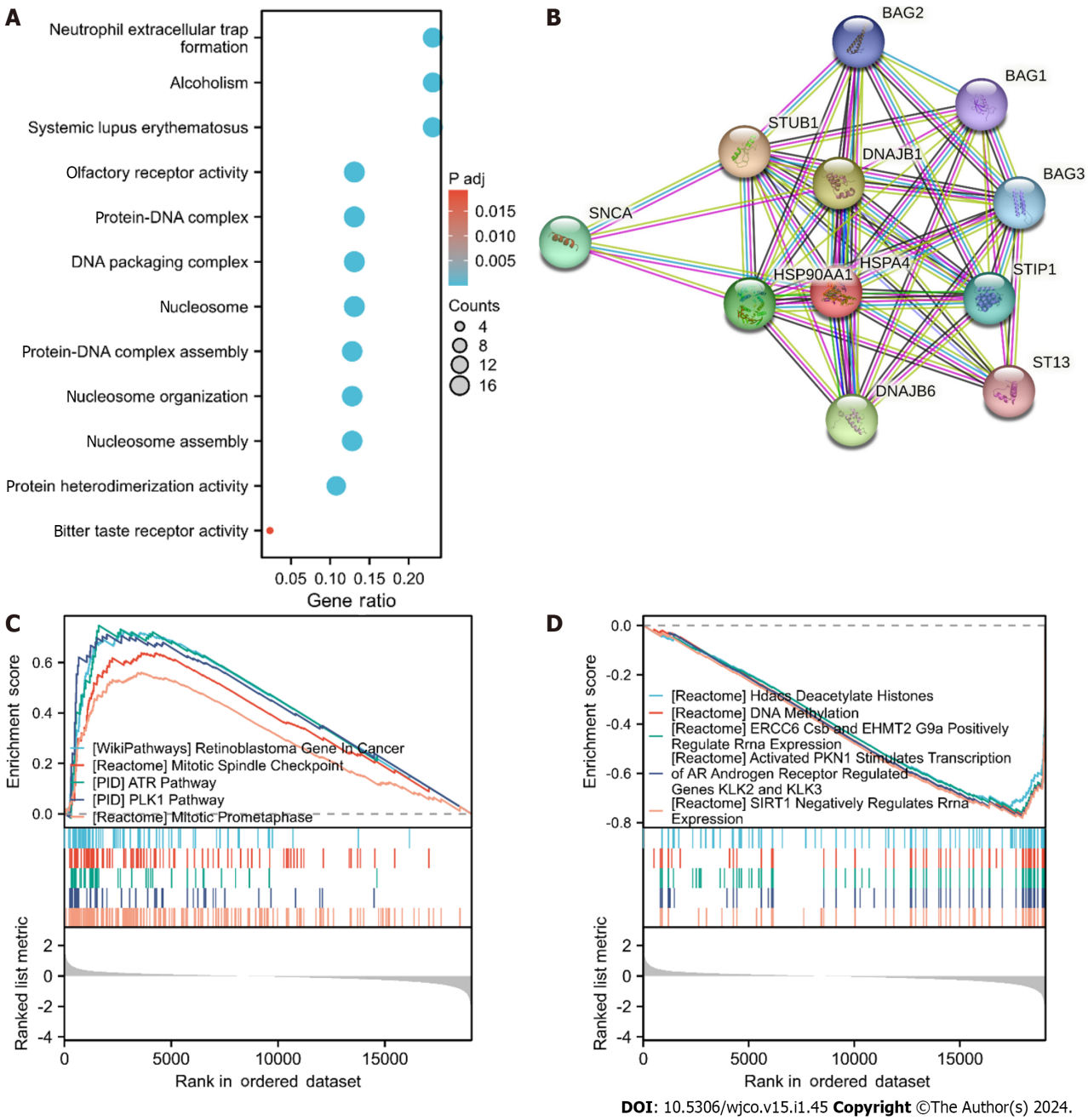

DOI: 10.5306/wjco.v15.i1.45

Figure 2 Enrichment analysis of HSPA4 in lung adenocarcinoma. A: Biological process enrichment related to HSPA4-related genes; B: A network of HSPA4 and its 10 potential co-interaction proteins; C and D: The results of enrichment analysis from gene set enrichment analysis.

Functional enrichment analysis of DEGs

GO analysis suggested that the DEG-related HSPA4 had important regulation on neutrophil extracellular trap formation, alcoholism, systemic lupus erythematosus, olfactory receptor activity, protein-DNA complex, DNA packaging complex, nucleosome, protein-DNA complex assembly, nucleosome organization, nucleosome assembly, protein heterodimerization activity, and bitter taste receptor activity (Figure 2A). And, the PPI network of HSPA4 and the potential co-expression genes in HSPA4-related DEGs were exhibited in Figure 2B.

To further explore the underlying biological function of HSPA4, GSEA analysis between the low and the high HSPA4 expression groups were executed to identify the GO terms and KEGG pathways related to HSPA4. A total of 425 pathways were significantly different in the enrichment of GO terms and KEGG signaling pathways within the high HSPA4 expression samples (FDR < 0.25 and adjusted P < 0.05). The GSEA analysis revealed that retinoblastoma gene in cancer, mitotic spindle checkpoint, ATR pathway, PLK1 pathway, and cell cycle were positively associated with high expression levels of HSPA4 (Figure 2C). HDACS deacetylate histones, DNA methylation, ERCC6 CSB and EHMT2 G9A positively regulate RRNA expression, activated PKN1 stimulates transcription of AR androgen receptor regulated genes KLK2 AND KLK3, SIRT1 negatively regulates RRNA expression were negatively associated with high expression levels of HSPA4 (Figure 2D). These results showed that the signaling pathways that regulated the immunoglobulin complex, DNA methylation, and cell cycle control were strongly related to HSPA4 expression.

Table 2 The COX regression analysis about clinicopathological characteristics associated with the survival of lung adenocarcinoma patients

Characteristics	Total (*N*)	Univariate analysis		Multivariate analysis	
		Hazard ratio (95%CI)	*P* value	Hazard ratio (95%CI)	*P* value
Pathologic T stage	527				
T1	176	Reference		Reference	
T2	285	1.507 (1.059-2.146)	0.023	1.086 (0.726-1.624)	0.687
T3 & T4	66	3.095 (1.967-4.868)	< 0.001	1.571 (0.827-2.984)	0.168
Pathologic N stage	514				
N0	345	Reference		Reference	
N1	96	2.293 (1.632-3.221)	< 0.001	1.293 (0.653-2.560)	0.461
N2 & N3	73	2.993 (2.057-4.354)	< 0.001	1.774 (0.906-3.471)	0.094
Pathologic stage	522				
Stage I	292	Reference		Reference	
Stage II & stage III & stage IV	230	2.889 (2.141-3.897)	< 0.001	1.587 (0.789-3.193)	0.195
Age	520				
≤ 65	257	Reference			
> 65	263	1.216 (0.910-1.625)	0.186		
Gender	530				
Female	283	Reference			
Male	247	1.087 (0.816-1.448)	0.569		
Number pack years smoked	363				
< 40	183	Reference			
≥ 40	180	1.073 (0.753-1.528)	0.697		
HSPA4	530				
Low	266	Reference		Reference	
High	264	1.476 (1.104-1.972)	0.009	1.356 (0.967-1.901)	0.078

Correlation between HSPA4 expression and immune cell infiltration

The correlation between the HSPA4 expression and the immune cell infiltrates quantified as the ssGSEA score was evaluated by Spearman correlation analysis. Both the infiltration levels of T cells and CD8 T cells display a significantly negative correlation with HSPA4 expression ($P = 0.001$) (Figure 3A and B). The infiltration levels of B cells and cytotoxic cells also display a significantly negative correlation with HSPA4 expression ($P < 0.001$) (Figure 3C and D). On the other hand, the infiltration levels of Th2 cells and T helper cells showed a significantly positive correlation with HSPA4 expression ($P < 0.05$) (Figure 3E and F). Th2 cells, Tcm, T helper cells, dendritic cell (DC), aDC, neutrophils, macrophages, and eosinophils, have also shown a positive relation with HSPA4. Treg, natural killer (NK) CD56dim cells, NK cells, Tgd, mast cells, Tem, Th1 cells, iDC, Th17 cells, CD8 T cells, T cells, NK CD56bright cells, cytotoxic cells, TFH, pDC, and B cells were negatively related to HSPA4 expression (Figure 3G). These above results showed the significant value of HSPA4 in immune cell infiltration of LUAD tissues. A heatmap was used to evaluate and visualize the varying degrees of correlation between 24 subtypes of tumor-infiltrating immune cells (Figure 3H).

Correlation between HSPA4 expression and clinicopathological variables

The result of Welch one-way ANOVA with Bonferroni correction analysis demonstrated that increased HSPA4 expression was significantly associated with advanced pathologic TNM stages (Figure 4A-C). And, the t-test also showed that high HSPA4 expression indicated advanced pathologic stage, and PD of primary therapy outcome (Figure 4D and E). Thus, increased HSPA4 expression indicated advanced tumor stage and poor primary therapy outcome. In addition, the female patients with LUAD had increased HSPA4 expression levels compared with male patients with LUAD (Figure 4F).

In this Cox regression analysis model, the univariate Cox regression analysis revealed that the TN stage, pathologic stage, and HSPA4 expression significantly correlated with poor survival of patients with LUAD ($P < 0.05$) (Table 2).

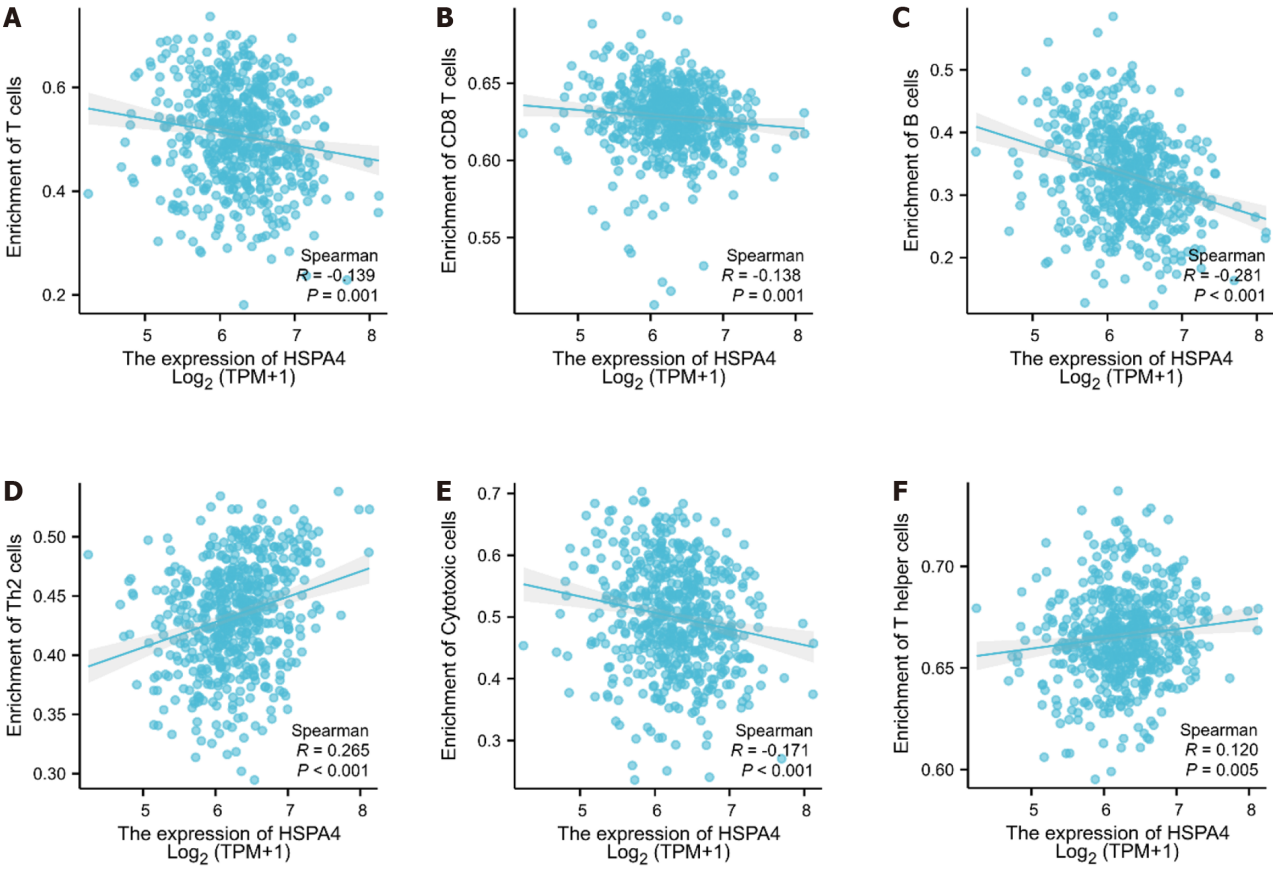
A
Enrichment of T cells
Spearman
R = -0.139
P = 0.001
The expression of HSPA4
Log2 (TPM+1)
B
Enrichment of CD8 T cells
Spearman
R = -0.138
P = 0.001
The expression of HSPA4
Log2 (TPM+1)
C
Enrichment of B cells
Spearman
R = -0.281
P < 0.001
The expression of HSPA4
Log2 (TPM+1)
D
Enrichment of Th2 cells
Spearman
R = 0.265
P < 0.001
The expression of HSPA4
Log2 (TPM+1)
E
Enrichment of Cytotoxic cells
Spearman
R = -0.171
P < 0.001
The expression of HSPA4
Log2 (TPM+1)
F
Enrichment of T helper cells
Spearman
R = 0.120
P = 0.005
The expression of HSPA4
Log2 (TPM+1)

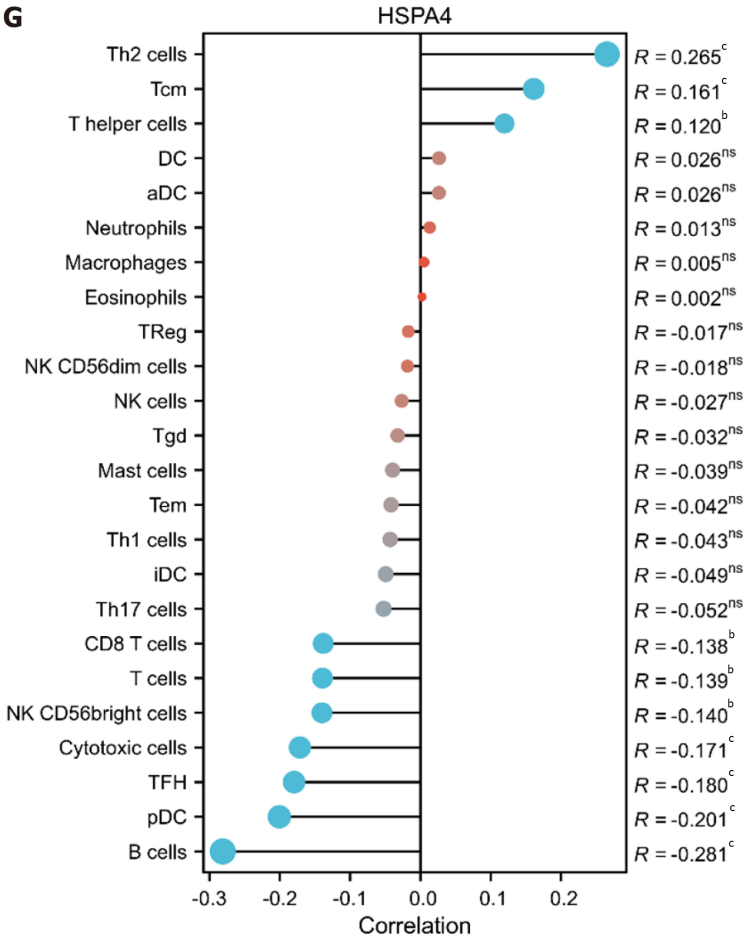
G
HSPA4
Th2 cells R = 0.265c
Tcm R = 0.161c
T helper cells R = 0.120b
DC R = 0.026ns
aDC R = 0.026ns
Neutrophils R = 0.013ns
Macrophages R = 0.005ns
Eosinophils R = 0.002ns
TReg R = -0.017ns
NK CD56dim cells R = -0.018ns
NK cells R = -0.027ns
Tgd R = -0.032ns
Mast cells R = -0.039ns
Tem R = -0.042ns
Th1 cells R = -0.043ns
iDC R = -0.049ns
Th17 cells R = -0.052ns
CD8 T cells R = -0.138b
T cells R = -0.139b
NK CD56bright cells R = -0.140b
Cytotoxic cells R = -0.171c
TFH R = -0.180c
pDC R = -0.201c
B cells R = -0.281c
Correlation

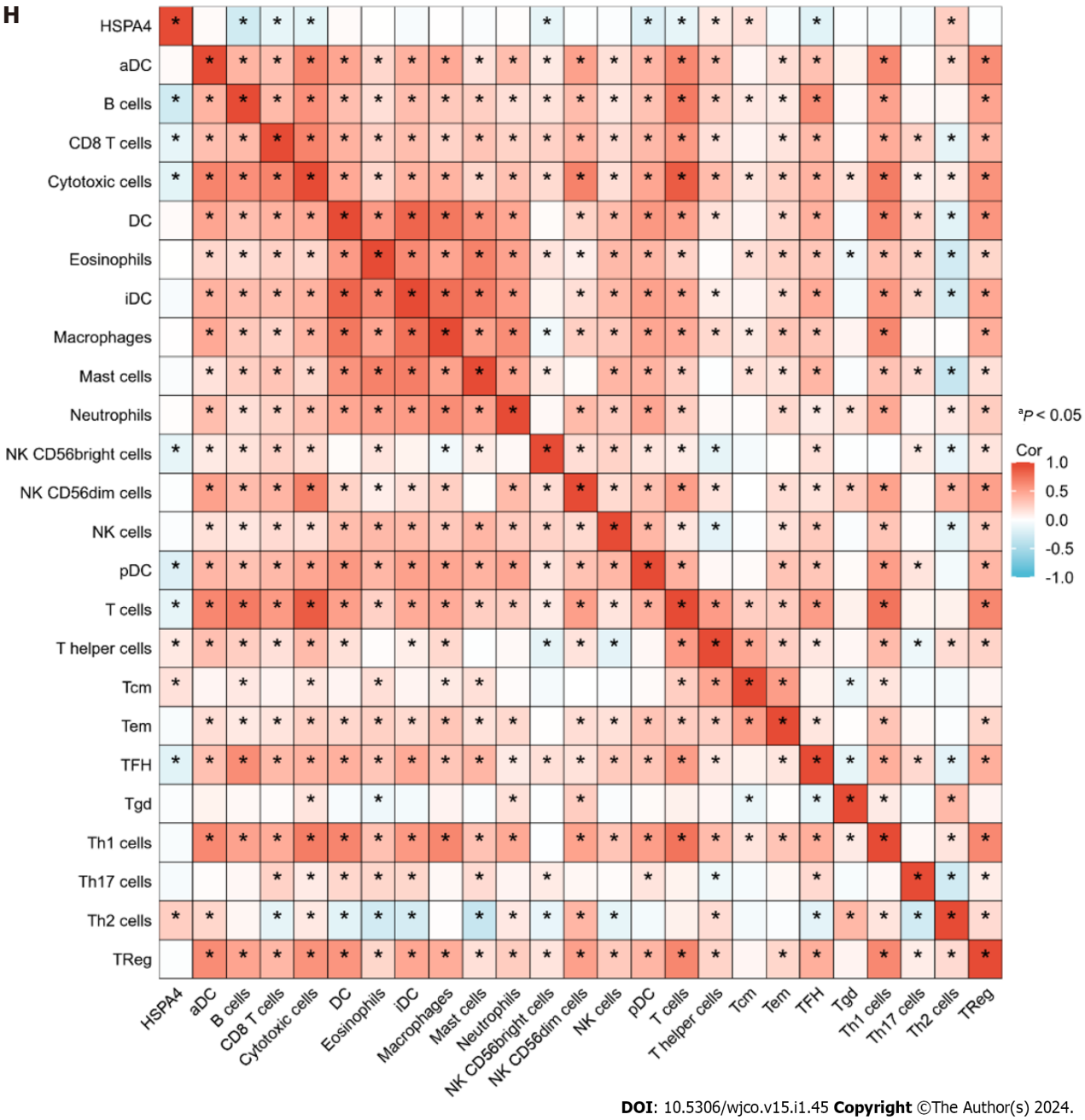

DOI: 10.5306/wjco.v15.i1.45

Figure 3 The results of analysis between HSPA4 expression and immune infiltration. A: The negative correlation between HSPA4 expression and T cells; B: CD8 T cells; C: B cells; D: Cytotoxic cells; E: The negative correlation between HSPA4 expression and Th2 cells; F: T helper cells; G: Correlation between HSPA4 expression level and the relative abundances of 24 immune cells; H: Heatmap of 24 immune infiltration cells in lung adenocarcinoma.

Multivariate Cox regression analysis indicated that T, N stage, pathologic stage and HSPA4 expression were independent factors for the survival of LUAD patients ($P < 0.05$) (Figure 5A).

Additionally, we evaluated the association between survival status and distribution of HSPA4 expression, and expression profile among LUAD samples. The plot features blue dots to depict surviving samples, while red dots represent dead samples. The upper line signifies the median risk score, with the left side denoting low-risk group characterized by less HSPA4 expression (Figure 5B). Conversely, right side of dotted line indicates high-risk samples, displaying higher levels of HSPA4 expression. As the risk score increases, there is a gradual rise in the number of orange dots, indicating an increase in deceased LUAD patients. This observation suggests that individuals categorized in the high-risk group face inferior survival outcomes and a heightened risk of mortality.

Furthermore, to assess the potential clinical use of HSPA4 expression, we developed a nomogram with the HSPA4 expression and traditional clinical prognostic factors, including TN stage, pathologic stage, and age, to predict the survival status in patients with LUAD (Figure 5C).

The Kaplan–Meier survival curve was drawn to assess the prognostic value of HSPA4 in patients with LUAD by R package survminer. LUAD samples were subsequently assigned into low and high HSPA4 expression groups based on the median expression value. The increased HSPA4 expression group tend to be significantly related to poor overall

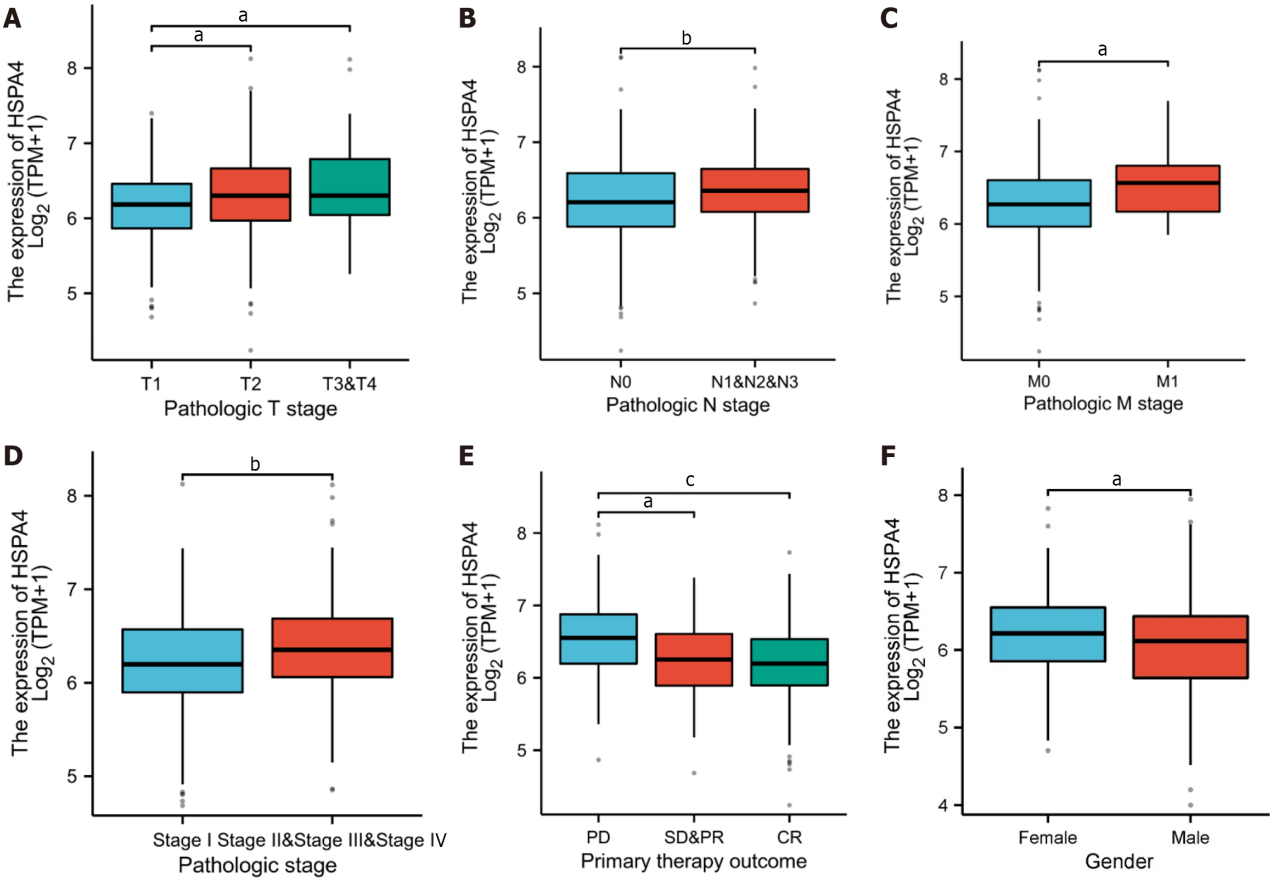

DOI: 10.5306/wjco.v15.i1.45

Figure 4 Correlation between the HSPA4 expression and different clinicopathologic characteristics. A: Correlation between the HSPA4 expression and the pathologic T stage; B: N stage; C: M stage; D: Pathologic stage; E: Primary therapy outcome; F: Gender. Statistical significance is expressed as [a] $P < 0.05$, [b]$P < 0.01$, [c]$P < 0.0001$.

survival (HR = 1.51, $P = 0.056$) and disease specific survival (HR = 1.40, $P = 0.071$) (Figure 6A and B).

The increased HSPA4expression of was also related to worse survival in the T2 subgroup of T stage ($P = 0.038$), M0 subgroup of M stage ($P = 0.006$), age > 65 subgroup ($P = 0.003$), female subgroup ($P = 0.021$), smoker subgroup ($P = 0.03$), and stage III subgroup of pathologic stage ($P = 0.061$) (Figure 6C-H).

Data validation

In all three independent datasets, Kaplan–Meier survival curves showed that high HSPA4 mRNA expression group exhibited a significantly poor survival compared to the low HSPA4 mRNA expression group ($P < 0.05$) (Figure 7).

HSPA4 methylation in patients with LUAD

The MethSurv tool was utilized to examine the association between DNA methylation levels of HSPA4 and the prognostic value of individual CpG sites. The analysis identified 13 methylation CpG sites, with cg05996250 and cg07474441 displaying the highest levels of DNA methylation (Figure 8). Among these CpG sites, seven of them, namely cg02067788, cg23946014, cg05996250, and cg07474441, exhibited a significant correlation with prognosis ($P < 0.05$) (Figure 8). Patients with decreased methylation levels of these CpG sites in HSPA4 experienced poorer overall survival compared to those with elevated HSPA4 methylation levels. Since increased methylation level means low expression of HSPA4, which indicates that patients with elevated expression of HSPA4 have a poor prognosis, which is consistent with the results in Figures 6 and 7.

DISCUSSION

LUAD is a common malignant tumor with prognosis influenced by various factors. Treatment options for patients with LUAD are limited, especially for those without actionable drug targets. However, some immunotherapy approaches, including immune checkpoint inhibitors (ICIs), and adoptive cellular therapy, have been shown effective for some LUADs. Nevertheless, there are also many challenges, including the lack of initial response and resistance overtime to ICIs in certain subgroups of cancers, that need to be addressed in order to broaden the application[28]. Therefore, it is necessary to study the molecular mechanisms underlying ICIs resistance to develop strategies to enhance Immuno-

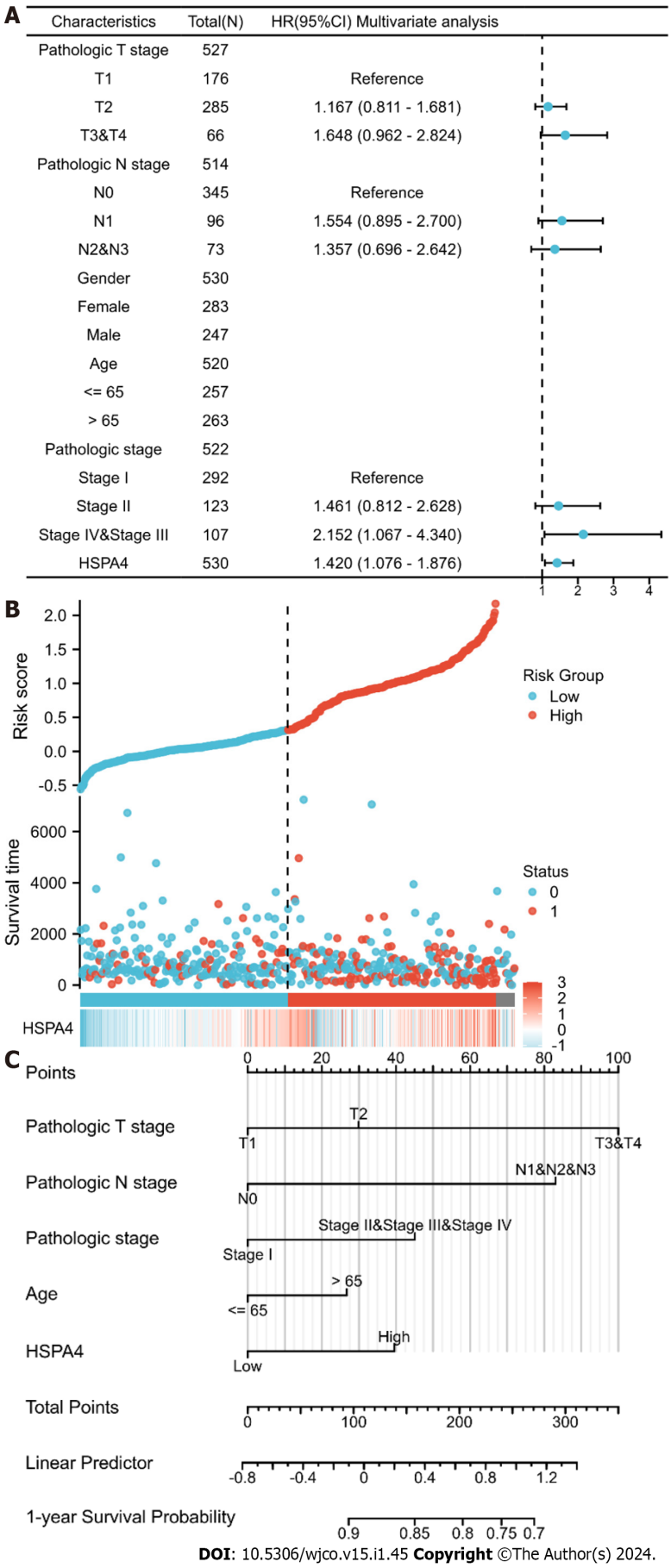

DOI: 10.5306/wjco.v15.i1.45 **Copyright** ©The Author(s) 2024.

Figure 5 The prognostic value of HSPA4 in lung adenocarcinoma. A: Multivariate Cox regression visualized in the forest plot; B: HSPA4 expression distribution and survival status. 0: dead, 1: alive; C: Nomogram with the HSPA4 expression and traditional clinical prognostic factors.

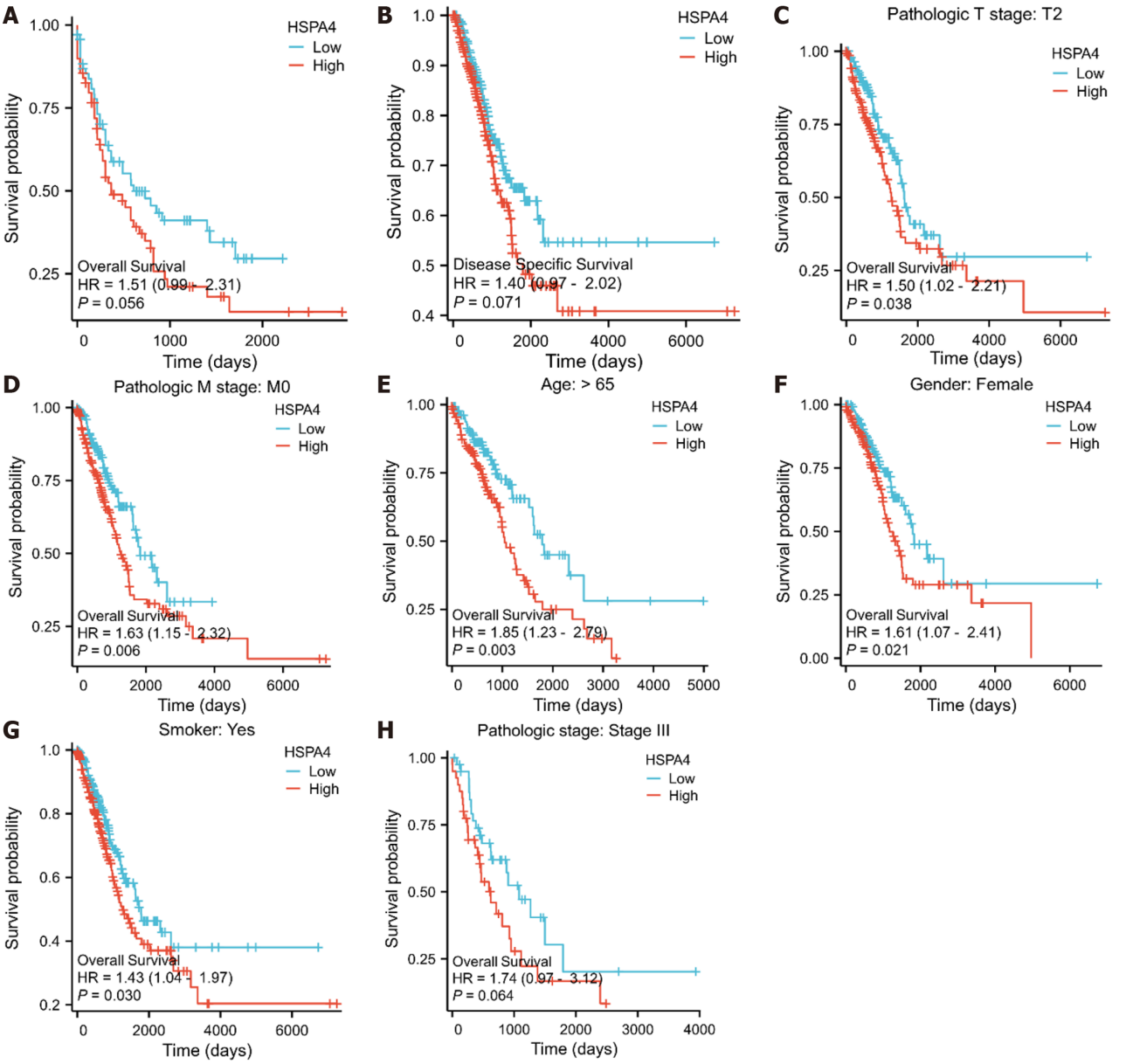

DOI: 10.5306/wjco.v15.i1.45 **Copyright** ©The Author(s) 2024.

Figure 6 The prognostic value of HSPA4 in the different subgroups. A and B: The prognostic value of HSPA4 in overall survival and disease specific survival of lung adenocarcinoma patients; C–H: High expression of HSPA4 was associated with worse overall survival in different subgroups.

therapy response.

In this study, we found that LUAD patients with high HSPA4 expression had worse overall survival and disease-specific survival, which is consistent with previous research evidences, supporting HSPA4 as a potential biomarker for evaluating the prognosis of LUAD patients. Previous evidences have shown that abnormal expression of HSPA4 is related to the occurrence and development of various tumors[23,29].

In addition, further subgroup analysis showed a positive correlation between high HSPA4 expression and worse survival in the T2 stage, M0 stage, age > 65 years, female, smoker, and pathological stage III subgroups. This indicates that HSPA4 may have promising predictive value in these specific subgroups and provide important information for individualized treatment decisions. For example, more aggressive treatment strategies may be needed for those with higher pathological stages in response to the malignant biological behavior represented by high HSPA4 expression.

When it comes to immune regulation in LUAD, the functional enrichment analysis demonstrated that HSPA4 plays crucial roles in the antigen presentation process, which is essential for the activation of T cells and the initiation of an immune response against cancer cells. It assists in the proper folding and assembly of antigens, facilitating their presentation on major histocompatibility complex molecules. This process enables immune cells to recognize and target cancer cells more effectively[30]. Furthermore, in our study, HSPA4 has been found to regulate the function of various immune cells involved in the anti-tumor immune response. It modulates the activity of dendritic cells, macrophages, and natural killer cells, among others, influencing their ability to recognize and eliminate cancer cells. HSPA4 can promote antigen cross-presentation by DCs and enhance the cytotoxicity of natural killer cells, thus improving the immune response against cancer. HSPA4 expression in the tumor microenvironment can influence immune cell infiltration. It has

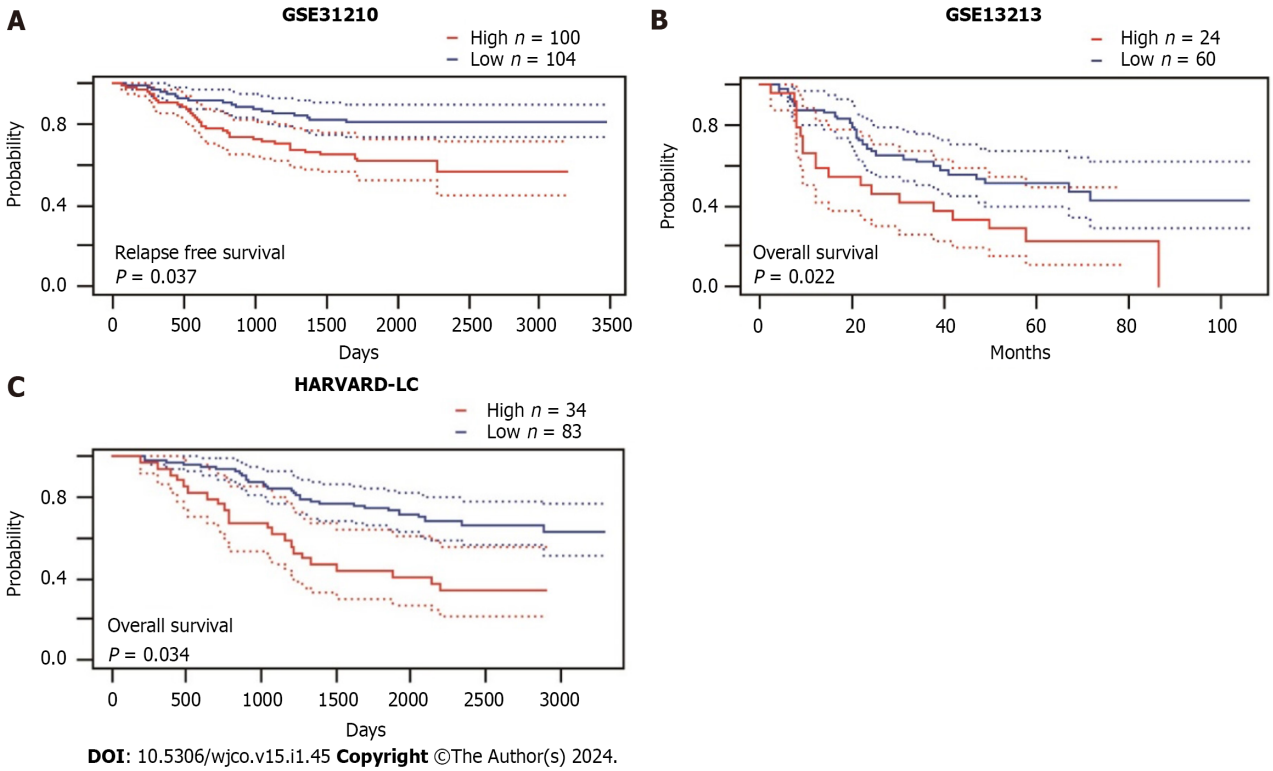

DOI: 10.5306/wjco.v15.i1.45 **Copyright** ©The Author(s) 2024.

Figure 7 The prognostic value of HSPA4 in three independent datasets. A: The prognostic value of HSPA4 in GSE31210 database; B: GSE13213 database; C: HARVARD-LC database.

been observed that high levels of HSPA4 are associated with decreased infiltration of immune cells, such as cytotoxic T cells and CD 8 T cells, into tumors. This infiltration is linked to improved prognosis in certain cancers[31].

Overall, HSPA4 plays a multifaceted role in immune regulation in LUAD. It facilitates antigen presentation, promotes immunogenic cell death, modulates immune cell function, and influences the tumor microenvironment. Further research is still needed to fully understand the molecular mechanisms underlying the correlation between HSPA4 and immune regulation in LUAD.

Subsequently, we developed a Nomogram model that combines HSPA4 expression with traditional clinical prognostic factors such as TNM stage, pathological stage, and age. This Nomogram model provides clinicians with an intuitive tool to more accurately assess the prognosis of LUAD patients and tailor individualized treatment strategies. The comprehensive predictive model integrating clinical and molecular biology information allows for a more comprehensive evaluation of patient prognostic risk and provides robust support for clinical decision-making. The HSPA4 expression and the combined nomogram model were of great significance in prognostic prediction for LUAD patients. The increased HSPA4 expression had been shown to indicate an immunosuppressive microenvironment, which maybe contribute to the immunotherapy resistance in the treatment of LUAD patients. The HSPA4 inhibitor addition may enhance the therapeutic response to immune checkpoint blockade, thereby optimizing treating strategies and drug application.

Although this study provides preliminary exploration of the potential of HSPA4 as a prognostic biomarker for LUAD patients, there are still some limitations. Firstly, our study is based on retrospective analysis and may have selection bias. Further prospective and multicenter validation studies will help better define the prognostic value of HSPA4. Moreover, this study only focused on the expression level of the HSPA4 gene and did not investigate its regulatory mechanisms and functions. Future research can delve into the biological characteristics of HSPA4 to reveal the specific role in the initiation and progression of LUAD.

CONCLUSION

Above all, this study suggests that HSPA4 is a potential prognostic indicator, with high expression correlating with worse prognosis in LUAD patients. The expression level of HSPA4 may have differential predictive value in different subgroups and can be used in combination with traditional clinical prognostic factors through the Nomogram model. The findings provide new clues for better evaluating prognostic risk and devising individualized treatment strategies for LUAD patients and serve as useful references for relevant clinical practice and research. Future studies should explore the biological functions and regulatory mechanisms of HSPA4 and validate its clinical applicability as a prognostic biomarker.

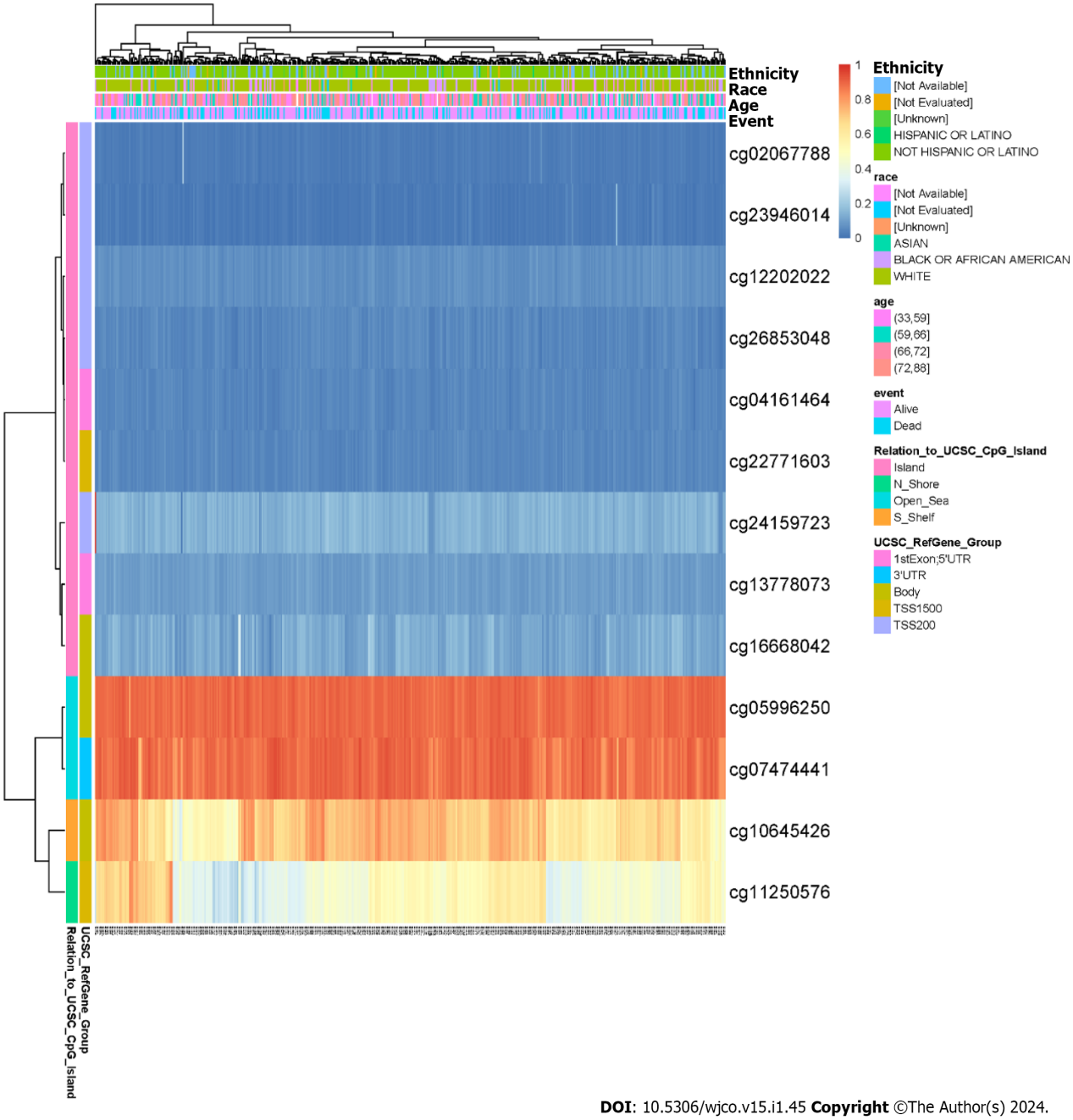

DOI: 10.5306/wjco.v15.i1.45

Figure 8 Visualization between the methylation level and HSPA4 expression.

ARTICLE HIGHLIGHTS

Research background

Heat shock 70 kDa protein 4 (HSPA4) is a member of the HSP110 family. Previous studies showed HSPA4 is significantly associated with prognosis and immune regulation in different cancer types. However, the role of HSPA4 in lung adenocarcinoma (LUAD) has not been revealed yet.

Research motivation

We tried to explore the prognostic and immunological roles of HSPA4 in the Bio informatics methods based on the public databases. We confirmed the role of HSPA4 in LUAD prognosis and verified the correlation between HSPA4 and immune regulation. This study can assist us better comprehend the biological characteristics of the disease and provide new therapeutic target for precision therapy.

Research objectives

We aim to comprehensively analyzed the correlation between HSPA4 expression and the clinical characteristic, prognosis and immunology based on the RNA-seq data from the public database. We showed HSPA4 is significantly associated

with prognosis and immune regulation and is a potential prognostic and new therapeutic target in LUAD.

Research methods

The primary research method used in my study was bioinformatics. This technique is an advanced technology used in recent years to study genetics and genomics. It is widely used due to its ability to analyze large datasets and identify patterns and relationships that might be difficult to detect using other methods. The novelty of bioinformatics lies in its ability to integrate multiple technologies and methodologies, such as computer science, statistics, and molecular biology, to provide a comprehensive understanding of biological systems. In my study, I applied various bioinformatics tools and algorithms to analyze genomic data and identify potential genetic targets for further investigation.

Research results

The study found that overexpression of HSPA4 was significantly associated with advanced disease stage, progression disease status, and worse survival outcomes in LUAD. Additionally, HSPA4 expression was correlated with alterations in cell cycle regulation, immune response, and the balance of infiltrating immune cells within the tumor microenvironment. These findings suggest that HSPA4 may play a role in tumor progression and immune evasion in LUAD. However, this study only focused on the expression level of the HSPA4 gene and did not investigate its regulatory mechanisms and functions. Future research can delve into the biological characteristics of HSPA4 to reveal the specific role in the initiation and progression of LUAD.

Research conclusions

This study proposed that HSPA4 may play a role in tumor progression and immune evasion in LUAD. This study comprehensively analyzed the correlation between HSPA4 expression and the clinical characteristic, prognosis and immunology in bioinformatics method based on the RNA-seq data from the public database.

Research perspectives

The regulatory mechanisms and functions of HSPA4 and the specific role in the initiation and progression of LUAD are direction of the future research.

FOOTNOTES

Author contributions: Wu X and Yang SY contributed equally to this work; Wu X, Yang SY and Zhang XJ designed the research study; Wu X, Yang SY and Fang JZ performed the analysis; Wu X, Yang SY, and Wang S analyzed the data and wrote the manuscript; all authors have read and approve the final manuscript.

Institutional review board statement: This study was reviewed and approved by the Ethics Committee of Zhengzhou University People's Hospital.

Clinical trial registration statement: Since our paper is not a clinical research study but a bioinformatics analysis to assess the prognostic and immunological significance of HSPA4 in LUAD using data from public database. So, it is not applicable to provide the Clinical Trial Registration Statement.

Informed consent statement: Since our paper is not a clinical research study but a bioinformatics analysis to assess the prognostic and immunological significance of HSPA4 in LUAD using data from public database. So, it is not applicable to provide the Signed Informed Consent Form(s) or Document(s).

Conflict-of-interest statement: All the authors declare that the research was conducted in the absence of any commercial or financial relationships that could be construed as a potential conflict of interest.

Data sharing statement: The datasets presented in this study can be found in online repositories. The names of the repository/repositories and accession number(s) can be found in the article/Supplementary material.

Country/Territory of origin: China

ORCID number: Xuan Wu 0000-0001-8539-6611; Xiao-Ju Zhang 0000-0002-2833-8746.

S-Editor: Liu JH
L-Editor: A
P-Editor: Zhang XD

REFERENCES

1 **Koundouros N**, Poulogiannis G. Reprogramming of fatty acid metabolism in cancer. *Br J Cancer* 2020; **122**: 4-22 [PMID: 31819192 DOI: 10.1038/s41416-019-0650-z]

2 **Sun N**, Zhao X. Therapeutic Implications of FABP4 in Cancer: An Emerging Target to Tackle Cancer. *Front Pharmacol* 2022; **13**: 948610 [PMID: 35899119 DOI: 10.3389/fphar.2022.948610]

3 **Hotamisligil GS**, Bernlohr DA. Metabolic functions of FABPs--mechanisms and therapeutic implications. *Nat Rev Endocrinol* 2015; **11**: 592-605 [PMID: 26260145 DOI: 10.1038/nrendo.2015.122]

4 **Lei C**, Fan B, Tian J, Li M, Li Y. PPARγ regulates fabp4 expression to increase DHA content in golden pompano (Trachinotus ovatus) hepatocytes. *Br J Nutr* 2022; **127**: 3-11 [PMID: 33663633 DOI: 10.1017/S0007114521000775]

5 **Zeng J**, Sauter ER, Li B. FABP4: A New Player in Obesity-Associated Breast Cancer. *Trends Mol Med* 2020; **26**: 437-440 [PMID: 32359475 DOI: 10.1016/j.molmed.2020.03.004]

6 **Mukherjee A**, Chiang CY, Daifotis HA, Nieman KM, Fahrmann JF, Lastra RR, Romero IL, Fiehn O, Lengyel E. Adipocyte-Induced FABP4 Expression in Ovarian Cancer Cells Promotes Metastasis and Mediates Carboplatin Resistance. *Cancer Res* 2020; **80**: 1748-1761 [PMID: 32054768 DOI: 10.1158/0008-5472.CAN-19-1999]

7 **Tian W**, Zhang W, Zhang Y, Zhu T, Hua Y, Li H, Zhang Q, Xia M. FABP4 promotes invasion and metastasis of colon cancer by regulating fatty acid transport. *Cancer Cell Int* 2020; **20**: 512 [PMID: 33088219 DOI: 10.1186/s12935-020-01582-4]

8 **Dum D**, Ocokoljic A, Lennartz M, Hube-Magg C, Reiswich V, Höflmayer D, Jacobsen F, Bernreuther C, Lebok P, Sauter G, Luebke AM, Burandt E, Marx AH, Simon R, Clauditz TS, Minner S, Menz A, Büscheck F, Gorbokon N, Steurer S, Blessin NC, Krech T. FABP1 expression in human tumors: a tissue microarray study on 17,071 tumors. *Virchows Arch* 2022; **481**: 945-961 [PMID: 35951102 DOI: 10.1007/s00428-022-03394-5]

9 **Xu B**, Chen L, Zhan Y, Marquez KNS, Zhuo L, Qi S, Zhu J, He Y, Chen X, Zhang H, Shen Y, Chen G, Gu J, Guo Y, Liu S, Xie T. The Biological Functions and Regulatory Mechanisms of Fatty Acid Binding Protein 5 in Various Diseases. *Front Cell Dev Biol* 2022; **10**: 857919 [PMID: 35445019 DOI: 10.3389/fcell.2022.857919]

10 **O'Sullivan SE**, Kaczocha M. FABP5 as a novel molecular target in prostate cancer. *Drug Discov Today* 2020 [PMID: 32966866 DOI: 10.1016/j.drudis.2020.09.018]

11 **Tang Z**, Kang B, Li C, Chen T, Zhang Z. GEPIA2: an enhanced web server for large-scale expression profiling and interactive analysis. *Nucleic Acids Res* 2019; **47**: W556-W560 [PMID: 31114875 DOI: 10.1093/nar/gkz430]

12 **Li Y**, Zhao ZG, Luo Y, Cui H, Wang HY, Jia YF, Gao YT. Dual targeting of Polo-like kinase 1 and baculoviral inhibitor of apoptosis repeat-containing 5 in TP53-mutated hepatocellular carcinoma. *World J Gastroenterol* 2020; **26**: 4786-4801 [PMID: 32921957 DOI: 10.3748/wjg.v26.i32.4786]

13 **Zhu W**, Zhang Q, Liu M, Yan M, Chu X, Li Y. Identification of DNA repair-related genes predicting pathogenesis and prognosis for liver cancer. *Cancer Cell Int* 2021; **21**: 81 [PMID: 33516217 DOI: 10.1186/s12935-021-01779-1]

14 **Ohata T**, Yokoo H, Kamiyama T, Fukai M, Aiyama T, Hatanaka Y, Hatanaka K, Wakayama K, Orimo T, Kakisaka T, Kobayashi N, Matsuno Y, Taketomi A. Fatty acid-binding protein 5 function in hepatocellular carcinoma through induction of epithelial-mesenchymal transition. *Cancer Med* 2017; **6**: 1049-1061 [PMID: 28374947 DOI: 10.1002/cam4.1020]

15 **Boettcher S**, Miller PG, Sharma R, McConkey M, Leventhal M, Krivtsov AV, Giacomelli AO, Wong W, Kim J, Chao S, Kurppa KJ, Yang X, Milenkowic K, Piccioni F, Root DE, Rücker FG, Flamand Y, Neuberg D, Lindsley RC, Jänne PA, Hahn WC, Jacks T, Döhner H, Armstrong SA, Ebert BL. A dominant-negative effect drives selection of TP53 missense mutations in myeloid malignancies. *Science* 2019; **365**: 599-604 [PMID: 31395785 DOI: 10.1126/science.aax3649]

16 **Dearth LR**, Qian H, Wang T, Baroni TE, Zeng J, Chen SW, Yi SY, Brachmann RK. Inactive full-length p53 mutants lacking dominant wild-type p53 inhibition highlight loss of heterozygosity as an important aspect of p53 status in human cancers. *Carcinogenesis* 2007; **28**: 289-298 [PMID: 16861262 DOI: 10.1093/carcin/bgl132]

17 **Lu Y**, Wu M, Xu Y, Yu L. The Development of p53-Targeted Therapies for Human Cancers. *Cancers (Basel)* 2023; **15**: 3560 [PMID: 37509223 DOI: 10.3390/cancers15143560]

18 **Farrell M**, Fairfield H, Karam M, D'Amico A, Murphy CS, Falank C, Pistofidi RS, Cao A, Marinac CR, Dragon JA, McGuinness L, Gartner CG, Iorio RD, Jachimowicz E, DeMambro V, Vary C, Reagan MR. Targeting the fatty acid binding proteins disrupts multiple myeloma cell cycle progression and MYC signaling. *Elife* 2023; **12** [PMID: 36880649 DOI: 10.7554/eLife.81184]

19 **Tontonoz P**, Graves RA, Budavari AI, Erdjument-Bromage H, Lui M, Hu E, Tempst P, Spiegelman BM. Adipocyte-specific transcription factor ARF6 is a heterodimeric complex of two nuclear hormone receptors, PPAR gamma and RXR alpha. *Nucleic Acids Res* 1994; **22**: 5628-5634 [PMID: 7838715 DOI: 10.1093/nar/22.25.5628]

20 **Icard P**, Fournel L, Wu Z, Alifano M, Lincet H. Interconnection between Metabolism and Cell Cycle in Cancer. *Trends Biochem Sci* 2019; **44**: 490-501 [PMID: 30655165 DOI: 10.1016/j.tibs.2018.12.007]

21 **Chiappa M**, Petrella S, Damia G, Broggini M, Guffanti F, Ricci F. Present and Future Perspective on PLK1 Inhibition in Cancer Treatment. *Front Oncol* 2022; **12**: 903016 [PMID: 35719948 DOI: 10.3389/fonc.2022.903016]

22 **Wheatley SP**, Altieri DC. Survivin at a glance. *J Cell Sci* 2019; **132** [PMID: 30948431 DOI: 10.1242/jcs.223826]

23 **Jia H**, Zhang X, Liu X, Qiao R, Liu Y, Lv S, Zhu H, Wang J, Kong Q, Zhang H, Zhang Z. FABP5, a Novel Immune-Related mRNA Prognostic Marker and a Target of Immunotherapy for Multiple Myeloma. *Front Med (Lausanne)* 2021; **8**: 667525 [PMID: 34249967 DOI: 10.3389/fmed.2021.667525]

24 **Field CS**, Baixauli F, Kyle RL, Puleston DJ, Cameron AM, Sanin DE, Hippen KL, Loschi M, Thangavelu G, Corrado M, Edwards-Hicks J, Grzes KM, Pearce EJ, Blazar BR, Pearce EL. Mitochondrial Integrity Regulated by Lipid Metabolism Is a Cell-Intrinsic Checkpoint for Treg Suppressive Function. *Cell Metab* 2020; **31**: 422-437.e5 [PMID: 31883840 DOI: 10.1016/j.cmet.2019.11.021]

25 **Zhang M**, Dai W, Li Z, Tang L, Chen J, Chen C. HSPA4 Knockdown Retarded Progression and Development of Colorectal Cancer. *Cancer Manag Res* 2021; **13**: 4679-4690 [PMID: 34163243 DOI: 10.2147/CMAR.S310729]

26 **Shang BB**, Chen J, Wang ZG, Liu H. Significant correlation between HSPA4 and prognosis and immune regulation in hepatocellular carcinoma. *PeerJ* 2021; **9**: e12315 [PMID: 34754620 DOI: 10.7717/peerj.12315]

27 **Shen B**, Zhang G, Liu Y, Wang J, Jiang J. Identification and Analysis of Immune-Related Gene Signature in Hepatocellular Carcinoma. *Genes (Basel)* 2022; **13** [PMID: 36292719 DOI: 10.3390/genes13101834]

28 **Morad G**, Helmink BA, Sharma P, Wargo JA. Hallmarks of response, resistance, and toxicity to immune checkpoint blockade. *Cell* 2021; **184**: 5309-5337 [PMID: 34624224 DOI: 10.1016/j.cell.2021.09.020]

29 **Gu Y**, Liu Y, Fu L, Zhai L, Zhu J, Han Y, Jiang Y, Zhang Y, Zhang P, Jiang Z, Zhang X, Cao X. Tumor-educated B cells selectively promote breast cancer lymph node metastasis by HSPA4-targeting IgG. *Nat Med* 2019; **25**: 312-322 [PMID: 30643287 DOI: 10.1038/s41591-018-0309-y]

30 **Jhunjhunwala S**, Hammer C, Delamarre L. Antigen presentation in cancer: insights into tumour immunogenicity and immune evasion. *Nat Rev Cancer* 2021; **21**: 298-312 [PMID: 33750922 DOI: 10.1038/s41568-021-00339-z]

31 **Oh DY**, Fong L. Cytotoxic CD4(+) T cells in cancer: Expanding the immune effector toolbox. *Immunity* 2021; **54**: 2701-2711 [PMID: 34910940 DOI: 10.1016/j.immuni.2021.11.015]

World Journal of Clinical Oncology

Submit a Manuscript: https://www.f6publishing.com

World J Clin Oncol 2024 January 24; 15(1): 62-88

DOI: 10.5306/wjco.v15.i1.62

ISSN 2218-4333 (online)

ORIGINAL ARTICLE

Clinical and Translational Research

Identification of the key genes and mechanisms associated with transcatheter arterial chemoembolisation refractoriness in hepatocellular carcinoma

Jie-Zhuang Huang, Jian-Di Li, Gang Chen, Rong-Quan He

Specialty type: Biochemistry and molecular biology

Provenance and peer review: Unsolicited article; Externally peer reviewed.

Peer-review model: Single blind

Peer-review report's scientific quality classification

Grade A (Excellent): 0
Grade B (Very good): B
Grade C (Good): 0
Grade D (Fair): 0
Grade E (Poor): 0

P-Reviewer: Lykoudis PM, United Kingdom

Received: October 23, 2023
Peer-review started: October 23, 2023
First decision: November 23, 2023
Revised: December 12, 2023
Accepted: December 28, 2023
Article in press: December 28, 2023
Published online: January 24, 2024

Jie-Zhuang Huang, Rong-Quan He, Department of Medical Oncology, The First Affiliated Hospital of Guangxi Medical University, Nanning 530021, Guangxi Zhuang Autonomous Region, China

Jian-Di Li, Gang Chen, Department of Pathology, The First Affiliated Hospital of Guangxi Medical University, Nanning 530021, Guangxi Zhuang Autonomous Region, China

Corresponding author: Rong-Quan He, MD, PhD, Doctor, Researcher, Department of Medical Oncology, The First Affiliated Hospital of Guangxi Medical University, No. 6 Shuangyong Road, Nanning 530021, Guangxi Zhuang Autonomous Region, China.
herongquan@gxmu.edu.cn

Abstract

BACKGROUND

Transcatheter arterial embolisation (TACE) is the primary treatment for intermediate-stage hepatocellular carcinoma (HCC) patients while some HCC cases have shown resistance to TACE.

AIM

To investigate the key genes and potential mechanisms correlated with TACE refractoriness in HCC.

METHODS

The microarray datasets of TACE-treated HCC tissues, HCC and non-HCC tissues were collected by searching multiple public databases. The respective differentially expressed genes (DEGs) were attained *via limma* R package. Weighted gene co-expression network analysis was employed for identifying the significant modules related to TACE non-response. TACE refractoriness-related genes were obtained by intersecting up-regulated TACE-associated and HCC-associated DEGs together with the genes in significant modules related to TACE non-response. The key genes expression in the above two pairs of samples was compared respectively *via Wilcoxon* tests and standard mean differences model. The prognostic value of the key genes was evaluated by Kaplan-Meier curve. Multivariate analysis was utilised to investigate the independent prognostic factor in key genes. Single-cell RNA (scRNA) sequencing analysis was conducted to explore the cell types in HCC. TACE refractoriness-related genes activity was

calculated *via* AUCell packages. The CellChat R package was used for the investigation of the cell–cell communication between the identified cell types.

RESULTS

HCC tissues of TACE non-responders (n = 66) and TACE responders (n = 81), HCC (n = 3941) and non-HCC (n = 3443) tissues were obtained. The five key genes, DLG associated protein 5 (DLGAP5), Kinesin family member 20A (KIF20A), Assembly factor for spindle microtubules (ASPM), Kinesin family member 11 (KIF11) and TPX2 microtubule nucleation factor (TPX2) in TACE refractoriness-related genes, were identified. The five key genes were all up-regulated in the TACE non-responders group and the HCC group. High expression of the five key genes predicted poor prognosis in HCC. Among the key genes, TPX2 was an independent prognostic factor. Four cell types, hepatocytes, embryonic stem cells, T cells and B cells, were identified in the HCC tissues. The TACE refractoriness-related genes expressed primarily in hepatocytes and embryonic stem cells. Hepatocytes, as the providers of ligands, had the strongest interaction with embryonic stem cells that provided receptors.

CONCLUSION

Five key genes (DLGAP5, KIF20A, ASPM, KIF11 and TPX2) were identified as promoting refractory TACE. Hepatocytes and embryonic stem cells were likely to boost TACE refractoriness.

Key Words: Hepatocellular carcinoma; Transcatheter arterial embolisation refractoriness; Weighted gene co-expression network analysis; Single-cell RNA sequencing; AUCell; CellChat

Core Tip: This is a study that explored the key genes and mechanisms related to transcatheter arterial chemoembolisation (TACE) refractoriness in hepatocellular carcinoma. Through the combination of tissue microarrays and RNA-seq with single-cell RNA sequencing, the TACE refractoriness-related genes were identified and five key genes (DLGAP5, KIF20A, ASPM, KIF11 and TPX2) associated with TACE refractoriness were revealed. The TACE refractoriness-related genes were found to mainly express in hepatocytes and embryonic stem cells. Hepatocytes providing ligands had the strongest interaction with embryonic stem cells as receptors providers.

Citation: Huang JZ, Li JD, Chen G, He RQ. Identification of the key genes and mechanisms associated with transcatheter arterial chemoembolisation refractoriness in hepatocellular carcinoma. *World J Clin Oncol* 2024; 15(1): 62-88
URL: https://www.wjgnet.com/2218-4333/full/v15/i1/62.htm
DOI: https://dx.doi.org/10.5306/wjco.v15.i1.62

INTRODUCTION

Hepatocellular carcinoma (HCC) is a major primary liver tumour, accounting for more than 90% of primary liver tumour cases[1]. HCC is currently the fifth most common cancer worldwide and the second leading cause of cancer death in men, with the five-year survival rate of 18% second only to pancreatic cancer[1]. The complex pathogenesis of HCC and its various risk factors like chronic hepatitis B virus infection and alcohol abuse lead to the increasing incidence of HCC[2,3]. A retrospective study showed that the incidence of HCC increased markedly in America from 1975 to 2016[4]. It is worth noting that HCC is generally diagnosed in its advance stage[5]. The appearance of symptoms stage means the rapid progress of HCC with the poor therapeutic effect and slim survival[6].

Transcatheter arterial embolisation (TACE) is a strategy in which catheters, with the support of various embolisation drugs, are placed in the large arteries, typically the femoral arteries, to block the tumour's blood supply[7,8]. The selection of the treatment is based on the Barcelona Clinic Liver Cancer staging system, which was created according to the number size of the HCC and the performance of the patient[9]. TACE is a standard therapy for intermediate-stage HCC patients[10]. Currently, surgical treatment, liver transplantation and ablation are available for early-HCC patients and contribute to a high survival rate[8,11]. However, metastatic disease may be a barrier to surgical therapy[12]. Local ablation is regarded as a safer alternative to surgery, but it is also not suitable for patients who have tumours in the subcapsular or domed position or near the main bile duct, large blood vessels or the intestine[13]. Patients who cannot benefit from the above treatments despite the early stage of the disease may be candidates for TACE[14]. Chemotherapy is universally considered the first choice for advanced HCC when there is a low pharmaceutical response or the formation of portal vein tumour thrombosis[15]. In clinical practice, multiple combinations of liver-directed therapies (LDT) pave the way for the curative treatment[16], and TACE is still the most widely used as an LDT for locally advanced HCC patients[17]. Therefore, TACE is an important method for treating HCC at all stages.

Unfortunately, some investigations have shown that a load of HCC patients did not respond to TACE, which reduces the efficacy of the systematic therapy significantly[18]. One recent study employed a cohort of HCC patients after TACE treatment, and a series of vitro experiments revealed that pyruvate kinase M1/2 was highly expressed, which may

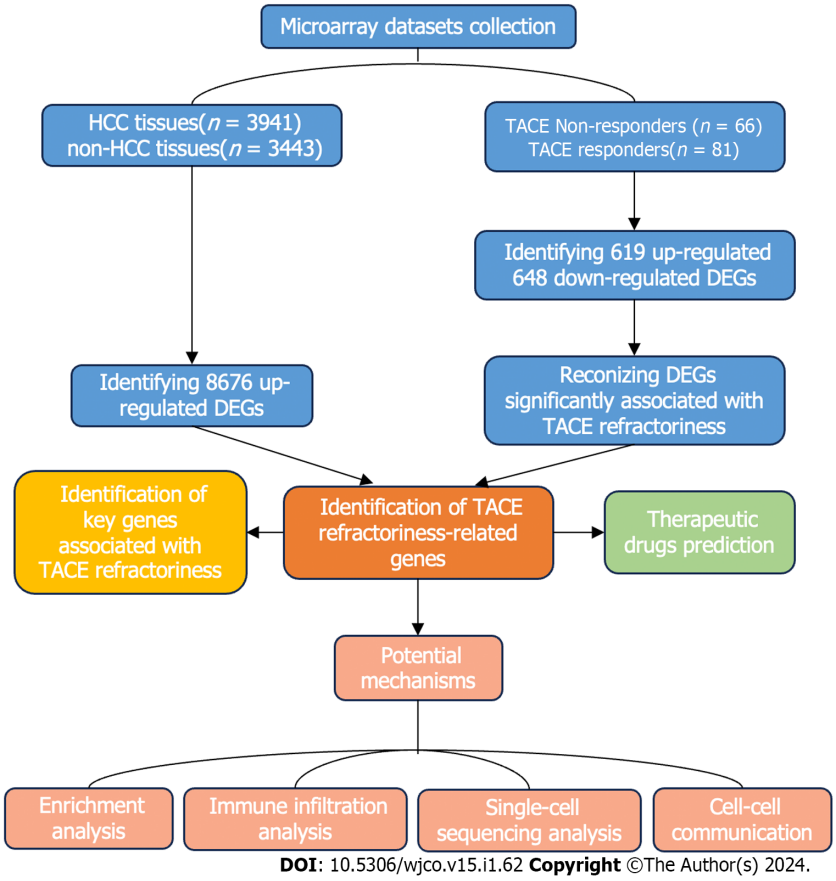

DOI: 10.5306/wjco.v15.i1.62 **Copyright** ©The Author(s) 2024.

Figure 1 The flow chart of the present study. HCC: Hepatocellular carcinoma; DEGs: Differentially expressed genes; TACE: Transcatheter arterial chemoembolisation; WGCNA analysis: Weighted gene co-expression network analysis.

promote HCC tolerance to TACE through glycolysis dysregulation[19], and was associated with a low survival rate in TACE non-response HCC patients. Additionally, another study found that the low expression of miRNA-125b induced an HCC tolerance to TACE through a transcriptome analysis of 680 HCC patients[20]. However, HCC is featured in the high heterogeneity of genetic drivers leading to therapeutic susceptibility[21]. Therefore, individual genes heterogeneity requires the exploration of other potential factors through systematic measures.

In this study, we aimed to identify the key genes of TACE refractoriness in HCC. Additionally, the potential mechanisms of TACE refractoriness in HCC were explored. Finally, potential therapeutic drugs against TACE refractoriness in HCC were discovered. The flow chart of this study is shown in Figure 1.

MATERIALS AND METHODS

Data collection and processing

We retrieved the datasets including TACE non-responders and TACE responders from the Cancer Genome Atlas (TCGA), Gene Expression Omnibus (GEO), International Cancer Genome Consortium and ArrayExpress databases, with the query formulation 'Hepatocellular carcinoma AND Transcatheter arterial embolisation'. The datasets included were required to belong to *Homo sapiens* and contained HCC tissues from TACE non-responders and TACE responders who had not received any prior treatment. Simultaneously, we collected HCC and its control samples from the TCGA, GEO, Genotype-tissue Expression (GTEx) and ArrayExpress databases with keywords 'hepatocellular carcinoma' based on the following criteria: (1) The matrix must be *Homo sapiens*; (2) the data sets should include HCC and normal liver tissues or one of the above groups and can be merged; and (3) the collected samples should not be influenced by any chemicals or physical treatment. Subsequently, the profiles of all of the screened datasets downloaded from the above database were annotated according to the platform annotation files and then conducted by $\log_2(x+1)$ conversion. To integrate the expression matrix from the same platforms or append the lack of normal liver tissue samples in some matrices, the R software (Version 3.6.2) was used to merge and normalise datasets with different sequencing and background through *limma* and surrogate variable analysis (sva) packages.

The screening of differentially expressed genes

The *limma* package was applied to identify the differentially expressed genes (DEGs). The DEGs between TACE non-responders and TACE responders (TACE-associated DEGs) had to meet the requirement of P value < 0.05 and $|\log_2$

(Foldchange)| > 0.5. The DEGs between HCC and non-HCC tissues (HCC-associated DEGs) from the datasets were integrated by calculating the standardised mean difference (SMD). DEGs with $P < 0.05$ and |SMD| > 0 were recorded as the DEGs in HCC.

Weighted gene co-expression network analysis

Weighted gene co-expression network analysis (WGCNA) is a systematic biological method for calculating the correlation among genes for finding gene clusters (modules) and connecting gene modules with external sample traits using eigengene network methodology[22]. In this study, we utilised WGCNA analysis to identify more reliable hub genes associated with TACE refractoriness in HCC.

The co-expression network construction

WGCNA R package was utilised to construct the co-expression network using the expression profile of the TACE-associated DEGs in GSE104580. Firstly, Pearson's correlation matrix and average linkage methods were both used for all pair-wise genes. Secondly, an adjacency matrix was established to calculate the correlation value. The soft threshold was used to emphasise the correlation between two genes and eliminate weak correlations. Thirdly, adjacency was transformed into a topological overlap matrix (TOM) to measure the similarity of the nodes by comparing the weighted correlation between each of the nodes. At the same time, the corresponding dissimilarity (1-TOM) was calculated.

Identification of the clinically significant modules

Module eigengene was the first principal component of the module and was defined as the expression file of the whole genes in the module. The correlation coefficient between module eigengene and the clinical trait, namely the reactivity to TACE, was calculated to identify the clinically significant module. Module membership was regarded as the correlation between the genes and the module eigengene and was used to evaluate whether the genes belonged to the module or not. Additionally, gene significance was defined as the mediated *P* in the linear regression between expression and clinical traits. In addition, module significance was the average absolute gene significance of whole genes in the module. Finally, the modules with the top-two correlation coefficients between module eigengene and clinical status TACE non-responders were selected as the clinically significant modules for further analysis.

The screening of key genes in the protein–protein interaction network

The up-regulated genes in TACE-associated DEGs, up-regulated HCC-associated DEGs and the genes in the clinically significant modules were intersected and their shared genes were considered as TACE refractoriness-related genes. TACE refractoriness-related genes were utilised for protein–protein interaction (PPI) network construction *via* STRING database. Then, the key genes were identified using the Maximal Clique Centrality (MCC) method of cytoHubba plugin in Cytoscape software (Version 3.7.2). MCC algorithm is a method of scoring each protein in the PPI network. A higher score means the protein is associated with more proteins in the network.

The validation of the key genes in expression and prognosis

The mRNA expression level of the key genes between TACE non-responders and TACE responders was compared through *Wilcoxon* tests. Then, to verify that the key genes were differentially expressed in HCC, SMD model and a 95% confidence interval (95%CI) were carried out using Meta R packages and STATA 12.0 by integrating the datasets containing HCC and non-HCC tissues. A random-effect model or fixed-effect model was selected in the light of the I^2 test and Chi-square test. The random-effect model was chosen when there was high heterogeneity ($I^2 > 50\%$ or $P < 0.05$). Otherwise, the fixed-effect model was chosen. Sensibility analysis was conducted to detect the high heterogeneous datasets. The protein expression of key genes in HCC tissues was compared to that in non-HCC tissues by browsing The Human Protein Atlas (THPA) database. We then gathered the clinical information of the HCC tissues in the datasets. The clinical information was required to include survival status and survival time, and only the clinical information in TCGA datasets was eligible. To identify the independent prognostic factors in the key genes, multivariate analysis was used. For survival analysis, the optimum cut-off for division into high expression and low expression group was determined by running Survminer and Survival packages and the hazard ratio (HR) was calculated by Cox-proportional hazards regression model. Finally, the Kaplan–Meier was visualised using the Survival package.

Gene sets enrichment analysis

TACE refractoriness-related genes were utilised in gene ontology (GO) annotation analysis, Kyoto Encyclopaedia of Genes and Genomes (KEGG) pathway using the clusterProfiler R package and Reactome pathway using Reactome pathway database. The terms with $P < 0.05$ and FDR < 0.25 were considered statistically significant. The top-five GO terms in respect to biological process (BP), cellular component (CC) and molecular function (MF) were investigated. Finally, the KEGG pathways and the top-ten Reactome pathways were visualised.

Single-cell RNA sequencing data pre-processing and cell type identification

To further explore the cell types involved in TACE refractoriness, single-cell RNA sequencing (scRNA-seq) analysis was adopted. The scRNA-seq data were obtained from the GEO database with the search strategy 'ScRNA OR Single Cell AND Hepatocellular Carcinoma'. The samples in the scRNA-seq data had to be HCC samples that were not treated using any chemical or physical factors. The quality control process of the scRNA-seq data was performed with the Seurat R package. Cells with < 500 genes, > 6000 genes or > 20% mitochondrial genes were filtered out. Then, the gene expression matrix was normalised and scaled. Subsequently, the Harmony R package was employed for eliminating batch effect. A

uniform manifold approximation and projection (UMAP) analysis was performed for dimensional reduction. The FindClusters function was able to classify the cells into different clusters with a resolution of 0.5, and the annotation of the cell clusters depended on the SingleR package. The activity of TACE refractoriness-related genes in each cell line was determined using the AUCell R package. Cells expressing more TACE refractoriness-related genes had higher area under-the-curve (AUC) values. The 'AUCell_exploreThresholds' function was used to determine the threshold for identifying TACE refractoriness-related genes' active cells. The AUC score of each cell was then mapped to the UMAP plot embedding using the ggplot2 R package to visualise the active clusters.

Cell–cell communication analysis

CellChat, an open R package, was utilised for the analysis of intercellular communications using scRNA-seq data[23]. After identifying the cell types in the HCC tissues, the CellChat R package (Version 1.1.3) was employed to investigate the number of interactions, the communication strength and the over-expressed ligands and receptors between each identified cell type. The discovery of overexpressed ligand-receptor pairs was based on the data of ligand-receptor pairs related to 'Secreted Signalling' in datasets CellChatDB. The communication probability was calculated by means of the function 'computeCommunProb' in the CellChat R package. Subsequently, the cell–cell communication was predicted and aggregated. The number of interactions was visualised to show integrated communication.

Immune infiltration analysis

To elucidate the correlation between the TACE resistance and tumour microenvironment in the HCC, we conducted immune infiltration analysis based on CIBERSORT and xCell algorithm. The CIBERSORT algorithm is a deconvolution method used, in this case, to process marker gene expression values to estimate the proportion of various types of immune cells[24]. The xCell algorithm was performed for cell-type enrichment analysis from gene expression data of 64 immune and stroma cell types[25]. In this study, the CIBERSORT algorithm assessed the proportions of 22 kinds of immune cells between TACE non-responders and TACE responders. Meanwhile, the relationship between the expression of the five key genes and the 22 kinds of immune cells' infiltration in the HCC samples from TACE non-responders was explored. The xCell algorithm evaluated the immune score, stromal score, microenvironment score and proportions of the cell types of the scRNA-seq analysis. Statistical significance required $P < 0.05$.

The exploration of potential therapeutic drugs

The pRRophetic R package was adopted to predict the half maximal inhibitory concentration (IC50) of chemotherapeutic agents antagonising HCC in the Genomics of Drug Sensitivity in Cancer database. IC_{50} represented the effectiveness of each kind of chemotherapeutic agent inhibiting specific biological or biochemical functions. The comparison of the IC_{50}s of the TACE non-responders group and the TACE responders group was tested by *Wilcoxon* signed-rank test.

RESULTS

Data collection and differentially expressed gene screening

The gene expression matrix GSE104580 including HCC samples of 66 TACE non-responders and 81 TACE- responders was obtained from the GEO database. The screening procedure can be seen in Figure 2. Additionally, a total of 3941 HCC and 3443 non-HCC samples were obtained from the TCGA, GEO, GTEx and ArrayExpress databases. The 85 studies that included HCC and non-HCC tissues were collected according to the procedure in Figure 3. The detailed information of the 84 datasets (datasets from TCGA and GTEx databases have been merged as one dataset) are listed in Supplementary Table 1. A total of 619 up-regulated and 648 down-regulated TACE-associated DEGs were screened and visualised (Figure 4A). The expression levels of the 30 top up-regulated and down-regulated DEGs were respectively performed (Figure 4B). In addition, 8676 up-regulated and 7125 down-regulated HCC-associated DEGs were obtained after integrating DEGs from 85 studies.

Constructing the co-expression modules

The expression file of 1267 TACE-associated DEGs and the clinical traits in GSE104580 were used for the WGCNA analysis. The soft-threshold $\beta = 7$ with the highest scan-free topology model fit ($R^2 = 0.88$) and the mean connectivity lower than 100 was set to construct a scan-free network (Figure 5A and B). Subsequently, the adjacency matrix was built and turned into a TOM to establish a gene-clustering dendrogram (Figure 5C). As shown in Figure 5C, each colour in the merge-dynamic row corresponds to a gene module after they were merged based on the cut line 0.25, and, finally, a total of five modules were identified.

The identification of clinically significant modules and the key genes

The clinical traits, namely reactivity to TACE in GSE104580, were combined with the five identified modules to screen for the clinically significant module(s) (Figure 5D). Finally, the blue and grey modules were identified as the clinically significant modules due to having the highest correlation coefficient with the clinical trait TACE non-responders. A total of 195 genes were in the blue and grey modules. After intersecting 619 up-regulated TACE-associated DEGs, 8676 up-regulated HCC-associated DEGs and 195 genes in the clinically significant modules, a total of 112 shared genes were identified as TACE refractoriness-related genes for further analysis (Figure 5E). According to the scoring results from the MCC algorithm, the top-five genes had relatively high scores, while the rest had extremely low scores. To ensure

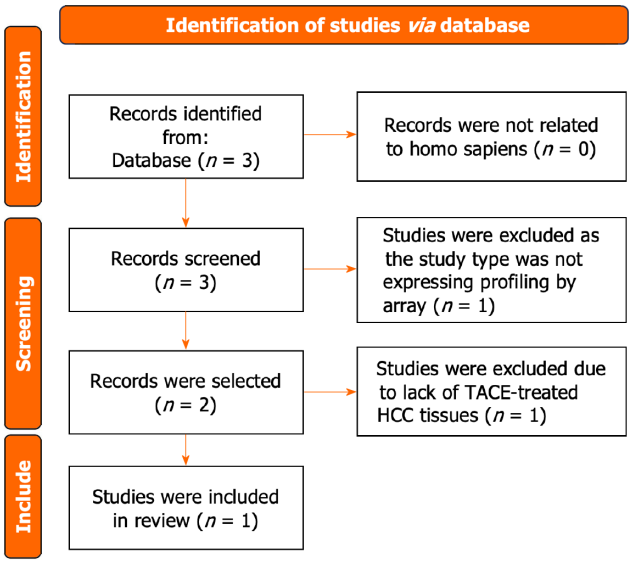

DOI: 10.5306/wjco.v15.i1.62 **Copyright** ©The Author(s) 2024.

Figure 2 Flow chart showing the collection of the transcatheter arterial embolisation-treated hepatocellular carcinoma samples. Finally, one study was included. HCC: Hepatocellular carcinoma; TACE: Transcatheter arterial chemoembolization.

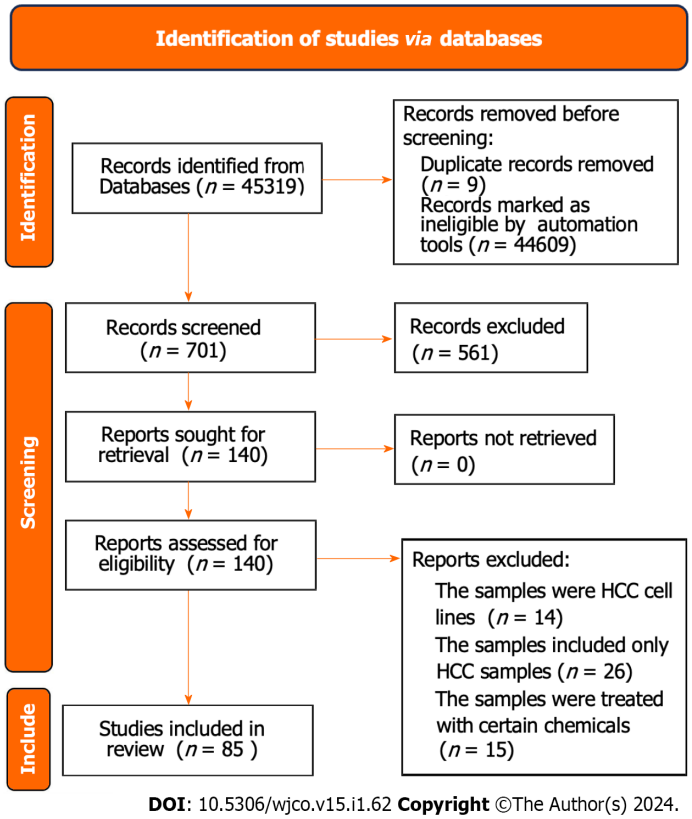

DOI: 10.5306/wjco.v15.i1.62 **Copyright** ©The Author(s) 2024.

Figure 3 Flow chart of the acquisition of hepatocellular carcinoma and non- hepatocellular carcinoma samples *via* database. The information from 85 studies is displayed in Supplementary Table 1. HCC: Hepatocellular carcinoma.

reliability and accuracy, we selected the top-five genes as the key genes among the TACE refractoriness-related genes. The five key genes, DLG associated protein 5 (DLGAP5), Kinesin family member 20A (KIF20A), Assembly factor for spindle microtubules (ASPM), Kinesin family member 11 (KIF11) and TPX2 microtubule nucleation factor (TPX2), were identified using the MCC methods in the CytoHubb plugin contained in Cytoscape software (Figure 6A).

The expression validation of key genes in TACE-treated HCC samples

To ascertain the key genes' differential expression in the HCC samples of the TACE non-responders and TACE responders, the mRNA expression of DLGAP5, KIF20A, ASPM, KIF11 and TPX2 was analysed. The results showed that

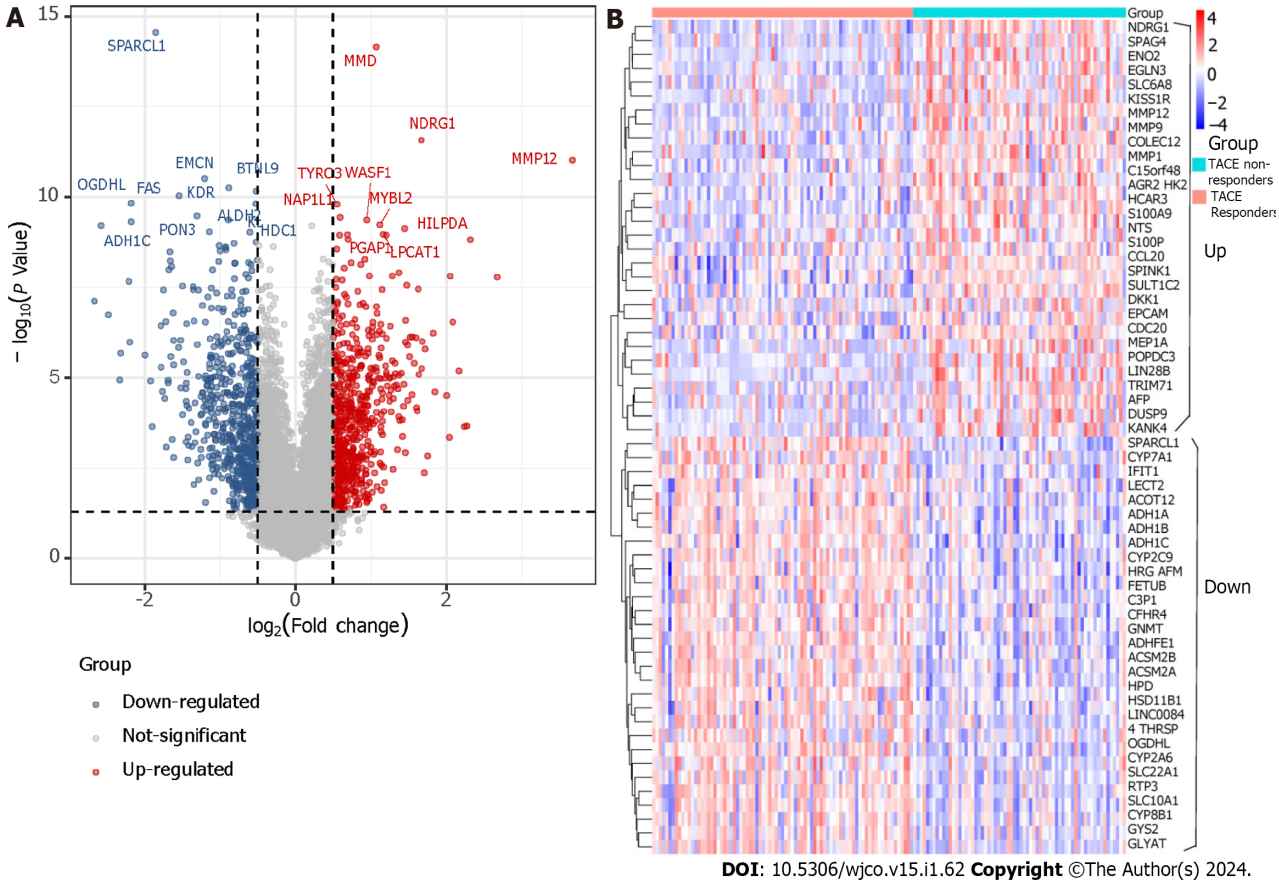

DOI: 10.5306/wjco.v15.i1.62 **Copyright** ©The Author(s) 2024.

Figure 4 Differentially expressed genes screening. A: The screening of differentially expressed genes (DEGs) between transcatheter arterial embolisation (TACE) non-responders and TACE responders (TACE-associated DEGs) in GSE104580. B: The expression level of the top-30 up-regulated and down-regulated TACE-associated DEGs.

the five key genes were all more highly expressed in the TACE non-responders group compared with TACE responders group (Figure 6B).

The expression validation of key genes in HCC via integrated data

After integrating all enrolled data including HCC and non-HCC tissues, we found that the SMD and 95%CI of the five key genes under random effects were as follows: DLGAP5 (SMD: 1.54, 95%CI: 1.38–1.90), KIF20A (SMD: 1.88, 95%CI: 1.63–2.13), ASPM (SMD: 2.00, 95%CI: 1.74–2.25), KIF11 (SMD: 1.45, 95%CI: 1.20–1.70) and TPX2 (SMD: 1.64, 95%CI: 1.43–1.85) (Figure 7). These indicated that the expression level of the five key genes was remarkably higher in the HCC than in the non-HCC tissues. The protein expression of key genes DLGAP5, KIF20A, KIF11 and TPX2 in the HCC tissues was higher than in the non-HCC tissues (Figure 8). The IHC resource for protein expression of ASPM was lack in THPA database.

The prognostic value of key genes

TPX2 was considered an independent prognostic factor in HCC *via* multivariate analysis (Figure 9A). The results showed that a high expression of the key genes was correlated with a low overall survival. To verify the key genes participating in HCC poor prognosis, the survival curves are shown in Figure 9B–F. In addition, HR was as follows: DLGAP5 (HR: 2.197, $P < 0.0001$), KIF20A (HR: 3.940, $P < 0.0001$), ASPM (HR: 2.702, $P = 0.0011$), KIF11 (HR: 4.021, $P < 0.0001$) and TPX2 (HR: 3.287, $P < 0.0001$).

GO enrichment and pathway analysis

For BP, the 112 TACE refractoriness-related genes were mainly enriched in nuclear division, organelle fission, mitotic nuclear division, chromosome segregation and mitotic sister chromatid segregation. CC involved spindle, chromosomal region, chromosome, centromeric region, microtubule and midbody. As for MF, these TACE refractoriness-related genes were associated with microtubule binding, tubulin binding, microtubule motor activity, cytoskeletal motor activity and peptidase regulator activity (Figure 10A). With regards to the pathways, these TACE refractoriness-related genes were mainly active in cell cycle pathways in the KEGG pathway enrichment analysis, and the relevant reactome pathways are shown in Figure 10B.

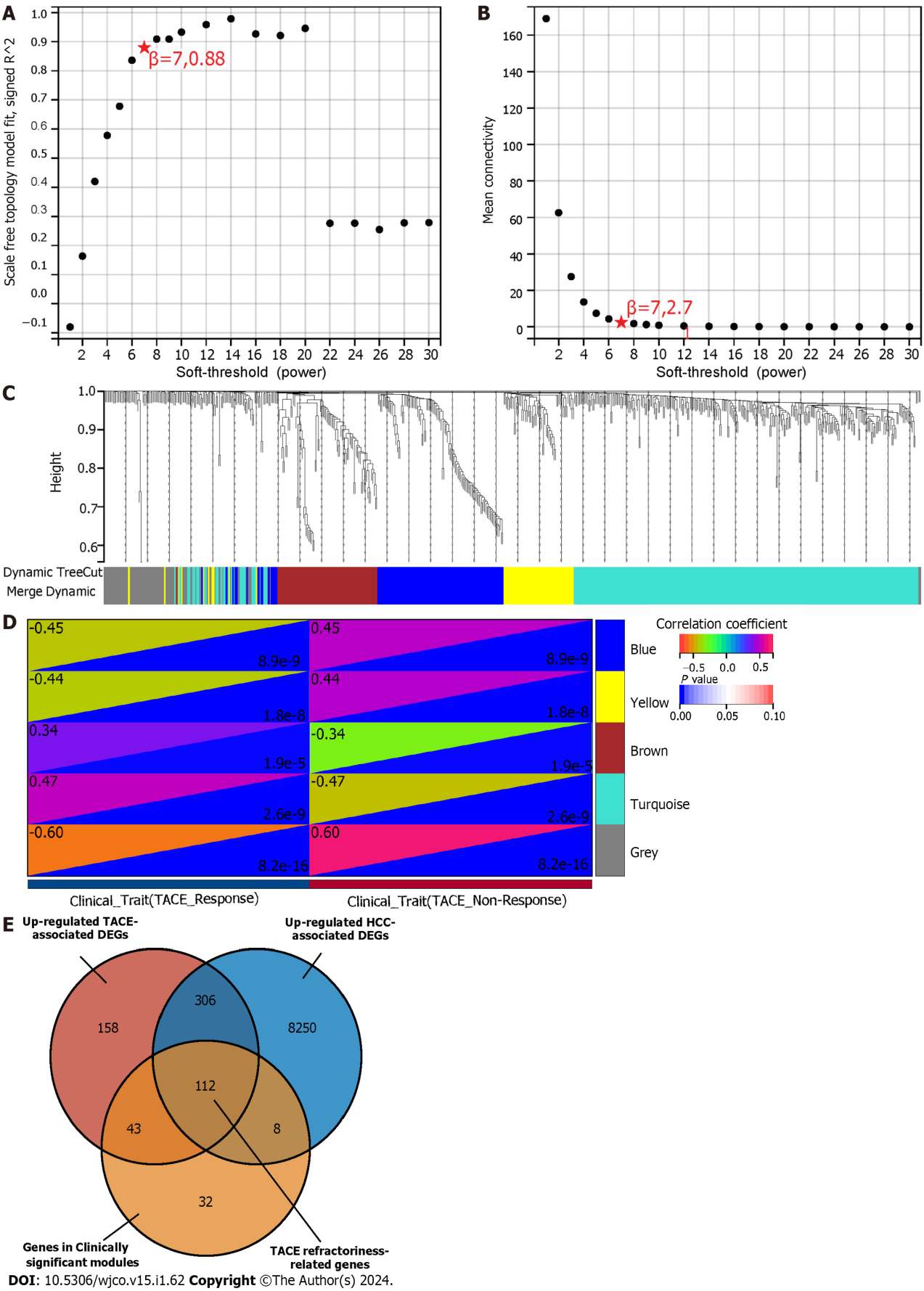

DOI: 10.5306/wjco.v15.i1.62 **Copyright** ©The Author(s) 2024.

Figure 5 Weighted gene co-expression network analysis and identification of transcatheter arterial embolisation refractoriness-related genes. A: The scale-free index for various soft-threshold powers; B: Analysis of the mean connectivity for various soft-threshold powers; C: Gene clustering dendrogram, with dissimilarity based on topological overlap, together with assigned module colours; D: Module-trait association. Blue and grey modules were

identified as the clinically significant modules due to their highest coefficient correlations; E: The identification of 112 TACE refractoriness-associated genes. TACE: Transcatheter arterial embolisation.

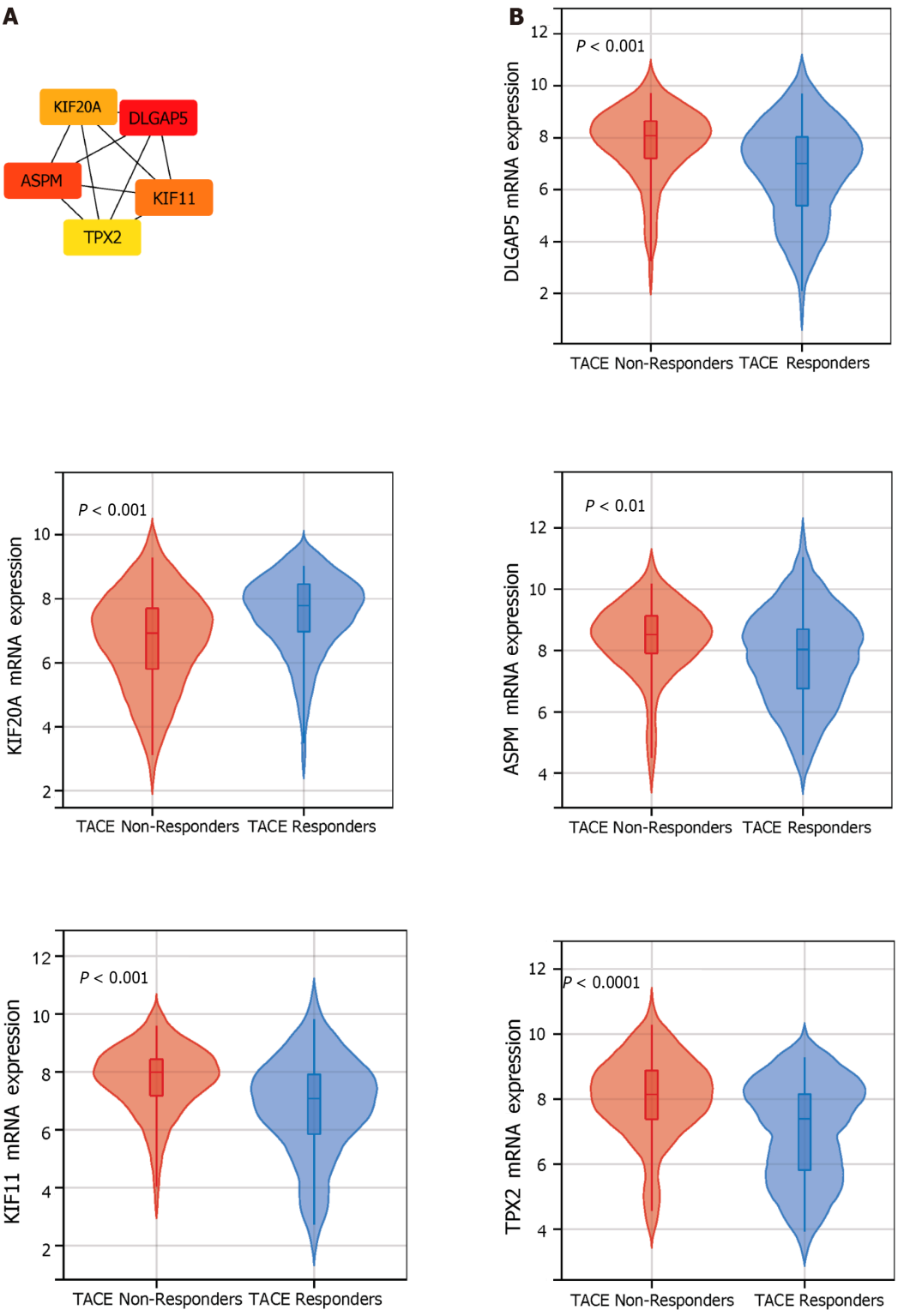

DOI: 10.5306/wjco.v15.i1.62

Figure 6 The identification and mRNA expression of five key genes in transcatheter arterial embolisation treated hepatocellular carcinoma. A: Five key genes were identified using Maximal Clique Centrality method of the cytoHubba plugin. B: The mRNA expression level of the five key genes in hepatocellular carcinoma samples of transcatheter arterial embolisation (TACE) non-responders and TACE responders. DLGAP5: DLG-associated protein 5; KIF20A: Kinesin family member 20A; ASPM: Assembly factor for spindle microtubules; KIF11: Kinesin family member 11; TPX2: TPX2 microtubule nucleation factor.

A

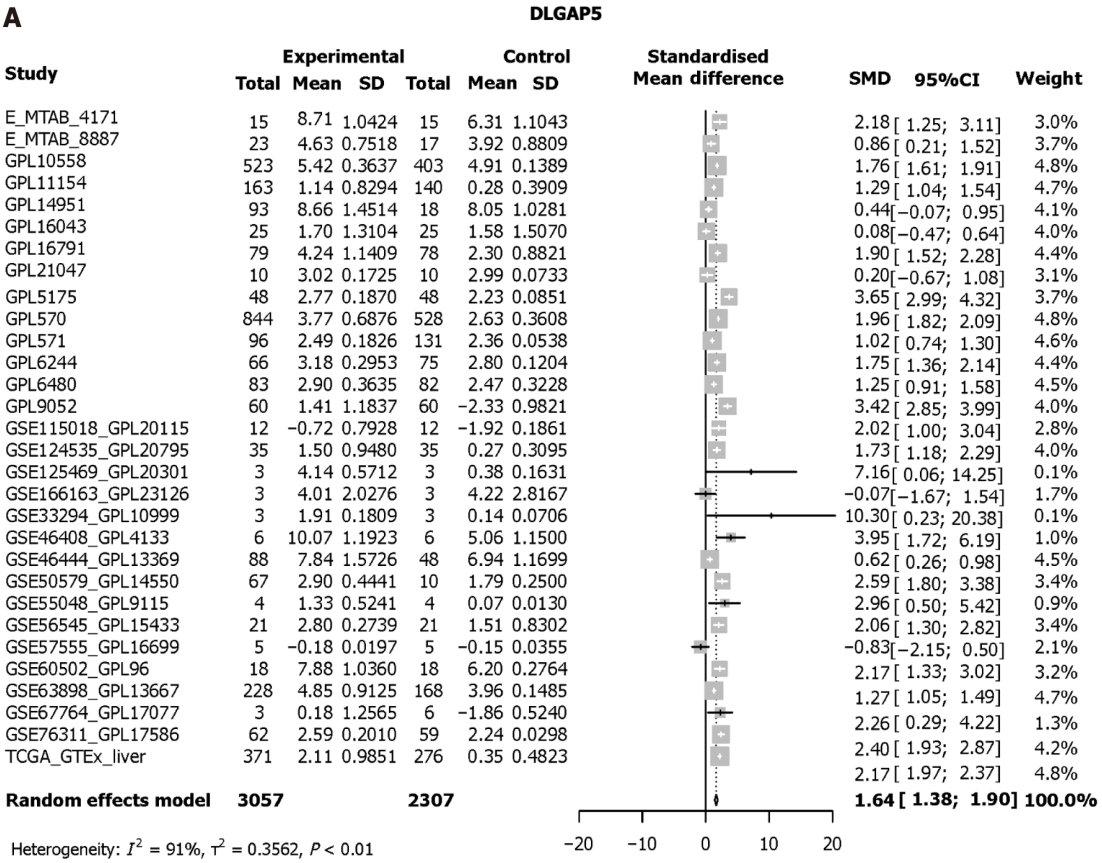
DLGAP5
Study
Experimental Total Mean SD
Control Total Mean SD
Standardised Mean difference
SMD 95%CI Weight
E_MTAB_4171 15 8.71 1.0424 15 6.31 1.1043 2.18 [1.25; 3.11] 3.0%
E_MTAB_8887 23 4.63 0.7518 17 3.92 0.8809 0.86 [0.21; 1.52] 3.7%
GPL10558 523 5.42 0.3637 403 4.91 0.1389 1.76 [1.61; 1.91] 4.8%
GPL11154 163 1.14 0.8294 140 0.28 0.3909 1.29 [1.04; 1.54] 4.7%
GPL14951 93 8.66 1.4514 18 8.05 1.0281 0.44 [−0.07; 0.95] 4.1%
GPL16043 25 1.70 1.3104 25 1.58 1.5070 0.08 [−0.47; 0.64] 4.0%
GPL16791 79 4.24 1.1409 78 2.30 0.8821 1.90 [1.52; 2.28] 4.4%
GPL21047 10 3.02 0.1725 10 2.99 0.0733 0.20 [−0.67; 1.08] 3.1%
GPL5175 48 2.77 0.1870 48 2.23 0.0851 3.65 [2.99; 4.32] 3.7%
GPL570 844 3.77 0.6876 528 2.63 0.3608 1.96 [1.82; 2.09] 4.8%
GPL571 96 2.49 0.1826 131 2.36 0.0538 1.02 [0.74; 1.30] 4.6%
GPL6244 66 3.18 0.2953 75 2.80 0.1204 1.75 [1.36; 2.14] 4.4%
GPL6480 83 2.90 0.3635 82 2.47 0.3228 1.25 [0.91; 1.58] 4.5%
GPL9052 60 1.41 1.1837 60 −2.33 0.9821 3.42 [2.85; 3.99] 4.0%
GSE115018_GPL20115 12 −0.72 0.7928 12 −1.92 0.1861 2.02 [1.00; 3.04] 2.8%
GSE124535_GPL20795 35 1.50 0.9480 35 0.27 0.3095 1.73 [1.18; 2.29] 4.0%
GSE125469_GPL20301 3 4.14 0.5712 3 0.38 0.1631 7.16 [0.06; 14.25] 0.1%
GSE166163_GPL23126 3 4.01 2.0276 3 4.22 2.8167 −0.07 [−1.67; 1.54] 1.7%
GSE33294_GPL10999 3 1.91 0.1809 3 0.14 0.0706 10.30 [0.23; 20.38] 0.1%
GSE46408_GPL4133 6 10.07 1.1923 6 5.06 1.1500 3.95 [1.72; 6.19] 1.0%
GSE46444_GPL13369 88 7.84 1.5726 48 6.94 1.1699 0.62 [0.26; 0.98] 4.5%
GSE50579_GPL14550 67 2.90 0.4441 10 1.79 0.2500 2.59 [1.80; 3.38] 3.4%
GSE55048_GPL9115 4 1.33 0.5241 4 0.07 0.0130 2.96 [0.50; 5.42] 0.9%
GSE56545_GPL15433 21 2.80 0.2739 21 1.51 0.8302 2.06 [1.30; 2.82] 3.4%
GSE57555_GPL16699 5 −0.18 0.0197 5 −0.15 0.0355 −0.83 [−2.15; 0.50] 2.1%
GSE60502_GPL96 18 7.88 1.0360 18 6.20 0.2764 2.17 [1.33; 3.02] 3.2%
GSE63898_GPL13667 228 4.85 0.9125 168 3.96 0.1485 1.27 [1.05; 1.49] 4.7%
GSE67764_GPL17077 3 0.18 1.2565 6 −1.86 0.5240 2.26 [0.29; 4.22] 1.3%
GSE76311_GPL17586 62 2.59 0.2010 59 2.24 0.0298 2.40 [1.93; 2.87] 4.2%
TCGA_GTEx_liver 371 2.11 0.9851 276 0.35 0.4823 2.17 [1.97; 2.37] 4.8%
Random effects model 3057 2307 1.64 [1.38; 1.90] 100.0%
Heterogeneity: I^2 = 91%, τ^2 = 0.3562, P < 0.01
−20 −10 0 10 20

B

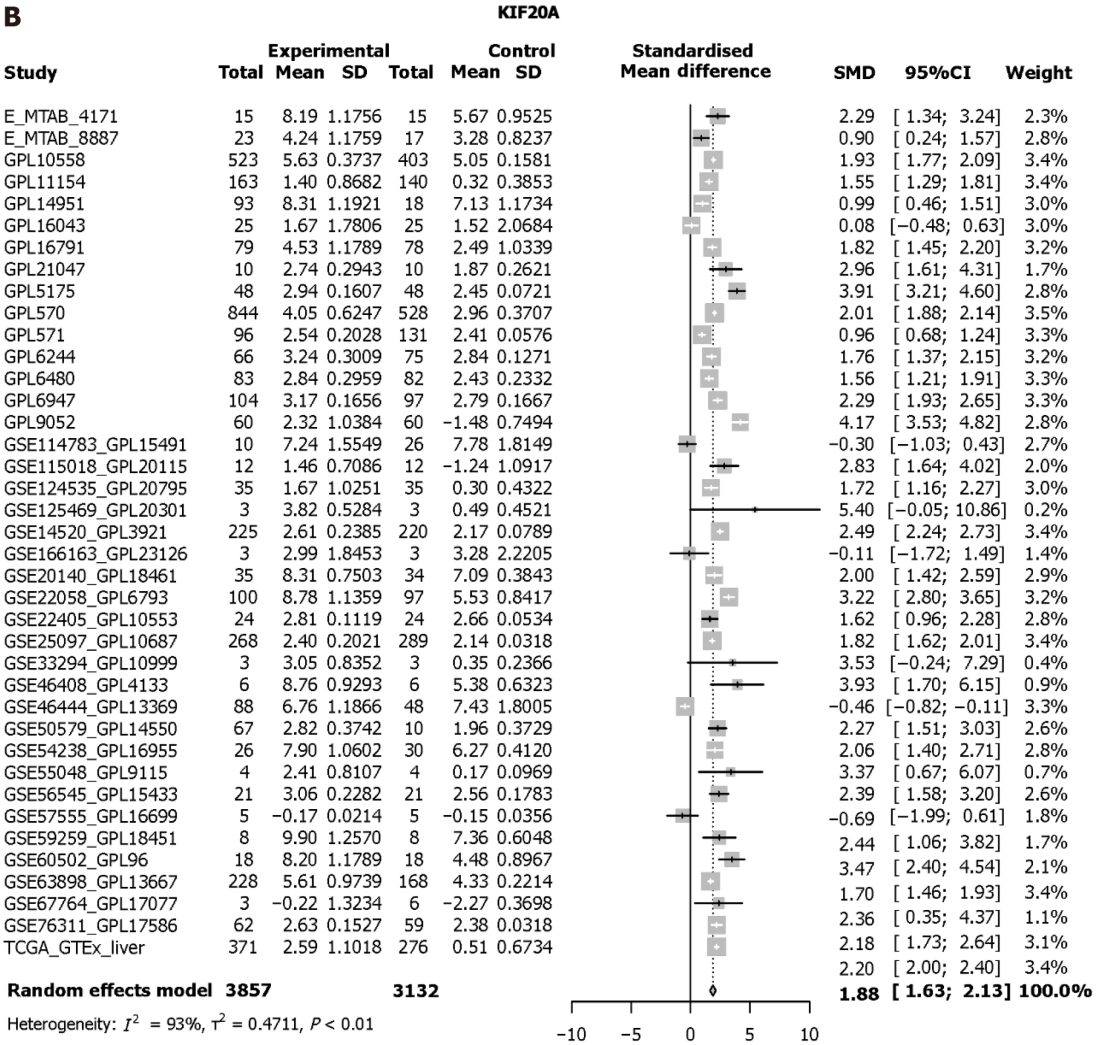
KIF20A
Study
Experimental Total Mean SD
Control Total Mean SD
Standardised Mean difference
SMD 95%CI Weight
E_MTAB_4171 15 8.19 1.1756 15 5.67 0.9525 2.29 [1.34; 3.24] 2.3%
E_MTAB_8887 23 4.24 1.1759 17 3.28 0.8237 0.90 [0.24; 1.57] 2.8%
GPL10558 523 5.63 0.3737 403 5.05 0.1581 1.93 [1.77; 2.09] 3.4%
GPL11154 163 1.40 0.8682 140 0.32 0.3853 1.55 [1.29; 1.81] 3.4%
GPL14951 93 8.31 1.1921 18 7.13 1.1734 0.99 [0.46; 1.51] 3.0%
GPL16043 25 1.67 1.7806 25 1.52 2.0684 0.08 [−0.48; 0.63] 3.0%
GPL16791 79 4.53 1.1789 78 2.49 1.0339 1.82 [1.45; 2.20] 3.2%
GPL21047 10 2.74 0.2943 10 1.87 0.2621 2.96 [1.61; 4.31] 1.7%
GPL5175 48 2.94 0.1607 48 2.45 0.0721 3.91 [3.21; 4.60] 2.8%
GPL570 844 4.05 0.6247 528 2.96 0.3707 2.01 [1.88; 2.14] 3.5%
GPL571 96 2.54 0.2028 131 2.41 0.0576 0.96 [0.68; 1.24] 3.3%
GPL6244 66 3.24 0.3009 75 2.84 0.1271 1.76 [1.37; 2.15] 3.2%
GPL6480 83 2.84 0.2959 82 2.43 0.2332 1.56 [1.21; 1.91] 3.3%
GPL6947 104 3.17 0.1656 97 2.79 0.1667 2.29 [1.93; 2.65] 3.3%
GPL9052 60 2.32 1.0384 60 −1.48 0.7494 4.17 [3.53; 4.82] 2.8%
GSE114783_GPL15491 10 7.24 1.5549 26 7.78 1.8149 −0.30 [−1.03; 0.43] 2.7%
GSE115018_GPL20115 12 1.46 0.7086 12 −1.24 1.0917 2.83 [1.64; 4.02] 2.0%
GSE124535_GPL20795 35 1.67 1.0251 35 0.30 0.4322 1.72 [1.16; 2.27] 3.0%
GSE125469_GPL20301 3 3.82 0.5284 3 0.49 0.4521 5.40 [−0.05; 10.86] 0.2%
GSE14520_GPL3921 225 2.61 0.2385 220 2.17 0.0789 2.49 [2.24; 2.73] 3.4%
GSE166163_GPL23126 3 2.99 1.8453 3 3.28 2.2205 −0.11 [−1.72; 1.49] 1.4%
GSE20140_GPL18461 35 8.31 0.7503 34 7.09 0.3843 2.00 [1.42; 2.59] 2.9%
GSE22058_GPL6793 100 8.78 1.1359 97 5.53 0.8417 3.22 [2.80; 3.65] 3.2%
GSE22405_GPL10553 24 2.81 0.1119 24 2.66 0.0534 1.62 [0.96; 2.28] 2.8%
GSE25097_GPL10687 268 2.40 0.2021 289 2.14 0.0318 1.82 [1.62; 2.01] 3.4%
GSE33294_GPL10999 3 3.05 0.8352 3 0.35 0.2366 3.53 [−0.24; 7.29] 0.4%
GSE46408_GPL4133 6 8.76 0.9293 6 5.38 0.6323 3.93 [1.70; 6.15] 0.9%
GSE46444_GPL13369 88 6.76 1.1866 48 7.43 1.8005 −0.46 [−0.82; −0.11] 3.3%
GSE50579_GPL14550 67 2.82 0.3742 10 1.96 0.3729 2.27 [1.51; 3.03] 2.6%
GSE54238_GPL16955 26 7.90 1.0602 30 6.27 0.4120 2.06 [1.40; 2.71] 2.8%
GSE55048_GPL9115 4 2.41 0.8107 4 0.17 0.0969 3.37 [0.67; 6.07] 0.7%
GSE56545_GPL15433 21 3.06 0.2282 21 2.56 0.1783 2.39 [1.58; 3.20] 2.6%
GSE57555_GPL16699 5 −0.17 0.0214 5 −0.15 0.0356 −0.69 [−1.99; 0.61] 1.8%
GSE59259_GPL18451 8 9.90 1.2570 8 7.36 0.6048 2.44 [1.06; 3.82] 1.7%
GSE60502_GPL96 18 8.20 1.1789 18 4.48 0.8967 3.47 [2.40; 4.54] 2.1%
GSE63898_GPL13667 228 5.61 0.9739 168 4.33 0.2214 1.70 [1.46; 1.93] 3.4%
GSE67764_GPL17077 3 −0.22 1.3234 6 −2.27 0.3698 2.36 [0.35; 4.37] 1.1%
GSE76311_GPL17586 62 2.63 0.1527 59 2.38 0.0318 2.18 [1.73; 2.64] 3.1%
TCGA_GTEx_liver 371 2.59 1.1018 276 0.51 0.6734 2.20 [2.00; 2.40] 3.4%
Random effects model 3857 3132 1.88 [1.63; 2.13] 100.0%
Heterogeneity: I^2 = 93%, τ^2 = 0.4711, P < 0.01
−10 −5 0 5 10

C

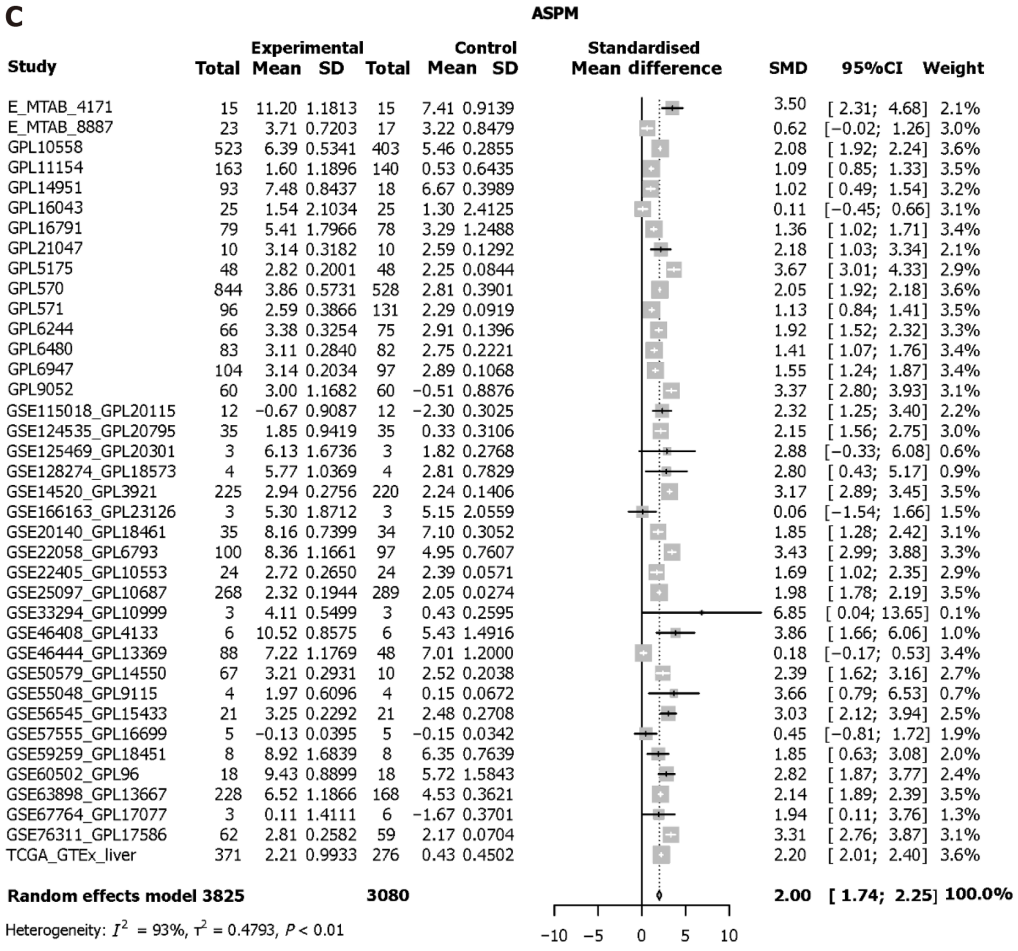
ASPM
Experimental
Control
Standardised Mean difference
Study Total Mean SD Total Mean SD SMD 95%CI Weight
E_MTAB_4171 15 11.20 1.1813 15 7.41 0.9139 3.50 [2.31; 4.68] 2.1%
E_MTAB_8887 23 3.71 0.7203 17 3.22 0.8479 0.62 [−0.02; 1.26] 3.0%
GPL10558 523 6.39 0.5341 403 5.46 0.2855 2.08 [1.92; 2.24] 3.6%
GPL11154 163 1.60 1.1896 140 0.53 0.6435 1.09 [0.85; 1.33] 3.5%
GPL14951 93 7.48 0.8437 18 6.67 0.3989 1.02 [0.49; 1.54] 3.2%
GPL16043 25 1.54 2.1034 25 1.30 2.4125 0.11 [−0.45; 0.66] 3.1%
GPL16791 79 5.41 1.7966 78 3.29 1.2488 1.36 [1.02; 1.71] 3.4%
GPL21047 10 3.14 0.3182 10 2.59 0.1292 2.18 [1.03; 3.34] 2.1%
GPL5175 48 2.82 0.2001 48 2.25 0.0844 3.67 [3.01; 4.33] 2.9%
GPL570 844 3.86 0.5731 528 2.81 0.3901 2.05 [1.92; 2.18] 3.6%
GPL571 96 2.59 0.3866 131 2.29 0.0919 1.13 [0.84; 1.41] 3.5%
GPL6244 66 3.38 0.3254 75 2.91 0.1396 1.92 [1.52; 2.32] 3.3%
GPL6480 83 3.11 0.2840 82 2.75 0.2221 1.41 [1.07; 1.76] 3.4%
GPL6947 104 3.14 0.2034 97 2.89 0.1068 1.55 [1.24; 1.87] 3.4%
GPL9052 60 3.00 1.1682 60 −0.51 0.8876 3.37 [2.80; 3.93] 3.1%
GSE115018_GPL20115 12 −0.67 0.9087 12 −2.30 0.3025 2.32 [1.25; 3.40] 2.2%
GSE124535_GPL20795 35 1.85 0.9419 35 0.33 0.3106 2.15 [1.56; 2.75] 3.0%
GSE125469_GPL20301 3 6.13 1.6736 3 1.82 0.2768 2.88 [−0.33; 6.08] 0.6%
GSE128274_GPL18573 4 5.77 1.0369 4 2.81 0.7829 2.80 [0.43; 5.17] 0.9%
GSE14520_GPL3921 225 2.94 0.2756 220 2.24 0.1406 3.17 [2.89; 3.45] 3.5%
GSE166163_GPL23126 3 5.30 1.8712 3 5.15 2.0559 0.06 [−1.54; 1.66] 1.5%
GSE20140_GPL18461 35 8.16 0.7399 34 7.10 0.3052 1.85 [1.28; 2.42] 3.1%
GSE22058_GPL6793 100 8.36 1.1661 97 4.95 0.7607 3.43 [2.99; 3.88] 3.3%
GSE22405_GPL10553 24 2.72 0.2650 24 2.39 0.0571 1.69 [1.02; 2.35] 2.9%
GSE25097_GPL10687 268 2.32 0.1944 289 2.05 0.0274 1.98 [1.78; 2.19] 3.5%
GSE33294_GPL10999 3 4.11 0.5499 3 0.43 0.2595 6.85 [0.04; 13.65] 0.1%
GSE46408_GPL4133 6 10.52 0.8575 6 5.43 1.4916 3.86 [1.66; 6.06] 1.0%
GSE46444_GPL13369 88 7.22 1.1769 48 7.01 1.2000 0.18 [−0.17; 0.53] 3.4%
GSE50579_GPL14550 67 3.21 0.2931 10 2.52 0.2038 2.39 [1.62; 3.16] 2.7%
GSE55048_GPL9115 4 1.97 0.6096 4 0.15 0.0672 3.66 [0.79; 6.53] 0.7%
GSE56545_GPL15433 21 3.25 0.2292 21 2.48 0.2708 3.03 [2.12; 3.94] 2.5%
GSE57555_GPL16699 5 −0.13 0.0395 5 −0.15 0.0342 0.45 [−0.81; 1.72] 1.9%
GSE59259_GPL18451 8 8.92 1.6839 8 6.35 0.7639 1.85 [0.63; 3.08] 2.0%
GSE60502_GPL96 18 9.43 0.8899 18 5.72 1.5843 2.82 [1.87; 3.77] 2.4%
GSE63898_GPL13667 228 6.52 1.1866 168 4.53 0.3621 2.14 [1.89; 2.39] 3.5%
GSE67764_GPL17077 3 0.11 1.4111 6 −1.67 0.3701 1.94 [0.11; 3.76] 1.3%
GSE76311_GPL17586 62 2.81 0.2582 59 2.17 0.0704 3.31 [2.76; 3.87] 3.1%
TCGA_GTEx_liver 371 2.21 0.9933 276 0.43 0.4502 2.20 [2.01; 2.40] 3.6%
Random effects model 3825 3080 2.00 [1.74; 2.25] 100.0%
Heterogeneity: I^2 = 93%, τ^2 = 0.4793, P < 0.01
−10 −5 0 5 10

D

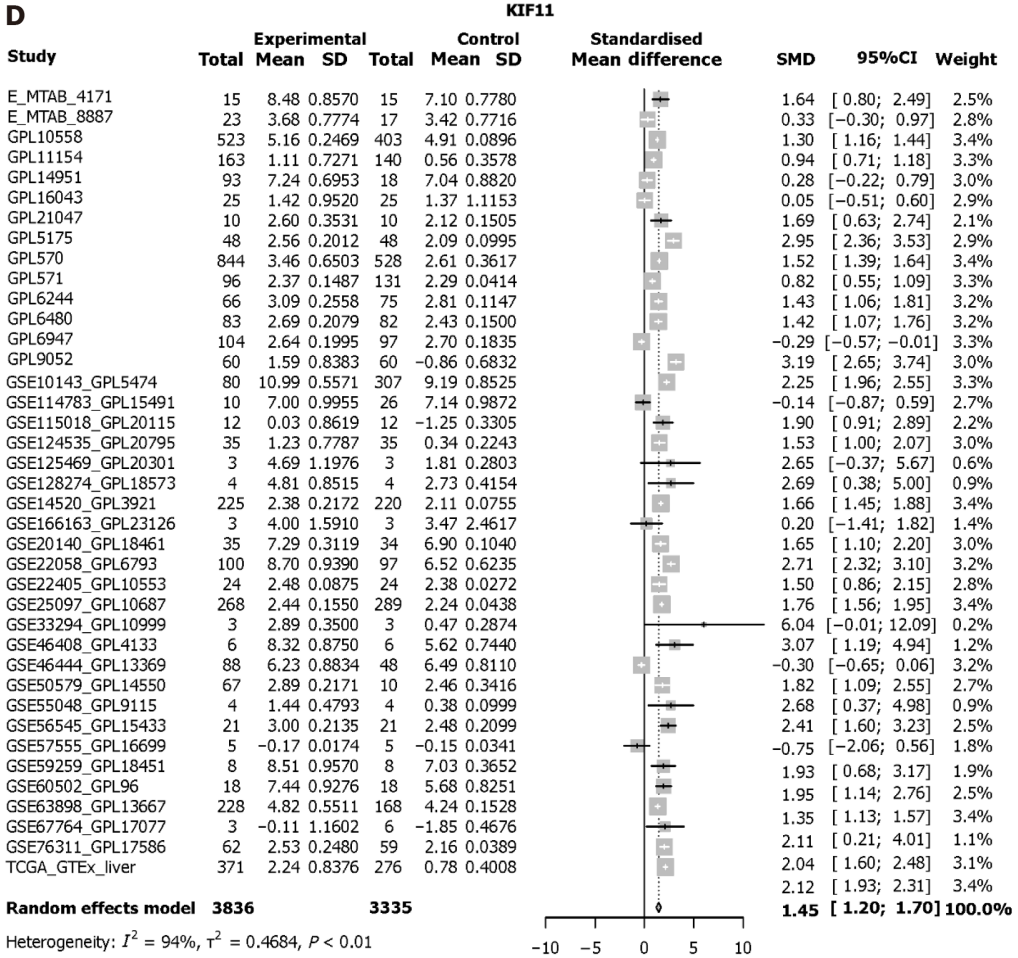
KIF11
Experimental
Control
Standardised Mean difference
Study Total Mean SD Total Mean SD SMD 95%CI Weight
E_MTAB_4171 15 8.48 0.8570 15 7.10 0.7780 1.64 [0.80; 2.49] 2.5%
E_MTAB_8887 23 3.68 0.7774 17 3.42 0.7716 0.33 [−0.30; 0.97] 2.8%
GPL10558 523 5.16 0.2469 403 4.91 0.0896 1.30 [1.16; 1.44] 3.4%
GPL11154 163 1.11 0.7271 140 0.56 0.3578 0.94 [0.71; 1.18] 3.3%
GPL14951 93 7.24 0.6953 18 7.04 0.8820 0.28 [−0.22; 0.79] 3.0%
GPL16043 25 1.42 0.9520 25 1.37 1.1153 0.05 [−0.51; 0.60] 2.9%
GPL21047 10 2.60 0.3531 10 2.12 0.1505 1.69 [0.63; 2.74] 2.1%
GPL5175 48 2.56 0.2012 48 2.09 0.0995 2.95 [2.36; 3.53] 2.9%
GPL570 844 3.46 0.6503 528 2.61 0.3617 1.52 [1.39; 1.64] 3.4%
GPL571 96 2.37 0.1487 131 2.29 0.0414 0.82 [0.55; 1.09] 3.3%
GPL6244 66 3.09 0.2558 75 2.81 0.1147 1.43 [1.06; 1.81] 3.2%
GPL6480 83 2.69 0.2079 82 2.43 0.1500 1.42 [1.07; 1.76] 3.2%
GPL6947 104 2.64 0.1995 97 2.70 0.1835 −0.29 [−0.57; −0.01] 3.3%
GPL9052 60 1.59 0.8383 60 −0.86 0.6832 3.19 [2.65; 3.74] 3.0%
GSE10143_GPL5474 80 10.99 0.5571 307 9.19 0.8525 2.25 [1.96; 2.55] 3.3%
GSE114783_GPL15491 10 7.00 0.9955 26 7.14 0.9872 −0.14 [−0.87; 0.59] 2.7%
GSE115018_GPL20115 12 0.03 0.8619 12 −1.25 0.3305 1.90 [0.91; 2.89] 2.2%
GSE124535_GPL20795 35 1.23 0.7787 35 0.34 0.2243 1.53 [1.00; 2.07] 3.0%
GSE125469_GPL20301 3 4.69 1.1976 3 1.81 0.2803 2.65 [−0.37; 5.67] 0.6%
GSE128274_GPL18573 4 4.81 0.8515 4 2.73 0.4154 2.69 [0.38; 5.00] 0.9%
GSE14520_GPL3921 225 2.38 0.2172 220 2.11 0.0755 1.66 [1.45; 1.88] 3.4%
GSE166163_GPL23126 3 4.00 1.5910 3 3.47 2.4617 0.20 [−1.41; 1.82] 1.4%
GSE20140_GPL18461 35 7.29 0.3119 34 6.90 0.1040 1.65 [1.10; 2.20] 3.0%
GSE22058_GPL6793 100 8.70 0.9390 97 6.52 0.6235 2.71 [2.32; 3.10] 3.2%
GSE22405_GPL10553 24 2.48 0.0875 24 2.38 0.0272 1.50 [0.86; 2.15] 2.8%
GSE25097_GPL10687 268 2.44 0.1550 289 2.24 0.0438 1.76 [1.56; 1.95] 3.4%
GSE33294_GPL10999 3 2.89 0.3500 3 0.47 0.2874 6.04 [−0.01; 12.09] 0.2%
GSE46408_GPL4133 6 8.32 0.8750 6 5.62 0.7440 3.07 [1.19; 4.94] 1.2%
GSE46444_GPL13369 88 6.23 0.8834 48 6.49 0.8110 −0.30 [−0.65; 0.06] 3.2%
GSE50579_GPL14550 67 2.89 0.2171 10 2.46 0.3416 1.82 [1.09; 2.55] 2.7%
GSE55048_GPL9115 4 1.44 0.4793 4 0.38 0.0999 2.68 [0.37; 4.98] 0.9%
GSE56545_GPL15433 21 3.00 0.2135 21 2.48 0.2099 2.41 [1.60; 3.23] 2.5%
GSE57555_GPL16699 5 −0.17 0.0174 5 −0.15 0.0341 −0.75 [−2.06; 0.56] 1.8%
GSE59259_GPL18451 8 8.51 0.9570 8 7.03 0.3652 1.93 [0.68; 3.17] 1.9%
GSE60502_GPL96 18 7.44 0.9276 18 5.68 0.8251 1.95 [1.14; 2.76] 2.5%
GSE63898_GPL13667 228 4.82 0.5511 168 4.24 0.1528 1.35 [1.13; 1.57] 3.4%
GSE67764_GPL17077 3 −0.11 1.1602 6 −1.85 0.4676 2.11 [0.21; 4.01] 1.1%
GSE76311_GPL17586 62 2.53 0.2480 59 2.16 0.0389 2.04 [1.60; 2.48] 3.1%
TCGA_GTEx_liver 371 2.24 0.8376 276 0.78 0.4008 2.12 [1.93; 2.31] 3.4%
Random effects model 3836 3335 1.45 [1.20; 1.70] 100.0%
Heterogeneity: I^2 = 94%, τ^2 = 0.4684, P < 0.01
−10 −5 0 5 10

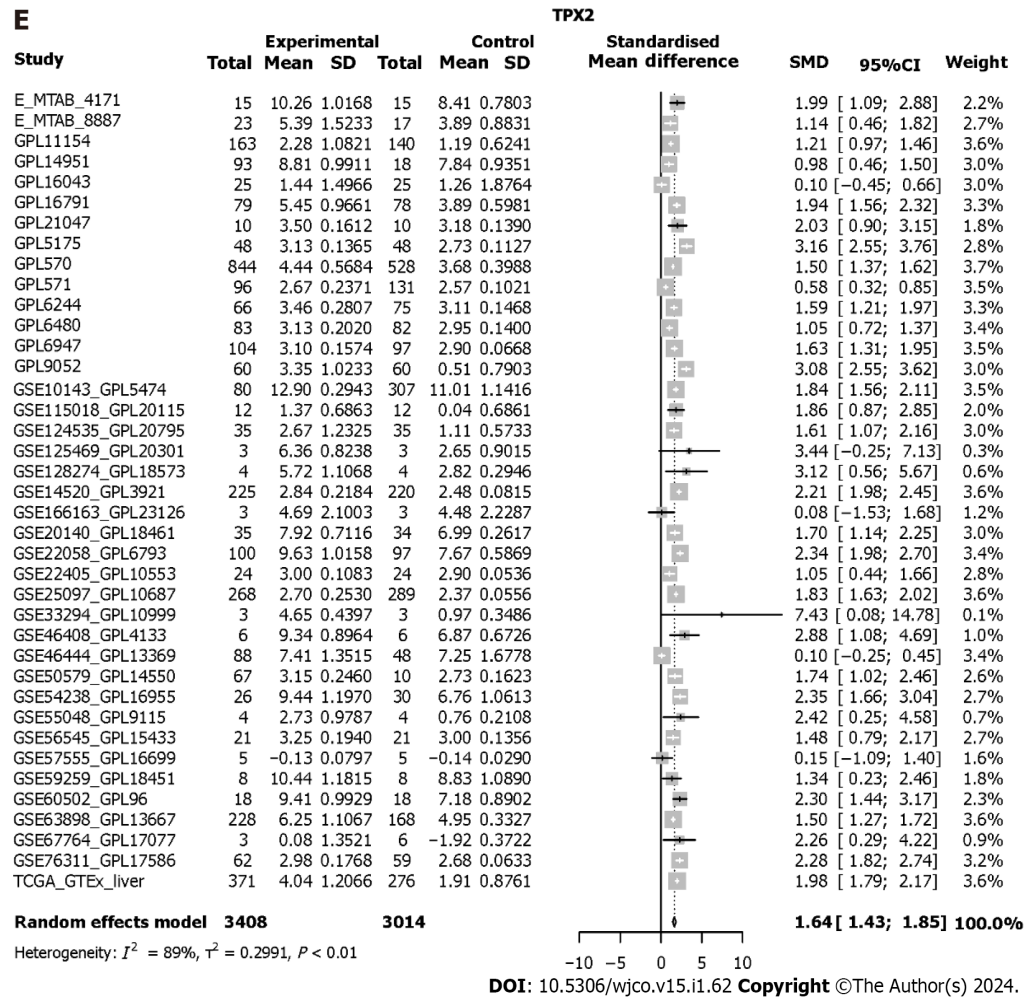

Figure 7 The expression of five key genes in hepatocellular carcinoma. A-E: The expression level of the five key genes in hepatocellular carcinoma (HCC) samples *via* the integration of all of the included HCC samples. DLGAP5: DLG associated protein 5; KIF20A: Kinesin family member 20A; ASPM: Assembly factor for spindle microtubules; KIF11: Kinesin family member 11; TPX2: TPX2 microtubule nucleation factor; SD: Standard deviation; SMD: Standard mean difference; CI: Confidence interval.

ScRNA analysis and AUCell

The dataset GSE103867 satisfied our requirements and was obtained for scRNA analysis. After quality control, a total of 3363 cells from HCC samples were identified. Four cell types were identified: hepatocytes, embryonic stem cells, T cells and B cells (Figure 11A). The expression level of five key genes in the four cell types is shown in Figures 11B and C. The AUCell R package was used for determining the TACE refractoriness-related activity in each cell line (Figure 11D). TACE refractoriness-related genes were mainly active in hepatocytes and embryonic stem cells (Figure 11E).

Prediction of cell–cell communication

As shown in Figure 12A–F, hepatocytes as providers of ligands and embryonic stem cells as the providers of receptors had the highest interaction strength. When hepatocytes expressed ligands and embryonic stem cells provided the corresponding receptors, some ligand-receptor pairs like MDK-SDC2 and MDK-NCL had the greatest communication probability of accomplishing cell–cell communication (Figure 12G).

Immune landscape exploration for refractory TACE-treated HCC

TACE non-responders had a higher level of infiltration of follicular helper T cells, macrophages M0 and active mast cells than TACE responders. While TACE non-responders were associated with a lower level of infiltration of active memory $CD4^+$ T cells, macrophages M1 and M2 macrophages (Figure 13A). The analysis of the connection between the expression of key genes and the infiltration of 22 kinds of immune cell in CIBERSORT algorithm was performed (Figure 13B–F). The correlation among hepatocytes, phenotypes of T cells and phenotypes of B cells was computed using the xCell algorithm (Figure 14A). TACE non-responders were calculated as having lower stroma and microenvironment scores (Figure 14B).

The potential therapeutic drugs discovery

There were 27 kinds of drugs used in the treatment of HCC in the pRRophetic R package. The IC_{50} values of the 27 chemotherapeutics were compared between TACE non-responders and TACE responders. Five chemotherapeutics

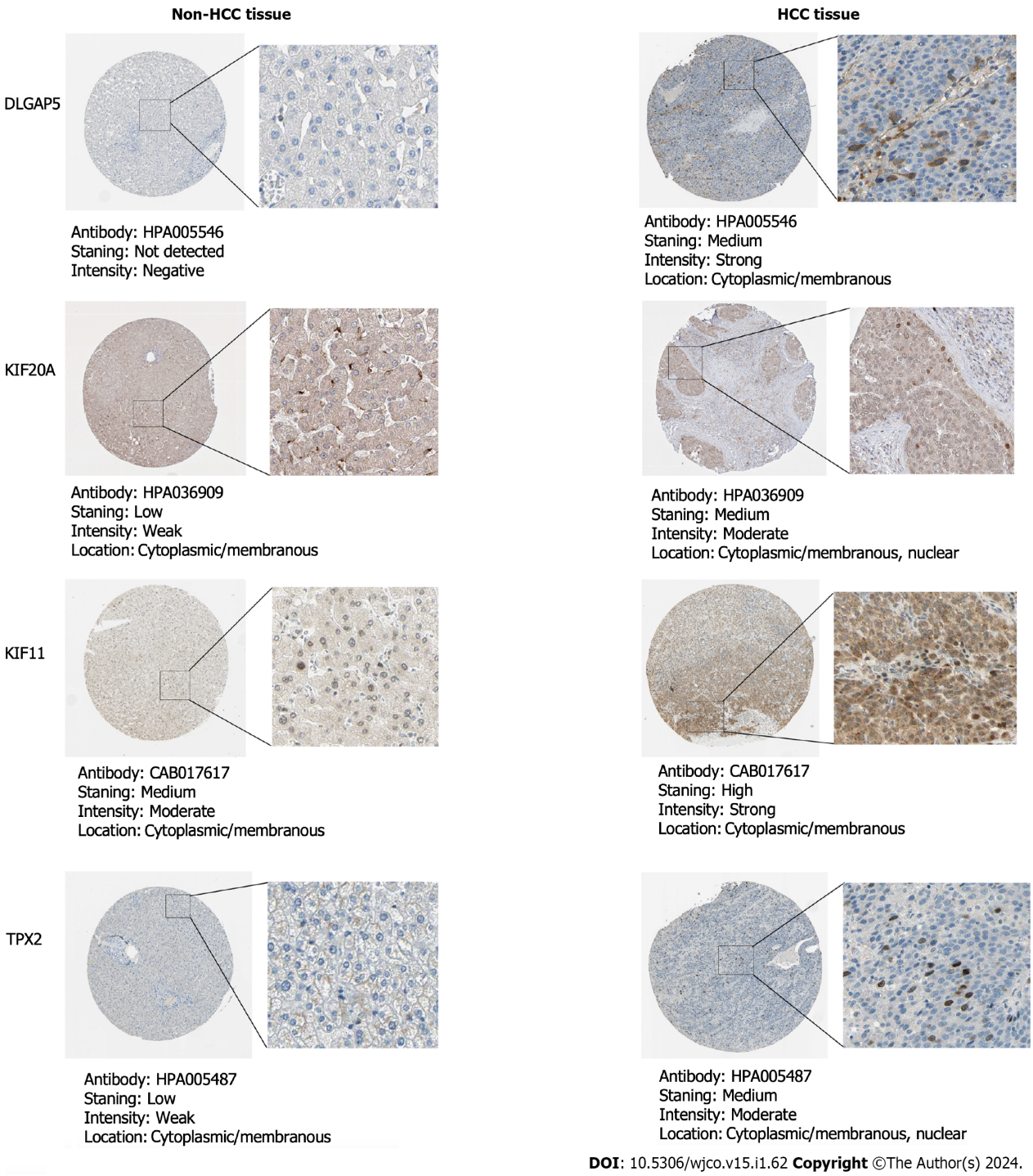

DOI: 10.5306/wjco.v15.i1.62

Figure 8 The protein expression of the key genes in non-hepatocellular carcinoma and hepatocellular carcinoma tissues *via* immunohistochemistry derived from The Human Protein Atlas database. The immunohistochemistry for protein expression of key-gene assembly factor for spindle microtubules was deficient in THPA database. DLGAP5: DLG associated protein 5; KIF20A: Kinesin family member 20A; KIF11: Kinesin family member 11; TPX2: TPX2 microtubule nucleation factor.

(CCT007093, Dasatinib, Erlotinib, Bortezomib and Lapatinib) had the potential for reversing TACE non-response (Figure 15).

DISCUSSION

In this study, we have achieved the following targets: (1) Five key genes (DLGAP5, KIF20A, ASPM, KIF11 and TPX2) were identified among TACE refractoriness-related genes and all overexpressed in the TACE non-responders group and the HCC group; (2) a higher expression of five key genes predicted a worse overall survival (OS) probability in HCC, and TPX2 was considered to be an independent prognostic factor in HCC; (3) cell cycle pathway was likely to play a role in

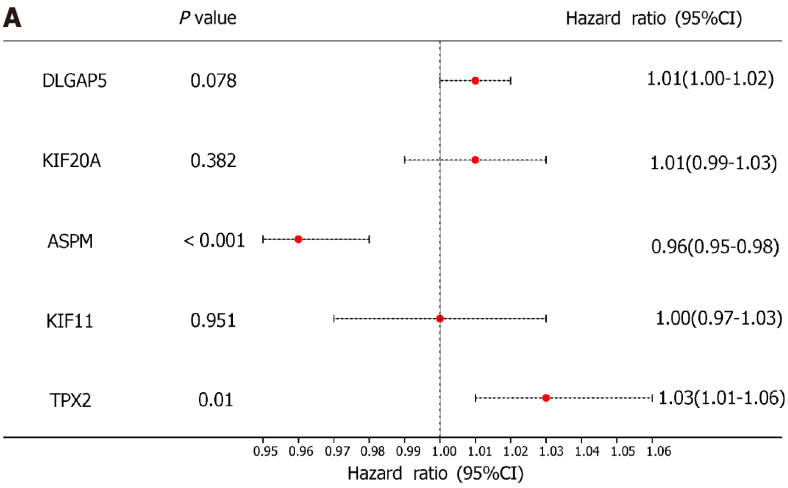
A
P value
Hazard ratio (95%CI)
DLGAP5
0.078
1.01(1.00-1.02)
KIF20A
0.382
1.01(0.99-1.03)
ASPM
< 0.001
0.96(0.95-0.98)
KIF11
0.951
1.00(0.97-1.03)
TPX2
0.01
1.03(1.01-1.06)
0.95 0.96 0.97 0.98 0.99 1.00 1.01 1.02 1.03 1.04 1.05 1.06
Hazard ratio (95%CI)

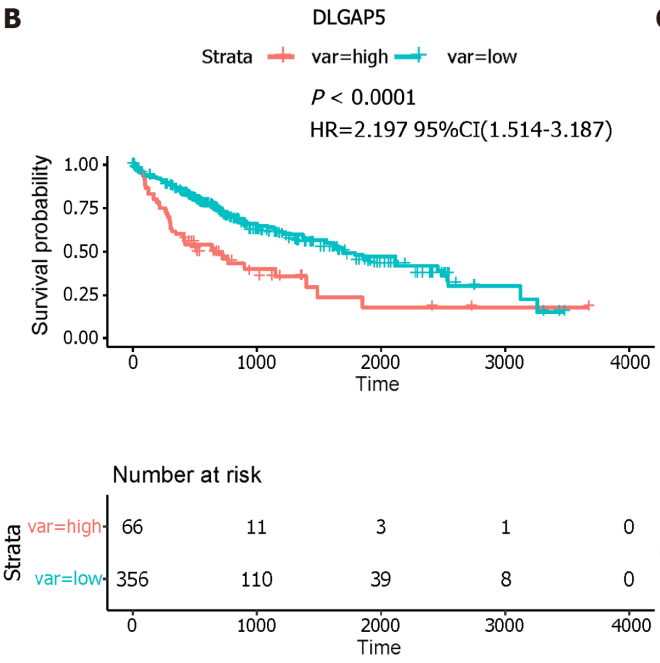
B
DLGAP5
Strata var=high var=low
P < 0.0001
HR=2.197 95%CI(1.514-3.187)
Survival probability
Time
Number at risk
var=high 66 11 3 1 0
var=low 356 110 39 8 0

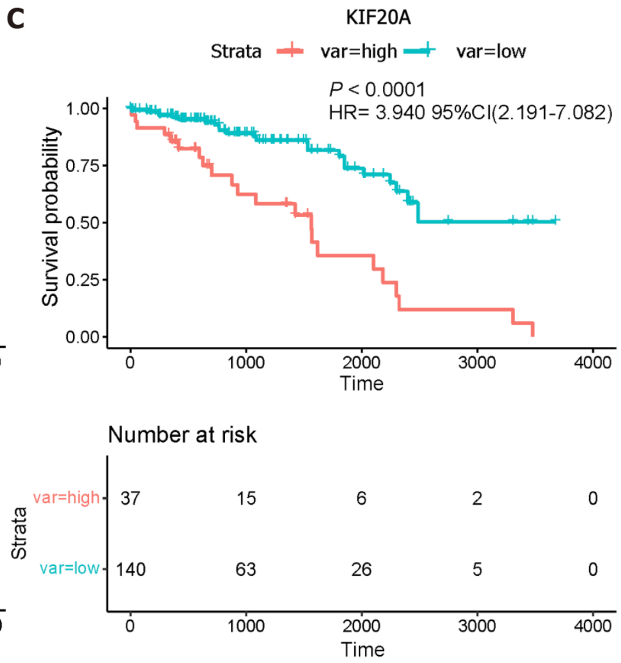
C
KIF20A
Strata var=high var=low
P < 0.0001
HR= 3.940 95%CI(2.191-7.082)
Survival probability
Time
Number at risk
var=high 37 15 6 2 0
var=low 140 63 26 5 0

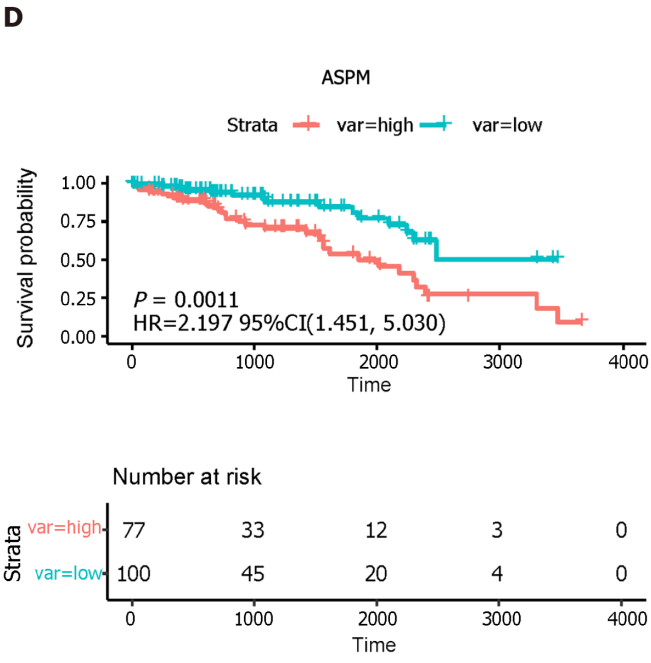
D
ASPM
Strata var=high var=low
P = 0.0011
HR=2.197 95%CI(1.451, 5.030)
Survival probability
Time
Number at risk
var=high 77 33 12 3 0
var=low 100 45 20 4 0

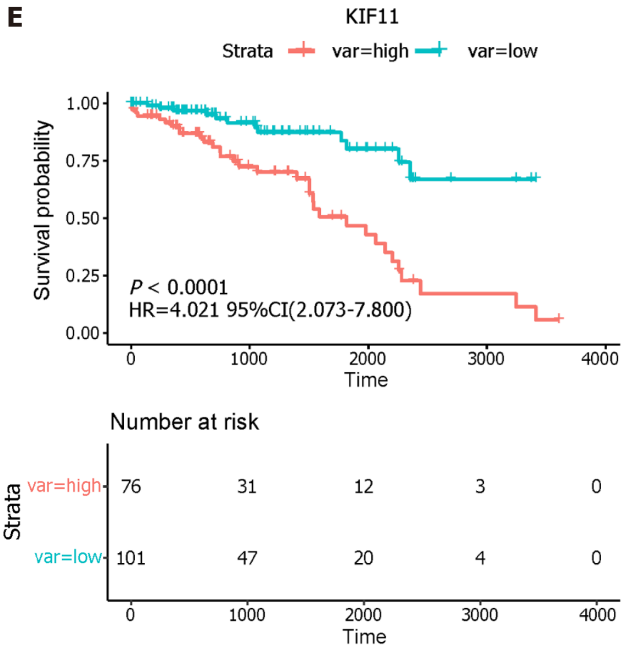
E
KIF11
Strata var=high var=low
P < 0.0001
HR=4.021 95%CI(2.073-7.800)
Survival probability
Time
Number at risk
var=high 76 31 12 3 0
var=low 101 47 20 4 0

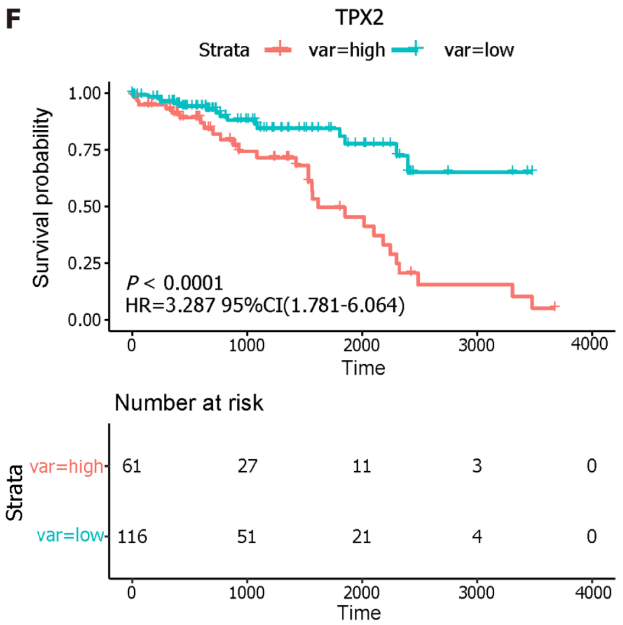

DOI: 10.5306/wjco.v15.i1.62

Figure 9 The Kaplan-Meier curve analysis. A: The multivariate analysis of five key genes; B–F: Survival curves for the five key genes. DLGAP5: DLG associated protein 5; KIF20A: kinesin family member 20A; ASPM: Assembly factor for spindle microtubules; KIF11: Kinesin family member 11; TPX2: TPX2 microtubule nucleation factor; HR: Hazard ratio; CI: Confidence interval.

resisting TACE therapy with enrichment analysis using TACE refractoriness-related genes; (4) four cell types, hepatocytes, embryonic stem cells, T cells and B cells, were identified in HCC samples *via* scRNA sequencing analysis, and hepatocytes and embryonic stem cells were seen as possibly promoting TACE refractoriness *via* AUCell and CellChat analysis; (5) the immune environment landscapes of the TACE non-response group and the TACE response group were revealed; (6) some compounds, like CCT007093, Dasatinib, Erlotinib, Bortezomib and Lapatinib, might be effective for the TACE non-response group according to drug-sensitivity analysis.

Some advanced imaging techniques have been reported as predicting the therapeutic response of TACE in HCC through the detection of liver hemodynamics, water molecule diffusion capacity, metabolic changes and blood-oxygen level[26]. One study found that the blood-oxygen level significantly decreased in the cancerous region of 30 HCC patients after receiving TACE but saw no notable changes in 30 healthy volunteers[27]. TACE creates a hypoxic microenvironment due to arterial embolisation, which contributes to a surge in the vascular endothelial growth factor, p53, which enlarges tumour size and decreases the survival rate[28,29]. Cheng *et al*[30] found that TPX2, as one of the hypoxia-related genes, was obviously and clearly expressed in a high-risk HCC group and participated in TACE refractoriness. Our study has identified TPX2 as a key gene for possibly inducing TACE refractoriness.

On the basis of some studies, autophagy may be a significant mechanism mediating the therapeutic efficacy of TACE in HCC. Autophagy protects the cancer cells from abominable conditions such as hypoxia, starvation and cell apoptosis induced by chemotherapy and enhances the cancer cells' resistance to hypoxic and chemotherapy[27]. Mao *et al*[29] demonstrated that apoptosis-stimulating p53 protein 2 (ASPP2) was low-expression in recurrent HCC patients after TACE treatment and confirmed that ASPP2, as a co-expression factor of the cancer suppressor p53, was responsible for decreasing the autophagy maker Beclin-1. Gao *et al*[31] concluded that TACE in combination with the autophagic inhibitor chloroquine shown to be more efficient at curing tumours in rabbit liver than TACE alone.

Further investigation of research showed that MicroRNA (miRNA) also has a substantial effect on the low therapeutic efficacy of TACE in HCC. Wei *et al*[20] found that down-regulated miR-125b was related to the recurrence of HCC after TACE treatment. They concluded that the low miR-125b expression attenuated the HIF1α translation to activate the HIF1α/pAKT loop and block the autocrine HIF1α/platelet-derived growth factor β (PDGFβ)/pAKT/HIF1α loop of HIF1α translation by targeting PDGFβ. Tumour-initiating cells (T-ICs) or cancer stem cells (CSCs) are a phenotype of cancer cells with a self-renewal and tumorigenesis faculty[32]. T-ICs and CSCs are connected to cancer proliferation and anti-cancer therapy resistance[33]. Clinical cohort analysis indicates that HCC patients with high miR-186 expression benefit from TACE[34]. Yao *et al*[34] found that a miR-186 knockdown led to the expansion of CSCs while a high expression of miR-186 inhibited the process. Additionally, other miRNA, like miR-26a, miR-107 and miR-106, were differentially expressed between TACE non-responders and TACE responders, and their differential expression was correlated with OS and progression-free survival[35].

Consistent with the description above, the engagement of T-IC and CSCs is another critical mechanism in the resistance of TACE in HCC. Zeng *et al*[36] stated that the CSC makers like epithelial cell adhesion molecule had a higher expression in TACE-treated specimens than non-TACE specimens, which indicated that HCC with abundant CSCs phenotype had a high risk of recurrence after TACE treatment. Subsequently, Xiang *et al*[37] explained that a low expression of Src-homology 2 domain-containing phosphatase 2 (Shp2) was favourable for a high therapeutic effect from TACE. As for the mechanism, they found that Shp2 appeared in sorted epithelial cell adhesion molecule-positive or clusters of differen-

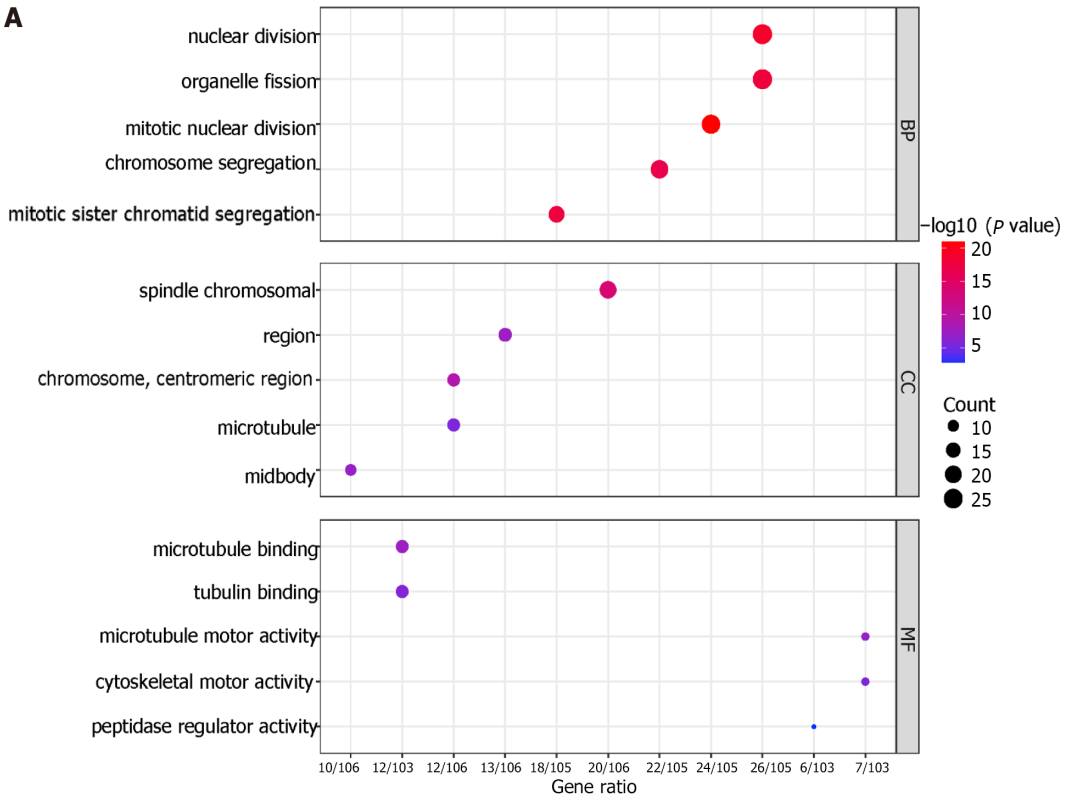

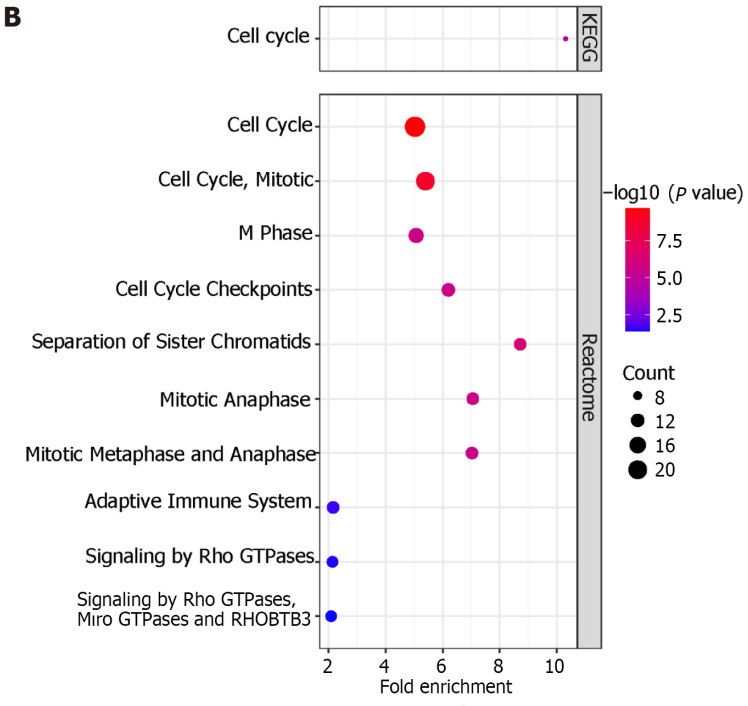

DOI: 10.5306/wjco.v15.i1.62

Figure 10 Enrichment analysis. A: Gene Ontology analysis of transcatheter arterial chemoembolisation (TACE) refractoriness-related genes. The top-five biological processes, the top-five cellular components, and the top-five molecular functions are shown; B: The Kyoto Encyclopaedia of Genes and Genomes and Reactome pathways of TACE refractoriness-related genes.

tiation 133-positive liver CSCs and in CSC-enriched hepatoma spheroids from patients, and that a high expression of Shp2 promoted the proliferation of liver CSCs by enhancing an accumulation of β-catenin[37]. Some transcription factors of embryonic stem cells had the ability to regulate the CSCs in pancreatic cancer[38]. Zhou *et al*[39] identified some potential methylation-related genes that become enriched in the embryonic stem cell pathway to characterise HCC, which indicated embryonic stem cells might play a role in HCC progression. The derivatives of embryonic stem cells were able to generate hepatocytes[40]. Hepatocytes were found to create a profound metabolic rewiring when preparing to proliferate in HCC[41]. However, there was little evidence to show the function of hepatocytes and embryonic stem cells

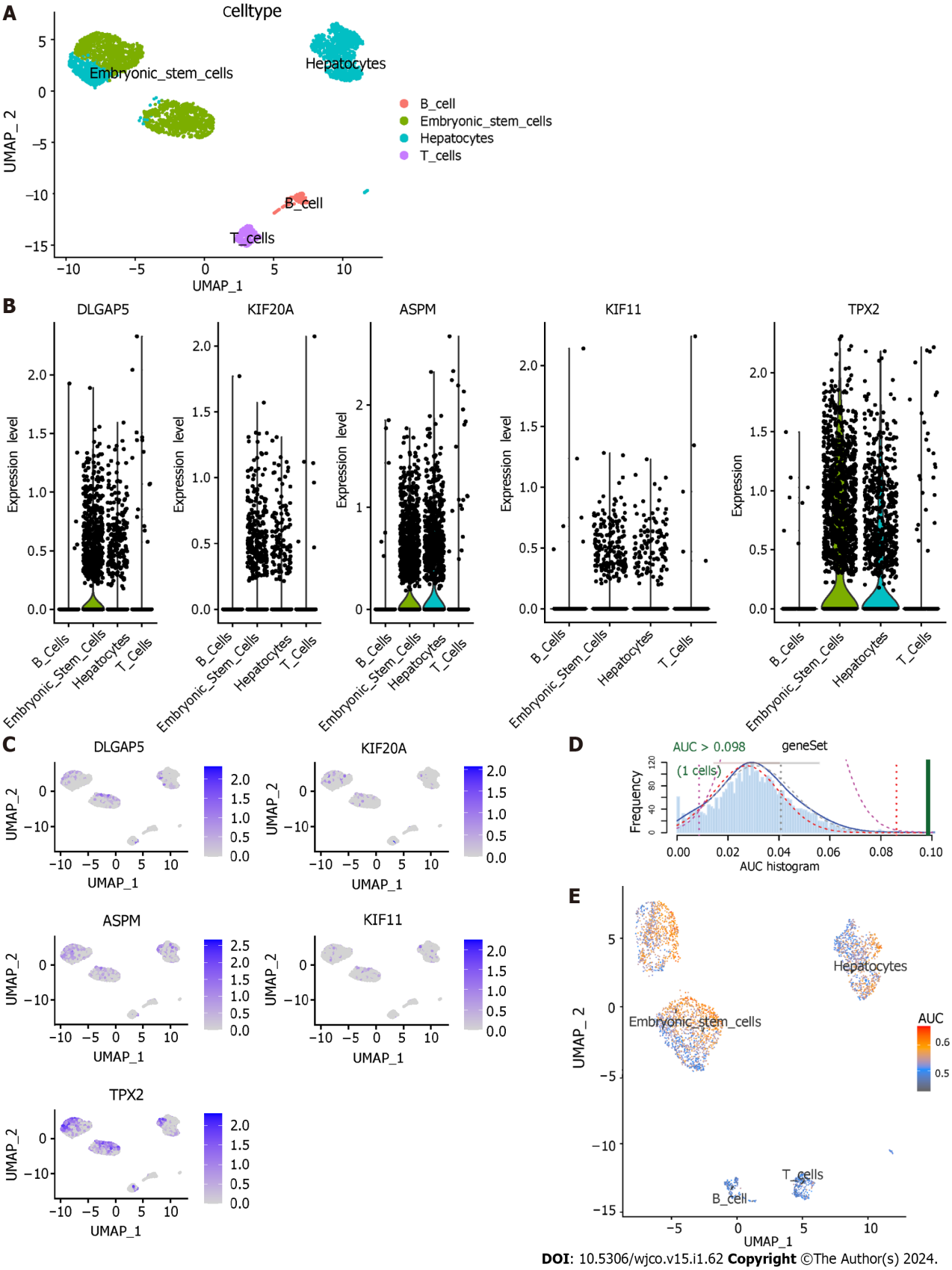

DOI: 10.5306/wjco.v15.i1.62 **Copyright** ©The Author(s) 2024.

Figure 11 Single-cell RNA sequencing analysis and AUCell. A: Uniform manifold approximation and projection (UMAP) plot showing four cell types in hepatocellular carcinoma samples; B: Violin plots showing the expression level of five key genes in four cell types. C: Expression level of five key genes in four cell types were drawn on UMAP; D: AUCell score distribution curves of 112 transcatheter arterial chemoembolisation (TACE) refractoriness-related genes; E: Scatter plot showing the distribution of AUCell scores in 112 TACE refractoriness-related genes. DLGAP5: DLG associated protein 5; KIF20A: Kinesin family member 20A; ASPM: Assembly factor for spindle microtubules; KIF11: Kinesin family member 11; TPX2: TPX2 microtubule nucleation factor; AUC: Area under the curve.

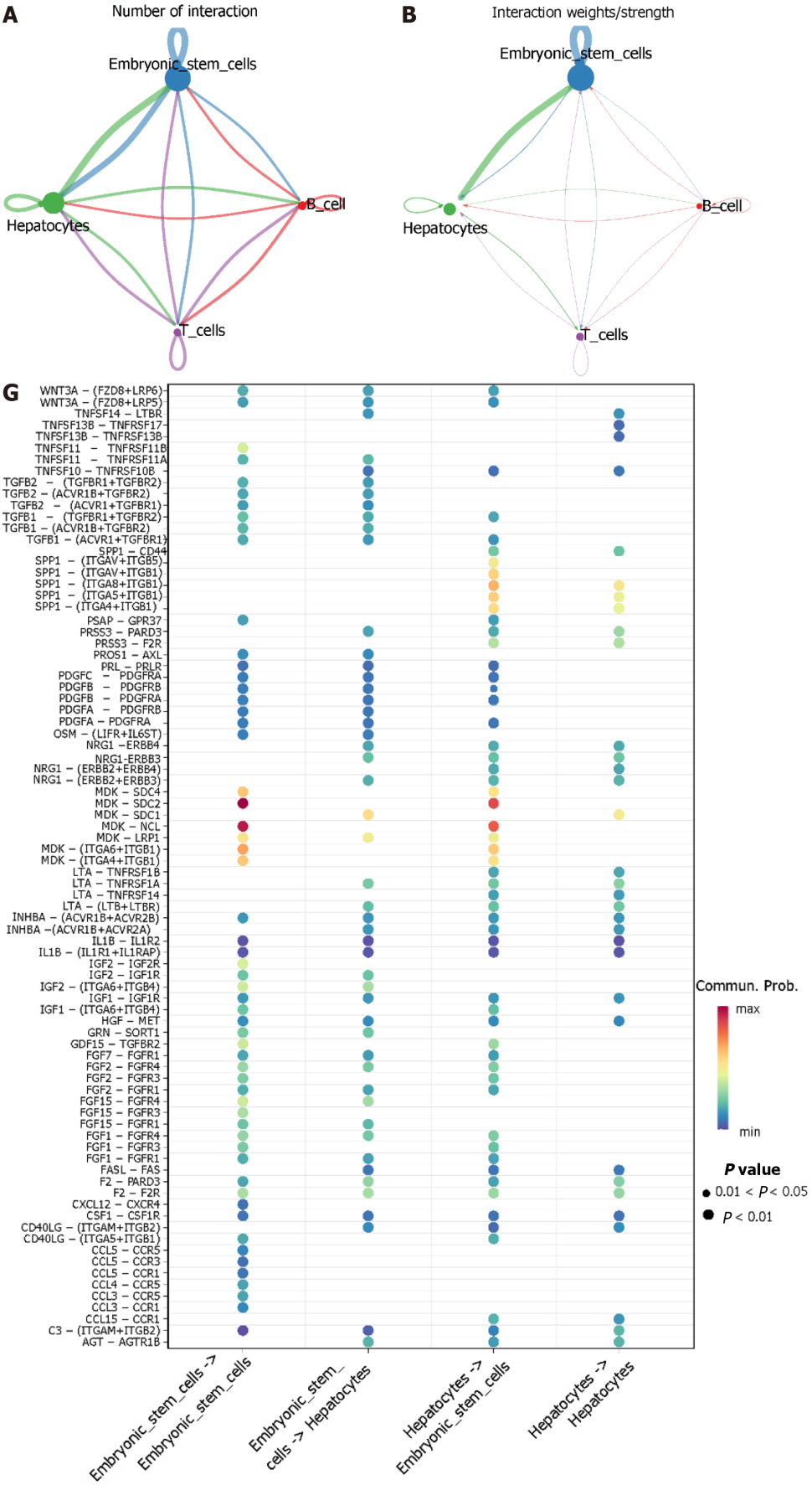

DOI: 10.5306/wjco.v15.i1.62

Figure 12 Cell–cell communication. A and B: The aggregated intercellular communication between any two cell groups. The colours of the periphery circle referred to one cell group and the vertex of periphery circle represented the numbers of cells. The cells in the starting site of edge expressed ligand and the cells the

arrow pointed in expressed receptor. The thickness of the line signified the numbers of ligand-receptor pairs, and the thicker the line meant more ligand-receptor pairs; B: The thickness of edge represented the interaction strength of any two cell groups. The thicker the edge was, the bigger the interaction strength; C–F: The intercellular communication of each cell group. Hepatocytes providing ligands had strongest communication with embryonic stem cells that expressed receptors; G: The identification of ligand-receptor pairs between hepatocytes and embryonic stem cells. (Ligands provider)→(receptors provider).

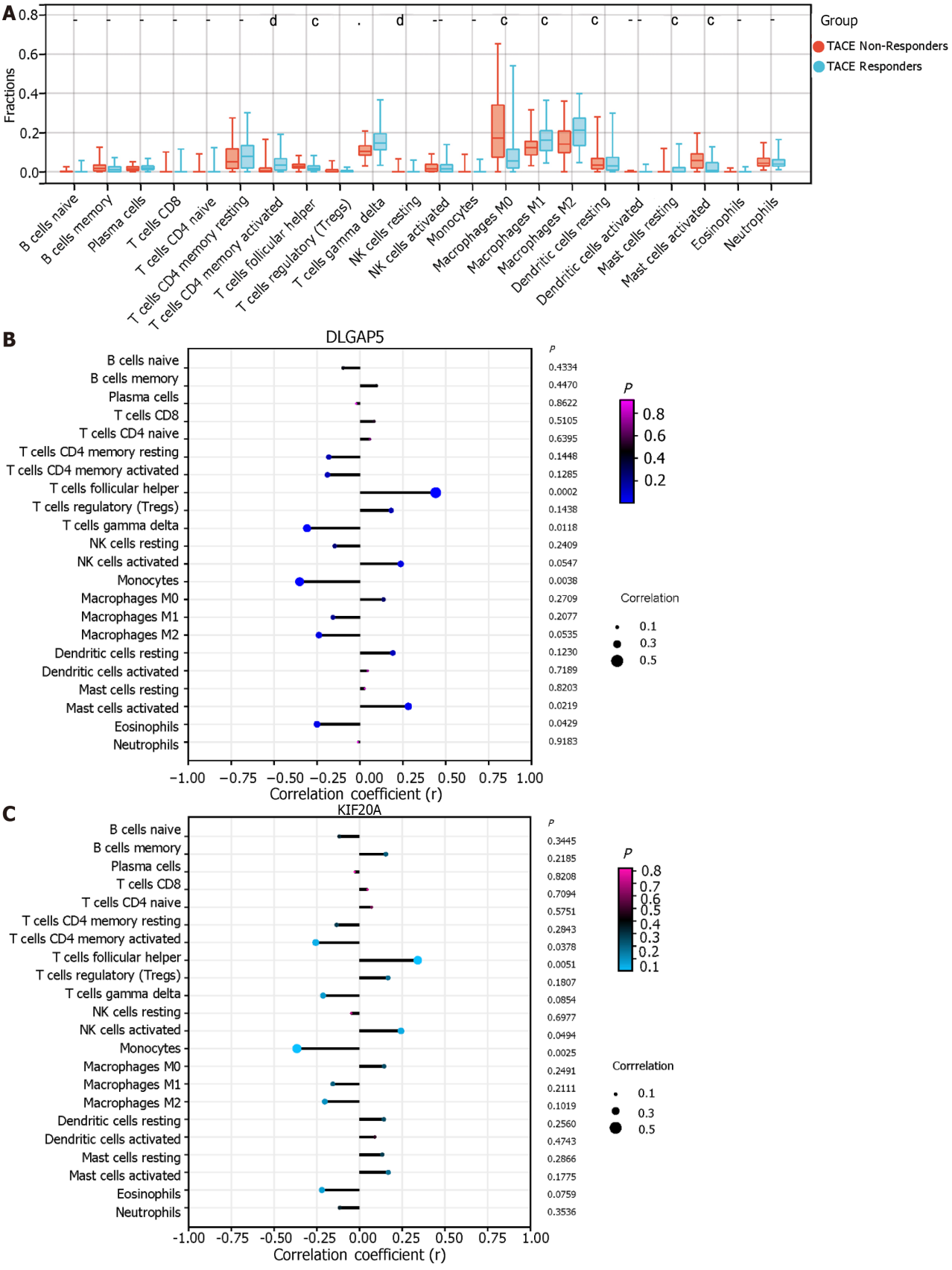

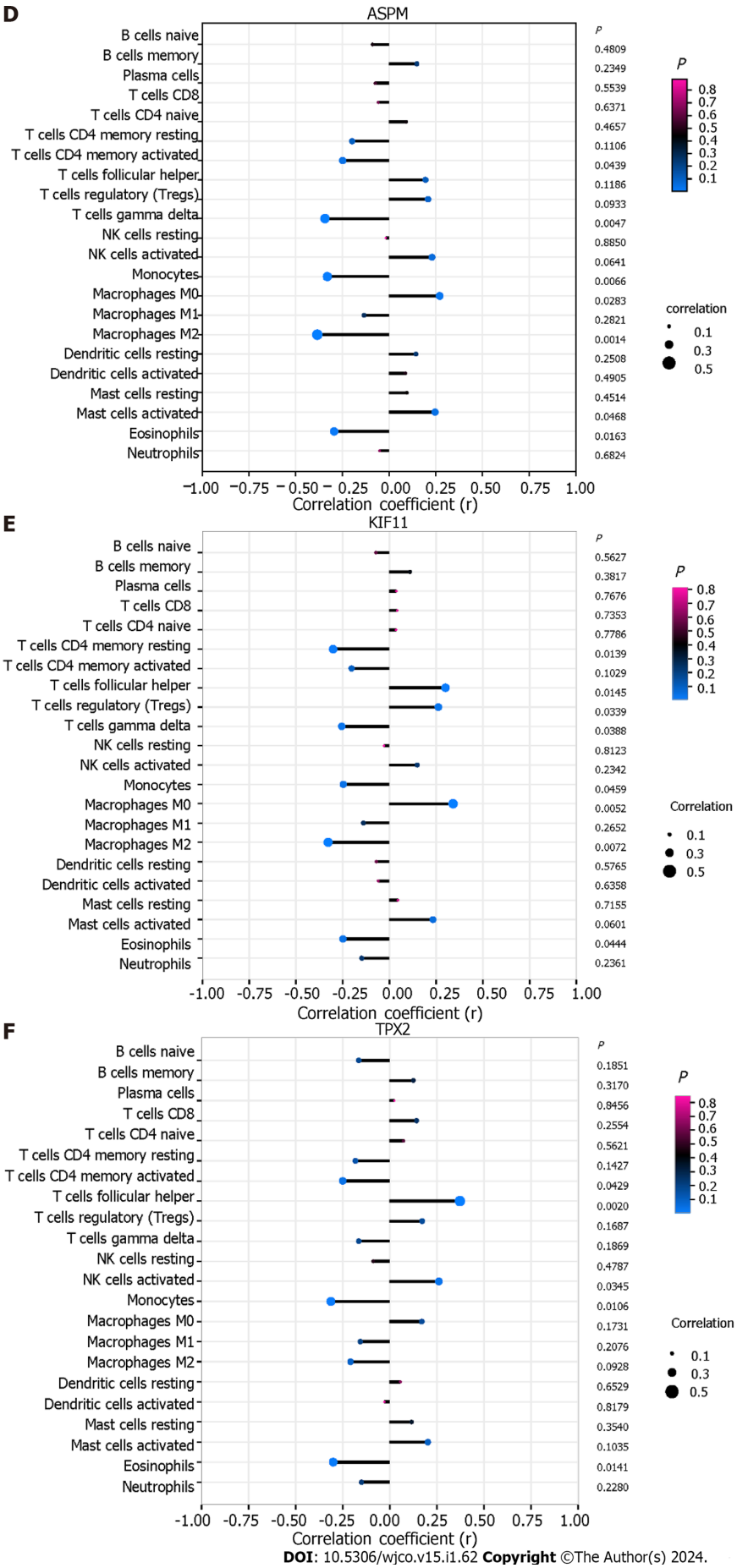

Figure 13 Immune infiltration analysis. A: The immune landscape of 22 kinds of immune cells between transcatheter arterial chemoembolisation (TACE) non-

responders and TACE responders using CIBERSORT algorithm. ([a]*P* < 0.05, [b]*P* < 0.01, [c]*P* < 0.001, [d]*P* < 0.0001); B-F: The relationship between expression of five key genes and the infiltration of 22 kinds of immune cells in TACE non-responders group. DLGAP5: DLG associated protein 5; KIF20A: Kinesin family member 20A; ASPM: Assembly factor for spindle microtubules; KIF11: Kinesin family member 11; TPX2: TPX2 microtubule nucleation factor; AUC: Area under the curve.

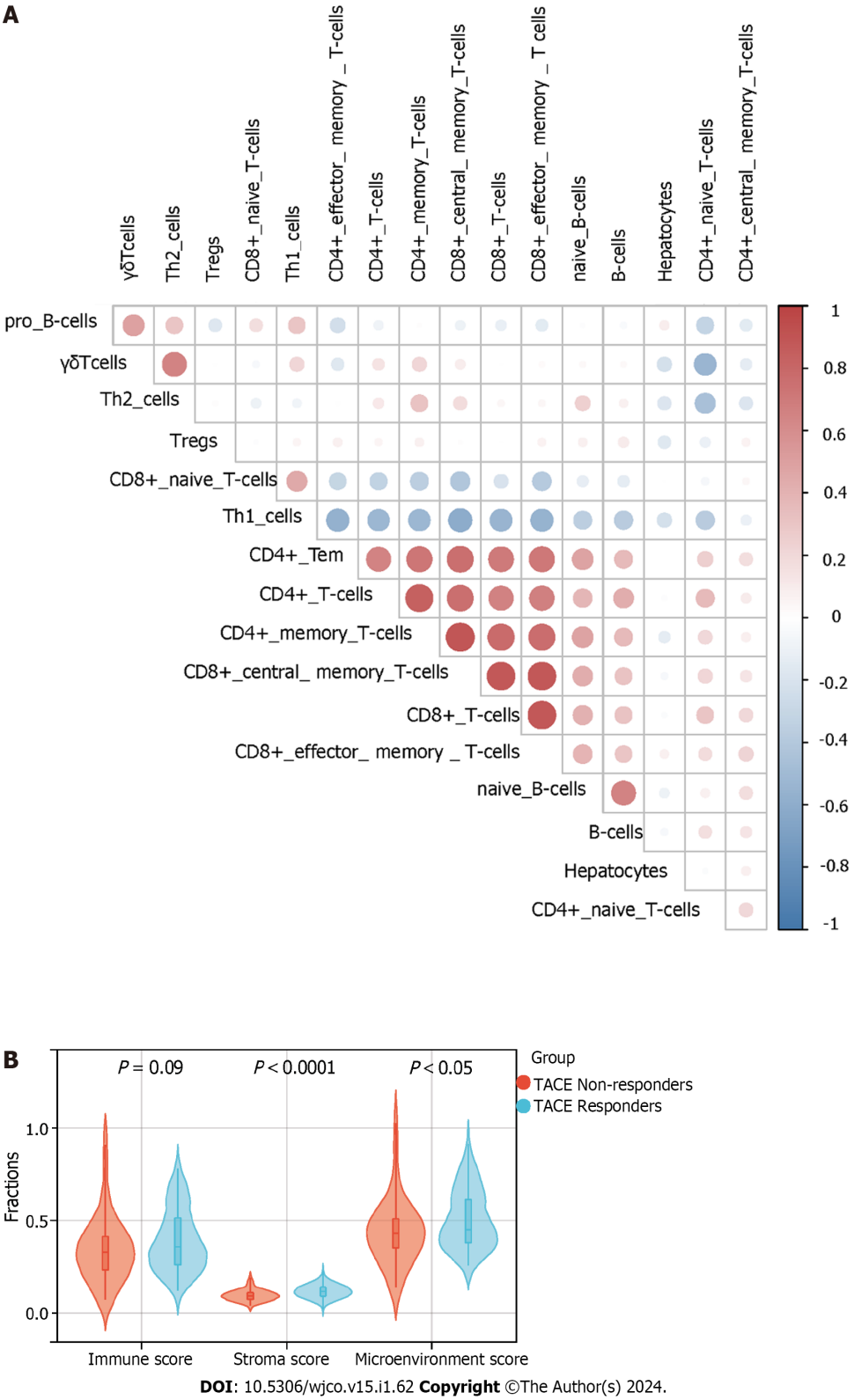

DOI: 10.5306/wjco.v15.i1.62

Figure 14 xCell immune infiltration analysis. A: The correlation between hepatocytes, phenotypes of T cells and phenotypes of B cells by xCell algorithm; B: The comparison of immune, stromal and microenvironment score between transcatheter arterial chemoembolisation (TACE) non-responders and TACE responders by xCell algorithm.

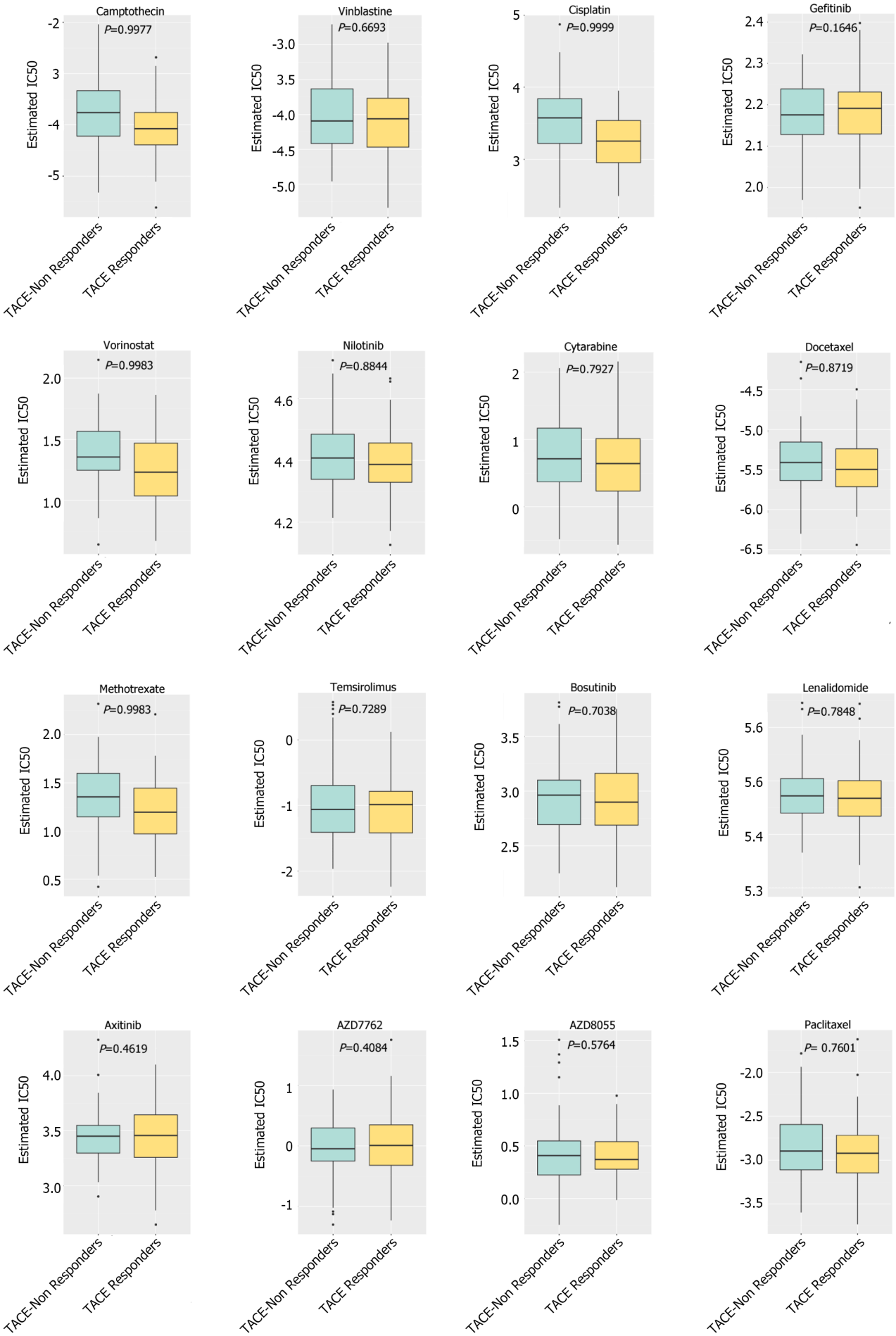
Camptothecin
P=0.9977
Vinblastine
P=0.6693
Cisplatin
P=0.9999
Gefitinib
P=0.1646
Vorinostat
P=0.9983
Nilotinib
P=0.8844
Cytarabine
P=0.7927
Docetaxel
P=0.8719
Methotrexate
P=0.9983
Temsirolimus
P=0.7289
Bosutinib
P=0.7038
Lenalidomide
P=0.7848
Axitinib
P=0.4619
AZD7762
P=0.4084
AZD8055
P=0.5764
Paclitaxel
P= 0.7601
Estimated IC50
TACE-Non Responders
TACE Responders

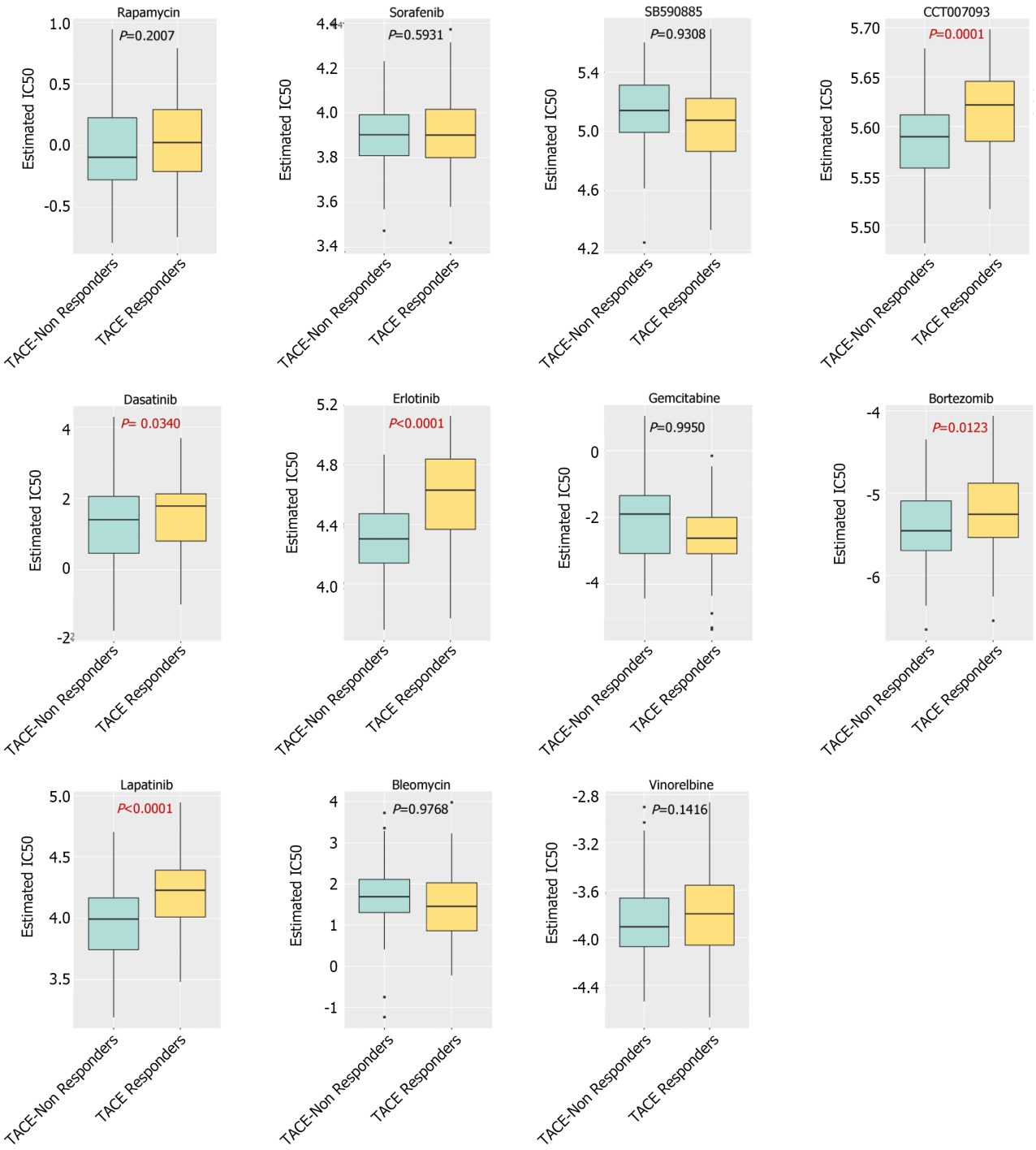

DOI: 10.5306/wjco.v15.i1.62

Figure 15 The prediction of potential drugs for refractory transcatheter arterial chemoembolisation treated hepatocellular carcinoma.
IC_{50}: Half maximal inhibitory concentration.

in TACE refractoriness.

The metabolic process is considered to play a part in the occurrence of TACE refractoriness in HCC. Aberrant glutamine metabolism (GM) is involved in tumorigenesis and poor prognosis[42,43]. Ying *et al*[43] employed 41 GM-associated genes to construct a transcriptome-based approach named 'GM score' and validated it using two independent HCC cohorts. The results showed that a high GM score had a positive correlation with a slim OS of HCC patients after TACE treatment. Therefore, it is plausible that the metabolic process and immune infiltration level may be connected to TACE refractoriness in HCC.

In this study, five key genes have been identified as being highly correlated with TACE refractoriness in HCC, and its potential mechanisms have been discussed. However, some limitations exist in this study. Firstly, although the five key genes (DLGAP5, KIF20A, ASPM, KIF11 and TPX2) were verified as being associated with TACE refractoriness, the clinical applicability of these genes requires more cases as confirmation due to the limited number of TACE-treated patients in this study and the heterogeneity in the diagnosis. Secondly, due to insufficient samples of HCC cells and

stroma treated by TACE, we have no scope for the further validation of the five key genes. Thirdly, the results of the AUCell analysis that TACE refractoriness-related genes were mainly active in hepatocytes and embryonic stem cells require further verification due to only one cell reaching the AUC threshold of TACE refractoriness-related genes list. Lastly, the potential mechanisms identified also need further proof through additional vivo and vitro experiments.

CONCLUSION

Five key genes (DLGAP5, KIF20A, ASPM, KIF11 and TPX2) were all up-regulated to facilitate TACE refractoriness. Hepatocytes and embryonic stem cells had intimate intercellular communication and were likely to boost TACE refractoriness. CCT007093, Dasatinib, Erlotinib, Bortezomib and Lapatinib possibly played a curable role in TACE non-responders.

ARTICLE HIGHLIGHTS

Research background

Transcatheter arterial embolisation (TACE) is a primary therapeutic strategy for hepatocellular carcinoma (HCC) patients in the intermediate and advanced stages. In China, TACE refractoriness is defined as the intrahepatic target lesion that remains in a disease progression state after receiving standardised and refined TACE treatment for three or more times consecutively.

Research motivation

It is essential to identify biomarkers for predicting TACE refractoriness and to explore the potential mechanisms of TACE refractoriness.

Research objectives

The purpose of our study is to identify the key genes associated with TACE refractoriness and investigate the potential mechanisms of TACE refractoriness.

Research methods

The gene expression profile was obtained from the public databases. Weighted gene co-expression network analysis and the cytoHubba plugin were utilised to identify the key genes in TACE refractoriness. Multivariate Cox regression and Kaplan–Meier were employed. ScRNA analysis was used for exploring the potential mechanisms of TACE refractoriness.

Research results

Five key genes (DLGAP5, KIF20A, ASPM, KIF11, and TPX2) were all up-regulated in TACE non-responders, which predicted poor prognosis. TPX2 is recognised as an independent prognostic factor. TACE refractoriness-related genes were mainly active in hepatocytes and embryonic stem cells. Hepatocytes and embryonic stem cells showed strong cellular interactions in HCC.

Research conclusions

Five key genes (DLGAP5, KIF20A, ASPM, KIF11, and TPX2) were identified as being associated with TACE refractoriness. Hepatocytes and embryonic stem cells probably promoted TACE refractoriness.

Research perspectives

More vivo and vitro experiments are essential to elaborate and verify the significance of the key genes and the potential mechanisms involved in TACE refractoriness.

ACKNOWLEDGEMENTS

The authors thank Guangxi Key Laboratory of Medical Pathology for their technical support.

FOOTNOTES

Author contributions: Huang JZ and Li JD took part in data collection, statistical analysis, interpretation and paper drafting; He RQ and Chen G were responsible for study design, statistical analysis guidance and paper correction.

Supported by Guangxi Higher Education Undergraduate Teaching Reform Project, No. 2021JGA142; Guangxi Educational Science Planning Key Project, No. 2022ZJY2791; Guangxi Medical University Education and Teaching Reform Project, No. 2021XJGA02; and

Guangxi Zhuang Autonomous Region Health Commission Self-financed Scientific Research Project, No. Z20201147.

Institutional review board statement: The study did not involve any human or animal related experiments, so no statement of ethics will be provided.

Informed consent statement: The letter is to state that "informed consent" is not apply for our manuscript because the data of this study are from the public database TCGA, GEO and GTEx database.

Conflict-of-interest statement: We have no financial relationships to disclose.

Data sharing statement: The datasets analysed in this study are publicly available in the TCGA (https://portal.gdc.cancer.gov/), GEO (https://www.ncbi.nlm.nih.gov/geo/) and GTEx (https://gtexportal.org/home/) databases.

Country/Territory of origin: China

ORCID number: Jie-Zhuang Huang 0009-0006-8471-3826; Jian-Di Li 0000-0001-7050-371X; Gang Chen 0000-0003-2402-2987; Rong-Quan He 0000-0002-7752-2080.

S-Editor: Liu JH
L-Editor: A
P-Editor: Zhang XD

REFERENCES

1 **Chen X**, Lu Y, Shi X, Han G, Zhang L, Ni C, Zhao J, Gao Y, Wang X. Epidemiological and Clinical Characteristics of Five Rare Pathological Subtypes of Hepatocellular Carcinoma. *Front Oncol* 2022; **12**: 864106 [PMID: 35463333 DOI: 10.3389/fonc.2022.864106]
2 **Zhang X**, Zou H, Chen Y, Zhang H, Tian R, Meng J, Zhu Y, Guo H, Dai E, Zhu B, Liu Z, Jin Y, Li Y, Feng L, Zhuang H, Pan CQ, Li J, Duan Z. The effects of increased dose of hepatitis B vaccine on mother-to-child transmission and immune response for infants born to mothers with chronic hepatitis B infection: a prospective, multicenter, large-sample cohort study. *BMC Med* 2021; **19**: 148 [PMID: 34253217 DOI: 10.1186/s12916-021-02025-1]
3 **Gufler S**, Seeboeck R, Schatz C, Haybaeck J. The Translational Bridge between Inflammation and Hepatocarcinogenesis. *Cells* 2022; **11** [PMID: 35159342 DOI: 10.3390/cells11030533]
4 **Yao J**, Liang X, Liu Y, Li S, Zheng M. Trends in Incidence and Prognostic Factors of Two Subtypes of Primary Liver Cancers: A Surveillance, Epidemiology, and End Results-Based Population Study. *Cancer Control* 2022; **29**: 10732748211051548 [PMID: 35147456 DOI: 10.1177/10732748211051548]
5 **Yang C**, Zhang H, Zhang L, Zhu AX, Bernards R, Qin W, Wang C. Evolving therapeutic landscape of advanced hepatocellular carcinoma. *Nat Rev Gastroenterol Hepatol* 2023; **20**: 203-222 [PMID: 36369487 DOI: 10.1038/s41575-022-00704-9]
6 **Chidambaranathan-Reghupaty S**, Fisher PB, Sarkar D. Hepatocellular carcinoma (HCC): Epidemiology, etiology and molecular classification. *Adv Cancer Res* 2021; **149**: 1-61 [PMID: 33579421 DOI: 10.1016/bs.acr.2020.10.001]
7 **Kim H**, Choi B, Mouli SK, Choi H, Harris KR, Kulik LM, Lewandowski RJ, Kim DH. Preclinical Development and Validation of Translational Temperature Sensitive Iodized Oil Emulsion Mediated Transcatheter Arterial Chemo-Immuno-Embolization for the Treatment of Hepatocellular Carcinoma. *Adv Healthc Mater* 2023; **12**: e2300906 [PMID: 37163283 DOI: 10.1002/adhm.202300906]
8 **Yang Y**, Lin K, Liu L, Qian Y, Yang Y, Yuan S, Zhu P, Huang J, Liu F, Gu F, Fu S, Jiang B, Liu H, Pan Z, Lau WY, Zhou W. Impact of preoperative TACE on incidences of microvascular invasion and long-term post-hepatectomy survival in hepatocellular carcinoma patients: A propensity score matching analysis. *Cancer Med* 2021; **10**: 2100-2111 [PMID: 33650288 DOI: 10.1002/cam4.3814]
9 **Khan AR**, Wei X, Xu X. Portal Vein Tumor Thrombosis and Hepatocellular Carcinoma - The Changing Tides. *J Hepatocell Carcinoma* 2021; **8**: 1089-1115 [PMID: 34522691 DOI: 10.2147/JHC.S318070]
10 **Hatanaka T**, Yata Y, Naganuma A, Kakizaki S. Treatment Strategy for Intermediate-Stage Hepatocellular Carcinoma: Transarterial Chemoembolization, Systemic Therapy, and Conversion Therapy. *Cancers (Basel)* 2023; **15** [PMID: 36980684 DOI: 10.3390/cancers15061798]
11 **Wang P**, Song X, Cao D, Cui K, Wang J, Utpatel K, Shang R, Wang H, Che L, Evert M, Zhao K, Calvisi DF, Chen X. Oncogene-dependent function of BRG1 in hepatocarcinogenesis. *Cell Death Dis* 2020; **11**: 91 [PMID: 32019910 DOI: 10.1038/s41419-020-2289-3]
12 **Yang S**, Pang L, Dai W, Wu S, Ren T, Duan Y, Zheng Y, Bi S, Zhang X, Kong J. Role of Forkhead Box O Proteins in Hepatocellular Carcinoma Biology and Progression (Review). *Front Oncol* 2021; **11**: 667730 [PMID: 34123834 DOI: 10.3389/fonc.2021.667730]
13 **Reig M**, Darnell A, Forner A, Rimola J, Ayuso C, Bruix J. Systemic therapy for hepatocellular carcinoma: the issue of treatment stage migration and registration of progression using the BCLC-refined RECIST. *Semin Liver Dis* 2014; **34**: 444-455 [PMID: 25369306 DOI: 10.1055/s-0034-1394143]
14 **Liu B**, Zhang Y, Chen H, Li W, Tsochatzis E. The combination of transcatheter arterial chemoembolisation (TACE) and thermal ablation *versus* TACE alone for hepatocellular carcinoma. *Cochrane Database Syst Rev* 2022; **1**: CD013345 [PMID: 34981511 DOI: 10.1002/14651858.CD013345.pub2]
15 **Kosaka Y**, Kimura T, Kawaoka T, Ogawa Y, Amioka K, Naruto K, Yoshikawa Y, Kikukawa C, Suehiro Y, Yamaoka K, Ando Y, Uchikawa

S, Morio K, Nakahara T, Murakami E, Takahashi S, Tsuge M, Hiramatsu A, Imamura M, Chosa K, Awai K, Nagata Y, Chayama K, Aikata H. Hepatic Arterial Infusion Chemotherapy Combined with Radiation Therapy for Advanced Hepatocellular Carcinoma with Tumor Thrombosis of the Main Trunk or Bilobar of the Portal Vein. *Liver Cancer* 2021; **10**: 151-160 [PMID: 33977091 DOI: 10.1159/000513706]

16 **Núñez KG**, Sandow T, Fort D, Hibino M, Wright P, Cohen AJ, Thevenot PT. PD-1 expression in hepatocellular carcinoma predicts liver-directed therapy response and bridge-to-transplant survival. *Cancer Immunol Immunother* 2022; **71**: 1453-1465 [PMID: 34689234 DOI: 10.1007/s00262-021-03087-z]

17 **Zhao P**, Zhao J, Deng Y, Zeng G, Jiang Y, Liao L, Zhang S, Tao Q, Liu Z, Tang X, Tu X, Jiang L, Zhang H, Zheng Y. Application of iron/barium ferrite/carbon-coated iron nanocrystal composites in transcatheter arterial chemoembolization of hepatocellular carcinoma. *J Colloid Interface Sci* 2021; **601**: 30-41 [PMID: 34058551 DOI: 10.1016/j.jcis.2021.05.102]

18 **Fako V**, Martin SP, Pomyen Y, Budhu A, Chaisaingmongkol J, Franck S, Lee JM, Ng IO, Cheung TT, Wei X, Liu N, Ji J, Zhao L, Liu Z, Jia HL, Tang ZY, Qin LX, Kloeckner R, Marquardt J, Greten T, Wang XW. Gene signature predictive of hepatocellular carcinoma patient response to transarterial chemoembolization. *Int J Biol Sci* 2019; **15**: 2654-2663 [PMID: 31754337 DOI: 10.7150/ijbs.39534]

19 **Martin SP**, Fako V, Dang H, Dominguez DA, Khatib S, Ma L, Wang H, Zheng W, Wang XW. PKM2 inhibition may reverse therapeutic resistance to transarterial chemoembolization in hepatocellular carcinoma. *J Exp Clin Cancer Res* 2020; **39**: 99 [PMID: 32487192 DOI: 10.1186/s13046-020-01605-y]

20 **Wei X**, Zhao L, Ren R, Ji F, Xue S, Zhang J, Liu Z, Ma Z, Wang XW, Wong L, Liu N, Shi J, Guo X, Roessler S, Zheng X, Ji J. MiR-125b Loss Activated HIF1α/pAKT Loop, Leading to Transarterial Chemoembolization Resistance in Hepatocellular Carcinoma. *Hepatology* 2021; **73**: 1381-1398 [PMID: 32609900 DOI: 10.1002/hep.31448]

21 **Myojin Y**, Kodama T, Maesaka K, Motooka D, Sato Y, Tanaka S, Abe Y, Ohkawa K, Mita E, Hayashi Y, Hikita H, Sakamori R, Tatsumi T, Taguchi A, Eguchi H, Takehara T. ST6GAL1 Is a Novel Serum Biomarker for Lenvatinib-Susceptible FGF19-Driven Hepatocellular Carcinoma. *Clin Cancer Res* 2021; **27**: 1150-1161 [PMID: 33288659 DOI: 10.1158/1078-0432.CCR-20-3382]

22 **Li X**, Duan Y, Hao Y. Identification of super enhancer-associated key genes for prognosis of germinal center B-cell type diffuse large B-cell lymphoma by integrated analysis. *BMC Med Genomics* 2021; **14**: 69 [PMID: 33663517 DOI: 10.1186/s12920-021-00916-z]

23 **Jin S**, Guerrero-Juarez CF, Zhang L, Chang I, Ramos R, Kuan CH, Myung P, Plikus MV, Nie Q. Inference and analysis of cell-cell communication using CellChat. *Nat Commun* 2021; **12**: 1088 [PMID: 33597522 DOI: 10.1038/s41467-021-21246-9]

24 **Huang J**, Chen T, Wang J, Wang Z, Huang S. Weighted gene co-expression network analysis and CIBERSORT screening of key genes related to m6A methylation in Hirschsprung's disease. *Front Genet* 2023; **14**: 1183467 [PMID: 37144136 DOI: 10.3389/fgene.2023.1183467]

25 **Teng L**, Shen L, Zhao W, Wang C, Feng S, Wang Y, Bi Y, Rong S, Shushakova N, Haller H, Chen J, Jiang H. SLAMF8 Participates in Acute Renal Transplant Rejection *via* TLR4 Pathway on Pro-Inflammatory Macrophages. *Front Immunol* 2022; **13**: 846695 [PMID: 35432371 DOI: 10.3389/fimmu.2022.846695]

26 **Yang K**, Zhang XM, Yang L, Xu H, Peng J. Advanced imaging techniques in the therapeutic response of transarterial chemoembolization for hepatocellular carcinoma. *World J Gastroenterol* 2016; **22**: 4835-4847 [PMID: 27239110 DOI: 10.3748/wjg.v22.i20.4835]

27 **Su H**, Yang F, Fu R, Li X, French R, Mose E, Pu X, Trinh B, Kumar A, Liu J, Antonucci L, Todoric J, Liu Y, Hu Y, Diaz-Meco MT, Moscat J, Metallo CM, Lowy AM, Sun B, Karin M. Cancer cells escape autophagy inhibition *via* NRF2-induced macropinocytosis. *Cancer Cell* 2021; **39**: 678-693.e11 [PMID: 33740421 DOI: 10.1016/j.ccell.2021.02.016]

28 **Lin ZH**, Jiang JR, Ma XK, Chen J, Li HP, Li X, Wu XY, Huang MS, Lin Q. Prognostic value of serum HIF-1α change following transarterial chemoembolization in hepatocellular carcinoma. *Clin Exp Med* 2021; **21**: 109-120 [PMID: 33037574 DOI: 10.1007/s10238-020-00667-8]

29 **Mao J**, Tan Z, Pan X, Meng F. ASPP2 expression predicts the prognosis of patients with hepatocellular carcinoma after transcatheter arterial chemoembolization. *Exp Ther Med* 2021; **21**: 397 [PMID: 33680119 DOI: 10.3892/etm.2021.9828]

30 **Cheng X**, Li J, Feng L, Feng S, Wu X, Li Y. The role of hypoxia-related genes in TACE-refractory hepatocellular carcinoma: Exploration of prognosis, immunological characteristics and drug resistance based on onco-multi-OMICS approach. *Front Pharmacol* 2022; **13**: 1011033 [PMID: 36225568 DOI: 10.3389/fphar.2022.1011033]

31 **Gao L**, Song JR, Zhang JW, Zhao X, Zhao QD, Sun K, Deng WJ, Li R, Lv G, Cheng HY, Wei LX. Chloroquine promotes the anticancer effect of TACE in a rabbit VX2 Liver tumor model. *Int J Biol Sci* 2013; **9**: 322-330 [PMID: 23569437 DOI: 10.7150/ijbs.5925]

32 **Sadasivam S**, Subramanian R. A perspective on challenges and opportunities in characterizing oral cancer stem cells. *Front Biosci (Landmark Ed)* 2020; **25**: 1011-1021 [PMID: 32114422 DOI: 10.2741/4845]

33 **Han J**, Won M, Kim JH, Jung E, Min K, Jangili P, Kim JS. Cancer stem cell-targeted bio-imaging and chemotherapeutic perspective. *Chem Soc Rev* 2020; **49**: 7856-7878 [PMID: 32633291 DOI: 10.1039/d0cs00379d]

34 **Yao H**, Yang Z, Lou Y, Huang J, Yang P, Jiang W, Chen S. miR-186 Inhibits Liver Cancer Stem Cells Expansion *via* Targeting PTPN11. *Front Oncol* 2021; **11**: 632976 [PMID: 33816273 DOI: 10.3389/fonc.2021.632976]

35 **Ali HEA**, Emam AA, Zeeneldin AA, Srour R, Tabashy R, El-Desouky ED, Abd Elmageed ZY, Abdel-Wahab AA. Circulating miR-26a, miR-106b, miR-107 and miR-133b stratify hepatocellular carcinoma patients according to their response to transarterial chemoembolization. *Clin Biochem* 2019; **65**: 45-52 [PMID: 30653948 DOI: 10.1016/j.clinbiochem.2019.01.002]

36 **Zeng Z**, Ren J, O'Neil M, Zhao J, Bridges B, Cox J, Abdulkarim B, Schmitt TM, Kumer SC, Weinman SA. Impact of stem cell marker expression on recurrence of TACE-treated hepatocellular carcinoma post liver transplantation. *BMC Cancer* 2012; **12**: 584 [PMID: 23216644 DOI: 10.1186/1471-2407-12-584]

37 **Xiang D**, Cheng Z, Liu H, Wang X, Han T, Sun W, Li X, Yang W, Chen C, Xia M, Liu N, Yin S, Jin G, Lee T, Dong L, Hu H, Wang H, Ding J. Shp2 promotes liver cancer stem cell expansion by augmenting β-catenin signaling and predicts chemotherapeutic response of patients. *Hepatology* 2017; **65**: 1566-1580 [PMID: 28059452 DOI: 10.1002/hep.28919]

38 **Herreros-Villanueva M**, Bujanda L, Billadeau DD, Zhang JS. Embryonic stem cell factors and pancreatic cancer. *World J Gastroenterol* 2014; **20**: 2247-2254 [PMID: 24605024 DOI: 10.3748/wjg.v20.i9.2247]

39 Zhou S, Li M, Ostrow D, Ruble D, Mascarenhas L, Pawel B, Buckley JD, Triche TJ. Potential methylation-regulated genes and pathways in hepatocellular neoplasm, not otherwise specified. *Front Oncol* 2022; **12**: 952325 [PMID: 36212481 DOI: 10.3389/fonc.2022.952325]

40 **Mennen RH**, Oldenburger MM, Piersma AH. Endoderm and mesoderm derivatives in embryonic stem cell differentiation and their use in developmental toxicity testing. *Reprod Toxicol* 2022; **107**: 44-59 [PMID: 34861400 DOI: 10.1016/j.reprotox.2021.11.009]

41 **Hall Z**, Chiarugi D, Charidemou E, Leslie J, Scott E, Pellegrinet L, Allison M, Mocciaro G, Anstee QM, Evan GI, Hoare M, Vidal-Puig A, Oakley F, Vacca M, Griffin JL. Lipid Remodeling in Hepatocyte Proliferation and Hepatocellular Carcinoma. *Hepatology* 2021; **73**: 1028-1044 [PMID: 32460431 DOI: 10.1002/hep.31391]

42 **Li B**, Cao Y, Meng G, Qian L, Xu T, Yan C, Luo O, Wang S, Wei J, Ding Y, Yu D. Targeting glutaminase 1 attenuates stemness properties in hepatocellular carcinoma by increasing reactive oxygen species and suppressing Wnt/beta-catenin pathway. *EBioMedicine* 2019; **39**: 239-254 [PMID: 30555042 DOI: 10.1016/j.ebiom.2018.11.063]

43 **Ying L**, Cheng M, Lu Y, Tao Q, Chen X, Shen B, Xiong F, Hu Z, Wang D, Li X. Glutamine Metabolism Scoring Predicts Prognosis and Therapeutic Resistance in Hepatocellular Carcinoma. *Pathol Oncol Res* 2021; **27**: 1610075 [PMID: 34992505 DOI: 10.3389/pore.2021.1610075]

World Journal of Clinical Oncology

Submit a Manuscript: https://www.f6publishing.com

World J Clin Oncol 2024 January 24; 15(1): 89-114

DOI: 10.5306/wjco.v15.i1.89

ISSN 2218-4333 (online)

ORIGINAL ARTICLE

Clinical and Translational Research

Predicting colorectal cancer prognosis based on long noncoding RNAs of disulfidptosis genes

Kui-Ling Wang, Kai-Di Chen, Wen-Wen Tang, Ze-Peng Chen, Yu-Ji Wang, Guo-Ping Shi, Yu-Gen Chen

Specialty type: Medicine, research and experimental

Provenance and peer review: Unsolicited article; Externally peer reviewed.

Peer-review model: Single blind

Peer-review report's scientific quality classification

Grade A (Excellent): A
Grade B (Very good): 0
Grade C (Good): 0
Grade D (Fair): 0
Grade E (Poor): 0

P-Reviewer: Lim YC, Brunei Darussalam

Received: October 25, 2023
Peer-review started: October 26, 2023
First decision: December 12, 2023
Revised: December 17, 2023
Accepted: January 4, 2024
Article in press: January 4, 2024
Published online: January 24, 2024

Kui-Ling Wang, Kai-Di Chen, Wen-Wen Tang, Ze-Peng Chen, Yu-Ji Wang, Guo-Ping Shi, Yu-Gen Chen, Department of Colorectal Surgery, The Affiliated Hospital of Nanjing University of Chinese Medicine, Nanjing 210029, Jiangsu Province, China

Corresponding author: Yu-Gen Chen, Doctor, MD, PhD, Chief Doctor, Professor, Surgeon, Department of Colorectal Surgery, The Affiliated Hospital of Nanjing University of Chinese Medicine, No. 155 Hanzhong Road, Qinhuai District, Nanjing 210029, Jiangsu Province, China. yugen.chen@njucm.edu.cn

Abstract

BACKGROUND

A recently hypothesized cause of cell death called disulfidptosis has been linked to the expansion, emigration, and vascular rebuilding of cancer cells. Cancer can be treated by targeting the pathways that trigger cell death.

AIM

To discover the long non-coding RNA of the disulfidaptosis-related lncRNAs (DRLs), prognosis clinical survival, and treat patients with colorectal cancer with medications.

METHODS

Initially, we queried the Cancer Genome Atlas database to collect transcriptome, clinical, and genetic mutation data for colorectal cancer (CRC). Training and testing sets for CRC patient transcriptome data were generated randomly. Key long non-coding RNAs (lncRNAs) related to DRLs were then identified and evaluated using a least absolute shrinkage and selection operator procedure, as well as univariate and multivariate Cox regression models. A prognostic model was then created after risk scoring. Also, Immune infiltration analysis, immune checkpoint analysis, and medication susceptibility analysis were used to investigate the causes of the different prognoses between high and low risk groups. Finally, we validated the differential expression and biomarker potential of risk-predictive lncRNAs through induction using both NCM460 and HT-29 cell lines, as well as a disulfidptosis model.

RESULTS

In this work, eight significant lncRNAs linked to disulfidptosis were found. Gene ontology and Kyoto Encyclopedia of Genes and Genomes pathway enrichment analyses of differentially expressed genes between high- and low-risk groups

from the prognostic model showed a close relationship with the immune response as well as significant enrichment in neutrophil extracellular trap formation and the IL-17 signaling pathway. Furthermore, significant immune cell variations between the high-risk and low-risk groups were seen, as well as a higher incidence of immunological escape risk in the high-risk group. Finally, Epirubicin, bortezomib, teniposide, and BMS-754807 were shown to have the lowest sensitivity among the four immunotherapy drugs.

CONCLUSION
Our findings emphasizes the role of disulfidptosis in regulating tumor development, therapeutic response, and patient survival in CRC patients. For the clinical treatment of CRC, these important LncRNAs could serve as viable therapeutic targets.

Key Words: Colorectal cancer; Clinical outcomes; Disulfidptosis; Drug sensitivity; Immunotherapy

Core Tip: Disulfidoptosis is a recently identified form of programmed cell death that is being intensely studied in the fields of tumor formation and therapy. Various studies have demonstrated the crucial predictive accuracy of biomarkers linked to disulfidoptosis for the diagnosis and management of cancer. In the mean time, there is increasing confirmation that lncRNA regulates the growth and progression of colorectal cancer (CRC). This study scrutinized out lncRNA closely correlated with disulfidoptosis and assessed its prognostic significance in CRC patients *via* integrating bioinformatics technology with a clinical patient database.

Citation: Wang KL, Chen KD, Tang WW, Chen ZP, Wang YJ, Shi GP, Chen YG. Predicting colorectal cancer prognosis based on long noncoding RNAs of disulfidptosis genes. *World J Clin Oncol* 2024; 15(1): 89-114
URL: https://www.wjgnet.com/2218-4333/full/v15/i1/89.htm
DOI: https://dx.doi.org/10.5306/wjco.v15.i1.89

INTRODUCTION

Colorectal cancer (CRC), the third most prevalent cancer in the world, accounting for over 1.8 million new cases and 881000 fatalities per year[1]. Via the use of auxiliary diagnostic procedures such as biochemical testing, digital rectal examination, sigmoidoscopy, and colonoscopy, the detection and survival rates of CRC have gradually improved[2,3]. However, among people under 50, the incidence and metastatic rates have been steadily increasing[4,5], with the incidence of CRC among adults under 50 years old increasing annually between 2012 to 2016 at a rate of 2.2%[6]. Nevertheless, CRC is also a heterogeneous disease[7], and challenges like microsatellite instability and chromosomal instability brought on by gene mutations, as well as multidrug resistance caused by tumor heterogeneity can affect treatment outcomes[8]. Thus, to choose the best chemotherapeutic treatments, identify sensitive groups, diagnose early stages of the disease, and increase the efficacy of diagnosis and treatment, it is desirable to investigate new biomarkers[9].

Recently, a process of cellular death known as, which is associated with the buildup of intracellular disulfide compounds, was postulated. This may therefore signify a change in how tumors are treated. Solute Carrier Family 7 Member 11 (SLC7A11) is overexpressed in the tumor microenvironment, where it speeds up the transport of cysteine into cells. In addition, injured immune cells and tumor cells have high metabolic rates and eat large amounts of glucose, which therefore causes a shortage of the reducing agent nicotinamide adenine dinucleotide phosphate (NADPH) and triggers glucose deprivation[10]. The reduction of cysteine to cystine is impacted by enhanced cysteine transport and the absence of NADPH, and in turn causes an accumulation of intracellular disulfide compounds. This accumulation then causes cell death following alteration of the cytoskeletal protein shape[11]. When cells overexpressing SLC7A11 are starved of glucose, Liu *et al*[12] found that supplementing culture media with 2-mercaptoethanol—a chemical that breaks disulfide bonds—can prevent defects induced by oxidative stress and therefore prevent cell death. Overall, disulfidptosis is a novel target for tumor therapy because it disturbs the integrity of the tumor microenvironment[13].

Noncoding RNAs longer than 200 nucleotides are known as long noncoding RNAs (lncRNAs). They are known to control the proliferation, differentiation, invasion, and metastasis of cancer cells by interacting with DNA, RNA, proteins, or lipids[14,15]. In addition, lncRNAs can control how metabolically relevant proteins undergo post-translational changes and support cancer energy metabolism[16]. Moreover, it has been widely documented that lncRNAs and CRC have a regulatory link. LncRNAs function as signaling molecules in pathways relevant to CRC or as competitive endogenous RNAs (ceRNAs) by competitively binding to common microRNA (miRNA) binding sites. This sequesters miRNAs and changes the expression of downstream target genes[17]. For example, by controlling the focal adhesion signaling pathway, the lncRNA ITGB8-AS1 functions as a ceRNA to enhance CRC cell proliferation and tumor formation[18]. Moreover, CRC can be efficiently inhibited by targeting ITGB8-AS1. In addition, studies have shown that lncRNAs play a role in many stages of CRC, including intestinal polyps and distant metastases, making them attractive prospective targets for treatment[19].

At present, there is no published data regarding the regulatory connection between disulfidaptosis-related lncRNAs (DRLs) and CRC. Consequently, the objective of this study is to determine whether DRLs can be used as a tumor biomarker for CRC to forecast patients prognoses and responses to treatment. Our study therefore offers a novel approach for forecasting how cancer patients respond to treatment and how they may fare clinically.

MATERIALS AND METHODS

Data sources

First, we obtained transcriptomic data for the Cancer Genome Atlas (TCGA)-COAD and TCGA-READ, including 564 CRC tumor samples and 44 normal tissue samples. Next, we ran Perl version 5.30.0 to extract RNA information from transcriptomic data and matched them with clinical datasets containing variables such as sex, age, stage, and survival time[20].

Screening for lncRNAs co-expressed with disulfidptosis genes

First, we searched for "disulfidptosis" in PubMed (https://pubmed.ncbi.nlm.nih.gov/?db=pubmed) and identified several genes connected to this molecular function. Next, we used the R packages "BiocManager" and "limma" as implemented in R version 4.2.0[21] to obtain an LncRNA expression matrix for disulfidptosis. |Pearson R| > 0.5 and P < 0.001 were used as filter conditions to produce an expression matrix for DRLs. We then used the "ggplot2" and "ggalluvial" R packages to create a Sankey association between genes related to disulfidptosis and DRLs[22].

Building and validating a risk prognosis model

Next, we combined clinical survival data with the LncRNA expression matrix, and omitted patients with missing information. CRC patients were then randomly allocated to training and testing groups. The testing group and the full dataset were used to validate the accuracy of the prognostic model, while the training group was used to construct the prognostic model. Next, to test the DRLs of the prognostic model, we used least absolute shrinkage and selection operator (LASSO) and univariate Cox regression analysis, followed by multivariate Cox regression analysis, at a significance threshold of P < 0.05. Eight DRLs were obtained. Relevant risk curves and heatmaps were then plotted using the "survival," "glmnet," "survminer," and "timeROC" R packages[23,24]. The following equation was then used to obtain the risk score[25]: Risk score = Σi = lnCoef (i) × Expr (i). The risk expression (Expr(i)) and risk coefficient (Coef(i)) functions represent the corresponding risk coefficient and risk expression. The samples in the training and testing groups were split into high-risk and low-risk groups based on the median values of the risk ratings assigned to each patient in the training group. The R packages "survival," "replot," and "rms" were used to create receiver operating characteristic (ROC) curves, c-index plots, column line plots, and calibration plots to evaluate the independence and accuracy of the prognostic model[26].

Gene ontology, Kyoto encyclopedia of genes and genomes, and gene set enrichment analysis pathway enrichment analysis

Next, we performed gene ontology (GO) functional enrichment analysis, Kyoto encyclopedia of genes and genomes (KEGG) pathway enrichment analysis, and gene set enrichment analysis (GSEA) enrichment analysis on the identified differentially expressed genes (DEGs) in the high-risk and low-risk groups, respectively. These analyses used a P value cutoff of 0.05 and a q-value cutoff of 0.05, and was implemented using the R software packages colorspace, stringi, DOSE, clusterProfiler, and enrichplot.

Tumor mutational burden and immune dysfunction and exclusion analyses

The tumor mutational burden (TMB) for each patient was determined using Perl scripts to analyze CRC mutation data. We carried out differential analysis using the R software packages "ggpubr," "limma," "survival," and "survminer." The "ggpubr" and "limma" packages. Next, the tumor immune dysfunction and exclusion (TIDE) score file was acquired from the TIDE website (http://tide.dfci.harvard.edu), and violin plots were created to compare the immune escape capabilities of high- and low-risk groups with respect to CRC TIDE[27].

Analysis of differences in the tumor microenvironment

We then used the "reshape2" and "ggpubr" packages to compare the immunological characteristics of the high- and low-risk cluster groups, and used box plots to illustrate the abundances of 22 tumor-infiltrating immune cells. We also used the "limma," "reshape2," "tidyverse," "ggplot2," "ggpubr," and "ggExtra" R packages to create a correlation heatmap for risk score, immune cell infiltration, and immune checkpoint analysis.

Analyses of drug susceptibility

The Genomics of Drug Sensitivity in Cancer (GDSC) website (https://www.cancerrxgene.org) was used to extract drug sensitivity and expression data for targeted therapies. OncoPredict software was used to forecast how responsive patients in the high- and low-risk groups would be to therapeutic medications[28,29].

Cell lines and cell culture

Human colorectal adenocarcinoma cells (HT-29) and normal colonic epithelial cells (NCM460) were procured from the Cell Repository at the Shanghai Institute of Cell Research (Shanghai, China). Both cell lines were authenticated using short tandem repeat analysis, and mycoplasma testing results were negative. NCM460 cells were cultured in RPMI-1640 medium (Gibco, California, United States), while HT29 cells were grown in Dulbecco's Modified Eagle Medium (DMEM) (Gibco, United States). Both culture media were supplemented with 10% fetal bovine serum (FBS, Sangon Biotech, China), as well as 100 U/mL penicillin and streptomycin (PS, Gibco, Shanghai, China). Additionally, both cell lines were maintained in a humidified incubator at 37 ◦C with 5% CO2.

Disulfidoptosis cell model establishment and cell proliferation assay

The experimental procedure was based on previously established protocols. 2-fluoro-6- (m-hydroxybenzoyloxy) phenyl m-hydroxybenzoate (WZB117) is a glucose transporter 1 (Glut1) inhibitor, effectively suppressing glucose uptake. In cancer cells with overexpression or underexpression of SLC7A11, WZB117 treatment creates a glucose-deficient intracellular environment, significantly reducing the production of NADPH in the pentose phosphate pathway. Insufficient NADPH impairs the ability to reduce accumulated intracellular cysteine, inducing disulfide stress and leading to cell death[12]. Therefore, WZB117 can mimic the intracellular conditions of glucose starvation, making it an inducer of disulfidoptosis.

Cell proliferation was assessed using the cell counting kit-8 (CCK8) assay kit (Bio-Rad Laboratories, Inc.) according to the manufacturer's instructions[30]. HT-29 cells were seeded at a density of 5-6 × 10^3 cells per well in a 96-well plate and cultured at 37°C for 24 h. After removing the culture medium, different concentrations of WZB117 (0, 1, 3, 10, 15, 30, 50, 100, 300 μmol/L) were added, and the cells were incubated for an additional 24 h. Subsequently, the culture medium was removed, and 100 μL of basal culture medium and 10 μL of CCK8 reagent were added to each well. The cells were then cultured for 4 h, and the absorbance at 450 nanometers was measured to assess cell viability under various drug concentrations.

Quantitative real-time polymerase chain reaction analysis

NCM460 cells and HT29 cells were seeded in 6-well plates (1-2 × 10^5 cells per well). HT-29 cells were treated with WZB117 (0 and 300 μmol/L) for 24 h. After 24 h, the culture medium was removed, and cells were washed 2-3 times with PBS at 4°C, harvested, and lysed. Total RNA from NCM460 and HT-29 cells was extracted using the RNA isolator (Vazyme, Nanjing, China). Complementary DNA (cDNA) was synthesized from 1 ng of total RNA using the NovoScript Plus All-in-one 1st Strand cDNA Synthesis SuperMix Kit, which contains genomic DNA (gDNA) removal (Jiangsu Novogene Bioinformatics Technology Co., Ltd.). Real-time quantitative polymerase chain reaction (qPCR) was performed using the QuantStudio 5 Real-Time PCR System (Applied Biosystems, United States) with the Hieff qPCR SYBR Green Master Mix (Shanghai Yisen Biological Technology Co., Ltd.). The primers listed in Table 1 were synthesized by Sangon Biotechnology (Shanghai) Co., Ltd.

RESULTS

Expression of LncRNA associated with co-expression of the disulfidptosis gene in CRC

A total of 571 CRC expression sequences and normal sample expression sequences were discovered using the TCGA transcriptome data. In addition, a literature search identified ten disulfidptosis genes (Supplementary Table 1). We then identified 564 differentially regulated lncRNAs following a correlation analysis between the disulfidptosis genes and CRC LncRNA dataset (|Pearson's R| > 0.5 and $P < 0.001$; Supplementary Table 2). Subsequent patients with incomplete data were then eliminated and the CRC LncRNA expression matrix was combined with clinical survival data, so we then obtained a total of 542 CRC patients in an expression matrix who satisfied all criteria. We found no significant variation in the clinical characteristics of the two groups between the 542 CRC patients randomly between the training group ($n = 271$) and the testing group ($n = 271$; Table 2). The relationship between DRLs and disulfide death genes was depicted using a Sankey diagram (Figure 1A). Next, using LASSO and univariate Cox regression analyses, 12 DRLs associated with CRC prognosis were identified, including five protective DRLs (*i.e.*, SNHG16, AC093157.1, AC005034.5, TNFRSF10A-AS1, and AC011815.1) and seven DRLs with a hazard ratio (HR) > 1, which indicate adverse prognostic factors (Figure 1B-D). Finally, eight DRLs were discovered that were related to overall survival (OS) in the TCGA-COAD and TCGA-READ cohorts based on multivariate Cox regression analysis (Supplementary Table 3). A correlation heatmap was then created to show the co-expression patterns of these eight DRLs (*i.e.*, AC005034.5, AC006213.7, AC011815.1, AC013652.1, AC093157.1, AL354993.2, AL683813.1, and TNFRSF10A-AS1), which were thought to have the most significant impact on CRC prognosis (Figure 1E).

Building a risk prediction model to predict OS in CRC patients

Subsequently, the risk score formula was utilized to calculate each score to generate the risk curve. The patient sample, ranked from low risk to high risk, is the abscissa in Figure 2A-C, while the ordinate represents the risk score value. 542 CRC patients were categorized as high risk or low risk based on the training group risk score's median risk score value. The survival time of the patients in the training group, test group, and all sets were subsequently analyzed (Figure 2D-F). That was discovered that the number of dead patients increased as the risk of the abscissa increased, and that the survival life of the deceased patients, represented by the red circle chart, was more brief than that of the surviving patients,

Table 1 Primers for disulfidptosis-related lncRNAs/Genes

LncRNA/Gene	Forward primer	Reverse primer
AC005034.5	TGCAAGGTGTCATCTGTAAGG	TGACAGTTCCAACAGGGCTA
AC011815.1	GGCCAGCGACAGATCCTTT	TGGCCCACTGTTGCCATCAA
AC013652.1	AGGGCATCAGACTGCATTTCA	GACAAGCAGAAAATGGGGCA
AC093157.1	GAGATGGGCAAGCCTACACC	TGGGTCCAGAAAGAAGTTGC
AL354993.2	TGCATTCCAGAGGGAGGAGA	CCACTCCTTGGAAGCTGTCT
AL683813.1	GCGGCTGAGTTTCTGACTCT	GTTTGGGATACAGGAGGCCG
TNFRSF10A-AS1	TCAGTGATAGCAACAGAAAACAG	ACTGCACCTAGCCAAGATGTC
TCAP	GAGTTCCCAAAGGGAGGGTG	TTTTCCTGGATCAGGGCCAC
NNAT	AATCAAAACACCGCACCAGC	ACCACCCTCCTTCCTCAACT
CHGB	GGTCCTCTCAAGGAGGGAGT	AGTGGGTTGAATGGTGGTCC
COL2A1	GCTCCCAGAACATCACCTACC	CGATAACAGTCTTGCCCCAC
β-actin	CGCGAGAAGATGCCCAGATC	TCACCGGAGTCCATCACGA

Table 2 Clinical characteristics of colorectal cancer patients in the training and testing groups, *n* (%)

Covariates	Type	Total	Test	Train	*P* value
Age	≤ 70	312 (57.56)	160 (59.04)	152 (56.09)	0.543
Age	> 70	230 (42.44)	111 (40.96)	119 (43.91)	-
Gender	FEMALE	255 (47.05)	137 (50.55)	118 (43.54)	0.1214
Gender	MALE	287 (52.95)	134 (49.45)	153 (56.46)	-
Stage	StageI	93 (17.16)	43 (15.87)	50 (18.45)	0.3949
Stage	StageII	208 (38.38)	100 (36.9)	108 (39.85)	-
Stage	StageIII	148 (27.31)	82 (30.26)	66 (24.35)	-
Stage	StageIV	78 (14.39)	36 (13.28)	42 (15.5)	-
Stage	Unknow	15 (2.77)	10 (3.69)	5 (1.85)	-
T	T1	15 (2.77)	6 (2.21)	9 (3.32)	0.8475
T	T2	93 (17.16)	45 (16.61)	48 (17.71)	-
T	T3	370 (68.27)	188 (69.37)	182 (67.16)	-
T	T4	63 (11.62)	32 (11.81)	31 (11.44)	-
T	Unknow	1 (0.18)	0 (0)	1 (0.37)	-
M	M0	402 (74.17)	205 (75.65)	197 (72.69)	0.4435
M	M1	77 (14.21)	35 (12.92)	42 (15.5)	-
M	Unknow	63 (11.62)	31 (11.44)	32 (11.81)	-
N	N0	318(58.67)	154 (56.83)	164 (60.52)	0.5238
N	N1	129 (23.8)	70 (25.83)	59 (21.77)	-
N	N2	94 (17.34)	46 (16.97)	48 (17.71)	-
N	Unknow	1 (0.18)	1 (0.37)	0 (0)	-

represented by the blue circle chart. In the test group, low risk patients tended to have higher OS than high risk patients, but the distinction was not statistically significant (P = 0.089; Figure 2K), possibly caused by the small sample size. Following that, the survival analysis of the three groups revealed that the low risk patients exceeded the OS in the training and all sets (P < 0.001; Figure 2J and L). The aforementioned findings demonstrate how well the risk score model predicts patient survival. The concentrations of AL354993.2, AC006213.7, AC013652.1, and AL683813.1 were more abundant in the high-risk group, according to an analysis of the risk score heatmap of the two groups. This suggested that

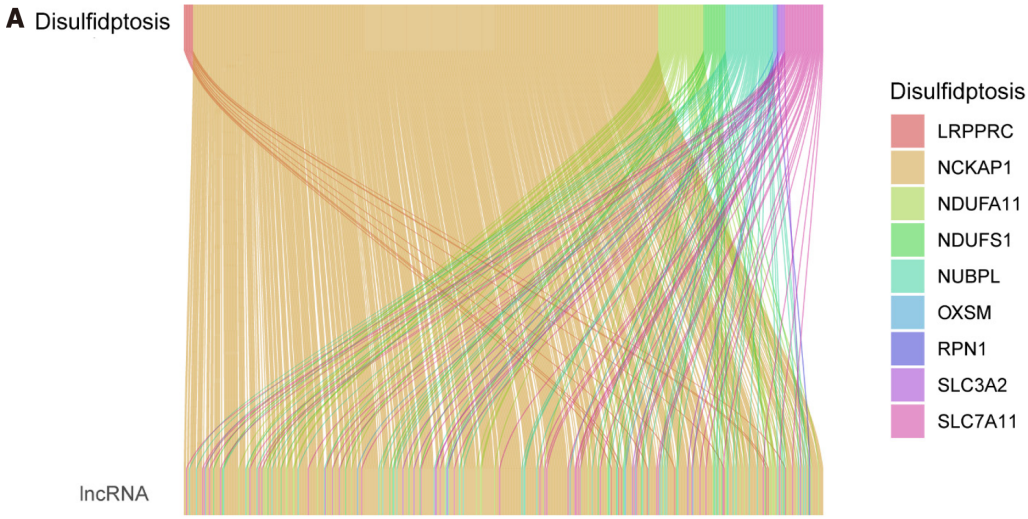
A Disulfidptosis
lncRNA
Disulfidptosis
LRPPRC
NCKAP1
NDUFA11
NDUFS1
NUBPL
OXSM
RPN1
SLC3A2
SLC7A11

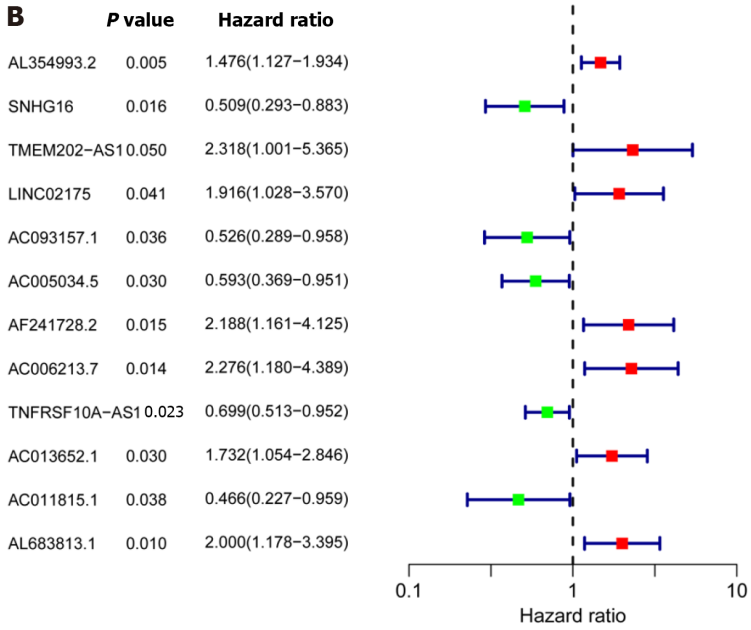
B
P value
Hazard ratio
AL354993.2 0.005 1.476(1.127−1.934)
SNHG16 0.016 0.509(0.293−0.883)
TMEM202−AS1 0.050 2.318(1.001−5.365)
LINC02175 0.041 1.916(1.028−3.570)
AC093157.1 0.036 0.526(0.289−0.958)
AC005034.5 0.030 0.593(0.369−0.951)
AF241728.2 0.015 2.188(1.161−4.125)
AC006213.7 0.014 2.276(1.180−4.389)
TNFRSF10A−AS1 0.023 0.699(0.513−0.952)
AC013652.1 0.030 1.732(1.054−2.846)
AC011815.1 0.038 0.466(0.227−0.959)
AL683813.1 0.010 2.000(1.178−3.395)
0.1
1
10
Hazard ratio

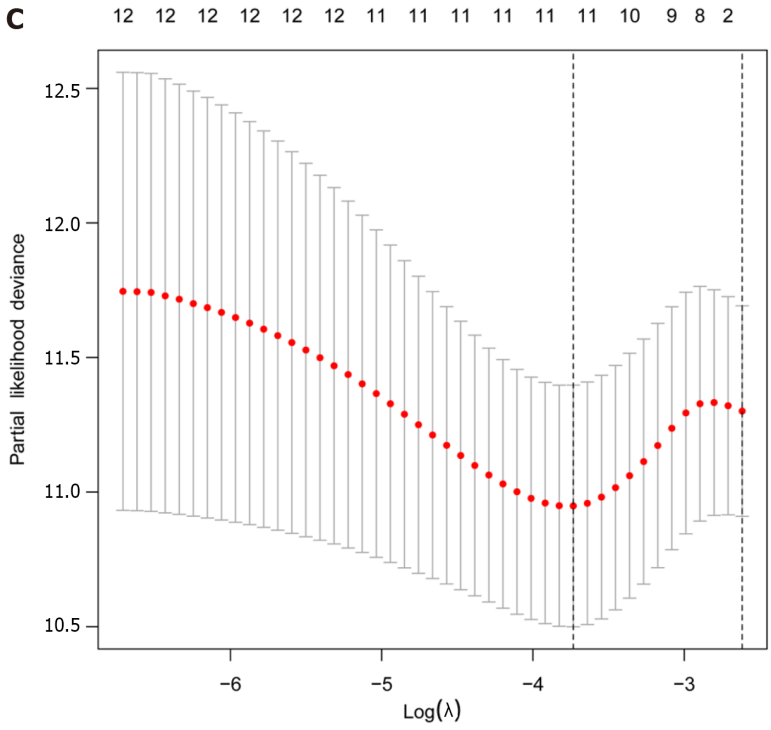
C
12 12 12 12 12 12 11 11 11 11 11 11 10 9 8 2
12.5
12.0
11.5
11.0
10.5
Partial likelihood deviance
−6
−5
−4
−3
Log(λ)

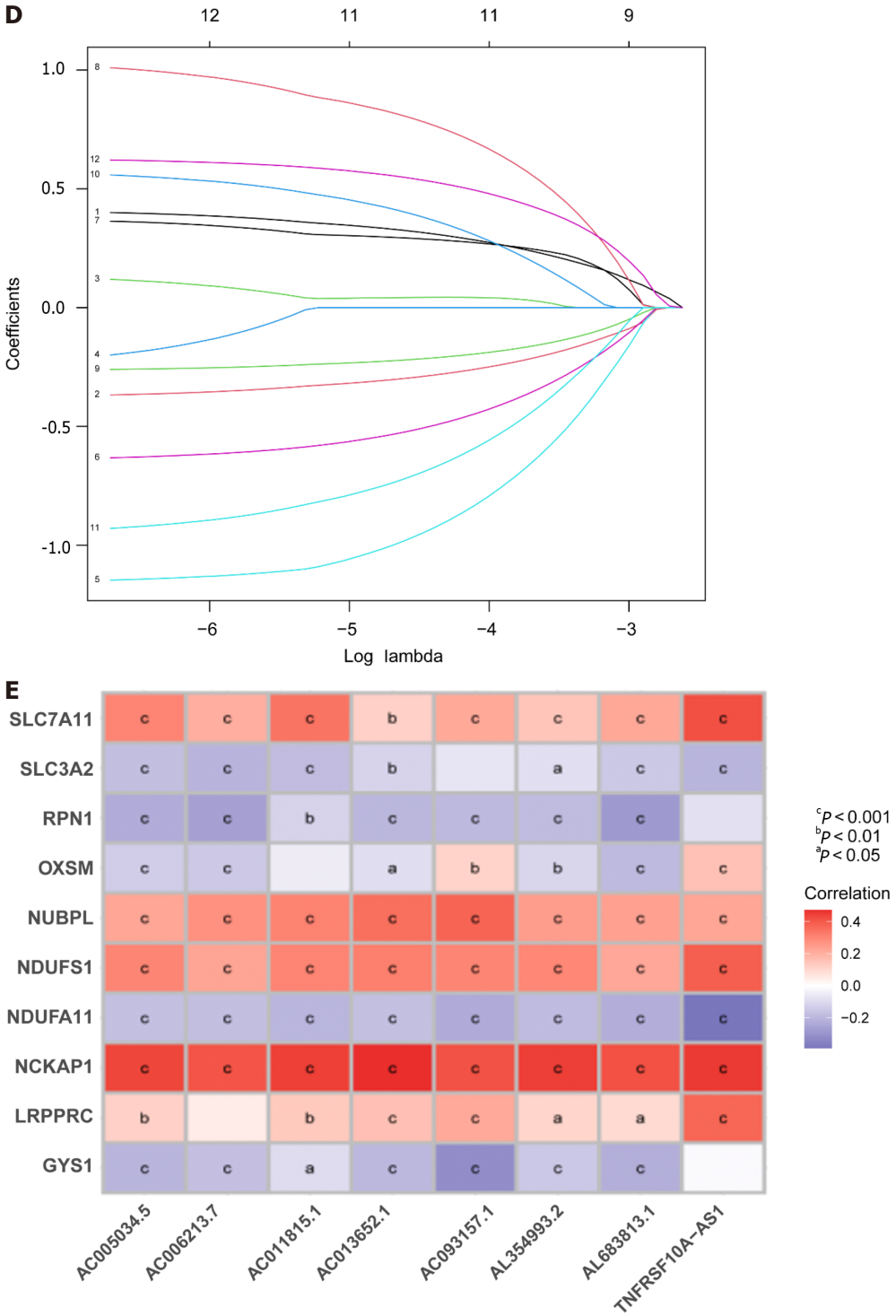

DOI: 10.5306/wjco.v15.i1.89 **Copyright** ©The Author(s) 2024.

Figure 1 Prognostic features of disulfidaptosis-related lncRNAs in colorectal cancer. A: Sankey diagram showing the relationship between disulfidaptosis-related genes and disulfidaptosis-related lncRNAs (DRLs); B: Forest plot of prognostic genes associated with DRLs; C: The least absolute shrinkage and selection operator (LASSO) coefficients of DRLs obtained *via* LASSO analysis; D: Cross-validation of DRLs in LASSO regression; E: Multivariable Cox regression analysis and correlation between disulfidaptosis genes and DRLs. $^{a}P < 0.05$; $^{b}P < 0.01$; $^{c}P < 0.001$.

these four DRLs may act as biomarkers for poor CRC prognosis. Comparing the high-risk group to the low-risk group revealed that AC093157.1, AC005034.5, TNFRSF10A-AS1, and AC011815.1 were less abundant, suggesting that these four DRLs may be valuable prognostic indicators for CRC (Figure 2G-I). All patients were also subjected to a progression-free survival analysis, with the results demonstrating that the low-risk group had a longer period of high-quality survival (Figure 2M). This observation is consistent with the finding that the low-risk group had a higher OS than the high-risk group. In addition, based on clinical factors such age, gender, and stage, we then compared the chance of survival and clinical traits of CRC patients. These findings demonstrated that high-risk patients had shorter OS than low-risk patients regardless of clinical characteristics, with the exception of stage I–II (Figure 3). We also note that inconsistency in results

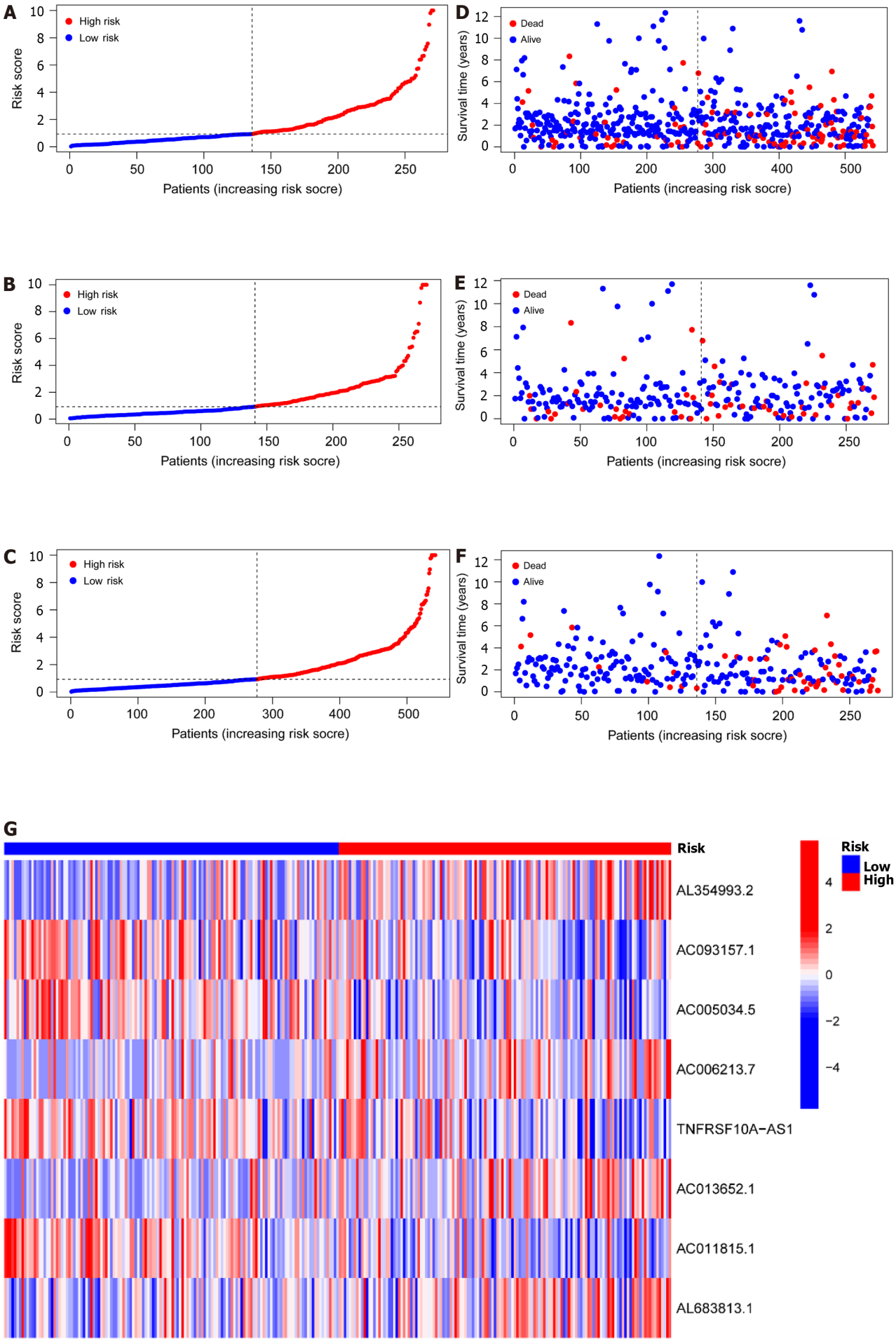
A
High risk
Low risk
Risk score
Patients (increasing risk socre)
D
Dead
Alive
Survival time (years)
Patients (increasing risk socre)
B
High risk
Low risk
Risk score
Patients (increasing risk socre)
E
Dead
Alive
Survival time (years)
Patients (increasing risk socre)
C
High risk
Low risk
Risk score
Patients (increasing risk socre)
F
Dead
Alive
Survival time (years)
Patients (increasing risk socre)
G
Risk
Low
High
AL354993.2
AC093157.1
AC005034.5
AC006213.7
TNFRSF10A-AS1
AC013652.1
AC011815.1
AL683813.1

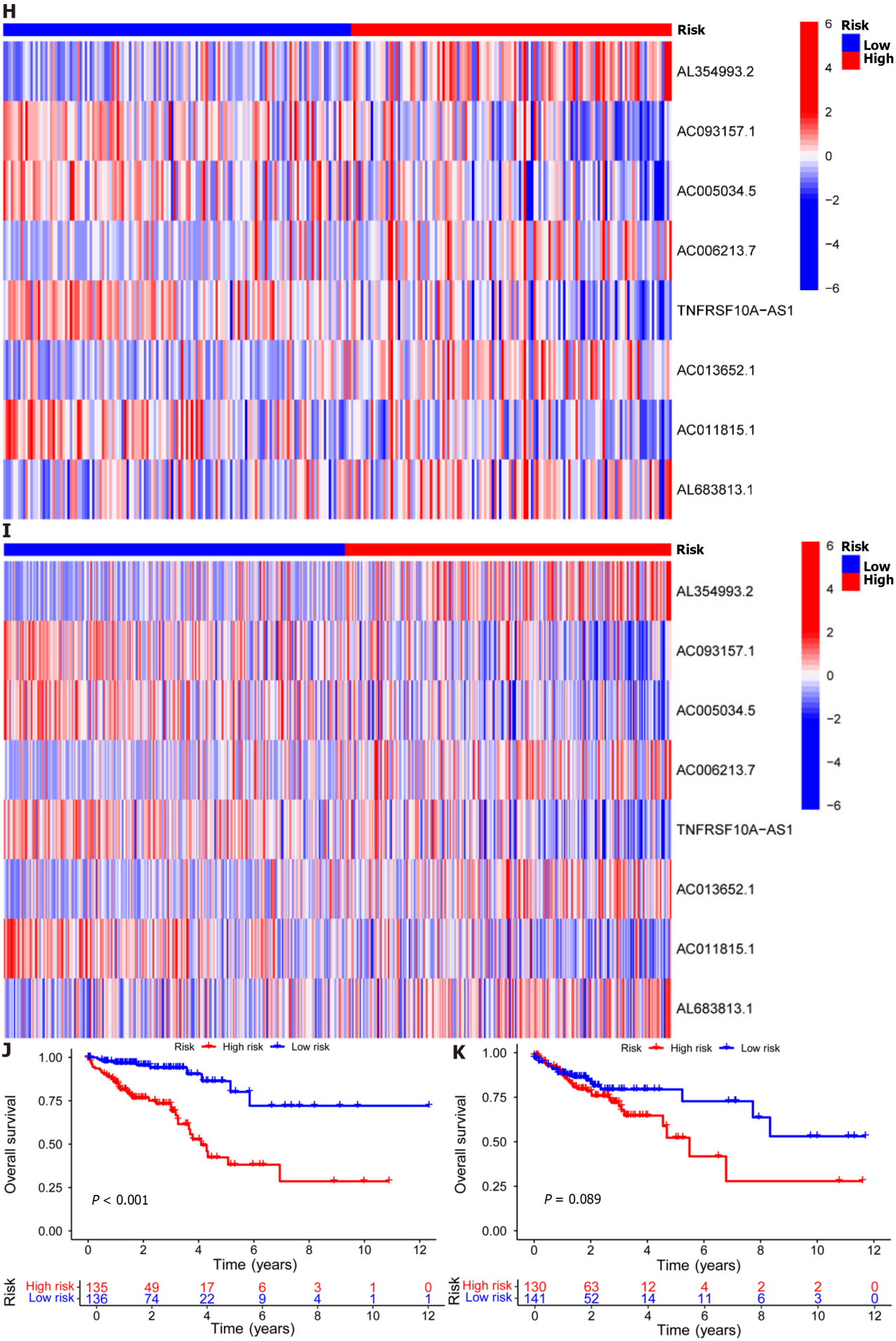
H
Risk
AL354993.2
AC093157.1
AC005034.5
AC006213.7
TNFRSF10A-AS1
AC013652.1
AC011815.1
AL683813.1
6
4
2
0
−2
−4
−6
Risk
Low
High
I
Risk
AL354993.2
AC093157.1
AC005034.5
AC006213.7
TNFRSF10A-AS1
AC013652.1
AC011815.1
AL683813.1
6
4
2
0
−2
−4
−6
Risk
Low
High
J
Risk
High risk
Low risk
Overall survival
1.00
0.75
0.50
0.25
0.00
P < 0.001
0
2
4
6
8
10
12
Time (years)
Risk
High risk 135 49 17 6 3 1 0
Low risk 136 74 22 9 4 1 1
Time (years)
K
Risk
High risk
Low risk
Overall survival
1.00
0.75
0.50
0.25
0.00
P = 0.089
Time (years)
Risk
High risk 130 63 12 4 2 2 0
Low risk 141 52 14 11 6 3 0
Time (years)

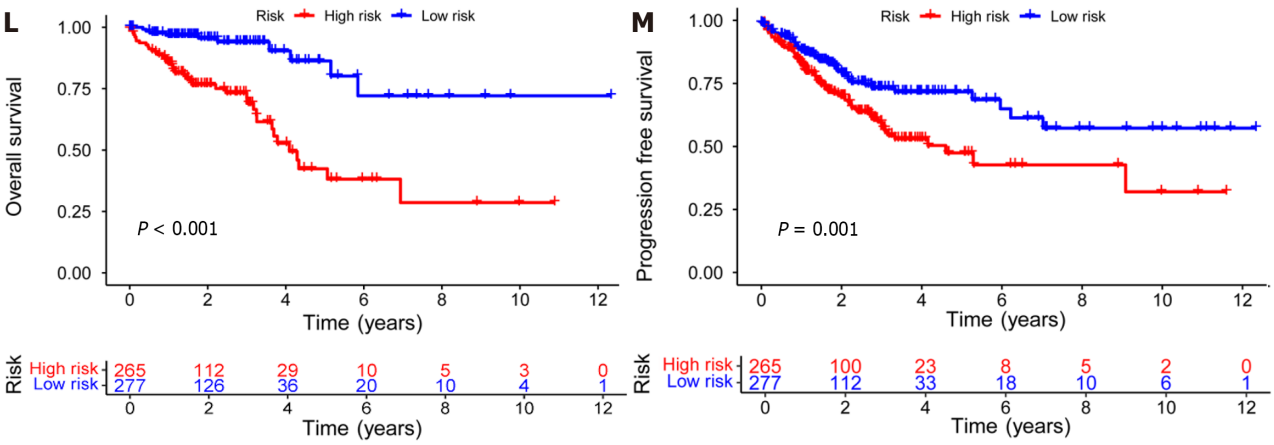

DOI: 10.5306/wjco.v15.i1.89 **Copyright** ©The Author(s) 2024.

Figure 2 Establishment of a risk prediction model for predicting overall survival in colorectal cancer patients. A-C: Distribution of patients in the training, testing, and combined sets with increasing risk scores; D-F: Survival time and risk scores of patients in the three groups; G-I: Risk score heatmaps for eight key disulfidaptosis-related lncRNAs in the three groups; J-L: Kaplan–Meier survival analysis of overall survival in the three groups of colorectal cancer patients; M: Progression-free survival analysis of the combined dataset.

may be due to the small patient population within this group and the poor prognosis associated with advanced CRC, both of which may impact the accuracy of results for stage I-stage II patients. In conclusion, the clinical outcomes of CRC patients can be predicted using a prognostic model developed using on DRLs risk assessment. Patients' DRLs risk scores were negatively associated with OS, with greater risk scores being accompanied by shorter OS and a poorer outlook.

DRLs risk prognosis model is a robust determinant of clinical outcomes of CRC patients

Patient age, gender, cancer stage, and risk score were subjected to single- and multi-factor Cox regression analyses. We discovered that both methods indicated risk scores that were statistically significant ($P < 0.001$), indicating that risk score is an independent prognostic factor for CRC apart from other clinical variables (Figure 4A and B). The areas under the curve (AUCs) for the 1-, 3-, and 5-year ROCs curves were also plotted (Figure 4C) indicates the high accuracy of the DRLs risk prognostic model for predicting the OS of patients. Furthermore, the AUC of the risk score was 0.665 (Figure 4D), which shows that the model's predictive power is greater than the additional clinical variables besides staging. Consistent with these findings, the C-index curve (Figure 4E) also revealed that the risk model had a higher concordance index than all clinical factors other than staging. A calibration plot was then created to compute OS *via* risk score and patient clinical parameters. According to these findings, patients had survival rates of 0.933, 0.803, and 0.722 after one, three, and five years, respectively (Figure 4F). A calibration curve (Figure 4G) verified the accuracy of the calibration plot. The DRLs risk prognostic model, in conclusion, reliably predicts the CRC patient survival and functions as an exceptional predictive indicator that is independent of other clinical characteristics.

GO, KEGG, and GSEA

DEGs were identified using the average gene expression levels of samples from the high- and low-risk group samples (Padj < 0.05, |log2 (fold change)|1, Supplementary Table 4). We used the "Bioconductor" R package in R software to perform GO enrichment analysis and KEGG pathway analysis to investigate the biological roles of DEGs. The biological processes (BP) that DEGs were found to be involved in included "chromatin remodeling," "protein-DNA complex subunit organization," "nucleosome organization," and "positive regulation of secretion," among others. We also observed significant increases in the expression of DEGs annotated as "DNA packaging complex," "protein-DNA complex," "nucleosome," and "endoplasmic reticulum lumen" have been noted in cellular components (CC). DEGs have been correlated to "signaling receptor activator activity," "receptor ligand activity," "peptidase regulator activity," and "peptidase inhibitor activity," among other molecular functions (MF; Figure 5A and 5B, Supplementary Table 5). These findings suggest that DEGs significantly participate in the control of the immunological response. In addition, KEGG pathway analysis showed that DEGs were primarily involved in "Neutrophil extracellular trap formation," "IL-17 signaling pathway," and "PPAR signaling pathway" (Figure 5C). The biological pathways "skeletal system development" and "Cell surface receptor signaling pathway involved in cell–cell signaling" were also discovered to be activated in the high-risk group by GSEA enrichment analysis. In terms of CC, enrichment was observed in the "Collagen-containing extracellular matrix" and "Endoplasmic reticulum lumen" terms. The biological functions "Nucleosome assembly" and "Nucleosome organization" were higher in the low-risk population, as well as the biological elements "DNA packaging complex" and "Nucleosome" (Figure 5D and E).

Analysis of the tumor immune microenvironment for high- and low-risk CRC patients

The tumor immune microenvironment controls immune-related tumors in CRC. Immunological cell subsets in CRC have many roles, and may exert either immunosuppressive or antitumor immunological effects to accelerate tumor growth [31]. The percentages of immune cells that infiltrate tumors were then calculated for the high- and low-risk groups

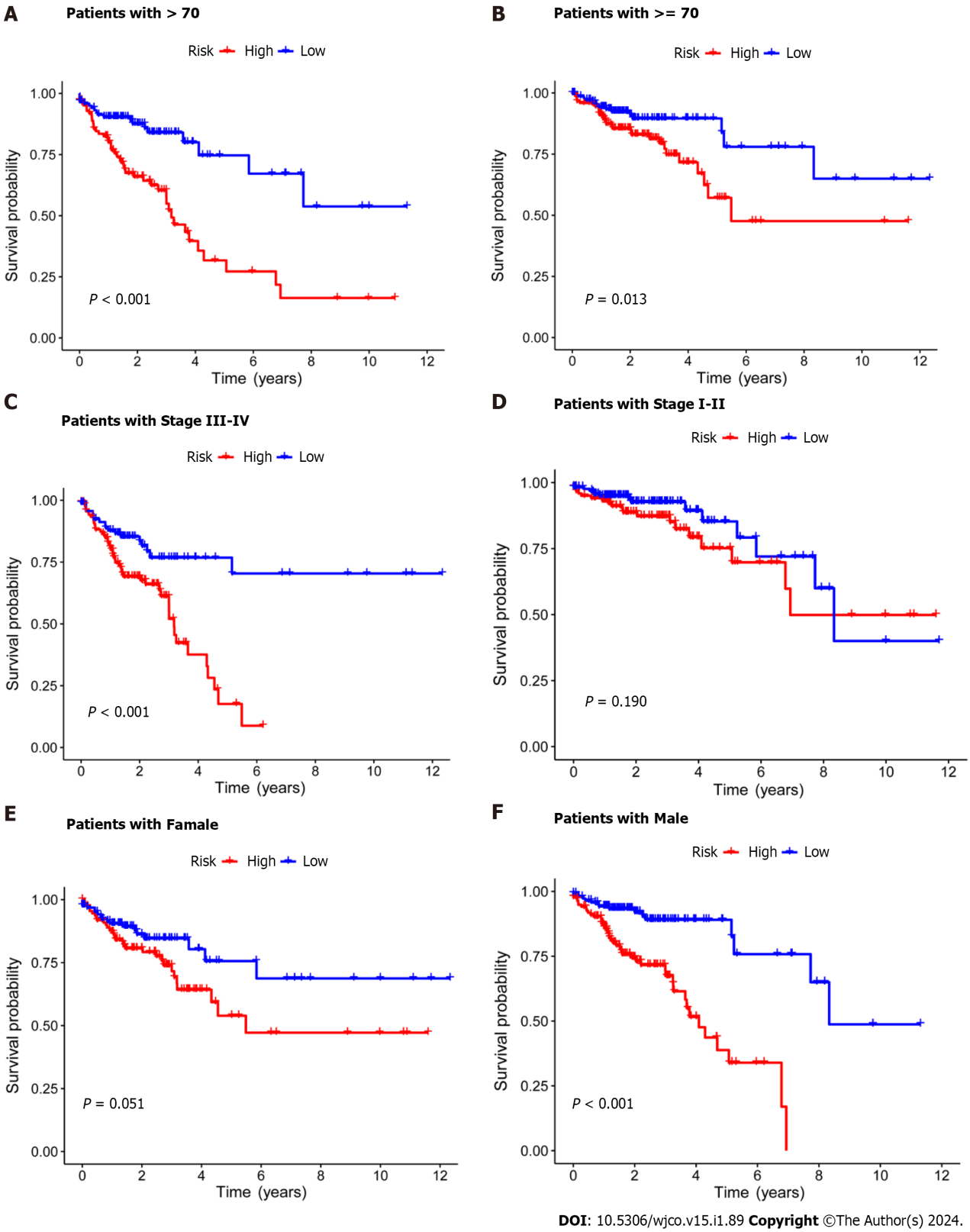

DOI: 10.5306/wjco.v15.i1.89

Figure 3 Kaplan–Meier survival analysis of high- and low-risk patients based on different clinical variables. A and B: Age; C and D: Stage; E and F: Gender.

(Supplementary Table 6). We discovered that the high-risk group had a lower percentage of inactive T cells with CD4 memory, inactive dendritic cells, active dendritic cells, and active eosinophils relative to the low-risk group. Moreover, compared to the high-risk group, the low-risk group had lower percentages of regulatory T cells (Tregs), dormant NK cells, and M0 macrophages (Figure 6A). Gene Set Variation Analysis (GSVA) is a gene set enrichment method that evaluates differences between different samples by performing pathway-centric analysis of gene sets. Next, using GSVA, we then examined variation in immune-related activities between high- and low-risk groups. According to these findings,

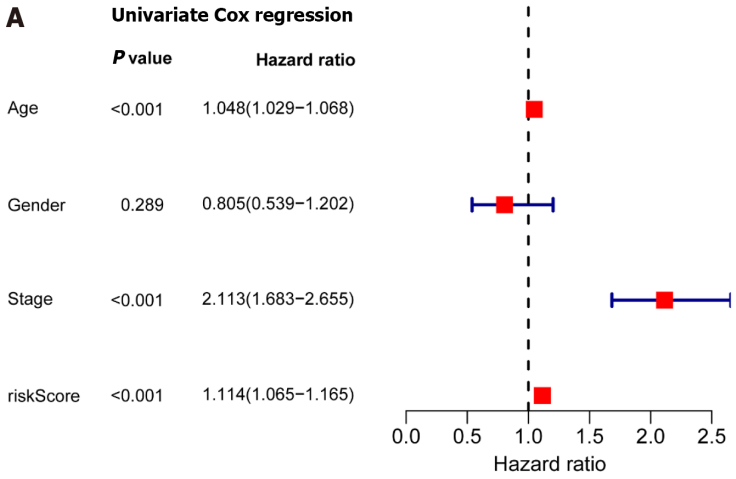
A
Univariate Cox regression
P value
Hazard ratio
Age
<0.001
1.048(1.029−1.068)
Gender
0.289
0.805(0.539−1.202)
Stage
<0.001
2.113(1.683−2.655)
riskScore
<0.001
1.114(1.065−1.165)
0.0 0.5 1.0 1.5 2.0 2.5
Hazard ratio

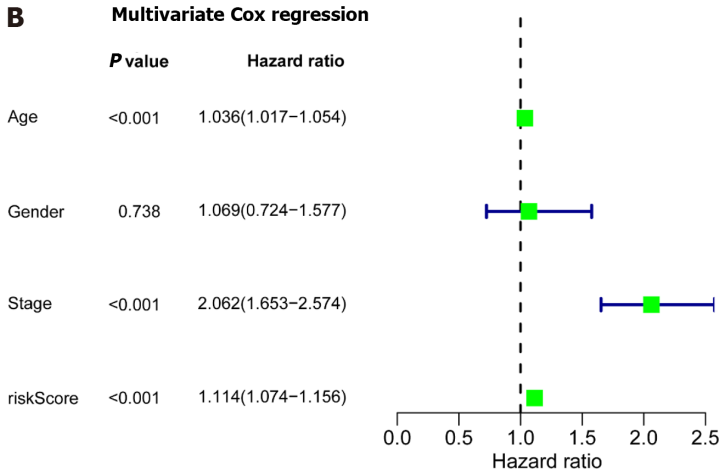
B
Multivariate Cox regression
P value
Hazard ratio
Age
<0.001
1.036(1.017−1.054)
Gender
0.738
1.069(0.724−1.577)
Stage
<0.001
2.062(1.653−2.574)
riskScore
<0.001
1.114(1.074−1.156)
0.0 0.5 1.0 1.5 2.0 2.5
Hazard ratio

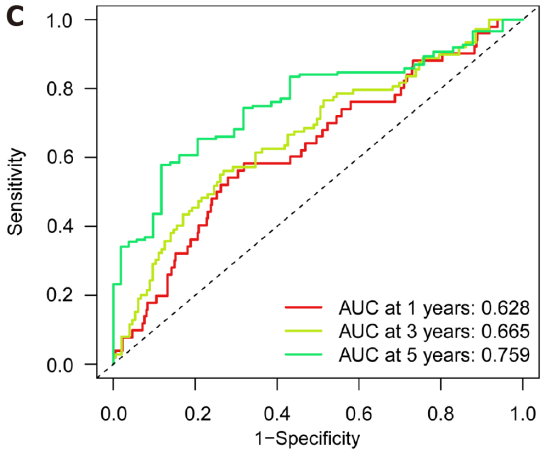
C
Sensitivity
1−Specificity
AUC at 1 years: 0.628
AUC at 3 years: 0.665
AUC at 5 years: 0.759

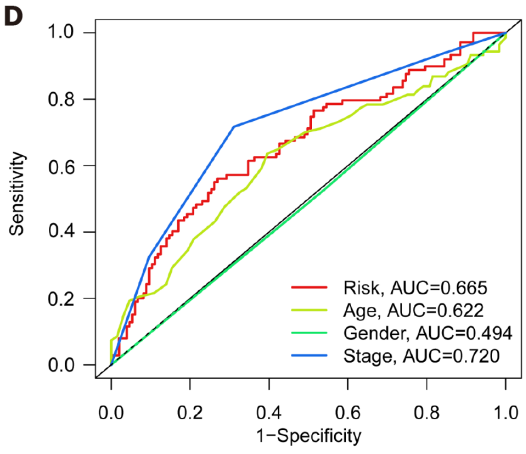
D
Sensitivity
1−Specificity
Risk, AUC=0.665
Age, AUC=0.622
Gender, AUC=0.494
Stage, AUC=0.720

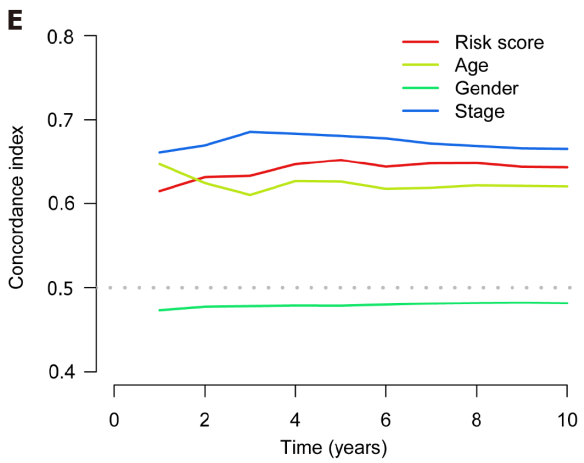
E
Concordance index
Time (years)
Risk score
Age
Gender
Stage

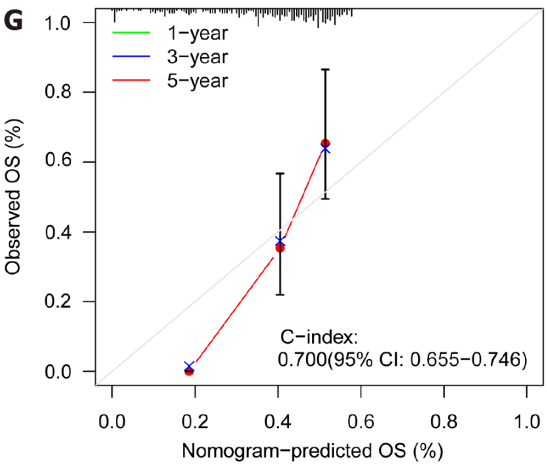
G
Observed OS (%)
Nomogram−predicted OS (%)
1−year
3−year
5−year
C−index:
0.700(95% CI: 0.655−0.746)

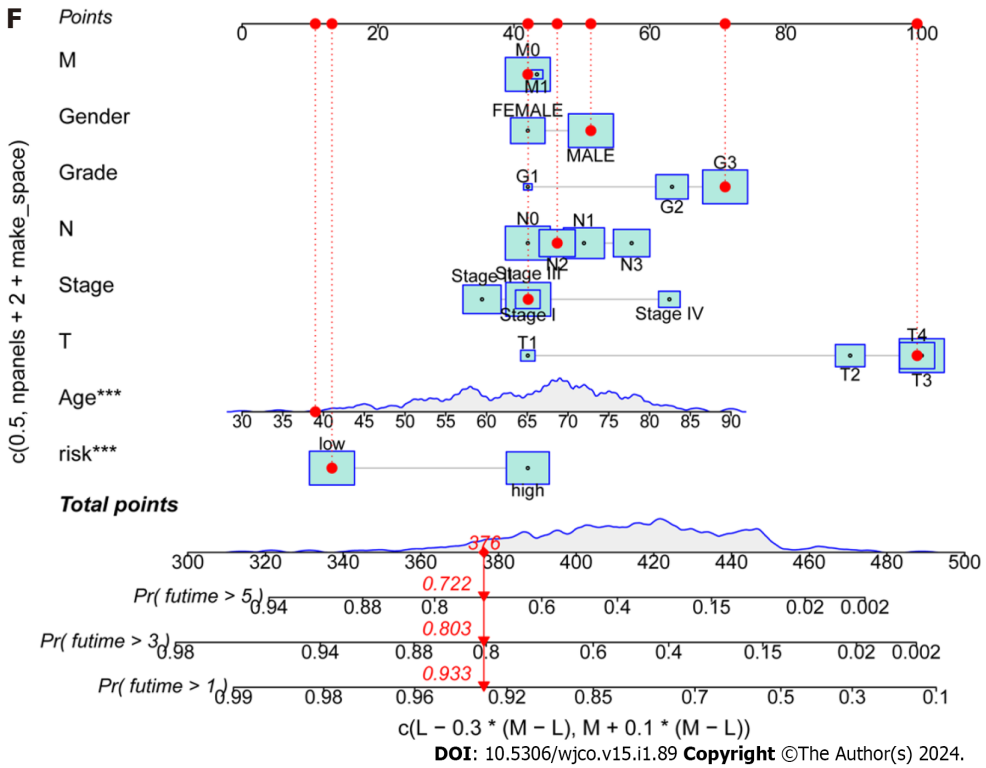

DOI: 10.5306/wjco.v15.i1.89 **Copyright** ©The Author(s) 2024.

Figure 4 Independent prognostic ability and predictability of clinical outcomes of the disulfidaptosis-related lncRNA risk scoring model.
A: Univariate Cox regression analysis of clinical variables and risk scores; B: Multivariate Cox regression analysis of clinical variables and risk scores; C: Prediction of 1-, 3-, and 5-year overall survival (OS) for all enrolled colorectal cancer (CRC) patients; D: Comparison of risk scoring model and clinical variables in predicting OS in CRC patients; E: C-index ROC curve of the risk model; F: Column chart of risk and clinical variable features predicting 1, 3, and 5-year OS in CRC patients; G: Calibration curves demonstrate the accuracy of the risk model in predicting 1, 3, and 5-year OS in CRC patients.

the low-risk group was more substantially connected with cytolytic activity, MHC class I, and neutrophils (Figure 6B). Moreover, a correlational study between the quantity of tumor-infiltrating immune cells and the eight important DRLs revealed a positive link between plasma cells, CD8 T cells, regulatory T cells (Tregs), and the eight critical DRLs (Figure 6C). In addition, we conducted a correlational analysis between immunological checkpoints and risk scores. This revealed a positive association between cancer associated fibroblast (CAF) and M2-like tumor-associated macrophage (TAM M2), a negative correlation between interferon gamma (IFNG) and CD274, and no significant correlation between these correlations (Figure 6D). Taken together, these findings imply that the tumor immunological milieu in the high- and low-risk groups differs significantly. Due to its strong immune surveillance position, the low-risk group displays a higher abundance of resting immune cells. Moreover, T cells, NK cells, and other immune cells, which are linked to tumor invasion, metastasis, and CRC development, are present in higher amounts in the high-risk group.

CRC mutation landscape, differential analysis of TMB, and TIDE

Next, we retrieved somatic mutation data from the TCGA database and generated waterfall plots to conduct intergroup comparisons using the maftools R package. This analysis was performed to investigate genetic alterations in patients from the high- and low-risk CRC groups. These plots revealed the existence of 15 highly altered genes, including APC, TP53, TTN, KRAS, MUC16, SYNE1, PIK3CA, FAT4, RYR2, ZFHX4, OBSCN, DNAH5, LRP1B, and CSMD3. APC, TP53, and TTN were found to have higher mutation frequencies in the high-risk population compared to the low-risk population, whereas MUC16, SYNE1, LRP1B, CSMD3, and CSMD1 showed higher mutation rates in the low-risk population (Figure 7A and B). The immunotherapy response has been linked to TMB[32], and here the low-risk group showed a larger mutation burden according to differential analysis of TMB (Figure 7C). The term TIDE describes a tumor cell's capacity to elude immune monitoring and suppress an immunological response; this can happen *via* a variety of methods. In contrast to the low-risk group, the high-risk group showed a higher TIDE score, as shown in Figure 7D. These findings demonstrate that immune evasion and tumor cell mutations are more common in the low-risk group of CRC patients, suggesting that there is a substantial therapeutic potential for immune checkpoint inhibitors for the management of low-risk CRC.

Identification of potential drugs for CRC

GDSC project is a database that focuses on the molecular indicators of therapeutic response and drug sensitivity in cancer cells. It is used to find novel therapeutic cancer biomarkers[33]. Here, an analysis using the oncoPredict identified four medicines *i.e.*, epirubicin, bortezomib, teniposide, and BMS-754807 that showed limited sensitivity toward CRC (Figure 8A-D). Of these, Forkhead box protein p3 (Foxp3) modulates epirubicin and has been identified as a suppressor of

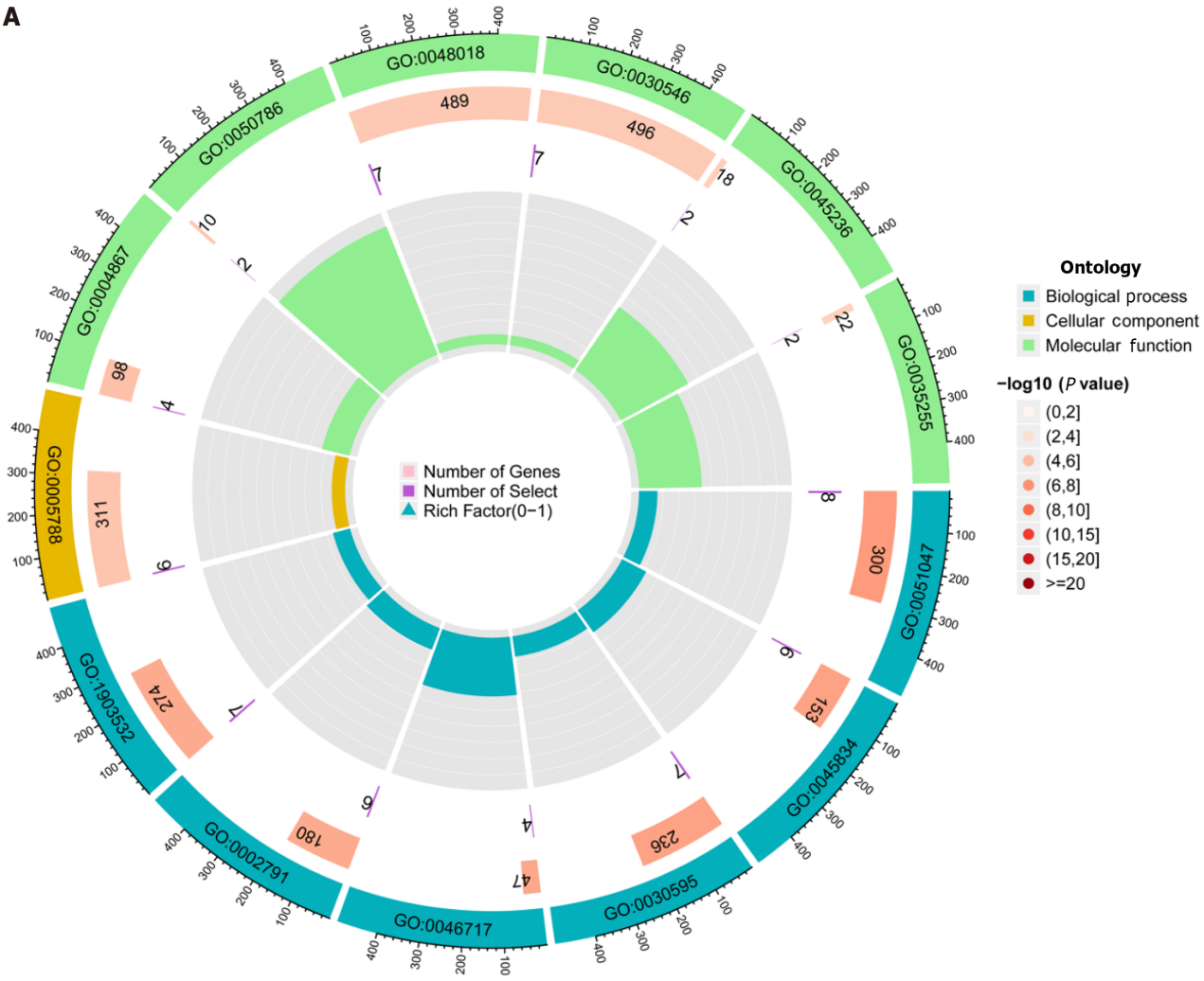
A
GO:0048018
GO:0030546
GO:0045236
GO:0035255
GO:0051047
GO:0045834
GO:0030595
GO:0046717
GO:0002791
GO:1903532
GO:0005788
GO:0004867
GO:0050786
489
496
18
22
300
153
236
47
180
274
311
98
Number of Genes
Number of Select
Rich Factor(0–1)
Ontology
Biological process
Cellular component
Molecular function
−log10 (P value)
(0,2]
(2,4]
(4,6]
(6,8]
(8,10]
(10,15]
(15,20]
>=20

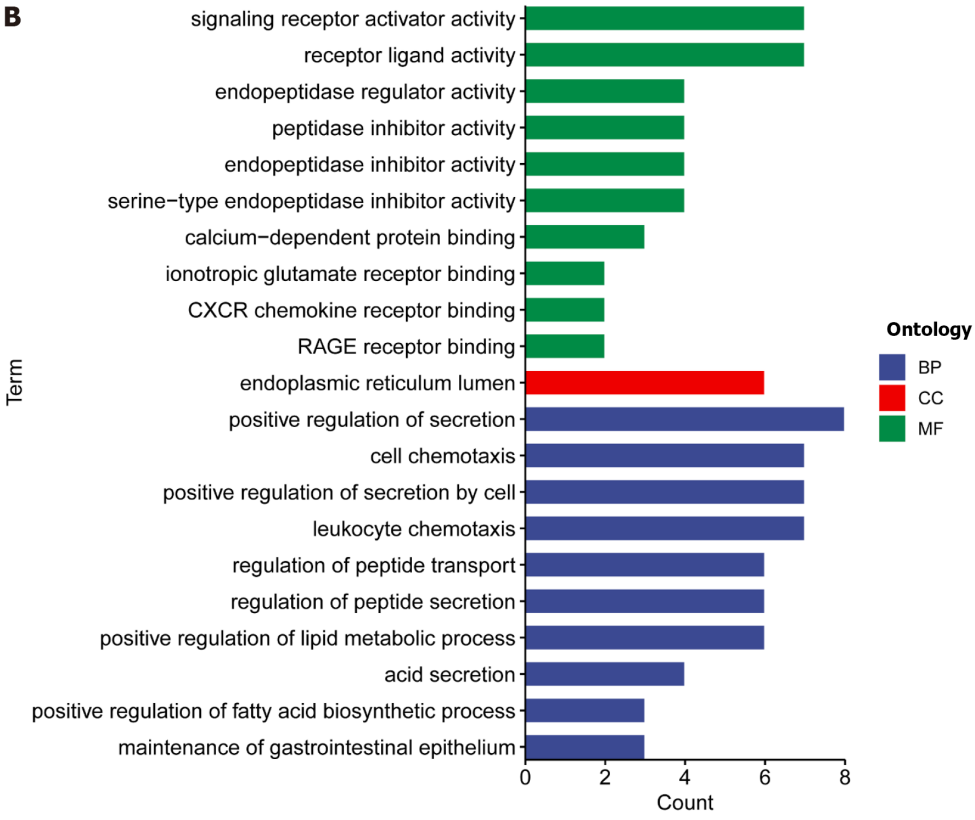
B
signaling receptor activator activity
receptor ligand activity
endopeptidase regulator activity
peptidase inhibitor activity
endopeptidase inhibitor activity
serine−type endopeptidase inhibitor activity
calcium−dependent protein binding
ionotropic glutamate receptor binding
CXCR chemokine receptor binding
RAGE receptor binding
endoplasmic reticulum lumen
positive regulation of secretion
cell chemotaxis
positive regulation of secretion by cell
leukocyte chemotaxis
regulation of peptide transport
regulation of peptide secretion
positive regulation of lipid metabolic process
acid secretion
positive regulation of fatty acid biosynthetic process
maintenance of gastrointestinal epithelium
Term
0
2
4
6
8
Count
Ontology
BP
CC
MF

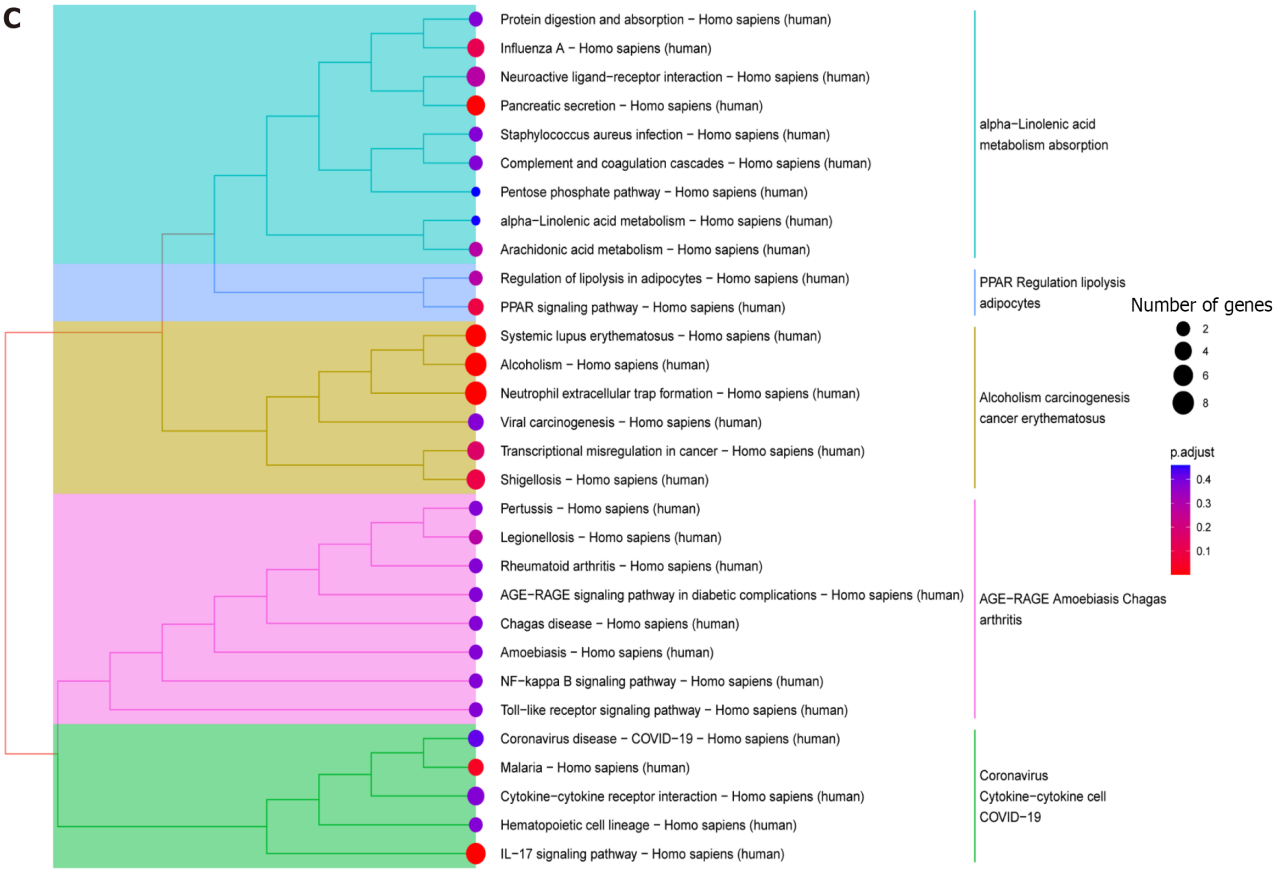
C
Protein digestion and absorption − Homo sapiens (human)
Influenza A − Homo sapiens (human)
Neuroactive ligand−receptor interaction − Homo sapiens (human)
Pancreatic secretion − Homo sapiens (human)
Staphylococcus aureus infection − Homo sapiens (human)
Complement and coagulation cascades − Homo sapiens (human)
Pentose phosphate pathway − Homo sapiens (human)
alpha−Linolenic acid metabolism − Homo sapiens (human)
Arachidonic acid metabolism − Homo sapiens (human)
Regulation of lipolysis in adipocytes − Homo sapiens (human)
PPAR signaling pathway − Homo sapiens (human)
Systemic lupus erythematosus − Homo sapiens (human)
Alcoholism − Homo sapiens (human)
Neutrophil extracellular trap formation − Homo sapiens (human)
Viral carcinogenesis − Homo sapiens (human)
Transcriptional misregulation in cancer − Homo sapiens (human)
Shigellosis − Homo sapiens (human)
Pertussis − Homo sapiens (human)
Legionellosis − Homo sapiens (human)
Rheumatoid arthritis − Homo sapiens (human)
AGE−RAGE signaling pathway in diabetic complications − Homo sapiens (human)
Chagas disease − Homo sapiens (human)
Amoebiasis − Homo sapiens (human)
NF−kappa B signaling pathway − Homo sapiens (human)
Toll−like receptor signaling pathway − Homo sapiens (human)
Coronavirus disease − COVID−19 − Homo sapiens (human)
Malaria − Homo sapiens (human)
Cytokine−cytokine receptor interaction − Homo sapiens (human)
Hematopoietic cell lineage − Homo sapiens (human)
IL−17 signaling pathway − Homo sapiens (human)
alpha−Linolenic acid
metabolism absorption
PPAR Regulation lipolysis
adipocytes
Alcoholism carcinogenesis
cancer erythematosus
AGE−RAGE Amoebiasis Chagas
arthritis
Coronavirus
Cytokine−cytokine cell
COVID−19
Number of genes
2
4
6
8
p.adjust
0.4
0.3
0.2
0.1

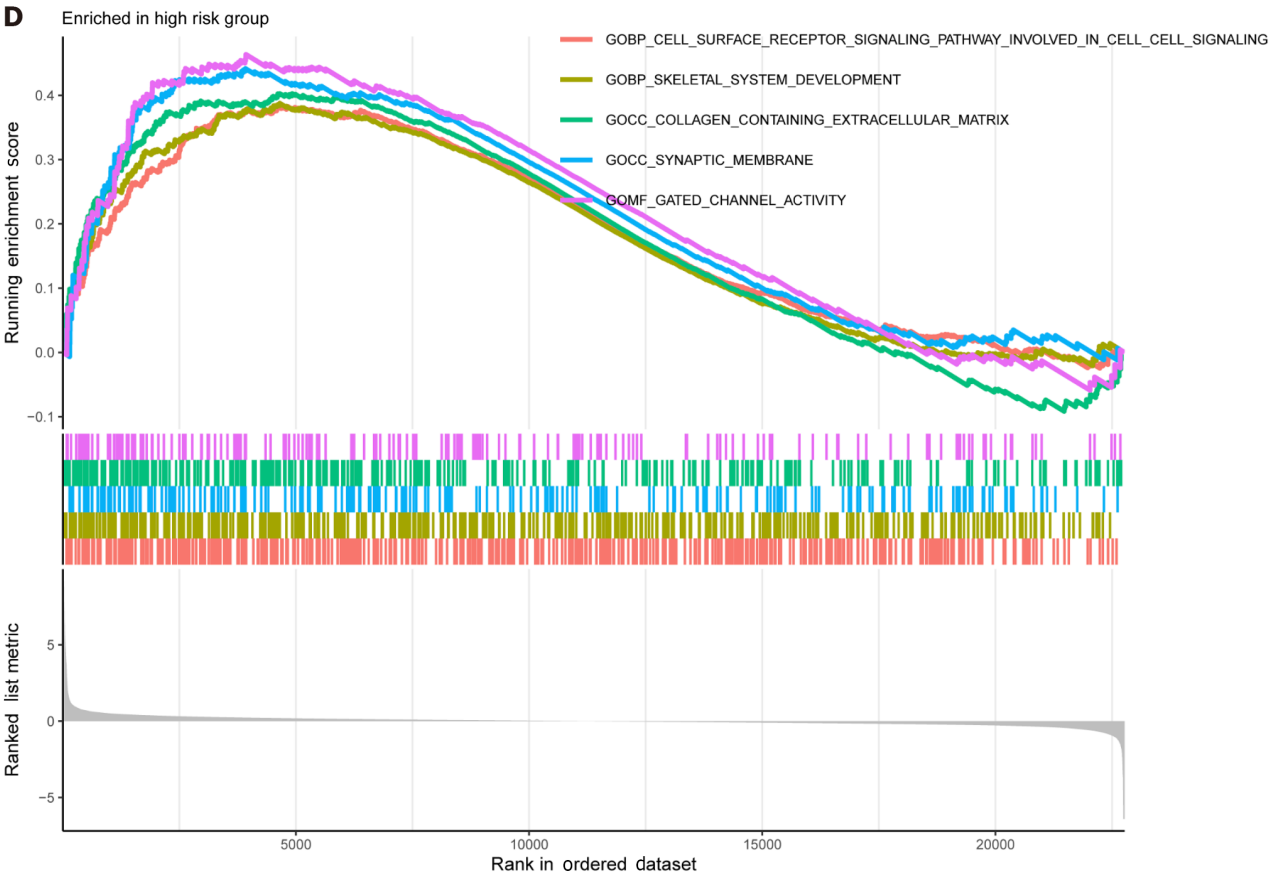
D
Enriched in high risk group
GOBP_CELL_SURFACE_RECEPTOR_SIGNALING_PATHWAY_INVOLVED_IN_CELL_CELL_SIGNALING
GOBP_SKELETAL_SYSTEM_DEVELOPMENT
GOCC_COLLAGEN_CONTAINING_EXTRACELLULAR_MATRIX
GOCC_SYNAPTIC_MEMBRANE
GOMF_GATED_CHANNEL_ACTIVITY
Running enrichment score
0.4
0.3
0.2
0.1
0.0
−0.1
Ranked list metric
5
0
−5
5000
10000
15000
20000
Rank in ordered dataset

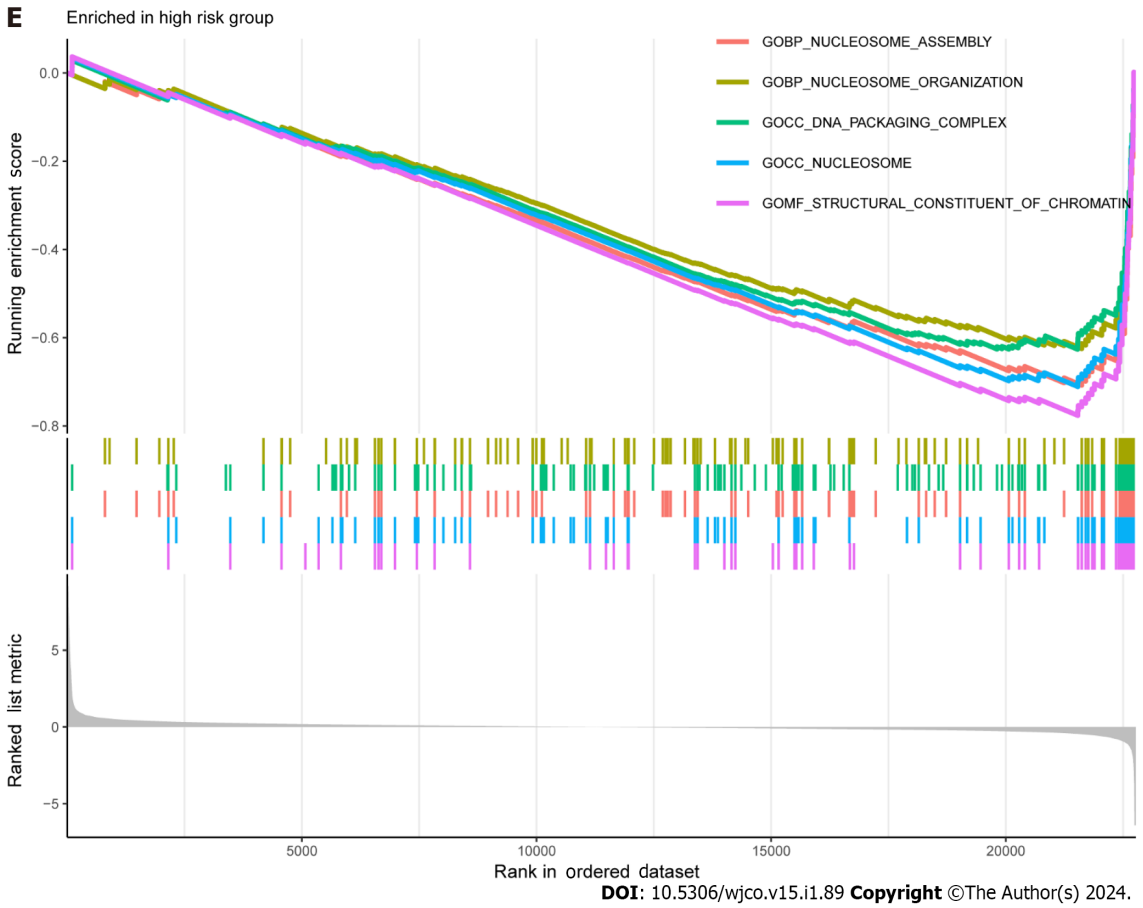

DOI: 10.5306/wjco.v15.i1.89

Figure 5 Enrichment analysis using the gene ontology, Kyoto encyclopedia of genes and genomes, and gene sets using gene set enrichment analysis frameworks. A and B: Gene ontology analysis reveals the diversity of molecular biology processes, cellular components, and molecular functions; C: Kyoto encyclopedia of genes and genomes pathway analysis identifies significantly enriched pathways; D and E: The top five pathways enriched between high and low-risk populations as identified by gene set enrichment analysisanalysis.

Treg cell function[34]. Moreover, the proteasome inhibitor bortezomib prevents CRC cells from forming spheres and thereby from self-renewing by inhibiting the fundamental transcription factor CTNNB1[35]. Teniposide, a topoisomerase II inhibitor, also strongly affects CRC gene expression[36]. Finally, the insulin-like growth factor 1 receptor (IGF-1R) inhibitor BMS-754807 has been found to have an impact on the growth and survival of tumor cells[37]. Drug sensitivity (also known as the half-maximal inhibitory concentration, or IC_{50} is the degree to which an organism responds to a particular drug, and the potency of the medicine decreases as the IC_{50} value rises. Epirubicin, Bortezomib, and teniposide all demonstrated greater sensitivity in the high-risk group, which suggests that the low-risk group may benefit from greater efficacy. The high-risk group, however, benefited the most from BMS-754807.

Validation of disulfidoptosis-related features in NCM460 and HT-29 cells

In this study, through multifactorial Cox regression analysis, we identified eight Disulfidoptosis-related lncRNAs that exhibited differential expression in CRC prognosis within the TCGA-COAD and TCGA-READ datasets. These lncRNAs include AL354993.2, AC006213.7, AC013652.1, AL683813.1, AC093157.1, AC005034.5, TNFRSF10A-AS1, and AC011815.1. Among these, the first four showed higher expression in the high-risk group associated with poor prognosis, while the latter four displayed an inverse trend. To validate the expression of these eight prognosis-related lncRNAs, we conducted qPCR experiments in two cell lines: normal colonic epithelial cells NCM460 and colorectal tumor cells HT-29. Our experiments revealed that AL354993.2, AL683813.1, AC093157.1, AC005034.5, and AC011815.1 exhibited significant differences in expression levels between HT-29 and NCM460 cells, with the former displaying higher expression levels. AC013652.1 and TNFRSF10A-AS1 exhibited a trending pattern but did not demonstrate significant differences (Figure 9). AC006213.7 was not found in the lncRNA database, and therefore, we do not discuss its expression levels at this time. TCAP, NNAT, CHGB, and COL2A1 were among the top four differentially expressed genes between the high and low-risk groups, with higher abundance in the high-risk group. Using qPCR technology, we also assessed the mRNA levels of these four genes and found that their expression was higher in HT-29 cells compared to NCM460 cells.

Induction of the disulfidoptosis cell model and in vitro validation of the risk prediction model

We constructed a disulfidoptosis cell model to investigate changes in the mRNA expression levels of LncRNAs in the CRC risk prediction model. Different concentrations of WZB117 (0, 1, 3, 10, 15, 30, 50, 100, 300 μmol/L) were applied to HT-29 cells to assess cell viability. As shown in Figure 10, cell viability was significantly inhibited at WZB117 concen-

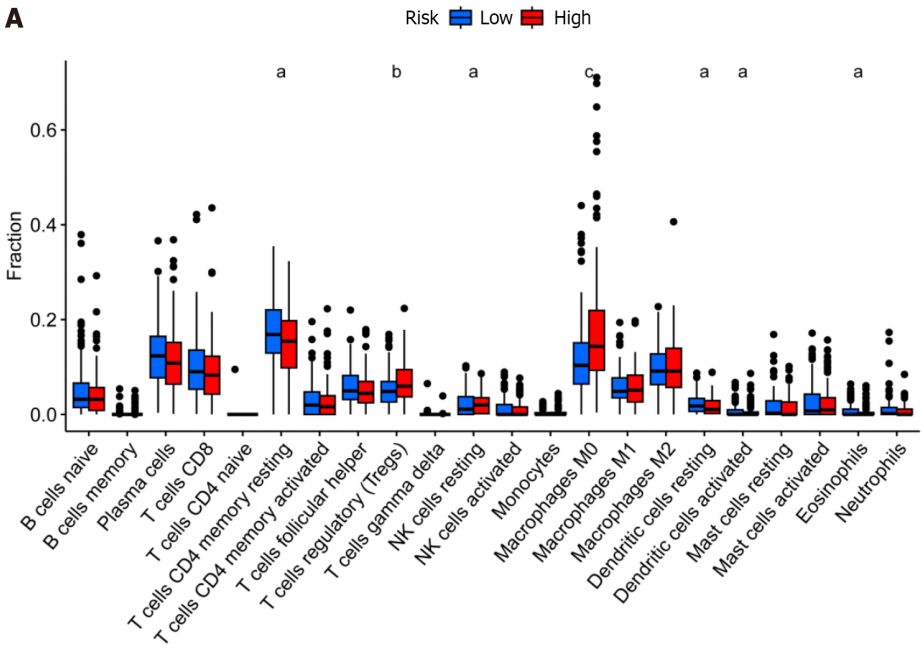
A
Risk Low High
Fraction
0.0
0.2
0.4
0.6
a
b
a
c
a
a
a
B cells naive
B cells memory
Plasma cells
T cells CD8
T cells CD4 naive
T cells CD4 memory resting
T cells CD4 memory activated
T cells follicular helper
T cells regulatory (Tregs)
T cells gamma delta
NK cells resting
NK cells activated
Monocytes
Macrophages M0
Macrophages M1
Macrophages M2
Dendritic cells resting
Dendritic cells activated
Mast cells resting
Mast cells activated
Eosinophils
Neutrophils

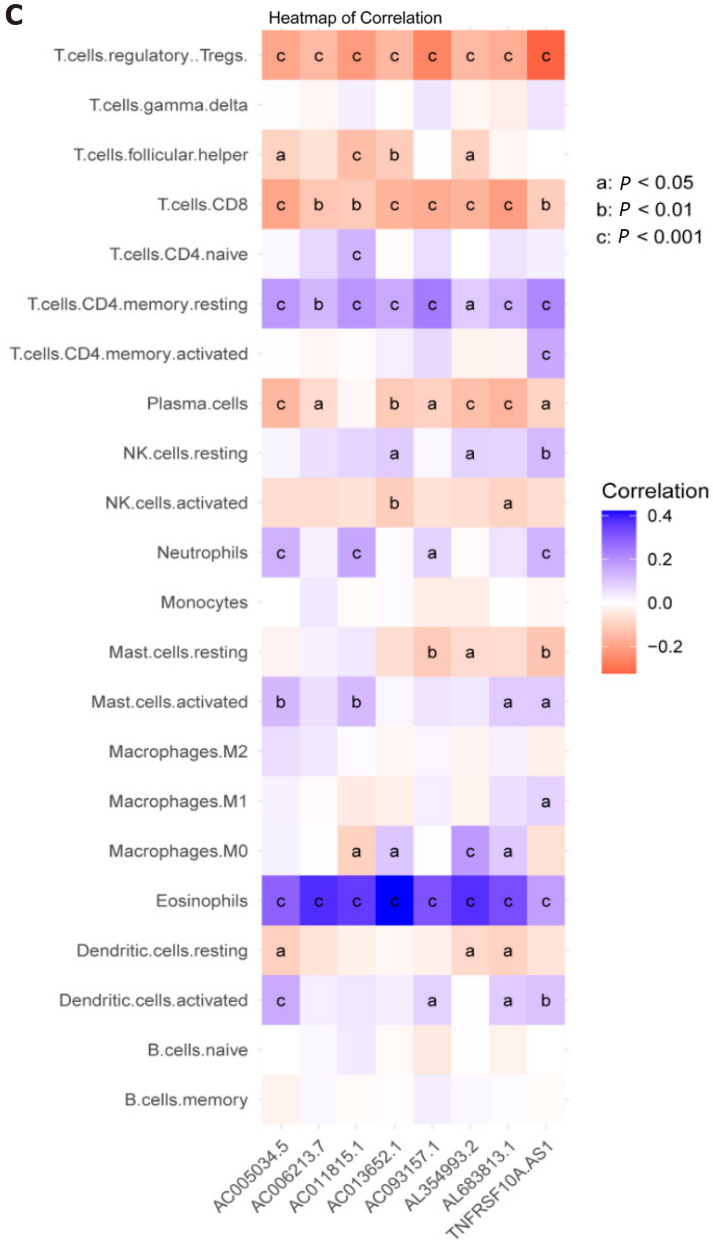
C
Heatmap of Correlation
T.cells.regulatory..Tregs.
T.cells.gamma.delta
T.cells.follicular.helper
T.cells.CD8
T.cells.CD4.naive
T.cells.CD4.memory.resting
T.cells.CD4.memory.activated
Plasma.cells
NK.cells.resting
NK.cells.activated
Neutrophils
Monocytes
Mast.cells.resting
Mast.cells.activated
Macrophages.M2
Macrophages.M1
Macrophages.M0
Eosinophils
Dendritic.cells.resting
Dendritic.cells.activated
B.cells.naive
B.cells.memory
AC005034.5
AC006213.7
AC011815.1
AC013652.1
AC093157.1
AL354993.2
AL683813.1
TNFRSF10A.AS1
a: P < 0.05
b: P < 0.01
c: P < 0.001
Correlation
0.4
0.2
0.0
−0.2

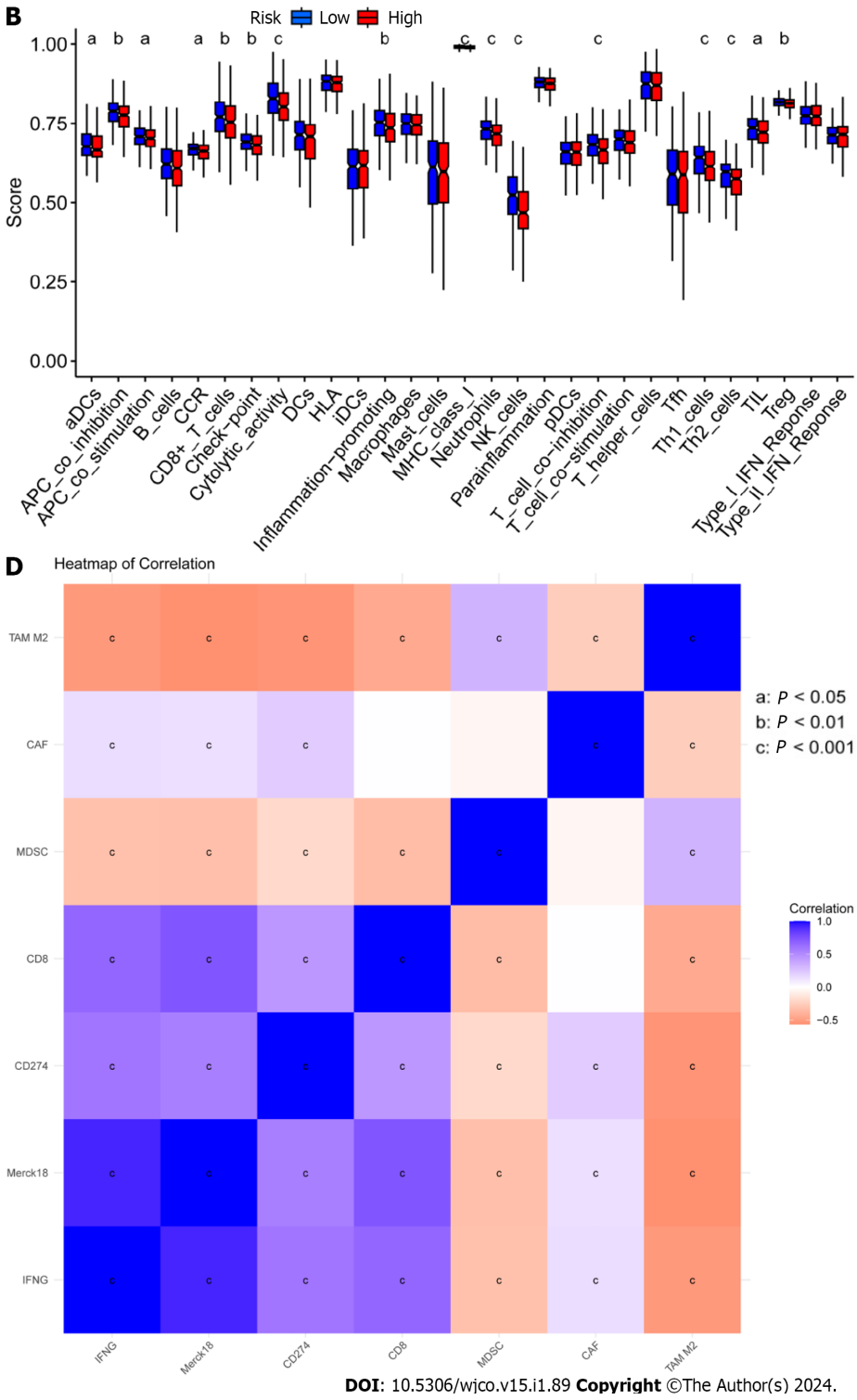

DOI: 10.5306/wjco.v15.i1.89 **Copyright** ©The Author(s) 2024.

Figure 6 Analysis of the tumor immune microenvironment for high- and low-risk patient groups. A: Shown are (A) Violin plots of the proportions of 22 tumor-infiltrating immune cells; B: Differential analysis of immune-related functions between high- and low-risk groups; C: Correlation analysis between infiltrating immune cells and eight key disulfidaptosis-related lncRNAs (disease risk factors); D: Correlation analysis between immune checkpoints and risk scores. [a]*P* < 0.05; [b]*P* < 0.01; [c]*P* < 0.001.

trations of 50 μmol, 100 μmol, and 300 μmol. Therefore, we selected 300 μmol as the effective induction concentration for Disulfidoptosis. Q-PCR results indicated that after WZB117 induction at 300 μmol, AL354993.2, AC013652.1, and AL683813.1 were upregulated in HT-29 cells, while AC005034.5, TNFRSF10A-AS1, and AC011815.1 were downregulated. The expression of TCAP, NNAT, CHGB, and COL2A1 was upregulated (Figure 11). Surprisingly, AC093157.1 increased after WZB117 induction, which was contrary to the risk model trend, possibly due to cell line-specific factors.

In summary, Disulfidoptosis can influence the expression of LncRNAs and differential genes in the risk prediction model. Therefore, these key LncRNAs and differential genes have the potential to serve as diagnostic markers for CRC, aiding in the treatment and prediction of the degree of CRC disease risk.

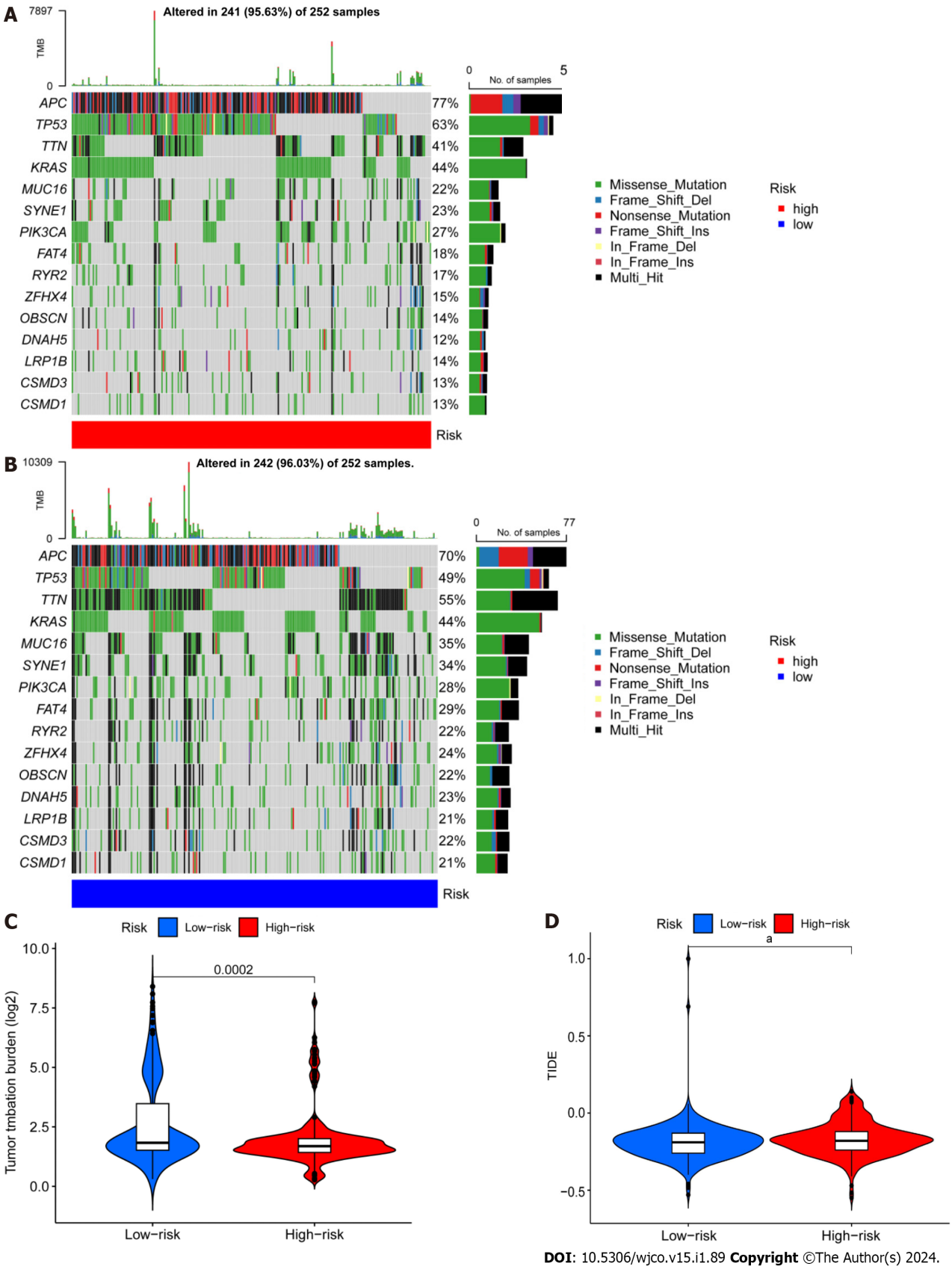

DOI: 10.5306/wjco.v15.i1.89 **Copyright** ©The Author(s) 2024.

Figure 7 Differential analysis of tumor mutation burden and tumor immune dysfunction and exclusion. A and B: Waterfall plots depicting 15 highly mutated genes in the high- and low-risk colorectal cancer (CRC) groups; C: Differential analysis of TMB in patients from the high- and low-risk CRC groups; D: Tumor immune dysfunction and exclusion analysis in patients from the high and low-risk groups. [a]$P < 0.05$; [b]$P < 0.01$; [c]$P < 0.001$.

DISCUSSION

CRC tumors have unique characteristics, including a high incidence, a high rate of metastasis, and a high fatality rate. Moreover, both the aberrant expression and regulation of multiple genes are involved in its onset and development. lncRNAs, which participate in vital BP such cell proliferation, apoptosis, invasion, and metastasis, have been demonstrated to play significant roles in CRC. For instance, the overexpression of LncRNA LINC00460 triggers the epithelial–mesenchymal transition and aids in the development of cancer. In CRC, LINC00460 interacts with the ATP-dependent RNA helicase A (DHX9) and insulin-like growth factor 2 mRNA-binding protein 2 (IGF2BP2) to recognize the high mobility group AT-hook 1 (HMGA1) and control its m6A modification. This in turn controls HMGA1 expression, improves mRNA stability, and aids tumor metastasis[38]. This suggests that lncRNAs may be useful therapeutic targets for CRC. Moreover, a novel type of cell death called disulfidptosis is known to take place under conditions of glucose starvation. Related to this process, SLC7A11 is upregulated in CRC, which speeds up the loss of cytoplasmic NADPH, thereby causing disulfide linkages to form in protein molecules and instigating the collapse of the actin network and cytoskeleton, finally resulting in cell death[39]. This study therefore analyzes the roles and regulatory mechanisms of lncRNAs connected to disulfidptosis in CRC, and offers new targets and methods for determining CRC prognosis.

Through bioinformatics analyses, we discovered eight key DRLs: AC005034.5, AC006213.7, AC011815.1, AC013652.1, AC093157.1, AL354993.2, AL683813.1, and TNFRSF10A-AS1. Previous reports suggested that the osteosarcoma protective factor AC005034.5 is downregulated in cases of increased disease risk[40]. Moreover, the elevated abundance of AC013652.1, a key prognostic marker for colorectal and stomach malignancy, predicts a poor prognosis for the patient[41, 42]. By facilitating cell apoptosis and controlling immune cell infiltration *via* the overexpression of zinc finger protein 268 [43], AC093157.1 has been shown to slow the development of clear cell renal cell carcinoma. In addition, the ability of gastric cancer cells to proliferate, advance through the cell cycle, and invade other tissues has been found to be strongly enhanced by TNFRSF10A-AS1[44]. Here, we created a risk prognosis model that divides patients into high- and low-risk groups based on these eight key DRLs. Using column plots, ROC curve analysis, c-indexes, calibration curves, and univariate and multivariate Cox regression analyses, we then validated the robustness and independence of the model (Figure 4). Next, we used the model's risk scores to contrast the survival rates of high- and low-risk groups. We observed that increased risk scores were associated with higher mortality in CRC patients (Figure 2D-F). This result shows that the risk score can be used as a reliable measure to predict patient survival. To enhance the reliability of the risk prediction model, we assessed the mRNA expression levels of the 8 Disulfidoptosis-Related LncRNAs (DRLs) in two cell lines, NCM460 and HT-29. Subsequently, induction of the Disulfidoptosis cell model using the Glut1 inhibitor WZB117 demonstrated that the accumulation of disulfides leads to increased cell death and alters the expression levels of DRLs.

Next, GO enrichment analysis of DEGs from the high- and low-risk groups revealed that DEGs were primarily engaged in the immune response. DRLs were strongly enriched in KEGG annotation terms for "Neutrophil extracellular trap formation (NET)," "IL-17 signaling pathway," and "PPAR signaling pathway." According to GSEA, the BP "Cell surface receptor signaling pathway involved in cell–cell signaling" and "skeletal system development" were active in the high-risk group (Figure 5). Releasing chromatin DNA threads encircling granule proteins, neutrophils release NET to capture microorganisms. Research points to a connection between NET growth and cancer pathogenesis. Vascular NETs can increase vascular permeability, which makes it easier for cancer cells to enter organs from vessels. Via its transmembrane receptor, the transmembrane protein CCDC25, NET-DNA performs as a chemoattractant for cancer cells. Through activating the ILK-β-parvin pathway, this interaction improves the motility of tumor cells[45]. The IL-17 signaling pathway is hazardous for the occurrence of cancer and strongly related to the advancement of inflammation. Adenomatous polyposis coli (Apc)-carrying intestinal epithelial cells proliferate in response to IL-17 signaling in the intestine, which facilitates the production of adenomas[46]. Intestinal barrier function is compromised by adenomas, which additionally increase IL-17 responses in tumors and hence accelerate tumor growth[47]. The ligand-activated nuclear receptor PPAR influences energy homeostasis and lipid metabolism[48]. Findings indicates that CRC tumor cells have abnormal activation of the PPAR signaling system. When PPARγ inhibitors are administered for blocking this pathway, tumor epithelial cell proliferation is dramatically suppressed and apoptosis is increased[49]. Here, the low-risk group exhibited a larger mutational load and a lower TIDE score during the study of differences in TMB (Figure 7). This suggests that the low-risk group may respond better to immune checkpoint inhibitor medication and has a lower chance of immunological escape. Furthermore, relative to the high-risk group, the expression levels of the immunological checkpoints CD274 (PD-L1) and IFNG were higher in the low-risk group. Conversely, the high-risk group exhibited higher levels of CAF and TAM M2 expression. However, additional experimental validation is necessary to ascertain whether these checkpoint inhibitors can be used as antitumor medications for CRC. Previous research has shown that solid CRC tumors typically exhibit disruptions in the IFNG-JAK-STAT-TET signaling pathway, which facilitates anti-PD-L1/PD-1 immunotherapy. Furthermore, IFNG is an important antiangiogenic mediator of tumor immunity. As a result, CD274 and IFNG may serve as promising targets for the therapy of CRC[50]. Finally, we showed that epirubicin, Bortezomib, teniposide, and BMS-754807 represent four possible CRC therapy medicines. Drug sensitivity results revealed that the first three medications showed greater efficacy in the low-risk group, while BMS-754807 was better suited to treat the high-risk group (Figure 8). Although teniposide has not yet undergone clinical trials for colorectal cancer, a check of the ClinicalTrials.gov database (https://clinicaltrials.gov) indicated that epirubicin, Bortezomib, and BMS-754807 are currently involved in several CRC-related clinical trials. We anticipate clinical study results for these four medications in the hope that they will show beneficial therapeutic benefits for the treatment of CRC.

As a result, the findings of the research we conducted highlight the complex role that disulfidptosis plays in the onset and course of colorectal cancer. We created a prognostic risk assessment feature by utilizing DRLs. This model illustrates the processes behind cellular disulfidptosis and predicts CRC patients' prognosis with consistency. Relevant pathways correlated to CRC immunity and prognosis were found by our analysis of genes that are DEGs in high- and low-risk

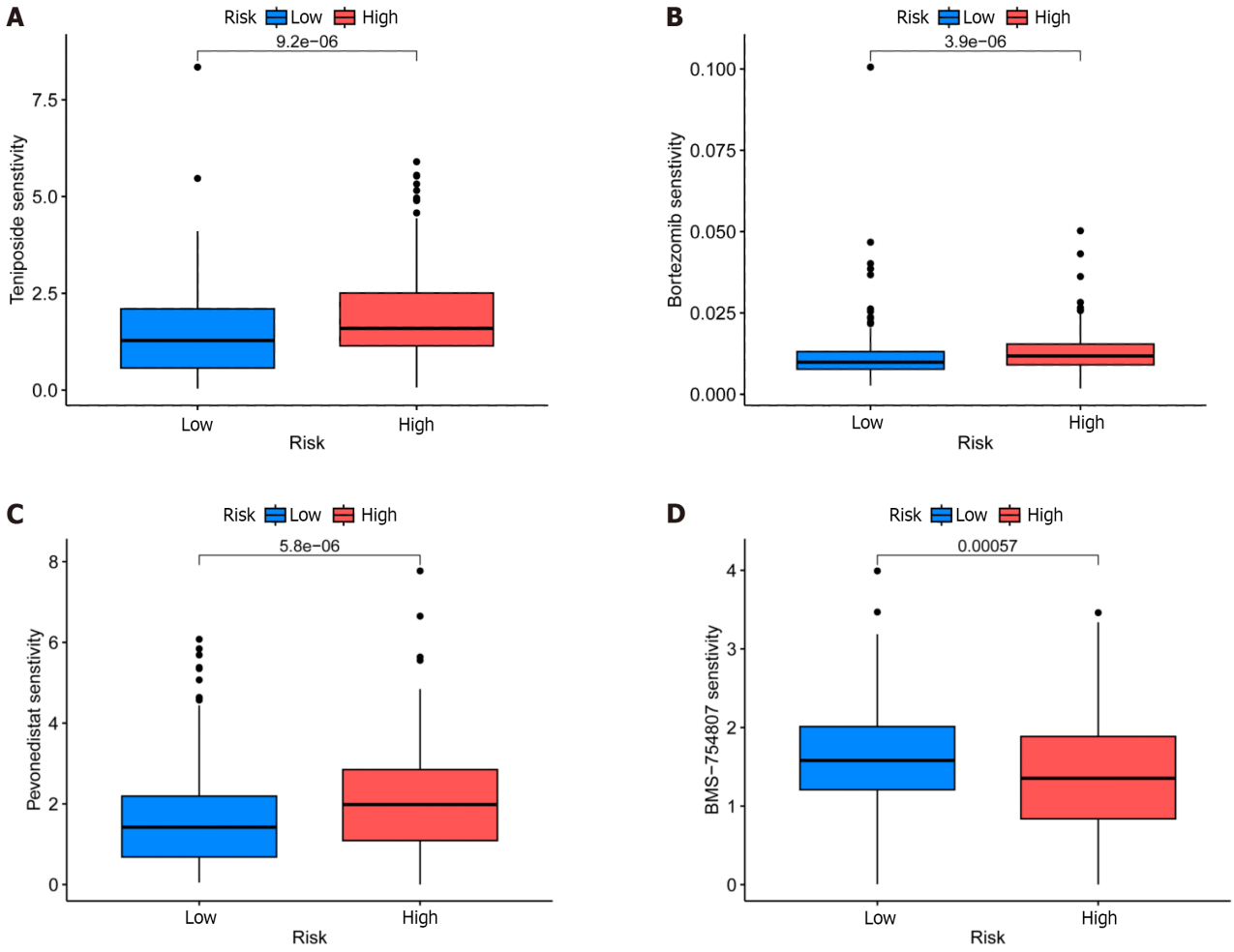

DOI: 10.5306/wjco.v15.i1.89 **Copyright** ©The Author(s) 2024.

Figure 8 Identification of potential drugs for the treatment of colorectal cancer. A: Epirubicin; B: Borte zomib; C: TeniposideD: BMS-754807.

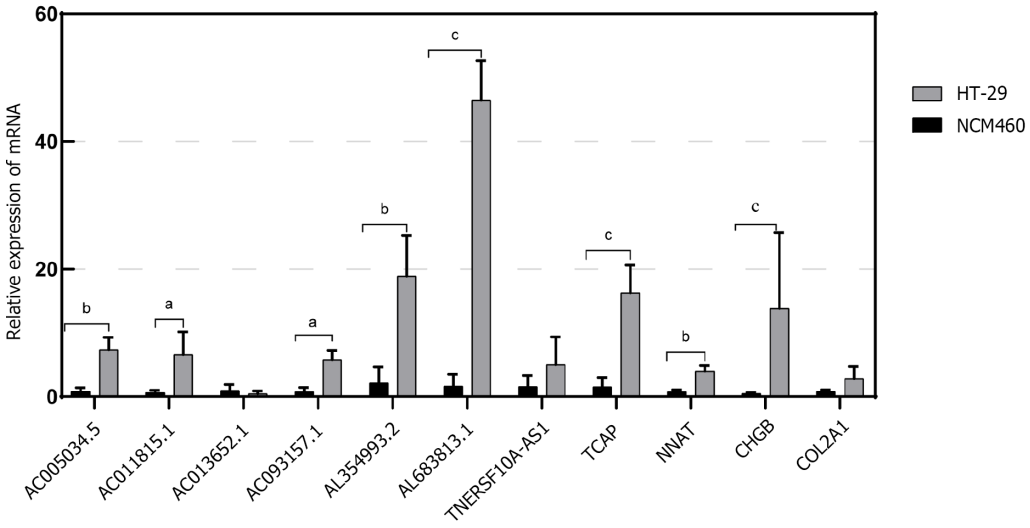

DOI: 10.5306/wjco.v15.i1.89 **Copyright** ©The Author(s) 2024.

Figure 9 Validation of the relationship between lncRNAs/Genes and cell death induced by disulfidoptosis. The expression of lncRNAs/Genes in NCM460 and HT-29 cells was measured by quantitative real-time polymerase chain reaction (n = 3). $^{a}P < 0.05$; $^{b}P < 0.01$; $^{c}P < 0.001$.

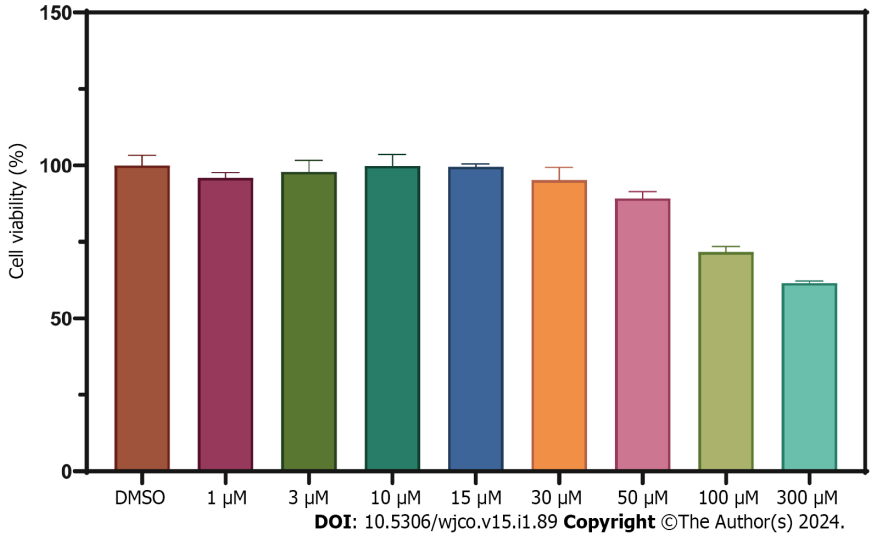

DOI: 10.5306/wjco.v15.i1.89 **Copyright** ©The Author(s) 2024.

Figure 10 Cell viability assessment of HT-29 cells treated with WZB117 at different concentrations for 24 h.

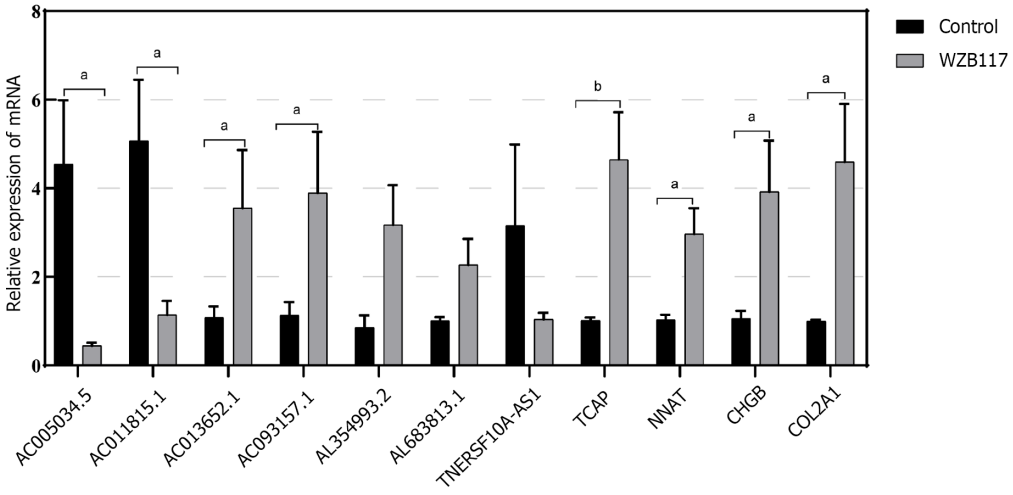

DOI: 10.5306/wjco.v15.i1.89 **Copyright** ©The Author(s) 2024.

Figure 11 Validation of the relationship between lncRNAs/Genes and cell death induced by disulfidoptosis. The expression of lncRNAs/Genes in HT-29 cells was measured by quantitative real-time polymerase chain reaction (n = 3) after treatment with 300 μmol/L WZB117 for 24 h. $^{a}P < 0.05$; $^{b}P < 0.01$; $^{c}P < 0.001$.

sample groups." This the discovery holds significant therapeutic implications for both the prevention and the treatment of CRC, as it is the first in the history of CRC research to combine disulfidptosis, LncRNA, and immunotherapy. However, there are limitations related to our database selection and analysis. Firstly, the sample size was small in our study. A study using a bigger sample size should be conducted in the future. Secondly, all data sources were derived from the TCGA database, which lacks significant experimental and clinical data to evaluate the accuracy of our results. Finally to confirm the functional properties of DEGs and the anticancer mechanisms of immunological checkpoints, we must refine the experimental design in future studies.

CONCLUSION

In conclusion, this is the first attempt to apply bioinformatics methods to examine the immune cell infiltration and the expression patterns of LncRNAs associated with the disulfidptosis genes in high- and low-risk groups of colorectal cancer patients. It is stressed the significance of LncRNAs in the diagnosis and treatment of colorectal cancer. Disulfidptosis is the name given to the accumulation of intracellular disulfide compounds that leads to the breakdown of cytoskeletal proteins, which may affect host homeostasis and promote tumor growth. The eight significant LncRNAs that have been discovered are closely associated to the disulfidptosis genes, which can be used as prognostic indicators to predict the clinical course of colorectal cancer patient. Furthermore, they have the capacity to act as regulators to restrain the

development, differentiation, invasion, and metastasis of cancer cells, providing fresh approaches for the focused treatment of colorectal cancer.

ARTICLE HIGHLIGHTS

Research background

Colorectal cancer (CRC) is an extremely fatal disease that is the third fastest-growing cause of cancer-related death globally. Disulfidptosis is one particular type of cell death that has been associated to the growth, escape, and regeneration of cancer cells. With disulfidptosis, colorectal cancer treatments and survival predictions could be altered.

Research motivation

A large number of clinical studies incorporate statistical significance to present their results. However, to be able to assess a therapy's adaptability and relevance in routine clinical practice, clinical measurements of significance are necessary.

Research objectives

The main goal of this work is to construct a stable biological biomarker that utilizes long non-coding RNA (LncRNA) linked to disulfidptosis-induced cell death. This may provide innovative viewpoints on the assessment of immunotherapy response and prognosis in patients suffering from CRC.

Research methods

The Cancer Genome Atlas (TCGA) database offered transcriptome, clinical, and genetic mutation data relating to CRC. The minimal absolute shrinkage and selection operator approach and univariate and multivariate Cox regression models were applied to discover and assess critical LncRNA correlated with disulfidptosis. Ultimately, the critical LncRNA served as the foundation for the prognostic model.

Research results

Through multivariate analysis, we succeeded to identify eight critical long non-coding RNAs linked to disulfidptosis. These LncRNAs had significant accuracy for the consequences of CRCs. Compared to the high-risk group, patients in the low-risk group had a higher rate of overall survival. As a result, the nomogram prediction model we created exhibits good predictive validity and incorporates clinical characteristics and risk scores.

Research conclusions

As a way to predict the prognosis of patients with colorectal cancer, we constructed a prediction model of disulfidptosis-related LncRNAs based on the TCGA-COAD and TCGA-READ cohort using bioinformatics technology and clinical patient data. The application of this model in clinical practice makes it much simpler to classify CRC patients precisely, pinpoint subgroups that are more likely to benefit from immunotherapy and radiation therapy, and provide evidence-based, targeted therapies for CRC patients.

Research perspectives

In subsequent research, we must enhance the animal and cell experiments in order to validate the functional characteristics of disulfidaptosis-related lncRNA and the immune checkpoints' anticancer mechanisms.

ACKNOWLEDGEMENTS

We are very grateful for data provided by databases such as TCGA. Thanks to reviewers and editors for their sincere comments.

FOOTNOTES

Author contributions: Chen YG provided the acquisition of funding and formulated research goals; Wang KL wrote the original manuscript; Chen KD, and Chen ZP were involved in the software analysis; Tang WW, Wang YJ, and Shi GP performed the data collation; All authors have read and agreed to the published version of the manuscript.

Supported by Jiangsu Province Science and Technology Plan Project-Youth Fund Project, No. BK2020040973.

Institutional review board statement: The ethical approval is not applicable to this article.

Informed consent statement: There were no human subjects included in this article, and therefore informed consent is not applicable.

Conflict-of-interest statement: All the authors declare that the study was carried out without any commercial or financial relationships

which could be considered a potential conflict of interest.

Data sharing statement: The original contributions presented in the study are included in the article. Further inquiries can be directed to the corresponding authors.

Country/Territory of origin: China

ORCID number: Yu-Gen Chen 0000-0001-9221-218X.

S-Editor: Liu JH
L-Editor: A
P-Editor: Zhang XD

REFERENCES

1 **Baidoun F**, Elshiwy K, Elkeraie Y, Merjaneh Z, Khoudari G, Sarmini MT, Gad M, Al-Husseini M, Saad A. Colorectal Cancer Epidemiology: Recent Trends and Impact on Outcomes. *Curr Drug Targets* 2021; **22**: 998-1009 [PMID: 33208072 DOI: 10.2174/1389450121999201117115717]
2 **U**. . Screening for colorectal cancer: U.S. Preventive Services Task Force recommendation statement. *Ann Intern Med* 2008; **149**: 627-637 [PMID: 18838716 DOI: 10.7326/0003-4819-149-9-200811040-00243]
3 **Li J**, Ma X, Chakravarti D, Shalapour S, DePinho RA. Genetic and biological hallmarks of colorectal cancer. *Genes Dev* 2021; **35**: 787-820 [PMID: 34074695 DOI: 10.1101/gad.348226.120]
4 **Chambers AC**, Dixon SW, White P, Williams AC, Thomas MG, Messenger DE. Demographic trends in the incidence of young-onset colorectal cancer: a population-based study. *Br J Surg* 2020; **107**: 595-605 [PMID: 32149386 DOI: 10.1002/bjs.11486]
5 **Done JZ**, Fang SH. Young-onset colorectal cancer: A review. *World J Gastrointest Oncol* 2021; **13**: 856-866 [PMID: 34457191 DOI: 10.4251/wjgo.v13.i8.856]
6 **Kim BJ**, Hanna MH. Colorectal cancer in young adults. *J Surg Oncol* 2023; **127**: 1247-1251 [PMID: 37222697 DOI: 10.1002/jso.27320]
7 **Zygulska AL**, Pierzchalski P. Novel Diagnostic Biomarkers in Colorectal Cancer. *Int J Mol Sci* 2022; **23** [PMID: 35055034 DOI: 10.3390/ijms23020852]
8 **Dariya B**, Aliya S, Merchant N, Alam A, Nagaraju GP. Colorectal Cancer Biology, Diagnosis, and Therapeutic Approaches. *Crit Rev Oncog* 2020; **25**: 71-94 [PMID: 33389859 DOI: 10.1615/CritRevOncog.2020035067]
9 **Lech G**, Słotwiński R, Słodkowski M, Krasnodębski IW. Colorectal cancer tumour markers and biomarkers: Recent therapeutic advances. *World J Gastroenterol* 2016; **22**: 1745-1755 [PMID: 26855534 DOI: 10.3748/wjg.v22.i5.1745]
10 **Reinfeld BI**, Madden MZ, Wolf MM, Chytil A, Bader JE, Patterson AR, Sugiura A, Cohen AS, Ali A, Do BT, Muir A, Lewis CA, Hongo RA, Young KL, Brown RE, Todd VM, Huffstater T, Abraham A, O'Neil RT, Wilson MH, Xin F, Tantawy MN, Merryman WD, Johnson RW, Williams CS, Mason EF, Mason FM, Beckermann KE, Vander Heiden MG, Manning HC, Rathmell JC, Rathmell WK. Cell-programmed nutrient partitioning in the tumour microenvironment. *Nature* 2021; **593**: 282-288 [PMID: 33828302 DOI: 10.1038/s41586-021-03442-1]
11 **Liu X**, Nie L, Zhang Y, Yan Y, Wang C, Colic M, Olszewski K, Horbath A, Chen X, Lei G, Mao C, Wu S, Zhuang L, Poyurovsky MV, James You M, Hart T, Billadeau DD, Chen J, Gan B. Actin cytoskeleton vulnerability to disulfide stress mediates disulfidptosis. *Nat Cell Biol* 2023; **25**: 404-414 [PMID: 36747082 DOI: 10.1038/s41556-023-01091-2]
12 **Liu X**, Olszewski K, Zhang Y, Lim EW, Shi J, Zhang X, Zhang J, Lee H, Koppula P, Lei G, Zhuang L, You MJ, Fang B, Li W, Metallo CM, Poyurovsky MV, Gan B. Cystine transporter regulation of pentose phosphate pathway dependency and disulfide stress exposes a targetable metabolic vulnerability in cancer. *Nat Cell Biol* 2020; **22**: 476-486 [PMID: 32231310 DOI: 10.1038/s41556-020-0496-x]
13 **Zhao S**, Wang L, Ding W, Ye B, Cheng C, Shao J, Liu J, Zhou H. Crosstalk of disulfidptosis-related subtypes, establishment of a prognostic signature and immune infiltration characteristics in bladder cancer based on a machine learning survival framework. *Front Endocrinol (Lausanne)* 2023; **14**: 1180404 [PMID: 37152941 DOI: 10.3389/fendo.2023.1180404]
14 **Xing C**, Sun SG, Yue ZQ, Bai F. Role of lncRNA LUCAT1 in cancer. *Biomed Pharmacother* 2021; **134**: 111158 [PMID: 33360049 DOI: 10.1016/j.biopha.2020.111158]
15 **Yang J**, Liu F, Wang Y, Qu L, Lin A. LncRNAs in tumor metabolic reprogramming and immune microenvironment remodeling. *Cancer Lett* 2022; **543**: 215798 [PMID: 35738332 DOI: 10.1016/j.canlet.2022.215798]
16 **Tan YT**, Lin JF, Li T, Li JJ, Xu RH, Ju HQ. LncRNA-mediated posttranslational modifications and reprogramming of energy metabolism in cancer. *Cancer Commun (Lond)* 2021; **41**: 109-120 [PMID: 33119215 DOI: 10.1002/cac2.12108]
17 **Wang L**, Cho KB, Li Y, Tao G, Xie Z, Guo B. Long Noncoding RNA (lncRNA)-Mediated Competing Endogenous RNA Networks Provide Novel Potential Biomarkers and Therapeutic Targets for Colorectal Cancer. *Int J Mol Sci* 2019; **20** [PMID: 31744051 DOI: 10.3390/ijms20225758]
18 **Lin X**, Zhuang S, Chen X, Du J, Zhong L, Ding J, Wang L, Yi J, Hu G, Tang G, Luo X, Liu W, Ye F. lncRNA ITGB8-AS1 functions as a ceRNA to promote colorectal cancer growth and migration through integrin-mediated focal adhesion signaling. *Mol Ther* 2022; **30**: 688-702 [PMID: 34371180 DOI: 10.1016/j.ymthe.2021.08.011]
19 **Ye LC**, Zhu X, Qiu JJ, Xu J, Wei Y. Involvement of long non-coding RNA in colorectal cancer: From benchtop to bedside (Review). *Oncol Lett* 2015; **9**: 1039-1045 [PMID: 25663854 DOI: 10.3892/ol.2015.2846]
20 **Conesa A**, Madrigal P, Tarazona S, Gomez-Cabrero D, Cervera A, McPherson A, Szcześniak MW, Gaffney DJ, Elo LL, Zhang X, Mortazavi

A. Erratum to: A survey of best practices for RNA-seq data analysis. *Genome Biol* 2016; **17**: 181 [PMID: 27565134 DOI: 10.1186/s13059-016-1047-4]

21 **Ritchie ME**, Phipson B, Wu D, Hu Y, Law CW, Shi W, Smyth GK. limma powers differential expression analyses for RNA-sequencing and microarray studies. *Nucleic Acids Res* 2015; **43**: e47 [PMID: 25605792 DOI: 10.1093/nar/gkv007]

22 **Gustavsson EK**, Zhang D, Reynolds RH, Garcia-Ruiz S, Ryten M. ggtranscript: an R package for the visualization and interpretation of transcript isoforms using ggplot2. *Bioinformatics* 2022; **38**: 3844-3846 [PMID: 35751589 DOI: 10.1093/bioinformatics/btac409]

23 **Blanche P**, Dartigues JF, Jacqmin-Gadda H. Estimating and comparing time-dependent areas under receiver operating characteristic curves for censored event times with competing risks. *Stat Med* 2013; **32**: 5381-5397 [PMID: 24027076 DOI: 10.1002/sim.5958]

24 **Friedman J**, Hastie T, Tibshirani R. Regularization Paths for Generalized Linear Models *via* Coordinate Descent. *J Stat Softw* 2010; **33**: 1-22 [PMID: 20808728]

25 **Pang Y**, Wang Y, Zhou X, Ni Z, Chen W, Liu Y, Du W. Cuproptosis-Related LncRNA-Based Prediction of the Prognosis and Immunotherapy Response in Papillary Renal Cell Carcinoma. *Int J Mol Sci* 2023; **24** [PMID: 36674979 DOI: 10.3390/ijms24021464]

26 **Mogensen UB**, Ishwaran H, Gerds TA. Evaluating Random Forests for Survival Analysis using Prediction Error Curves. *J Stat Softw* 2012; **50**: 1-23 [PMID: 25317082 DOI: 10.18637/jss.v050.i11]

27 **Jiang P**, Gu S, Pan D, Fu J, Sahu A, Hu X, Li Z, Traugh N, Bu X, Li B, Liu J, Freeman GJ, Brown MA, Wucherpfennig KW, Liu XS. Signatures of T cell dysfunction and exclusion predict cancer immunotherapy response. *Nat Med* 2018; **24**: 1550-1558 [PMID: 30127393 DOI: 10.1038/s41591-018-0136-1]

28 **Wang T**, Guo K, Zhang D, Wang H, Yin J, Cui H, Wu W. Disulfidptosis classification of hepatocellular carcinoma reveals correlation with clinical prognosis and immune profile. *Int Immunopharmacol* 2023; **120**: 110368 [PMID: 37247499 DOI: 10.1016/j.intimp.2023.110368]

29 **Rodriguez J**, Point D, Castellanos R, Brugère J. [Cancers of the hypopharynx. Course of surgical salvage]. *Ann Otolaryngol Chir Cervicofac* 1987; **104**: 565-568 [PMID: 3426068 DOI: 10.1093/bib/bbab260]

30 **Zheng X**, Chen L, Zhou Y, Wang Q, Zheng Z, Xu B, Wu C, Zhou Q, Hu W, Jiang J. A novel protein encoded by a circular RNA circPPP1R12A promotes tumor pathogenesis and metastasis of colon cancer *via* Hippo-YAP signaling. *Mol Cancer* 2019; **18**: 47 [PMID: 30925892 DOI: 10.1186/s12943-019-1010-6]

31 **Peña-Romero AC**, Orenes-Piñero E. Dual Effect of Immune Cells within Tumour Microenvironment: Pro- and Anti-Tumour Effects and Their Triggers. *Cancers (Basel)* 2022; **14** [PMID: 35406451 DOI: 10.3390/cancers14071681]

32 **Heeke S**, Hofman P. Tumor mutational burden assessment as a predictive biomarker for immunotherapy in lung cancer patients: getting ready for prime-time or not? *Transl Lung Cancer Res* 2018; **7**: 631-638 [PMID: 30505707 DOI: 10.21037/tlcr.2018.08.04]

33 **Yang W**, Soares J, Greninger P, Edelman EJ, Lightfoot H, Forbes S, Bindal N, Beare D, Smith JA, Thompson IR, Ramaswamy S, Futreal PA, Haber DA, Stratton MR, Benes C, McDermott U, Garnett MJ. Genomics of Drug Sensitivity in Cancer (GDSC): a resource for therapeutic biomarker discovery in cancer cells. *Nucleic Acids Res* 2013; **41**: D955-D961 [PMID: 23180760 DOI: 10.1093/nar/gks1111]

34 **Kashima H**, Momose F, Umehara H, Miyoshi N, Ogo N, Muraoka D, Shiku H, Harada N, Asai A. Epirubicin, Identified Using a Novel Luciferase Reporter Assay for Foxp3 Inhibitors, Inhibits Regulatory T Cell Activity. *PLoS One* 2016; **11**: e0156643 [PMID: 27284967 DOI: 10.1371/journal.pone.0156643]

35 **Yang Z**, Liu S, Zhu M, Zhang H, Wang J, Xu Q, Lin K, Zhou X, Tao M, Li C, Zhu H. PS341 inhibits hepatocellular and colorectal cancer cells through the FOXO3/CTNNB1 signaling pathway. *Sci Rep* 2016; **6**: 22090 [PMID: 26915315 DOI: 10.1038/srep22090]

36 **Carvalho RF**, do Canto LM, Cury SS, Frøstrup Hansen T, Jensen LH, Rogatto SR. Drug Repositioning Based on the Reversal of Gene Expression Signatures Identifies TOP2A as a Therapeutic Target for Rectal Cancer. *Cancers (Basel)* 2021; **13** [PMID: 34771654 DOI: 10.3390/cancers13215492]

37 **Wang Q**, Zhang Y, Zhu J, Zheng H, Chen S, Chen L, Yang HS. IGF-1R inhibition induces MEK phosphorylation to promote survival in colon carcinomas. *Signal Transduct Target Ther* 2020; **5**: 153 [PMID: 32843616 DOI: 10.1038/s41392-020-0204-0]

38 **Hou P**, Meng S, Li M, Lin T, Chu S, Li Z, Zheng J, Gu Y, Bai J. LINC00460/DHX9/IGF2BP2 complex promotes colorectal cancer proliferation and metastasis by mediating HMGA1 mRNA stability depending on m6A modification. *J Exp Clin Cancer Res* 2021; **40**: 52 [PMID: 33526059 DOI: 10.1186/s13046-021-01857-2]

39 **Zheng P**, Zhou C, Ding Y, Duan S. Disulfidptosis: a new target for metabolic cancer therapy. *J Exp Clin Cancer Res* 2023; **42**: 103 [PMID: 37101248 DOI: 10.1186/s13046-023-02675-4]

40 **Wang X**, Xie C, Lin L. Development and validation of a cuproptosis-related lncRNA model correlated to the cancer-associated fibroblasts enable the prediction prognosis of patients with osteosarcoma. *J Bone Oncol* 2023; **38**: 100463 [PMID: 36569351 DOI: 10.1016/j.jbo.2022.100463]

41 **Li N**, Shen J, Qiao X, Gao Y, Su HB, Zhang S. Long Non-Coding RNA Signatures Associated with Ferroptosis Predict Prognosis in Colorectal Cancer. *Int J Gen Med* 2022; **15**: 33-43 [PMID: 35018112 DOI: 10.2147/IJGM.S331378]

42 **Wang W**, Pei Q, Wang L, Mu T, Feng H. Construction of a Prognostic Signature of 10 Autophagy-Related lncRNAs in Gastric Cancer. *Int J Gen Med* 2022; **15**: 3699-3710 [PMID: 35411177 DOI: 10.2147/IJGM.S348943]

43 **Wang K**, Gu Y, Ni J, Zhang H, Wang Y, Zhang Y, Sun X, Xu T, Mao W, Peng B. Noncoding-RNA mediated high expression of zinc finger protein 268 suppresses clear cell renal cell carcinoma progression by promoting apoptosis and regulating immune cell infiltration. *Bioengineered* 2022; **13**: 10467-10481 [PMID: 35735115 DOI: 10.1080/21655979.2022.2060787]

44 **Sun D**, Gou H, Wang D, Li C, Li Y, Su H, Wang X, Zhang X, Yu J. LncRNA TNFRSF10A-AS1 promotes gastric cancer by directly binding to oncogenic MPZL1 and is associated with patient outcome. *Int J Biol Sci* 2022; **18**: 3156-3166 [PMID: 35637954 DOI: 10.7150/ijbs.68776]

45 **Yang L**, Liu Q, Zhang X, Liu X, Zhou B, Chen J, Huang D, Li J, Li H, Chen F, Liu J, Xing Y, Chen X, Su S, Song E. DNA of neutrophil extracellular traps promotes cancer metastasis *via* CCDC25. *Nature* 2020; **583**: 133-138 [PMID: 32528174 DOI: 10.1038/s41586-020-2394-6]

46 **Wang K**, Kim MK, Di Caro G, Wong J, Shalapour S, Wan J, Zhang W, Zhong Z, Sanchez-Lopez E, Wu LW, Taniguchi K, Feng Y, Fearon E, Grivennikov SI, Karin M. Interleukin-17 receptor a signaling in transformed enterocytes promotes early colorectal tumorigenesis. *Immunity* 2014; **41**: 1052-1063 [PMID: 25526314 DOI: 10.1016/j.immuni.2014.11.009]

47 **Li X**, Bechara R, Zhao J, McGeachy MJ, Gaffen SL. IL-17 receptor-based signaling and implications for disease. *Nat Immunol* 2019; **20**: 1594-1602 [PMID: 31745337 DOI: 10.1038/s41590-019-0514-y]

48 **Fan S**, Gao Y, Qu A, Jiang Y, Li H, Xie G, Yao X, Yang X, Zhu S, Yagai T, Tian J, Wang R, Gonzalez FJ, Huang M, Bi H. YAP-TEAD mediates PPAR α-induced hepatomegaly and liver regeneration in mice. *Hepatology* 2022; **75**: 74-88 [PMID: 34387904 DOI: 10.1002/hep.32105]

49 **Wang R**, Li J, Zhou X, Mao Y, Wang W, Gao S, Gao Y, Chen K, Yu S, Wu X, Wen L, Ge H, Fu W, Tang F. Single-cell genomic and

transcriptomic landscapes of primary and metastatic colorectal cancer tumors. *Genome Med* 2022; **14**: 93 [PMID: 35974387 DOI: 10.1186/s13073-022-01093-z]

50 **Yue T**, Cai Y, Zhu J, Liu Y, Chen S, Wang P, Rong L. Autophagy-related IFNG is a prognostic and immunochemotherapeutic biomarker of COAD patients. *Front Immunol* 2023; **14**: 1064704 [PMID: 36756126 DOI: 10.3389/fimmu.2023.1064704]

World Journal of Clinical Oncology

Submit a Manuscript: https://www.f6publishing.com

World J Clin Oncol 2024 January 24; 15(1): 115-129

DOI: 10.5306/wjco.v15.i1.115

ISSN 2218-4333 (online)

ORIGINAL ARTICLE

Clinical and Translational Research

Gene signatures to therapeutics: Assessing the potential of ivermectin against t(4;14) multiple myeloma

Yang Song, Hao-Jun Zhang, Xia Song, Jie Geng, Hong-Yi Li, Li-Zhong Zhang, Bo Yang, Xue-Chun Lu

Specialty type: Oncology

Provenance and peer review: Unsolicited article; Externally peer reviewed.

Peer-review model: Single blind

Peer-review report's scientific quality classification

Grade A (Excellent): 0
Grade B (Very good): B
Grade C (Good): 0
Grade D (Fair): 0
Grade E (Poor): 0

P-Reviewer: Blanc R, France

Received: November 20, 2023
Peer-review started: November 20, 2023
First decision: December 5, 2023
Revised: December 13, 2023
Accepted: January 2, 2024
Article in press: January 2, 2024
Published online: January 24, 2024

Yang Song, Hong-Yi Li, School of Basic Medicine, Medical School of Chinese PLA, Beijing 100853, China

Hao-Jun Zhang, Xia Song, Jie Geng, Li-Zhong Zhang, School of Basic Medicine, Shanxi Medical University, Taiyuan 030001, Shanxi Province, China

Bo Yang, Xue-Chun Lu, Department of Hematology, The Second Medical Centre, Chinese PLA General Hospital, Beijing 100853, China

Corresponding author: Xue-Chun Lu, PhD, Chief Doctor, Professor, Research Scientist, Department of Hematology, The Second Medical Center, Chinese PLA General Hospital, No. 28 Fuxing Road, Haidian District, Beijing 100853, China. luxuechun@301hospital.com.cn

Abstract

BACKGROUND

Multiple myeloma (MM) is a terminal differentiated B-cell tumor disease characterized by clonal proliferation of malignant plasma cells and excessive levels of monoclonal immunoglobulins in the bone marrow. The translocation, (t)(4;14), results in high-risk MM with limited treatment alternatives. Thus, there is an urgent need for identification and validation of potential treatments for this MM subtype. Microarray data and sequencing information from public databases could offer opportunities for the discovery of new diagnostic or therapeutic targets.

AIM

To elucidate the molecular basis and search for potential effective drugs of t(4;14) MM subtype by employing a comprehensive approach.

METHODS

The transcriptional signature of t(4;14) MM was sourced from the Gene Expression Omnibus. Two datasets, GSE16558 and GSE116294, which included 17 and 15 t(4;14) MM bone marrow samples, and five and four normal bone marrow samples, respectively. After the differentially expressed genes were identified, the Cytohubba tool was used to screen for hub genes. Then, the hub genes were analyzed using Gene Ontology and Kyoto Encyclopedia of Genes and Genomes analysis. Using the STRING database and Cytoscape, protein–protein interaction networks and core targets were identified. Potential small-molecule drugs were identified and validated using the Connectivity Map database and molecular

docking analysis, respectively.

RESULTS

In this study, a total of 258 differentially expressed genes with enriched functions in cancer pathways, namely cytokine receptor interactions, nuclear factor (NF)-κB signaling pathway, lipid metabolism, atherosclerosis, and Hippo signaling pathway, were identified. Ten hub genes (*cd45, vcam1, ccl3, cd56, app, cd48, btk, ccr2, cybb,* and *cxcl12*) were identified. Nine drugs, including ivermectin, deforolimus, and isoliquiritigenin, were predicted by the Connectivity Map database to have potential therapeutic effects on t (4;14) MM. In molecular docking, ivermectin showed strong binding affinity to all 10 identified targets, especially *cd45* and *cybb*. Ivermectin inhibited t(4;14) MM cell growth *via* the NF-κB pathway and induced MM cell apoptosis in vitro. Furthermore, ivermectin increased reactive oxygen species accumulation and altered the mitochondrial membrane potential in t(4;14) MM cells.

CONCLUSION

Collectively, the findings offer valuable molecular insights for biomarker validation and potential drug development in t(4;14) MM diagnosis and treatment, with ivermectin emerging as a potential therapeutic alternative.

Key Words: Multiple myeloma; Functional enrichment analysis; Molecular docking simulation; Gene expression profiling; Therapeutic target; Ivermectin

Core Tip: Multiple myeloma is a hematological malignancy with a significant impact on public health, and the t(4;14) subtype is particularly aggressive and resistant to existing treatments. Our study addresses the urgent need for new therapeutic approaches by employing a comprehensive approach that includes bioinformatics analysis, molecular docking, and experimental validation. We identified ten key genes associated with t(4;14) multiple myeloma (MM), shedding light on the molecular basis of this subtype. We explored the potential of ivermectin to assess whether it may be "repurposed" as a therapeutic agent for t(4;14) MM. Our findings indicate that ivermectin not only inhibits MM cell growth but also induces apoptosis *via* the nuclear factor-κB signaling pathway.

Citation: Song Y, Zhang HJ, Song X, Geng J, Li HY, Zhang LZ, Yang B, Lu XC. Gene signatures to therapeutics: Assessing the potential of ivermectin against t(4;14) multiple myeloma. *World J Clin Oncol* 2024; 15(1): 115-129
URL: https://www.wjgnet.com/2218-4333/full/v15/i1/115.htm
DOI: https://dx.doi.org/10.5306/wjco.v15.i1.115

INTRODUCTION

Multiple myeloma (MM) represents a severe hematological malignancy, affecting 176404 individuals and resulting in117077 fatalities annually[1]. MM is characterized by uncontrolled plasma cell proliferation in the bone marrow, leading to severe complications, such as bone and kidney damage, anemia, and hypercalcemia[2]. Of particular concern is the t(4;14) subtype, comprising up to 15% of new MM cases, with notably low survival rates and strong resistance to existing therapies[3]. Thus, effectively addressing this subtype remains an important medical challenge. Although the seminal research of Foltz *et al*[4] and Ashby *et al*[5] have provided insights into the pivotal facets of t(4;14) MM (Supplementary Table 1),which have advanced our understanding of this malignancy, certain aspects remain elusive.

Translational medicine is increasingly considering drug repurposing as a potential strategy to develop efficient, safe, cost-effective, and readily available anticancer treatments[6]. Advances in high-throughput sequencing technology have expanded biomedical and computational resources, facilitating a deeper understanding of cancer etiology and drug-target interactions, thus enabling drug repurposing[7]. Notably, the Connectivity Map (CMap) tool, housing a comprehensive dataset of 7000 microarrays from various cancer cells treated with 1309 molecular compounds, has been instrumental in identifying potential treatments for various cancers[8]. Notably, Shi *et al*[9] used CMap to identify eugenol as a potential treatment for triple-negative breast cancer, and Qiu *et al*[10] computationally identified small-molecule drugs with the potential to treat cervical cancer.

There is an urgent need for identification and validation of potential treatments for this MM subtype, therefore, we aim to elucidate the molecular basis and search for potential effective drugs by employing a comprehensive approach. We hope to contribute to advancing early MM diagnosis and tailoring its treatment.

MATERIALS AND METHODS

Differential expression analysis

The Gene Expression Omnibus (GEO) database (https://www.ncbi.nlm.nih.gov/gds) is a key public repository housing high-throughput gene expression data, microarray data, and gene chip information. For this study, we sourced the t(4;14) MM-related expression dataset from GEO. Our search parameters were tailored to t(4;14) MM across all fields, combined with filters for "Homo sapiens" as the organism and "dataset." Two datasets, GSE16558 and GSE116294, which included 17 and 15 t(4;14) MM bone marrow samples, and five and four normal bone marrow samples, respectively (Supplementary Table 2), were further considered for our analysis. To identify DEGs between the t(4;14) MM samples and normal samples, we used the "limma" package in R software [version 4.2.2, (http://www.R-project.org/)]. Our selection criteria were a P value < 0.05 and absolute log2 fold change (FC) > 1.

PPI network analysis

To construct a functional PPI network for the identified DEGs, we used the STRING online database tool (https://string-db.org/)[11]. Our selected threshold required a credibility score of > 0.4 for inclusion within the network. The Cytoscape software [version 3.10.1, (https://cytoscape.org/)] was used to visually map the PPI, offering a clear understanding of protein interactions.

Hub gene mapping

Using Cytoscape, the molecular complex detection (MCODE) plugin was activated to highlight prominent clusters, abiding by criteria, such as an MCODE score > 6 and a node count > 4. The CytoHubba plugin[12] within Cytoscape, paired with the Maximal Clique Centrality (MCC) method, was used to filter and identify the top-ranking genes. A combination of results drawn from the MCODE, MCC, and degree scores led to the identification of 10 key hub genes.

Functional enrichment analysis

The enrichment analysis was performed using the "GSEApy" package within Python (v.3.11.4, [https://www.python.org]), using the Kyoto Encyclopedia of Genes and Genomes (KEGG) and Gene Ontology. Subsequently, statistical significance was evaluated using the p-value, whereas the visualization of data was achieved using the "ggplot2" package in R. Gene Set Enrichment Analysis (GSEA) was performed using its dedicated software, sourcing gene sets from the Molecular Signature Database (http://software.broadinstitute.org/gsea/index.jsp).

Drug screening using CMap

The CMap database (https://clue.io)[13], a key tool in systems biology, was used to identify potential therapeutic candidates. Our criteria were rigorous, with a cutoff score of < −80.

Molecular docking

For our molecular docking investigations, 3D structural models of the proteins encoded by target genes were retrieved from UniProt[14] and Protein Data Bank databases and augmented with AlphaFold data. Focusing on structures determined *via* X-ray diffraction with a co-crystal resolution < 2.5 Å, we downloaded the 2D structural model of ivermectin from PubChem[15] and converted it into a 3D structure using the LigPrep module in Maestro. AutoDockTools were used to preprocess the ligands. Optimization included water removal, hydrogenation, charge determination, and torsion centers and bond selection, yielding a pdbqt file suitable for docking studies. Macromolecular docking calculations were performed using Vina software [version 1.1.2, (http://vina.scripps.edu/)]. To illustrate the post-docking ligand-receptor interactions, we used Ligplot+[16] for 2D mapping and PyMOL[17] for in-depth 3D analysis.

Reagents and antibodies

Ivermectin was purchased from Aladdin Biological Technology (Shanghai, China). The following primary antibodies were purchased from CST (Danvers, MA, United States): Anti- poly (ADP-ribose) polymerase (PARP) (9532; 1:1000), anti-cleaved PARP (5625; 1:1000), anti-cleaved caspase 3 (9661; 1:500), anti-cleaved caspase 9 (20750; 1:1000), and β-actin (3700; 1:1000). The following primary antibodies were purchased from Abcam (Cambridge, United Kingdom): Anti-B-cell lymphoma 2 (Bcl2; ab182858; 1:1000), anti-Bcl-2-associated X protein (Bax; ab32503; 1:1000), anti-NF-κB p65 (ab32536; 1:1000), anti-NF-κB p65 (phospho S536) (ab86299; 1:1000), anti-inhibitor of NF-κB (IκB) alpha (ab32518; 1:1000), and anti-IκB alpha (phospho-S36) (ab133462; 1:1000). The following secondary antibodies were purchased from Beyotime Biotechnology (Shanghai, China): anti-rabbit IgG (A0208; 1:5000) and anti-mouse IgG (A0216; 1:5000).

Cell culture

NCI-H929, a t(4;14) MM cell line, was obtained from the Cell Bank of the Type Culture Collection of the Chinese Academy of Sciences (Shanghai, China). The cells were cultured in RPMI-1640 medium (Gibco, Billings, MO, United States) with 10% fetal bovine serum (Gibco) and 1% penicillin/streptomycin (Gibco) at 37 °C with 5% CO_2. Preliminary tests confirmed that the cell lines were *Mycoplasma*-free.

Cytotoxic activity assay

To assess cytotoxic activity, 5000 cells were seeded per well into a 96-well plate and exposed to ivermectin concentrations ranging from 0–20 μmol/L for 24–48 h. After incubation, cell viability was evaluated using Cell Counting Kit-8 (CCK8)

(DojinDo, Shanghai, China), which required an additional 2-h incubation with 10 μL of CCK8 solution at 37 °C. The absorbance of the reaction mixture was measured at 450 nm using a microplate reader (Thermo Fisher Scientific, California, United States). The inhibitory concentration 50% (IC_{50}) of ivermectin for each cell type was determined from the viability data using GraphPad Prism v.10 and the following equation:

[(As−Ab)/(Ac−Ab)] × 100%, where "As," "Ac," and "Ab" are the absorbance values in the experimental, control, and blank wells, respectively.

Apoptosis assay

Cells were seeded into 6-well plates and treated with ivermectin for 24 h. After treatment, the cells were collected by centrifugation. They were then stained using the fluorescein isothiocyanate (FITC) Annexin V Apoptosis Detection Kit with 7-aminoactinomycin D (7-AAD; 640922; BioLegend, San Diego, CA, United States) by adding 5 μL of FITC conjugated with annexin V and 5 μL of 7-AAD solution. This was followed by 15 min incubation in the dark at 25 °C. Subsequently, the stained cells were analyzed using a flow cytometer (LSRFortessa; BD, Franklin Lakes, NJ, United States), and the data obtained were processed and interpreted using FlowJo software (v.10.4).

Reactive oxygen species assay

The cells were cultured in 6-well plates overnight. Fresh RPMI-1640 medium containing the indicated concentrations of ivermectin was added, and the cells were cultured for 24 h. A reactive oxygen species (ROS) assay kit (S0033S; Beyotime) was used to detect intracellular ROS levels using the following protocol: treated cells were incubated with 2′,7′-dichlorodihydrofluorescein diacetate for 20 min at 37 °C. Cells were washed thrice with serum-free medium, and images were acquired using a fluorescent inverted microscope (Olympus, Tokyo, Japan).

Mitochondrial membrane potential assay

Cells were first allowed to settle in 6-well plates, after which they were treated with ivermectin for 24 h. A JC-1 assay kit (M34152; Thermo Fisher Scientific) was used to evaluate the mitochondrial membrane potential within these cells. The assessment was performed in strict accordance with the manufacturer's guidelines. Readings from this assessment were captured using a flow cytometer (LSRFortessa; BD).

Western blot analysis

After 48 h of ivermectin treatment, the cells were harvested and lysed using Cell Lysis Buffer (P0013; Beyotime), which included a protease inhibitor. The subsequent lysate was subjected to a 30-min ice bath before centrifugation at 12000 rpm for 20 min at 4 °C. Proteins were quantified using a BCA assay kit (P0010; Beyotime), separated by sodium dodecyl-sulfate polyacrylamide gel electrophoresis, and transferred onto polyvinylidene fluoride membranes. Subsequently, these membranes were blocked with 5% skim milk for 2 h and incubated with primary antibodies overnight at 4 °C. After thorough washing, the membranes were incubated with horseradish peroxidase-conjugated secondary antibodies for 1 h at 25 °C. The proteins were visualized using an electrochemiluminescence kit (NCM Biotech, Suzhou, China).

Statistical analysis

All statistical evaluations were performed using both the R package and GraphPad Prism v.9.0 (GraphPad Software Inc., San Diego, CA, United States). Student's *t*-test was used to compare the means between two groups. Comparisons across multiple groups were conducted using one- and two-way ANOVA. All results are presented as the mean ± SD. Statistical significance was set at P levels < 0.05.

RESULTS

Identification of DEGs

We identified 1,100 DEGs (270 upregulated and 830 downregulated) and 1746 DEGs (808 upregulated and 938 downregulated) in the GSE16558 and GSE116294 datasets, respectively. These microarray findings have been presented using heat maps and volcano graphs, applying a threshold of P < 0.05, logFC<1 for downregulated genes, and logFC>1 for upregulated genes (Supplementary Figure 1).

Potential targets involved in t(4;14) MM and PPI network: To better understand the therapeutic pathways involved in t(4;14) MM, we constructed a Venn diagram and identified 258 probable targets related to t(4;14) MM (Figure 1A). Subsequently, a PPI network containing these targets was constructed to elucidate the target interrelations. The PPI network comprised 175 nodes and 697 edges (Figure 1B). Three targets that lacked interactions with other targets were excluded from the assessment. The top five identified nodes were cd45, btk, ccl3, cdh1, and cxcl12, highlighting their pivotal roles in the network.

Identification of clusters and hub targets in the PPI network

Using the Cytoscape MCODE plugin, we identified two clusters with scores > 6 (Figure 1C). The first group, with 57 nodes and 343 edges, was centered on the seed gene, *CD45*, and was predominantly related to altered transcriptional regulation in cancer. The second smaller cluster, which included 15 nodes and 66 edges, had *TLR1* as its seed gene and was primarily related to the negative regulation of apoptosis and signal transduction. Subsequently, the CytoHubba score

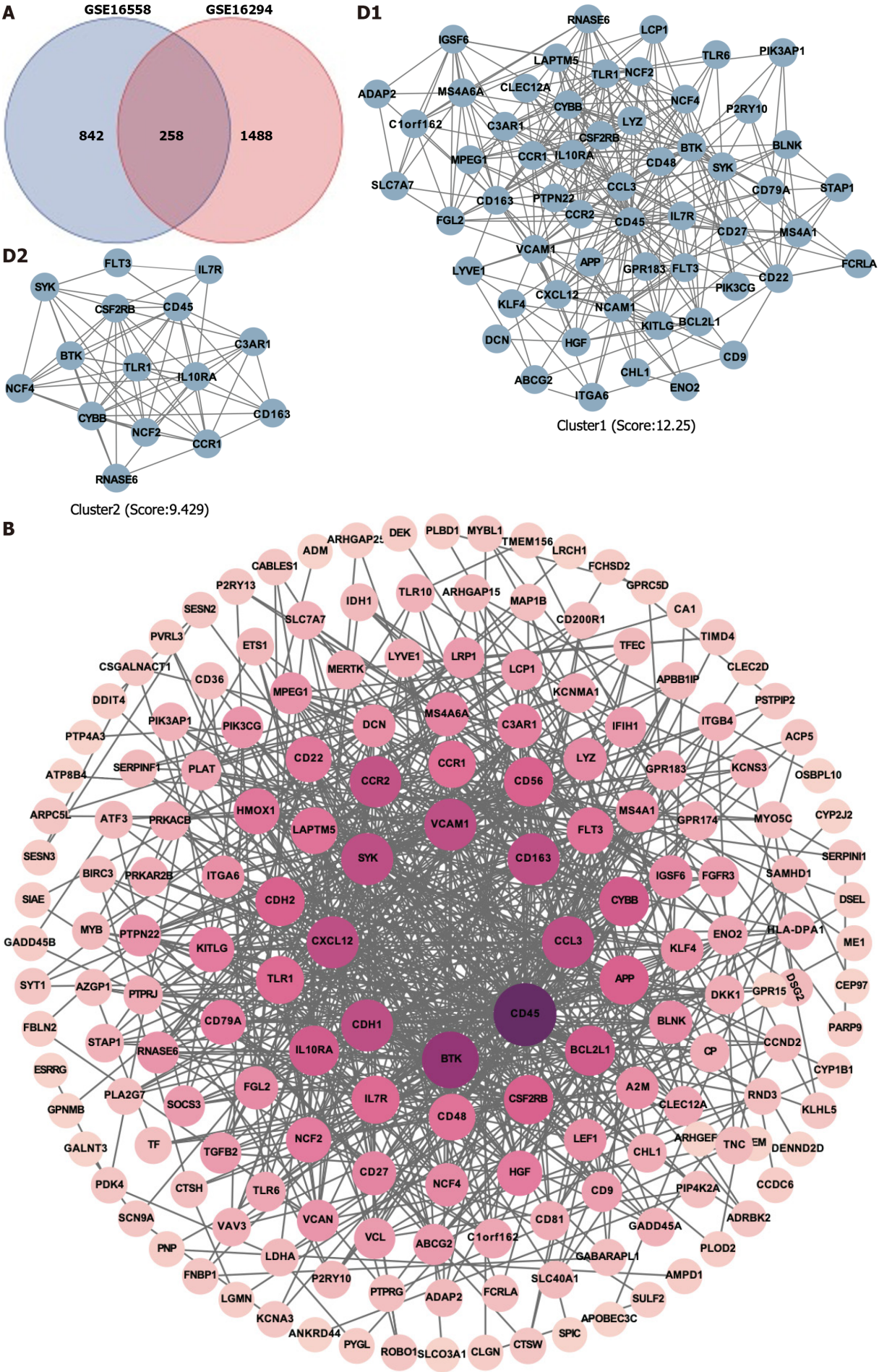
A
GSE16558
GSE16294
842
258
1488
D1
Cluster1 (Score:12.25)
D2
Cluster2 (Score:9.429)
B

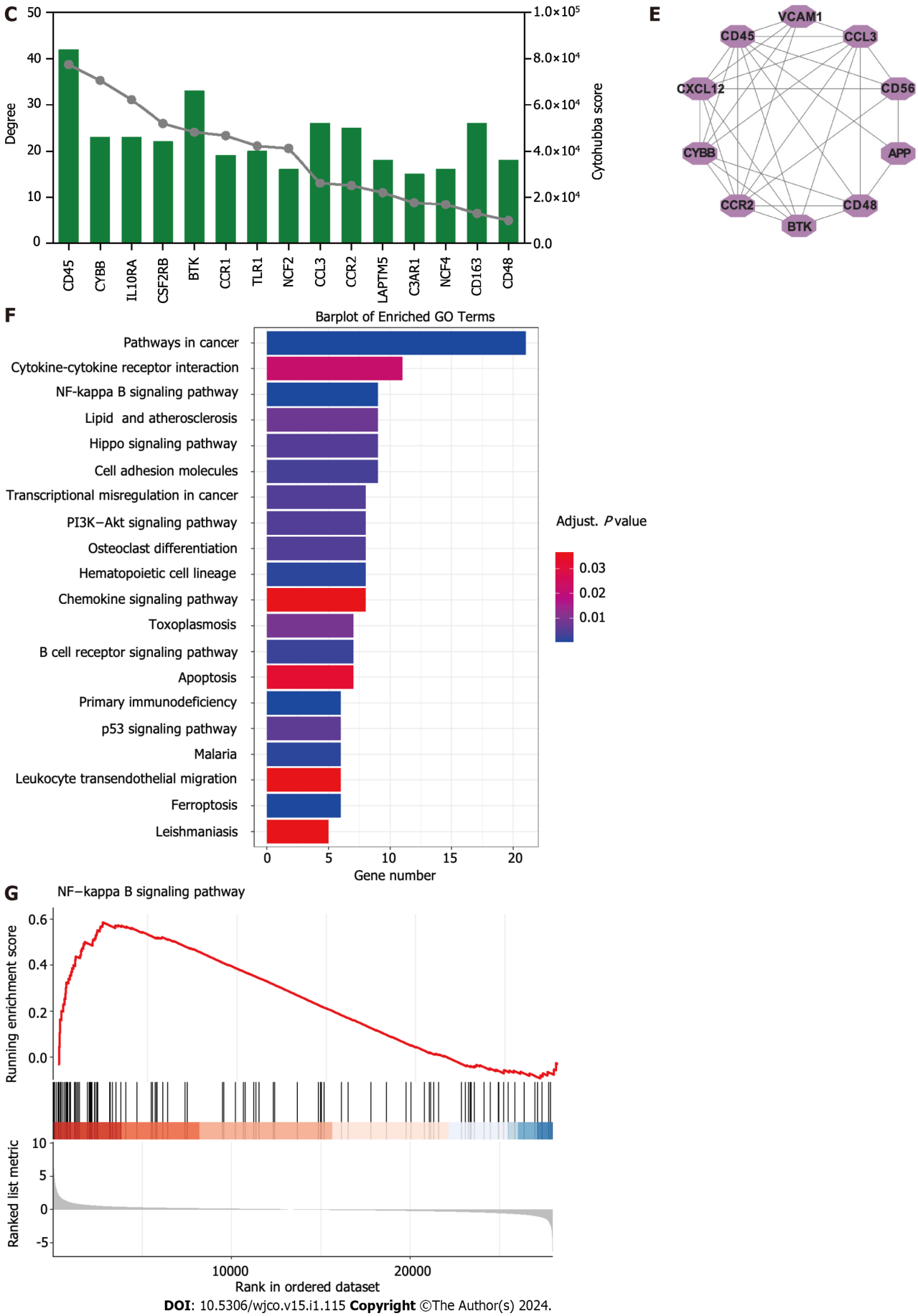

DOI: 10.5306/wjco.v15.i1.115

Figure 1 Identification of hub targets and the Kyoto Encyclopedia of Genes and Genomes pathways. A: Venn diagram illustrating overlap of

targets between GSE16558 and GSE116294 datasets; B: Target protein–protein interaction (PPI) network; C: Top 15 hub genes identified using CytoHubba plugin; D: Two primary clusters of PPI scored using themolecular complex detection plugin; E: Ranking of top 10 hub genes within PPI network; F: The Kyoto Encyclopedia of Genes and Genomes pathway enrichment analysis; G: Gene Set Enrichment Analysis of nuclear factor -κB signaling pathway. NK: Nuclear factor.

was used to identify the top 15 genes (Figure 1D). Each of these 15 genes had a degree score >15, indicating comprehensive interactions among them. Combining insights from MCODE, MCC, and degree scores, we identified 10 central hub genes: *cd45*, *vcam1*, *ccl3*, *cd56*, *app*, *cd48*, *btk*, *ccr2*, *cybb*, and *cxcl12* (Figure 1E).

Functional enrichment analysis

To better understand the potential therapeutic targets of t(4;14) MM, we performed functional enrichment analysis of the 255 shared targets. Using the KEGG database, we identified 232 enriched signal pathway terms through enrichment analysis. With an adjusted *P* value of < 0.05, the top 20 pathways, including those related to cancer, cytokine-cytokine receptor interaction, NF-κB signaling, and the Hippo signaling pathway, were identified (Figure 1F). The GSEA for the NF-κB signaling pathway is illustrated in Figure 1G. Based on these findings, we focused on the NF-κB signaling pathway to elucidate the potential mechanisms related to t(4;14) MM.

Ivermectin identified as a potential drug using CMap

We used 258 DEGs as potential drug targets for t(4; 14) MM and assessed the CMap database to identify small compounds that could serve as prospective drugs. Table 1 lists the top nine small-molecule drugs believed to hold therapeutic potential in countering the gene expression pattern of t(4;14) MM (with a cut-off score of < −80). Notably, ivermectin, which was listed among the identified small molecules, was considered for further investigation, as it is a high-ranking approved non-chemotherapeutic drug. Thus, we evaluated the potential inhibitory effects of ivermectin on t(4;14) MM cells.

Table 1 Potential drugs identified using the Connectivity Map database

ID	Name	Score	Mechanism of action
BRD-K29733039	Deforolimus	−92.69	mTOR inhibitor
BRD-A48570745	Ivermectin	−91.74	GABA receptor regulator
BRD-K33583600	Isoliquiritigenin	−91.69	Guanylate cyclase activator
BRD-K59456551	Methotrexate	−90.69	Dihydrofolate reductase inhibitor
BRD-A43150328	Penicillic acid	−87.56	Another antibiotic
BRD-A64479082	Quinidine	−85.76	Sodium channel blocker
BRD-K35377380	I-OMe-AG-538	−83.43	IGF-1 inhibitor
BRD-K59570838	Homoveratrylamine	−82.67	Dopamine analog
BRD-A50675702	Fipronil	−80.55	GABA gated chloride channel blocker

mTOR: Mammalian target of rapamycin; GABA: Gamma-aminobutyric acid; IGF-1: Insulin-like growth factor-1.

Molecular docking

Molecular docking is a pivotal technique for the design of structure-based drugs. It facilitates the assessment of molecular interactions by determining the most favorable conformation between small-molecule targets and compounds. The 2D structure of ivermectin is shown in Figure 2A. In molecular docking simulations, ivermectin displayed strong binding affinity to all 10 identified targets, with docking energy scores below −7 kcal/mol (Figure 2B). Notably, CD45 and CYBB demonstrated the most potent binding, with binding energies of −10.2 kcal/mol and −9.9 kcal/mol, respectively. The 3D structural analysis revealedfavorable binding sites for ivermectin in both CD45 (Figure 2E) and CYBB (Figure 2F). Additionally, 2D interaction diagrams indicated hydrogen bond formation between ivermectin and specific amino acid residues in CD45 (Glu1030 and Glu1003) and CYBB (Art73), along with hydrophobic interactions in CD45 (Figure 2C) and water-mediated interactions in CYBB (Figure 2D). These findings shed light on the binding mechanisms underlying the strong affinity between ivermectin and its targets, providing valuable insights for future drug design.

Ivermectin inhibits the proliferation of t(4;14) MM cells

We evaluated the impact of ivermectin on t(4;14) MM cell proliferation by subjecting cells to varying concentrations (0, 4, 6, 8, 10, and 20 μmol/L) of ivermectin and time intervals (24 and 48 h) of exposure. Cell viability, determined using CCK8, demonstrated a significant, concentration- and time-dependent decrease in cancer cell viability (Figure 3A and B). The half-maximum inhibitory concentration (IC_{50}) of ivermectin was approximately 9.4 μmol/L in NCI-H929 cells.

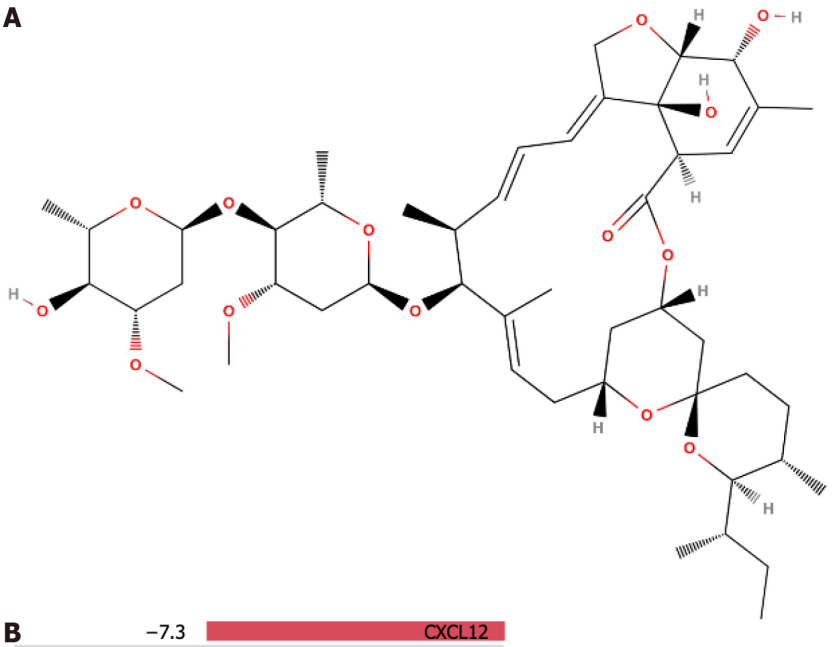
A

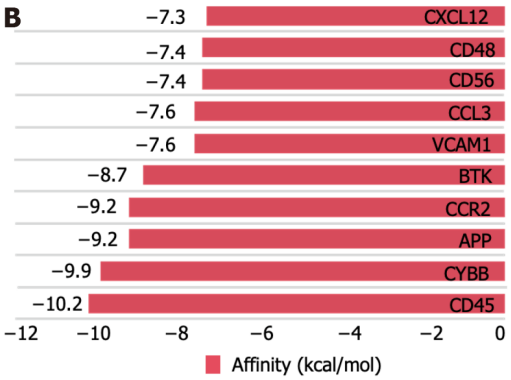
B
−7.3 CXCL12
−7.4 CD48
−7.4 CD56
−7.6 CCL3
−7.6 VCAM1
−8.7 BTK
−9.2 CCR2
−9.2 APP
−9.9 CYBB
−10.2 CD45
−12 −10 −8 −6 −4 −2 0
Affinity (kcal/mol)

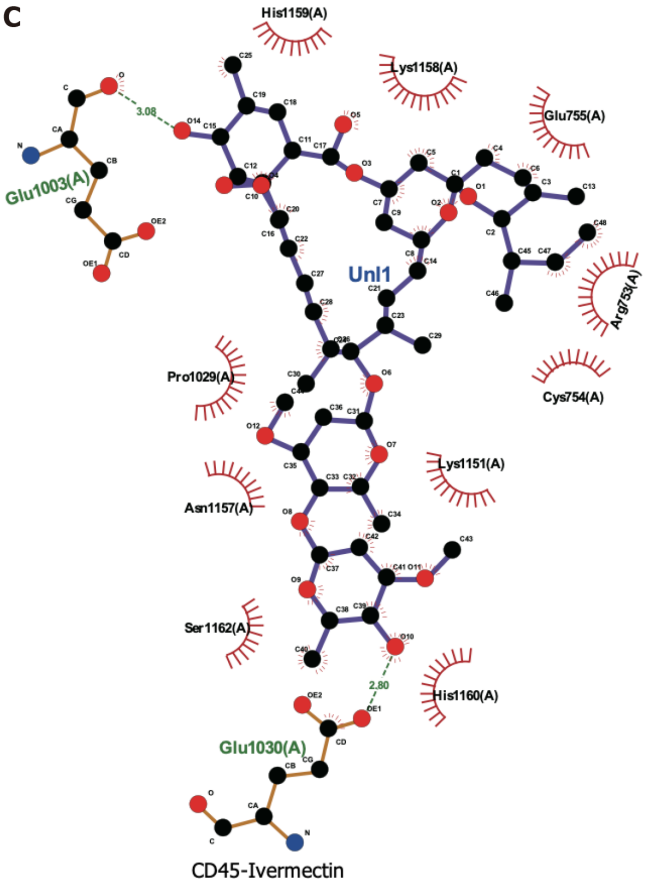
C
His1159(A)
Lys1158(A)
Glu755(A)
Glu1003(A)
Unl1
Arg753(A)
Pro1029(A)
Cys754(A)
Lys1151(A)
Asn1157(A)
Ser1162(A)
His1160(A)
Glu1030(A)
CD45-Ivermectin

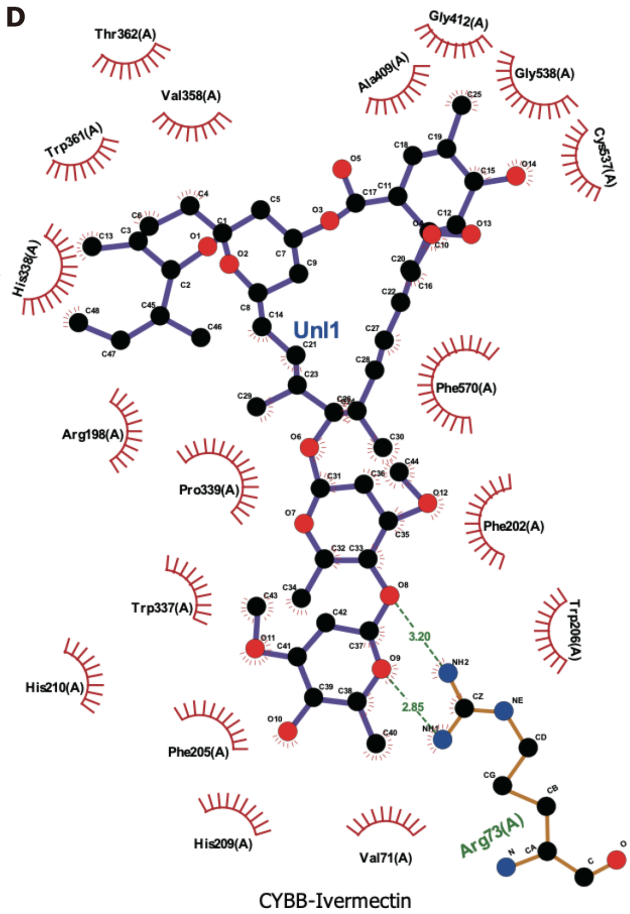
D
Thr362(A)
Gly412(A)
Ala409(A)
Gly538(A)
Val358(A)
Trp361(A)
Cys537(A)
His338(A)
Unl1
Phe570(A)
Arg198(A)
Pro339(A)
Phe202(A)
Trp337(A)
Trp206(A)
His210(A)
Phe205(A)
His209(A)
Val71(A)
Arg73(A)
CYBB-Ivermectin

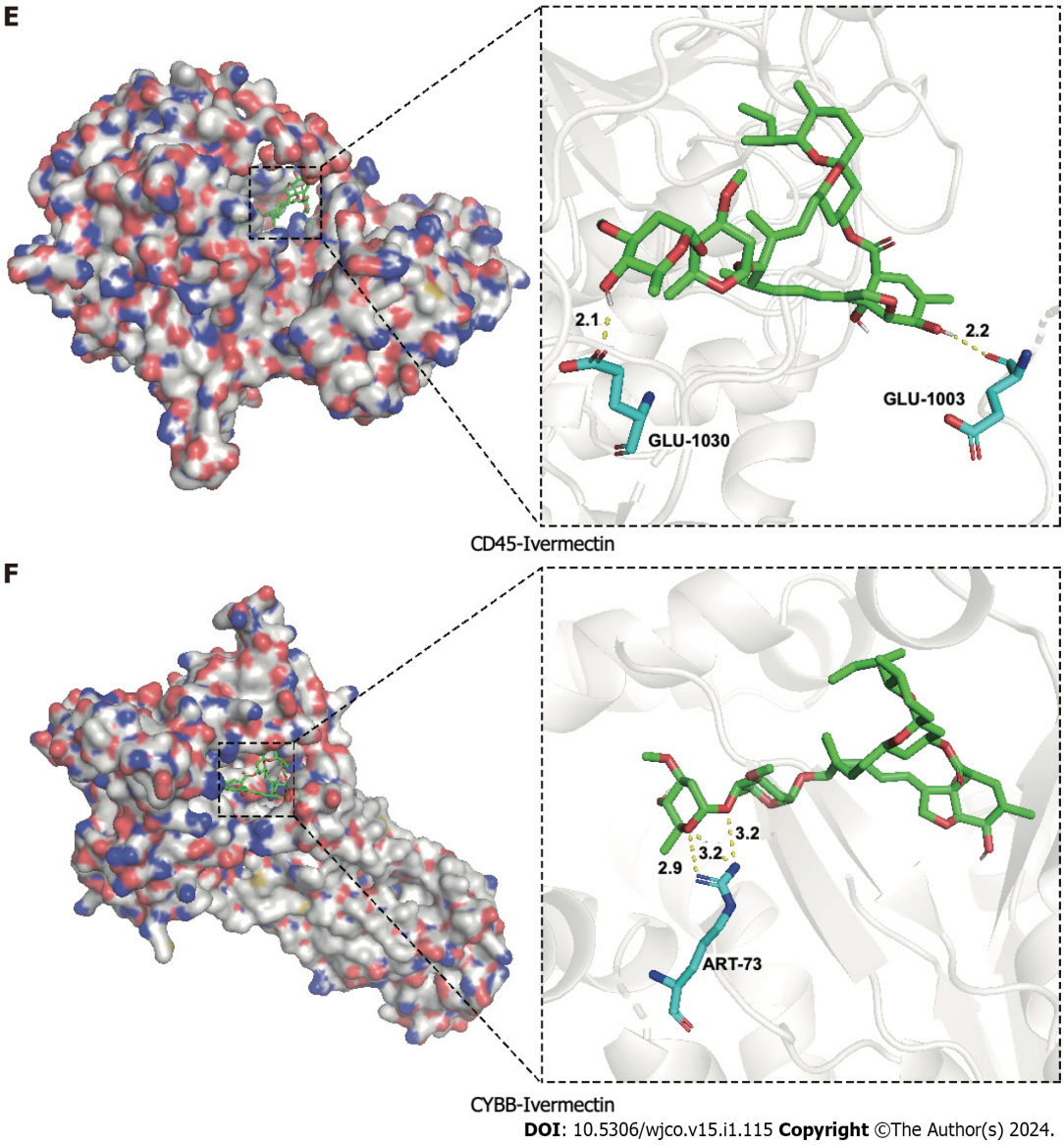

DOI: 10.5306/wjco.v15.i1.115 **Copyright** ©The Author(s) 2024.

Figure 2 Molecular docking analysis of ivermectin with hub target genes. A: Chemical structure of ivermectin; B: Binding affinity of ivermectin with the top 10 hub- target genes. A longer bar indicates a lower binding affinity; C: 2D interaction diagrams of ivermectin with CYBB; D: 2D interaction diagrams of ivermectin with CD45; E: 3D docking structures and interactions of ivermectin with CD45; F: 3D docking structures and interactions of ivermectin with CYBB.

Ivermectin induces apoptosis in t(4;14) MM cells

Drug-induced apoptosis is the primary mechanism underlying cancer cell death[18]. To assess this, we analyzed the expression of the pro- and anti-apoptotic proteins BAX and BCL2, respectively, after treatment and further inspected the BAX/BCL2 ratio. We observed that ivermectin induced apoptosis in t(4;14) MM cells, as evidenced by the upregulation of pro-apoptotic protein BAX and a decrease in anti-apoptotic protein BCL2 levels (Figure 3C). The BAX/BCL2 ratio significantly increased (Figure 3D), and the intrinsic mitochondrial apoptotic pathway was activated, as indicated by elevated caspase-9, caspase-3, downstream effector caspase-3, and PARP expression levels (Figure 3E and F). Annexin V-FITC/propidium iodide staining revealed a substantial increase in the proportion of apoptotic t(4;14) MM cells after ivermectin treatment compared with that of the control (Figure 3G and H), highlighting that the suppressive effect of ivermectin on t(4; 14) MM cells was associated with apoptosis.

Ivermectin increases ROS accumulation and alters the mitochondrial membrane potential in t(4;14) MM cells

Mitochondria are widely known to be the intracellular source of ROS. These species can trigger oxidative damage, leading to a series of mitochondria-related events, including apoptosis[19]. We detected a significant accumulation of ROS in t(4;14) MM cells treated with ivermectin compared with that in untreated controls (Figure 4A). We also observed a notable reduction in the mitochondrial membrane potential (Figure 4B and C), suggesting that ivermectin-induced apoptosis in t(4;14) MM cells was related to mitochondrial function. Collectively, these findings suggest a relationship between ivermectin-induced apoptosis in t(4;14) MM cells and altered mitochondrial dynamics.

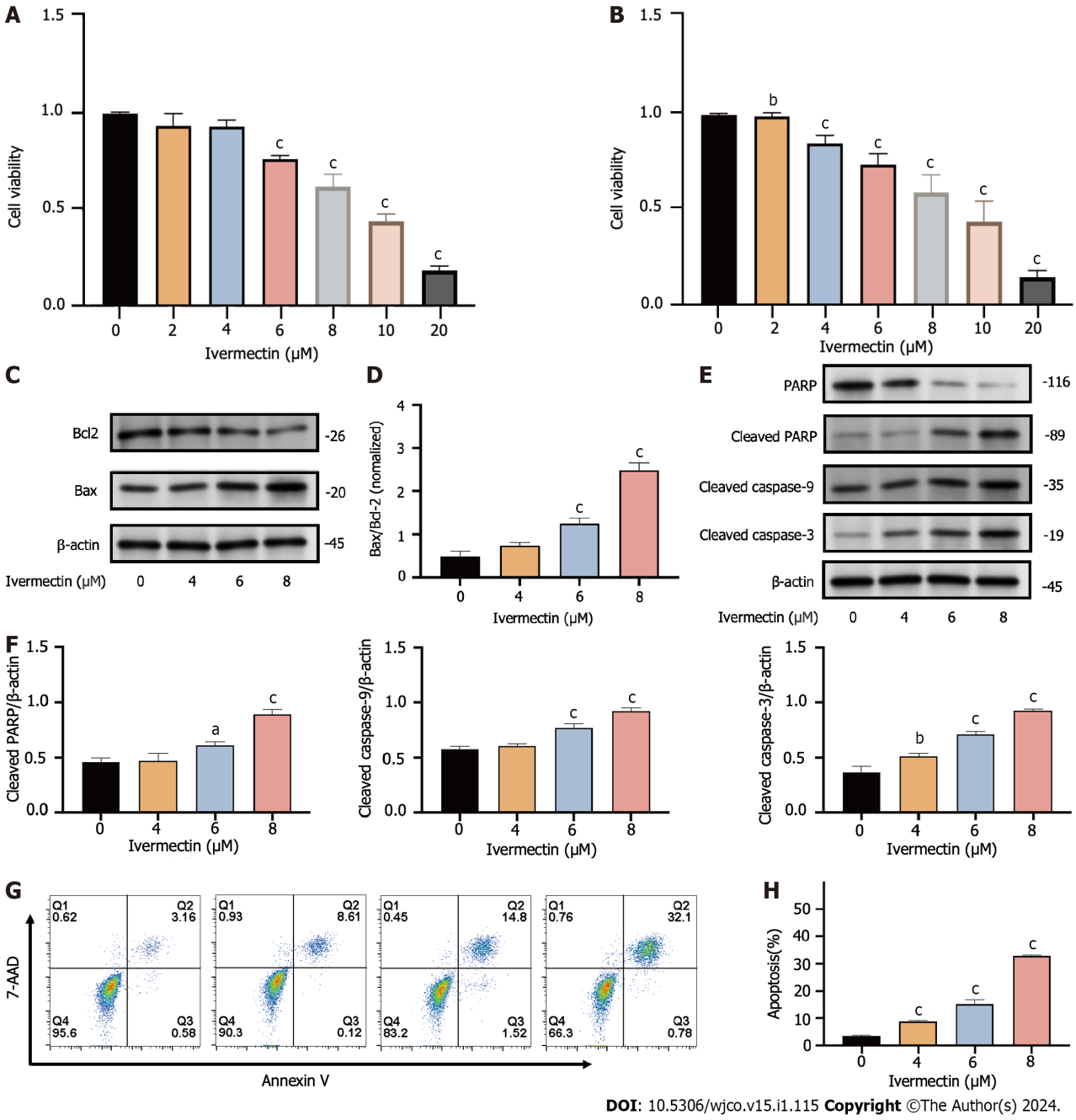

DOI: 10.5306/wjco.v15.i1.115

Figure 3 Ivermectin inhibits proliferation and promotes apoptosis in t(4; 14) multiple myeloma cells. A: CCK-8 analysis of cell viability in cells treated with ivermectin for 24 h; B: CCK-8 analysis of cell viability in cells treated with ivermectin for 48 h; C: Western blot analysis revealing Bax and Bcl-2 protein expression levels in cells treated with ivermectin; D: The relative Bax protein expression levels to Bcl-2 protein expression levels are presented as the means ± SD of three independent experiments; E: Western blot analysis displaying protein expression levels of caspase cascade (including cleaved-caspase 9, cleaved-caspase 3, PARP, and cleaved PARP); F: The data are shown as the means ± SD of three independent experiments. G: Apoptosis in t(4;14) multiple myeloma cells post-ivermectin treatment using 7-AAD/Annexin-V flow cytometry assay. H: The data are shown as the means ± SD of three independent experiments. $^{a}P < 0.05$, $^{b}P < 0.01$, and $^{c}P < 0.001$ compared with the control group.

Ivermectin triggers apoptosis in t(4;14) MM cells via NF-κB signaling pathway

The NF-κB signaling pathway plays a crucial role in the onset and progression of the disease in t(4;14) MM, often exhibiting overactivation in these cells and promoting their survival[20]. Our results revealed that ivermectin treatment substantially reduced both the protein expression and phosphorylation levels of NF-κB p65 in a dose-dependent manner (Figure 4D and E). Furthermore, the protein expression and phosphorylation levels of IκBα, a regulator upstream of NF-κB, were also suppressed in t(4;14) MM cells post-ivermectin treatment.

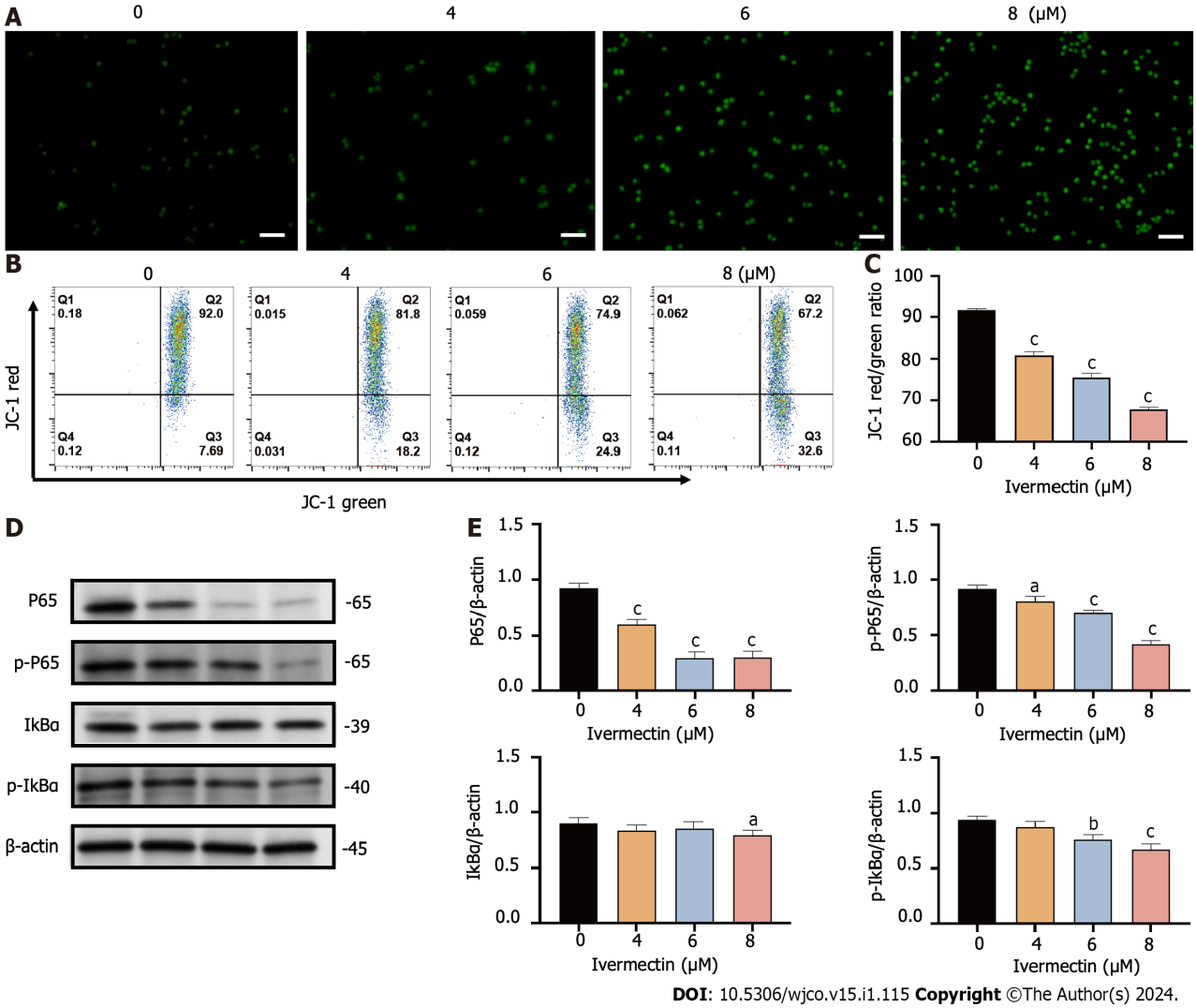

DOI: 10.5306/wjco.v15.i1.115

Figure 4 Ivermectin induces apoptosis in t(4;14) multiple myeloma cells *via* mitochondrial and nuclear factor-κB signaling pathway. A: Visualization of intracellular reactive oxygen species (ROS) in t(4;14) multiple myeloma (MM) cells after treatment with ivermectin using 2',7'-dichlorodihydrofluorescein (DCF) diacetate staining. ROS is represented by the green DCF fluorescence viewed under a fluorescence microscope at 200× magnification. Scale bar: 50 μm. B: Mitochondrial membrane potential in t(4;14) MM cells post-ivermectin treatment assessed using JC-1 staining; C: The data are shown as the means ± SD of three independent experiments; D: Expression patterns of p65, p-p65, p-IκBα, and IκBα in t(4;14) MM cells after exposure to ivermectin, analyzed by western blotting; E: The data are shown as the means ± SD of three independent experiments. $^{a}P < 0.05$, $^{b}P < 0.01$, and $^{c}P < 0.001$ compared with the control group.

DISCUSSION

MM is a multifaceted and incurable disease that displays vast heterogeneity in its clinical manifestations, genetic changes, therapeutic responses, and overall prognosis[2]. Guidelines from bodies, such as the International Myeloma Working Group, recognize t(4;14) MM as a high-risk cytogenetic abnormality[21]. The t(4;14) MM subtype continues to present a challenging prognosis despite advances in drug therapies[22]. Therefore, there is an urgent need to develop new therapeutic drugs to treat t(4;14) MM. Recent studies have highlighted the potential of identifying molecular targets and therapeutic drugs for MM through expression profiling and functional enrichment analyses. Di Meo *et al*[23] identified ILT3 as an immunotherapeutic target for MM, whereas Mereu *et al*[24] revealed that UNC0642 increasedcarfilzomib sensitivity and counteracted drug resistance in MM cell lines. In this study, we identified the key genes and prospective therapeutic agents for t(4;14) MM using gene expression profile analysis.

The regulation of the immune response is fundamental for the development and progression of MM[25]. We identified CD45, CD48, and CD56 as the key genes in t(4;14) MM. Compared with healthy bone marrow controls, patients with t(4;14) MM exhibited decreased CD45 expression levels, whereas CD48 and CD56 levels were notably increased. CD45, also known as protein tyrosine phosphatase receptor type C, was previously called the common leukocyte antigen. This protein is essential for modulating antigen receptor signaling, which is crucial for lymphocyte development, survival, and function[26]. However, the role of CD45 in MM remains elusive. Evidence suggests thatCD45 expression decreases during MM progression[27]. As mature MM cells are predominantly CD45-negative and have inactive SRC family kinases, they remain unaffected by elotuzumab[28]. Moreover, MM cells in high-risk genetic categories tend to express

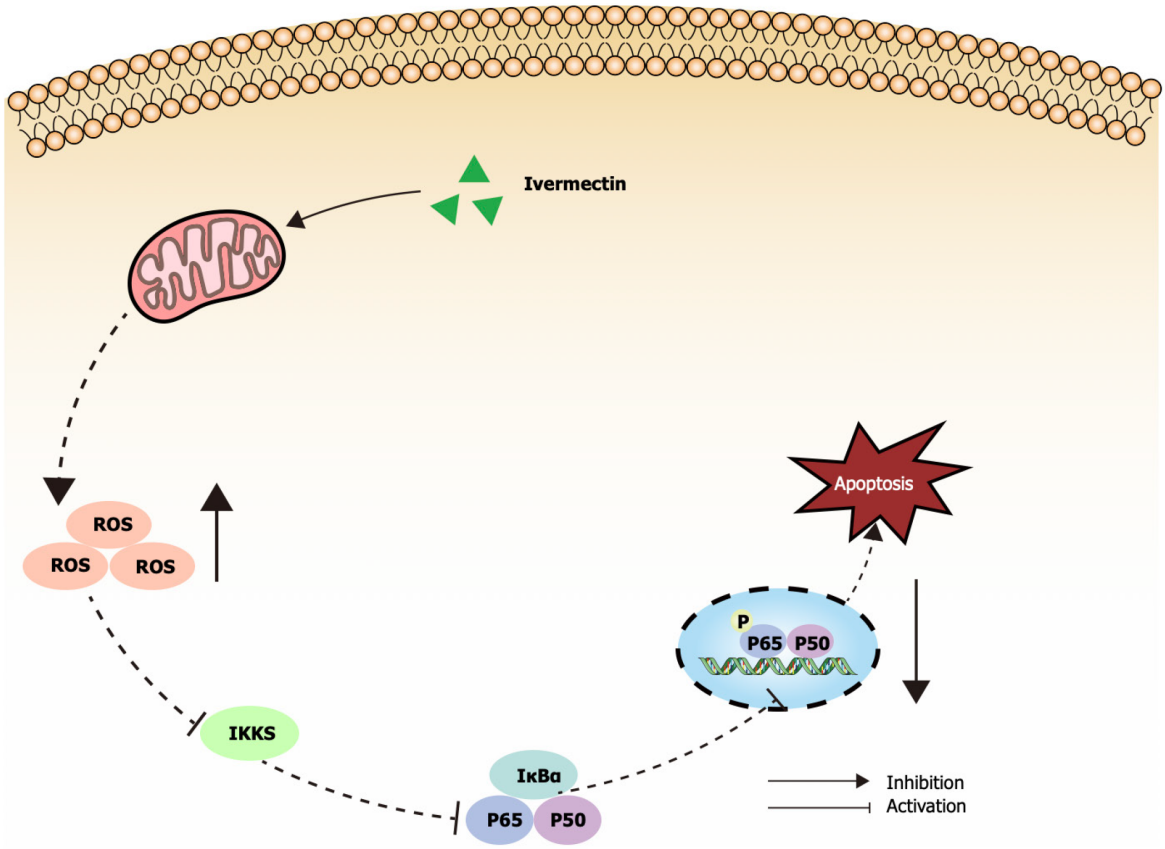

DOI: 10.5306/wjco.v15.i1.115 **Copyright** ©The Author(s) 2024.

Figure 5 Illustrated overview of ivermectin promoting apoptosis in t(4;14) multiple myeloma cells. IκBα: Anti-inhibitor of NF-κB; IKKs: Inhibitors of kappa B kinase; ROS: Reactive oxygen species.

reduced CD45 levels[29]. CD48[30], a member of the signaling lymphocytic activation molecule family, plays a role in immune cell adhesion and activation. Although it is present in almost all MM plasma cells, it is absent from non-hematopoietic tissues. Van Acker *et al*[31] identified CD48 as a promising molecular target for the therapy of MM antibody therapy. CD56, a neural cell adhesion molecule, is a glycoprotein present in neural and muscle tissues, as well as in myeloma cells. Cottini *et al*[32] observed its high expression levels in the t(4;14) MM cell line NCI-H929. CD56 boosts MM cell growth and influences adhesion to stromal cells. Collectively, these findings highlight the potential for a deeper evaluation of immune phenotypes for both diagnosis and treatment of t(4;14) MM.

In this study, we also utilized the CMap database to identify potential small-molecule drugs targeting t(4;14) MM. Our primary focus was on molecular docking and subsequent experimental validation of the predicted drug, ivermectin. Traditionally, ivermectin is a macrocyclic lactone antibiotic used to treat parasitic diseases[33]. Recent studies have revealed its potential antitumor capabilities in various cancers, including breast[34] and pancreatic[35] cancer. Emerging evidence also suggests its synergistic lethal effects on MM cells when combined with proteasome inhibitors[36]. However, a comprehensive understanding of the specific action mechanisms of ivermectin against MM, especially the t(4;14) subtype, remains elusive. Our findings demonstrate that ivermectin suppresses the growth of t(4;14) MM cells, as well as triggers apoptosis.

The NF-κB signaling pathway is crucial for driving cancer progression, angiogenesis, and shaping the tumor microenvironment[37]. It orchestrates the production of pro-inflammatory cytokines, inflammatory mediators, and cell adhesion molecules, creating a favorable microenvironment for MM initiation and progression[38]. Consequently, many leading anti-MM drugs indirectly target the NF-κB signaling pathway[39]. Bortezomib hinders the proteasomal degradation of NF-κB and IκB proteins, inhibiting gene transcription activation[40]. Our findings revealed a pronounced suppression of the NF-κB signaling pathway in ivermectin-treated t(4;14) MM cells (Figure 5). This suggests that ivermectin, by acting as an external signaling agent, inhibits the activation of this pathway, reducing anti-apoptotic effects and thereby enhancing cell apoptosis.

Mitochondria are essential for cell survival, functioning as the primary source of ROS and producing adenosine triphosphate (ATP) through oxidative phosphorylation[41]. In a pathological state, mitochondrial dysfunction results inATP depletion[42]. In the current study, treatment of t(4;14) MM with ivermectin led to elevated ROS levels and decreased cell membrane potential. These findings, along with previous reports, suggest that ivermectin exposure can induce oxidative stress and disrupt the mitochondrial balance, facilitating the apoptosis of t(4;14) MM cells.

There are also some limitations of the present study. Firstly, the sample size may be insufficient, potentially leading to selection bias. Secondly, regarding the experiments on ivermectin against t(4;14) MM, this study has only completed a portion of the *in vitro* experiments, and further validation of its effectiveness and safety is still required in *in vivo*

experiments. Furthermore, additional genetic and experimental studies are needed to elucidate the mechanisms and functions of these key genes in the occurrence and development of t(4;14) translocated multiple myeloma.

CONCLUSION

In conclusion, we utilized bioinformatics tools, molecular docking, and experimental validation to identify key genes and potential treatments for t(4;14) MM. Notably, we confirmed that ivermectin induced apoptosis in t(4;14) MM cells *via* the NF-κB signaling pathway. However, these insights require additional exploration and robust validation in further studies.

ARTICLE HIGHLIGHTS

Research background

Multiple myeloma (MM) is a terminally differentiated B-cell tumor disease with a challenging prognosis. Specifically, the t(4;14) MM is categorized as a high-risk subtype within MM.

Research motivation

The t(4;14) MM tends to relapse, and currently, there is a lack of effective clinical treatment strategies.

Research objectives

This study aimed to elucidate the molecular basis of the t(4;14) MM and search for potential effective drugs through a comprehensive approach.

Research methods

The transcriptional characteristics of t(4;14) multiple myeloma were obtained from the Gene Expression Omnibus and subjected to gene ontology and pathway enrichment analysis. Utilizing the STRING database and Cytoscape, a protein-protein interaction network was constructed, and core targets were identified. Connectivity Map identified potential small-molecule drugs, and these findings were validated through molecular docking analysis. One of these drugs, ivermectin, was further tested for its effects on t(4;14) multiple myeloma cells.

Research results

We identified 258 differentially expressed genes with enriched functions in cancer pathways, cytokine receptor interactions, the nuclear factor (NF)-kappa B signaling pathway. Ten key genes were pinpointed. Ivermectin emerged as a potential treatment. *In vitro*, ivermectin inhibited t(4;14) MM cell growth *via* the NF-kappa B pathway and induced t(4;14) MM cell apoptosis.

Research conclusions

Ivermectin induced apoptosis in t(4;14) MM cells *via* the NF-κB signaling pathway.

Research perspectives

Our study offers valuable molecular insights for biomarker validation and potential drug development in t(4;14) MM diagnosis and treatment.

FOOTNOTES

Author contributions: Song Y and Lu XC conceived and designed the experiments. Zhang HJ, Geng J, and Song Y conducted the experiments and drafted the manuscript; Zhong LZ and Song X contributed to the techniques used and commented on the manuscript; Li HY performed the data analysis; Yang B and Lu XC assisted with revising the manuscript; All the authors reviewed the results and approved the final version of the manuscript.

Supported by the National Key Research and Development Program of China, No. 2021YFC2701704; the National Clinical Medical Research Center for Geriatric Diseases, "Multicenter RCT" Research Project, No. NCRCG-PLAGH-20230010; and the Military Logistics Independent Research Project, No. 2022HQZZ06.

Institutional review board statement: This study does not involve research on humans/animals and does not include the initial version formally approved by the Institutional Review Board in the official language of the authors' country.

Informed consent statement: This study does not involve clinical research and does not include the initial version of the informed consent form signed by all subjects and investigators.

Conflict-of-interest statement: The authors declare that they have no known competing financial interests or personal relationships that could have appeared to influence the work reported in this paper.

Data sharing statement: No additional data are available.

Country/Territory of origin: China

ORCID number: Xue-Chun Lu 0000-0002-8937-2278.

S-Editor: Liu JH
L-Editor: A
P-Editor: Zhang XD

REFERENCES

1 **Siegel RL**, Miller KD, Wagle NS, Jemal A. Cancer statistics, 2023. *CA Cancer J Clin* 2023; **73**: 17-48 [PMID: 36633525 DOI: 10.3322/caac.21763]
2 **Cowan AJ**, Green DJ, Kwok M, Lee S, Coffey DG, Holmberg LA, Tuazon S, Gopal AK, Libby EN. Diagnosis and Management of Multiple Myeloma: A Review. *JAMA* 2022; **327**: 464-477 [PMID: 35103762 DOI: 10.1001/jama.2022.0003]
3 **Abdallah N**, Rajkumar SV, Greipp P, Kapoor P, Gertz MA, Dispenzieri A, Baughn LB, Lacy MQ, Hayman SR, Buadi FK, Dingli D, Go RS, Hwa YL, Fonder A, Hobbs M, Lin Y, Leung N, Kourelis T, Warsame R, Siddiqui M, Lust J, Kyle RA, Bergsagel L, Ketterling R, Kumar SK. Cytogenetic abnormalities in multiple myeloma: association with disease characteristics and treatment response. *Blood Cancer J* 2020; **10**: 82 [PMID: 32782240 DOI: 10.1038/s41408-020-00348-5]
4 **Foltz SM**, Gao Q, Yoon CJ, Sun H, Yao L, Li Y, Jayasinghe RG, Cao S, King J, Kohnen DR, Fiala MA, Ding L, Vij R. Evolution and structure of clinically relevant gene fusions in multiple myeloma. *Nat Commun* 2020; **11**: 2666 [PMID: 32471990 DOI: 10.1038/s41467-020-16434-y]
5 **Ashby C**, Boyle EM, Bauer MA, Mikulasova A, Wardell CP, Williams L, Siegel A, Blaney P, Braunstein M, Kaminetsky D, Keats J, Maura F, Landgren O, Walker BA, Davies FE, Morgan GJ. Structural variants shape the genomic landscape and clinical outcome of multiple myeloma. *Blood Cancer J* 2022; **12**: 85 [PMID: 35637217 DOI: 10.1038/s41408-022-00673-x]
6 **Zhang Z**, Zhou L, Xie N, Nice EC, Zhang T, Cui Y, Huang C. Overcoming cancer therapeutic bottleneck by drug repurposing. *Signal Transduct Target Ther* 2020; **5**: 113 [PMID: 32616710 DOI: 10.1038/s41392-020-00213-8]
7 **Hernández-Lemus E**, Martínez-García M. Pathway-Based Drug-Repurposing Schemes in Cancer: The Role of Translational Bioinformatics. *Front Oncol* 2020; **10**: 605680 [PMID: 33520715 DOI: 10.3389/fonc.2020.605680]
8 **Martin KH**, Slack JK, Boerner SA, Martin CC, Parsons JT. Integrin connections map: to infinity and beyond. *Science* 2002; **296**: 1652-1653 [PMID: 12040184 DOI: 10.1126/science.296.5573.1652]
9 **Shi X**, Zhang W, Bao X, Liu X, Yang M, Yin C. Eugenol modulates the NOD1-NF-κB signaling pathway *via* targeting NF-κB protein in triple-negative breast cancer cells. *Front Endocrinol (Lausanne)* 2023; **14**: 1136067 [PMID: 36923216 DOI: 10.3389/fendo.2023.1136067]
10 **Qiu HZ**, Huang J, Xiang CC, Li R, Zuo ED, Zhang Y, Shan L, Cheng X. Screening and Discovery of New Potential Biomarkers and Small Molecule Drugs for Cervical Cancer: A Bioinformatics Analysis. *Technol Cancer Res Treat* 2020; **19**: 1533033820980112 [PMID: 33302814 DOI: 10.1177/1533033820980112]
11 **Szklarczyk D**, Gable AL, Lyon D, Junge A, Wyder S, Huerta-Cepas J, Simonovic M, Doncheva NT, Morris JH, Bork P, Jensen LJ, Mering CV. STRING v11: protein-protein association networks with increased coverage, supporting functional discovery in genome-wide experimental datasets. *Nucleic Acids Res* 2019; **47**: D607-D613 [PMID: 30476243 DOI: 10.1093/nar/gky1131]
12 **Chin CH**, Chen SH, Wu HH, Ho CW, Ko MT, Lin CY. cytoHubba: identifying hub objects and sub-networks from complex interactome. *BMC Syst Biol* 2014; **8** Suppl 4: S11 [PMID: 25521941 DOI: 10.1186/1752-0509-8-S4-S11]
13 **Yang K**, Dinasarapu AR, Reis ES, Deangelis RA, Ricklin D, Subramaniam S, Lambris JD. CMAP: Complement Map Database. *Bioinformatics* 2013; **29**: 1832-1833 [PMID: 23661693 DOI: 10.1093/bioinformatics/btt269]
14 **UniProt Consortium**. UniProt: a hub for protein information. *Nucleic Acids Res* 2015; **43**: D204-D212 [PMID: 25348405 DOI: 10.1093/nar/gku989]
15 **Kim S**, Chen J, Cheng T, Gindulyte A, He J, He S, Li Q, Shoemaker BA, Thiessen PA, Yu B, Zaslavsky L, Zhang J, Bolton EE. PubChem 2019 update: improved access to chemical data. *Nucleic Acids Res* 2019; **47**: D1102-D1109 [PMID: 30371825 DOI: 10.1093/nar/gky1033]
16 **Laskowski RA**, Swindells MB. LigPlot+: multiple ligand-protein interaction diagrams for drug discovery. *J Chem Inf Model* 2011; **51**: 2778-2786 [PMID: 21919503 DOI: 10.1021/ci200227u]
17 **Delano WL**. Pymol: an open-source molecular graphics tool. *CCP4 Newsl Protein Crystallogr* 2002; **40**: 82-92 [DOI: 10.1101/2020.06.16.154773]
18 **Singh P**, Lim B. Targeting Apoptosis in Cancer. *Curr Oncol Rep* 2022; **24**: 273-284 [PMID: 35113355 DOI: 10.1007/s11912-022-01199-y]
19 **Nakamura H**, Takada K. Reactive oxygen species in cancer: Current findings and future directions. *Cancer Sci* 2021; **112**: 3945-3952 [PMID: 34286881 DOI: 10.1111/cas.15068]
20 **Yu H**, Lin L, Zhang Z, Zhang H, Hu H. Targeting NF-κB pathway for the therapy of diseases: mechanism and clinical study. *Signal Transduct Target Ther* 2020; **5**: 209 [PMID: 32958760 DOI: 10.1038/s41392-020-00312-6]

21 **Hagen P**, Zhang J, Barton K. High-risk disease in newly diagnosed multiple myeloma: beyond the R-ISS and IMWG definitions. *Blood Cancer J* 2022; **12**: 83 [PMID: 35637223 DOI: 10.1038/s41408-022-00679-5]

22 **Sonneveld P**, Avet-Loiseau H, Lonial S, Usmani S, Siegel D, Anderson KC, Chng WJ, Moreau P, Attal M, Kyle RA, Caers J, Hillengass J, San Miguel J, van de Donk NW, Einsele H, Bladé J, Durie BG, Goldschmidt H, Mateos MV, Palumbo A, Orlowski R. Treatment of multiple myeloma with high-risk cytogenetics: a consensus of the International Myeloma Working Group. *Blood* 2016; **127**: 2955-2962 [PMID: 27002115 DOI: 10.1182/blood-2016-01-631200]

23 **Di Meo F**, Iyer A, Akama K, Cheng R, Yu C, Cesarano A, Kurihara N, Tenshin H, Aljoufi A, Marino S, Soni RK, Roda J, Sissons J, Vu LP, Guzman M, Huang K, Laskowski T, Broxmeyer HE, Roodman DG, Perna F. A target discovery pipeline identified ILT3 as a target for immunotherapy of multiple myeloma. *Cell Rep Med* 2023; **4**: 101110 [PMID: 37467717 DOI: 10.1016/j.xcrm.2023.101110]

24 **Mereu E**, Abbo D, Paradzik T, Cumerlato M, Bandini C, Labrador M, Maccagno M, Ronchetti D, Manicardi V, Neri A, Piva R. Euchromatic Histone Lysine Methyltransferase 2 Inhibition Enhances Carfilzomib Sensitivity and Overcomes Drug Resistance in Multiple Myeloma Cell Lines. *Cancers (Basel)* 2023; **15** [PMID: 37190128 DOI: 10.3390/cancers15082199]

25 **Swamydas M**, Murphy EV, Ignatz-Hoover JJ, Malek E, Driscoll JJ. Deciphering mechanisms of immune escape to inform immunotherapeutic strategies in multiple myeloma. *J Hematol Oncol* 2022; **15**: 17 [PMID: 35172851 DOI: 10.1186/s13045-022-01234-2]

26 **Al Barashdi MA**, Ali A, McMullin MF, Mills K. Protein tyrosine phosphatase receptor type C (PTPRC or CD45). *J Clin Pathol* 2021; **74**: 548-552 [PMID: 34039664 DOI: 10.1136/jclinpath-2020-206927]

27 **Robillard N**, Pellat-Deceunynck C, Bataille R. Phenotypic characterization of the human myeloma cell growth fraction. *Blood* 2005; **105**: 4845-4848 [PMID: 15741217 DOI: 10.1182/blood-2004-12-4700]

28 **Guo H**, Cruz-Munoz ME, Wu N, Robbins M, Veillette A. Immune cell inhibition by SLAMF7 is mediated by a mechanism requiring src kinases, CD45, and SHIP-1 that is defective in multiple myeloma cells. *Mol Cell Biol* 2015; **35**: 41-51 [PMID: 25312647 DOI: 10.1128/MCB.01107-14]

29 **Radzevičius M**, Dirsė V, Klimienė I, Matuzevičienė R, Kučinskienė ZA, Pečeliūnas V. Multiple Myeloma Immunophenotype Related to Chromosomal Abnormalities Used in Risk Assessment. *Diagnostics (Basel)* 2022; **12** [PMID: 36140450 DOI: 10.3390/diagnostics12092049]

30 **McArdel SL**, Terhorst C, Sharpe AH. Roles of CD48 in regulating immunity and tolerance. *Clin Immunol* 2016; **164**: 10-20 [PMID: 26794910 DOI: 10.1016/j.clim.2016.01.008]

31 **Van Acker HH**, Capsomidis A, Smits EL, Van Tendeloo VF. CD56 in the Immune System: More Than a Marker for Cytotoxicity? *Front Immunol* 2017; **8**: 892 [PMID: 28791027 DOI: 10.3389/fimmu.2017.00892]

32 **Cottini F**, Rodriguez J, Hughes T, Sharma N, Guo L, Lozanski G, Liu B, Cocucci E, Yang Y, Benson D. Redefining CD56 as a Biomarker and Therapeutic Target in Multiple Myeloma. *Mol Cancer Res* 2022; **20**: 1083-1095 [PMID: 35380709 DOI: 10.1158/1541-7786.MCR-21-0828]

33 **Laing R**, Gillan V, Devaney E. Ivermectin - Old Drug, New Tricks? *Trends Parasitol* 2017; **33**: 463-472 [PMID: 28285851 DOI: 10.1016/j.pt.2017.02.004]

34 **Draganov D**, Han Z, Rana A, Bennett N, Irvine DJ, Lee PP. Ivermectin converts cold tumors hot and synergizes with immune checkpoint blockade for treatment of breast cancer. *NPJ Breast Cancer* 2021; **7**: 22 [PMID: 33654071 DOI: 10.1038/s41523-021-00229-5]

35 **Lee DE**, Kang HW, Kim SY, Kim MJ, Jeong JW, Hong WC, Fang S, Kim HS, Lee YS, Kim HJ, Park JS. Ivermectin and gemcitabine combination treatment induces apoptosis of pancreatic cancer cells *via* mitochondrial dysfunction. *Front Pharmacol* 2022; **13**: 934746 [PMID: 36091811 DOI: 10.3389/fphar.2022.934746]

36 **Luo H**, Feng Y, Wang F, Lin Z, Huang J, Li Q, Wang X, Liu X, Zhai X, Gao Q, Li L, Zhang Y, Wen J, Zhang L, Niu T, Zheng Y. Combinations of ivermectin with proteasome inhibitors induce synergistic lethality in multiple myeloma. *Cancer Lett* 2023; **565**: 216218 [PMID: 37149018 DOI: 10.1016/j.canlet.2023.216218]

37 **Napetschnig J**, Wu H. Molecular basis of NF-κB signaling. *Annu Rev Biophys* 2013; **42**: 443-468 [PMID: 23495970 DOI: 10.1146/annurev-biophys-083012-130338]

38 **Wong AH**, Shin EM, Tergaonkar V, Chng WJ. Targeting NF-κB Signaling for Multiple Myeloma. *Cancers (Basel)* 2020; **12** [PMID: 32781681 DOI: 10.3390/cancers12082203]

39 **Vrábel D**, Pour L, Ševčíková S. The impact of NF-κB signaling on pathogenesis and current treatment strategies in multiple myeloma. *Blood Rev* 2019; **34**: 56-66 [PMID: 30501907 DOI: 10.1016/j.blre.2018.11.003]

40 **Paramore A**, Frantz S. Bortezomib. *Nat Rev Drug Discov* 2003; **2**: 611-612 [PMID: 12908468 DOI: 10.1038/nrd1159]

41 **Zhang B**, Pan C, Feng C, Yan C, Yu Y, Chen Z, Guo C, Wang X. Role of mitochondrial reactive oxygen species in homeostasis regulation. *Redox Rep* 2022; **27**: 45-52 [PMID: 35213291 DOI: 10.1080/13510002.2022.2046423]

42 **Ma Z**, Han H, Zhao Y. Mitochondrial dysfunction-targeted nanosystems for precise tumor therapeutics. *Biomaterials* 2023; **293**: 121947 [PMID: 36512861 DOI: 10.1016/j.biomaterials.2022.121947]

World Journal of Clinical Oncology

Submit a Manuscript: https://www.f6publishing.com

World J Clin Oncol 2024 January 24; 15(1): 130-144

DOI: 10.5306/wjco.v15.i1.130

ISSN 2218-4333 (online)

ORIGINAL ARTICLE

Basic Study

Fatty acid binding protein 5 is a novel therapeutic target for hepatocellular carcinoma

Yan Li, William Lee, Zhen-Gang Zhao, Yi Liu, Hao Cui, Hao-Yu Wang

Specialty type: Gastroenterology and hepatology

Provenance and peer review: Unsolicited article; Externally peer reviewed.

Peer-review model: Single blind

Peer-review report's scientific quality classification

Grade A (Excellent): 0
Grade B (Very good): 0
Grade C (Good): C
Grade D (Fair): 0
Grade E (Poor): 0

P-Reviewer: Banerjee S, India

Received: August 30, 2023
Peer-review started: August 30, 2023
First decision: November 20, 2023
Revised: December 2, 2023
Accepted: December 25, 2023
Article in press: December 25, 2023
Published online: January 24, 2024

Yan Li, Zhen-Gang Zhao, Yi Liu, Hao Cui, Hao-Yu Wang, Department of Gastroenterology, Tianjin Third Central Hospital, Tianjin 300170, China

William Lee, Biomedical Engineering, Texas A&M University, College Station, TX 77843, United States

Corresponding author: Yan Li and William Lee, MD, Chief Physician, Department of Gastroenterology, Tianjin Third Central Hospital, No. 83 Jintang Road, Hedong District, Tianjin 300170, China.
li13821177880@126.com

Abstract

BACKGROUND

Hepatocellular carcinoma (HCC) is an aggressive subtype of liver cancer and is one of the most common cancers with high mortality worldwide. Reprogrammed lipid metabolism plays crucial roles in HCC cancer cell survival, growth, and evolution. Emerging evidence suggests the importance of fatty acid binding proteins (FABPs) in contribution to cancer progression and metastasis; however, how these FABPs are dysregulated in cancer cells, especially in HCC, and the roles of FABPs in cancer progression have not been well defined.

AIM

To understand the genetic alterations and expression of FABPs and their associated cancer hallmarks and oncogenes in contributing to cancer malignancies.

METHODS

We used The Cancer Genome Atlas datasets of pan cancer and liver hepatocellular carcinoma (LIHC) as well as patient cohorts with other cancer types in this study. We investigated genetic alterations of FABPs in various cancer types. mRNA expression was used to determine if FABPs are abnormally expressed in tumor tissues compared to non-tumor controls and to investigate whether their expression correlates with patient clinical outcome, enriched cancer hallmarks and oncogenes previously reported for patients with HCC. We determined the protein levels of FABP5 and its correlated genes in two HCC cell lines and assessed the potential of FABP5 inhibition in treating HCC cells.

RESULTS

We discovered that a gene cluster including five FABP family members (*FABP4, FABP5, FABP8, FABP9* and *FABP12*) is frequently co-amplified in cancer. Amplification, in fact, is the most common genetic alteration for FABPs, leading to overexpression of FABPs. *FABP5* showed the greatest differential mRNA expression comparing tumor with non-tumor tissues. High *FABP5* expression correlates well with worse patient outcomes ($P < 0.05$). *FABP5* expression highly correlates with enrichment of G2M checkpoint ($r = 0.33$, $P = 1.1e-10$), TP53 signaling pathway ($r = 0.22$, $P = 1.7e-5$) and many genes in the gene sets such as *CDK1* ($r = 0.56$, $P = 0$), *CDK4* ($r = 0.49$, $P = 0$), and *TP53* ($r = 0.22$, $P = 1.6e-5$). Furthermore, *FABP5* also correlates well with two co-expressed oncogenes *PLK1* and *BIRC5* in pan cancer especially in LIHC patients ($r = 0.58$, $P = 0$; $r = 0.58$, $P = 0$; respectively). FABP5^{high} Huh7 cells also expressed higher protein levels of p53, BIRC5, CDK1, CDK2, and CDK4 than FABP5^{low} HepG2 cells. FABP5 inhibition more potently inhibited the tumor cell growth in Huh7 cells than in HepG2 cells.

CONCLUSION

We discovered that *FABP5* gene is frequently amplified in cancer, especially in HCC, leading to its significant elevated expression in HCC. Its high expression correlates well with worse patient outcome, enriched cancer hallmarks and oncogenes in HCC. FABP5 inhibition impaired the cell viability of FABP5^{high} Huh7 cells. All these support that FABP5 is a novel therapeutic target for treating FABP5^{high} HCC.

Key Words: Hepatocellular carcinoma; Fatty acid binding protein; Novel target; Amplification; Correlated expression

Core Tip: Several recent studies reported that fatty acid binding proteins (FABPs) contribute to reprogrammed lipid metabolism and cancer progression; however, how these FABPs are dysregulated in cancer, especially in hepatocellular carcinoma (HCC), has not been carefully addressed. We discovered that a *FABP* gene cluster including *FABP5* are frequently amplified in cancer. *FABP5* is significantly upregulated in HCC and its high expression correlates well with worse patient outcomes, enrichment of top enriched cancer hallmarks involved in cell cycle progression, and two oncogenes *PLK1* and *BIRC5* in HCC. FABP5 inhibition impaired the cell viability of FABP5^{high} HCC cells. Our data supported that FABP5 is a novel therapeutic target for treating HCC.

Citation: Li Y, Lee W, Zhao ZG, Liu Y, Cui H, Wang HY. Fatty acid binding protein 5 is a novel therapeutic target for hepatocellular carcinoma. *World J Clin Oncol* 2024; 15(1): 130-144
URL: https://www.wjgnet.com/2218-4333/full/v15/i1/130.htm
DOI: https://dx.doi.org/10.5306/wjco.v15.i1.130

INTRODUCTION

Cancer cells are heavily dependent on cellular metabolism pathways for their disease malignancy and progression. Lipid metabolism has been increasingly recognized to be reprogrammed and plays crucial roles in cancer cell survival, growth, and evolution[1].

There is emerging evidence suggesting the critical roles of fatty acid binding proteins (FABPs) in contribution to cancer progression and metastasis[2,3]. FABPs are a family of chaperone proteins that bind to long-chain fatty acids, retinoids, and other hydrophobic molecules[3]. There are ten FABP genes identified in the human genome, each with restricted tissue distribution in healthy individuals. Some of the family members including *FABP4*, *FABP5*, and *FABP7* are abnormally expressed in cancer cells beyond tissue expression restriction and play important roles in cancer malignancy and progression[2,3]. *FABP4* is normally expressed in adipocytes at high levels and its expression is controlled by peroxisome proliferator-activated receptor gamma (PPARγ)[4]. Accumulating evidence shows that FABP4 plays important roles in cancer progression in multiple cancer types, including breast cancer[5], ovarian cancer[6], and colon cancer[7]. In contrast, loss of *FABP1* expression in colorectal cancer is associated with poor patient outcome[8]. *FABP5* is normally expressed in cells of epidermal origin and emerging evidence shows that it functions to regulate fatty acid trafficking, lipid metabolism and cell growth[9]. *FABP5* was found to be upregulated in many cancer types[10]. However, the mechanism leading to abnormal FABP expression in cancer is not clear and the roles of these FABPs in contributing to cancer progression have not been well defined. In this study, we aimed to investigate the genetic alterations leading to abnormal expression of FABPs in cancer and the missing links of abnormal FABP expression to cancer gene signatures and patient survival.

MATERIALS AND METHODS

Cells and reagents

Hepatocellular carcinoma (HCC) cell lines HepG2 and Huh7 were obtained from our laboratory for long-term storage and cultured in high glucose Dulbecco's modified Eagle medium containing 10% fetal bovine serum and 1% penicillin/streptomycin. SBFI-26 (S9957) was purchased from Selleck Chemicals (Houston, TX, United States). The antibodies against FABP5 (39926), p53 (9282), BIRC5 (2808), CDK1 (77055), CDK2 (2546), CDK4 (12790), MCL-1 (94296) and GAPDH (2118) were purchased from Cell Signaling Technology (Danvers, MA, United States). A CellTiter-Glo 2.0 cell viability assay kit (G9241) was purchased from Promega (Madison, WI, United States).

Collection of datasets and bioinformation analysis platforms

We performed data analysis for The Cancer Genome Atlas (TCGA) pan-cancer and liver hepatocellular carcinoma (LIHC) patient cohort through cBioPortal (https://www.cbioportal.org/) and a well-established web bioinformatic platform Gene Expression Profiling Interactive Analysis 2 (GEPIA2, http://gepia2.cancer-pku.cn/#index), developed by Zhang Lab, Peking University[11]. GEPIA2 collected RNA sequencing data of 9,736 tumors and 8,587 non-tumor samples from the TCGA and the Genotype-Tissue Expression projects.

Identification of genetic alterations of FABP family members

To find out the genetic alterations of FABPs (*FABP1*, *FABP2*, *FABP3*, *FABP4*, *FABP5*, *FABP6*, *FABP7*, *PMP2*, *FABP9* and *FABP12*) in cancer cells, we used cBioPortal tools. We checked the frequencies of each genetic alteration using TCGA pan-cancer (70655 samples from 217 non-redundant studies) and LIHC cohort (1829 samples from eleven studies) and their correlation with *FABP5* mRNA expression and HCC cancer stages.

Expression of FABP5 in tumor and non-tumor cells and its correlation with patient survival

We compared mRNA expression of FABPs in tumor *vs* non-tumor tissues using TCGA pan-cancer (9664 tumor tissue samples and 711 non-tumor tissue samples) and LIHC cohort (360 tumor tissue samples and 50 non-tumor tissue samples) and checked if high expression correlates with poor patient outcomes using the GEAIP2 platform.

Correlation of FABP5 expression with cancer hallmarks and oncogenes in HCC cells

We assessed correlation of *FABP5* expression with cancer hallmarks enriched in HCC cells (G2M checkpoint and TP53 signaling) and highlighted genes within the gene sets using the GEAIP2 platform.

Cell viability assay

The cell viability assay was performed as described in our earlier study[12]. Briefly, 2000 HepG2 or Huh7 cells per well were pre-seeded into white 96-well plates overnight. The cells were then treated with a 2-fold serial dilution of SBFI-26 (0-100 μmol/L). The cell viability was measured using a VICTOR Nivo Multimode Microplate Reader (PerkinElmer Health Sciences Inc, Shelton, CT, United States) at 72 h post treatment by using CellTiter-Glo 2.0 Reagent.

Statistical and computational analysis

We performed Pearson's or Spearman's correlation test to determine whether there was a significant link between the two variables. The log-rank test was used to determine the statistical significance of gene expression in correlation with patient outcome. $^{a}P < 0.05$; $^{b}P < 0.01$; $^{c}P < 0.001$; $^{d}P < 0.0001$.

RESULTS

FABP4, FABP5, FABP8, FABP9 and FABP12 are frequently co-amplified in cancer

We discovered that a cluster of FABP genes *FABP4, FABP5, FABP8, FABP9* and *FABP12* at the adjacent loci of chromosome 8, but not other FABPs located at different chromosomes, showed high frequencies of genetic alteration (3%) in the pan-cancer cohort (Figure 1A). The frequency of genetic alterations of these FABPs reaches 5%-6% in the LIHC cohort (Figure 1B). The prevalent type of alteration is amplification and co-occurrence of amplification of these genes *FABP4, FABP5, FABP8, FABP9* and *FABP12* is highly significant ($P < 0.001$) (Figure 1C). Other genetic alterations such as mutations, structural variants and homo-deletion also occur but at much lower frequencies (Figure 1A and B).

FABP5 and FABP4 amplifications occur at the highest frequencies in patients with prostate adenocarcinoma or HCC

Interestingly, when we checked genetic alterations of FABPs in different cancer types, we discovered that patients with prostate adenocarcinoma (PRAD) or HCC have the highest genetic alteration frequencies among others and again with genetic amplification as the prevalent type. *FABP4* showed the highest frequency in PRAD (7.9%) followed by HCC (7.8%) using TCGA pan cancer cohort, while *FABP5* showed the highest frequency in HCC (8.1%) followed by prostate PRAD (Figure 2A and C). Consistent with these, when we checked their genetic status in various liver cancer cohorts, we observed high *FABP4* alteration frequencies up to 12.5% and *FABP5* up to 12.2% in the aggressive subtype HCC (Figure 2B and D). Importantly, *FABP5* mRNA expression is much higher in the patients with *FABP5* amplification than those with *FABP5* gain, diploid, or deletion ($P < 0.0001$) (Figure 2E). Moreover, HCC cases at stage II-IV showed higher

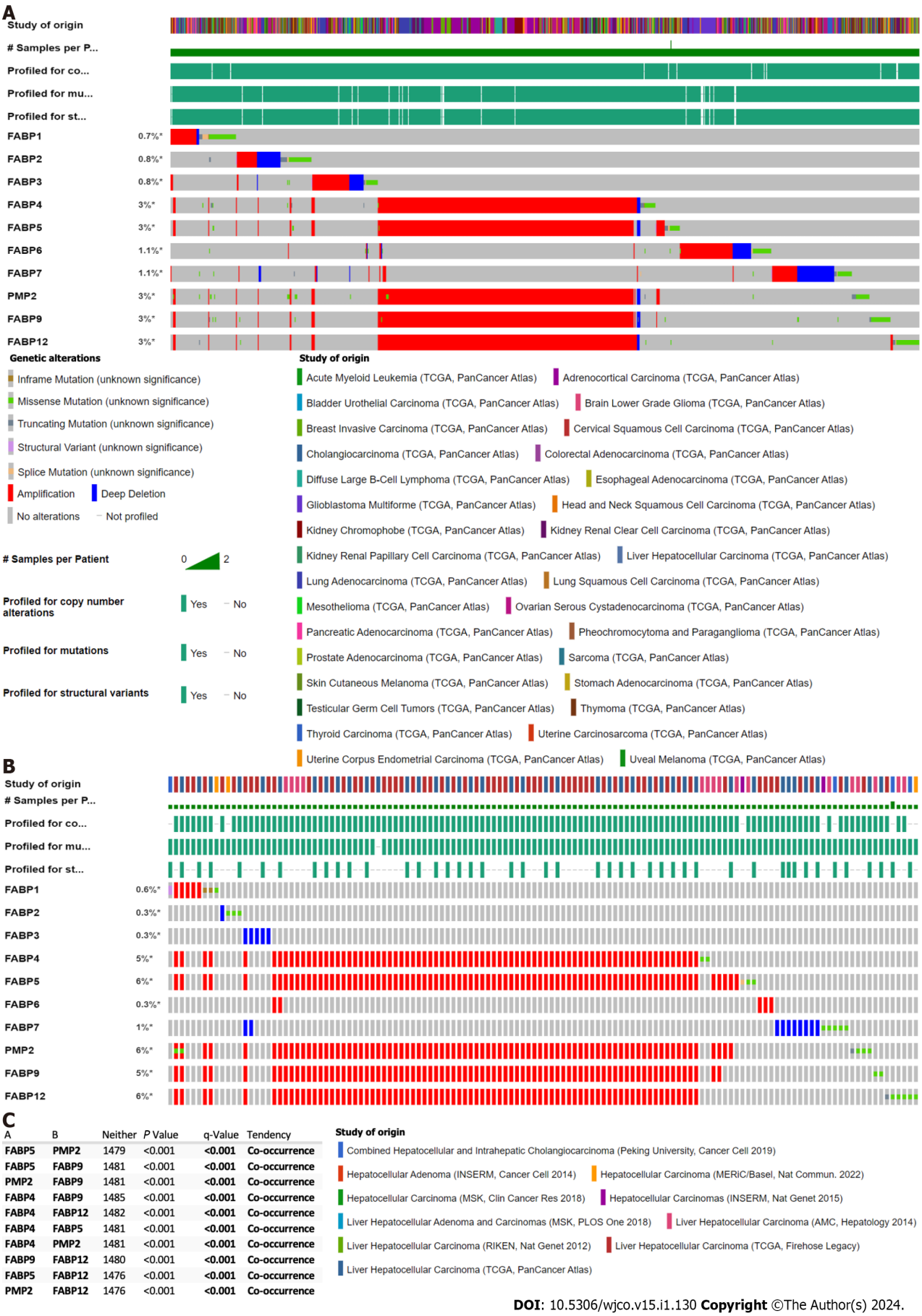

A	B	Neither	*P* Value	q-Value	Tendency
FABP5	**PMP2**	1479	<0.001	**<0.001**	**Co-occurrence**
FABP5	**FABP9**	1481	<0.001	**<0.001**	**Co-occurrence**
PMP2	**FABP9**	1481	<0.001	**<0.001**	**Co-occurrence**
FABP4	**FABP9**	1485	<0.001	**<0.001**	**Co-occurrence**
FABP4	**FABP12**	1482	<0.001	**<0.001**	**Co-occurrence**
FABP4	**FABP5**	1481	<0.001	**<0.001**	**Co-occurrence**
FABP4	**PMP2**	1481	<0.001	**<0.001**	**Co-occurrence**
FABP9	**FABP12**	1480	<0.001	**<0.001**	**Co-occurrence**
FABP5	**FABP12**	1476	<0.001	**<0.001**	**Co-occurrence**
PMP2	**FABP12**	1476	<0.001	**<0.001**	**Co-occurrence**

DOI: 10.5306/wjco.v15.i1.130

Figure 1 Genetic alternation of FABP family members in various cancer types. A-B: Genetic alternation of each FABP family member (*FABP1*, *FABP2*, *FABP3*, *FABP4*, *FABP5*, *FABP6*, *FABP7*, *PMP2*, *FABP9* and *FABP12*) in pan-cancer types (70655 samples from 217 non-redundant studies) (A) and in various liver

cancer subtypes (1829 samples from eleven studies) (B) using The Cancer Genome Atlas datasets. The mutation frequency for each FABP gene was shown next to the gene name; C: Co-occurrence of genetic alternation of the gene loci of FABP family members in liver cancer.

expression of *FABP5* (P = 0.071), but not *FABP4* (P = 0.179) (Figure 2F).

FABP5 and FABP4 are expressed at much higher levels in tumor tissues compared to non-tumor counterparts in HCC

To find out whether amplification and resulting high expression of FABP family members has clinical significance in cancer, we compared their expression in tumor tissues and non-tumor controls for various cancer types (Figure 3A). Among all family members, *FABP3*, *FABP4*, and *FABP5* are expressed ubiquitously across various cancer types (Figure 3A), while *FABP1*, *FABP6*, *FABP7*, and *FABP8* are expressed selectively in restricted cancer types. In contrast, *FABP2*, *FABP9*, and *FABP12* are expressed at extremely low levels, if any (Figure 3A). *FABP1*, *FABP3*, *FABP4*, and *FABP5*, but not other family members, are selectively expressed in LIHC patients (Figure 3A and Supplementary Figure 1A), while *FABP3*, *FABP4* and *FABP5* are also selectively expressed in PRAD patients (Figure 3A and Supplementary Figure 1A). When we checked the expression of FABPs in tumor tissues compared to non-tumor controls, we found that *FABP5* is significantly upregulated in adrenocortical carcinoma (ACC), glioblastoma multiforme (GBM), kidney renal clear cell carcinoma (KIRC), brain lower-grade glioma (LGG), liver hepatocellular carcinoma (LIHC), lung adenocarcinoma (LUAD), skin cutaneous melanoma (SKCM), and uveal melanoma (UVM), while *FABP4* is significantly upregulated only in colon adenocarcinoma (COAD), lung squamous cell carcinoma and stomach adenocarcinoma (Figure 3B). In patients with LIHC, among the selectively expressed FABPs, only *FABP5* and *FABP4* showed significant upregulation of mRNA expression in tumor tissues compared to non-tumor controls. Other FABPs, such as *FABP1* (restricted expression in normal liver), did not show differential expression in tumor and non-tumor tissues, even though it is expressed at prominent levels in patients with LIHC (Figure 3C and Supplementary Figure 1A-C). More importantly, high *FABP5* expression significantly correlates with overall patient survival (P = 6.6e-5) and disease-free survival (P = 6.6e-5) (Figure 3D-E). We found that high *FABP5* expression significantly correlates with overall survival not only in LIHC but also in other cancer types including ACC, GBM, KIRC, LGG, LUAD, SKCM, and UVM, where *FABP5* is found to be upregulated in tumor tissues compared to non-tumor control (Figure 3B and Supplementary Figure 1D). In contrast, high *FABP4* expression showed less significant correlation with poor overall survival (P = 0.047) (Figure 3E). In addition, expression of other FABPs (*FABP1* and *FABP3*) expressed in LIHC, does not significantly correlate with overall survival (P = 0.21 and 0.091, respectively) (Supplementary Figure 1E-G). Together, these data indicate that *FABP5*, among other FABPs, is selectively upregulated in tumor tissues and its expression correlates well with poor clinical outcomes in patients with HCC.

High FABP5 expression selectively associated with enrichment of cancer hallmarks G2M checkpoint and TP53 signaling

E2F targets, G2M checkpoint and DNA repair have been identified to be the top three cancer hallmarks enriched in HCC tumor cells compared to non-tumor controls[13], which supported that cell cycle and DNA repair signaling networks are critical for HCC cancer malignancies and progression. Therefore, we are interested in checking if *FABP5* overexpression correlates with enrichment of these important cancer hallmarks in HCC. We found that *FABP5* expression correlates well with G2M checkpoint gene signature (r = 0.33, P = 1.1e-10) (Figure 4A and B), and most of the genes in the dataset, including *ATR* (r = 0.35, P = 3.9e-12)[13], *BRCA1* (r = 0.23, P = 8.1e-6), *CCNB1* (r = 0.61, P = 0), *CDK1* (r = 0.56, P = 0), *CDKN2D* (r = 0.37, P = 121e-13), *CHEK1* (r = 0.46, P = 0), *CHEK2* (r = 0.17, P = 0.001), *PI4KA* (r = 0.29, P = 9.3e-9), *PRKDC* (r = 0.43, P = 1.4e-11), *RPS6K1* (r = 0.3, P = 3.6e-9), and *YWHAH* (r = 0.38, P = 5.7e-14) (Figure 4C). Among these, expressions of *CCNB1* and *CDK1* showed the highest correlation with *FABP5* expression (Figure 4C). The strong *CCNB1-FABP5* correlation is observed in LIHC but also in many other cell types including COAD (r = 0.43, P = 6.5e-14), DLBCL (r = 0.54, P = 6.5e-14), KICH (r = 0.8, P = 6.7e-16), KIRC (r = 0.46, P = 0), READ (r = 0.36, P = 0.00043), tenosynovial giant cell tumor (r = 0.43, P = 1.3e-7), and UVM (r = 0.75, P = 1.3e-15) (Supplementary Figure 2A and B).

In an independent analysis using cBioportal platform, we found that most genes involved in cell cycle network are dysregulated with *TP53* as the top gene (Figure 4D). Therefore, we checked if *FABP5* expression is associated with expression of *TP53* and p53 signaling gene signature. We found that *FABP5* expression correlates well with *TP53* expression (r = 0.22, P = 1.6e-5), its signaling gene signature (r = 0.33, P = 1.1e-10) (Figure 5A and B), and almost half of the genes in the dataset, including *BCL2* (r = 0.15, P = 0.0044), *CDK2* (r = 0.28, P = 6.6e-8), *CDK4* (r = 0.49, P = 0), *E2F1* (r = 0.15, P = 0029), *PCNA* (r = 0.31, P = 2.2e-9), and *RB1* (r = 0.21, P = 5.2e-5) (Figure 5C). In an independent analysis using cBioportal platform, we found that most genes involved in TP53 signaling network are dysregulated with *TP53* as the top gene (Figure 5D).

High FABP5 expression correlated well with PLK1 and BIRC5 expression

In our previous study, we demonstrated that that *PLK1*, a master regulator of cell cycle, and *BIRC5*, a multifunctional gene only expressed at G2M phase, are two important oncogenes that are highly co-expressed in HCC and the co-targeting of PLK1 and BIRC5 synergistically inhibited tumor growth of HCC preclinical models *in vitro* and *in vivo*[12]. To investigate the relationship between *FABP5* expression and *PLK1-BIRC5* co-expression in cancer, we first checked expression of selected FABPs together with *CCNB1*, *TP53*, *BIRC5* and *PLK1* (Figure 6A). Expression of *FABP5*, but not other FABPs including *FABP1, FABP3, FABP4* and *FABP6* appeared to be well-correlated with expression of *PLK1* and *BIRC5* across cancer types, in addition to *CCNB1* and *TP53* (Figure 6A). Consistent with our previous findings[12],

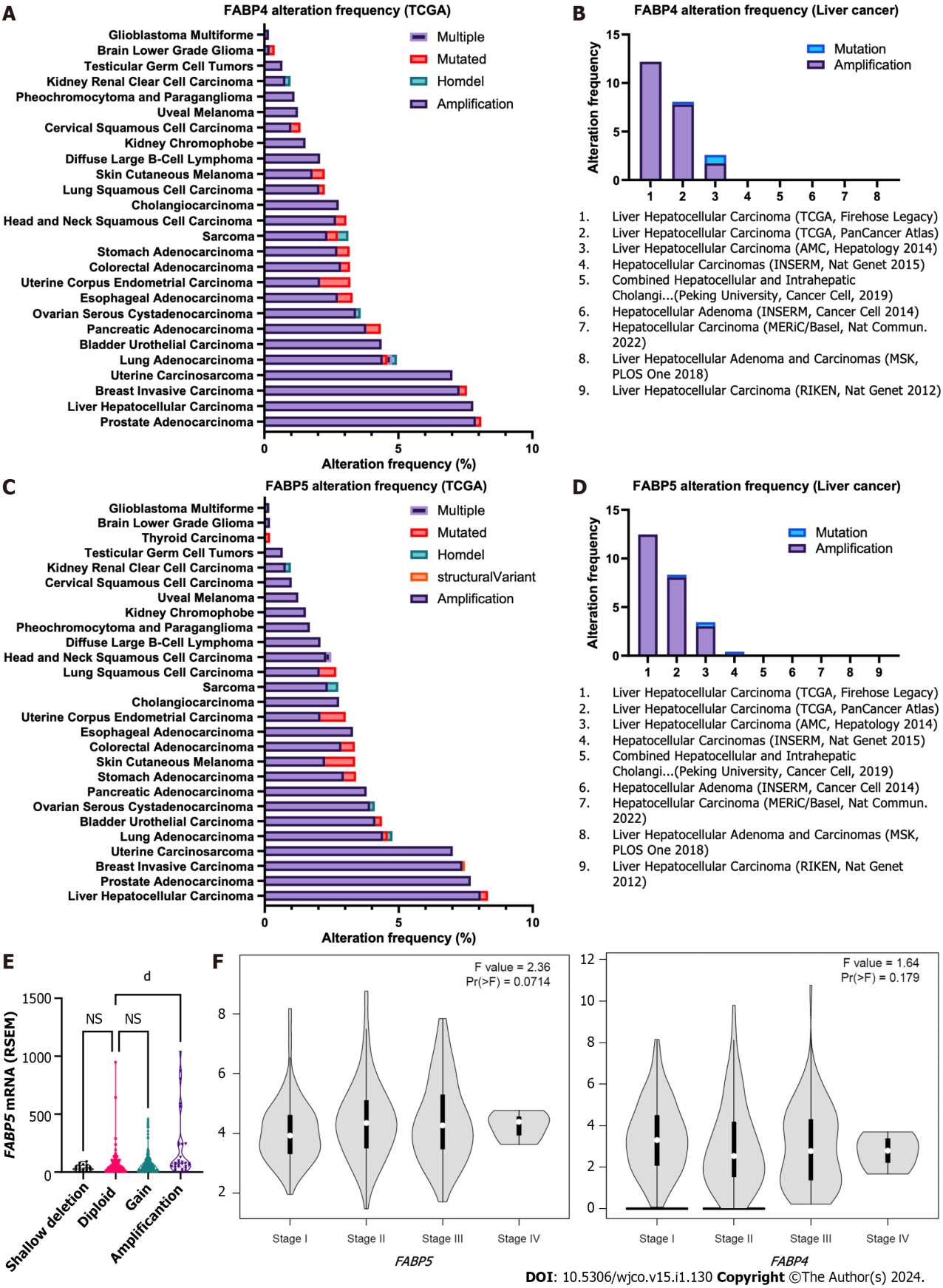

DOI: 10.5306/wjco.v15.i1.130

Figure 2 Frequencies of genetic alternations and expression of *FABP4* and *FABP5* in various cancer types. A-B: Frequencies of genetic alternations of *FABP4* in major cancer types using The Cancer Genome Atlas (TCGA) datasets *via* cBioportal (A) and in various liver cancer subtypes (B) using TCGA datasets *via* cBioportal; C-D: Frequencies of genetic alternations of *FABP5* in pan-cancer types (C) and in various liver cancer subtypes (D) using TCGA datasets *via* cBioportal; E: *FABP5* expression in liver cancer with different *FABP5* genetic alteration types using TCGA datasets *via* cBioportal; F: Expression of

FABP5 (left panel) and *FABP4* (right panel) in liver cancer at stage I-IV using TCGA datasets *via* GEPIA2 portal. [d]*P* < 0.0001; NS: Not significant.

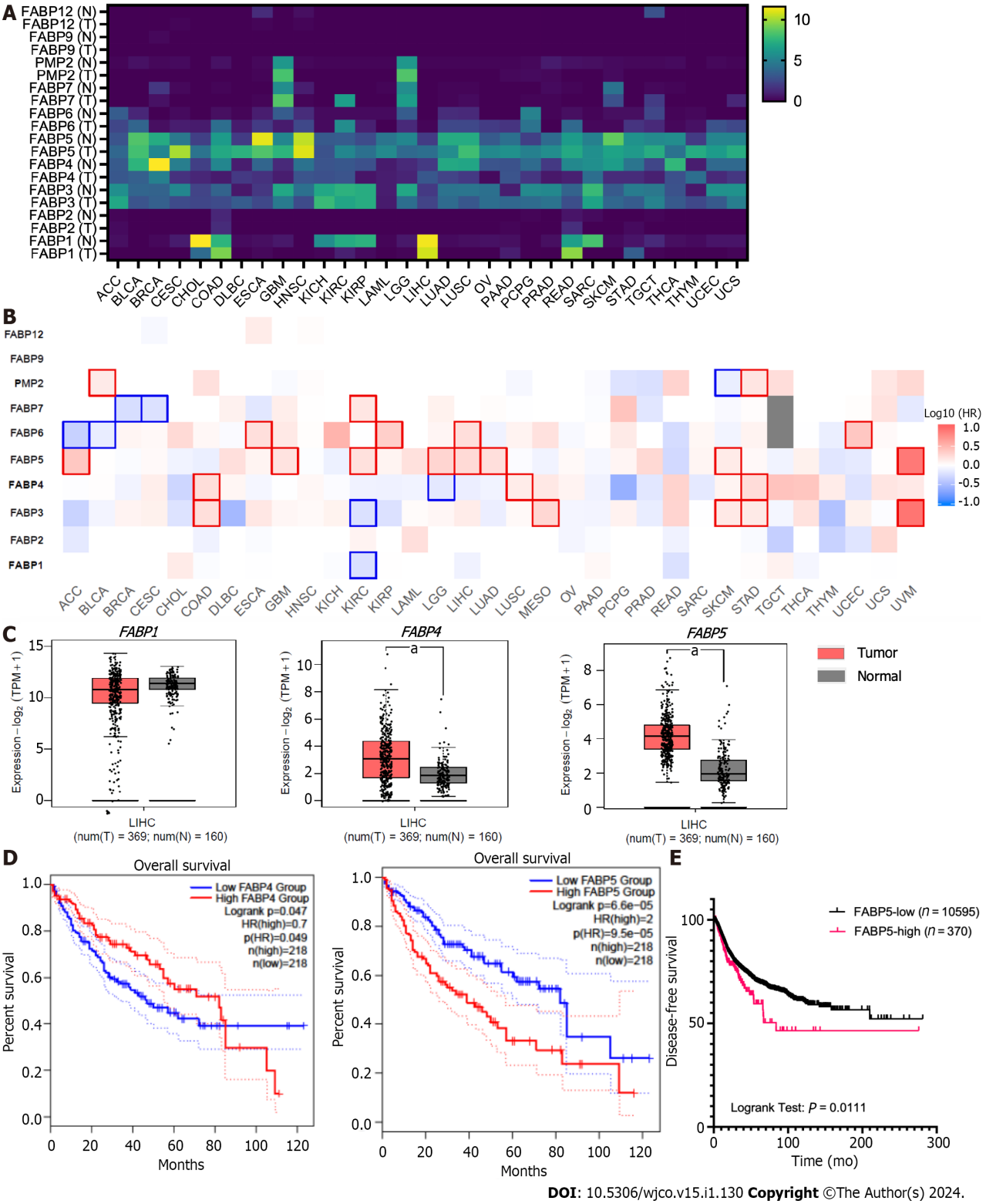

DOI: 10.5306/wjco.v15.i1.130

Figure 3 Expression of FABP family members in tumor tissues and non-tumor tissue control in various cancer types. A-B: Expression of each FABP family member (*FABP1*, *FABP2*, *FABP3*, *FABP4*, *FABP5*, *FABP6*, *FABP7*, *PMP2*, *FABP9* and *FABP12*) in tumor tissues and non-tumor tissue control in various cancer types (A) and statistical significance when comparing their expression in tumor tissues with non-tumor tissue control (B) using GEPIA2 portal; C: Higher expression of *FABP4* and *FABP5*, but not *FABP1*, was observed in liver tumor tissues comparing to non-tumor tissue control; D-E: High expression levels of *FABP5*, but not *FABP1* or *FABP4*, in liver cancer correlate with overall patient survival (D) and disease-free survival (E). [a]*P* < 0.05.

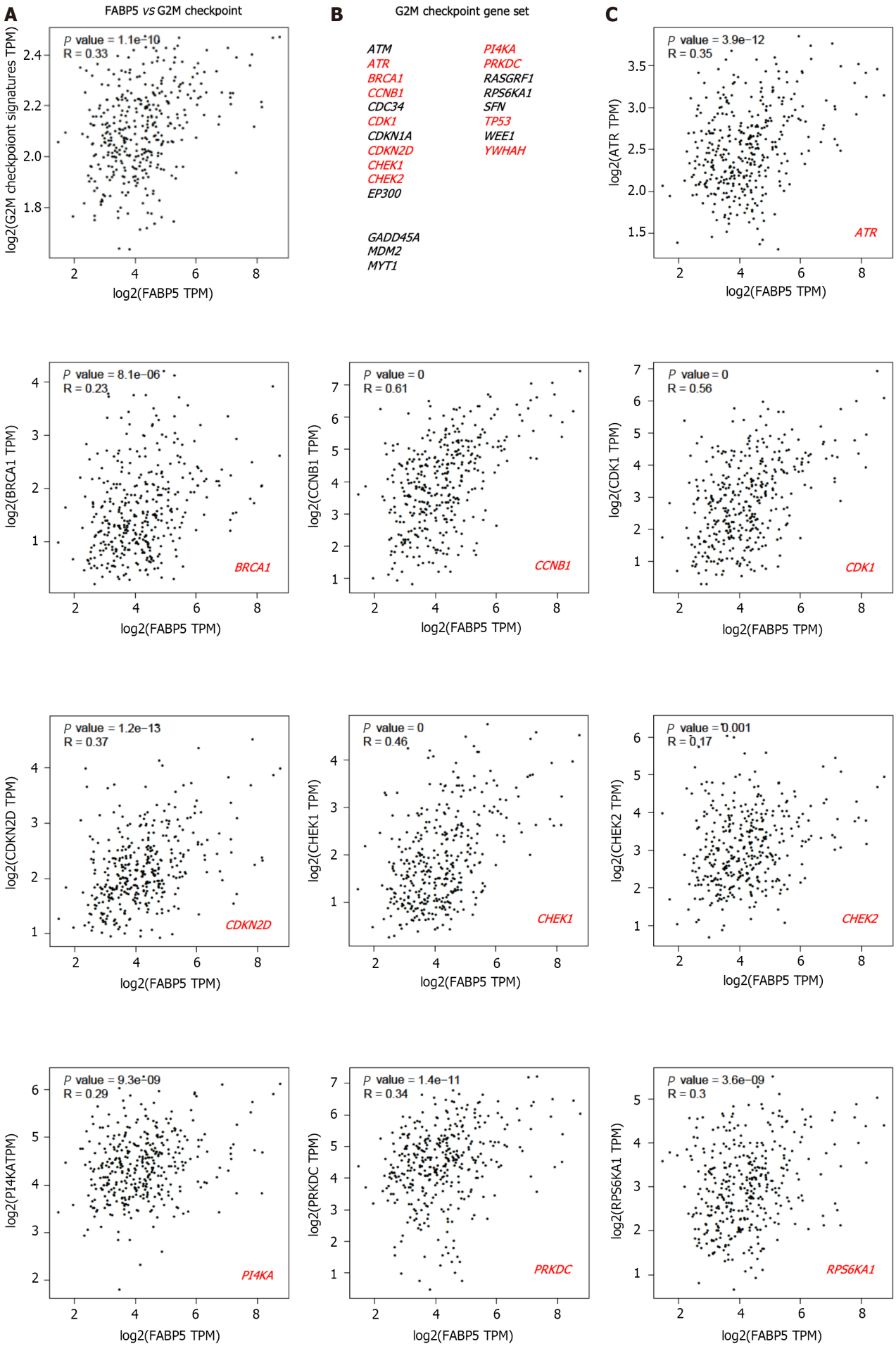
A
FABP5 *vs* G2M checkpoint
P value = 1.1e-10
R = 0.33
log2(G2M checkpoint signatures TPM)
log2(FABP5 TPM)
B
G2M checkpoint gene set
ATM
ATR
BRCA1
CCNB1
CDC34
CDK1
CDKN1A
CDKN2D
CHEK1
CHEK2
EP300
GADD45A
MDM2
MYT1
PI4KA
PRKDC
RASGRF1
RPS6KA1
SFN
TP53
WEE1
YWHAH
C
P value = 3.9e-12
R = 0.35
log2(ATR TPM)
ATR
P value = 8.1e-06
R = 0.23
log2(BRCA1 TPM)
BRCA1
P value = 0
R = 0.61
log2(CCNB1 TPM)
CCNB1
P value = 0
R = 0.56
log2(CDK1 TPM)
CDK1
P value = 1.2e-13
R = 0.37
log2(CDKN2D TPM)
CDKN2D
P value = 0
R = 0.46
log2(CHEK1 TPM)
CHEK1
P value = 0.001
R = 0.17
log2(CHEK2 TPM)
CHEK2
P value = 9.3e-09
R = 0.29
log2(PI4KATPM)
PI4KA
P value = 1.4e-11
R = 0.34
log2(PRKDC TPM)
PRKDC
P value = 3.6e-09
R = 0.3
log2(RPS6KA1 TPM)
RPS6KA1

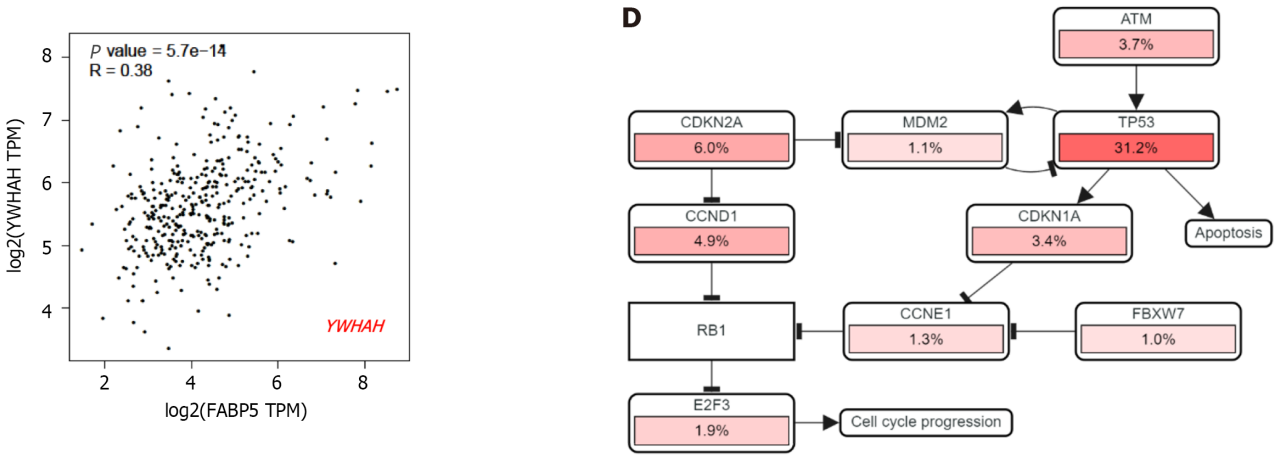

DOI: 10.5306/wjco.v15.i1.130

Figure 4 Expression of FABP5 correlates with cancer hallmark G2M checkpoint and genes within. A: *FABP5* positively correlated with enrichment of cancer hallmark G2M checkpoint in patients with liver hepatocellular carcinoma (LIHC); B: Gene list included in the cancer hallmark G2M checkpoint. The genes that showed positive correlation with *FABP5* are highlighted in red ($P < 0.01$); C: Highlighted genes in the G2M checkpoint gene set positively correlate with *FABP5* expression in patients with LIHC. *P* values show the statistical significance of the correlation; *R* values indicate the correlation coefficient; D: Altered expression of individual genes in the G2M checkpoint gene set showed in the context of signaling network. Pink bars show upregulation of gene expression.

expression of *PLK1* and *BIRC5* showed remarkable correlation in pan cancer ($r = 0.73$, $P = 0$) and even higher in LIHC ($r = 0.83$, $P = 0$) (Figure 6B and C). Expression of *FABP5* also showed some correlation with *PLK1* ($r = 0.19$, $P = 0$) or *BIRC5* ($r = 0.15$, $P = 0$) in cancer and much better correlation in LIHC patient cohort ($r = 0.58$, $P = 0$; $r = 0.58$, $P = 0$, respectively) (Figure 6D-G and Supplementary Figure 3A and B). These data demonstrate that *FABP5* is highly correlated to the expression of *PLK1-BIRC5* co-expression, which is selectively in patients with HCC.

HCC cells with high FABP5 expression are sensitive to FABP5 inhibition

The stabilizing *TP53* mutation Y220C in Huh7 cells resulted in overexpression of p53, which is much higher than that in HepG2 cells harboring wild type *TP53* gene. Interestingly, FABP5 protein expression is also expressed at a much higher level in Huh7 cells than HepG2 cells (Figure 7A). BIRC5, CDK1, CDK2, and CDK4, but not MCL-1, are also expressed at much higher levels in FABP5^{high} Huh7 cells than FABP5^{low} HepG2 cells (Figure 7A). Huh7 cells are more sensitive to FABP5 inhibition by SBFI-26, a specific inhibitor of FABP5, than in HepG2 cells (IC_{50} = 89 and 145 μmol/L) at 6 d upon treatment (Figure 7B and C). Long treatment for 6 d led to further inhibition of cell viability of Huh7 cells than shorter treatment for 3 d (IC_{50} = 89 and 749 μmol/L, respectively) (Figure 7D and E). This demonstrated that like many other compounds targeting regulators of cellular mechanism, the anti-tumor effect of FABP5 inhibitor SBFI-26 is a slow process, which requires time to show the anti-tumor effect. Together, these data indicate that HCC cells with high FABP5 expression are sensitive to FABP5 inhibition.

DISCUSSION

In this study, we discovered the *FABP5* gene is frequently amplified together with other adjacent family members *FABP4*, *FABP8*, *FABP9* and *FABP12* as a gene cluster. However, only *FABP5* and *FABP4* are highly expressed in HCC patients and are significantly upregulated in tumor cells compared to non-tumor controls. Compared to *FABP4*, *FABP5* is expressed at higher levels in cancer including LIHC and more differentially expressed in tumor cells compared to non-tumor controls. Consistent with our data, Ohata *et al*[14] performed immunohistochemical staining of FABP5 for 243 paired HCC and adjacent non-tumor liver tissue samples. The study confirmed that all normal liver cells were stained negatively, while liver tumor cells can be divided into two groups, FABP5 positive (57.2%) and FABP5 negative (42.8%). Therefore, this data supports that FABP5 is overexpressed in 57.2% of patients with liver tumors. Our data of FABP5 expression in HepG2 and Huh7 cells is consistent with published data in this study as well. This study showed a positive correlation of high FABP5 expression with distant metastasis and invasion. However, Huh7 and HepG2 are both considered to be low metastatic. Our data showed that high expression of *FABP5* mRNA correlated well with G2M checkpoint (P = 1.1e-10, r = 0.33) and TP53 signaling in liver cancer cells (P = 1.7e-5, r = 0.22) (Figures 4 and 5). We confirmed some of these gene expression differences involved in these two signaling networks including CDK1, CDK2, CDK4, and BIRC5 by western blotting in FABP5 low expressing HepG2 cells and FABP5-high expressing Huh7 cells (Figure 7A). The hotspot mutation Y220C of *TP53* gene results in its decreased DNA binding and reduced p53 tumor suppressor function, leading to cancer progression[15-17]. This may explain that Huh7 cells carrying TP53 Y220C mutation grow much faster than hepG2 cells with wild type TP53 (cell doubling time, 24 and 48 h, respectively). Therefore, it is possible that the TP53 genetic status affects the cell proliferation and expression of FABP5, which requires further validation.

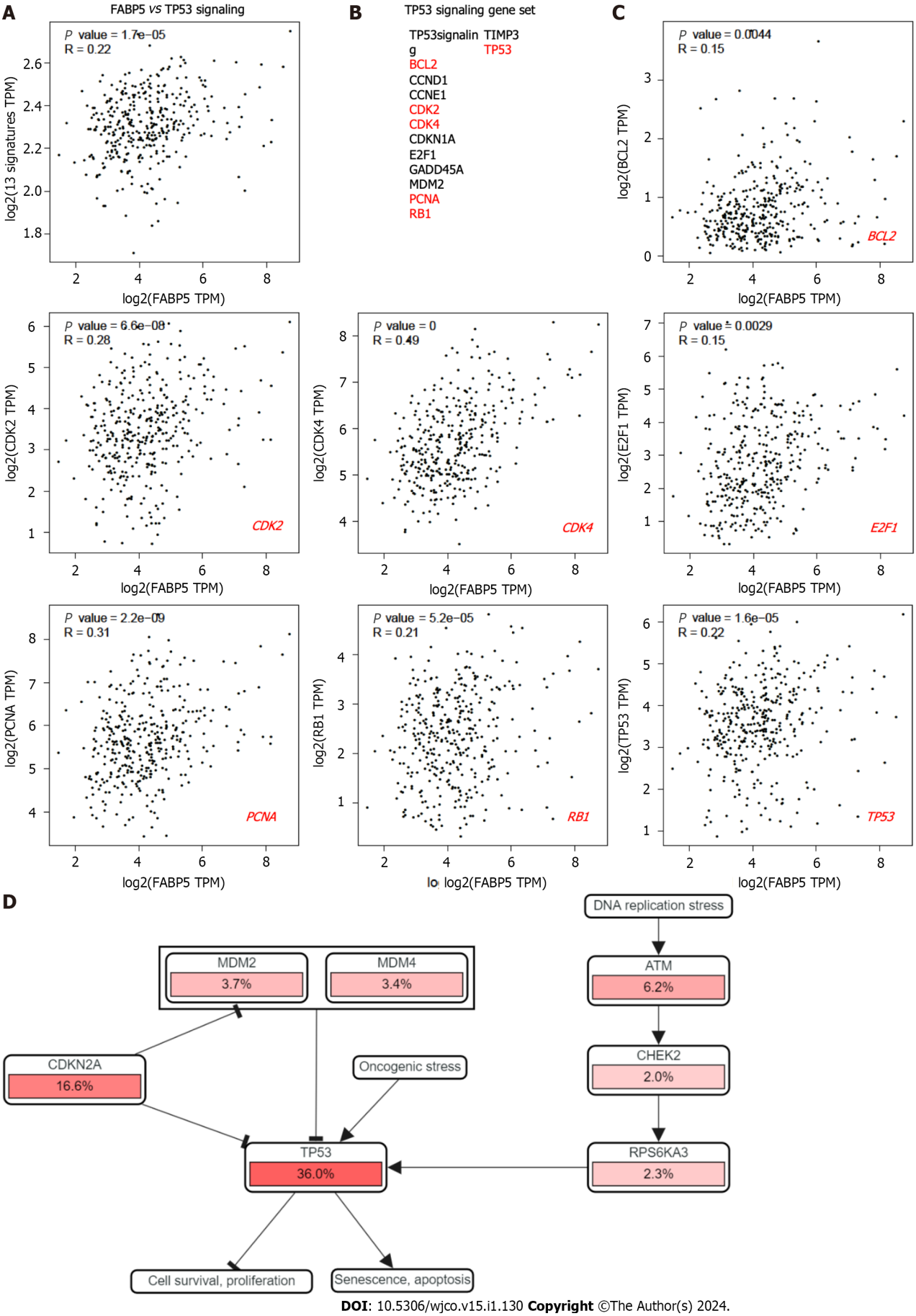

DOI: 10.5306/wjco.v15.i1.130 **Copyright** ©The Author(s) 2024.

Figure 5 Expression of *FABP5* correlates with cancer hallmark TP53 signaling and genes within. A: *FABP5* positively correlated with enrichment

of cancer hallmark TP53 signaling in patients with liver hepatocellular carcinoma; B: Gene list included in TP53 signaling. The genes that showed positive correlation with *FABP5* are highlighted in red; C: Highlighted genes in the TP53 signaling gene set positively correlate with *FABP5* expression. *P* values show the statistical significance of the correlation; *R* values show the correlation coefficient; D: Altered expression of individual genes in the TP53 signaling gene set shown in the context of signaling network. Pink bars show upregulation of gene expression.

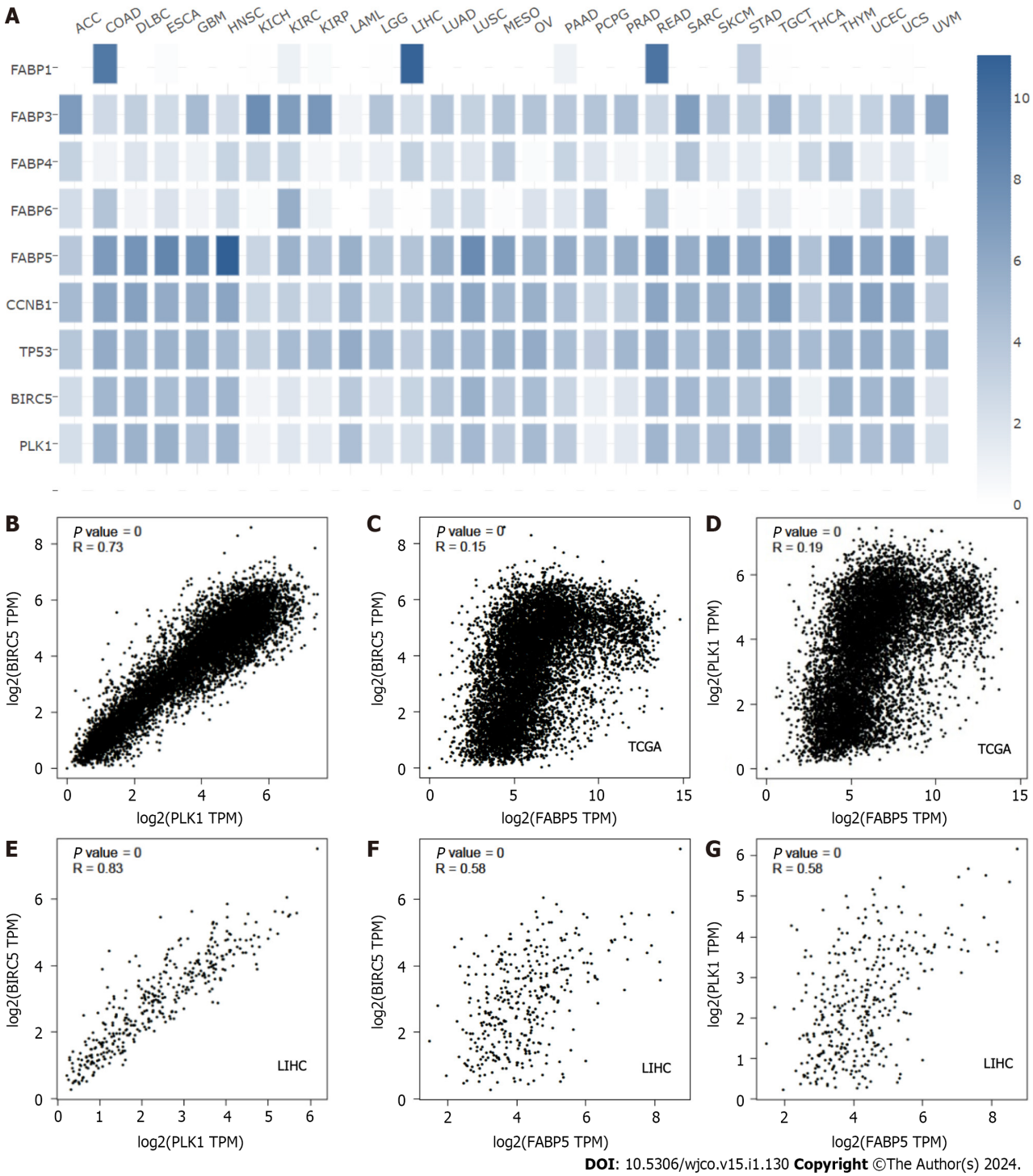

DOI: 10.5306/wjco.v15.i1.130

Figure 6 Expression of *FABP5* correlates with *PLK1* and *BIRC5* expression in pan cancer and liver cancer. A: Expression of *FABP5* and other FABP family members as well as several highlighted genes *CCNB1, TP53, BIRC5* and *PLK1* in each cancer type using GEPIA2 portal; B and C: *FABP5* expression positively correlated with expression of *BIRC5* at pan cancer (B) and liver cancer (C); D and E: *FABP5* expression positively correlated with expression of *PLK1* at pan cancer (D) and liver cancer (E); F and G: *BIRC5* expression positively correlated with expression of *PLK1* at pan cancer (F) and liver cancer (G). *P* values show the statistical significance of the correlation; *R* values show the correlation coefficient.

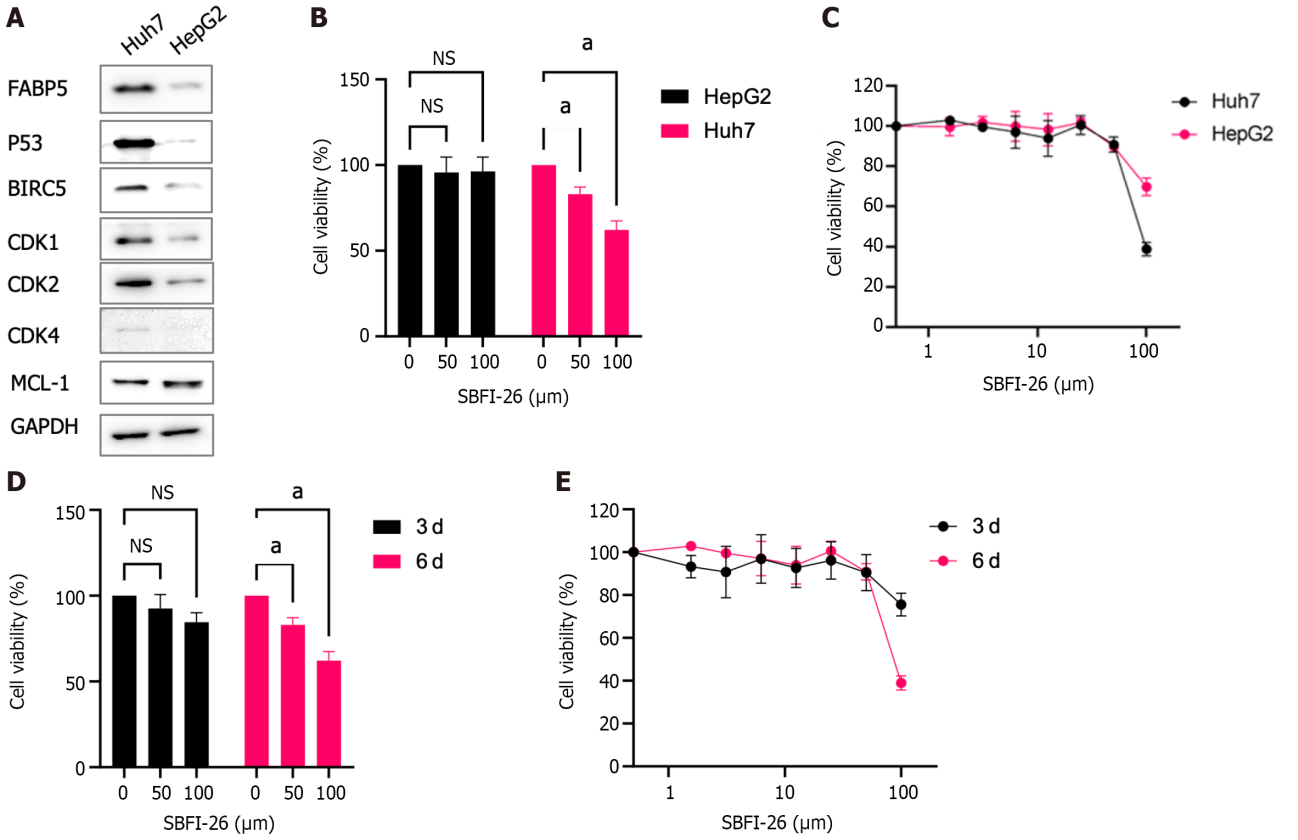

DOI: 10.5306/wjco.v15.i1.130 **Copyright** ©The Author(s) 2024.

Figure 7 Huh7 cells are sensitive to FABP5 inhibition by SFBI-26. A: Western blot shows the expression of FABP5, p53, and other proteins in Huh7 and HepG2 cells; B: 3-dose (0, 50 and 100 μmol/L) cell viability assay shows SBFI-26 inhibited the cell viability of hepatocellular carcinoma (HCC) cell lines Huh7 and HepG2 cells post treatment for 6 d; C: 8-dose (2-fold serial doses up to 100 μmol/L) cell viability assay showed SBFI-26 inhibited the cell viability of HCC cell lines post treatment for 6 d; D: 3-dose (0, 50 and 100 μmol/L) cell viability assay shows SBFI-26 inhibited the cell viability of Huh7 cells in time-dependent manner; E: 8-dose cell viability assay showed SBFI-26 inhibited the cell viability of Huh7 cells at 3- and 6-d post treatment; NS: Not significant.

Furthermore, the correlation of *FABP5* expression with poor patient survival is more significant than that of *FABP4* expression. These data suggest *FABP5* is the predominant gene across FABPs that are dysregulated in cancer, and it is the most important member that contributes significantly to cancer malignancy and progression, especially in patients with HCC. It is interesting to find out that high *FABP5* expression correlates well with top cancer hallmarks and two oncogenes *PLK1* and *BIRC5* that were identified in HCC patients in our and other studies earlier[12,13]. These data strongly suggest that *FABP5* is a novel therapeutic target for treating HCC and provides valuable insights for potential therapeutic development in treating patients with HCC.

Small molecule inhibitors targeting FABP proteins, especially FABP4, are currently under development by multiple efforts. Early preclinical data provide evidence that targeting FABP4 by BMS309403 is promising in treating cancer for multiple cancer disease models[2,7,18]. In this study, our data suggests that FABP5 is a novel therapeutic target in patients with HCC and other cancer types. FABP5 inhibitors such as SFBI-26 are emerging and demonstrate that targeting FABP5 is feasible and promising in treating cancer[13].

We found that the gene cluster with *FABP4, FABP5, FABP8, FABP9,* and *FABP12* in adjacent loci in chromosome 8 are often co-amplified in many cancer types but with highest frequencies in PRAD and HCC. Amplification is the most common genetic alteration type for these FABPs. In contrast, other family members *FABP1, FABP2, FABP3, FABP6* and *FABP7* also showed expression in cancer, ubiquitously or selectively, but are not frequently altered at genetic level. Interestingly, not all co-amplified family members are expressed in cancer due to amplification. Only *FABP4* and *FABP5* are expressed across various cancer types, suggesting that genetic amplification itself is necessary but not sufficient for their abnormal expression in cancer. Expression of *FABP4*, as a major target of PPARγ[19], has been shown to be controlled by PPARγ[4], and *FABP4* has been shown to negatively regulate PPARγ expression level, likely through a negative feedback signaling loop. In contrast to *FABP4*, *FABP5* has been shown to facilitate fatty-acid induced PPARγ activation and downstream signaling, and activated PPARγ in turn upregulates FABP5 expression levels in prostate cancer[10]. Whether this is also the case in HCC requires further investigation. In this study, we discovered that *FABP5* is the one with greatest changes in mRNA expression across family members in patients with LIHC comparing tumor with non-tumor tissues and its expression highly correlates with poor patient outcome and enriched cancer hallmarks involved in cell cycle progression.

Dysregulated cell metabolism and cell cycle progression are key interconnecting events for cancer malignancy and progression[20]. The top three cancer hallmarks previously reported in HCC patients are E2F targets, G2M checkpoint

and DNA repair[13]. All these lead to dysregulated cell cycle progression. Interestingly, we discovered that *FABP5* expression highly correlates with top cancer hallmarks enriched in LIHC patients (G2M checkpoint), which likely drive cancer cell survival and proliferation[13]. In our previous study, we demonstrated that two oncogenes, *PLK1* and *BIRC5*, are highly co-expressed in HCC and co-targeting of PLK1 and BIRC5 synergistically inhibited tumor growth of HCC preclinical models *in vitro* and *in vivo*[12]. Both PLK1 and BIRC5 are master regulators in cell cycle, powerful in promoting cell cycle progression and inhibiting cell death[21,22]. In this study, we confirmed that *PLK1* and *BIRC5* are co-expressed in cancer including HCC. More interestingly, *FABP5* expression correlates very well with expression of *PLK1* and *BIRC5* in multiple cancer types. The strong correlation of *FABP5* with cell cycle hallmark and cell cycle master regulators suggests its critical role in contribution to cancer cell progression when overexpressed.

In addition to its upregulation and functions in tumor cells, FABP5 is also found to be dysregulated in multiple immune cell types and can serve as a novel immune-related prognostic marker and a target of immunotherapy[23]. FABP5 was reported to regulate mitochondrial integrity and functions as cell-intrinsic checkpoint for Treg suppressive function in tumor microenvironment[24]. However, how FABP5 is dysregulated and the underlying mechanism in anti-tumor immunity have not been fully understood and requires further investigation.

CONCLUSION

FABP5 is frequently amplified in HCC, leading to its abnormal expression. High *FABP5* expression correlates well with worse patient outcome, enriched cancer hallmarks and oncogenes in HCC. Targeting FABP5 by SBFI-26 is more effective in FABP5-high expressing cells than FABP5-low expressing cells.

ARTICLE HIGHLIGHTS

Research background

FABP5 amplification can serve as a prognosis biomarker for the prediction of patient outcome and as a novel therapeutic target for treating hepatocellular carcinoma (HCC) with *FABP5* amplification.

Research motivation

FABP5 is frequently amplified in cancer, especially in HCC, which leads to its abnormal expression in HCC. High *FABP5* expression correlates well with worse patient outcome, enriched cancer hallmarks and oncogenes in HCC. Targeting FABP5 by SBFI-26 is more effective in FABP5-high expressing cells (Huh7) than FABP5-low expressing cells (HepG2).

Research objectives

FABP4, FABP5, FABP8, FABP9 and *FABP12* as a gene cluster is frequently amplified in cancer, which is the most common genetic alteration for FABPs. *FABP5* is highly overexpressed in cancer and its expression correlates well with worse patient outcomes. *FABP5* expression highly correlates with enrichment of G2M checkpoint, TP53 signaling pathway, and many genes in the gene sets such as *CDK1*, *CDK4*, and *TP53*. Furthermore, *FABP5* also correlates well with two co-expressed oncogenes *PLK1* and *BIRC5* in liver hepatocellular carcinoma (LIHC) patients. FABP5-high expressing Huh7 cells also expressed higher protein levels of p53, BIRC5, CDK1, CDK2, and CDK4 than FABP5-low expressing HepG2 cells. Huh7 is more sensitive to FABP5 inhibition than HepG2 cells.

Research methods

In this study, we accessed the public available portal of The Cancer Genome Atlas datasets of pan cancer and liver hepatocellular carcinoma LIHC by using cBioPortal and GEPIA2 portal. Based on mutation and CNA (copy number variation) datasets, we investigated genetic alterations of FABP family members in various cancer types. Based on mRNA datasets, we investigated FABP expression and their correlation with patient clinical outcome, enriched cancer hallmarks and oncogenes. For validation, we determined the protein levels of FABP5 and its correlated genes in Huh7 and HepG2 and evaluated the potential of targeting FABP5 in treating HCC.

Research results

The present study aimed to understand the genetic alterations and expression of FABP family members and their associated cancer hallmarks and oncogenes in contributing to cancer malignancies, especially HCC.

Research conclusions

Several family members including *FABP4*, *FABP5*, and *FABP7* are abnormally expressed in cancer cells beyond tissue expression restriction and play important roles in cancer malignancy and progression. However, the mechanism leading to their abnormal expression is not clear.

Research perspectives

Reprogrammed lipid metabolism plays crucial roles in cell survival, growth, and evolution in many cancer types including HCC, an aggressive subtype of liver cancer. Fatty acid binding protein (FABP) family members including

FABP5 play important roles in contribution to cancer progression and metastasis; however, how these FABP members, especially FABP5, are dysregulated in HCC and their contribution to HCC cancer progression have not been well defined.

ACKNOWLEDGEMENTS

We would like to thank the patients and their families who contributed to this research study. We also appreciate the availability of the TCGA dataset and the built-in analysis *via* the web-based bioinformatic platforms cBioportal and GEPIA2.

FOOTNOTES

Co-first authors: Yan Li and William Lee.

Author contributions: Li Y conceived and designed the study; Li Y, Lee W, Zhao ZG, Liu Y, Cui H, and Wang HY performed the experiments and analyzed the data; Li Y, Lee W, Zhao ZG, Liu Y, Cui H, and Wang HY interpreted the data; Li Y and Lee W drafted the manuscript; Liu Y, Cui H, and Wang HY revised the manuscript; All authors approved the final version of the article. Lee W contributed primarily to the bioinformatics analysis and therefore Lee W and Li Y contributed equally to the study. Li Y conceived and designed the study, performed the experiments, analyzed and interpreted the data, drafted and revised the manuscript. Lee W contributed to the bioinformatics analysis, data analysis and interpretation, as well as manuscript drafting and revision. Both authors have made substantial contributions to the study and are therefore qualified as co-first authors of the paper.

Supported by Tianjin Key Medical Discipline Construction Project, No. TJYXZDXK-034A.

Institutional review board statement: This study was approved by the Institutional Review Board (IRB) of Tianjin Third Central Hospital.

Conflict-of-interest statement: All authors have seen and agreed with the contents of the manuscript and there is no conflict of interest to declare.

Data sharing statement: For this bioinformatics analysis, we acquired the TCGA data and LIHC data as well as the data for other cancer patients from cBioPortal (https://www.cbioportal.org/). The bioinformatic platform GEPIA2 also used the TCGA datasets for the built-in analysis. No additional data are available.

Country/Territory of origin: China

ORCID number: Yan Li 0000-0003-2602-7423; William Lee 0009-0008-2736-6025; Zhen-Gang Zhao 0000-0001-7249-4474; Yi Liu 0000-0001-8082-8868; Hao Cui 0000-0002-5629-7814; Hao-Yu Wang 0000-0001-6672-2733.

S-Editor: Liu JH
L-Editor: Filipodia
P-Editor: Zhang XD

REFERENCES

1 **Koundouros N**, Poulogiannis G. Reprogramming of fatty acid metabolism in cancer. *Br J Cancer* 2020; **122**: 4-22 [PMID: 31819192 DOI: 10.1038/s41416-019-0650-z]
2 **Sun N**, Zhao X. Therapeutic Implications of FABP4 in Cancer: An Emerging Target to Tackle Cancer. *Front Pharmacol* 2022; **13**: 948610 [PMID: 35899119 DOI: 10.3389/fphar.2022.948610]
3 **Hotamisligil GS**, Bernlohr DA. Metabolic functions of FABPs--mechanisms and therapeutic implications. *Nat Rev Endocrinol* 2015; **11**: 592-605 [PMID: 26260145 DOI: 10.1038/nrendo.2015.122]
4 **Lei C**, Fan B, Tian J, Li M, Li Y. PPARγ regulates fabp4 expression to increase DHA content in golden pompano (Trachinotus ovatus) hepatocytes. *Br J Nutr* 2022; **127**: 3-11 [PMID: 33663633 DOI: 10.1017/S0007114521000775]
5 **Zeng J**, Sauter ER, Li B. FABP4: A New Player in Obesity-Associated Breast Cancer. *Trends Mol Med* 2020; **26**: 437-440 [PMID: 32359475 DOI: 10.1016/j.molmed.2020.03.004]
6 **Mukherjee A**, Chiang CY, Daifotis HA, Nieman KM, Fahrmann JF, Lastra RR, Romero IL, Fiehn O, Lengyel E. Adipocyte-Induced FABP4 Expression in Ovarian Cancer Cells Promotes Metastasis and Mediates Carboplatin Resistance. *Cancer Res* 2020; **80**: 1748-1761 [PMID: 32054768 DOI: 10.1158/0008-5472.CAN-19-1999]
7 **Tian W**, Zhang W, Zhang Y, Zhu T, Hua Y, Li H, Zhang Q, Xia M. FABP4 promotes invasion and metastasis of colon cancer by regulating fatty acid transport. *Cancer Cell Int* 2020; **20**: 512 [PMID: 33088219 DOI: 10.1186/s12935-020-01582-4]

8 **Dum D**, Ocokoljic A, Lennartz M, Hube-Magg C, Reiswich V, Höflmayer D, Jacobsen F, Bernreuther C, Lebok P, Sauter G, Luebke AM, Burandt E, Marx AH, Simon R, Clauditz TS, Minner S, Menz A, Büscheck F, Gorbokon N, Steurer S, Blessin NC, Krech T. FABP1 expression in human tumors: a tissue microarray study on 17,071 tumors. *Virchows Arch* 2022; **481**: 945-961 [PMID: 35951102 DOI: 10.1007/s00428-022-03394-5]

9 **Xu B**, Chen L, Zhan Y, Marquez KNS, Zhuo L, Qi S, Zhu J, He Y, Chen X, Zhang H, Shen Y, Chen G, Gu J, Guo Y, Liu S, Xie T. The Biological Functions and Regulatory Mechanisms of Fatty Acid Binding Protein 5 in Various Diseases. *Front Cell Dev Biol* 2022; **10**: 857919 [PMID: 35445019 DOI: 10.3389/fcell.2022.857919]

10 **O'Sullivan SE**, Kaczocha M. FABP5 as a novel molecular target in prostate cancer. *Drug Discov Today* 2020 [PMID: 32966866 DOI: 10.1016/j.drudis.2020.09.018]

11 **Tang Z**, Kang B, Li C, Chen T, Zhang Z. GEPIA2: an enhanced web server for large-scale expression profiling and interactive analysis. *Nucleic Acids Res* 2019; **47**: W556-W560 [PMID: 31114875 DOI: 10.1093/nar/gkz430]

12 **Li Y**, Zhao ZG, Luo Y, Cui H, Wang HY, Jia YF, Gao YT. Dual targeting of Polo-like kinase 1 and baculoviral inhibitor of apoptosis repeat-containing 5 in TP53-mutated hepatocellular carcinoma. *World J Gastroenterol* 2020; **26**: 4786-4801 [PMID: 32921957 DOI: 10.3748/wjg.v26.i32.4786]

13 **Zhu W**, Zhang Q, Liu M, Yan M, Chu X, Li Y. Identification of DNA repair-related genes predicting pathogenesis and prognosis for liver cancer. *Cancer Cell Int* 2021; **21**: 81 [PMID: 33516217 DOI: 10.1186/s12935-021-01779-1]

14 **Ohata T**, Yokoo H, Kamiyama T, Fukai M, Aiyama T, Hatanaka Y, Hatanaka K, Wakayama K, Orimo T, Kakisaka T, Kobayashi N, Matsuno Y, Taketomi A. Fatty acid-binding protein 5 function in hepatocellular carcinoma through induction of epithelial-mesenchymal transition. *Cancer Med* 2017; **6**: 1049-1061 [PMID: 28374947 DOI: 10.1002/cam4.1020]

15 **Boettcher S**, Miller PG, Sharma R, McConkey M, Leventhal M, Krivtsov AV, Giacomelli AO, Wong W, Kim J, Chao S, Kurppa KJ, Yang X, Milenkowic K, Piccioni F, Root DE, Rücker FG, Flamand Y, Neuberg D, Lindsley RC, Jänne PA, Hahn WC, Jacks T, Döhner H, Armstrong SA, Ebert BL. A dominant-negative effect drives selection of TP53 missense mutations in myeloid malignancies. *Science* 2019; **365**: 599-604 [PMID: 31395785 DOI: 10.1126/science.aax3649]

16 **Dearth LR**, Qian H, Wang T, Baroni TE, Zeng J, Chen SW, Yi SY, Brachmann RK. Inactive full-length p53 mutants lacking dominant wild-type p53 inhibition highlight loss of heterozygosity as an important aspect of p53 status in human cancers. *Carcinogenesis* 2007; **28**: 289-298 [PMID: 16861262 DOI: 10.1093/carcin/bgl132]

17 **Liu X**, Wilcken R, Joerger AC, Chuckowree IS, Amin J, Spencer J, Fersht AR. Small molecule induced reactivation of mutant p53 in cancer cells. *Nucleic Acids Res* 2013; **41**: 6034-6044 [PMID: 23630318 DOI: 10.1093/nar/gkt305]

18 **Farrell M**, Fairfield H, Karam M, D'Amico A, Murphy CS, Falank C, Pistofidi RS, Cao A, Marinac CR, Dragon JA, McGuinness L, Gartner CG, Iorio RD, Jachimowicz E, DeMambro V, Vary C, Reagan MR. Targeting the fatty acid binding proteins disrupts multiple myeloma cell cycle progression and MYC signaling. *Elife* 2023; **12** [PMID: 36880649 DOI: 10.7554/eLife.81184]

19 **Tontonoz P**, Graves RA, Budavari AI, Erdjument-Bromage H, Lui M, Hu E, Tempst P, Spiegelman BM. Adipocyte-specific transcription factor ARF6 is a heterodimeric complex of two nuclear hormone receptors, PPAR gamma and RXR alpha. *Nucleic Acids Res* 1994; **22**: 5628-5634 [PMID: 7838715 DOI: 10.1093/nar/22.25.5628]

20 **Icard P**, Fournel L, Wu Z, Alifano M, Lincet H. Interconnection between Metabolism and Cell Cycle in Cancer. *Trends Biochem Sci* 2019; **44**: 490-501 [PMID: 30655165 DOI: 10.1016/j.tibs.2018.12.007]

21 **Chiappa M**, Petrella S, Damia G, Broggini M, Guffanti F, Ricci F. Present and Future Perspective on PLK1 Inhibition in Cancer Treatment. *Front Oncol* 2022; **12**: 903016 [PMID: 35719948 DOI: 10.3389/fonc.2022.903016]

22 **Wheatley SP**, Altieri DC. Survivin at a glance. *J Cell Sci* 2019; **132** [PMID: 30948431 DOI: 10.1242/jcs.223826]

23 **Jia H**, Zhang X, Liu X, Qiao R, Liu Y, Lv S, Zhu H, Wang J, Kong Q, Zhang H, Zhang Z. FABP5, a Novel Immune-Related mRNA Prognostic Marker and a Target of Immunotherapy for Multiple Myeloma. *Front Med (Lausanne)* 2021; **8**: 667525 [PMID: 34249967 DOI: 10.3389/fmed.2021.667525]

24 **Field CS**, Baixauli F, Kyle RL, Puleston DJ, Cameron AM, Sanin DE, Hippen KL, Loschi M, Thangavelu G, Corrado M, Edwards-Hicks J, Grzes KM, Pearce EJ, Blazar BR, Pearce EL. Mitochondrial Integrity Regulated by Lipid Metabolism Is a Cell-Intrinsic Checkpoint for Treg Suppressive Function. *Cell Metab* 2020; **31**: 422-437.e5 [PMID: 31883840 DOI: 10.1016/j.cmet.2019.11.021]

World Journal of Clinical Oncology

Submit a Manuscript: https://www.f6publishing.com

World J Clin Oncol 2024 January 24; 15(1): 145-158

DOI: 10.5306/wjco.v15.i1.145

ISSN 2218-4333 (online)

SCIENTOMETRICS

What are the changes in the hotspots and frontiers of microRNAs in hepatocellular carcinoma over the past decade?

Lu Zhang, Zu-Yuan Chen, Xiao-Xian Wei, Jian-Di Li, Gang Chen

Specialty type: Oncology

Provenance and peer review: Unsolicited article; Externally peer reviewed.

Peer-review model: Single blind

Peer-review report's scientific quality classification

Grade A (Excellent): 0
Grade B (Very good): B
Grade C (Good): 0
Grade D (Fair): 0
Grade E (Poor): 0

P-Reviewer: Beenet L, United States

Received: October 22, 2023
Peer-review started: October 22, 2023
First decision: November 23, 2023
Revised: December 8, 2023
Accepted: December 28, 2023
Article in press: December 28, 2023
Published online: January 24, 2024

Lu Zhang, Zu-Yuan Chen, Xiao-Xian Wei, Jian-Di Li, Gang Chen, Department of Pathology, The First Affiliated Hospital of Guangxi Medical University, Nanning 530021, Guangxi Zhuang Autonomous Region, China

Corresponding author: Gang Chen, PhD, Professor, Department of Pathology, The First Affiliated Hospital of Guangxi Medical University, No. 6 Shuangyong Road, Nanning 530021, Guangxi Zhuang Autonomous Region, China. chengang@gxmu.edu.cn

Abstract

BACKGROUND

Emerging research suggests that microRNAs (miRNAs) play an important role in the development of hepatocellular carcinoma (HCC). A comprehensive analysis of recent research concerning miRNAs in HCC development could provide researchers with a valuable reference for further studies.

AIM

To make a comprehensive analysis of recent studies concerning miRNAs in HCC.

METHODS

All relevant publications were retrieved from the Web of Science Core Collection database. Bibliometrix software, VOSviewer software and CiteSpace software were used to visually analyze the distribution by time, countries, institutions, journals, and authors, as well as the keywords, burst keywords and thematic map.

RESULTS

A total of 9426 publications on this topic were found worldwide. According to the keywords analysis, we found that the studies of miRNAs focused on their expression level, effects, and mechanisms on the biological behaviour of HCC. Keywords bursting analysis showed that in the early years (2013–2017), "microRNA expression", "gene expression", "expression profile", "functional polymorphism", "circulating microRNA", "susceptibility" and "mir 21" started to attract attention. In the latest phase (2018–2022), the hot topics turned to "sorafenib resistance", "tumor microenvironment" and so on.

CONCLUSION

This study provides a comprehensive overview of the role of miRNAs in HCC development based on bibliometric analysis. The hotspots in this field focus on miRNAs expression level, effects, and mechanisms on the biological behavior of HCC. The frontiers turned to sorafenib resistance, tumor microenvironment and

so on.

Key Words: miRNA; Hepatocellular carcinoma; Bibliometric; VOSviewer; CiteSpace

Core Tip: The main objective of this work is to systematically analyse the recent research concerning microRNAs (miRNAs) in hepatocellular carcinoma (HCC). Annual publications provided an overview of the trends in this area, while distribution by countries, institutions, journals, and authors analysis were outstandingly representative and provided some cooperation situation information. According to the keywords analysis, the studies of miRNAs focused on their expression level, effects, and mechanisms on the biological behaviour of HCC. Keywords bursting analysis showed that in the latest phase (2018–2022), the hot topics turned to "sorafenib resistance", "tumor microenvironment" and so on.

Citation: Zhang L, Chen ZY, Wei XX, Li JD, Chen G. What are the changes in the hotspots and frontiers of microRNAs in hepatocellular carcinoma over the past decade? *World J Clin Oncol* 2024; 15(1): 145-158
URL: https://www.wjgnet.com/2218-4333/full/v15/i1/145.htm
DOI: https://dx.doi.org/10.5306/wjco.v15.i1.145

INTRODUCTION

It is estimated that in 2020, 905700 people were diagnosed with liver cancer worldwide and 830200 died from liver cancer, with China accounting for 45.3% of the world's liver cancer cases and 47.1% of the world's liver cancer deaths[1]. In southern China, where liver cancer death rates are high (22.3 per 100000), especially in rural areas (26.6 per 100000), Fusui County in Guangxi Province is one of the nine regions with the highest incidence of liver cancer in the country[2]. As the understanding of the carcinogenic factors that cause liver cancer has improved worldwide, researchers have developed new treatment strategies, such as immunotherapy and targeted therapies. The continuous development of new technologies and drugs provides hope for further diagnosis and treatment of liver cancer[3]. Hepatocellular carcinoma (HCC) accounts for 85%-90% of primary liver cancers and is highly drug-resistant, making it difficult to treat. Most patients are diagnosed at an advanced stage, greatly affecting the prognosis and five-year survival rate[4]. Therefore, new therapies for HCC remain an unmet medical need. In this regard, important insights into the biology of the disease have been obtained through genomics, transcriptomics and epigenomics studies[5]. In recent years, exploration in the field of noncoding genes has provided a new understanding of the pathogenesis and development of HCC, early diagnostic markers, and novel therapeutic targets.

MicroRNA (miRNA), a small noncoding RNA molecule approximately 22 nucleotides in length, is estimated to regulate almost 60% of human protein-coding genes[6]. miRNA is closely associated with the pathogenesis of various types of tumors[7]. Previous research has shown that a great quantity of miRNAs are aberrantly expressed in various cancer cell lines and tissues, and they participate in the biological processes such as the tumor invasion, metastasis, autophagy, regulation of the tumor microenvironment, chemotherapy resistance, and immunotherapy modulation[8-12]. As competitive endogenous RNAs, long noncoding RNAs (lncRNAs) and circRNAs contain miRNA binding sites and promote miRNA target gene expression through competition with miRNAs[13-17]. For example, Wang *et al*[18] identified and verified a novel MAGI2-AS3/miRNA-374-5p/FOXO1 network that was associated with HBV-related HCC. Therefore, the identification of miRNAs and their binding sites on tumor will help to explore new mechanisms of tumor occurrence and development, as well as to discover new tumor diagnostic markers and therapeutic targets[19,20].

In our research, we used bibliometrics to explore the research relationship between miRNAs and HCC. Bibliometrics are able to study the distribution focus, number relationship and change pattern of literature in related fields using mathematical, statistical and other econometric research methods[21]. Potential relationships between large amounts of literature were presented in bibliometric plots, and large bibliometric plots were visualized and analysed with VOSviewer and CiteSpace. Related software was used to summarize and display the relationships between countries, institutions, journals, authors, and keywords. Then, the topic was examined at a macro level to discuss future directions and the extent of progress, providing a better overview and new ideas for the researchers involved.

MATERIALS AND METHODS

Search strategy

All relevant publications were retrieved from the Web of Science Core Collection (WOSCC) database with the following search strategies: ((“hepatocellular carcinoma” OR “hepatocarcinoma” OR “HCC” OR “liver cancer” OR “liver carcinoma” OR “hepatic cancer” OR “hepatic carcinoma”) AND (“miRNA” OR “microRNA” OR “miR”)) AND Document types = (Article OR Review) AND Language = English, index = Science Citation Index Expanded (SCI-

EXPANDED), with a limited time frame from 2013 to 2022. In total, 9,426 publications were ultimately included.

Data extraction

The bibliographic information was downloaded from the WOSCC database, including title, authors, year of publications, country, institution, keywords, citations, abstract and reference. The Bibliometrix software was used to extract all data eligible for inclusion in this study by two investigators alone and then imported into Microsoft Excel. Where there was any disagreement between the two investigators, a third investigator resolved it.

Statistical analysis

Microsoft Excel was used to calculate descriptive statistical analysis, including institutions, journals, and authors. Visualization analysis was based on the Bibliometrix software, VOSviewer software and CiteSpace software. Visual network analysis consisted of the node size, distance, and colour. Nodes represent specific elements, and the size of the node indicates the quantity or frequency of publication. The larger the node, the more often the element presented. A line between nodes meant that these nodes appeared together in the same article in the 9426 publications. The thicker the line, the more often they appeared together.

RESULTS

Publication output

A total of 9426 records were initially found based on the search criteria. Annual publications provided an overview of the research field of miRNA in HCC. Figure 1 shows the distribution of publications related to the field of miRNAs in HCC development from 2013 to 2022. Noticeably, the annual output of papers was nearly tripled compared to 2013 (380 publications) in 2017 (1067 publications). A turning point occurred in 2020, and the number of publications began to decline. In 2021 and 2022, the number of publications was 1132 and 931, respectively. The change in the average annual number of citations is also shown in Figure 1. The result reflects that the average yearly citations decreased yearly.

Distribution by countries and institutions

Figure 2 shows the number of articles in each country. Figure 3 shows the top 10 productive countries based on total citations in the research field of miRNA in HCC. China, the United States, Japan, and Italy contributed to the majority of scientific publications. China was the country with the most publications (7186 articles) and had the highest number of total citations (193462), followed by the United States (962 publications and 46707 total citations) and Japan (271 publications and 9038 total citations). According to the network map, the larger a node was, the more articles a country produced, while the thickness of lines between nodes indicated the strength of collaboration (Figure 4). The results show that China was the most prolific country and collaborated substantially with other countries. Table 1 shows the top 10 productive institutions based on citations concerning miRNA research in HCC. Sun Yat Sen University published 346 articles and had the most total citations (12488), followed by Nanjing Med University (337 publications and 11397 total citations) and Fudan University (311 publications and 11612 total citations).

Distribution by journals

Table 2 shows the top 10 productive journals, their impact factor and their JCR ranking. Oncotarget (335) has the largest number of publications, followed by Oncology Letters (248) and PLoS One (200). Among the top 10 productive journals, Biomedicine and Pharmacotherapy has an impact factor greater than 5, and two journals (Biomedicine and Pharmacotherapy, Scientific Reports) belong to JCR quartile 1 (Q1).

Distribution by authors

The author distribution was examined to identify the author with the strongest influence. Supplementary Table 1 shows the top 10 most prolific researchers. The most prolific author was Masaki Tsutomu from Kagawa University (42 publications), followed by Fan Jia from Fudan University (40 publications) and Morishita Asahiro from Kagawa University (40 publications).

Analysis of keywords and burst keywords

We analysed the high-frequency keywords mentioned most frequently in the research articles related to miRNAs in HCC to help us understand the main research hot spots in this field. The top 20 keywords with the highest frequency are shown in Figure 5. “Expression”, “cancer”, “metastasis”, “proliferation”, “invasion”, “growth”, “down-regulation”, “apoptosis”, “progression”, and “cells” comprised the top 10, suggesting that the research on miRNAs focuses on their expression level in HCC and their impact on the biological behaviour of HCC. “Migration”, “breast-cancer”, “cell-proliferation”, “tumor-suppressor”, “promotes”, “epithelial-mesenchymal transition”, “gene”, “colorectal-cancer”, “identification”, and “gastric-cancer” are the next 10 keywords, indicating that the research focuses on the effects and mechanisms of miRNAs on the biological behaviour of HCC, and applies to other tumors.

Burst keywords were regarded as an indicator for the frontiers of the specific field during a period of time. We used CiteSpace to explore the 20 keywords with the strongest citation bursts of the last 10 years (Figure 6). From 2013 to 2022, “microRNA expression”, “gene”, “in vivo”, “human hepatocellular carcinoma”, “gene expression”, “functional polymorphism”, “circulating microRNA”, “expression profile”, “hepatocarcinogenesis”, “susceptibility”, “pre

Table 1 Top 10 productive institutions based on citations

Institutions	Publications	Citations
Sun Yat Sen University	346	12488
Nanjing Med University	337	11397
Fudan University	311	11612
Shanghai Jiao Tong University	267	11300
Xi'an Jiao Tong University	262	7411
Zhejiang University	261	8164
Zhengzhou University	230	5638
Huazhong University Sci & Technol	209	5223
Wuhan University	189	5180
Shandong University	346	4749

Table 2 Top 10 productive journals and their impact factor and JCR ranking

Rank	Journal	Publications	2021 impact factor	2022 JCR quartile
1	*Oncotarget*	335	Removed	-
2	*Oncology Letters*	248	3.111	Q4
3	*PLoS One*	200	3.752	Q2
4	*Oncology Reports*	198	4.136	Q3
5	*Molecular Medicine Reports*	189	3.432	Q3
6	*Oncotargets and Therapy*	188	4.345	Q2
7	*European Review for Medical and Pharmacological Sciences*	162	3.784	Q2
8	*Biomedicine and Pharmacotherapy*	160	7.419	Q1
9	*Tumor Biology*	156	Removed	-
10	*Scientific Reports*	154	4.996	Q1

microRNA", "tumor suppressor gene", "liver" and "mir 21" started to attract attention in the early years (2013–2017). Regarding the latest phase (2018–2022), "statistics", "ceRNA", "lncRNA", "sorafenib resistance", "circular RNA" and "tumor microenvironment" became trend topics.

The timeline spectrum of keywords can clearly represent the time span of each cluster and the development trend of a specific cluster, explore the time characteristics of the research field reflected by each cluster, and thereby verify the evolutionary trend of hotspots. According to Figure 7, the articles on miRNA research in the HCC field published from 2013 to 2022 could be categorized into 6 main clusters. The first cluster was "#0 hepatitis c virus", and followed by "#1 hepatocellular carcinoma", "#2 proliferation", "#3 circular RNA", "#4 DNA methylation" and "#5 polymorphism". The tree-rings with different sizes on the timeline indicate which keywords have a higher frequency.

We used Bibliometrix software to draw a thematic map of miRNA in the field of HCC research, and the results indicate that topics such as "expression", "cancer", "metastasis", "proliferation", "invasion", "mircoRNAs", "growth", "apoptosis", "progression" and "cells" were in the Motor Themes, as well as the topics such as "circulating microRNAs", "in-vivo", "serum", "infection", "mir-122", "hepatitis-b-virus", "replication", "DNA", "fibrosis" and "potential biomarkers"; the topic "nanoparticles" was in the Niche Themes; and the topics such as "susceptibility", "functional polymorphism" were in the Emerging or Declining Themes, as well as the topics such as "risk", "squamous-cell carcinoma" and "association"; "hepatocellular-carcinoma", "down-regulation", "breast-cancer", "tumor-suppressor", "colorectal-cancer", "gastric-cancer", "microRNA", "up-regulation", "lung-cancer" and "prostate-cancer" were in the Basic Themes (Figure 8).

DISCUSSION

In this study, we conducted a bibliometric and visualized analysis of the last 10 years focusing on studies based on miRNAs in HCC. We achieve insight into the role of miRNAs in HCC. Annual publications provided an overview of the trends in this area, while distribution by countries, institutions, journals, and authors analysis were outstandingly repres-

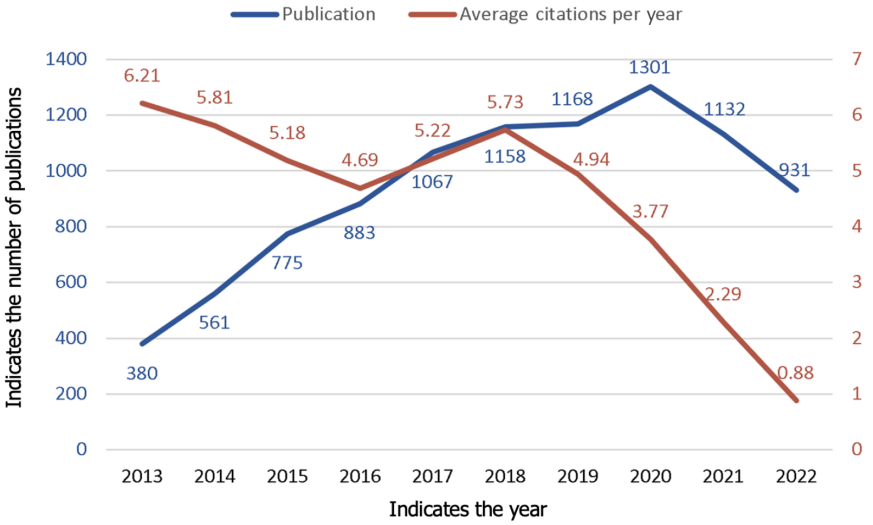

DOI: 10.5306/wjco.v15.i1.145 **Copyright** ©The Author(s) 2024.

Figure 1 Yearly changes in the number of publications and average number of citations. The change in the number of publication in corresponding year is shown with a blue line, and the change in the average annual number of citations is shown with a brown line.

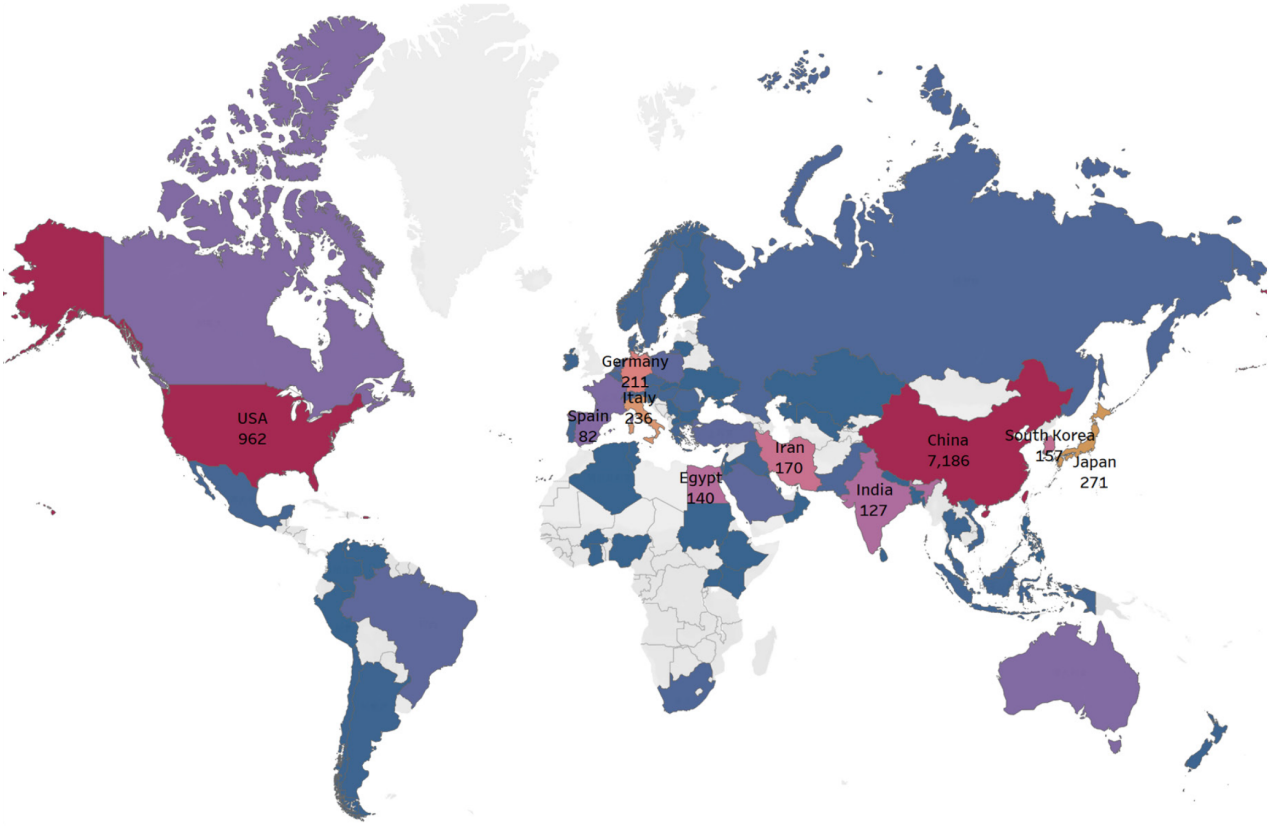

DOI: 10.5306/wjco.v15.i1.145 **Copyright** ©The Author(s) 2024.

Figure 2 The number of articles in each country. The closer the color is to red, the higher the number of articles issued in this country.

entative and provided some cooperation situation information.

Keywords analysis could discover emerging trends or study frontiers in the field of miRNAs in HCC. In our study, we used Bibliometrix and CiteSpace software to analyze the active keywords mentioned most frequently in the research papers related to miRNA in HCC. The top 20 keywords with the highest frequency were "expression", "cancer", "metastasis", "proliferation", "invasion", "growth", "down-regulation", "apoptosis", "progression", "cells", "migration", "breast-cancer", "cell-proliferation", "tumor-suppressor", "promotes", "epithelial-mesenchymal transition", "gene", "colorectal-cancer", "identification" and "gastric-cancer". Based on this result, we conclude that the studies of miRNAs focus on their expression level and impact on the biological behaviour in HCC, as well as the mechanism exploration.

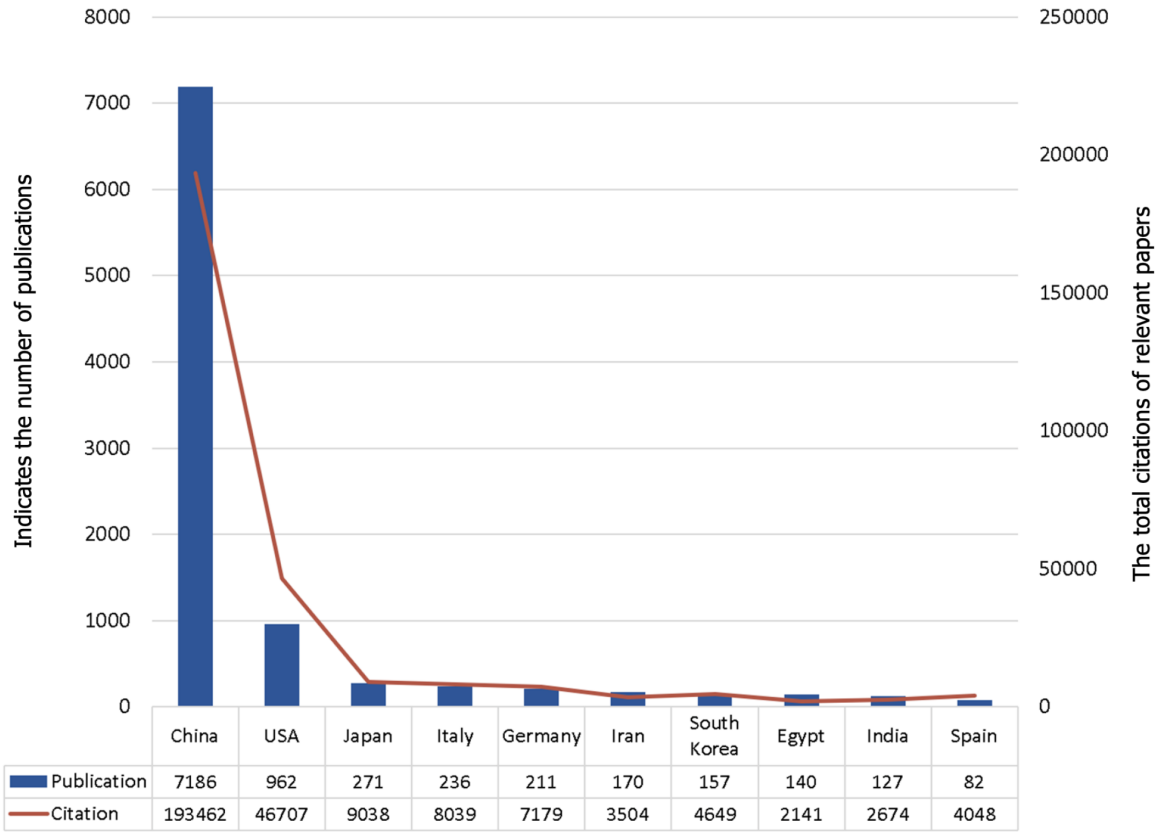

DOI: 10.5306/wjco.v15.i1.145

Figure 3 Top 10 countries with most publications and citations.

Interestingly, other tumor types also appeared in our results. After carefully reviewing the included literature, we found studies on tumors having different miRNA, and the miRNA in one tumor can also be applied to other tumors. This suggests that searching for specific miRNAs in one type of tumor and finding miRNAs with similar effects in multiple types of tumors is routine in tumor research. For example, we found that miR-21-3p plays an important role in the progression of multiple tumors, such as HCC, lung cancer, colorectal cancer, breast cancer and ovarian cancer[22-26].

Keywords bursting analysis shows that in the early years (2013–2017), "microRNA expression", "gene", "*in vivo*", "human hepatocellular carcinoma", "gene expression", "functional polymorphism", "circulating microRNA", "expression profile", "hepatocarcinogenesis", "susceptibility", "pre microRNA", "tumor suppressor gene", "liver" and "mir 21" started to attract attention. In the latest phase (2018–2022), the hot topics turned to "statistics", "ceRNA", "lncRNA", "sorafenib resistance", "circular RNA" and "tumor microenvironment". At the early exploration stage, laboratory techniques such as Northern blotting and quantitative polymerase chain reaction were the main methods for studying miRNA expression. Further exploration of miRNAs was limited to some extent by the limitations of these techniques. The development of sequencing technology has greatly promoted the research of miRNAs in various diseases [27]. For example, Murakami *et al*[28] used next-generation sequencing and microarrays to evaluate the miRNA expression profile of HCC and detected novel miRNAs that could not be detected by microarrays, providing diagnostic insights for the study of miRNAs in HCC.

Polymorphism is mainly concentrated in the early stages of relevant research in the timeline spectrum, and as a major keyword, it shows significant significance. The same gene or protein exhibits different functions in different environments or cells, indicating polymorphism. Therefore, the high-frequency occurrence periods of polymorphism, gene, and gene expression are basically coincident. This polymorphism is closely related to the risk of HCC occurrence and progression[29-32]. For example, after long-term alcohol exposure, liver cells lacking ALDH2 produce a large amount of harmful oxidative mitochondrial DNA, which can be received by adjacent HCC cells. Subsequently, multiple carcinogenic pathways are activated, thereby promoting alcohol-related liver cancer[33]. With the growing understanding of the mechanism of miRNA action, research on polymorphism in HCC has shifted towards clinical drug therapy research, resulting in a decrease in the frequency of keyword occurrences. The deepening of miRNA research is often accompanied by the synchronization of circulating miRNA research, partly because circulating miRNAs exist in body fluids and have the characteristics of simple collection and detection for cancer prediction, showing high clinical application value and can be used as biomarkers for cancer[34-37].

The high-frequency occurrence period of the keyword susceptibility was almost in the early and middle stages of the entire related research. This is because studying the sensitivity of miRNAs can help determine which miRNAs have therapeutic potential in HCC and provide a basis for individualized treatment of HCC. From the selection of miRNAs related to HCC to the predictive role of miRNAs in HCC, it has important research significance. In the study by Zhang *et*

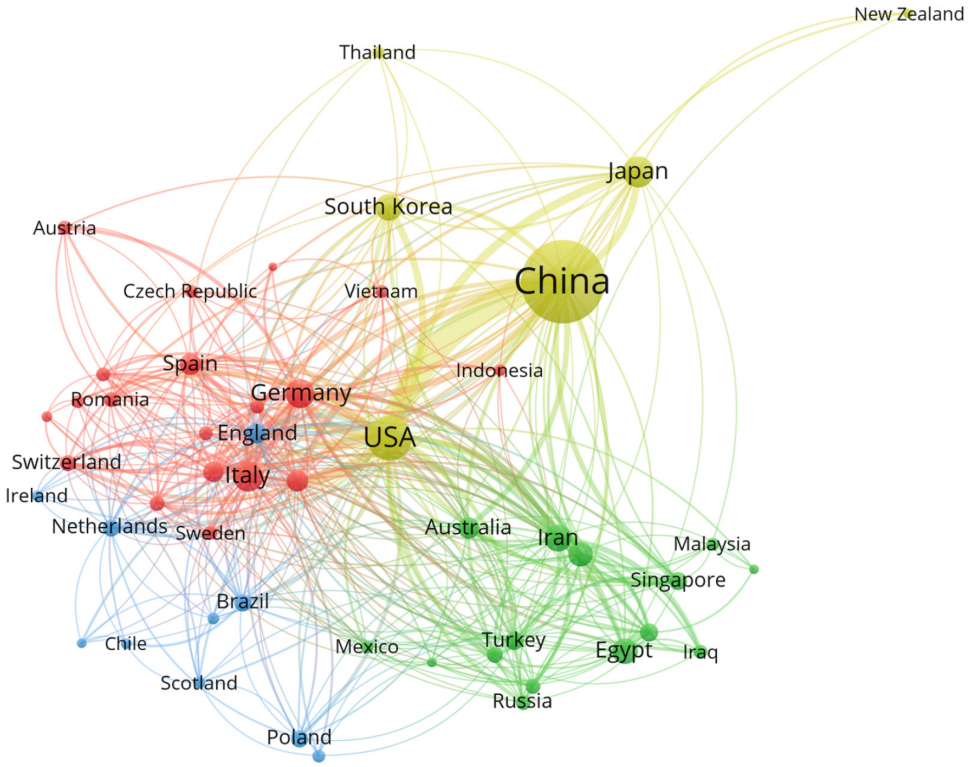

DOI: 10.5306/wjco.v15.i1.145 **Copyright** ©The Author(s) 2024.

Figure 4 Country-level cooperation network map. Each node represents a country, and the connecting lines indicate that there were associations between these countries, different colors identified different research communities.

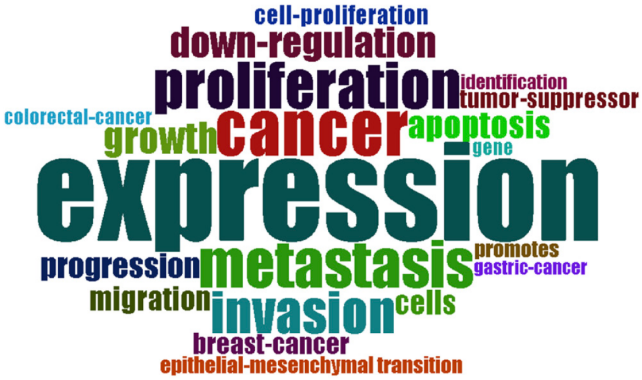

DOI: 10.5306/wjco.v15.i1.145 **Copyright** ©The Author(s) 2024.

Figure 5 Word cloud. A word cloud of the 20 most frequently used research keywords, the larger the font size the higher the frequency of occurrence.

al[38], it was found that miR-196a2 can be used as a predictive indicator of HCC sensitivity, especially for HBV-related HCC. Previous and mid-term studies have focused on understanding the occurrence and development of HCC; therefore, the keyword hepatocarcinogenesis contains the high-frequency occurrence period of relevant keywords. Existing preclinical studies and clinical trials have discovered different miRNA profiles in hepatocarcinogenesis. For example, miR-122 and miR-34a play important roles in hepatic lipid metabolism, which is associated with HCC[39,40]. miR-122 also has important roles in hepatic inflammation, as do miR-132 and miR-155[41-43]. miR-21 can mediate the activation of hepatic stellate cells *via* the PTEN/AKT pathway during hepatic fibrosis[44]. Hepatitis B virus (HBV) is the most common cause of HCC in China, and the miR-99 family can promote HBV replication, while miR-199-3p and miR-201 can suppress HBV replication[45,46]. A cohort study suggested that miR-221 and miR-222 play pivotal roles in the progression of liver fibrosis due to persistent hepatitis C virus (HCV) infection[47]. Another study demonstrated that miR-182 is associated with alcoholic hepatitis[48].

In 2013, Liu *et al*[49] used TargetScan, PicTar, and miRanda prediction algorithms based on the discovery of a new class of small molecule regulatory RNAs closely related to HCC and found that pre-microRNAs play important roles in cell differentiation and mitosis. Subsequent studies have proven that pre-microRNAs can not only mediate RNA splicing and cell signal transduction but also induce G1/S stagnation and may play a role in cancer. Meanwhile, Giacomo Diaz detected a complete set of 2226 human miRNAs, including 1121 pre-miRNAs, 1105 mature miRNAs, and several tumor

Top 20 Keywords with the strongest citation bursts

Keywords	Year	Strength	Begin	End	2013 - 2022
microrna expression	2013	28.26	**2013**	2016	
gene	2013	24.61	**2013**	2014	
in vivo	2013	19.75	**2013**	2016	
human hepatocellular carcinoma	2013	18.74	**2013**	2016	
gene expression	2013	18.7	**2013**	2014	
functional polymorphism	2013	16.84	**2013**	2014	
circulating microrna	2013	16.51	**2013**	2015	
expression profile	2013	15.18	**2013**	2015	
hepatocarcinogenesis	2013	15.08	**2013**	2017	
susceptibility	2013	15.02	**2013**	2016	
pre microrna	2013	14.96	**2013**	2014	
tumor suppressor gene	2013	14.74	**2013**	2016	
liver	2013	13.08	**2013**	2014	
mir 21	2013	12.99	**2013**	2015	
statistics	2018	14.15	**2018**	2020	
cerna	2018	17.67	**2019**	2022	
lncrna	2018	16.27	**2019**	2022	
sorafenib resistance	2019	12.77	**2019**	2022	
circular rna	2017	50.28	**2020**	2022	
tumor microenvironment	2020	15.03	**2020**	2022	

DOI: 10.5306/wjco.v15.i1.145 **Copyright** ©The Author(s) 2024.

Figure 6 Top 20 keywords with the strongest citation burst. In the graph on the right, the red line indicates the keyword burst during this period.

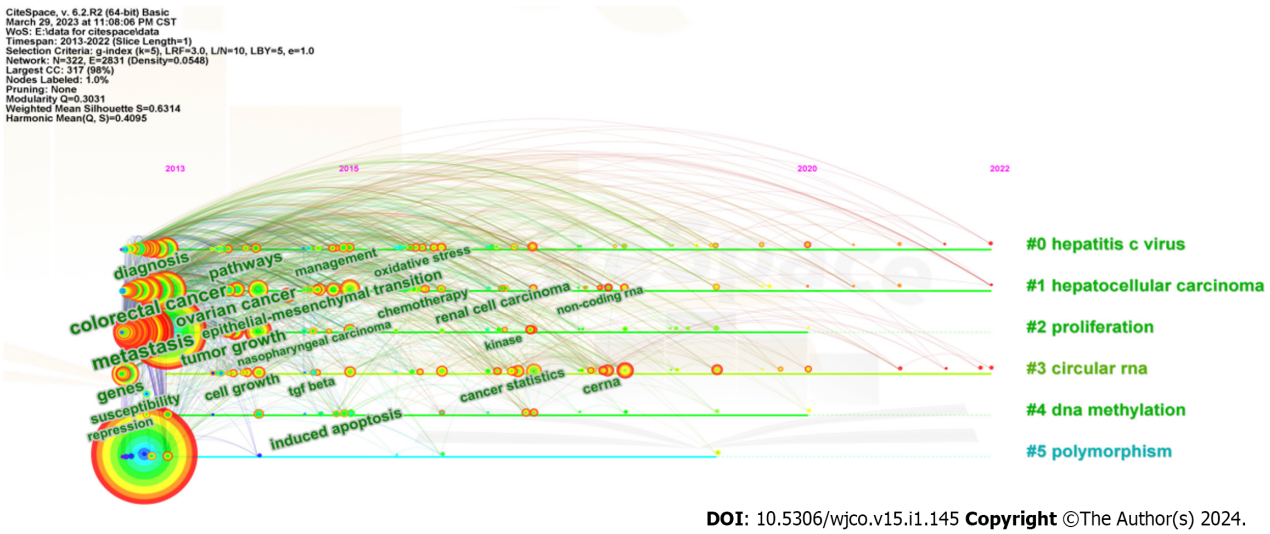

DOI: 10.5306/wjco.v15.i1.145 **Copyright** ©The Author(s) 2024.

Figure 7 The timeline spectrum of keywords in the research articles related to microRNAs in hepatocellular carcinoma.

suppressors, by comparing tumor tissue with a wide range of liver specimens, further confirming that inactivation of tumor suppressors is the cause of most human cancer development[50]. In the following years, a large amount of research was conducted on tumor suppressor factors. Hishida *et al*[51] invented the triple array analysis method, which identified genes with altered expression through gene expression profiles, single nucleotide polymorphisms, and methylation arrays and subsequently identified tumor suppressor genes. Subsequently, a large number of tumor suppressors were confirmed.

From 2013 to 2015, studies were conducted on miR-21 (one of the most frequently overexpressed small RNAs in cancer). Wagenaar *et al*[52] used cell culture and found that miR-21 is related to the regulation of cell metabolism and is cell environment dependent. In 2019-2022, Wang, Antonio, and others identified the carcinogenic lncRNA lncUCID and

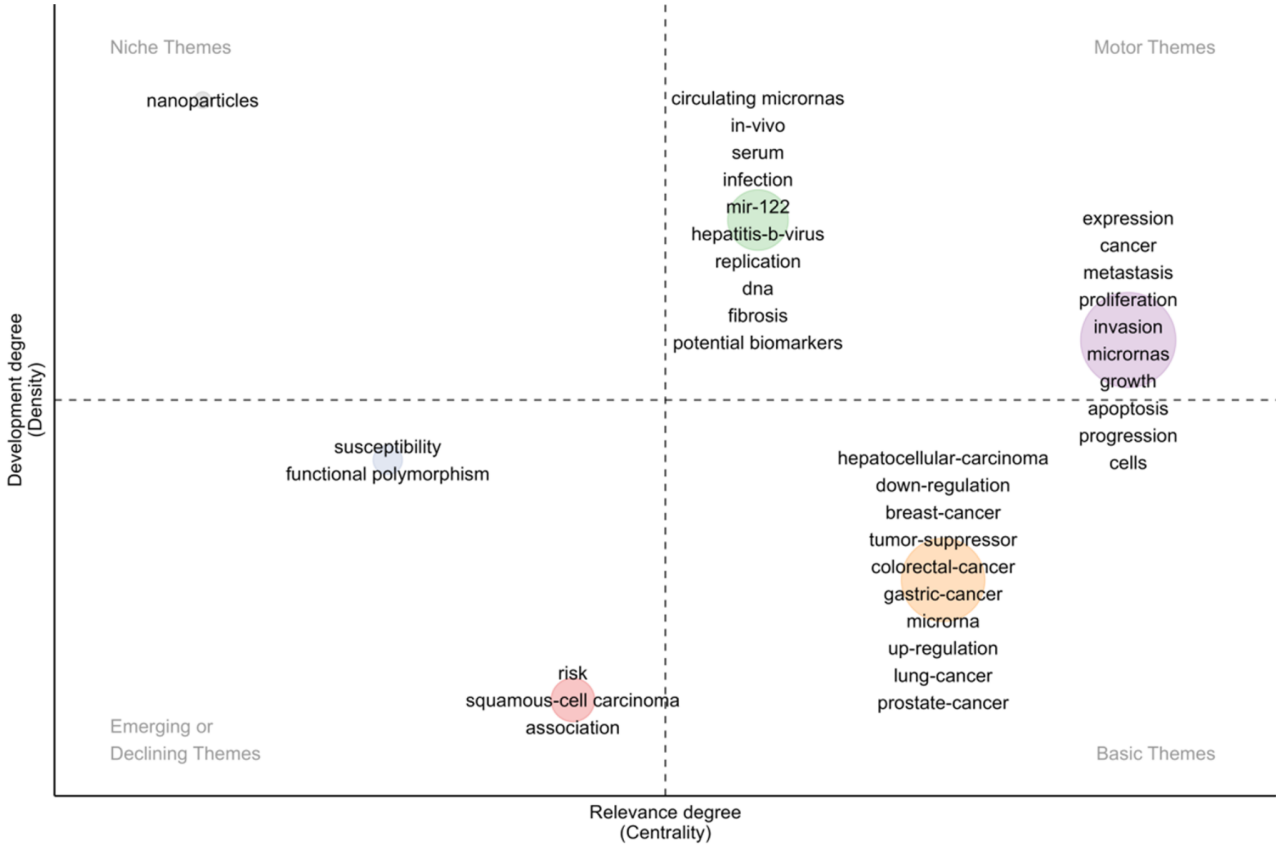

DOI: 10.5306/wjco.v15.i1.145

Figure 8 Thematic map of keywords in the research articles related to microRNAs in hepatocellular carcinoma.

its role in the BRAF pathway. They found that upregulation of lncUCID can enhance CDK6 expression and promote HCC growth. The lncRNA of BRAF is associated with cancer proliferation and tyrosine kinase inhibitor escape in HCC, and inhibiting the use of lncRNA in the BRAF pathway may become a possible therapeutic strategy for HCC. These findings provide insights into the biological function of lncRNAs, the regulatory network of cell cycle control, and the development mechanism of HCC[53,54].

The keyword "sorafenib resistance" appeared frequently in 2019-2022 because sorafenib became the first-line treatment drug for HCC and has been shown to effectively improve the prognosis of patients with advanced HCC by strong evidence and clinical experience[55-60]. However, according to the research of Tang Weiwei and others, the number of patients who can benefit from sorafenib is small (30%), and the population usually develops drug resistance within 6 months. The adverse events found in patients receiving sorafenib treatment mainly include digestive and skin diseases and may even cause hypertension and abdominal pain, leading to treatment interruption. Therefore, it is urgent to study the drug resistance mechanism of sorafenib and more reasonable clinical treatment methods[61]. Studies have explored various relationships between miRNAs and sorafenib. For example, miR-23a-3p contributes to sorafenib resistance in HCC by regulating ferroptosis[62]. miR-10b-3p can be a biomarker for predicting sorafenib efficacy[63]. miR-494-3p promotes sorafenib resistance in HCC cells by targeting PTEN[64]. Wang *et al*[65] found that compared with patients with HCC treated with sorafenib, patients treated with lenvatinib developed 3 differentially expressed miRNAs, including miR-548ah, miR-888 and miR-196a-1. Wang *et al*[65] further investigated the adverse events of sorafenib and lenvatinib and found that the patients in the sorafenib group and lenvatinib group developed different frequent symptoms, such as hypertension, diarrhoea and hand-foot skin reactions. At present, systemic therapy has become the standard therapy for unresectable HCC in the middle and late stages. Small molecule antiangiogenic targeted drugs and immune checkpoint inhibitors are the main systemic therapy options. The combination of the two often has a synergistic effect and improves the prognosis of HCC patients. During the use of these systems for treatment, changes in miRNA expression profiles and levels in HCC patients may have important value in predicting drug efficacy, drug-related adverse events and prognosis [66].

From 2020 to 2022, research in the field of miRNAs in HCC began to focus on the "tumor microenvironment". The tumor microenvironment is a complex environment in which tumor cells survive and develop, including surrounding blood vessels, immune cells, fibroblasts, bone marrow-derived inflammatory cells, various signaling molecules and the extracellular matrix. As the location of tumor cells survival, the tumor microenvironment plays a vital role in the occurrence, development, and metastasis of tumors. The amount of research on the tumor microenvironment in HCC has gradually increased, and some studies have focused on the mechanism, which involves some miRNAs. For example, Zhou *et al*[67] found that exosomal miR-761 modulated the tumor microenvironment *via* SOCS2/JAK2/STAT3 pathway-dependent activation of cancer-associated fibroblasts. In the research of Yugawa *et al*[68], the findings suggested that the

loss of antitumoral miR-150-3p in cancer-associated fibroblast-derived exosomes greatly promotes HCC progression. Research on the effect of miRNAs on the tumor microenvironment can provide more therapeutic strategies for HCC.

The thematic map is a two-dimensional map constructed with the density index as the vertical axis and the centrality index as the horizontal axis. Density represents the strength of the connections between basic knowledge units within a single topic. If the density value of a certain topic is higher, it indicates that the maturity of the topic is higher. Centrality represents the strength of the connection between a certain topic and other topics. If the centrality value of a certain topic is higher, it indicates that the topic is closely related to other topics and is at the core of all research topics. According to the density and centrality value, the rectangular coordinate system is divided into four regions: Motor Themes, a core theme with high maturity; Niche Themes, a highly mature isolated theme; Emerging or Declining Themes, new or disappearing themes; Basic Themes, a basic theme with low maturity and some influence but has not been well developed and should continue to be strengthened in the future. According to our results, themes such as "susceptibility", "functional polymorphism", "risk", "squamous-cell carcinoma" and "association" are the new or disappearing themes, while "nanoparticles" is a highly mature but isolated theme. "Expression", "cancer", "metastasis", "proliferation", "invasion", "microRNAs", "growth", "apoptosis", "progression", "cells", "circulating microRNAs", "in-vivo", "serum", "infection", "mir-122", "hepatitis-b-virus", "replication", "DNA", "fibrosis" and "potential biomarkers" are the mainstream themes. "Hepatocellular-carcinoma", "down-regulation", "breast-cancer", "tumor-suppressor", "colorectal-cancer", "gastric-cancer", "microRNA", "up-regulation", "lung-cancer" and "prostate-cancer" are the basic themes with low maturity, which have some influence but have not been well developed and should continue to be strengthened in the future.

Strengths and limitations

This study is novel for its comprehensive extraction and evaluation of research outputs from the available global data to explore the relationship between miRNA and HCC. However, there are also some limitations in this study. For example, it did not include all relevant literature and was limited to the Web of Science Core Collection database, which may lead to selection bias. Meanwhile, some recently published high-quality papers might not be highlighted due to low citation frequency because of the short time since their publication.

CONCLUSION

Our study provides a comprehensive overview of the role of miRNAs in HCC development from 2013 to 2022 based on bibliometric analysis. According to the keywords analysis, we found that the studies of miRNAs focused on their expression level, effects, and mechanisms on the biological behaviour of HCC. Keywords bursting analysis showed that in the early years (2013–2017), "microRNA expression", "gene expression", "expression profile", "functional polymorphism", "circulating microRNA", "susceptibility" and "mir 21" started to attract attention. In the latest phase (2018–2022), the hot topics turned to "sorafenib resistance", "tumor microenvironment" and so on.

ARTICLE HIGHLIGHTS

Research background

Over the past 10 years, studies have increasingly focused on the role of microRNAs (miRNAs) in hepatocellular carcinoma (HCC), generating significant scientific output. The accumulated knowledge needs to be systematically organized in order to improve research efficiency.

Research motivation

The purpose of this article is to make a comprehensive analysis of recent studies concerning miRNAs in HCC.

Research objectives

We aim to systematically analyze the research on miRNAs in HCC in the past decade. A comprehensive analysis of recent research concerning miRNAs in HCC development could provide researchers with a valuable reference for further studies.

Research methods

This study collected relevant publications from the Web of Science Core Collection database (https://www.webofscience.com/) with a specific search strategy and the limited time frame was from 2013 to 2022. Bibliometrix software, VOSviewer software and CiteSpace software were used to visually analyze the distribution by time, countries, institutions, journals, and authors, as well as the keywords, burst keywords and thematic map.

Research results

A total of 9426 publications on this topic were found worldwide. According to the keywords analysis, we found that the studies of miRNAs focused on their expression level, effects, and mechanisms on the biological behaviour of HCC. Keywords bursting analysis showed that in the early years (2013–2017), "microRNA expression", "gene expression",

"expression profile", "functional polymorphism", "circulating microRNA", "susceptibility" and "mir 21" started to attract attention. In the latest phase (2018–2022), the hot topics turned to "sorafenib resistance", "tumor microenvironment" and so on.

Research conclusions

This study provides a comprehensive overview of the role of miRNAs in HCC development based on bibliometric analysis. The hotspots in this field focus on miRNAs expression level, effects, and mechanisms on the biological behavior of HCC. The frontiers turned to sorafenib resistance, tumor microenvironment and so on.

Research perspectives

Future research should focus on the application value of miRNAs as biomarkers in predicting clinical treatment outcomes and prognosis in HCC patients.

ACKNOWLEDGEMENTS

We would like to thank "Guangxi Zhuang Autonomous Region Clinical Medicine Research Center for Molecular Pathology and Intelligent Pathology Precision Diagnosis" for providing technical support.

FOOTNOTES

Author contributions: Zhang L and Chen G conceived and designed the study. Zhang L, Chen ZY, Wei XX and Li JD searched the publications from Web of Science and decided which paper to be included, analyzed the data and made all the graphs; Zhang L drafted the manuscript; Chen G revised the manuscript.

Supported by Guangxi Zhuang Autonomous Region Health Commission Self-Financed Scientific Research Project, No. Z20201174; Innovation Project of Guangxi Graduate Education, No. YCBZ2023110; Guangxi Higher Education Undergraduate Teaching Reform Project, No. 2022JGA146; Guangxi Educational Science Planning Key Project, No. 2022ZJY2791; and Guangxi Medical High-level Key Talents Training "139" Program (2020).

Conflict-of-interest statement: All the authors report no relevant conflicts of interest for this article.

PRISMA 2009 Checklist statement: The authors have read the PRISMA 2009 Checklist, and the manuscript was prepared and revised according to the PRISMA 2009 Checklist.

Country/Territory of origin: China

ORCID number: Lu Zhang 0009-0004-0981-995X; Gang Chen 0000-0003-2402-2987.

S-Editor: Liu JH
L-Editor: A
P-Editor: Zhang XD

REFERENCES

1 **Rumgay H**, Arnold M, Ferlay J, Lesi O, Cabasag CJ, Vignat J, Laversanne M, McGlynn KA, Soerjomataram I. Global burden of primary liver cancer in 2020 and predictions to 2040. *J Hepatol* 2022; **77**: 1598-1606 [PMID: 36208844 DOI: 10.1016/j.jhep.2022.08.021]
2 **Li Q**, Cao M, Lei L, Yang F, Li H, Yan X, He S, Zhang S, Teng Y, Xia C, Chen W. Burden of liver cancer: From epidemiology to prevention. *Chin J Cancer Res* 2022; **34**: 554-566 [PMID: 36714347 DOI: 10.21147/j.issn.1000-9604.2022.06.02]
3 **Wei Q**, Zhou H, Hou X, Liu X, Chen S, Huang X, Chen Y, Liu M, Duan Z. Current status of and barriers to the treatment of advanced-stage liver cancer in China: a questionnaire-based study from the perspective of doctors. *BMC Gastroenterol* 2022; **22**: 351 [PMID: 35871649 DOI: 10.1186/s12876-022-02425-4]
4 **Vogel A**, Meyer T, Sapisochin G, Salem R, Saborowski A. Hepatocellular carcinoma. *Lancet* 2022; **400**: 1345-1362 [PMID: 36084663 DOI: 10.1016/S0140-6736(22)01200-4]
5 **Llovet JM**, Montal R, Sia D, Finn RS. Molecular therapies and precision medicine for hepatocellular carcinoma. *Nat Rev Clin Oncol* 2018; **15**: 599-616 [PMID: 30061739 DOI: 10.1038/s41571-018-0073-4]
6 **Shi YH**, Wen TF, Xiao DS, Dai LB, Song J. Predicting miRNA targets for hepatocellular carcinoma with an integrated method. *Transl Cancer Res* 2020; **9**: 1752-1760 [PMID: 35117522 DOI: 10.21037/tcr.2020.02.46]

7 **Ho PTB**, Clark IM, Le LTT. MicroRNA-Based Diagnosis and Therapy. *Int J Mol Sci* 2022; **23** [PMID: 35806173 DOI: 10.3390/ijms23137167]

8 **Chen S**, Wang Y, Li D, Wang H, Zhao X, Yang J, Chen L, Guo M, Zhao J, Chen C, Zhou Y, Liang G, Xu L. Mechanisms Controlling MicroRNA Expression in Tumor. *Cells* 2022; **11** [PMID: 36139427 DOI: 10.3390/cells11182852]

9 **Zeng Z**, Cai J, Liao Y, Sun S, Xie L. Progress in the effect of microRNA-21 on diseases *via* autophagy. *Zhong Nan Da Xue Xue Bao Yi Xue Ban* 2022; **47**: 936-941 [PMID: 36039591 DOI: 10.11817/j.issn.1672-7347.2022.210647]

10 **Hamidi AA**, Taghehchian N, Basirat Z, Zangouei AS, Moghbeli M. MicroRNAs as the critical regulators of cell migration and invasion in thyroid cancer. *Biomark Res* 2022; **10**: 40 [PMID: 35659780 DOI: 10.1186/s40364-022-00382-4]

11 **Luo Y**, Peng L, Shan W, Sun M, Luo L, Liang W. Machine learning in the development of targeting microRNAs in human disease. *Front Genet* 2022; **13**: 1088189 [PMID: 36685965 DOI: 10.3389/fgene.2022.1088189]

12 **Kousar K**, Ahmad T, Abduh MS, Kanwal B, Shah SS, Naseer F, Anjum S. miRNAs in Regulation of Tumor Microenvironment, Chemotherapy Resistance, Immunotherapy Modulation and miRNA Therapeutics in Cancer. *Int J Mol Sci* 2022; **23** [PMID: 36430305 DOI: 10.3390/ijms232213822]

13 **Entezari M**, Taheriazam A, Orouei S, Fallah S, Sanaei A, Hejazi ES, Kakavand A, Rezaei S, Heidari H, Behroozaghdam M, Daneshi S, Salimimoghadam S, Mirzaei S, Hashemi M, Samarghandian S. LncRNA-miRNA axis in tumor progression and therapy response: An emphasis on molecular interactions and therapeutic interventions. *Biomed Pharmacother* 2022; **154**: 113609 [PMID: 36037786 DOI: 10.1016/j.biopha.2022.113609]

14 **Yao D**, Nong L, Qin M, Wu S, Yao S. Identifying circRNA-miRNA interaction based on multi-biological interaction fusion. *Front Microbiol* 2022; **13**: 987930 [PMID: 36620017 DOI: 10.3389/fmicb.2022.987930]

15 **Huang T**, Wu Z, Zhu S. The roles and mechanisms of the lncRNA-miRNA axis in the progression of esophageal cancer: a narrative review. *J Thorac Dis* 2022; **14**: 4545-4559 [PMID: 36524088 DOI: 10.21037/jtd-22-1449]

16 **Nishita-Hiresha V**, Varsha R, Jayasuriya R, Ramkumar KM. The role of circRNA-miRNA-mRNA interaction network in endothelial dysfunction. *Gene* 2023; **851**: 146950 [PMID: 36228866 DOI: 10.1016/j.gene.2022.146950]

17 **Ishaq Y**, Ikram A, Alzahrani B, Khurshid S. The Role of miRNAs, circRNAs and Their Interactions in Development and Progression of Hepatocellular Carcinoma: An Insilico Approach. *Genes (Basel)* 2022; **14** [PMID: 36672755 DOI: 10.3390/genes14010013]

18 **Wang C**, Su K, Lin H, Cen B, Zheng S, Xu X. Identification and Verification of a Novel MAGI2-AS3/miRNA-374-5p/FOXO1 Network Associated with HBV-Related HCC. *Cells* 2022; **11** [PMID: 36359865 DOI: 10.3390/cells11213466]

19 **Hwang H**, Chang HR, Baek D. Determinants of Functional MicroRNA Targeting. *Mol Cells* 2023; **46**: 21-32 [PMID: 36697234 DOI: 10.14348/molcells.2023.2157]

20 **Wang H**, Meng Q, Qian J, Li M, Gu C, Yang Y. Review: RNA-based diagnostic markers discovery and therapeutic targets development in cancer. *Pharmacol Ther* 2022; **234**: 108123 [PMID: 35121000 DOI: 10.1016/j.pharmthera.2022.108123]

21 **Ninkov A**, Frank JR, Maggio LA. Bibliometrics: Methods for studying academic publishing. *Perspect Med Educ* 2022; **11**: 173-176 [PMID: 34914027 DOI: 10.1007/s40037-021-00695-4]

22 **Hong Y**, Ye M, Wang F, Fang J, Wang C, Luo J, Liu J, Liu L, Zhao Q, Chang Y. MiR-21-3p Promotes Hepatocellular Carcinoma Progression *via* SMAD7/YAP1 Regulation. *Front Oncol* 2021; **11**: 642030 [PMID: 33763375 DOI: 10.3389/fonc.2021.642030]

23 **Zhang YQ**, Chen RL, Shang LQ, Yang SM. Nicotine-induced miR-21-3p promotes chemoresistance in lung cancer by negatively regulating FOXO3a. *Oncol Lett* 2022; **24**: 260 [PMID: 35765274 DOI: 10.3892/ol.2022.13380]

24 **Jiao W**, Leng X, Zhou Q, Wu Y, Sun L, Tan Y, Ni H, Dong X, Shen T, Liu Y, Li J. Different miR-21-3p isoforms and their different features in colorectal cancer. *Int J Cancer* 2017; **141**: 2103-2111 [PMID: 28734015 DOI: 10.1002/ijc.30902]

25 **Amirfallah A**, Knutsdottir H, Arason A, Hilmarsdottir B, Johannsson OT, Agnarsson BA, Barkardottir RB, Reynisdottir I. Hsa-miR-21-3p associates with breast cancer patient survival and targets genes in tumor suppressive pathways. *PLoS One* 2021; **16**: e0260327 [PMID: 34797887 DOI: 10.1371/journal.pone.0260327]

26 **Fang W**, Xia Y. LncRNA HLA-F-AS1 attenuates the ovarian cancer development by targeting miR-21-3p/PEG3 axis. *Anticancer Drugs* 2022; **33**: 671-681 [PMID: 35276697 DOI: 10.1097/CAD.0000000000001288]

27 **Lokhande HA**. Bioinformatics Analysis of miRNA Sequencing Data. *Methods Mol Biol* 2023; **2595**: 225-237 [PMID: 36441466 DOI: 10.1007/978-1-0716-2823-2_16]

28 **Murakami Y**, Tanahashi T, Okada R, Toyoda H, Kumada T, Enomoto M, Tamori A, Kawada N, Taguchi YH, Azuma T. Comparison of hepatocellular carcinoma miRNA expression profiling as evaluated by next generation sequencing and microarray. *PLoS One* 2014; **9**: e106314 [PMID: 25215888 DOI: 10.1371/journal.pone.0106314]

29 **Rao K**, Zheng K, Zhao Q, He J, Zhou B, Hou G, Sha N, Wang W, Yan M, Zhou Y, Jin Y, Jiang Y, Xia Q. The negative effect of G1958A polymorphism on MTHFD1 protein stability and HCC growth. *Cell Oncol (Dordr)* 2023; **46**: 735-744 [PMID: 36913067 DOI: 10.1007/s13402-023-00780-2]

30 **Ambrozkiewicz F**, Trailin A, Červenková L, Vaclavikova R, Hanicinec V, Allah MAO, Palek R, Třeška V, Daum O, Tonar Z, Liška V, Hemminki K. CTNNB1 mutations, TERT polymorphism and CD8+ cell densities in resected hepatocellular carcinoma are associated with longer time to recurrence. *BMC Cancer* 2022; **22**: 884 [PMID: 35962322 DOI: 10.1186/s12885-022-09989-0]

31 **Mohamed AA**, Esmail OE, Ibrahim AMA, Makled S, Al-Hussain E, Elsaid A, Alboraie M, El-Awady RR. The role of PRDM1 gene polymorphism in the progression of hepatocellular carcinoma in Egyptian patients. *J Med Virol* 2023; **95**: e28343 [PMID: 36424348 DOI: 10.1002/jmv.28343]

32 **Youssef SS**, Youness RA, Abbas EAE, Osman NM, ELFiky A, El-Kassas M. miR-516a-3P, a potential circulating biomarker in hepatocellular carcinoma, correlated with rs738409 polymorphism in PNPLA3. *Per Med* 2022; **19**: 483-493 [PMID: 36239555 DOI: 10.2217/pme-2022-0005]

33 **Seo W**, Gao Y, He Y, Sun J, Xu H, Feng D, Park SH, Cho YE, Guillot A, Ren T, Wu R, Wang J, Kim SJ, Hwang S, Liangpunsakul S, Yang Y, Niu J, Gao B. ALDH2 deficiency promotes alcohol-associated liver cancer by activating oncogenic pathways *via* oxidized DNA-enriched extracellular vesicles. *J Hepatol* 2019; **71**: 1000-1011 [PMID: 31279903 DOI: 10.1016/j.jhep.2019.06.018]

34 **Yu B**, Zhou S, Liang H, Ye Q, Wang Y. Development and Validation of a Novel Circulating miRNA-Based Diagnostic Score for Early Detection of Hepatocellular Carcinoma. *Dig Dis Sci* 2022; **67**: 2283-2292 [PMID: 33982217 DOI: 10.1007/s10620-021-07031-0]

35 **Yousuf T**, Dar SB, Bangri SA, Choh NA, Rasool Z, Shah A, Rather RA, Rah B, Bhat GR, Ali S, Afroze D. Diagnostic implication of a circulating serum-based three-microRNA signature in hepatocellular carcinoma. *Front Genet* 2022; **13**: 929787 [PMID: 36457743 DOI: 10.3389/fgene.2022.929787]

36 **Ding LH**, Fallgren CM, Yu Y, McCarthy M, Edmondson EF, Ullrich RL, Weil MM, Story MD. Orthologs of human circulating miRNAs associated with hepatocellular carcinoma are elevated in mouse plasma months before tumour detection. *Sci Rep* 2022; **12**: 10927 [PMID: 35764780 DOI: 10.1038/s41598-022-15061-5]

37 **Tork ASE**, Kamel AAF, Zaki MA, Abo El-Wafa RAH, El-Assar OS, Ibrahim Abdelkarem OA. Circulating MiRNA-373 as a Predictor of Response to Super-selective Transarterial Chemoembolization Bridging Therapy in Hepatocellular Carcinoma Patients Awaiting Liver Transplantation. *Asian Pac J Cancer Prev* 2023; **24**: 291-299 [PMID: 36708579 DOI: 10.31557/APJCP.2023.24.1.291]

38 **Zhang Q**, Xu X, Wu M, Qin T, Wu S, Liu H. MiRNA Polymorphisms and Hepatocellular Carcinoma Susceptibility: A Systematic Review and Network Meta-Analysis. *Front Oncol* 2020; **10**: 562019 [PMID: 33542895 DOI: 10.3389/fonc.2020.562019]

39 **Cheung O**, Puri P, Eicken C, Contos MJ, Mirshahi F, Maher JW, Kellum JM, Min H, Luketic VA, Sanyal AJ. Nonalcoholic steatohepatitis is associated with altered hepatic MicroRNA expression. *Hepatology* 2008; **48**: 1810-1820 [PMID: 19030170 DOI: 10.1002/hep.22569]

40 **Ding J**, Li M, Wan X, Jin X, Chen S, Yu C, Li Y. Effect of miR-34a in regulating steatosis by targeting PPARα expression in nonalcoholic fatty liver disease. *Sci Rep* 2015; **5**: 13729 [PMID: 26330104 DOI: 10.1038/srep13729]

41 **Hsu SH**, Wang B, Kota J, Yu J, Costinean S, Kutay H, Yu L, Bai S, La Perle K, Chivukula RR, Mao H, Wei M, Clark KR, Mendell JR, Caligiuri MA, Jacob ST, Mendell JT, Ghoshal K. Essential metabolic, anti-inflammatory, and anti-tumorigenic functions of miR-122 in liver. *J Clin Invest* 2012; **122**: 2871-2883 [PMID: 22820288 DOI: 10.1172/JCI63539]

42 **Strum JC**, Johnson JH, Ward J, Xie H, Feild J, Hester A, Alford A, Waters KM. MicroRNA 132 regulates nutritional stress-induced chemokine production through repression of SirT1. *Mol Endocrinol* 2009; **23**: 1876-1884 [PMID: 19819989 DOI: 10.1210/me.2009-0117]

43 **Bala S**, Petrasek J, Mundkur S, Catalano D, Levin I, Ward J, Alao H, Kodys K, Szabo G. Circulating microRNAs in exosomes indicate hepatocyte injury and inflammation in alcoholic, drug-induced, and inflammatory liver diseases. *Hepatology* 2012; **56**: 1946-1957 [PMID: 22684891 DOI: 10.1002/hep.25873]

44 **Wei J**, Feng L, Li Z, Xu G, Fan X. MicroRNA-21 activates hepatic stellate cells *via* PTEN/Akt signaling. *Biomed Pharmacother* 2013; **67**: 387-392 [PMID: 23643356 DOI: 10.1016/j.biopha.2013.03.014]

45 **Lin Y**, Deng W, Pang J, Kemper T, Hu J, Yin J, Zhang J, Lu M. The microRNA-99 family modulates hepatitis B virus replication by promoting IGF-1R/PI3K/Akt/mTOR/ULK1 signaling-induced autophagy. *Cell Microbiol* 2017; **19** [PMID: 27886437 DOI: 10.1111/cmi.12709]

46 **Zhang GL**, Li YX, Zheng SQ, Liu M, Li X, Tang H. Suppression of hepatitis B virus replication by microRNA-199a-3p and microRNA-210. *Antiviral Res* 2010; **88**: 169-175 [PMID: 20728471 DOI: 10.1016/j.antiviral.2010.08.008]

47 **Abdel-Al A**, El-Ahwany E, Zoheiry M, Hassan M, Ouf A, Abu-Taleb H, Abdel Rahim A, El-Talkawy MD, Zada S. miRNA-221 and miRNA-222 are promising biomarkers for progression of liver fibrosis in HCV Egyptian patients. *Virus Res* 2018; **253**: 135-139 [PMID: 29932949 DOI: 10.1016/j.virusres.2018.06.007]

48 **Blaya D**, Coll M, Rodrigo-Torres D, Vila-Casadesús M, Altamirano J, Llopis M, Graupera I, Perea L, Aguilar-Bravo B, Díaz A, Banales JM, Clària J, Lozano JJ, Bataller R, Caballería J, Ginès P, Sancho-Bru P. Integrative microRNA profiling in alcoholic hepatitis reveals a role for microRNA-182 in liver injury and inflammation. *Gut* 2016; **65**: 1535-1545 [PMID: 27196584 DOI: 10.1136/gutjnl-2015-311314]

49 **Liu RY**, Diao CF, Zhang Y, Wu N, Wan HY, Nong XY, Liu M, Tang H. miR-371-5p down-regulates pre mRNA processing factor 4 homolog B (PRPF4B) and facilitates the G1/S transition in human hepatocellular carcinoma cells. *Cancer Lett* 2013; **335**: 351-360 [PMID: 23466643 DOI: 10.1016/j.canlet.2013.02.045]

50 **Diaz G**, Melis M, Tice A, Kleiner DE, Mishra L, Zamboni F, Farci P. Identification of microRNAs specifically expressed in hepatitis C virus-associated hepatocellular carcinoma. *Int J Cancer* 2013; **133**: 816-824 [PMID: 23390000 DOI: 10.1002/ijc.28075]

51 **Hishida M**, Nomoto S, Inokawa Y, Hayashi M, Kanda M, Okamura Y, Nishikawa Y, Tanaka C, Kobayashi D, Yamada S, Nakayama G, Fujii T, Sugimoto H, Koike M, Fujiwara M, Takeda S, Kodera Y. Estrogen receptor 1 gene as a tumor suppressor gene in hepatocellular carcinoma detected by triple-combination array analysis. *Int J Oncol* 2013; **43**: 88-94 [PMID: 23695389 DOI: 10.3892/ijo.2013.1951]

52 **Wagenaar TR**, Zabludoff S, Ahn SM, Allerson C, Arlt H, Baffa R, Cao H, Davis S, Garcia-Echeverria C, Gaur R, Huang SM, Jiang L, Kim D, Metz-Weidmann C, Pavlicek A, Pollard J, Reeves J, Rocnik JL, Scheidler S, Shi C, Sun F, Tolstykh T, Weber W, Winter C, Yu E, Yu Q, Zheng G, Wiederschain D. Anti-miR-21 Suppresses Hepatocellular Carcinoma Growth *via* Broad Transcriptional Network Deregulation. *Mol Cancer Res* 2015; **13**: 1009-1021 [PMID: 25758165 DOI: 10.1158/1541-7786.MCR-14-0703]

53 **Gnoni A**, Licchetta A, Memeo R, Argentiero A, Solimando AG, Longo V, Delcuratolo S, Brunetti O. Role of BRAF in Hepatocellular Carcinoma: A Rationale for Future Targeted Cancer Therapies. *Medicina (Kaunas)* 2019; **55** [PMID: 31766556 DOI: 10.3390/medicina55120754]

54 **Wang YL**, Liu JY, Yang JE, Yu XM, Chen ZL, Chen YJ, Kuang M, Zhu Y, Zhuang SM. Lnc-UCID Promotes G1/S Transition and Hepatoma Growth by Preventing DHX9-Mediated CDK6 Down-regulation. *Hepatology* 2019; **70**: 259-275 [PMID: 30865310 DOI: 10.1002/hep.30613]

55 **Zhang Z**, He CZ, Qin YQ, Liao JJ, Huang ST, Mo S, Li HM, Lin JY. Exploring the mechanism of resistance to sorafenib in two hepatocellular carcinoma cell lines. *Aging (Albany NY)* 2020; **12**: 24255-24269 [PMID: 33234725 DOI: 10.18632/aging.104195]

56 **Lin Z**, Xia S, Liang Y, Ji L, Pan Y, Jiang S, Wan Z, Tao L, Chen J, Lin C, Liang X, Xu J, Cai X. LXR activation potentiates sorafenib sensitivity in HCC by activating microRNA-378a transcription. *Theranostics* 2020; **10**: 8834-8850 [PMID: 32754282 DOI: 10.7150/thno.45158]

57 **Xu Y**, Huang J, Ma L, Shan J, Shen J, Yang Z, Liu L, Luo Y, Yao C, Qian C. MicroRNA-122 confers sorafenib resistance to hepatocellular carcinoma cells by targeting IGF-1R to regulate RAS/RAF/ERK signaling pathways. *Cancer Lett* 2016; **371**: 171-181 [PMID: 26655273 DOI: 10.1016/j.canlet.2015.11.034]

58 **Ji L**, Lin Z, Wan Z, Xia S, Jiang S, Cen D, Cai L, Xu J, Cai X. miR-486-3p mediates hepatocellular carcinoma sorafenib resistance by targeting FGFR4 and EGFR. *Cell Death Dis* 2020; **11**: 250 [PMID: 32313144 DOI: 10.1038/s41419-020-2413-4]

59 **Chen MY**, Yadav VK, Chu YC, Ong JR, Huang TY, Lee KF, Lee KH, Yeh CT, Lee WH. Correction: Chen *et al* Hydroxychloroquine (HCQ) Modulates Autophagy and Oxidative DNA Damage Stress in Hepatocellular Carcinoma to Overcome Sorafenib Resistance *via* TLR9/SOD1/hsa-miR-30a-5p/Beclin-1 Axis. Cancers 2021, 13, 3227. *Cancers (Basel)* 2023; **15** [PMID: 36831696 DOI: 10.3390/cancers15041028]

60 **Pratama MY**, Pascut D, Massi MN, Tiribelli C. The role of microRNA in the resistance to treatment of hepatocellular carcinoma. *Ann Transl Med* 2019; **7**: 577 [PMID: 31807558 DOI: 10.21037/atm.2019.09.142]

61 **Tang W**, Chen Z, Zhang W, Cheng Y, Zhang B, Wu F, Wang Q, Wang S, Rong D, Reiter FP, De Toni EN, Wang X. The mechanisms of sorafenib resistance in hepatocellular carcinoma: theoretical basis and therapeutic aspects. *Signal Transduct Target Ther* 2020; **5**: 87 [PMID: 32532960 DOI: 10.1038/s41392-020-0187-x]

62 **Lu Y**, Chan YT, Tan HY, Zhang C, Guo W, Xu Y, Sharma R, Chen ZS, Zheng YC, Wang N, Feng Y. Epigenetic regulation of ferroptosis *via*

ETS1/miR-23a-3p/ACSL4 axis mediates sorafenib resistance in human hepatocellular carcinoma. *J Exp Clin Cancer Res* 2022; **41**: 3 [PMID: 34980204 DOI: 10.1186/s13046-021-02208-x]

63 **Shao YY**, Chen PS, Lin LI, Lee BS, Ling A, Cheng AL, Hsu C, Ou DL. Low miR-10b-3p associated with sorafenib resistance in hepatocellular carcinoma. *Br J Cancer* 2022; **126**: 1806-1814 [PMID: 35236936 DOI: 10.1038/s41416-022-01759-w]

64 **Gao Y**, Yin Z, Qi Y, Peng H, Ma W, Wang R, Li W. Golgi phosphoprotein 3 promotes angiogenesis and sorafenib resistance in hepatocellular carcinoma *via* upregulating exosomal miR-494-3p. *Cancer Cell Int* 2022; **22**: 35 [PMID: 35073936 DOI: 10.1186/s12935-022-02462-9]

65 **Wang L**, Wang L, Xiao B, Cui M, Zhang B. Differences Between Sorafenib and Lenvatinib Treatment from Genetic and Clinical Perspectives for Patients with Hepatocellular Carcinoma. *Med Sci Monit* 2022; **28**: e934936 [PMID: 35473892 DOI: 10.12659/MSM.934936]

66 **Li J**, Bao H, Huang Z, Liang Z, Wang M, Lin N, Ni C, Xu Y. Little things with significant impact: miRNAs in hepatocellular carcinoma. *Front Oncol* 2023; **13**: 1191070 [PMID: 37274242 DOI: 10.3389/fonc.2023.1191070]

67 **Zhou XH**, Xu H, Xu C, Yan YC, Zhang LS, Sun Q, Wang WL, Shi YJ. Hepatocellular carcinoma-derived exosomal miRNA-761 regulates the tumor microenvironment by targeting the SOCS2/JAK2/STAT3 pathway. *World J Emerg Med* 2022; **13**: 379-385 [PMID: 36119773 DOI: 10.5847/wjem.j.1920-8642.2022.089]

68 **Yugawa K**, Yoshizumi T, Mano Y, Itoh S, Harada N, Ikegami T, Kohashi K, Oda Y, Mori M. Cancer-associated fibroblasts promote hepatocellular carcinoma progression through downregulation of exosomal miR-150-3p. *Eur J Surg Oncol* 2021; **47**: 384-393 [PMID: 32883551 DOI: 10.1016/j.ejso.2020.08.002]

World Journal of Clinical Oncology

Submit a Manuscript: https://www.f6publishing.com

World J Clin Oncol 2024 January 24; 15(1): 159-164

DOI: 10.5306/wjco.v15.i1.159

ISSN 2218-4333 (online)

CASE REPORT

Radiotherapy for hyoid bone metastasis from lung adenocarcinoma: A case report

Jonathan Hsu, Kambridge Hribar, Joseph Poen

Specialty type: Oncology

Provenance and peer review: Unsolicited article; Externally peer reviewed.

Peer-review model: Single blind

Peer-review report's scientific quality classification
Grade A (Excellent): 0
Grade B (Very good): B
Grade C (Good): 0
Grade D (Fair): 0
Grade E (Poor): 0

P-Reviewer: Li HL, China

Received: November 28, 2023
Peer-review started: November 28, 2023
First decision: December 7, 2023
Revised: December 21, 2023
Accepted: January 3, 2024
Article in press: January 3, 2024
Published online: January 24, 2024

Jonathan Hsu, Medical School, California University of Science and Medicine, Colton, CA 92324, United States

Kambridge Hribar, Department of Otolaryngology, ENT Consultants of Marin, Greenbrae, CA 94904, United States

Joseph Poen, Radiation Oncology, Marin Cancer Care, Greenbrae, CA 94904, United States

Corresponding author: Jonathan Hsu, Medical Assistant, Medical School, California University of Science and Medicine, 1501 Violet Street, Colton, CA 92324, United States.
jonathan.hsu@student.cusm.edu

Abstract

BACKGROUND

Metastasis to the hyoid bone is an exceptionally rare occurrence, with documented cases limited to breast, liver, colon, skin, lung, and prostate cancers. This report highlights an unusual case involving the metastasis of lung adenocarcinoma to the hyoid bone, accompanied by a distinctive headache. Previous documentation involved surgical resection of the hyoid mass. We present a case displaying the benefits of palliative radiotherapy.

CASE SUMMARY

A 72-year-old non-smoking, non-alcoholic woman, initially under investigation for a year-long elevation in absolute lymphocyte count, presented with a month-long history of intermittent throat pain. Despite negative findings in gastroenterological and otolaryngologic examinations, a contrast-enhanced chest computed tomography scan revealed a mediastinal mass and questionable soft tissue thickening in her left anterolateral neck. Subsequent imaging and biopsies confirmed the presence of lung adenocarcinoma metastasis to the hyoid bone. The patient was treated with platinum-based chemo-immunotherapy along with pembrolizumab. Ultimately, the lung cancer was unresponsive. Our patient opted for palliative radiation therapy instead of surgical resection to address her throat pain. As a result, her throat pain was alleviated, and it also incidentally resolved her chronic headaches. This is the second documented case of lung adenocarcinoma metastasizing to the hyoid bone.

CONCLUSION

Palliative radiotherapy may add to the quality of life in symptomatic patients with cancer metastatic to the hyoid bone.

Key Words: Metastasis; Radiotherapy; Adenocarcinoma; Hyoid; Throat; Headache; Case report

Core Tip: Metastasis of lung adenocarcinoma to the hyoid bone is exceedingly rare. This case report spotlights the value of palliative radiation therapy for throat pain in patients with tumors metastatic to the hyoid bone.

Citation: Hsu J, Hribar K, Poen J. Radiotherapy for hyoid bone metastasis from lung adenocarcinoma: A case report. *World J Clin Oncol* 2024; 15(1): 159-164
URL: https://www.wjgnet.com/2218-4333/full/v15/i1/159.htm
DOI: https://dx.doi.org/10.5306/wjco.v15.i1.159

INTRODUCTION

This case report accounts for the second reported instance of hyoid metastasis from lung adenocarcinoma. Metastatic tumors to the hyoid bone are rare, with sporadic instances reported in breast, liver, colon, skin, lung, and prostate cancers [1-6]. We present the case of a 72-year-old female patient with stage IV terminal lung cancer presenting with throat pain attributed to a metastatic tumor on the hyoid. Choosing radiotherapy over surgery, she experienced significant relief from her throat pain.

CASE PRESENTATION

Chief complaints

A 72-year-old white female patient presents to an otolaryngology clinic complaining of intermittent throat pain for the past month.

History of present illness

Symptoms of throat pain persisted for a month with no response to antibiotics, antihistamines, or acid reflux medications. Alongside the throat pain, she was experiencing left, lateral, posterior headaches and intermittent episodes of vertigo.

History of past illness

Patient with no history of smoking or alcohol presented with a mildly elevated absolute lymphocyte count (ALC) of 4336 in February 2020. She denied systemic symptoms of fevers, night sweats, or unintentional weight loss.

Personal and family history

The patient reported only a paternal history of prostate cancer and denied melanoma, skin and squamous cell carcinomas in her family.

Physical examination

No masses were appreciated on palpation of her neck, flexible laryngoscopy, nor esophageal endoscopy.

Laboratory examinations

Mildly elevated ALC of 4336 in February 2020. A CBC in 2021 demonstrated an increase in lymphocyte count with an ALC of 5645. Given this increase in lymphocytosis, the patient was referred to a hematologist to be worked up for follicular lymphoma.

Imaging examinations

A computed tomography (CT) scan of the chest abdomen pelvis with contrast was performed, which incidentally showed a single para mediastinal 2.8 cm mass in the upper left lung lobe and questionable soft tissue thickening in her left antero-lateral neck. Flow cytometry of her peripheral blood revealed an abnormal CD10 positive B-cell population, co-expressing CD20, CD19, and CD45 with low CD23 present, which is consistent with a follicular lymphoma. A CT neck with contrast, followed by magnetic resonance imaging (MRI) of the neck with and without contrast were ordered to further evaluate the neck tissue. The CT and MRI of the neck confirmed a focal soft tissue lesion with residual calcifications measuring 1.4 cm × 1.9 cm × 1.7 cm centered on the left limb of the hyoid bone (Figure 1). MRI of the neck also revealed a suspicious thyroid nodule which required an ultrasound to be further evaluated.

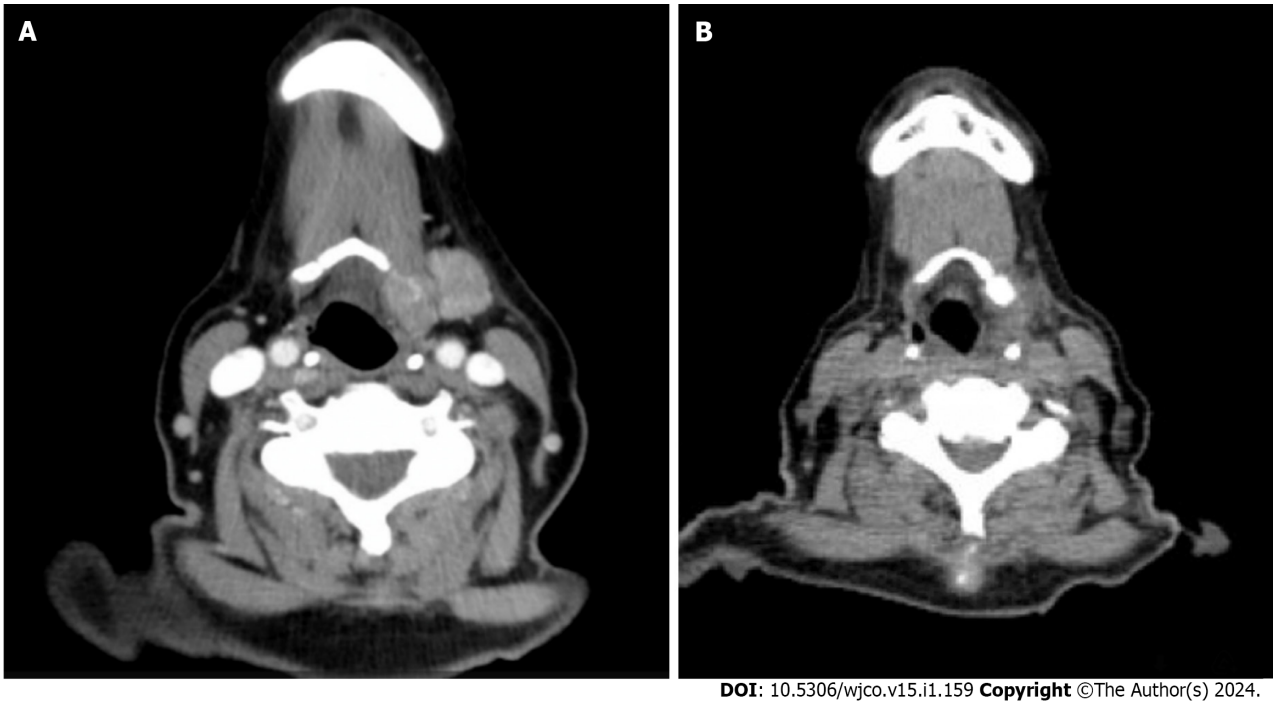

DOI: 10.5306/wjco.v15.i1.159

Figure 1 Computed tomography. A: Computed tomography (CT) neck w/ contrast pre-radiotherapy; B: CT neck w/contrast post radiotherapy.

Due to the improbability of follicular lymphoma in the anterior mediastinum without associated lymphadenopathy, a lung biopsy was recommended. A CT-guided biopsy of the mass in the upper left lung lobe mass identified it as invasive mucinous adenocarcinoma. Figure 2 displays the biomarkers tested for the diagnosis. Positron emission tomography (PET)/CT revealed both the ipsilateral hilar node lesion and the hyoid bone lesion exhibited significantly higher metabolic activity compared to the primary lung cancer (Figure 3). Ultrasound-guided fine needle aspiration biopsy of the left hyoid mass and the right thyroid nodule resulted in a diagnosis of metastatic mucinous adenocarcinoma and papillary thyroid carcinoma respectively. Correlation of the biopsy with PET/CT confirmed that the hyoid bone tumor had metastasized from the primary lung adenocarcinoma.

FINAL DIAGNOSIS

Metastatic lung adenocarcinoma of invasive mucinous type to the ipsilateral hilar node and hyoid bone. The patient was diagnosed as papillary thyroid carcinoma and follicular lymphoma.

TREATMENT

The patient, now diagnosed with metastatic lung adenocarcinoma to the ipsilateral hilar node and hyoid bone, was presented to a tumor board. The tumor board recommended against a lobectomy due to the higher recurrence risk with stage III lung cancer. Dissection of the hilar lymph node was not recommended as the node was situated in the aortopulmonary zone. Since the lung adenocarcinoma lacked targetable mutations and did not express PDL1, the patient was treated with a platinum-based chemo-immunotherapy along with pembrolizumab based on the outcomes of a clinical trial in 2018[7]. The patient was also referred to head and neck surgery for consideration of resecting the metastatic cancer that engulfed the hyoid bone. However, she elected not to proceed with the procedure due to her concerns about the potential debilitating risks to swallowing and speech function.

Chemotherapy for metastatic lung cancer was initiated with Pemetrexed, Carboplatin, and Pembrolizumab for three cycles before a PET/CT scan was repeated. Despite undergoing chemotherapy, the patient continued to experience left-sided neck pain so 2 mg of dexamethasone OD was prescribed for managing her pain. PET/CT skull base to mid-thigh was repeated and after comparison to the previous PET/CT, the left upper lobe mass appeared to be stable to slightly increased in size, decreased SUV max in the ipsilateral left supra hilar node, and stable to minimally increased SUV max in the left hilar lesion which appeared grossly similar in extent to prior with some increased sclerosis of the engulfed left hyoid. These results indicated that the lung cancer was unresponsive to chemotherapy.

With disease persistent in the hyoid region and significant pain, the oncologist suggested the patient discontinue carboplatin and introduce palliative radiation for the hyoid metastatic disease. The patient chose to pursue radiotherapy. Prior to each treatment, a cone beam CT scan was obtained on the linear accelerator for targeting precision down to about 1 mm. Three hundred cGy was delivered in each treatment fraction and a total of 3600 cGy was given in 12 treatments

Biomarker/Gene	Method	Analyte	Result
ERBB2	Seq	DNA-Tumor	Mutation Not Detected
FGFR3	Seq	RNA-Tumor	Fusion Not Detected
MET	Seq	RNA-Tumor	Variant Transcript Not Detected
NRG1	Seq	RNA-Tumor	Fusion Not Detected
PD-L1(22c3)	IHC	Protein	Negative TPS: 0%
PD-L1(28-8)	IHC	Protein	Negative: 0%
PD-L1(SP142)	IHC	Protein	Negative IC: 0%, Negative TC: 0%
RET	Seq	DNA-Tumor	Mutation Not Detected
STK11	Seq	DNA-Tumor	Mutation Not Detected
TP53	Seq	DNA-Tumor	Mutation Not Detected
ALK	IHC	Protein	Negative
PTEN	IHC	Protein	Positive
Keap1	Seq	DNA-Tumor	Pathogenic Variant
MLH1	IHC	Protein	Positive
MSH2	IHC	Protein	Positive
MSH6	IHC	Protein	Positive
PMS2	IHC	Protein	Positive
CK7	IHC	Protein	Positive
TTF-1	IHC	Protein	Positive
CK20	IHC	Protein	Negative
Napsin	IHC	Protein	Negative

DOI: 10.5306/wjco.v15.i1.159

Figure 2 Lung specimen biomarker/gene table. Cancer-type relevant biomarkers and genes of the lung tumor.

over 2-1/2 wk.

OUTCOME AND FOLLOW-UP

The patient responded well to the treatment, completely remediating the patient's complaint of throat pain and it also resolved the patient's headaches. A repeated PET/CT showed a decrease of SUV max of 16.6 to 5.4 in the hyoid region.

Post palliative radiotherapy treatment, the patient remained asymptomatic for a year until succumbing to the advancing lung cancer.

DISCUSSION

Lung cancer is the leading cause of cancer death and the second most diagnosed cancer in the world[8]. Approximately 13.2% of non-small cell lung cancer metastasizes to bone[9], which are most commonly found on the spine, chest, and pelvis[10]. The hyoid bone is an unusual site for secondary tumors. This is the second reported case of lung adenocarcinoma metastasizing to the hyoid bone.

The previously documented patient elected for surgical resection of the hyoid bone[1]. Our patient opted out of surgery, due to its significant risks which could negatively impact her quality of life. The hyoid bone is positioned in the anterior midline of the neck and situated axially between the mandible and thyroid cartilage[11]. It plays a considerable role in phonation, conserving airway integrity, swallowing, and mastication; therefore, surgical resection of this bone potentially will result in the debilitation of these physiologic functions.

The benefits of palliative radiotherapy for bone cancer pain are well documented[12]. The radiotherapy of 300 cGy with each treatment, totaling 3600 cGy over 2-1/2 wk was well tolerated by the patient, and successfully mitigated the patient's throat pain and headaches.

The relief of headaches was an unexpected positive outcome. One potential theory could be analogous to the Stylocarotid syndrome. Patients with irregular stylohyoid complex either from an elongation of the styloid process, ossification of the stylohyoid ligament, or elongation of the hyoid bone sometimes experience neurological symptoms like headaches and vertigo. This clinical presentation of neck pain, headache, otalgia, and vertigo is due to ischemia, compression of the internal and/or external carotid arteries[11,13,14].

In conclusion, palliative radiotherapy may increase the quality of life for symptomatic patients with metastatic cancer to the hyoid bone.

CONCLUSION

Palliative radiotherapy may add to the quality of life in symptomatic patients with cancer metastatic to the hyoid bone.

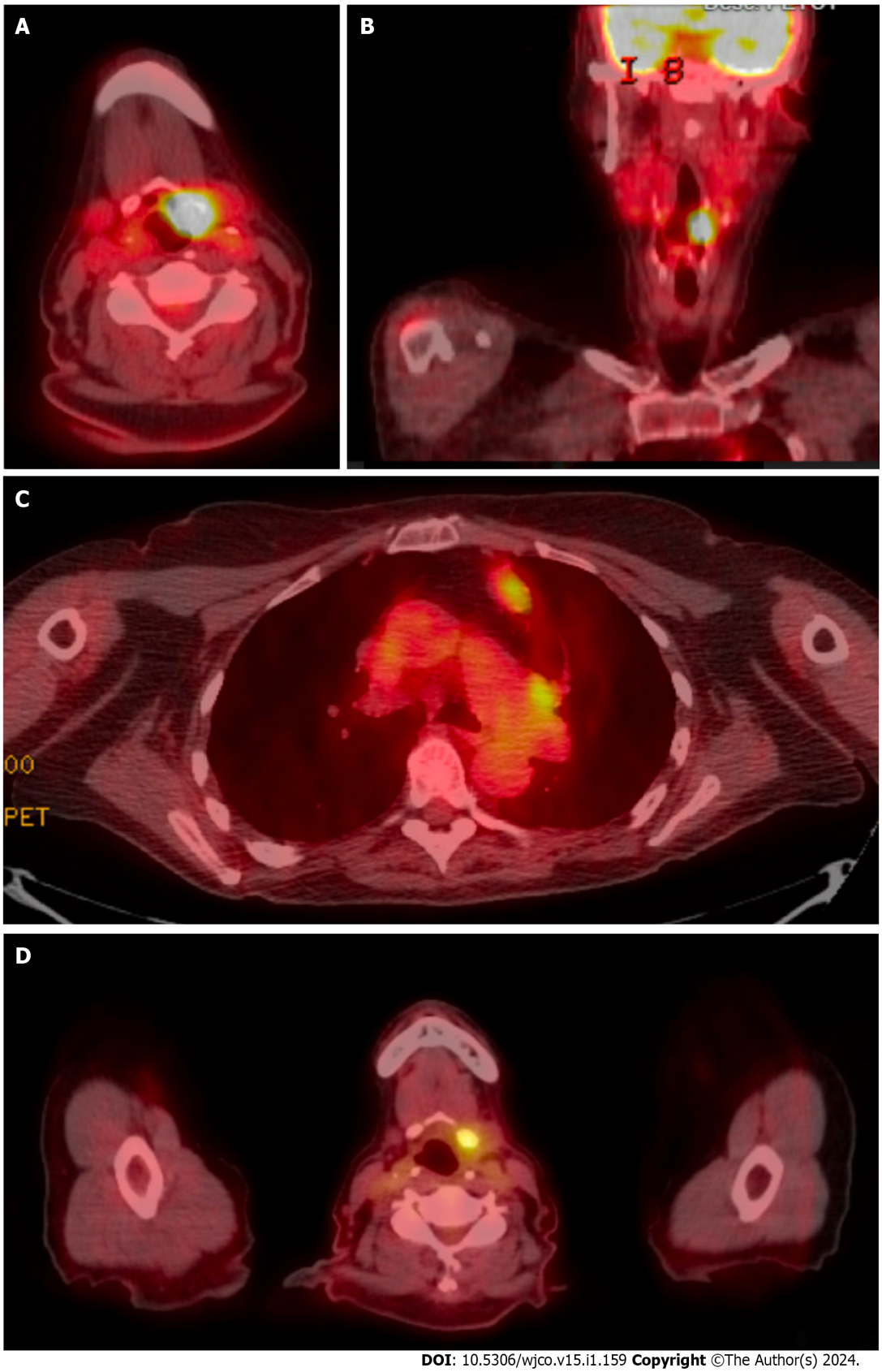

DOI: 10.5306/wjco.v15.i1.159

Figure 3 Positron emission tomography/computed tomography imaging. A and B: Positron emission tomography/computed tomography (PET/CT) imaging indicating hyoid bone tumor; C: PET/CT imaging indicating lung tumors; D: Hyoid region post radiotherapy.

FOOTNOTES

Author contributions: Hsu J contributed to data collection and manuscript writing; Hribar K and Poen J both provided patient data, conceptualization, and supervision; and all authors have read and approved the final manuscript.

Informed consent statement: Informed written consent was obtained from the patients for the publication of this report and any accompanying images.

Conflict-of-interest statement: The authors declare that they have no conflict of interest.

CARE Checklist (2016) statement: The authors have read the CARE Checklist (2016), and the manuscript was prepared and revised according to the CARE Checklist (2016).

Country/Territory of origin: United States

ORCID number: Jonathan Hsu 0009-0009-6054-8733.

S-Editor: Chen YL
L-Editor: A
P-Editor: Zhang XD

REFERENCES

1 **Zhang HY**, Shan Li S, Guo X, Zhao N. Hyoid Bone Metastasis in Patients With Lung Adenocarcinoma: A Case Report. *Ear Nose Throat J* 2021; **100**: NP373-NP376 [PMID: 32283978 DOI: 10.1177/0145561320916985]
2 **Kusama H**, Okishiro M, Ishida T, Sato Y, Morimoto Y, Matsushita K, Hashimoto T, Kimura K, Katsura Y, Nitta K, Kagawa Y, Takeno A, Sakisaka H, Nakahira S, Taniguchi K, Egawa C, Takeda Y, Kato T, Tamura S, Takatsuka Y, Oku K, Goto T, Nagano T, Nakatsuka S. [A case of hyoid bone metastasis from breast cancer]. *Gan To Kagaku Ryoho* 2014; **41**: 1915-1917 [PMID: 25731374]
3 **Iguchi H**, Okabe Y, Takayama M, Wada T, Hachiya K, Matsushita N, Yamane H. [Solitary hyoid bone metastasis from hepatocellular carcinoma treated with surgery]. *Nihon Jibiinkoka Gakkai Kaiho* 2012; **115**: 783-786 [PMID: 23016270 DOI: 10.3950/jibiinkoka.115.783]
4 **Bracanovic D**, Vukovic V, Janovic A, Radosavljevic D, Rakocevic Z. Hyoid Bone and Thyroid Cartilage Metastases from Sigmoid Colon Adenocarcinoma: A Case Report. *Balkan Med J* 2017; **34**: 278-280 [PMID: 28443578 DOI: 10.4274/balkanmedj.2015.1817]
5 **Ryan JF**, Xie DX, Eytan DF, McCarthy EF, Mandal R, Gourin CG, Lipson EJ, Meyer CF, Vosler PS. Melanoma metastatic to the hyoid bone. *Clin Case Rep* 2021; **9**: 522-525 [PMID: 33489207 DOI: 10.1002/ccr3.3571]
6 **Wang SH**, Lee JC, Liu TC. Occult prostate cancer detected by hyoid bone metastasis after resection of thyroglossal duct cyst. *Int J Oral Maxillofac Surg* 2011; **40**: 1326-1328 [PMID: 21601425 DOI: 10.1016/j.ijom.2011.04.010]
7 **Gandhi L**, Rodríguez-Abreu D, Gadgeel S, Esteban E, Felip E, De Angelis F, Domine M, Clingan P, Hochmair MJ, Powell SF, Cheng SY, Bischoff HG, Peled N, Grossi F, Jennens RR, Reck M, Hui R, Garon EB, Boyer M, Rubio-Viqueira B, Novello S, Kurata T, Gray JE, Vida J, Wei Z, Yang J, Raftopoulos H, Pietanza MC, Garassino MC; KEYNOTE-189 Investigators. Pembrolizumab plus Chemotherapy in Metastatic Non-Small-Cell Lung Cancer. *N Engl J Med* 2018; **378**: 2078-2092 [PMID: 29658856 DOI: 10.1056/NEJMoa1801005]
8 **Sung H**, Ferlay J, Siegel RL, Laversanne M, Soerjomataram I, Jemal A, Bray F. Global Cancer Statistics 2020: GLOBOCAN Estimates of Incidence and Mortality Worldwide for 36 Cancers in 185 Countries. *CA Cancer J Clin* 2021; **71**: 209-249 [PMID: 33538338 DOI: 10.3322/caac.21660]
9 **da Silva GT**, Bergmann A, Thuler LCS. Incidence and Risk Factors for Bone Metastasis in Non-Small Cell Lung Cancer. *Asian Pac J Cancer Prev* 2019; **20**: 45-51 [PMID: 30678379 DOI: 10.31557/APJCP.2019.20.1.45]
10 **Zhang L**, Gong Z. Clinical Characteristics and Prognostic Factors in Bone Metastases from Lung Cancer. *Med Sci Monit* 2017; **23**: 4087-4094 [PMID: 28835603 DOI: 10.12659/msm.902971]
11 **AlJulaih GH**, Menezes RG. Anatomy, Head and Neck: Hyoid Bone. 2023 Aug 14. In: StatPearls [Internet]. Treasure Island (FL): StatPearls Publishing; 2023 Jan- [PMID: 30969548]
12 **Zhu G**, Dong Y, He X, Zhao P, Yang A, Zhou R, Ma J, Xie Z, Song XJ. Radiotherapy Suppresses Bone Cancer Pain through Inhibiting Activation of cAMP Signaling in Rat Dorsal Root Ganglion and Spinal Cord. *Mediators Inflamm* 2016; **2016**: 5093095 [PMID: 26989332 DOI: 10.1155/2016/5093095]
13 **Jain S**, Bansal A, Paul S, Prashar DV. Styloid-stylohyoid syndrome. *Ann Maxillofac Surg* 2012; **2**: 66-69 [PMID: 23483633 DOI: 10.4103/2231-0746.95326]
14 **Colby CC**, Del Gaudio JM. Stylohyoid complex syndrome: a new diagnostic classification. *Arch Otolaryngol Head Neck Surg* 2011; **137**: 248-252 [PMID: 21422308 DOI: 10.1001/archoto.2011.25]

Published by **Baishideng Publishing Group Inc**
7041 Koll Center Parkway, Suite 160, Pleasanton, CA 94566, USA
Telephone: +1-925-3991568
E-mail: office@baishideng.com
Help Desk: https://www.f6publishing.com/helpdesk
https://www.wjgnet.com